frontiers | Research Topics

Systems biology in brain-gut axis research

Edited by
Chunhui Bao, Jianhua Chen, Xiaoming Jin and He Wang

Published in
Frontiers in Neuroscience

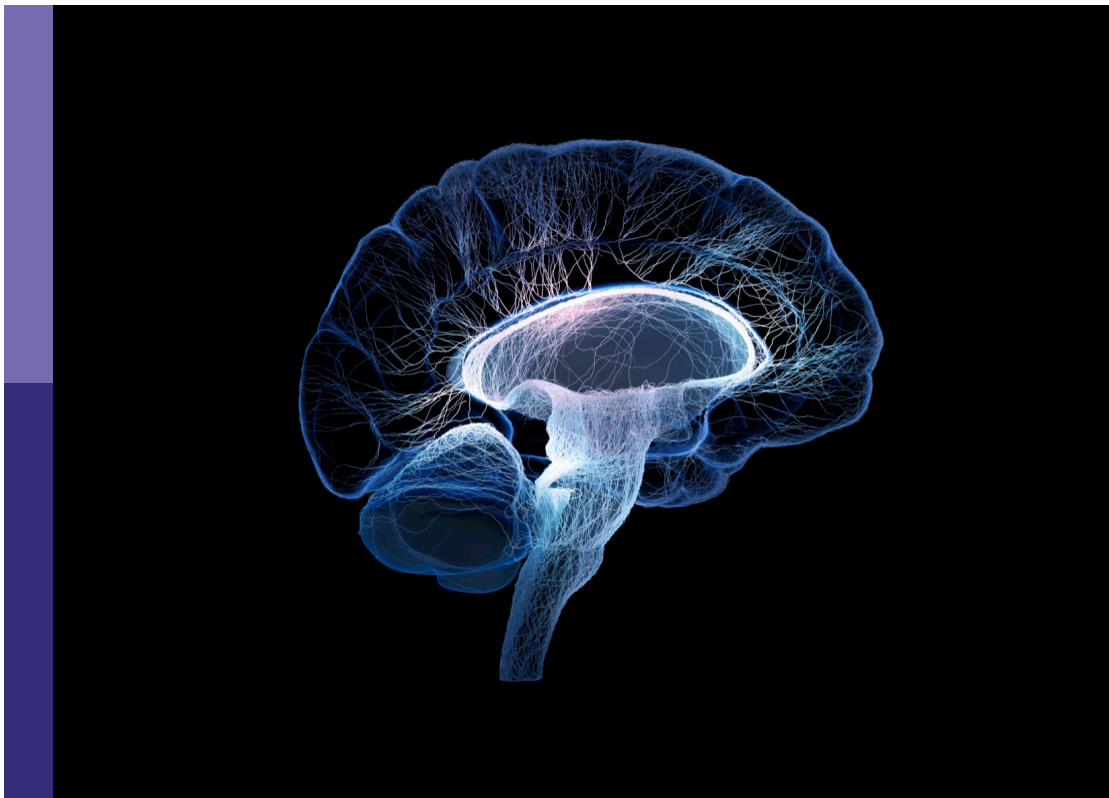

ISSN 1664-8714
ISBN 978-2-8325-2419-0
DOI 10.3389/978-2-8325-2419-0

About Frontiers

Frontiers is more than just an open access publisher of scholarly articles: it is a pioneering approach to the world of academia, radically improving the way scholarly research is managed. The grand vision of Frontiers is a world where all people have an equal opportunity to seek, share and generate knowledge. Frontiers provides immediate and permanent online open access to all its publications, but this alone is not enough to realize our grand goals.

Frontiers journal series

The Frontiers journal series is a multi-tier and interdisciplinary set of open-access, online journals, promising a paradigm shift from the current review, selection and dissemination processes in academic publishing. All Frontiers journals are driven by researchers for researchers; therefore, they constitute a service to the scholarly community. At the same time, the *Frontiers journal series* operates on a revolutionary invention, the tiered publishing system, initially addressing specific communities of scholars, and gradually climbing up to broader public understanding, thus serving the interests of the lay society, too.

Dedication to quality

Each Frontiers article is a landmark of the highest quality, thanks to genuinely collaborative interactions between authors and review editors, who include some of the world's best academicians. Research must be certified by peers before entering a stream of knowledge that may eventually reach the public - and shape society; therefore, Frontiers only applies the most rigorous and unbiased reviews. Frontiers revolutionizes research publishing by freely delivering the most outstanding research, evaluated with no bias from both the academic and social point of view. By applying the most advanced information technologies, Frontiers is catapulting scholarly publishing into a new generation.

What are Frontiers Research Topics?

Frontiers Research Topics are very popular trademarks of the *Frontiers journals series*: they are collections of at least ten articles, all centered on a particular subject. With their unique mix of varied contributions from Original Research to Review Articles, Frontiers Research Topics unify the most influential researchers, the latest key findings and historical advances in a hot research area.

Find out more on how to host your own Frontiers Research Topic or contribute to one as an author by contacting the Frontiers editorial office: frontiersin.org/about/contact

Systems biology in brain-gut axis research

Topic editors

Chunhui Bao — Shanghai University of Traditional Chinese Medicine, China
Jianhua Chen — Shanghai Jiao Tong University, China
Xiaoming Jin — Indiana University; Purdue University Indianapolis, United States
He Wang — Fudan University, China

Citation

Bao, C., Chen, J., Jin, X., Wang, H., eds. (2023). *Systems biology in brain-gut axis research*. Lausanne: Frontiers Media SA. doi: 10.3389/978-2-8325-2419-0

Table of contents

frontiers in Neuroscience

ORIGINAL RESEARCH
published: 16 February 2022
doi: 10.3389/fnins.2022.800976

Is It Worth It? Obesity Affects Snack Food Valuation Across the Menstrual Cycle

Larissa S. Heuberger[1†], Susanna Gobbi[2†], Susanna C. Weber[2], Gwendolyn Graf[3], Philippe N. Tobler[1,2], Lori Asarian[4], Nori Geary[5], Mareike Roth[3] and Brigitte Leeners[3,6*]*

[1] Swiss Federal Institute of Technology, Zurich, Switzerland, [2] Zurich Center for Neuroeconomics, University of Zurich, Zurich, Switzerland, [3] Department of Reproductive Endocrinology, University Hospital of Zurich, Zurich, Switzerland, [4] Department of Medicine, University of Vermont, Burlington, VT, United States, [5] Retired, Underhill, VT, United States, [6] Department of Reproductive Endocrinology, University of Zurich, Zurich, Switzerland

Background: The importance of menstrual cycle physiology in appetite and obesity is poorly understood. We investigated the effects of body mass index (BMI), menstrual cycle phase and sweet and salty taste on monetary valuation of snack foods.

Methods: We recruited 72 women and after the application of in- and exclusion criteria 31 participants with healthy weight and 25 with obesity remained. The participants completed a willingness to pay (WTP) task to measure subjective value of 30 snack food items in the pre-ovulatory and mid-luteal cycle phases.

Results: Generalized linear mixed model (GLMM) analysis revealed that BMI, cycle phase and snack taste interacted to influence WTP (−0.15 [−0.22, −0.03], $p = 0.002$). Hence, WTP was inversely related to BMI, but the strength of the relation depended on cycle phase and taste. The WTP of participants with healthy weight for salty taste changed across cycle phase but the WTP for sweet taste was not affected by cycle phase. Moreover, the cycle effect for the salty snacks ceased in participants with obesity.

Conclusion: The inverse effect of BMI on WTP valuation of snack foods contrasts with the positive effect of BMI on pleasantness ratings for milkshakes by the same women that we previously reported. This indicates that the two measures reflect different aspects of food-related valuative processing in obesity. Furthermore, the WTP data suggest that the selection of salty snacks may differ from that of sweet snacks in the pre-ovulatory phase of the menstrual cycle for individuals of healthy weight. The cycle phase does not seem to affect food valuation of participants with obesity. These findings are relevant to understanding and treating obesity in women.

Keywords: obesity, value-based decision making, food valuation, willingness to pay, ovarian hormones, menstrual cycle

OPEN ACCESS

Edited by:
Xiaoming Jin,
Indiana University-Purdue University Indianapolis, United States

Reviewed by:
Emmanuel N. Pothos,
Tufts University School of Medicine, United States
Derya Dikmen,
Hacettepe University, Turkey

***Correspondence:**
Brigitte Leeners
brigitte.leeners@usz.ch
Larissa S. Heuberger
larissa_heuberger@hotmail.com

[†]*These authors share first authorship*

Specialty section:
This article was submitted to Gut-Brain Axis, a section of the journal Frontiers in Neuroscience

Received: *24 October 2021*
Accepted: *21 January 2022*
Published: *16 February 2022*

Citation:
Heuberger LS, Gobbi S, Weber SC, Graf G, Tobler PN, Asarian L, Geary N, Roth M and Leeners B (2022) Is It Worth It? Obesity Affects Snack Food Valuation Across the Menstrual Cycle. Front. Neurosci. 16:800976. doi: 10.3389/fnins.2022.800976

INTRODUCTION

Obesity remains a pressing issue worldwide. In many countries, obesogenic environments are thought to contribute substantially to obesity's high incidence. These environments include easily available energy-dense foods, which has brought about a relatively novel way of eating known as snacking (Duffey and Popkin, 2011; Mattes, 2018). The calorie intake from snacks add to the calorie

intake from main meals, and therefore snacking is associated with a higher body mass index (BMI; kg/m^2) (Mattes, 2018).

Nevertheless, despite the wide-ranging academic attention devoted to obesity, the roles of reproductive hormones in obesity in women have not often been taken into account. This is important because more women than men suffer from obesity worldwide (NCD Risk Factor Collaboration, 2016). Emotional eating, which is frequently associated with obesity, seems most frequent in the mid-luteal phase of the menstrual cycle and to be influenced by increased levels of both progesterone and β-estradiol (Klump et al., 2013). Indeed, many studies have shown increased subjective appetite and food intake in the mid-luteal compared to the mid- to late-follicular and periovulatory phases of the cycle (Buffenstein et al., 1995; Dye and Blundell, 1997; Brennan et al., 2009; Asarian and Geary, 2013; Gorczyca et al., 2016). It is unclear whether these changes are related to altered macronutrient selection. Some studies did not detect changes (Martini et al., 1994; Brennan et al., 2009), whereas others reported increased protein or carbohydrate intake in the mid-luteal phase (Bowen and Grunberg, 1990; Gorczyca et al., 2016). This change in intake could influence the nutrient metabolism in the gut affecting reward signals. In a recent study (de Araujo et al., 2020), the authors suggest that internal signals *via* the gut-brain-axis generate an unconscious food reward which might constitute the prime driver of overeating. This mechanism is part of a two-roads-to-food-reward model, where food reward is substantially influenced by the flavor-nutrient learning process happening in the gut (i.e., the low-road) and results not only from conscious reward signals based on food perception, taste and oral somatosensation (the high-road). Furthermore, a number of differences in taste perception have been linked to obesity and reproductive hormone status (Asarian and Geary, 2013; Hardikar et al., 2017). These studies indicate that better understanding of the effects of reproductive physiology and food type are important for continued progress in obesity research.

Ovarian hormones may affect food intake by changing the motivation to eat. For example, in ovariectomized rats, administration of β-estradiol resulted in decreased motivation for sucrose rewards (Richard et al., 2017). Such data suggest that estrogens and other ovarian hormones might modulate value-based decision making in relation to food. In addition, diet-induced obesity of female rats is associated with decreased dopamine signaling independent of the menstrual cycle in the nucleus accumbens, which is a fundamental brain region for reward processing (Geiger et al., 2009). We previously analyzed perceived pleasantness of milkshakes in relation to patterns of brain activity detected with fMRI in women with obesity or healthy weight (Gobbi et al., 2020). In that study there was an apparent effect of menstrual cycle phase on perceived pleasantness of sweet milkshakes, but this did not reach statistical significance (Gobbi et al., 2020). Here we expand on these findings studying in the same group of women another aspect of appetite, food valuation as an integration of hunger signals, past experience of the food's flavor and its gastrointestinal and metabolomics effects. To this aim, we used the willingness to pay (WTP) paradigm. The WTP measures the motivation to eat using a bidding and auction method which was developed to quantify an option's utility (Becker et al., 1964). In this study, we aimed to determine if women's valuation of snack foods, first, varies between women with obesity and women with healthy weight, second, varies between the pre-ovulatory and mid-luteal phases of the menstrual cycle, and, third, whether these effects are similar for sweet and salty snack foods.

MATERIALS AND METHODS

All procedures were approved by the Ethics Commission of the Canton of Zurich, and the participants gave written informed consent. They were compensated for expenditures associated with study participation and received 500 Swiss Francs (CHF) for completing the study.

Participants

The participants were recruited and screened for eligibility at the department of Reproductive Endocrinology (University Hospital Zurich). In the pre-screening phase, general, endocrinologic and mental health were assessed through a Clinical Assessment Questionnaire designed for the present study. Only individuals fulfilling our previously described (Gobbi et al., 2020) in- and exclusion criteria were recruited. Women with healthy weight (BMI 18.5–24.9 kg/m^2) or with grade 1 or 2 obesity (BMI 30–39.9 kg/m^2) and who reported that they were weight stable and not dieting were invited to participate. Eligible women were provided with the Three-Factor Eating Questionnaire (TFEQ) and the Eating Disorder Examination-Questionnaire (EDE-Q) to complete at home before the first test visit and to return by mail.

We recruited 72 physically and psychiatrically healthy women who were cycling normally and not using hormonal contraception. Four women withdrew from the study prior to completion, one was excluded due to insufficient German language skills, and two were excluded because of technical difficulties with the tasks. The participants were invited to attend two test visits, one in the pre-ovulatory phase and one in the mid-luteal phase of the menstrual cycle, with order randomized. Tests were timed in relation to menstrual cycle phases, calculated based on cycle information obtained from the participants (i.e., cycle length and days since the last menstruation) and confirmed against progesterone levels. For this paper, the pre-ovulatory phase targeted measurements from 16 ± 2 days prior to menstruation, i.e., shortly before ovulation, with low progesterone levels (3.0 ± 7.9 nmol/l). The mid-luteal phase targeted 7 ± 3 days prior to menstruation with high progesterone levels (21.4 ± 18.5 nmol/l). Six participants were excluded because their blood hormone levels were not in agreement with calculated cycle phases in either cycle phase. Another six participants for which only one cycle phase could be confirmed were retained, with their missing data accounted for in the statistical analyses. Three participants were excluded because their

mean cycle length was not within the normal range (25–35 days).

Test Procedure

Participants were advised not to drink or eat anything after 10pm on the evening prior to both test visits. The study compensation fee served as credit for the WTP task. In this task, participants bid money on a scale from 0 to 2.5 CHF in accordance with their desire to obtain different food items, which were pictures of 15 sweet and 15 salty common snack foods displaying a serving size of the product in front of its package on a black background. The snacks predominantly comprised chocolate bars, nut bars, cookies, gummy bears, crackers, olives, crisps, and salted nuts. To account for potential successive contrast influences among food items, this procedure was done twice for each food item in different order, resulting in 60 WTP bids. The participants bid on a continuous scale using a trackball, which they moved to the desired bid amount and then pressed to confirm their choice. The compensation method for the task was determined by an incentive-compatible auction mechanism (Becker et al., 1964). At the end of each session, one trial was selected at random and implemented. If the participant's bid for the food item in that trial was greater than or equal to the auction price, they paid the auction price from their compensation fee and they received the snack to consume at the laboratory, before leaving. Otherwise, the participant did not obtain the food item and kept the entire compensation amount. The WTP task and several other tasks were completed whilst lying supine in a whole-body MRI scanner [Philips Medical Systems, Laboratory for Social and Neural Systems research (SNS Lab) in Zürich University Hospital, Zürich, Switzerland; more details regarding the scanning procedure and the other experiments are described elsewhere (Gobbi et al., 2020)]. In addition to the WTP task reported here, participants performed a task assessing food value measured by willingness to exert physical effort and a task related to experienced food value (milkshake sampling), which was previously reported (Gobbi et al., 2020). Trials of the different tasks were presented in random order. In addition, on each test day, participants performed the tasks in the MRI twice, once before and once after an *ad libitum* meal. The meal consisted of ham sandwiches and tap water, and the consumed amount was determined by comparing the weight of sandwiches before and after the meal. Weights were transformed to kcal and analyzed as *ad libitum* consumption level. Participants had 30 min to finish the meal and then returned to the scanner and repeated the three valuation tasks. Hence, the participant performed the tasks in two satiety states (fasted, fed) and two menstrual cycle phases (pre-ovulatory, mid-luteal), resulting in four sessions in total.

At different time points throughout the experiment, participants rated a number of subjective states. These included hunger, satiety, desire to eat, nausea, tiredness, feeling well, anxiety, discomfort, agitation, and dizziness. The participants provided these ratings using a generalized visual analog scale ranging from "not at all" to "as strong as possible" (Blundell et al., 2010). The participants answered by moving a trackball along the rating scale and clicking to indicate their response. For both WTP and subjective state ratings the scale direction was randomized across trials and sessions to disentangle brain activation from physical skills or habits related to moving the trackball.

Statistical Analysis

Statistical analyses were performed using Microsoft Excel 2013 and R version 4.0.2 (R Core Team, 2013). Participants were weighed during both visits, which resulted in two different BMIs per participant (kg/m^2). For the Spearman correlation analyses and the generalized linear mixed model (GLMM) analysis, BMI was treated as a continuous variable, whereas for group comparisons, we used the categorical variable weight status, i.e., healthy weight or obese.

Willingness to pay bids without confirmation (no trackball press) were considered invalid, i.e., entered the analysis as missing values. In addition, we excluded items with WTP bids of zero in all four experimental sessions due to an apparent dislike of these items. Visual inspection of the histograms and the quantile-quantile plots indicated that the WTP bids and several other dependent variables were not normally distributed. Therefore, non-parametric statistical analyses were done for all analysis except the GLMM, which was based on a beta distribution. We computed Spearman correlation coefficients (r_s) for WTP bids, BMI, *ad libitum* consumption levels, TFEQ scores, and the subjective state ratings from the time points around the WTP task, excluding missing values. A correlation matrix (**Figure 1**) was constructed using the R function corrplot (Wei et al., 2017). Magnitudes of the correlations are reported with the Spearman correlation coefficient r_s.

We also contrasted the mean WTP bids, the EDE-Q and the TFEQ scores of the groups with healthy weight and obesity using Wilcoxon signed-rank tests for independent samples and we conducted group comparisons for WTP differences for sweet or salty food items using Wilcoxon signed-rank tests for paired samples. To calculate effect sizes r for the Wilcoxon tests we used the R function wilcox_effsize (Kassambara, 2020). We further tested for mean differences in WTP across cycle phases. To account for seven participants who completed two test visits in the same cycle phase and six participants for whom only one cycle phase was confirmed, we applied a method designed for paired data with missing values (Fong et al., 2018) using the R function pm.wilcox.test with the SR-MW method, which consists of a combination of signed-rank statistics for paired data and Mann-Whitney statistics for unpaired data (Fong et al., 2018). Because this test results in a *Z*-value, the effect sizes were calculated as the *Z*-statistic divided by the square root of the number of observations (Rosenthal, 1994). Visualizations of group comparisons were obtained using ggplot (Wickham, 2006). The Spearman correlations and group contrasts were considered exploratory, so we used a significance level of $\alpha = 0.05$.

The dependent variable for the GLMM analysis was the WTP. As these data followed an extreme values distribution determined by the monetary rating boundaries of 0 and 2.5 (in CHF), we used a beta regression model and a logit function as link (Cribari-Neto and Zeileis, 2010). The data were divided by 2.5 to normalize WTP values (WTP_{Norm}) to between 0 and 1, as previously suggested (Smithson and Verkuilen, 2006), and transformed using the function $WTP_{conv} = ([WTP_{Norm}(n-1) + 0.5]/n)$ where

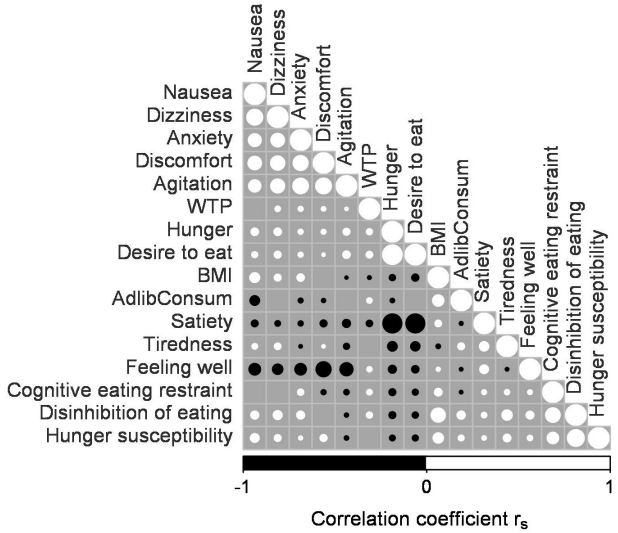

FIGURE 1 | Correlation matrix of willingness to pay (WTP), *ad libitum* consumption level, BMI, Three-Factor Eating Questionnaire (TFEQ) scores, and subjective state ratings. This correlation matrix displays the correlation of WTP, BMI, *ad libitum* consumption level, TFEQ Cognitive eating restraint, TFEQ Disinhibition of eating, TFEQ Hunger susceptibility, nausea, dizziness, anxiety, discomfort, agitation, hunger, desire to eat, satiety, tiredness, and feeling well. See Results for further explanations. The diameter of the filled and open circles are proportional to the correlation magnitude (r_s) where a large circle stands for a high r_s. Open circles indicate positive correlation, whereas filled circles indicate negative correlations. No circle is depicted at intersections where there was no significant correlation ($p > 0.05$).

n is the number of samples (Smithson and Verkuilen, 2006). We used the glmmTMB R package because it enables inclusion of random effects in the model (Brooks et al., 2017). We included random intercepts for participants and items as well as participant-specific random slopes for *Day* and *Satiety*. The model is defined as follows:

$$WTP_{ij} = (\beta_0 + u_{0j} + u_{0k}) + (\beta_1 + u_{1j})\, Day_{ij} + (\beta_2 + u_{2j})$$

$$Satiety_{ij} + \beta_3 CP_{ij} + \beta_4\, AdlibConsum_{ij} + \beta_5\, BMI_{ij} + \beta_6$$

$$Taste_{ij} + \beta_7\, AdLibConsum_{ij}\, BMI_{ij} + \beta_8\, CP_{ij}\, AdLibConsum_{ij} +$$

$$\beta_9 CP_{ij}\, BMI_{ij} + \beta_{10}\, BMI_{ij} Taste_{ij} + \beta_{11}\, CP_{ij}\, Taste_{ij} +$$

$$\beta_{12}\, AdLibConsum_{ij}\, Taste_{ij} + \beta_{13}\, CP_{ij}\, AdLibConsum_{ij}\, BMI_{ij} +$$

$$\beta_{14}\, CP_{ij}\, BMI_{ij}\, Taste_{ij} + \beta_{15}\, CP_{ij}\, AdLibConsum_{ij}\, Taste_{ij} + e_{ij}$$

The index i represents the trial, j the participant and k the item. The continuous variables *BMI* and *ad libitum* consumption level (*AdlibConsum*) were *z*-scored at a group level and day of test visit (*Day*; Day 1 or Day 2), *Satiety* (Fasted or Fed), cycle phase (*CP*; Pre-ovulatory or Mid-luteal), and *Taste* (Sweet or Salty) were used as binary variables. Two- and three-way interactions were included. We calculated the *p*-values using the Wald statistic. To correct for the multiple tests using WTP bids as dependent variable (correlation, three Wilcoxon tests and the GLMM), we applied the Bonferroni procedure, resulting in a nominal threshold of 0.01 (= 0.05/5), and only effects for which *p*-value < 0.01 were considered significant. To display significant interaction effects we used the R functions ggpredict and ggplot (Wickham, 2006; Lüdecke, 2018).

RESULTS

Subjects

We report the results for 56 women who fulfilled our selection criteria. **Table 1** shows the participants' demographic data. We assessed the cycle phases more conservatively than previously, resulting in fewer participants than in our previous paper (Gobbi et al., 2020). Forty-six (82%) women submitted complete questionnaires. These participants' global EDE-Q scores were 1.4 ± 1.1, which closely matches community norm values (Fairburn et al., 2014). The EDE-Q scores Restraint, Eating concern, Shape concern and Weight concern were all significantly lower for participants with healthy weight than for those with obesity (median Restraint 0.4 and 1.2, $r = 0.36$, $p = 0.016$; Eating concern 0.2 and 0.8, $r = 0.51$, $p < 0.001$; Weight concern 0.1 and 3.0, $r = 0.68$, $p < 0.001$; and Shape concern 1.1 and 3.5, $r = 0.65$, $p < 0.001$). The TFEQ scores cognitive eating restraint and hunger susceptibility did not differ between participants with healthy weight and with obesity ($p = 0.414$ and $p = 0.058$) but disinhibition of eating was higher in the obese than in the healthy weight group (median 9.0 and 7.0, $r = 0.40$, $p = 0.007$).

Spearman Correlations

Figure 1 summarizes the Spearman correlational data. The WTP bids correlated very weakly positively with desire to eat, hunger, feeling well, dizziness, anxiety, agitation and discomfort ($r_s \leq 0.1$, $p \leq 0.011$) and negatively with satiety rating ($r_s = -0.09$, $p < 0.001$) and BMI ($r_s = -0.03$, $p = 0.002$). Analysis of the TFEQ scores revealed a weak but significant correlation of BMI with cognitive eating restraint and hunger susceptibility ($r_s = 0.13$, $p < 0.001$ and $r_s = 0.25$, $p < 0.001$) and a moderate correlation of BMI with disinhibition of eating ($r_s = 0.46$, $p < 0.001$). We also found very weak correlations of WTP with cognitive restraint and with disinhibition of eating ($r_s \leq 0.1$, $p < 0.001$; **Figure 1**). Hence, the Spearman correlations of WTP bids with the subjective state ratings, TFEQ scores and *ad libitum* consumption level failed to reveal any strong relationships.

Group Comparisons

The WTP bids (in CHF) of participants with healthy weight were significantly reduced in the pre-ovulatory compared to the mid-luteal phase (median 0.95 and 1.10, $r = -0.14$, $p < 0.001$), whereas those of women with obesity did not change significantly across cycle phases ($p = 0.334$; **Figure 2**). Furthermore, group comparisons within cycle phase showed that the pre-ovulatory WTP bids were higher in participants with obesity than in

TABLE 1 | Demographics of the participants fulfilling the inclusion criteria.

	Mean ± SD	Range
Age (y)	25.5 ± 4.7	(18–40)
Healthy weight (*n* = 31)	26.0 ± 5.0	(19–40)
Obese (*n* = 25)	24.9 ± 4.4	(18–33)
BMI (kg/m^2)	26.9 ± 5.4	(18.8–37.4)
Healthy weight (*n* = 31)	22.3 ± 2.1	(18.8–25.9)
Obese (*n* = 25)	32.3 ± 2.2	(29.0–37.4)
Cycle length (d)	29 ± 2	(25–35)
Healthy weight (*n* = 31)	28 ± 2	(25–32)
Obese (*n* = 25)	29 ± 2	(27–35)
EDE-Q: restraint	1.0 ± 1.0	(0–3.6)
Healthy weight (*n* = 27)	0.6 ± 0.8	(0–3.2)
Obese (*n* = 19)	1.4 ± 1.2	(0–3.6)
EDE-Q: eating concern	0.6 ± 0.8	(0–3.0)
Healthy weight (*n* = 27)	0.3 ± 0.4	(0–1.4)
Obese (*n* = 19)	1.1 ± 1.0	(0–3.0)
EDE-Q: shape concern	2.1 ± 1.5	(0–5.4)
Healthy weight (*n* = 27)	1.3 ± 0.8	(0–3.6)
Obese (*n* = 19)	3.3 ± 1.4	(0.8–5.4)
EDE-Q: weight concern	1.8 ± 1.5	(0–5.2)
Healthy weight (*n* = 27)	0.9 ± 0.7	(0–2.4)
Obese (*n* = 19)	3.0 ± 1.4	(0.4–5.2)
TFEQ: cognitive eating restraint	6.9 ± 4.0	(1–15)
Healthy weight (*n* = 27)	6.5 ± 4.4	(1–14)
Obese (*n* = 19)	7.5 ± 3.5	(2–15)
TFEQ: disinhibition of eating	7.1 ± 3.1	(1–15)
Healthy weight (*n* = 27)	5.9 ± 3.2	(1–11)
Obese (*n* = 19)	8.7 ± 3.5	(2–15)
TFEQ: hunger susceptibility	5.3 ± 3.6	(0–13)
Healthy weight (*n* = 27)	4.6 ± 2.9	(0–11)
Obese (*n* = 19)	6.3 ± 3.1	(1–13)

Data are mean ± SD and range for all 56 participants except as noted. BMI [weight (kg)/height^2 (m^2)] are the data collected on the two test days. The women with healthy weight include three women whose BMI increased from below 25 at screening to between 25 and 26 during the tests, and the women with obesity include three women whose BMI decreased from above 30 at screening to between 29 and 30 during the tests.

participants with healthy weight (median 1.00 and 0.95, $r = 0.05$, $p = 0.012$) whereas the mid-luteal WTP bids were lower in participants with obesity than those with healthy weight (median 1.00 and 1.10, $r = 0.07$, $p < 0.001$). Thus, obesity eliminated the effect of the menstrual cycle on WTP for snack foods that was evident in women with healthy weight (**Figure 2**).

On average, the WTP bids for sweet snacks were higher than the ones for salty snacks (median 1.08 and 0.98, $r = 0.13$, $p < 0.001$). This difference arose in both cycle phases (pre-ovulatory $r = 0.14$, $p = 0.002$ and mid-luteal $r = 0.12$, $p = 0.010$) and weight groups (healthy weight $r = 0.12$, $p = 0.010$ and obese $r = 0.15$, $p = 0.002$). Hence, WTP differed depending on the taste of the snack foods presented, i.e., sweet or salty.

Generalized Linear Mixed Model

The GLMM outcomes are summarized in **Table 2**. The satiety state significantly affected WTP_{conv} ($p_{corrected} < 0.01$). Specifically, average WTP_{conv} was higher in fasted compared to fed satiety state ($Z = -5.13$, $p < 0.001$). The predictor snack type ("taste") showed a trend-level effect but did not survive Bonferroni correction. There were two significant interactions predicting WTP_{conv} bids ($p_{corrected} < 0.01$). The first interaction was between snack type and cycle phase ($Z = 4.27$, $p < 0.001$), the second one between snack type, cycle phase and BMI ($Z = -3.07$, $p = 0.002$). As shown in **Figure 3**, WTP_{conv} was inversely related to BMI but the strength of the relation depended on cycle phase and snack type. That is, for both snack types in the mid-luteal phase and for sweet snacks in the pre-ovulatory phase, mean WTP_{conv} decreased similarly from ∼0.50 in participants with the lowest BMI to ∼0.35 in participants with the highest BMI. In contrast, WTP_{conv} for salty snacks in the pre-ovulatory phase was less, ∼0.41, in participants with the lowest BMI, and decreased less steeply, to ∼0.37 for participants with the highest BMI. Furthermore, WTP bids for salty foods were generally higher in women with lower BMI than with high BMI, especially during the mid-luteal phase. In contrast, for sweet snacks, WTP bids were also generally higher in women with lower BMI, but were not affected by menstrual cycle phase.

DISCUSSION

Food Valuation Depends on Obesity, Cycle Phase, and Snack Taste

In this study we used a WTP method to measure the subjective value of snack foods in women with healthy weight or obesity. We report an inverse relationship between WTP and BMI, which depends on snack taste and cycle phase. The decreasing WTP with increasing BMI is opposite to what we found in a milkshake tasting task, where the same participants' pleasantness ratings increased with BMI (Gobbi et al., 2020). This indicates that the different tasks link to different parts of the reward and valuation systems. Specifically, rating milkshake pleasantness is a more sensory or consummatory process, whereas WTP is a more anticipatory process. Moreover, compared to typical anticipatory ratings, such as expected satiety (Brunstrom, 2014), the WTP task is a more complex decision-making and value-estimation task. Indeed, during the milkshake task our fMRI data indicated that predominantly hedonic and homeostatic brain circuits were activated (Gobbi et al., 2020) whereas WTP has been reported to be associated with activity in different regions of the prefrontal cortex (Plassmann et al., 2007; Tang et al., 2014). This might reflect involvement of cognition and value computation in the WTP task, which is in line with the prefrontal cortex being involved in cognitive control of goal-directed behavior (Miller and Cohen, 2001). Relatedly, cognitive restraint of eating may have influenced WTP bidding of participants with obesity. High cognitive restraint is positively associated with BMI [e.g., Banna et al. (2018) and Adams et al. (2019)] and has been reported to dampen cyclic eating changes (Asarian and Geary, 2013). We measured a small positive correlation of both WTP and BMI with the TFEQ score cognitive eating restraint and the EDE-Q scores Restraint and Eating concern were

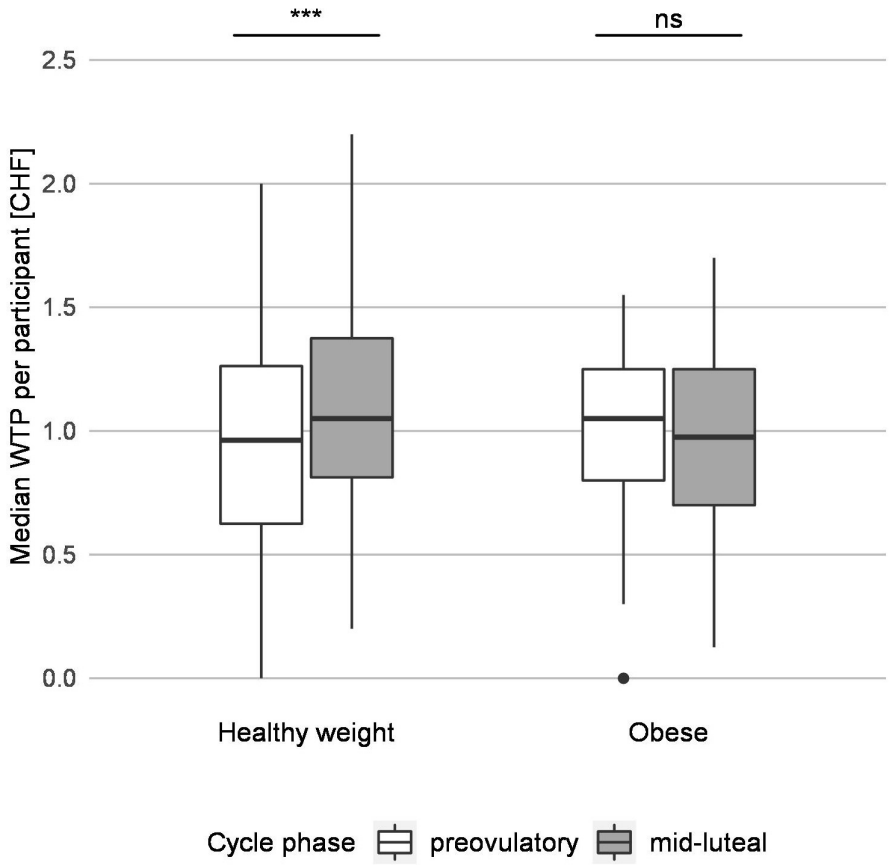

FIGURE 2 | Group testing reveals that pre-ovulatory and mid-luteal willingness to pay (WTP) differs for participants with healthy weight but not for participants with obesity. The median WTP per participant for participants with normal weight and with obesity are depicted. The white and the gray boxes represent the median WTP per participant in the pre-ovulatory and mid-luteal cycle phase, respectively, and indicate the range of the data from the first to the third quartile. The horizontal line represents the median, and the whiskers reach to the minimal and maximal values not considered outliers; one outlier is represented by a dot. Group comparisons revealed a significant difference in WTP between pre-ovulatory and mid-luteal cycle phase for participants with healthy weight but not for participants with obesity. ***$p < 0.001$, ns, not significant.

significantly increased in women with obesity. Hence, WTP of participants with obesity might be lower in part due to cognitive restraint.

Food Valuation Differs by Cycle Phase for Salty Snacks

Our findings reveal that valuation appears to be higher for sweet than for salty snack foods, especially for participants with obesity and in the pre-ovulatory cycle phase. In contrast, mid-luteal WTP bids of participants with healthy weight did not differ by taste. Hence, while the WTP for salty snacks increased from the pre-ovulatory to mid-luteal cycle phase, the WTP for sweet snacks did not depend on cycle phase. This absence of cycle effect for sweet food parallels the findings on pleasantness of milkshakes (Gobbi et al., 2020). The mid-luteal increase in women's value for salty food is in accordance with an apparent stronger dislike of unsalted popcorn in the luteal phase compared to the follicular phase (Frye and Demolar, 1994). However, neither intake of nor preference ratings for salty food changed between menstrual cycle phases (Bowen and Grunberg, 1990). Thus, further research is required to assess the relationship between the valuation change and actual intake of salty foods in snack and non-snack contexts. We conclude, first, that women's food valuation differs by taste and, second, that valuation for salty food but not for sweet food differs by cycle phase.

Possible Mechanisms

Previous neuroimaging studies demonstrated correlations between WTP and activity of different brain regions (Plassmann et al., 2007; Tang et al., 2014). Some of these are associated with subjective values, reinforcing the idea that the WTP approach is a valid measure of subjective value (Bartra et al., 2013). We found that WTP is lower in the pre-ovulatory than in the mid-luteal phase for participants with healthy weight. In line with this, another study found that the appeal of food images was lower in the second week of the menstrual cycle than in the last week (Frank et al., 2010). Such changes across the menstrual cycle have also been reported for brain activation in response to food images and uncertain monetary rewards

TABLE 2 | The generalized linear mixed model (GLMM) reveals a main effect of satiety state, an interaction of cycle phase with snack taste, and a three-way interaction of cycle phase with snack taste and BMI to significantly predict WTP_{conv}.

	Estimate	SE	*Z*-statistic	*P*-value
(Intercept)	−0.15 [−0.34, 0.09]	0.14	−1.12	0.264
Mid-luteal	−0.04 [−0.21, 0.15]	0.09	−0.40	0.687
AdlibConsum	0.08 [−0.11, 0.25]	0.09	0.86	0.391
BMI	−0.15 [−0.33, 0.06]	0.10	−1.45	0.146
Salty	−0.29 [−0.36, −0.23]	0.12	−2.37	0.018
Fed	−0.24 [−0.32, −0.14]	0.05	−5.13	< 0.001∗
Day 2	−0.03 [−0.18, 0.13]	0.08	−0.36	0.717
AdlibConsum × BMI	0.05 [−0.11, 0.22]	0.08	0.65	0.515
Mid-luteal × AdlibConsum	0.10 [−0.09, 0.30]	0.10	1.00	0.319
Mid-luteal × BMI	0.01 [−0.18, 0.18]	0.09	0.15	0.878
BMI × Salty	0.08 [−0.01, 0.13]	0.04	2.21	0.027
Mid-luteal × Salty	0.20 [0.09, 0.28]	0.05	4.27	< 0.001*
AdlibConsum × Salty	−0.04 [−0.11, 0.04]	0.04	−1.12	0.263
Mid-luteal × AdlibConsum × BMI	−0.07 [−0.25, 0.10]	0.09	−0.73	0.466
Mid-luteal × BMI × Salty	−0.15 [−0.22, −0.03]	0.05	−3.07	0.002*
Mid-luteal × AdlibConsum × Salty	−0.05 [−0.16, 0.04]	0.05	−1.03	0.303
Number of observations:		11,022		
BIC:		−14655.2		

*This table illustrates the GLMM results aiming to explain WTP_{conv} by the different predictors CP (Pre-ovulatory or Mid-luteal), AdlibConsum (Z score), Taste (Sweet or Salty), BMI (Z score), Satiety (Fasted or Fed), Day (Day 1 or Day 2), and interaction effects among predictor variables, according to Eq. 1. The confidence intervals were computed for the fixed terms considering the random effect for participants but not items because it was not possible to include both random effects due to algorithmic limitations of the package used in R. The p-values were obtained using the Wald Z-statistic. Bonferroni-corrected significant effects were found for Satiety (Fed), the interaction of CP and Taste (Mid-luteal × Salty) as well as the interaction of BMI, CP, and Taste (BMI × Mid-luteal × Salty). Data are mean regression coefficients [95% CI] and all continuous regressors were z-scored before entering the model. P-values are uncorrected; *Significant following Bonferroni-correction, $p_{corrected} < 0.01$.*

(Dreher et al., 2007; Frank et al., 2010). Furthermore, rat studies have revealed that estrogens enhance striatal dopamine signaling (Becker and Cha, 1989; Becker, 1999; Yoest et al., 2014). Although neither estrogens nor progestins are sufficient to explain increased energy intakes in the mid-luteal cycle phase in women or other anthropoid primates (Asarian and Geary, 2013), increases in the two hormones have been associated with increases in emotional eating during the mid-luteal phase (Klump et al., 2013) and progesterone and β-estradiol synergized to induce striatal dopamine release in rats (Yoest et al., 2018).

As described above, WTP bids decreased with increasing BMI, but changed across the menstrual cycle only in participants with healthy weight bidding for salty snacks. At least the former effect may be related to dopamine signaling. The reward behavior in the group with obesity, which did not depend on the menstrual cycle, supports results of experiments with female rats which showed that an obesity-inducing regimen decreased mesolimbic dopamine transmission (Geiger et al., 2009). Furthermore, reduced activation of reward-associated brain regions in individuals with obesity has been shown in human trials (Carnell et al., 2012), and striatal dopamine D_2 receptor expression was lower in individuals with severe obesity compared to humans with healthy weight (Wang et al., 2001). Relatedly, long term intake of energy-rich food (Burger and Stice, 2011) and high saturated-fat diets (Kleinridders and Pothos, 2019) decrease dopamine signaling in reward-associated brain areas. Thus, chronic downregulation of dopamine in certain brain regions of individuals with obesity may interfere with reward processing, which would otherwise depend on menstrual cycle. Further research should address how dopamine signaling affects valuation of different foods across the menstrual cycle and in women with different BMI.

Subjective State Ratings and Satiety State

The GLMM revealed a significant main effect of satiety state (fed or fasted) as a predictor for WTP_{conv}. This supports theoretical approaches suggesting that value-based decision making depends on hunger (Niv et al., 2006; Rangel et al., 2008) and that the food evaluation process is influenced by the gut-brain-axis (de Araujo et al., 2020). In apparent contrast, our correlational analyses suggested that WTP bids were not substantially related to subjective states. In view of the interactive effect of BMI, cycle phase and snack taste revealed by the GLMM, however, it is not surprising that simple correlational analyses failed. The lower power of non-parametric correlations may have also contributed. It is also possible that subjective ratings are weaker measures of food valuation than our behavioral and fMRI measures. For example, the weak correlation of satiety ratings and WTP contrasts with the clear main effect of satiety state as a predictor for WTP_{conv}. Additionally, our fMRI analysis revealed increased striatal and prefrontal activity in participants with obesity

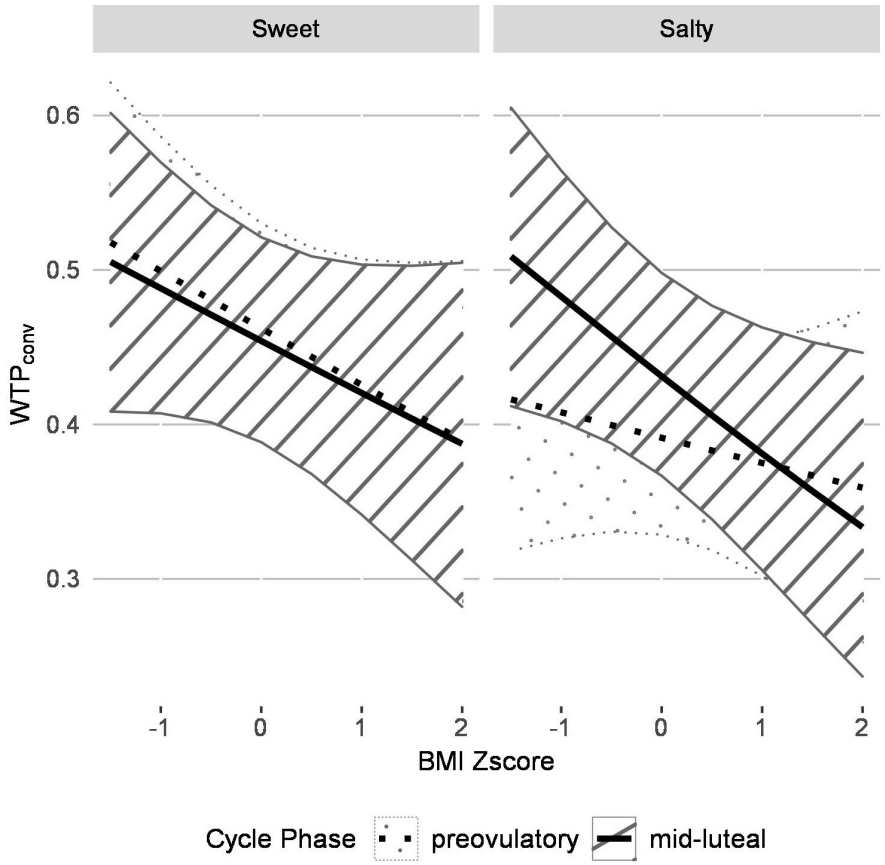

FIGURE 3 | The generalized linear mixed model (GLMM) reveals that the relationship between WTP_{conv} is inversely related to BMI for both sweet and salty snacks and menstrual cycling affects WTP_{conv} for salty, but not for sweet, snacks. The plot visualizes how cycle phase, taste and BMI interact to predict WTP_{conv} according to the GLMM. WTP_{conv} is inversely related to BMI and the strength of this relationship depends on cycle phase and taste. For sweet food items, average pre-ovulatory and mid-luteal WTP_{conv} both decrease with increasing BMI and the GLMM only predicted a slight difference between cycle phases. For salty food items, higher average WTP bids are predicted in the mid-luteal compared to the pre-ovulatory cycle phase for participants with low BMI whereas this effect diminishes with increasing BMI. Control analyses verified that the overall effect was reflected in the data of the individual groups.

despite their ratings of high satiety and low desire to eat (Gobbi et al., 2020).

Strengths and Limitations

We used BMI as a metric to discriminate between people with and without obesity rather than other methods like dual energy x-ray absorptiometry (DXA) because it remains a simple and accurate measure for obesity on a population level (The World Health Organization [WHO], 2022). However, the association between BMI and body fat content is limited because BMI does not consider age, physical activity level, and sex (The World Health Organization [WHO], 2022). Still, in our study, we controlled for the variables age and sex as only adult, premenopausal women were included. Moreover, we asked the participants to fill out the International Physical Activity Questionnaire (IPAQ) to determine their physical activity (Craig et al., 2013) because it has been shown that BMI can be especially inaccurate for individuals with a high muscle mass, e.g., athletes. Indeed, the literature suggests that athletes' food choices are influenced not only by the commonly found factors taste, convenience, and nutrition (Birkenhead and Slater, 2015). Sport requires a different type of energy supply and athletes choose food in order to optimize their performance (Parraga, 1990; Eertmans et al., 2005; Birkenhead and Slater, 2015). Likewise, weight-conscious individuals usually prioritize low-energy foods that are helpful for their diet and body composition compared to more palatable choices (Birkenhead and Slater, 2015). Thus, we could expect sports involvement to enhance inhibitory control and dietary self-control (Wills et al., 2007; Lowe et al., 2016) and consequentially to decrease the positive evaluation of food snacks in the WTP task implemented in the study. The IPAQ allowed us to control for differences in the level of physical activity between people with obesity and with healthy weight; on average between groups, we did not find any. Therefore, we can exclude high BMI due to increased muscle mass. Furthermore, the difference of body weight in an average Swiss woman (1.64 m tall; Eglitis-media, 2022) between a BMI of 22.3 and 32.3 (mean BMI of the two groups) corresponds to 26.9 kg, which is unlikely to be due to

differences in muscle mass alone. Hence, in view of these considerable differences of BMI between groups and the control for confounding factors such as age, sex, and physical activity, we considered BMI as a sufficient measure to differentiate participants with healthy weight from those with obesity. In general, our inclusion criteria were rather strict in order to increase the likelihood of detecting causal neuroendocrine effects. Although we invited only participants with a BMI greater than 30 or below 25, some participants changed body weight enough to bring their BMI outside the inclusion criteria. This was unlikely to be of high importance for the majority of our analysis in which BMI was used as a continuous variable. Participants were informed that the study was about steroid hormones and asked to maintain menstrual cycle records; this might have promoted response biases related to their beliefs about menstrual cycle and appetite. Timing may have affected some outcomes because food preferences are lower in the morning, when our experiment took place, than later in the day (Reichenberger et al., 2018). Lastly, other factors, such as prices, social information, habituation and labels, might have influenced WTP ratings in our test situation (List and Shogren, 1999; Niv et al., 2006; Rangel et al., 2008; Suzuki et al., 2017; Motoki and Suzuki, 2020). To minimize habituation bias, we organized the study sessions in random order with respect to cycle phase. Furthermore, the participants were provided with all instructions prior to the test sessions and they conducted the WTP task alone in the scanner.

CONCLUSION

This study aimed to measure food valuation and to investigate whether it changes with BMI, cycle phase, and taste. Our major findings were that WTP changes across the menstrual cycle for participants with healthy weight and for salty food items. This indicates that obesity research should focus more on the influences of, first, types of foods and eating occasions and, second, reproductive hormones on reward processing, in particular dopamine signaling and anticipatory food valuation. Furthermore, the reduction in the effect of menstrual cycle changes on food valuation in women with obesity is a novel finding which, if reproduced by future studies, may be critical for future obesity research.

DATA AVAILABILITY STATEMENT

The datasets generated and/or analyzed during the current study are available from the corresponding author on reasonable request. Requests to access the datasets should be directed to BL, brigitte.leeners@usz.ch.

ETHICS STATEMENT

The studies involving human participants were reviewed and approved by Ethics Commission of the Canton of Zurich. The patients/participants provided their written informed consent to participate in this study.

AUTHOR CONTRIBUTIONS

LH planned and performed the data analysis and wrote the first draft of the manuscript. SG collected and curated the data, planned and supported the data analysis. SW programmed the task and collected data. GG, MR, and BL realized recruitment and selected the participants. BL, LA, NG, PT, MR, and SW designed the study. All authors contributed to the manuscript and approved the final version.

FUNDING

This work was supported by funding from the Marlene Porsche Foundation, the Zurich Center for Integrative Human Physiology, Philhuman Foundation, Foundation for Nutrition Research, Foundation for Scientific Research University of Zurich, Baugarten Foundation, and the Swiss NSF (grants PP00P1 150739 and 100014_165884 to PT).

ACKNOWLEDGMENTS

We would like to thank the participants from this study, Ferdinand von Meyenn for his valuable comments and discussions, and Daria Hinz and Karl Treiber for their assistance with the data collection.

REFERENCES

Adams, R. C., Chambers, C. D., and Lawrence, N. S. (2019). Do restrained eaters show increased BMI, food craving and disinhibited eating? A comparison of the restraint scale and the restrained eating scale of the dutch eating behaviour questionnaire. *R. Soc. Open Sci.* 6:190174. doi: 10.1098/rsos.190174

Asarian, L., and Geary, N. (2013). Sex differences in the physiology of eating. *Am. J. Physiol. Regul. Integr. Comp. Physiol.* 305, R1215–R1267.

Banna, J. C., Panizza, C. E., Boushey, C. J., Delp, E. J., and Lim, E. (2018). Association between cognitive restraint, uncontrolled eating, emotional eating and BMI and the amount of food wasted in early adolescent girls. *Nutrients* 10:1279. doi: 10.3390/nu10091279

Bartra, O., McGuire, J. T., and Kable, J. W. (2013). The valuation system: a coordinate-based meta-analysis of BOLD fMRI experiments examining neural correlates of subjective value. *Neuroimage* 76, 412–427. doi: 10.1016/j.neuroimage.2013.02.063

Becker, G. M., Degroot, M. H., and Marschak, J. (1964). Measuring utility by a single-response sequential method. *Behav. Sci.* 9, 226–232. doi: 10.1002/bs.3830090304

Becker, J. B. (1999). Gender differences in dopaminergic function in striatum and nucleus accumbens. *Pharmacol. Biochem. Behav.* 64, 803–812. doi: 10.1016/s0091-3057(99)00168-9

Becker, J. B., and Cha, J.-H. (1989). Estrous cycle-dependent variation in amphetamine-induced behaviors and striatal dopamine release assessed with microdialysis. *Behav. Brain Res.* 35, 117–125. doi: 10.1016/s0166-4328(89)80112-3

Birkenhead, K. L., and Slater, G. (2015). A review of factors influencing athletes' food choices. *Sports Med.* 45, 1511–1522. doi: 10.1007/s40279-015-0372-1

Blundell, J., de Graaf, C., Hulshof, T., Jebb, S., Livingstone, B., Lluch, A., et al. (2010). Appetite control: methodological aspects of the evaluation of foods. *Obes. Rev.* 11, 251–270. doi: 10.1111/j.1467-789X.2010.00714.x

Bowen, D. J., and Grunberg, N. E. (1990). Variations in food preference and consumption across the menstrual cycle. *Physiol. Behav.* 47, 287–291. doi: 10.1016/0031-9384(90)90144-s

Brennan, I. M., Feltrin, K. L., Nair, N. S., Hausken, T., Little, T. J., Gentilcore, D., et al. (2009). Effects of the phases of the menstrual cycle on gastric emptying, glycemia, plasma GLP-1 and insulin, and energy intake in healthy lean women. *Am. J. Physiol. Gastrointest. Liver Physiol.* 297, G602–G610. doi: 10.1152/ajpgi.00051.2009

Brooks, M., Kristensen, K., van Benthem, K., Magnusson, A., Berg, C. W., Nielsen, A., et al. (2017). glmmTMB balances speed and flexibility among packages for zero-inflated generalized linear mixed modeling. *R. J.* 9, 378–400. doi: 10.32614/rj-2017-066

Brunstrom, J. M. (2014). Mind over platter: pre-meal planning and the control of meal size in humans. *Int. J. Obes.* 38(Suppl. 1), S9–S12. doi: 10.1038/ijo.2014.83

Buffenstein, R., Poppitt, S. D., McDevitt, R. M., and Prentice, A. M. (1995). Food intake and the menstrual cycle: a retrospective analysis, with implications for appetite research. *Physiol. Behav.* 58, 1067–1077. doi: 10.1016/0031-9384(95)02003-9

Burger, K. S., and Stice, E. (2011). Variability in reward responsivity and obesity: evidence from brain imaging studies. *Curr. Drug Abuse Rev.* 4, 182–189. doi: 10.2174/1874473711104030182

Carnell, S., Gibson, C., Benson, L., Ochner, C. N., and Geliebter, A. (2012). Neuroimaging and obesity: current knowledge and future directions. *Obes. Rev.* 13, 43–56. doi: 10.1111/j.1467-789X.2011.00927.x

Craig, C. L., Marshall, A. L., Sjöström, M., Bauman, A. E., Booth, M. L., Ainsworth, B. E., et al. (2013). International physical activity questionnaire: 12-country reliability and validity. *Med. Sci. Sports Exerc.* 35, 1381–1395.

Cribari-Neto, F., and Zeileis, A. (2010). Beta regression in R. *J. Statist. Softw.* 34, 1–24.

de Araujo, I. E., Schatzker, M., and Small, D. M. (2020). Rethinking food reward. *Annu. Rev. Psychol.* 71, 139–164. doi: 10.1007/978-1-137-21747-9_8

Dreher, J.-C., Schmidt, P. J., Kohn, P., Furman, D., Rubinow, D., and Berman, K. F. (2007). Menstrual cycle phase modulates reward-related neural function in women. *Proc. Natl. Acad. Sci. U.S.A.* 104:2465. doi: 10.1073/pnas.0605569104

Duffey, K. J., and Popkin, B. M. (2011). Energy density, portion size, and eating occasions: contributions to increased energy intake in the United States, 1977–2006. *PLoS Med.* 8:e1001050. doi: 10.1371/journal.pmed.1001050

Dye, L., and Blundell, J. E. (1997). Menstrual cycle and appetite control: implications for weight regulation. *Hum. Reprod.* 12, 1142–1151. doi: 10.1093/humrep/12.6.1142

Eertmans, A., Victoir, A., Vansant, G., and Van den Bergh, O. (2005). Food-related personality traits, food choice motives and food intake: mediator and moderator relationships. *Food Qual. Prefer.* 16, 714–726. doi: 10.1016/j.foodqual.2005.04.007

Eglitis-media (2022). *Average Height and Weight by Country*. Available online at: https://www.worlddata.info/average-bodyheight.php (accessed January 15, 2022).

Fairburn, C. G., Cooper, Z., and O'Connor, M. (2014). *Eating Disorder Examination, Edition 17.0D*. Available online at: https://www.corc.uk.net/media/1951/ede_170d.pdf (accessed August 04, 2020).

Fong, Y., Huang, Y., Lemos, M. P., and McElrath, M. J. (2018). Rank-based two-sample tests for paired data with missing values. *Biostatistics* 19, 281–294. doi: 10.1093/biostatistics/kxx039

Frank, T. C., Kim, G. L., Krzemien, A., and Van Vugt, D. A. (2010). Effect of menstrual cycle phase on corticolimbic brain activation by visual food cues. *Brain Res.* 1363, 81–92. doi: 10.1016/j.brainres.2010.09.071

Frye, C. A., and Demolar, G. L. (1994). Menstrual cycle and sex differences influence salt preference. *Physiol. Behav.* 55, 193–197. doi: 10.1016/0031-9384(94)90031-0

Geiger, B. M., Haburcak, M., Avena, N. M., Moyer, M. C., Hoebel, B. G., and Pothos, E. N. (2009). Deficits of mesolimbic dopamine neurotransmission in rat dietary obesity. *Neuroscience* 159, 1193–1199. doi: 10.1016/j.neuroscience.2009.02.007

Gobbi, S., Weber, S. C., Graf, G., Hinz, D., Asarian, L., Geary, N., et al. (2020). Reduced neural satiety responses in women affected by obesity. *Neuroscience* 447, 94–112. doi: 10.1016/j.neuroscience.2020.07.022

Gorczyca, A. M., Sjaarda, L. A., Mitchell, E. M., Perkins, N. J., Schliep, K. C., Wactawski-Wende, J., et al. (2016). Changes in macronutrient, micronutrient, and food group intakes throughout the menstrual cycle in healthy, premenopausal women. *Eur. J. Nutr.* 55, 1181–1188. doi: 10.1007/s00394-015-0931-0

Hardikar, S., Höchenberger, R., Villringer, A., and Ohla, K. (2017). Higher sensitivity to sweet and salty taste in obese compared to lean individuals. *Appetite* 111, 158–165. doi: 10.1016/j.appet.2016.12.017

Kassambara, A. (2020). *rstatix: Pipe-Friendly Framework for Basic Statistical Tests. R Package Version 0.6.0*. Available online at: https://rpkgs.datanovia.com/rstatix/ (accessed March 04, 2021).

Kleinridders, A., and Pothos, E. N. (2019). Impact of brain insulin signaling on dopamine function, food intake, reward, and emotional behavior. *Curr. Nutr. Rep.* 8, 83–91. doi: 10.1007/s13668-019-0276-z

Klump, K. L., Keel, P. K., Racine, S. E., Burt, S. A., Neale, M., Sisk, C. L., et al. (2013). The interactive effects of estrogen and progesterone on changes in emotional eating across the menstrual cycle. *J. Abnorm. Psychol.* 122, 131–137. doi: 10.1037/a0029524

List, J. A., and Shogren, J. F. (1999). Price information and bidding behavior in repeated second-price auctions. *Am. J. Agric. Econ.* 81, 942–949. doi: 10.2307/1244336

Lowe, C. J., Kolev, D., and Hall, P. A. (2016). An exploration of exercise-induced cognitive enhancement and transfer effects to dietary self-control. *Brain Cogn.* 110, 102–111. doi: 10.1016/j.bandc.2016.04.008

Lüdecke, D. (2018). ggeffects: tidy data frames of marginal effects from regression models. *J. Open Source Softw.* 3:772.

Martini, M. C., Lampe, J. W., Slavin, J. L., and Kurzer, M. S. (1994). Effect of the menstrual cycle on energy and nutrient intake. *Am. J. Clin. Nutr.* 60, 895–899. doi: 10.1093/ajcn/60.6.895

Mattes, R. D. (2018). Snacking: a cause for concern. *Physiol. Behav.* 193(Pt B), 279–283. doi: 10.1016/j.physbeh.2018.02.010

Miller, E. K., and Cohen, J. D. (2001). An integrative theory of prefrontal cortex function. *Annu. Rev. Neurosci.* 24, 167–202.

Motoki, K., and Suzuki, S. (2020). Extrinsic factors underlying food valuation in the human brain. *Front. Behav. Neurosci.* 14:131. doi: 10.3389/fnbeh.2020.00131

NCD Risk Factor Collaboration (2016). Trends in adult body-mass index in 200 countries from 1975 to 2014: a pooled analysis of 1698 population-based measurement studies with 19.2 million participants. *Lancet* 387, 1377–1396. doi: 10.1016/S0140-6736(16)30054-X

Niv, Y., Joel, D., and Dayan, P. (2006). A normative perspective on motivation. *Trends Cogn. Sci.* 10, 375–381. doi: 10.1016/j.tics.2006.06.010

Parraga, I. M. (1990). Determinants of food consumption. *J. Am. Diet. Assoc.* 90, 661–663.

Plassmann, H., O'Doherty, J., and Rangel, A. (2007). Orbitofrontal cortex encodes willingness to pay in everyday economic transactions. *J. Neurosci.* 27, 9984–9988. doi: 10.1523/JNEUROSCI.2131-07.2007

R Core Team (2013). *R: A Language and Environment for Statistical Computing*. Vienna: R Foundation for Statistical Computing.

Rangel, A., Camerer, C., and Montague, P. R. (2008). A framework for studying the neurobiology of value-based decision making. *Nat. Rev. Neurosci.* 9, 545–556. doi: 10.1038/nrn2357

Reichenberger, J., Richard, A., Smyth, J. M., Fischer, D., Pollatos, O., and Blechert, J. (2018). It's craving time: time of day effects on momentary hunger and food craving in daily life. *Nutrition* 55–56, 15–20. doi: 10.1016/j.nut.2018.03.048

Richard, J. E., López-Ferreras, L., Anderberg, R. H., Olandersson, K., and Skibicka, K. P. (2017). Estradiol is a critical regulator of food-reward behavior. *Psychoneuroendocrinology* 78, 193–202. doi: 10.1016/j.psyneuen.2017.01.014

Rosenthal, R. (1994). "Parametric measures of effect size," in *The Handbook of Research Synthesis*, eds H. Cooper and L. V. Hedges (New York, NY: Russell Sage Foundation), 237.

Smithson, M., and Verkuilen, J. (2006). A better lemon squeezer? Maximum-likelihood regression with beta-distributed dependent variables. *Psychol. Methods* 11, 54–71. doi: 10.1037/1082-989X.11.1.54

Suzuki, S., Cross, L., and O'Doherty, J. P. (2017). Elucidating the underlying components of food valuation in the human orbitofrontal cortex. *Nat. Neurosci.* 20, 1780–1786. doi: 10.1038/s41593-017-0008-x

Tang, D. W., Fellows, L. K., and Dagher, A. (2014). Behavioral and neural valuation of foods is driven by implicit knowledge of caloric content. *Psychol. Sci.* 25, 2168–2176. doi: 10.1177/0956797614552081

The World Health Organization [WHO] (2022). *Body Mass Index (BMI)*. Geneva: World Health Organization.

Wang, G.-J., Volkow, N. D., Logan, J., Pappas, N. R., Wong, C. T., Zhu, W., et al. (2001). Brain dopamine and obesity. *Lancet* 357, 354–357. doi: 10.1016/s0140-6736(00)03643-6

Wei, T., Simko, V., Levy, M., Xie, Y., Jin, Y., and Zemla, J. (2017). Package 'corrplot'. *Statistician* 56:e24.

Wickham, H. (ed.) (2006). *ggplot.: An Implementation of the Grammar of Graphics in R. R Package Version 3.3.3.*

Wills, T. A., Isasi, C. R., Mendoza, D., and Ainette, M. G. (2007). Self-control constructs related to measures of dietary intake and physical activity in adolescents. *J. Adolesc. Health* 41, 551–558. doi: 10.1016/j.jadohealth.2007.06.013

Yoest, K. E., Cummings, J. A., and Becker, J. B. (2014). Estradiol, dopamine and motivation. *Cent. Nerv. Syst. Agents Med. Chem.* 14, 83–89. doi: 10.2174/1871524914666141226103135

Yoest, K. E., Quigley, J. A., and Becker, J. B. (2018). Rapid effects of ovarian hormones in dorsal striatum and nucleus accumbens. *Horm. Behav.* 104, 119–129. doi: 10.1016/j.yhbeh.2018.04.002

Conflict of Interest: The authors declare that the research was conducted in the absence of any commercial or financial relationships that could be construed as a potential conflict of interest.

frontiers in Neuroscience

ORIGINAL RESEARCH
published: 17 February 2022
doi: 10.3389/fnins.2021.797598

Altered Brain Functional Asymmetry in Patients With Major Depressive Disorder Related to Gastrointestinal Symptoms

*Xiaoya Fu[1], Yudan Ding[1], Jindong Chen[1], Feng Liu[2], Huabing Li[3], Jingping Zhao[1] and Wenbin Guo[1,4]**

[1] National Clinical Research Center for Mental Disorders, Department of Psychiatry, The Second Xiangya Hospital of Central South University, Changsha, China, [2] Department of Radiology, Tianjin Medical University General Hospital, Tianjin, China, [3] Department of Radiology, The Second Xiangya Hospital of Central South University, Changsha, China, [4] Department of Psychiatry, The Third People's Hospital of Foshan, Foshan, China

Objective: Disrupted brain functional asymmetry has been reported in major depressive disorder (MDD). The comorbidity may be a crucial factor to this functional asymmetry. It is quite common that gastrointestinal (GI) symptoms are comorbid with MDD, but limited evidence focuses on the effect of GI comorbidity on the neuropathology of MDD from a functional lateralization perspective.

Methods: Resting-state functional magnetic resonance imaging was obtained in 28 healthy controls (HCs), 35 MDD patients with GI symptoms (GI-MDD patients), and 17 patients with MDD without GI symptoms (nGI-MDD patients). The parameter of asymmetry (PAS) was used to analyze the imaging data and evaluate the changes of functional asymmetry.

Results: The GI-MDD patients showed increased PAS scores in the left inferior frontal gyrus (IFG) and superior medial prefrontal cortex (MPFC) and decreased PAS scores in the right postcentral gyrus in comparison with nGI-MDD patients. The PAS scores of the left IFG and left superior MPFC were correlated with the severity of GI problems and could be applied to distinguish GI-MDD patients from nGI-MDD patients with an accuracy, a sensitivity, and a specificity of 92.31, 100, and 76.47%, respectively. Furthermore, GI-MDD and nGI-MDD patients both displayed increased PAS scores in the PCC/precuneus.

Conclusions: This study revealed the influence of concomitant GI symptoms on functional asymmetry in MDD patients. Increased PAS scores of the left IFG and superior MPFC might represent an unbalanced regulation of brain over GI function and had the potential to be regarded as distinctive features related to functional GI symptoms in MDD.

Keywords: parameter of asymmetry (PAS), major depressive disorder (MDD), gastrointestinal (GI) symptoms, asymmetry, interhemispheric connectivity

OPEN ACCESS

Edited by:
Jianhua Chen,
Shanghai Jiao Tong University, China

Reviewed by:
Haiqing Huang,
University of Pittsburgh, United States
Ning Sun,
First Hospital of Shanxi Medical University, China

***Correspondence:**
Wenbin Guo
guowenbin76@csu.edu.cn

Specialty section:
This article was submitted to Gut-Brain Axis, a section of the journal Frontiers in Neuroscience

Received: *19 October 2021*
Accepted: *22 December 2021*
Published: *17 February 2022*

Citation:
Fu X, Ding Y, Chen J, Liu F, Li H, Zhao J and Guo W (2022) Altered Brain Functional Asymmetry in Patients With Major Depressive Disorder Related to Gastrointestinal Symptoms. Front. Neurosci. 15:797598. doi: 10.3389/fnins.2021.797598

INTRODUCTION

Hemispheric asymmetry is widespread in various species and of great significance for human perception, emotion, cognition, and behavior (Güntürkün et al., 2020). The hemispheric specialization is advantageous for individuals to efficiently process information and reduce reaction time. Generally, the left hemisphere appears to be more specialized for language and motor coordination, while the right hemisphere is more relevant to memory and visuospatial attention (Gotts et al., 2013; Caeyenberghs and Leemans, 2014).

The right-left asymmetry in the process of emotional information sparks an interest to researchers. Many different hypotheses of brain lateralization in the emotional processing were proposed, like the right hemisphere model (the dominance of the right hemisphere) and the approach-avoidance model (the opposite dominance of the left hemisphere for approach/positive affect and the right for avoidance/negative affect) (Gainotti, 2019). But the results of neuroimaging studies suggested that brain functional lateralization in the emotional process might be region-specific (Wager et al., 2003; Beraha et al., 2012). Though the pattern of lateralization in the emotional processing is still controversial, disrupted functional lateralization has been reported in depression, a disease with abnormal emotional processing. A meta-analysis of electroencephalograph (EEG) studies reported a link of depression to altered resting frontal asymmetry with a moderate effect (Thibodeau et al., 2006). The psychosocial risk, especially maternal depression, showed an association to greater right-sided resting frontal EEG asymmetry in children (Peltola et al., 2014). These findings indicate that the anomalous hemispheric asymmetry may be of great importance for clinical diagnosis and treatment of depression. Bruder et al. (2017) reviewed electrophysiological and functional magnetic resonance imaging (fMRI) evidence of brain asymmetry in depression and revealed abnormalities in brain asymmetry and lateralized responses to emotional stimuli, but the comorbidity might be a confound factor to suppress or enhance the alteration of brain asymmetry.

It is not rare that patients with major depressive disorder (MDD) are comorbid with other mental or somatic symptoms. Gastrointestinal (GI) symptoms and decreased appetite are fairly common manifestations in MDD patients. Over 70% of patients suffered from concomitant GI symptoms in depressive episodes (Huang J. et al., 2021). The presence of GI symptoms would have a negative influence on the course of MDD, contributing to greater depressive severity (Huang M. H. et al., 2021). Previous studies have reported that the concomitant GI symptoms in MDD were related to abnormal brain functional activity (Liu et al., 2020; Yan et al., 2021). Some work in functional GI disorders also found abnormal functional connectivity in the patients (Li et al., 2021). But limited studies focused on the effect of GI comorbidity on the neuropathology of MDD from a perspective of functional lateralization. Thus, we intended to investigate the abnormality of brain functional asymmetry in MDD patients with GI discomfort for a better understanding of the neuropathological influence of comorbid with GI symptoms on MDD.

We employed parameter of asymmetry (PAS) to reflect the change of functional asymmetry. PAS is a novel voxel-wise quantitative index defined as the difference of functional connectivity (FC) of the given voxel between voxels in contralateral and ipsilateral hemisphere. According to a previous study, both intra- and inter-hemispheric connectivity should be taken into consideration when assessing hemispheric specialization (Mueller et al., 2015). The communication and coordination between two hemispheres are of great significance for efficient process of complex and complementary cognitive tasks (Hoptman and Davidson, 1994; Güntürkün et al., 2020). PAS has been applied in exploring the anomalous asymmetry in many psychiatric disorders (Zhu et al., 2018, 2019; Su et al., 2020; Ding et al., 2021; Jia et al., 2021). In the present study, we investigated functional asymmetry in MDD patients with concomitant GI symptoms with this novel approach.

MATERIALS AND METHODS

Participants

This study included 28 healthy controls (HCs) and 52 MDD patients following the DSM-5 criteria. Based on the existence of GI symptoms, 52 patients were classified as GI-MDD (MDD with at least one GI symptoms, $n = 35$) or nGI-MDD (MDD without GI symptoms, $n = 17$) patients. The GI symptoms mainly included medically unexplained nausea, vomit, constipation, diarrhea, gastralgia, heartburn, flatulence, and so on. All participants were Han Chinese and right-handed. Participants with organic digestive diseases, neurological disorders, severe physical diseases, brain structural abnormalities, pregnancy, and history of substance abuse or MRI scanning contraindications were excluded. HCs had no history of psychotic symptoms and were ruled out if they or their relatives had a history of mental disorders. All included patients scored 17 points or above in the 17-item Hamilton Rating Scale for Depression (HRSD-17) and had no history of antidepressants or electroconvulsive therapy. The severity of clinical symptoms of patients was assessed by HRSD-17 from the following five aspects: retardation symptoms (items 1, 7, 8, and 14), cognitive disturbances (items 2, 3, and 9), insomnia (items 4, 5, and 6), anxiety/somatization (items 10, 11, 12, 13, 15, and 17), and weight loss (item 16). The severity of GI symptoms was evaluated by GI symptoms item (item 12) in the HRSD-17.

This study was approved by the Medical Research Ethics Committee of the Second Xiangya Hospital of Central South University. All participants provided written informed consents.

Image Acquisition and Data Preprocessing

Scanning was conducted on a Siemens 3.0T scanner, with headphones and foam padding to minimize head motion and scanner noises. Participants were instructed to remain motionless, close their eyes, and stay awake during scan. Echo planar imaging sequence was employed to obtain functional magnetic resonance imaging (fMRI) data with the following parameters: repetition time/echo time = 2,000 ms/30 ms,

flip angle = 90°, field of view = 240 mm × 240 mm, matrix = 64 mm × 64, 4 mm slice thickness, 0.4 mm gap, 30 slices, number of volumes = 250.

The images were preprocessed by the Data Processing Assistant for Resting-State fMRI (DPARSF) software package (Yan and Zang, 2010). After removing the initial 10 volumes, slice-timing correction and head motion correction were conducted. Participants with excessive head movement (maximal translation > 2 mm or maximal rotation > 2°) would be excluded. The images were spatially normalized to a standard Montreal Neurological Institute template and resampled to 3 mm × 3 mm × 3 mm. A 4-mm Gaussian kernel of full-width at half-maximum was used in smoothing. Friston-24 head motion, signals of cerebrospinal fluid, and white matter were regressed out. After bandpass-filtered (0.01–0.08 Hz) and linearly detrended, the images were scrubbed (framewise displacement threshold of 0.2 mm).

Parameter of Asymmetry Calculation

As described in previous studies (Zhu et al., 2018; Ding et al., 2021), the calculation of PAS scores followed the formula:

$$PAS = FC_{inter} - FC_{intra}$$

FC_{inter} and FC_{intra} refer to interhemispheric FC and intrahemispheric FC, respectively. FC_{inter} is defined as the mean FC (Fisher's Z-transformed) of a given voxel between other voxels in the contralateral hemisphere, whereas FC_{intra} is the mean FC of the given voxel between the voxels in the ipsilateral hemisphere. Negative correlations were not included in calculation for their damaging effect on reliability (Wang et al., 2011). A threshold of $r > 0.2$ was set to remove weak correlations possibly resulting from signal noises (Wang et al., 2013).

Statistical Analysis

Two-sample t-tests, one-way analyses of variance, and chi-square test were used to analyze demographic and clinical data based on the scale of measure. A threshold of $p < 0.05$ was set as the significant level.

PAS scores were compared by using analyses of covariance (ANCOVA) across three groups, followed by *post hoc* t-tests for multiple comparison, with age, gender, years of education, and the mean framewise displacement as covariates. A threshold of $p < 0.05$ was set as the significant level for the false discovery rate correction.

The PAS scores of clusters showed significant group differences were extracted for further correlation and support vector machine (SVM) analysis. Spearman correlation followed by the Benjamini–Hochberg correction was used in correlation analysis between the extracted PAS scores and clinical variables in the patients. SVM analysis was applied to examine whether the extracted PAS scores were capable of discriminating GI-MDD and nGI-MDD patients. The analysis employed a "leave-one-out" strategy using the LIBSVM software package (Chang and Lin, 2011).

RESULTS

Demographic and Clinical Characteristics

No participant was excluded because of excessive head movement. As demographic and clinical details presented in **Table 1**, there was no apparent difference in age, sex ratio, and years of education across three group. Two patient groups had no significant differences in illness duration. Relative to nGI-MDD patients, GI-MDD patients experienced more severe depressive symptoms, indicated by higher HRSD-17 scores, particularly in the factors of anxiety/somatization, weight loss, and sleep disturbance.

Group Differences

ANCOVA results revealed significant PAS differences in predominantly left hemisphere. Basically, the regions with

TABLE 1 | Demographic and clinical characteristics of the participants.

	GI-MDD (n = 35)	nGI-MDD (n = 17)	HCs (n = 28)	F, t or χ^2 value	*Post hoc* t-tests or p-values
Age (years)	30.86 ± 6.84	30.29 ± 8.05	30.14 ± 5.00	0.102	0.90[a]
Gender (male/female)	13/22	6/11	14/14	1.377	0.50[b]
Education (years)	14.51 ± 3.28	12.94 ± 3.46	14.61 ± 2.69	1.797	0.17[a]
Illness duration (months)	6.23 ± 4.63	6.94 ± 3.98		0.544	0.59[c]
HRSD-17 scores	22.69 ± 3.41	20.18 ± 2.67	0.89 ± 0.88	585.979	GI-MDD > nGI-MDD > HC
Anxiety/somatization	7.31 ± 1.92	6.41 ± 1.66	0.39 ± 0.57	174.531	GI-MDD > nGI-MDD > HC
Weight loss	0.80 ± 0.83	0.06 ± 0.24	0	18.741	GI-MDD > nGI-MDD, HC
Cognitive disturbance	3.71 ± 1.78	3.41 ± 1.50	0	64.213	GI-MDD, nGI-MDD > HC
Retardation	6.40 ± 1.42	6.76 ± 1.56	0.18 ± 0.39	253.030	GI-MDD, nGI-MDD > HC
Sleep disturbance	4.46 ± 1.42	3.53 ± 1.28	0.32 ± 0.55	103.570	GI-MDD > nGI-MDD > HC

GI-MDD, major depressive disorder with gastrointestinal symptoms; HCs, healthy controls; HRSD-17 scores, 17-item Hamilton Rating Scale for Depression; nGI-MDD, major depressive disorder without gastrointestinal symptoms.

[a] *The p-value was obtained by analyses of variance.*

[b] *The p-value was obtained by a chi-square test.*

[c] *The p-value was obtained by two-sample t-tests.*

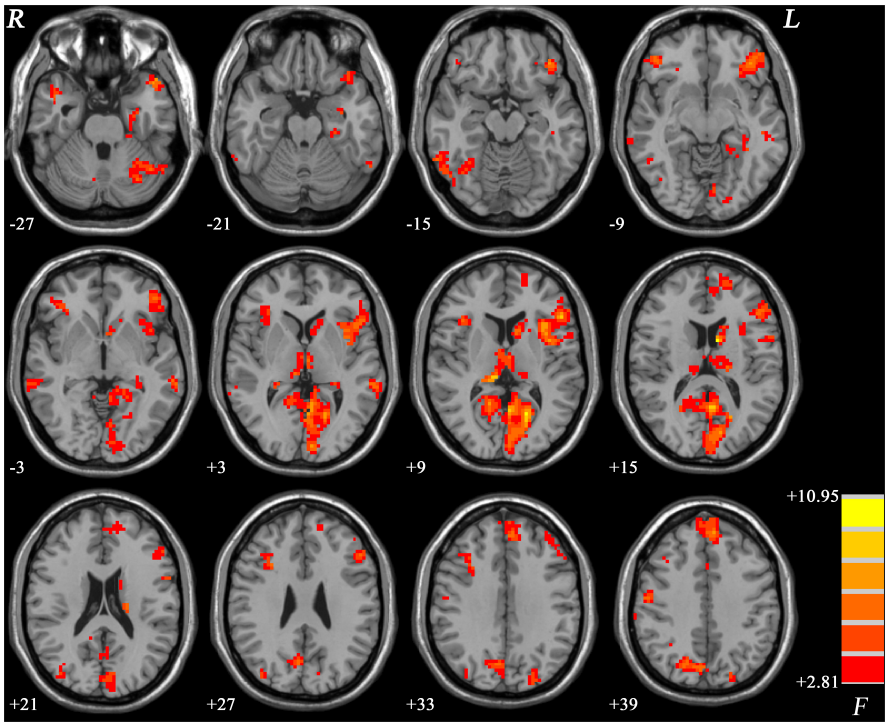

FIGURE 1 | Brain regions showing significantly different PAS scores across three groups. The color bar indicates F values based on ANCOVA. The results were FDR (false discovery rate) corrected at $p < 0.05$. PAS, parameter of asymmetry; ANCOVA, analysis of covariance.

PAS alterations mainly located in the default mode network (DMN) and left frontoparietal network, including the left parahippocampal gyrus, left caudate, bilateral middle temporal gyrus (MTG), and dorsolateral prefrontal cortex. Widespread regions of visual network such as the fusiform and some parts of the cerebellum also exhibited significant differences (**Figure 1**).

GI-MDD patients, relative to nGI-MDD patients, exhibited increased PAS scores in the left inferior frontal gyrus (IFG) and left superior medial prefrontal cortex (MPFC). Moreover, a reduction in PAS was observed in GI-MDD patients in the right postcentral gyrus of the somatomotor network (**Table 2** and **Figure 2**).

Comparing to HCs, increased PAS scores were shown in GI-MDD patients in the bilateral posterior cingulate cortex (PCC) and precuneus, which are key components of the DMN. Higher PAS scores were also found in the right cuneus of the frontoparietal network in the GI-MDD group. Left insula, bilateral thalamus, and left cerebellum Crus I showed decreased PAS scores in GI-MDD patients relative to HCs (**Table 2** and **Figure 3**).

Similar to GI-MDD group, increased PAS scores were found in the left PCC/precuneus in nGI-MDD patients relative to HCs. Decreased PAS scores were displayed in the bilateral superior MPFC, left IFG, and left insula (**Table 2** and **Figure 4**).

Correlation Analysis

For all MDD patients, their PAS scores of the left IFG and superior MPFC were positively correlated with the severity of GI symptoms and weight loss. Additionally, the severity of GI symptoms and insomnia was negatively correlated to the PAS scores of the right postcentral gyrus (**Figure 5**). Although

TABLE 2 | Significant PAS differences across groups.

Cluster location	Peak (MNI)			Number of voxels	*T*-value
	x	*y*	*z*		
GI-MDD vs. nGI-MDD					
Left IFG	−39	36	−12	61	4.0821
Left superior MPFC	−6	24	57	152	4.2209
Right postcentral gyrus	27	−39	57	67	−4.2251
GI-MDD vs. HCs					
Bilateral PCC/precuneus	−6	−57	15	102	4.0477
Right cuneus	9	−75	42	70	3.9449
Left insula	−33	15	6	76	−4.0040
Bilateral thalamus	9	−30	9	96	−4.2195
Left cerebellum Crus1	−39	−57	−30	42	−3.9492
nGI-MDD vs. HCs					
Left PCC/precuneus	−18	−69	9	361	4.2542
Left IFG/insula	−51	24	9	117	−3.9871
Bilateral superior MPFC	6	36	60	65	−3.6197

GI-MDD, major depressive disorder with gastrointestinal symptoms; HCs, healthy controls; IFG, inferior frontal gyrus; MNI, Montreal Neurological Institute; MPFC, medial prefrontal cortex; nGI-MDD, major depressive disorder without gastrointestinal symptoms; PCC, posterior cingulate cortex.

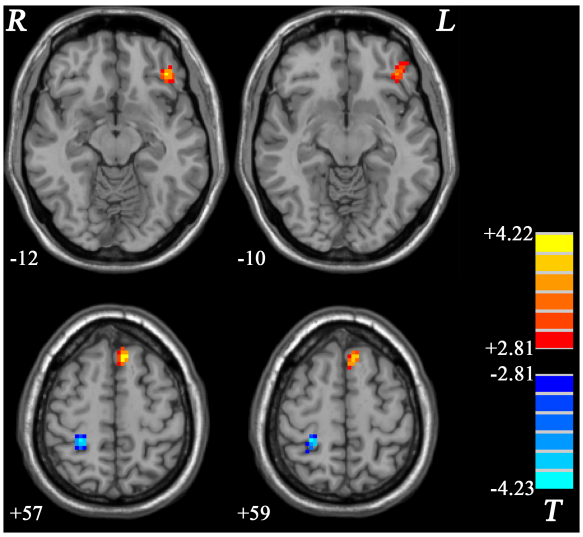

FIGURE 2 | Regions with significantly different PAS scores in comparison between GI-MDD and nGI-MDD patients without GI symptoms. The color bar indicates the *T*-values from *post hoc t*-tests. GI-MDD, major depressive disorder with gastrointestinal symptoms; nGI-MDD, major depressive disorder without gastrointestinal symptoms; PAS, parameter of asymmetry.

potential inverse associations were found between the scores of weight loss and the PAS scores of the right postcentral gyrus, as well as between the severity of retardation symptoms and the PAS scores of the left superior MPFC, their significances did not pass the Benjamini-Hochberg correction.

No correlation was found between clinical variables and PAS scores in GI-MDD or nGI-MDD patients after the Benjamini-Hochberg correction.

Support Vector Machine Results

Based on the results of group differences between GI-MDD and nGI-MDD, we performed the SVM analysis using the PAS scores of the left IFG, left superior MPFC, and right postcentral gyrus as features. As detailed results shown in **Table 3**, a combination of the left IFG and left superior MPFC reached a highest accuracy of 92.31%, with a sensitivity of 100% and a specificity of 76.47% (**Figure 6**). When combining the PAS scores of these three clusters to discriminate the GI-MDD and nGI-MDD patients, the accuracy, sensitivity, and specificity were 90.38, 100, and 70.59%, respectively.

DISCUSSION

This study investigated the effect of GI symptoms on functional asymmetry in first-episode, treatment-naive MDD patients. In comparison across three groups, we found that the regions with significant differences were dominantly distributed in the left hemisphere and involved multiple brain networks including the DMN, visual network, frontoparietal network, and cerebellum. Increased PAS scores in the left IFG and left superior MPFC and decreased PAS scores in the right postcentral gyrus were found

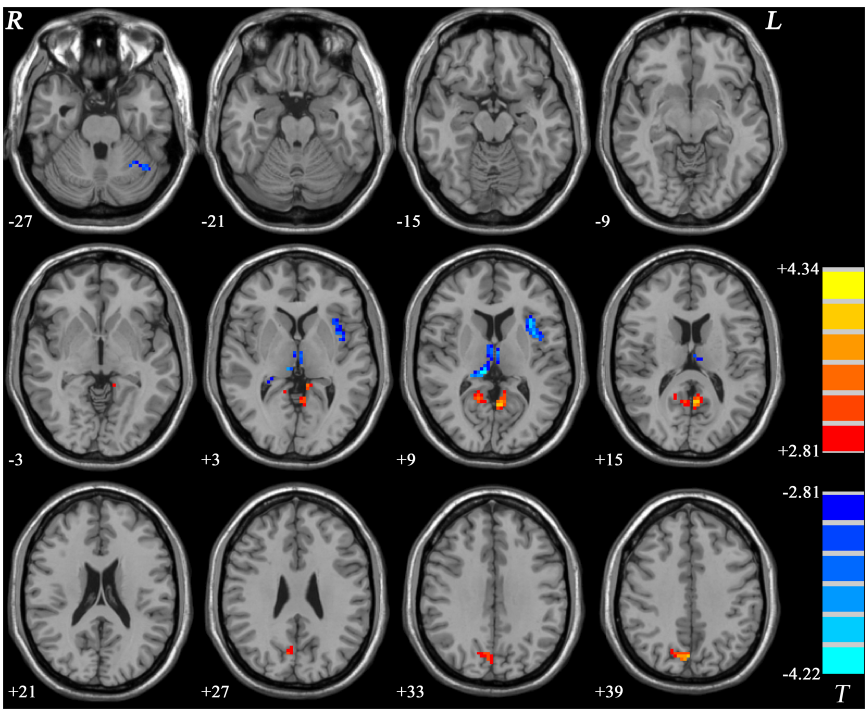

FIGURE 3 | Regions with significantly different PAS scores in GI-MDD patients compared to HCs. The color bar indicates the *T*-values from *post hoc t*-tests. GI-MDD, major depressive disorder with gastrointestinal symptoms; HCs, healthy controls; PAS, parameter of asymmetry.

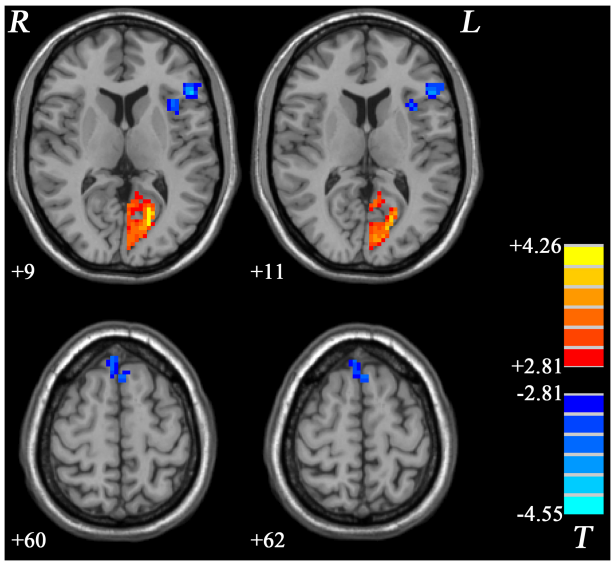

FIGURE 4 | Regions with significantly different PAS scores in nGI-MDD patients compared to HCs. The color bar indicates the *T*-values from *post hoc t*-tests. HCs, healthy controls; nGI-MDD, major depressive disorder without gastrointestinal symptoms; PAS, parameter of asymmetry.

in comparison between GI-MDD and nGI-MDD patients. The PAS scores of the left IFG and left superior MPFC were correlated with the severity of GI problems and, more importantly, they could better meet the requirment of discrimination between GI-MDD and nGI-MDD patients. In addition, increased PAS scores in the PCC/precuneus were found in both GI-MDD and nGI-MDD patients.

The nGI-MDD patients showed decreased PAS scores in the left IFG and left superior MPFCs compared to GI-MDD patients and HCs, which indicated both MDD and GI symptoms had potential influence on the alterations of function asymmetry of these regions. Compared to HCs, the nGI-MDD group had lower PAS scores in the left IFG and the bilateral superior MPFC, which indicated that these brain regions had stronger intrahemispheric FC and/or weaker interhemispheric FC possibly related to depression. However, the existence of GI symptoms changed the functional asymmetry of the left IFG and left superior MPFC to the other direction. These results indicated that either increased lateralization or increased interhemispheric connectivity might account for disrupted functions.

Lateralization as a feature occurring in various vertebrate and even invertebrate species was suggested to offer considerable advantages for individuals. For instance, brain functional asymmetry may increase neural capacity by reducing functional redundancy and conflicts between hemispheres (Vallortigara, 2006). In addition, the dominance of one hemisphere can leave the other hemisphere free to have an advantage of other functions, thereby helping to perform parallel processing of functionally separate tasks (Gerrits et al., 2020). Atypical asymmetry was reported to have an association with poor cognitive function (Gerrits et al., 2020) and a variety of neuropsychiatric disorders, such as schizophrenia (Sun et al., 2017), autism spectrum disorder (Carper et al., 2016), and attention deficit/hyperactivity disorder (Ahmadi et al., 2021).

Although the lateralization is more advantageous to process information efficiently, it did not mean that a reduced PAS

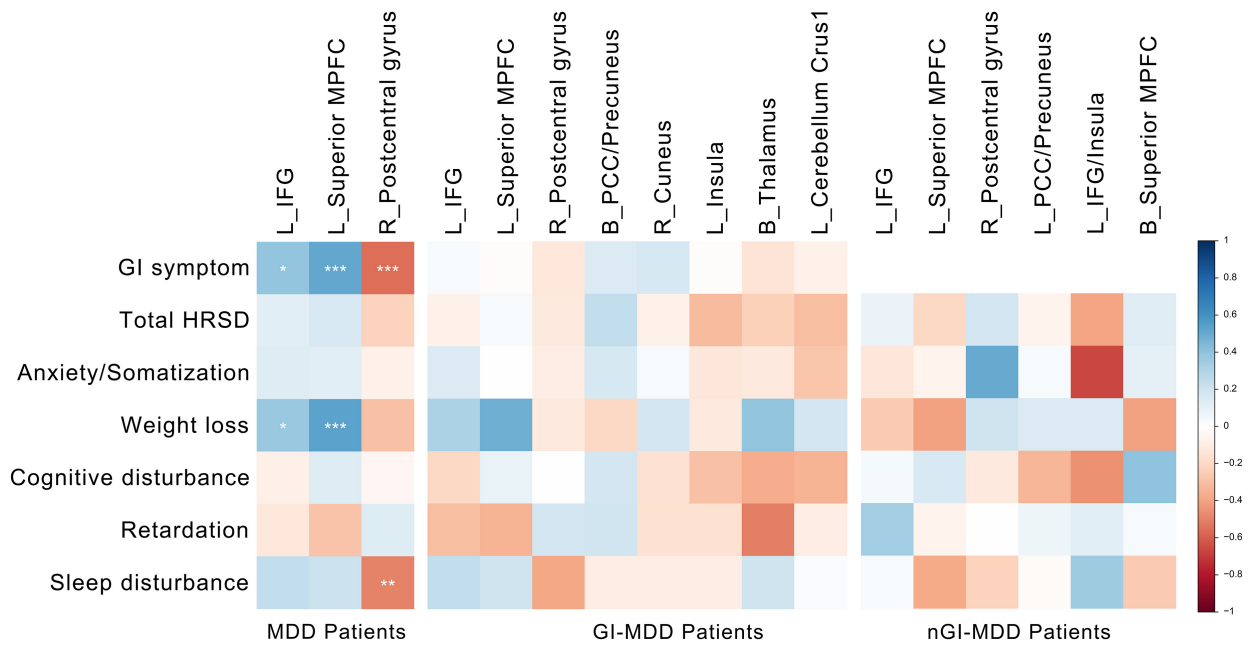

FIGURE 5 | Correlations between altered PAS scores and clinical variables. The color represents the Spearman correlation values. The significance levels are marked with asterisks (*$p < 0.05$, **$p < 0.01$, ***$p < 0.001$). PAS, parameter of asymmetry.

TABLE 3 | Support vector machine results of discrimination between GI-MDD patients and nGI-MDD patients by using PAS scores.

Brain region(s)	Accuracy	Sensitivity	Specificity
Left IFG	78.84%(41/52)	100%(35/35)	35.29%(6/17)
Left superior MPFC	76.92%(40/52)	85.71%(30/35)	58.82%(10/17)
Right postcentral gyrus	78.85%(41/52)	91.43%(32/35)	52.94%(9/17)
Left IFG + left superior MPFC	92.31%(48/52)	100%(35/35)	76.47%(13/17)
Left IFG + right postcentral gyrus	82.69%(43/52)	97.14%(34/35)	52.94%(9/17)
Left superior MPFC + right postcentral gyrus	84.62%(44/52)	94.29%(33/35)	64.71%(11/17)
Left IFG + left superior MPFC + right postcentral gyrus	90.38%(47/52)	100%(35/35)	70.59%(12/17)

GI-MDD, major depressive disorder with gastrointestinal symptoms; IFG, inferior frontal gyrus; MPFC, medial prefrontal cortex; nGI-MDD, major depressive disorder without gastrointestinal symptoms; PAS, parameter of asymmetry; SVM, support vector machine.

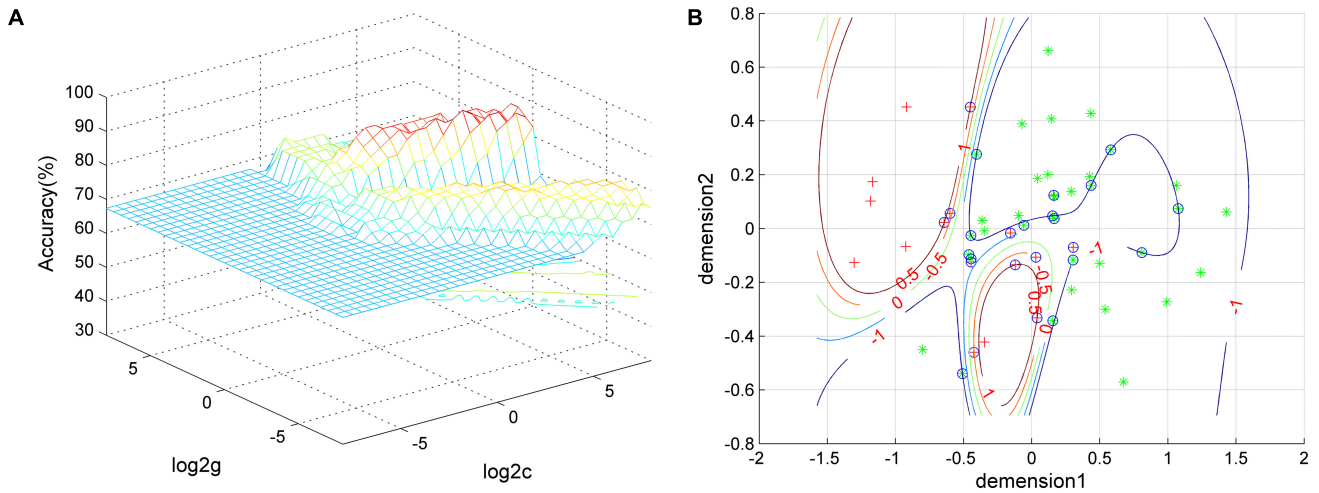

FIGURE 6 | The visualization of SVM classification using the combination of the PAS scores of the left IFG and left superior MPFC. **(A)** SVM parameter result of 3D view and **(B)** classified map of the results. Green asterisks represent the GI-MDD patients, and red crosses represent nGI-MDD patients. GI-MDD, major depressive disorder with gastrointestinal symptoms; IFG, inferior frontal gyrus; MPFC, medial prefrontal cortex; nGI-MDD, major depressive disorder without gastrointestinal symptoms; PAS, parameter of asymmetry; SVM, support vector machine.

score is definitely better. The connectivity between the two hemispheres is of great importance. The two hemispheres are connected by commissural system, by which neural information is exchanged between the left and the right half of brain. The commissures were necessary for the construction of functional asymmetry. It was proposed that one hemisphere could send excitatory or inhibitory neural information to the other hemisphere to reduce or enhance functional asymmetry through the commissural system (Bloom and Hynd, 2005). The interhemispheric transfer of multiple types of information, such as perceptual and motor information, would be severely impaired if the corpus callosum was fully severed (Gazzaniga, 2005). Likewise, emotional processing is under the influence of the commissural system. Subjects responded faster and more accurately to the faces with complex social emotions presented in the bilateral visual fields than in unilateral conditions, suggesting the advantage of interhemispheric cooperation in emotional processing (Tamietto et al., 2007). Disrupted interhemispheric connectivity was observed in functional anomalies and multiple psychiatric disorders. The schizophrenic and depressed patients showed altered transcallosal connectivity measured by interhemispheric signal propagation (Hui et al., 2021).

Some researchers proposed that one hemisphere would recruit the other hemisphere to increase processing power when its capability was not adequate for a given task (Banich and Belger, 1990). Therefore, increased interhemispheric connectivity or reduced functional asymmetry might be the manifestation of interhemispheric recruitment for compensation of disturbed functions. It was found in older individuals with functional deficiency of dominant hemisphere that the hemispheric asymmetry reduced (Cabeza, 2002). A study in mice indicated that interhemispheric interaction might be involved in remodeling of cortical plasticity if unilateral cortical sensory input was partially deprived (Jablonka et al., 2021). Another animal study in rats found that the interhemispheric FC was significantly reduced after stroke alongside serious deficits of sensorimotor function and subsequently restored during the recovery period of sensorimotor function (van Meer et al., 2010). A human study reported similar results that interhemispheric interaction played a crucial role in rehabilitation (Chen et al., 2021). When subjects needed to respond to the faces

with complex social emotion presented in the left or right visual field, the finding of no difference between unilateral presentations might support the hypothesis of interhemispheric recruitment, because the perception of basic emotion is right-lateralized (Tamietto et al., 2006, 2007). Therefore, increased interhemispheric might be a kind of complementary mechanism to counteract the functional deficiency. Given the perspectives of functional segregation and region-specific process in emotion, the alterations of functional asymmetry in specific regions might give us more information to understand the significance of altered functional asymmetry.

The left IFG and bilateral superior MPFC showed decreased PAS scores in nGI-MDD patients relative to HCs, that is, stronger intrahemispheric FC and/or weaker interhemispheric FC. IFG, a component of the semantic system, also involved in perceiving emotional expressions, is regarded as a region of integrating semantic content and emotional signals in communication. Several neurocognitive studies regarded IFG as a key node in process of affective voices (Schirmer and Kotz, 2006; Belyk et al., 2017). A meta-analysis study of IFG revealed that the perception of semantics was strongly left-lateralized, but emotional perceptions did not show lateralization (Belyk et al., 2017). Therefore, the exacerbated left lateralization of IFG, represented by decreased PAS scores in the left IFG might indicate a dysfunctional emotional perception when perceiving semantics with emotion. The superior MPFC, as a crucial component of the DMN, with close connection to both emotional modulation and interoception, was found to be involved in MDD (Zhou et al., 2010). A previous study investigating interhemispheric connectivity between the homotopic voxels of the two hemisphere using voxel-mirrored homotopic connectivity (VMHC) reported reduced VMHC of MPFC in MDD patients (Guo et al., 2013). The lower VMHC was correlated with poorer performance in Wisconsin Card Sorting Test (Guo et al., 2013). Decreased PAS scores of the superior MPFC in both hemispheres probably was attributed to the reduced interhemispheric connectivity.

However, the occurrences of GI discomfort led to increased PAS scores of the left IFG and left superior MPFC, along with decreased PAS score in the right postcentral gyrus. These aberrant functional asymmetries were not only correlated with the severity of GI dysfunction, but also could draw a clear distinction between GI-MDD and nGI-MDD. The MPFC could be activated by stress and regulated stress-related corticosterone secretion and autonomic function. Additionally, portions of cortical neurons in control of parasympathetic output of stomach are located in MPFC (Levinthal and Strick, 2020). A review concerning stress-induced gastric mucosal lesion has reported the role of MPFC in regulating gastric dysfunction (Zhao et al., 2020). An early study in rats found that bilateral or right lesions, but not the left lesion, of MPFC could reduce plasma corticosterone level and impair gastric stress pathology in the development of gastric ulcer. The lesion of left MPFC could result in stronger emotional and autonomic reactivity in restraint stress, which suggested that the right MPFC facilitated these physiological stress responses and the left MPFC regulated these responses (Sullivan and Gratton, 1999). Therefore, increased PAS scores in the left MPFC might suggest a recruitment to regulate the stress-induced gastric pathology.

The finding of increased PAS scores in the left IFG in comparison between GI-MDD and nGI-MDD patients has intrigued us. A previous study reported that ingestion could increase the cerebral blood flow in the bilateral IFG, implying that IFG might play a role in satiety (Camps et al., 2018). The right IFG was associated with peptide YY, a gut-derived hormone in regulating multiple GI function, including GI motility, secretion, and absorption (Weise et al., 2012; El-Salhy et al., 2020). Moreover, nausea induced by visual stimulation could activate the activity in the right IFG, but activity of the left IFG predominated when using transcutaneous electrical acupuncture to treat nausea (Sarosiek et al., 2017). This issue indicated that functional asymmetry of IFG might be involved in regulation of GI function, and increased PAS scores of the left IFG in our study might be on account of interhemispheric recruitment to regulate the GI dysfunction.

The postcentral gyrus showed significant differences in comparison between GI-MDD and nGI-MDD patients. The postcentral gyrus is a key component of sensorimotor network and contributes to the process of visceral stimulation. The cortical thickness of primary somatosensory cortex was associated with pain intensity in female irritable bowel syndrome (IBS) patients (Grinsvall et al., 2021). Previous studies have reported aberrant activity and function of sensorimotor network in functional GI disorders (Mayer et al., 2009; Duan et al., 2021; Liu G. et al., 2021). Moreover, we observed that altered PAS scores in the right postcentral gyrus had inverse correlation to sleep disturbance in MDD, implying that FC of postcentral gyrus corresponded with sleep quality, which was consistent with previous studies (Huang et al., 2012; Klumpp et al., 2018).

In both GI-MDD and nGI-MDD groups, we found increased PAS scores in the left PCC/precuneus. A previous study of our group using a large sample dataset from the REST-meta-MDD project, the largest MDD resting-state fMRI database, also reported increased PAS scores in the left PCC and precuneus (Ding et al., 2021). These results suggested stronger interhemispheric FC and/or weaker intrahemispheric FC in the left PCC and precuneus in MDD patients. Most studies using VMHC found decreased homotopic connectivity in the PCC and precuneus in MDD patients (Guo et al., 2013; Fan et al., 2018; Shan et al., 2021), though some increased VMHC was reported (Zhao et al., 2021). The inconsistency between these findings and our results might result from different analysis method. The focuses of VMHC and PAS were different. Specifically, the former shows an interest in abnormal interhemispheric FC and only limits to homotopic voxels, whereas the latter expresses interest in the change of functional lateralization. Therefore, it is not surprising that these findings pointed to conflicting results. Both PCC and precuneus are key regions of DMN and were implicated in the introspective processes (Broyd et al., 2009). The altered functional asymmetry in PCC and precuneus suggested less lateralization of these regions in depression.

Moreover, we found decreased PAS scores in the bilateral thalamus, left insula, and cerebellum Crus I and increased PAS scores in the right cuneus in GI-MDD patients compared to HCs,

which suggested altered connectivity involved in depression. But these abnormalities of functional asymmetry were only presented in comparison between GI-MDD and HCs, not between nGI-MDD and HCs, suggesting that the occurrence of GI symptoms had influence on functional asymmetry to some extent. Many studies have found that these regions have connections with functional GI disorders (Mayer et al., 2009; Tillisch et al., 2011). The insula was considered as an important region in functional GI disorders, as its role in integrating multimodal sensory information and processing multiple types of information related to visceral sensory, emotional pain, etc. The right insula was considered to have high association with visceral afferent; thus, left-lateralized insula might have adverse effect on the experience of visceral feelings (Mayer et al., 2009). Given that no significant correlation was found between these changes and clinical variables, these abnormalities of functional asymmetry need to be taken with more caution.

Some limitations should be noted. Firstly, we did not categorize the GI-MDD patients based on the types of their GI symptoms in consideration of the small sample size. It would be better to include more nGI-MDD patients since the sample size of GI-MDD group was twice the size of nGI-MDD group. Secondly, this is a cross-sectional study. Although we thought the increased interhemispheric connectivity might be a kind of compensation to counteract the disrupted function, further longitudinal research is required to elucidate that these alterations of functional asymmetry are the cause or the consequence of functional deficiency. Thirdly, as some previous studies, we only used the GI item in the HRSD-17 to evaluate the severity of GI symptoms (Liu et al., 2020; Liu P. et al., 2021). But a more specific evaluation of GI symptoms would be an ideal approach.

CONCLUSION

In summary, this study revealed the influence of concomitant GI symptoms on functional asymmetry in MDD patients. Increased PAS scores of the left IFG and superior MPFC might represent unbalanced regulation of brain over GI function and had the potential to be regarded as distinctive features in patients with MDD concomitant GI discomfort.

DATA AVAILABILITY STATEMENT

The data presented in this study are available upon request to the corresponding author WG.

ETHICS STATEMENT

The studies involving human participants were reviewed and approved by Medical Research Ethics Committee of the Second Xiangya Hospital of Central South University. The patients/participants provided their written informed consent to participate in this study.

AUTHOR CONTRIBUTIONS

All authors contributed to and approved the final manuscript. XF wrote the manuscript and contributed to data analysis. YD contributed to the manuscript writing. HL and WG conducted the study. JC, FL, and JZ contributed to data management and analysis. WG designed the study and analyzed the imaging data.

FUNDING

This study was supported by grants from the National Natural Science Foundation of China (Grant Nos. 82171508 and 81771447), Natural Science Foundation of Hunan (Grant No. 2020JJ4784), Science and Technology Program of Hunan Province (Grant No. 2020SK53413), Key-Area Research and Development Program of Guangdong Province (2018B030334001), and Natural Science Foundation of Tianjin (Grant No. 18JCQNJC10900).

ACKNOWLEDGMENTS

We appreciate all subjects who participated in research.

REFERENCES

Ahmadi, M., Kazemi, K., Kuc, K., Cybulska-Klosowicz, A., Helfroush, M. S., and Aarabi, A. (2021). Resting state dynamic functional connectivity in children with attention deficit/hyperactivity disorder. *J. Neural. Eng* 18:0460d1. doi: 10.1088/1741-2552/ac16b3

Banich, M. T., and Belger, A. (1990). Interhemispheric interaction: how do the hemispheres divide and conquer a task? *Cortex J. Devoted Study Nerv. Syst. Behav.* 26, 77–94. doi: 10.1016/s0010-9452(13)80076-7

Belyk, M., Brown, S., Lim, J., and Kotz, S. A. (2017). Convergence of semantics and emotional expression within the IFG pars orbitalis. *NeuroImage* 156, 240–248. doi: 10.1016/j.neuroimage.2017.04.020

Beraha, E., Eggers, J., Hindi Attar, C., Gutwinski, S., Schlagenhauf, F., Stoy, M., et al. (2012). Hemispheric asymmetry for affective stimulus processing in healthy subjects–A fMRI study. *PLoS One* 7:e46931. doi: 10.1371/journal.pone.0046931

Bloom, J. S., and Hynd, G. W. (2005). The role of the corpus callosum in interhemispheric transfer of information: excitation or inhibition? *Neuropsychol. Rev.* 15, 59–71. doi: 10.1007/s11065-005-6252-y

Broyd, S. J., Demanuele, C., Debener, S., Helps, S. K., James, C. J., and Sonuga-Barke, E. J. S. (2009). Default-mode brain dysfunction in mental disorders: a systematic review. *Neurosci. Biobehav. Rev.* 33, 279–296. doi: 10.1016/j.neubiorev.2008.09.002

Bruder, G. E., Stewart, J. W., and McGrath, P. J. (2017). Right brain, left brain in depressive disorders: clinical and theoretical implications of behavioral, electrophysiological and neuroimaging findings. *Neurosci. Biobehav. Rev.* 78, 178–191. doi: 10.1016/j.neubiorev.2017.04.021

Cabeza, R. (2002). Hemispheric asymmetry reduction in older adults: the HAROLD model. *Psychol. Aging* 17, 85–100. doi: 10.1037//0882-7974.17.1.85

Caeyenberghs, K., and Leemans, A. (2014). Hemispheric lateralization of topological organization in structural brain

networks. *Hum. Brain Mapp.* 35, 4944–4957. doi: 10.1002/hbm.22524

Camps, G., Veit, R., Mars, M., de Graaf, C., and Smeets, P. A. M. (2018). Just add water: effects of added gastric distention by water on gastric emptying and satiety related brain activity. *Appetite* 127, 195–202. doi: 10.1016/j.appet.2018.04.023

Carper, R. A., Treiber, J. M., DeJesus, S. Y., and Müller, R.-A. (2016). Reduced hemispheric asymmetry of white matter microstructure in autism spectrum disorder. *J. Am. Acad. Child Adolesc. Psychiatry* 55, 1073–1080. doi: 10.1016/j.jaac.2016.09.491

Chang, C.-C., and Lin, C.-J. (2011). LIBSVM: a library for support vector machines. *ACM Trans. Intell. Syst. Technol.* 2:27:1–27:27. doi: 10.1145/1961189.1961199

Chen, C., Yuan, K., Wang, X., Khan, A., Chu, W. C.-W., and Tong, R. K.-Y. (2021). Neural correlates of motor recovery after robot-assisted training in chronic stroke: a multimodal neuroimaging study. *Neural Plast.* 2021:8866613. doi: 10.1155/2021/8866613

Ding, Y.-D., Yang, R., Yan, C.-G., Chen, X., Bai, T.-J., Bo, Q.-J., et al. (2021). Disrupted hemispheric connectivity specialization in patients with major depressive disorder: evidence from the REST-meta-MDD Project. *J. Affect. Disord.* 284, 217–228. doi: 10.1016/j.jad.2021.02.030

Duan, S., Liu, L., Li, G., Wang, J., Hu, Y., Zhang, W., et al. (2021). Altered functional connectivity within and between salience and sensorimotor networks in patients with functional constipation. *Front. Neurosci.* 15:628880. doi: 10.3389/fnins.2021.628880

El-Salhy, M., Hatlebakk, J. G., and Hausken, T. (2020). Possible role of peptide YY (PYY) in the pathophysiology of irritable bowel syndrome (IBS). *Neuropeptides* 79:101973. doi: 10.1016/j.npep.2019.101973

Fan, H., Yang, X., Zhang, J., Chen, Y., Li, T., and Ma, X. (2018). Analysis of voxel-mirrored homotopic connectivity in medication-free, current major depressive disorder. *J. Affect. Disord.* 240, 171–176. doi: 10.1016/j.jad.2018.07.037

Gainotti, G. (2019). Emotions and the right hemisphere: can new data clarify old models? *Neurosci. Rev. J. Bringing Neurobiol. Neurol. Psychiatry* 25, 258–270. doi: 10.1177/1073858418785342

Gazzaniga, M. S. (2005). Forty-five years of split-brain research and still going strong. *Nat. Rev. Neurosci.* 6, 653–659. doi: 10.1038/nrn1723

Gerrits, R., Verhelst, H., and Vingerhoets, G. (2020). Mirrored brain organization: statistical anomaly or reversal of hemispheric functional segregation bias? *Proc. Natl. Acad. Sci. U.S.A.* 117, 14057–14065. doi: 10.1073/pnas.2002981117

Gotts, S. J., Jo, H. J., Wallace, G. L., Saad, Z. S., Cox, R. W., and Martin, A. (2013). Two distinct forms of functional lateralization in the human brain. *Proc. Natl. Acad. Sci. U.S.A.* 110, E3435–E3444. doi: 10.1073/pnas.1302581110

Grinsvall, C., Ryu, H. J., Van Oudenhove, L., Labus, J. S., Gupta, A., Ljungberg, M., et al. (2021). Association between pain sensitivity and gray matter properties in the sensorimotor network in women with irritable bowel syndrome. *Neurogastroenterol. Motil. Off. J. Eur. Gastrointest. Motil. Soc.* 33:e14027. doi: 10.1111/nmo.14027

Güntürkün, O., Ströckens, F., and Ocklenburg, S. (2020). Brain lateralization: a comparative perspective. *Physiol. Rev.* 100, 1019–1063. doi: 10.1152/physrev.00006.2019

Guo, W., Liu, F., Dai, Y., Jiang, M., Zhang, J., Yu, L., et al. (2013). Decreased interhemispheric resting-state functional connectivity in first-episode, drug-naive major depressive disorder. *Prog. Neuropsychopharmacol. Biol. Psychiatry* 41, 24–29. doi: 10.1016/j.pnpbp.2012.11.003

Hoptman, M. J., and Davidson, R. J. (1994). How and why do the two cerebral hemispheres interact? *Psychol. Bull.* 116, 195–219. doi: 10.1037/0033-2909.116.2.195

Huang, J., Cai, Y., Su, Y., Zhang, M., Shi, Y., Zhu, N., et al. (2021). Gastrointestinal symptoms during depressive episodes in 3256 patients with major depressive disorders: findings from the NSSD. *J. Affect. Disord.* 286, 27–32. doi: 10.1016/j.jad.2021.02.039

Huang, M.-H., Wang, Y.-P., Wu, P.-S., Chan, Y.-L. E., Cheng, C.-M., Yang, C.-H., et al. (2021). Association between gastrointestinal symptoms and depression among older adults in Taiwan: a cross-sectional study. *J. Chin. Med. Assoc.* 84, 331–335. doi: 10.1097/JCMA.0000000000000460

Huang, Z., Liang, P., Jia, X., Zhan, S., Li, N., Ding, Y., et al. (2012). Abnormal amygdala connectivity in patients with primary insomnia: evidence from resting state fMRI. *Eur. J. Radiol.* 81, 1288–1295. doi: 10.1016/j.ejrad.2011.03.029

Hui, J., Zomorrodi, R., Lioumis, P., Ensafi, E., Voineskos, D., Voineskos, A., et al. (2021). Altered interhemispheric signal propagation in schizophrenia and depression. *Clin. Neurophysiol.* 132, 1604–1611. doi: 10.1016/j.clinph.2021.03.039

Jablonka, J. A., Binkowski, R., Kazmierczak, M., Sadowska, M., Sredniawa, W., Szlachcic, A., et al. (2021). The role of interhemispheric interactions in cortical plasticity. *Front. Neurosci.* 15:631328. doi: 10.3389/fnins.2021.631328

Jia, C., Ou, Y., Chen, Y., Ma, J., Zhan, C., Lv, D., et al. (2021). Disrupted asymmetry of inter- and intra-hemispheric functional connectivity at rest in medication-free obsessive-compulsive disorder. *Front. Neurosci.* 15:634557. doi: 10.3389/fnins.2021.634557

Klumpp, H., Hosseini, B., and Phan, K. L. (2018). Self-reported sleep quality modulates amygdala resting-state functional connectivity in anxiety and depression. *Front. Psychiatry* 9:220. doi: 10.3389/fpsyt.2018.00220

Levinthal, D. J., and Strick, P. L. (2020). Multiple areas of the cerebral cortex influence the stomach. *Proc. Natl. Acad. Sci. U.S.A.* 117, 13078–13083. doi: 10.1073/pnas.2002737117

Li, J., He, P., Lu, X., Guo, Y., Liu, M., Li, G., et al. (2021). A resting-state functional magnetic resonance imaging study of whole-brain functional connectivity of voxel levels in patients with irritable bowel syndrome with depressive symptoms. *J. Neurogastroenterol. Motil.* 27, 248–256. doi: 10.5056/jnm20209

Liu, G., Li, S., Chen, N., Zhao, Z., Guo, M., Liu, H., et al. (2021). Inter-hemispheric functional connections are more vulnerable to attack than structural connection in patients with irritable bowel syndrome. *J. Neurogastroenterol. Motil.* 27, 426–435. doi: 10.5056/jnm20134

Liu, P., Li, G., Zhang, A., Yang, C., Liu, Z., Sun, N., et al. (2020). Brain structural and functional alterations in MDD patient with gastrointestinal symptoms: a resting-state MRI study. *J. Affect. Disord.* 273, 95–105. doi: 10.1016/j.jad.2020.03.107

Liu, P., Li, Y., Zhang, A.-X., Sun, N., Li, G.-Z., Chen, X., et al. (2021). Brain structural alterations in MDD patients with gastrointestinal symptoms: evidence from the REST-meta-MDD project. *Prog. Neuropsychopharmacol. Biol. Psychiatry* 111:110386. doi: 10.1016/j.pnpbp.2021.110386

Mayer, E. A., Aziz, Q., Coen, S., Kern, M., Labus, J., Lane, R., et al. (2009). Brain imaging approaches to the study of functional gi disorders. *Neurogastroenterol. Motil. Off. J. Eur. Gastrointest. Motil. Soc.* 21, j.1365–j.2982. doi: 10.1111/j.1365-2982.2009.01304.x

Mueller, S., Wang, D., Pan, R., Holt, D. J., and Liu, H. (2015). Abnormalities in hemispheric specialization of caudate nucleus connectivity in schizophrenia. *JAMA Psychiatry* 72, 552–560. doi: 10.1001/jamapsychiatry.2014.3176

Peltola, M. J., Bakermans-Kranenburg, M. J., Alink, L. R. A., Huffmeijer, R., Biro, S., and van IJzendoorn, M. H. (2014). Resting frontal EEG asymmetry in children: meta-analyses of the effects of psychosocial risk factors and associations with internalizing and externalizing behavior. *Dev. Psychobiol.* 56, 1377–1389. doi: 10.1002/dev.21223

Sarosiek, I., Song, G., Sun, Y., Sandoval, H., Sands, S., Chen, J., et al. (2017). Central and peripheral effects of transcutaneous acupuncture treatment for nausea in patients with diabetic gastroparesis. *J. Neurogastroenterol. Motil.* 23, 245–253. doi: 10.5056/jnm16097

Schirmer, A., and Kotz, S. A. (2006). Beyond the right hemisphere: brain mechanisms mediating vocal emotional processing. *Trends Cogn. Sci.* 10, 24–30. doi: 10.1016/j.tics.2005.11.009

Shan, X., Cui, X., Liu, F., Li, H., Huang, R., Tang, Y., et al. (2021). Shared and distinct homotopic connectivity changes in melancholic and non-melancholic depression. *J. Affect. Disord.* 287, 268–275. doi: 10.1016/j.jad.2021.03.038

Su, Q., Yu, M., Liu, F., Li, Y., Li, D., Deng, M., et al. (2020). Abnormal functional asymmetry in the salience and auditory networks in first-episode, drug-naive somatization disorder. *Neuroscience* 444, 1–8. doi: 10.1016/j.neuroscience.2020.07.043

Sullivan, R. M., and Gratton, A. (1999). Lateralized effects of medial prefrontal cortex lesions on neuroendocrine and autonomic stress responses in rats. *J. Neurosci.* 19, 2834–2840. doi: 10.1523/JNEUROSCI.19-07-02834.1999

Sun, Y., Chen, Y., Collinson, S. L., Bezerianos, A., and Sim, K. (2017). Reduced hemispheric asymmetry of brain anatomical networks is linked to schizophrenia: a connectome study. *Cereb. Cortex N. Y. N.* 1991, 602–615. doi: 10.1093/cercor/bhv255

Tamietto, M., Adenzato, M., Geminiani, G., and de Gelder, B. (2007). Fast recognition of social emotions takes the whole brain: interhemispheric

cooperation in the absence of cerebral asymmetry. *Neuropsychologia* 45, 836–843. doi: 10.1016/j.neuropsychologia.2006.08.012

Tamietto, M., Latini Corazzini, L., de Gelder, B., and Geminiani, G. (2006). Functional asymmetry and interhemispheric cooperation in the perception of emotions from facial expressions. *Exp. Brain Res.* 171, 389–404. doi: 10.1007/s00221-005-0279-4

Thibodeau, R., Jorgensen, R. S., and Kim, S. (2006). Depression, anxiety, and resting frontal EEG asymmetry: a meta-analytic review. *J. Abnorm. Psychol.* 115, 715–729. doi: 10.1037/0021-843X.115.4.715

Tillisch, K., Mayer, E. A., and Labus, J. S. (2011). Quantitative meta-analysis identifies brain regions activated during rectal distension in irritable bowel syndrome. *Gastroenterology* 140, 91–100. doi: 10.1053/j.gastro.2010.07.053

Vallortigara, G. (2006). The evolutionary psychology of left and right: costs and benefits of lateralization. *Dev. Psychobiol.* 48, 418–427. doi: 10.1002/dev.20166

van Meer, M. P. A., van der Marel, K., Wang, K., Otte, W. M., el Bouazati, S., Roeling, T. A. P., et al. (2010). Recovery of sensorimotor function after experimental stroke correlates with restoration of resting-state interhemispheric functional connectivity. *J. Neurosci.* 30, 3964–3972. doi: 10.1523/JNEUROSCI.5709-09.2010

Wager, T. D., Phan, K. L., Liberzon, I., and Taylor, S. F. (2003). Valence, gender, and lateralization of functional brain anatomy in emotion: a meta-analysis of findings from neuroimaging. *NeuroImage* 19, 513–531. doi: 10.1016/s1053-8119(03)00078-8

Wang, J.-H., Zuo, X.-N., Gohel, S., Milham, M. P., Biswal, B. B., and He, Y. (2011). graph theoretical analysis of functional brain networks: test-retest evaluation on short- and long-term resting-state functional MRI data. *PLoS One* 6:e21976. doi: 10.1371/journal.pone.0021976

Wang, L., Dai, Z., Peng, H., Tan, L., Ding, Y., He, Z., et al. (2013). Overlapping and segregated resting-state functional connectivity in patients with major depressive disorder with and without childhood neglect. *Hum. Brain Mapp.* 35, 1154–1166. doi: 10.1002/hbm.22241

Weise, C. M., Thiyyagura, P., Reiman, E. M., Chen, K., and Krakoff, J. (2012). Postprandial plasma PYY concentrations are associated with increased regional gray matter volume and rCBF declines in caudate nuclei – a combined MRI and H215O PET study. *NeuroImage* 60, 592–600. doi: 10.1016/j.neuroimage.2011.12.023

Yan, C., and Zang, Y. (2010). DPARSF: a MATLAB toolbox for "Pipeline". Data analysis of resting-state fMRI. *Front. Syst. Neurosci.* 4:13. doi: 10.3389/fnsys.2010.00013

Yan, M., Chen, J., Liu, F., Li, H., Huang, R., Tang, Y., et al. (2021). Disrupted regional homogeneity in major depressive disorder with gastrointestinal symptoms at rest. *Front. Psychiatry* 12:636820. doi: 10.3389/fpsyt.2021.636820

Zhao, D.-Q., Xue, H., and Sun, H.-J. (2020). Nervous mechanisms of restraint water-immersion stress-induced gastric mucosal lesion. *World J. Gastroenterol.* 26, 2533–2549. doi: 10.3748/wjg.v26.i20.2533

Zhao, W., Zhu, D., Zhang, Y., Zhang, C., Zhang, B., Yang, Y., et al. (2021). Relationship between illness duration, corpus callosum changes, and sustained attention dysfunction in major depressive disorder. *Quant. Imaging Med. Surg.* 11, 2980–2993. doi: 10.21037/qims-20-970

Zhou, Y., Yu, C., Zheng, H., Liu, Y., Song, M., Qin, W., et al. (2010). Increased neural resources recruitment in the intrinsic organization in major depression. *J. Affect. Disord.* 121, 220–230. doi: 10.1016/j.jad.2009.05.029

Zhu, F., Liu, F., Guo, W., Chen, J., Su, Q., Zhang, Z., et al. (2018). Disrupted asymmetry of inter- and intra-hemispheric functional connectivity in patients with drug-naive, first-episode schizophrenia and their unaffected siblings. *EBioMedicine* 36, 429–435. doi: 10.1016/j.ebiom.2018.09.012

Zhu, F., Liu, Y., Liu, F., Yang, R., Li, H., Chen, J., et al. (2019). Functional asymmetry of thalamocortical networks in subjects at ultra-high risk for psychosis and first-episode schizophrenia. *Eur. Neuropsychopharmacol.* 29, 519–528. doi: 10.1016/j.euroneuro.2019.02.006

Conflict of Interest: The authors declare that the research was conducted in the absence of any commercial or financial relationships that could be construed as a potential conflict of interest.

Publisher's Note: All claims expressed in this article are solely those of the authors and do not necessarily represent those of their affiliated organizations, or those of the publisher, the editors and the reviewers. Any product that may be evaluated in this article, or claim that may be made by its manufacturer, is not guaranteed or endorsed by the publisher.

frontiers | Frontiers in Neuroscience

ORIGINAL RESEARCH
published: 07 April 2022
doi: 10.3389/fnins.2022.801899

The Role of Medial Prefrontal Cortex in Acupuncture Treatment for Functional Dyspepsia

Yuke Teng[1†], Tao Yin[1†], Yue Yang[1†], Ruirui Sun[1], Zilei Tian[1], Peihong Ma[2], Zhaoxuan He[1], Yuzhu Qu[1], Liuyang Huang[1], Yuan Chen[3] and Fang Zeng[1]**

[1] Acupuncture and Tuina School/The 3rd Teaching Hospital, Chengdu University of Traditional Chinese Medicine, Chengdu, China, [2] School of Acupuncture-Moxibustion and Tuina, Beijing University of Chinese Medicine, Beijing, China, [3] International Education School, Chengdu University of Traditional Chinese Medicine, Chengdu, China

Acupuncture is an effective therapy for functional dyspepsia (FD). However, the efficacy of acupuncture in the treatment of FD varies among individuals in clinical practice. This study aimed to reveal the brain response patterns in acupuncture higher response/lower response FD patients. Firstly, we performed a within-group comparison of brain function activity before and after acupuncture treatment in 115 FD patients and analyzed the correlation between brain function activity changes and clinical improvements. Secondly, 115 subjects were divided into the acupuncture higher response group or the lower response group based on the median clinical improvement values. The changes in functional brain activity after acupuncture treatment were investigated in these two groups, respectively. Finally, the identified brain regions associated with the clinical improvements were set as regions of interest (ROI), and the ROI-to-voxel functional connectivity comparisons were also performed in both groups, respectively. The results demonstrated that the functional activities of the left cerebellum inferior, right middle temporal gyrus, and right medial prefrontal cortex (mPFC) were increased, and the left Heschl and right middle cingulate cortex were decreased in 115 FD patients after acupuncture treatment. The functional connectivity changes of mPFC were correlated with improving the Nepean Dyspepsia Symptom Index. The significant increase in mPFC functional activity was also found in acupuncture higher response FD patients but not in lower response FD patients. The functional connectivity between the mPFC and default mode network (DMN) was significantly diminished in the higher response group but not in the lower response group. In conclusion, this study suggested that modulating the functional activity of the mPFC and its connectivity to the DMN may be one of the important mechanisms of acupuncture for treating FD with a higher response.

Keywords: acupuncture, functional dyspepsia, curative effect, fMRI, mPFC, DMN

OPEN ACCESS

Edited by:
Chunhui Bao,
Shanghai University of Traditional Chinese Medicine, China

Reviewed by:
Yan Zhou,
Shanghai Jiao Tong University, China
Jing Tao,
Fujian University of Traditional Chinese Medicine, China

****Correspondence:***
Yuan Chen
1040539320@qq.com
Fang Zeng
zeng_fang@126.com;
zengfang@cdutcm.edu.cn

[†] These authors have contributed equally to this work and share first authorship

Specialty section:
This article was submitted to Gut-Brain Axis, a section of the journal Frontiers in Neuroscience

Received: *26 October 2021*
Accepted: *25 February 2022*
Published: *07 April 2022*

Citation:
Teng Y, Yin T, Yang Y, Sun R, Tian Z, Ma P, He Z, Qu Y, Huang L, Chen Y and Zeng F (2022) The Role of Medial Prefrontal Cortex in Acupuncture Treatment for Functional Dyspepsia. Front. Neurosci. 16:801899. doi: 10.3389/fnins.2022.801899

INTRODUCTION

As a functional gastrointestinal disorder (FGID) with high prevalence in the general population (Enck et al., 2017), functional dyspepsia (FD) is characterized by postprandial fullness, early satiation, epigastric pain, or burning (Ford et al., 2020). FD significantly affects the quality of life (QoL) of patients and families, results in severe medication overuse, and leads to substantial social

and financial burdens (Black et al., 2020; Oh et al., 2020). However, due to its complex etiology and unclear pathogenesis, the curative effect of FD is unsatisfactory (Ford et al., 2020), so efforts in seeking effective alternative therapies attract both patients and practitioners.

Acupuncture has been used to treat gastrointestinal symptoms for several millennia in China and some other Asian countries. It is increasingly accepted as an alternative treatment for FGIDs in western countries (Wang et al., 2021). In clinical practice, the efficacy of acupuncture in the treatment of FD varies among individuals (Yang et al., 2020). The varying effectiveness may be related to the different responses to acupuncture treatment. Therefore, it is necessary to explore the mechanism of the acupuncture effect to improve clinical efficacy.

The brain–gut axis is a conception of nerve anatomy. The central nervous system and myenteric nervous plexuses have a bidirectional connection that affects functions such as sensation and movement. With the development of neuroimaging technology, the study of the brain–gut axis is not limited to animal experiments. Non-invasive and high spatial and temporal resolution techniques, such as functional magnetic resonance imaging (fMRI), support brain–gut interaction studies based on human beings. For example, through fMRI techniques, studies have identified changes in brain activity in the medial prefrontal cortex, orbitofrontal cortex, cingulate gyrus, hippocampus, precuneus, and temporal pole in FD patients compared with healthy subjects (Liu et al., 2013; Chen et al., 2018; Qi et al., 2020). Thus, the Rome criteria have defined FD as a disease with abnormal brain–gut interaction (Drossman, 2016). In addition, these neuroimaging techniques have also been widely used to study the mechanisms of acupuncture treatment for FD. Multiple neuroimaging studies demonstrated that acupuncture treatment not only improved clinical symptoms (postprandial fullness, upper abdominal bloating, and early satiation) but also significantly modulated the abnormal brain function in FD patients, such as the posterior cingulate cortex, insula, and hippocampus, etc. (Zeng et al., 2015; Wang et al., 2020; Yang et al., 2020). However, whether the key to the therapeutic effects of acupuncture is related to the activity of some brain regions requires further research.

Therefore, based on the hypothesis that the brain response of acupuncture higher response FD patients is different from that of lower response patients, the present study aimed to (1) investigate the brain activity changes elicited by acupuncture treatment in all enrolled FD patients and analyze the correlation between symptom improvements and brain activity changes to explore the potential key regions involved in acupuncture treatment; (2) compare the differences in brain activity changes between the higher group (group exhibiting higher responses to acupuncture treatment) and the lower group (group exhibiting lower responses to acupuncture treatment) to verify further the key regions involved in acupuncture treatment; and (3) investigate the changes of connectivity pattern of the key regions in the higher response group, to explore the central mechanism of acupuncture for treating FD.

MATERIALS AND METHODS

This study is a secondary data analysis study. The data originate from two randomized controlled neuroimaging trials with acupuncture treatment for FD (The Chinese Clinical Trial Registry: ChiCTR-IOR-15006402 and ChiCTR-IOR-15006523) (Yin et al., 2017; Sun et al., 2018, 2021).

Patients

A total of 115 FD patients from the two studies mentioned above were included in this study. All FD patients were from the outpatient department of the Affiliated Hospital of Chengdu University of Traditional Chinese Medicine and the campus of Chengdu University of Traditional Chinese Medicine. FD patients were enrolled if they fulfilled the following inclusion criteria: (1) they match the Rome III criteria for functional dyspepsia and postprandial distress syndrome, (2) they are right-handed and aged 18 to 45 years old, (3) they are not attending any other clinical trials in last 3 months, and (4) they provide written informed consent. Patients were excluded if they: (1) had esophagitis, gastric atrophy, or erosive gastroduodenal lesions on endoscopy; cholecystitis; and gallstones; (2) were pregnant or lactating; (3) were suffering from cardiovascular, renal, or respiratory illnesses or other organic diseases; (4) had a history of psychiatric and neurological disorders or head trauma with loss of consciousness; or (5) were using dynamic gastrointestinal medicine or received acupuncture treatment during the last 15 metal stents or electronic implant, intraocular metal foreign body, claustrophobia, hyperpyrexia, etc. (Yin et al., 2017; Sun et al., 2018).

Acupuncture Interventions

The 115 FD patients received the 20 sessions' acupuncture treatment over 4 weeks (five sessions per week). In each week, acupuncture was performed once per day for 5 days continuously, with 2-day intervals to the next week. In each session, patients received manual acupuncture treatment with disposable sterile stainless-steel needles (25–40 × 0.25 mm; Suzhou Hua Tuo Medical Instrument Co., Ltd., China) for 30 min. Acupuncture treatment was performed by two licensed acupuncturists with experience of over 3 years. In the two original studies, one study used acupuncture ST36 combined with CV12 as the treatment group and acupuncture ST36 and acupuncture CV12 as the control groups, respectively; the other study used acupuncture ST36 with Deqi as the treatment group and without Deqi as the control group, respectively (Yin et al., 2017; Sun et al., 2018).

Outcome Measurements

The outcome measurements of the two studies included the Nepean Dyspepsia Symptom Index (NDSI) and Symptom Index of Dyspepsia (SID). The NDSI is a dyspepsia-specific index used to measure the dyspepsia symptoms over the previous 14 days. The scale measures the frequency, intensity, and level of discomfort of 15 upper gastrointestinal symptoms. It includes interference (13 items), knows/control (7 items), eats/drink (3 items), and sleep/disturb (2 items), and higher scores indicate more severe symptoms and poorer QoL. The SID includes

the evaluation of four primary symptoms of FD, including postprandial fullness discomfort, early satiety, epigastric pain, and epigastric burning. The scoring of each item from none to severe is 0–3, with 0 indicating no symptoms, 1 indicating mild symptoms, 2 indicating moderate symptoms, and 3 indicating severe symptoms. The total score of four items evaluated the symptom severity of FD patients.

fMRI Data Acquisition

All 115 FD patients received two fMRI scans, performed at baseline and after treatment. The parameters and sequences of the two fMRI scans were the same in all FD patients (Yin et al., 2017; Sun et al., 2018).

Data Analysis

fMRI Data Processing

The fMRI data preprocessing was performed using SPM12 (SPM12[1]) and DPARSF 4.5[2]. The procedure was conducted as follows: (1) The first 10 time points of the fMRI scan for each subject were discarded, and the retained data were corrected for slice timing and rearranged. (2) The functional image and T1 image were repositioned with six rigid body parameters and registered in the functional space together with segmentation. (3) The structural image was segmented uniformly and normalized. (4) White matter and cerebrospinal fluid signals were regressed with the Friston 24-parameter model, and the head motion was corrected again. (5) The image was resampled into a 3-mm cube element and then smoothed with a Gaussian kernel with a half-maximum width of 6 mm. (6) The imaging data were time filtered (0.01–0.08 Hz) to eliminate the effects of extremely low-frequency drift and high-frequency noise (such as respiration and heart rhythm) and generate fALFF map. (7) Conversion of an fALFF map to a zfALFF map using a normal Z transform.

Clinical Data and Correlation Analysis

Paired t-tests (normal distribution) or Wilcoxon signed rank tests (non-normal distribution) were selected for within-group comparisons. Two simple t-tests (normal distribution) or Mann–Whitney U-test (non-normal distribution) was chosen for between-group comparisons. The level of statistical significance was $p < 0.05$, and a two-tailed test was used. Correlation analysis was performed using Pearson correlation analysis (normal distribution) or Spearman correlation analysis (non-normal distribution). The level of statistical significance was $p < 0.05$, and a two-tailed test was used.

Analysis of Effect-Related Brain Regions

In the first step, the paired t-test was used to analyze the changed brain areas in 115 FD patients after acupuncture treatment and to extract the change values ($p < 0.05$, GRF-corrected) (Liu et al., 2021). In the second step, clinical improvement values were calculated for 115 FD patients after acupuncture treatment. In the third step, a correlation analysis of the results of the first and second steps was performed to obtain the brain areas associated with the efficacy of acupuncture.

Grouping of Higher or Lower Response to Acupuncture

The 115 FD patients were regrouped according to the efficacy. Referring to the study by Ma et al. (2015), patients with FD were divided into two subgroups based on a median SID improvement value of 2 points: the higher response group (greater than or equal to 2 points) and the lower response group (less than 2 points).

Resting-State Functional Connection Analysis

Paired t-test was used to analyze the brain activities of patients in the acupuncture higher/lower response group, and the brain regions related to efficacy in the higher response group were regarded as regions of interest (ROI). The paired t-test was used to analyze the resting-state functional connectivity (rsFC) before and after the acupuncture treatment in the higher response group. This study selected all comparison thresholds for brain regions with GRF-corrected $p < 0.05$ (Liu et al., 2021).

RESULTS

Cerebral Activity Changes and the Correlation With Symptom Improvement in All Functional Dyspepsia Patients

Cerebral Activity Changes Elucidated by Acupuncture Treatment in All Functional Dyspepsia Patients

The functional activities of the left cerebellum inferior, right middle temporal gyrus, and right medial prefrontal cortex increased while those of the left Heschl and the right middle cingulate cortex decreased after acupuncture treatment for all FD patients (**Table 1** and **Figure 1**).

The Correlation Between Cerebral Activity Changes and Symptom Improvement

The correlation analysis showed that the change of the right medial prefrontal cortex (mPFC) was correlated with the improvement of NDSI ($r = 0.20$, $p = 0.03$) but not with the improvement in SID. Other brain function activity areas were not associated with the clinical improvement value (**Table 1** and **Figure 1**).

Cerebral Activity Changes in the Acupuncture Higher/Lower Response Group

Grouping Results of Demographic Characteristics and Clinical Variables

Among the 115 FD patients, 66 FD patients were assigned to the higher response group, and 49 FD patients were assigned to the lower response group. The demographic characteristics and clinical variables of the two groups are described in **Table 2**. There was no significant difference between gender, age, height, and weight between the two groups.

[1]http://www.fil.ion.ucl.ac.uk/spm

[2]http://rfmri.org/DPARSF

TABLE 1 | Cerebral activity changes elucidated by acupuncture treatment in all FD patients.

			MNI				Cluster	Correlation with NDSI
Regions	**Side**	**Sign**	**X**	**Y**	**Z**	**T value**	**size**	***p* value**
Cerebelum_Crus2	L	↑	−15	−90	−33	3.62	57	0.34
Frontal_Mid	R	↑	39	21	51	3.30	54	0.55
Frontal_Sup_Medial	R	↑	9	48	48	4.01	59	0.03*
Frontal_Sup_Medial	R	↑	12	63	12	3.91	85	0.11
Heschl	L	↓	−45	−12	12	−4.80	51	0.23
Cingulum_Mid	R	↓	6	−15	51	−3.92	134	0.45

*MNI, Montreal Neurological Institute; Cerebelum_Crus2, cerebellum inferior; Frontal_Mid, middle temporal gyrus; Frontal_Sup_Medial, medial prefrontal cortex; Cingulum_Mid, middle cingulate cortex; ↑, increasing; ↓, decreasing; L, left; R, right; *p < 0.05.*

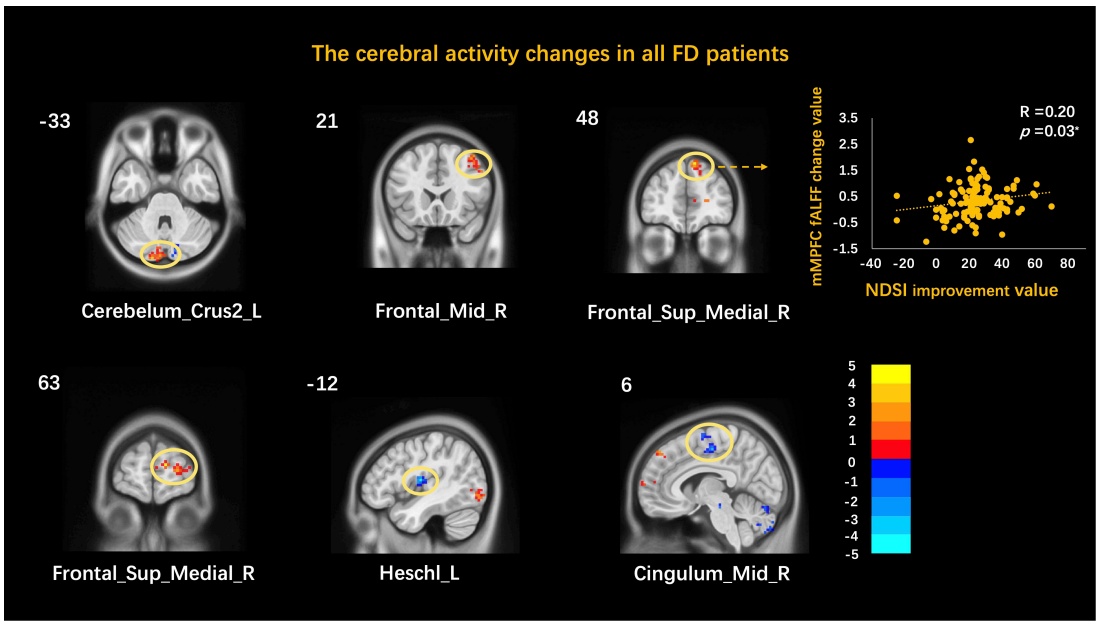

FIGURE 1 | Correlation between cerebral activity changes and symptom improvement. Cerebelum_Crus2, cerebellum inferior; Frontal_Mid, middle temporal gyrus; Frontal_Sup_Medial, medial prefrontal cortex; Cingulum_Mid, middle cingulate cortex; L, left; R, right; *$p < 0.05$.

TABLE 2 | Demographic characteristics and clinical variables in all FD patients/higher/lower groups.

	All FD patients (*n* = 115)	**Higher response group (*n* = 66)**	**Lower response group (*n* = 49)**	***p* value**
Gender (male/female)	28/88	16/50	11/38	1
Age (years), mean ± SD	22.22 ± 2.34	22.00 ± 1.98	22.55 ± 2.70	0.47
Height, mean ± SD	161.93 ± 7.64	162.12 ± 7.00	161.71 ± 8.56	0.63
Weight, mean ± SD	52.52 ± 8.61	51.62 ± 8.91	53.85 ± 8.13	0.24
NDSI score improvements, mean ± SD	23.67 ± 15.68	29.36 ± 13.40	15.90 ± 15.34	0.00**
SID score improvements, median (IQR)	2 (1,3)	3 (2,4)	1 (0,1)	0.00**

*NDSI, Nepean Dyspepsia Symptom Index; SID, Symptom Index of Dyspepsia; **p < 0.001.*

Cerebral Activity Changes of the Higher/Lower Groups

After acupuncture treatment, the functional activities of the right mPFC and the left caudate increased while those of the left anterior cingulate cortex, the left rectus, and the right lingual gyrus decreased in the higher response group. After acupuncture treatment, the functional activities of the right inferior temporal gyrus and the left inferior occipital gyrus increased while those of the right cerebellum inferior, the right cerebellum superior, and the left pallidus decreased in the lower response group. The two groups' detailed information of altered brain areas after acupuncture treatment is described in **Table 3** and **Figure 2**.

TABLE 3 | The cerebral activity changes in higher/lower group.

Regions	Side	Sign	MNI			T value	Cluster size
			X	Y	Z		
Higher response group							
Frontal_Sup_Medial	R	↑	9	48	48	4.10	61
Caudate	L	↑	−15	−6	18	3.95	63
Cingulum_Ant	L	↓	0	18	24	−3.50	72
Rectus	L	↓	−12	21	−15	−3.30	70
Lingual	R	↓	12	−54	−6	−3.15	79
Lower response group							
Temporal_Inf	R	↑	48	−69	−6	3.87	73
Occipital_Inf	L	↑	−42	−84	−12	3.51	53
Cerebelum_Crus2	R	↓	42	−75	−39	−4.08	76
Cerebelum_Crus1	R	↓	6	−78	−21	−3.06	68
Pallidum	L	↓	−18	3	6	−3.40	71

MNI, Montreal Neurological Institute; Frontal_Sup_Medial, medial prefrontal cortex; Cingulum_Ant, anterior cingulate cortex; Lingual, lingual gyrus; Temporal_Inf, inferior temporal gyrus; Occipital_Inf, inferior occipital gyrus; Cerebelum_Crus2, cerebellum inferior; Cerebelum_Crus1, cerebellum superior; ↑, increasing; ↓, decreasing; L, left; R, right.

TABLE 4 | Changes of mPFC rsFC in higher response group.

Regions	Side	Sign	MNI			T value	Cluster size
			X	Y	Z		
Temporal_Mid	L	↓	−63	−30	12	−4.01	176
Cerebelum_Crus1	R	↓	45	−81	−33	−3.75	103
Cingulum_Ant	L	↓	0	45	12	−4.45	409
Cingulum_Mid/ Cingulum_Post	R	↓	3	−18	33	−5.03	379
Angular	L/R	↓	60	−57	30	−4.79	187

MNI, Montreal Neurological Institute; Temporal_Mid, middle temporal gyrus; Cerebelum_Crus1, cerebellum superior; Cingulum_Ant, anterior cingulate cortex; Cingulum_Mid, middle cingulate cortex; Cingulum_Post, posterior cingulate cortex; ↓, decreasing; L, left; R, right.

Resting-State Cerebral Functional Connectivity in the Higher Response Group

After finding that mPFC correlated with clinical improvement values and significant changes in functional activity in the higher response group, the mPFC was used as an ROI to explore the brain network characteristics of FD patients in the higher response group to acupuncture. The results showed that the mPFC rsFC with the left middle temporal gyrus, the right cerebellum superior, the left anterior cingulate cortex, the right middle cingulate cortex/posterior cingulate cortex, and the bilateral angular gyrus decreased (**Table 4** and **Figure 3**). The correlation analysis showed no correlation between the mPFC rsFC and clinical symptom improvement values in the higher response group.

Resting-State Cerebral Functional Connectivity in the Lower Response Group

The mPFC was used as the ROI to explore the brain network characteristics of FD patients in the acupuncture low response

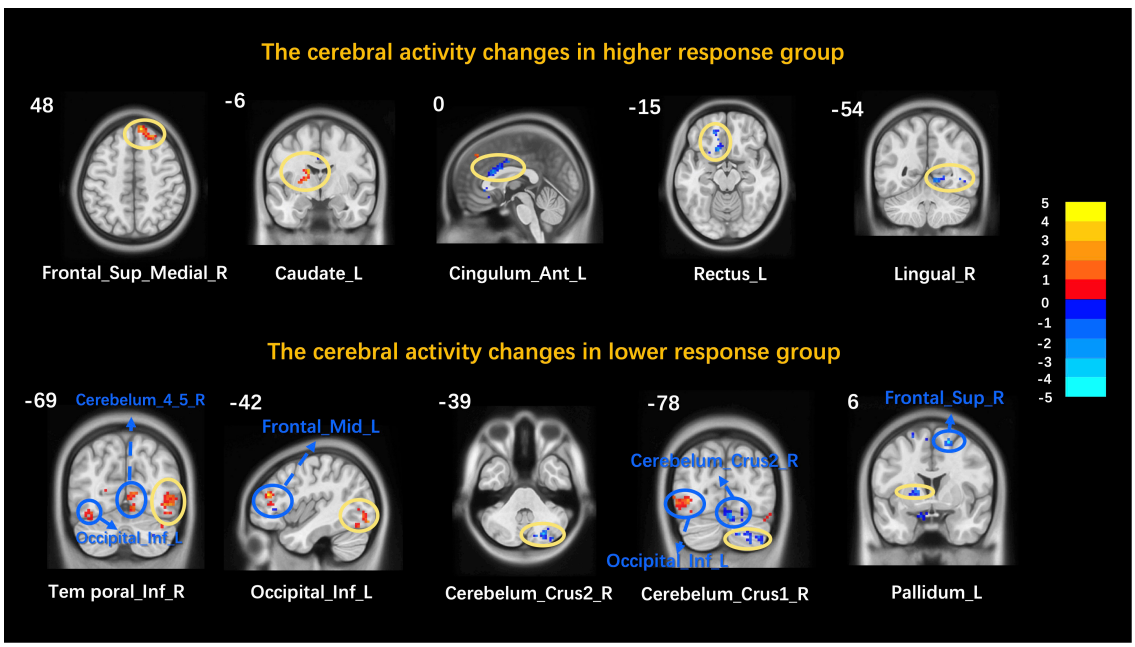

FIGURE 2 | Cerebral activity changes in the higher/lower response group. Frontal_Sup_Medial, medial prefrontal cortex; Cingulum_Ant, anterior cingulate cortex; Lingual, lingual gyrus; Temporal_Inf, inferior temporal gyrus; Occipital_Inf, inferior occipital gyrus; Cerebelum_Crus2, cerebellum inferior; Cerebelum_Crus1, cerebellum superior; L, left; R, right. Yellow circles mark peak points and blue marks non-peak areas.

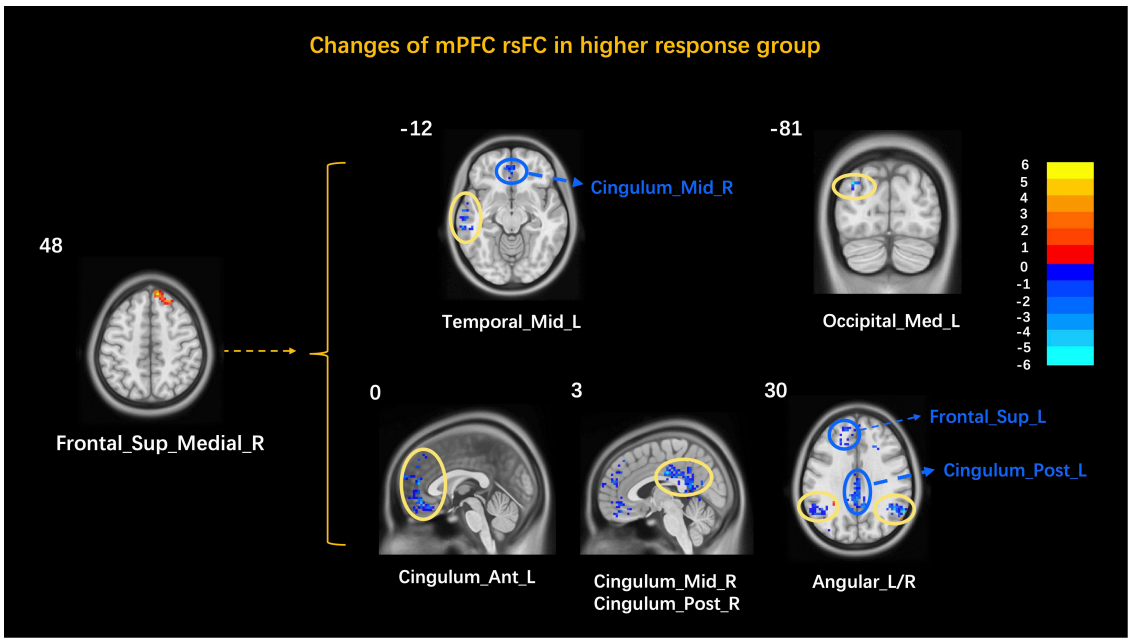

FIGURE 3 | Changes of the mPFC rsFC in the higher response group. Frontal_Sup_Medial, medial prefrontal cortex; Temporal_Mid, middle temporal gyrus; Cerebelum_Crus1, cerebellum superior; Cingulum_Ant, anterior cingulate cortex; Cingulum_Mid, middle cingulate cortex; Cingulum_Post, posterior cingulate cortex; L, left; R, right. Yellow circles mark peak points and blue marks non-peak areas.

TABLE 5 | Changes of mPFC rsFC in the lower response group.

			MNI				
Regions	**Side**	**Sign**	**X**	**Y**	**Z**	**T value**	**Cluster size**
Occipital_Mid	R	↑	33	−69	30	4.09	151
Frontal_Mid_Orb	R	↑	30	45	0	3.995	78

MNI, Montreal Neurological Institute; Occipital_Mid, middle occipital gyrus; Frontal_Mid_Orb, orbital middle frontal gyrus; ↑, increasing; ↓, decreasing; L, left; R, right.

group. The results showed that the mPFC rsFC with the right middle occipital gyrus and the right orbital middle frontal gyrus increased (**Table 5** and **Figure 4**). The correlation analysis showed no correlation between the mPFC rsFC and clinical symptom improvement values in the lower response group.

Between-Group Comparisons of Resting-State Cerebral Activity Changes in the Higher and Lower Response Groups

A comparison of the mPFC rsFC in the higher response and lower response groups was done to explore the brain network characteristics of FD patients with the acupuncture higher/lower response groups. The results showed that the mPFC rsFC with the left cerebellum inferior, the left inferior temporal gyrus, the right orbital middle frontal gyrus, the right angular gyrus, and the left posterior cingulate cortex decreased while that with the left inferior frontal gyrus triangular part increased (**Table 6** and **Figure 5**).

DISCUSSION

By analyzing the correlation between cerebral activity changes and symptom improvements of all FD patients after acupuncture treatment and comparing the differences in cerebral activity changes between the higher response and the lower response groups, this study found that mPFC might be involved in acupuncture for FD and demonstrated the alternations of functional connectivity between mPFC and default mode network (DMN).

Several studies have confirmed that the mPFC is involved in regulating gastrointestinal physiological function and in the central pathological changes of FD (Kano et al., 2020). In a physiological state, the mPFC is extensively involved in the cognitive process, visceral function regulation, emotional activity, etc. (Euston et al., 2012). The mPFC includes the infralimbic cortex (IL) and the prelimbic cortex (PL) (Hurley-Gius and Neafsey, 1986; Neafsey, 1990). The former exerts a pronounced influence on visceral/autonomic nervous activities through its direct projections to the medulla gastrointestinal motor centers. At the same time, some cortical neurons that affect the output of the gastric parasympathetic nerve originate from the mPFC, so IL is considered to belong to the "visceral motor cortex." PL is related to cognitive, emotional, and executive functions and is considered part of the "cognitive–emotional cortex" (Zhao et al., 2019). In a pathological state, the structural and

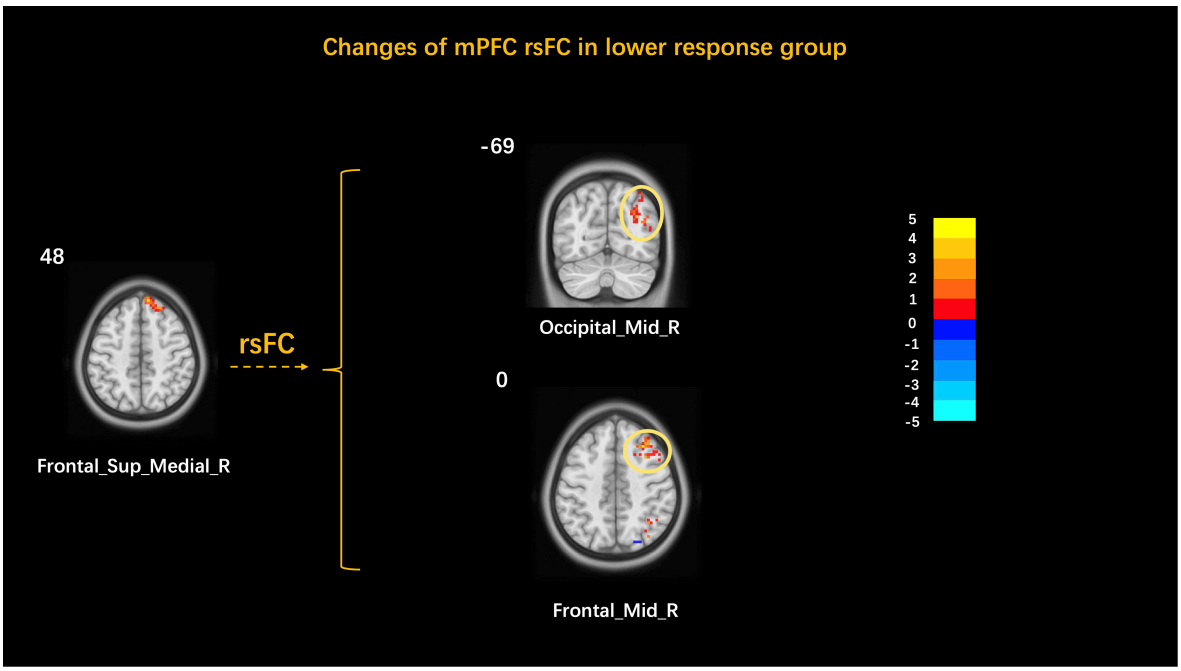

FIGURE 4 | Changes of the mPFC rsFC in the higher response group. Occipital_Mid, middle occipital gyrus; Frontal_Mid_Orb, orbital middle frontal gyrus; L, left; R, right.

functional changes in the mPFC in FD patients have been documented in multiple neuroimaging studies. For example, an 18F-FDG PET-CT study found that FD patients showed significant glucometabolic increase in mPFC, which suggests that the altered signal of mPFC might be related to patients' selective attention to sensations from the stomach, such as postprandial upper abdominal discomfort, early satiety, and abdominal distension (Zeng et al., 2011). A structural MRI study reported the changes of cortical thickness and subcortical volume in mPFC in FD patients compared with healthy subjects and suggested that these changes were closely related to the severity of symptoms (Liu et al., 2018). Similarly, a decreased gray matter density of mPFC was found in FD patients reporting meal-related symptoms compared with healthy subjects (Zeng et al., 2013). These studies demonstrated the role of mPFC in the central pathogenesis of FD. They suggested that mPFC may be a potential target brain region of gastrointestinal modulating effect of acupuncture treatment.

To investigate the role of mPFC in the acupuncture treatment for FD, three analyses were designed in this current study. Firstly, significant cerebral activity changes in mPFC were found in all FD patients after 4 weeks of acupuncture treatment. The increased activity of mPFC was markable related to the improvement in NDSI scores. It indicated that the more significant the decrease in mPFC activity, the more influential the dyspepsia symptoms. The results suggested that the regulation of mPFC function may be one of the mechanisms of acupuncture for treating FD. Secondly, to further confirm the involvement of mPFC in the therapeutic effect of acupuncture on FD, 115 FD patients included in this study were divided into the higher response group and the lower response group according to the clinical improvement of SID scores. The results showed increased activities in the mPFC of the higher response FD patients, while there were no significant activities in the mPFC of the lower response patients. These two results indicate that mPFC should be a critical region in the realization of acupuncture effect, and the adjustment of abnormal function of mPFC may be an important mechanism of acupuncture effectively treating FD. Thirdly, to further explore how mPFC participates in the realization of acupuncture effect, this study selected the mPFC as ROI and performed the ROI-based rsFC analysis. The results demonstrated that the rsFC of the mPFC with the left anterior cingulate cortex (ACC), the right middle cingulate cortex (MCC)/posterior cingulate cortex (PCC), and the bilateral angular gyrus (AG) significantly decreased in the

TABLE 6 | Between-group comparisons of mPFC rsFC changes.

			MNI				
Regions	**Side**	**Sign**	**X**	**Y**	**Z**	**T value**	**Cluster size**
Cerebelum_Crus2	L	↓	−36	−72	−45	−4.09	94
Temporal_Inf	L	↓	−57	−9	−27	−3.67	93
Frontal_Mid_Orb	R	↓	30	60	−9	−3.79	101
Frontal_Inf_Tri	L	↑	−42	36	18	3.76	124
Angular	R	↓	48	−60	39	−4.45	221
Cingulum_Post	L	↓	0	−36	33	−4.12	96

MNI, Montreal Neurological Institute; Cerebelum_Crus2, cerebellum inferior; Temporal_Inf, inferior temporal gyrus; Frontal_Mid_Orb, orbital middle frontal gyrus; Frontal_Inf_Tri, inferior frontal gyrus, triangular part; Cingulum_Post, posterior cingulate cortex; ↑, increasing; ↓, decreasing; L, left; R, right.

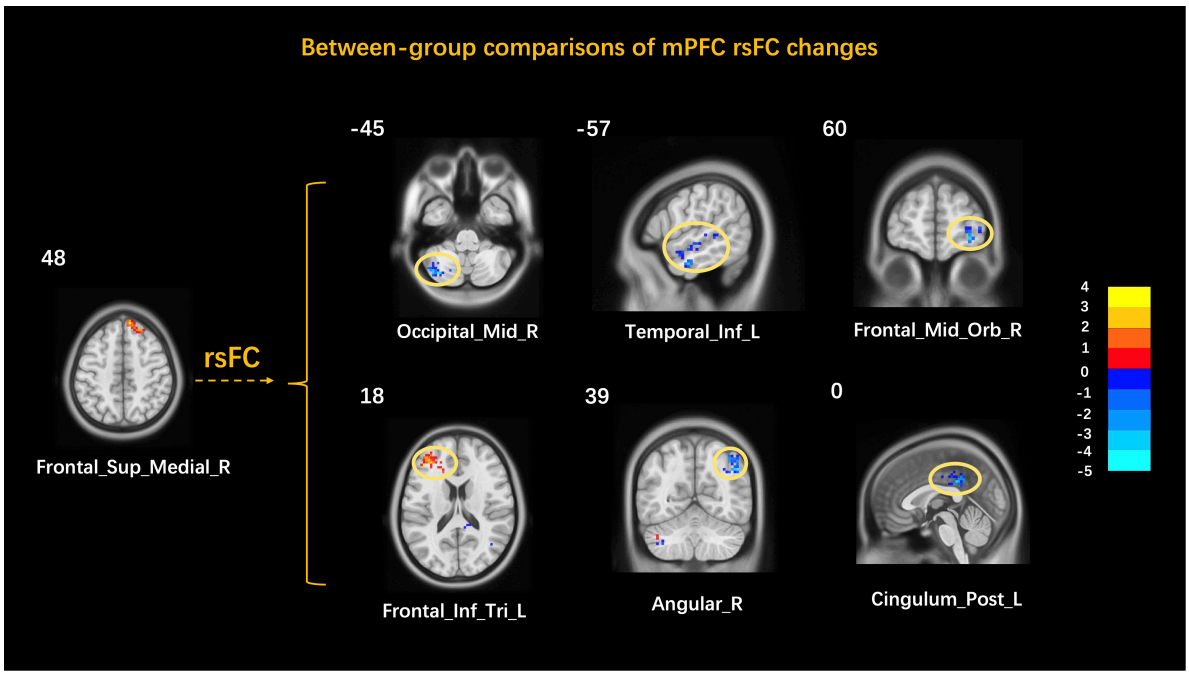

FIGURE 5 | Between-group comparisons of mPFC rsFC changes. MNI, Montreal Neurological Institute; Cerebellum_Crus2, cerebellum inferior; Temporal_Inf, inferior temporal gyrus; Frontal_Mid_Orb, orbital middle frontal gyrus; Frontal_Inf_Tri, inferior frontal gyrus, triangular part; Cingulum_Post, posterior cingulate cortex; L, left; R, right.

higher response group but not in the lower response group. Also, the results of the between-group comparison between the high and low response groups showed that the functional connectivity of mPFC rsFC with regions such as PCC and AG was decreased. These decreased regions are an important part of the DMN.

The DMN is a functional network composed of brain regions that maintain synchronous, low-frequency spontaneous neuronal activity in a resting state and continue to be negatively activated in a task state (Lei et al., 2013) and is thought to be associated with social behavior, emotional control, and sensory-visceral movements. Several neuroimaging studies have demonstrated the DMN alternations in patients with gastrointestinal diseases, including FD (Liu et al., 2013), functional constipation (FC) (Yin et al., 2021), irritable bowel syndrome (IBS) (Qi et al., 2016), Crohn's disease (CD) (Thomann et al., 2017), and ulcerative colitis (UC) (Skrobisz et al., 2020), and suggested the involvement of DMN in the abnormal process of brain–gut interaction in these gastrointestinal diseases. For example, a structural MRI indicated that, compared with healthy subjects, FD patients showed significant cortical thickness alterations in some regions of DMN such as mPFC, PCC, AG, etc. (Liu et al., 2018). Furthermore, a review indicated that functional connectivity changes in DMN were commonly seen in acupuncture studies with different participants. The involvement of DMN in acupuncture treatment is suggested to be a factor in the realization of treatment efficacy. For example, previous studies found that acupuncture could enhance the post-stimulus spatial extent of DMN in healthy subjects (Dhond et al., 2008) and could modulate the abnormal function of DMN in IBS patients (Zhao et al., 2018) and so on. In this study, the functional connectivity between mPFC and DMN was significantly decreased in the higher response group after acupuncture treatment. The results suggested that the efficacy of acupuncture for FD may be achieved by modulating the internal connectivity pattern between the mPFC and the DMN to improve the abnormal gastric sensory and cognitive/emotional processing. The limitations of this study are mainly that the results of this study are a secondary analysis of two randomized controlled neuroimaging studies of acupuncture for FD, and the results need to be verified in a subsequent strictly designed prospective study.

CONCLUSION

In conclusion, this study discovered that mPFC might play an important role in the acupuncture treatment for FD from three aspects. Based on finding the significantly decreased functional activity of mPFC and its negative correlation with symptom improvement in all FD patients after acupuncture treatment, a subgroup analysis further verified the participation of mPFC in acupuncture treatment efficacy, and a ROI-based functional connectivity analysis indicated the enhancement in functional connectivity between mPFC and DMN in the higher response group. These results suggest that modulating the functional activity of the mPFC and its connectivity to the DMN may be one of the important mechanisms of acupuncture for treating FD. This implies that mPFC and DMN might play a key role in the treatments for FD by acupuncture.

DATA AVAILABILITY STATEMENT

The original contributions presented in the study are included in the article/supplementary material, further inquiries can be directed to the corresponding author/s.

ETHICS STATEMENT

The studies involving human participants were reviewed and approved by Affiliated Hospital of Chengdu University of Traditional Chinese Medicine. The ethics committee waived the requirement of written informed consent for participation. Written informed consent was obtained from the individual(s) for the publication of any potentially identifiable images or data included in this article.

AUTHOR CONTRIBUTIONS

FZ, YT, and YY designed the study and drafted the manuscript. FZ, YC, and TY revised the study design and the manuscript. TY, RS, PM, ZH, YQ, and LH were involved in the study implementation and data collection. ZT was involved in the design of the diagrams in the manuscript. All authors contributed to the article and approved the submitted version.

FUNDING

This study was supported by the National Natural Science Foundation of China (Nos. 81973960, 81622052, and 81473602), the Ten Thousand Talent Program of China (No. W02020595), and the Sichuan Science and Technology Program (Nos. 2019JDTD0011 and 15QNJJ0008).

REFERENCES

Black, C. J., Drossman, D. A., Talley, N. J., Ruddy, J., and Ford, A. C. (2020). Functional gastrointestinal disorders: advances in understanding and management. *Lancet* 396, 1664–1674. doi: 10.1016/s0140-6736(20)32115-32112

Chen, Y., Wang, R., Hou, B., Feng, F., Fang, X., Zhu, L., et al. (2018). Regional brain activity during rest and gastric water load in subtypes of functional dyspepsia: a preliminary brain functional magnetic resonance imaging study. *J. Neurogastroenterol. Motil.* 24, 268–279. doi: 10.5056/jnm17076

Dhond, R. P., Yeh, C., Park, K., Kettner, N., and Napadow, V. (2008). Acupuncture modulates resting state connectivity in default and sensorimotor brain networks. *Pain* 136, 407–418. doi: 10.1016/j.pain.2008.01.011

Drossman, D. A. (2016). Functional gastrointestinal disorders: history, pathophysiology, clinical features and Rome IV. *Gastroenterology*. doi: 10.1053/j.gastro.2016.02.032 [Epub ahead of print].

Enck, P., Azpiroz, F., Boeckxstaens, G., Elsenbruch, S., Feinle-Bisset, C., Holtmann, G., et al. (2017). Functional dyspepsia. *Nat. Rev. Dis. Primers* 3:17081. doi: 10.1038/nrdp.2017.81

Euston, D. R., Gruber, A. J., and McNaughton, B. L. (2012). The role of medial prefrontal cortex in memory and decision making. *Neuron* 76, 1057–1070. doi: 10.1016/j.neuron.2012.12.002

Ford, A. C., Mahadeva, S., Carbone, M. F., Lacy, B. E., and Talley, N. J. (2020). Functional dyspepsia. *Lancet* 396, 1689–1702. doi: 10.1016/s0140-6736(20)30469-30464

Hurley-Gius, K. M., and Neafsey, E. J. (1986). The medial frontal cortex and gastric motility: microstimulation results and their possible significance for the overall pattern of organization of rat frontal and parietal cortex. *Brain Res.* 365, 241–248. doi: 10.1016/0006-8993(86)91635-91635

Kano, M., Oudenhove, L. V., Dupont, P., Wager, T. D., and Fukudo, S. (2020). Imaging brain mechanisms of functional somatic syndromes: potential as a biomarker? *Tohoku J. Exp. Med.* 250, 137–152. doi: 10.1620/tjem.250.137

Lei, X., Zhao, Z., and Chen, H. (2013). Extraversion is encoded by scale-free dynamics of default mode network. *Neuroimage* 74, 52–57. doi: 10.1016/j.neuroimage.2013.02.020

Liu, P., Wang, G., Zeng, F., Liu, Y., Fan, Y., Wei, Y., et al. (2018). Abnormal brain structure implicated in patients with functional dyspepsia. *Brain Imaging Behav.* 12, 459–466. doi: 10.1007/s11682-017-9705-z

Liu, P., Zeng, F., Zhou, G., Wang, J., Wen, H., von Deneen, K. M., et al. (2013). Alterations of the default mode network in functional dyspepsia patients: a resting-state fmri study. *Neurogastroenterol. Motil.* 25, e382–e388. doi: 10.1111/nmo.12131

Liu, W., Yue, Q., Gong, Q., Zhou, D., and Wu, X. (2021). Regional and remote connectivity patterns in focal extratemporal lobe epilepsy. *Ann. Transl. Med.* 9:1128. doi: 10.21037/atm-21-1374

Ma, T., Zeng, F., Li, Y., Wang, C. M., Tian, X., Yu, S., et al. (2015). Which subtype of functional dyspepsia patients responses better to acupuncture? a retrospective analysis of a randomized controlled trial. *Forsch Komplementmed.* 22, 94–100. doi: 10.1159/000380983

Neafsey, E. J. (1990). Prefrontal cortical control of the autonomic nervous system: anatomical and physiological observations. *Prog. Brain Res.* 85, 147–165. doi: 10.1016/s0079-6123(08)62679-62675

Oh, J. H., Kwon, J. G., Jung, H. K., Tae, C. H., Song, K. H., Kang, S. J., et al. (2020). Clinical practice guidelines for functional dyspepsia in Korea. *J. Neurogastroenterol. Motil.* 26, 29–50. doi: 10.5056/jnm19209

Qi, R., Ke, J., Schoepf, U. J., Varga-Szemes, A., Milliken, C. M., Liu, C., et al. (2016). Topological reorganization of the default mode network in irritable bowel syndrome. *Mol. Neurobiol.* 53, 6585–6593. doi: 10.1007/s12035-015-9558-9557

Qi, R., Shi, Z., Weng, Y., Yang, Y., Zhou, Y., Surento, W., et al. (2020). Similarity and diversity of spontaneous brain activity in functional dyspepsia subtypes. *Acta Radiol.* 61, 927–935. doi: 10.1177/0284185119883391

Skrobisz, K., Piotrowicz, G., Naumczyk, P., Sabisz, A., Markiet, K., Rydzewska, G., et al. (2020). Imaging of morphological background in selected functional and inflammatory Gastrointestinal diseases in fMRI. *Front. Psychiatry* 11:461. doi: 10.3389/fpsyt.2020.00461

Sun, R., He, Z., Ma, P., Yin, S., Yin, T., Liu, X., et al. (2021). The participation of basolateral amygdala in the efficacy of acupuncture with deqi treating for functional dyspepsia. *Brain Imaging Behav.* 15, 216–230. doi: 10.1007/s11682-019-00249-247

Sun, R., Hong, X., Guo, J., Yin, S., Feng, P., Lan, L., et al. (2018). The central mechanism of acupuncture treatment with a long-lasting effect for functional dyspepsia: study protocol for a randomized controlled trial. *Trials* 19:373. doi: 10.1186/s13063-018-2742-2740

Thomann, A. K., Griebe, M., Thomann, P. A., Hirjak, D., Ebert, M. P., Szabo, K., et al. (2017). Intrinsic neural network dysfunction in quiescent Crohn's Disease. *Sci. Rep.* 7:11579. doi: 10.1038/s41598-017-11792-y

Wang, X. Y., Wang, H., Guan, Y. Y., Cai, R. L., and Shen, G. M. (2021). Acupuncture for functional gastrointestinal disorders: a systematic review and meta-analysis. *J. Gastroenterol. Hepatol.* 36, 3015–3026. doi: 10.1111/jgh.15645

Wang, Y., Hou, Y. Q., Yang, J. W., Wang, L. Q., Shao, J. K., Zou, X., et al. (2020). Acupuncture of different treatment frequency in postprandial distress syndrome: a pilot randomized clinical trial. *Neurogastroenterol. Motil.* 32:e13812. doi: 10.1111/nmo.13812

Yang, J. W., Wang, L. Q., Zou, X., Yan, S. Y., Wang, Y., Zhao, J. J., et al. (2020). Effect of acupuncture for postprandial distress syndrome: a randomized clinical trial. *Ann. Intern. Med.* 172, 777–785. doi: 10.7326/m19-2880

Yin, S., Chen, Y., Lei, D., Sun, R. R., Ma, T. T., Feng, P. M., et al. (2017). Cerebral mechanism of puncturing at He-Mu point combination for functional dyspepsia: study protocol for a randomized controlled parallel trial. *Neural Regen. Res.* 12, 831–840. doi: 10.4103/1673-5374.206655

Yin, T., He, Z., Ma, P., Sun, R., Xie, K., Liu, T., et al. (2021). Aberrant functional brain network dynamics in patients with functional constipation. *Hum. Brain Mapp.* 42, 5985–5999. doi: 10.1002/hbm.25663

Zeng, F., Lan, L., Tang, Y., Liu, M., Liu, X., Song, W., et al. (2015). Cerebral responses to puncturing at different acupoints for treating meal-related functional dyspepsia. *Neurogastroenterol. Motil.* 27, 559–568. doi: 10.1111/nmo.12532

Zeng, F., Qin, W., Liang, F., Liu, J., Tang, Y., Liu, X., et al. (2011). Abnormal resting brain activity in patients with functional dyspepsia is related to symptom severity. *Gastroenterology* 141, 499–506. doi: 10.1053/j.gastro.2011.05.003

Zeng, F., Qin, W., Yang, Y., Zhang, D., Liu, J., Zhou, G., et al. (2013). Regional brain structural abnormality in meal-related functional dyspepsia patients: a voxel-based morphometry study. *PLoS One* 8:e68383. doi: 10.1371/journal.pone.0068383

Zhao, D. Q., Gong, S. N., Ma, Y. J., and Zhu, J. P. (2019). Medial prefrontal cortex exacerbates gastric dysfunction of rats upon restraint water-immersion stress. *Mol. Med. Rep.* 20, 2303–2315. doi: 10.3892/mmr.2019.10462

Zhao, J. M., Lu, J. H., Yin, X. J., Wu, L. Y., Bao, C. H., Chen, X. K., et al. (2018). Comparison of electroacupuncture and mild-warm moxibustion on brain-gut function in patients with constipation-predominant irritable bowel syndrome: a randomized controlled trial. *Chin. J. Integr. Med.* 24, 328–335. doi: 10.1007/s11655-018-2838-2830

Conflict of Interest: The authors declare that the research was conducted in the absence of any commercial or financial relationships that could be construed as a potential conflict of interest.

Publisher's Note: All claims expressed in this article are solely those of the authors and do not necessarily represent those of their affiliated organizations, or those of the publisher, the editors and the reviewers. Any product that may be evaluated in this article, or claim that may be made by its manufacturer, is not guaranteed or endorsed by the publisher.

frontiers | Frontiers in Neuroscience

REVIEW
published: 25 April 2022
doi: 10.3389/fnins.2022.852506

A Reciprocal Link Between Gut Microbiota, Inflammation and Depression: A Place for Probiotics?

Ahmed Eltokhi[1]* *and Iris E. Sommer*[2]

[1] Department of Pharmacology, University of Washington, Seattle, WA, United States, [2] Department of Biomedical Sciences of Cells & Systems, University Medical Centre Groningen, University of Groningen, Groningen, Netherlands

Depression is a severe mental disorder that places a significant economic burden on public health. The reciprocal link between the trillions of bacteria in the gut, the microbiota, and depression is a controversial topic in neuroscience research and has drawn the attention of public interest and press coverage in recent years. Mounting pieces of evidence shed light on the role of the gut microbiota in depression, which is suggested to involve immune, endocrine, and neural pathways that are the main components of the microbiota-gut-brain axis. The gut microbiota play major roles in brain development and physiology and ultimately behavior. The bidirectional communication between the gut microbiota and brain function has been extensively explored in animal models of depression and clinical research in humans. Certain gut microbiota strains have been associated with the pathophysiology of depression. Therefore, oral intake of probiotics, the beneficial living bacteria and yeast, may represent a therapeutic approach for depression treatment. In this review, we summarize the findings describing the possible links between the gut microbiota and depression, focusing mainly on the inflammatory markers and sex hormones. By discussing preclinical and clinical studies on probiotics as a supplementary therapy for depression, we suggest that probiotics may be beneficial in alleviating depressive symptoms, possibly through immune modulation. Still, further comprehensive studies are required to draw a more solid conclusion regarding the efficacy of probiotics and their mechanisms of action.

Keywords: gut microbiota, inflammation, depression, sex hormones, probiotics

OPEN ACCESS

Edited by:
He Wang,
Fudan University, China

Reviewed by:
Amy Mackos,
The Ohio State University, United States
Valentina Caputi,
University College Cork, Ireland

***Correspondence:**
Ahmed Eltokhi
Eltokhi@uw.edu

Specialty section:
This article was submitted to Gut-Brain Axis, a section of the journal Frontiers in Neuroscience

Received: *11 January 2022*
Accepted: *18 March 2022*
Published: *25 April 2022*

Citation:
Eltokhi A and Sommer IE (2022) A Reciprocal Link Between Gut Microbiota, Inflammation and Depression: A Place for Probiotics? Front. Neurosci. 16:852506. doi: 10.3389/fnins.2022.852506

GUT MICROBIOTA IN HEALTH

The trillions of bacteria inhabiting our gastrointestinal (GI) tract are referred to as "gut microbiota" and are well known to exert a marked influence on the host during homeostasis (Thursby and Juge, 2017). Approximately 160 species of bacteria are living in the human colon, with *Bacteroidetes* and *Firmicutes* being the dominant bacterial phyla in healthy individuals (Qin et al., 2010; Huttenhower et al., 2012; Sommer and Backhed, 2013; Rajilic-Stojanovic and de Vos, 2014). The gut microbiota are separated from immune cells by two mucus layers and a single layer of epithelial cells (Johansson et al., 2013; Mowat and Agace, 2014), allowing the regulation of the immune system and vice versa (Round and Mazmanian, 2009; Gensollen et al., 2016). They benefit the host by strengthening the

gut integrity (Natividad and Verdu, 2013), providing nutrients such as vitamins (LeBlanc et al., 2013; Rowland et al., 2018), promoting resistance to colonization by pathogenic species (Cameron and Sperandio, 2015; Pacheco and Sperandio, 2015; Sassone-Corsi and Raffatellu, 2015; Baumler and Sperandio, 2016) and harvesting energy (den Besten et al., 2013). Therefore, a pathological alteration of the gut microbiota composition, known as dysbiosis, can have serious consequences on the health of the host, ranging from chronic GI diseases to neuropsychiatric disorders (Guinane and Cotter, 2013; Petersen and Round, 2014; Schroeder and Backhed, 2016).

The high-throughput and low-cost sequencing methods that have become available over the last decade enabled the investigation of the gut microbiota (Thursby and Juge, 2017). The bacterial species are nowadays easily distinguished *via* targeting the bacterial 16S ribosomal RNA gene that is present in all bacteria with enough sequence conservation and nine highly variable regions for phylogenetic analyses (Mizrahi-Man et al., 2013; Poretsky et al., 2014). To characterize the nature of the human microbiota and pave the way for a better understanding of human health and disease, the Human Microbiome Project (HMP) was carried out over 10 years and two phases (Turnbaugh et al., 2007; Proctor et al., 2019). Additionally, it can identify new diagnostic biomarkers of health, which will enhance our knowledge of the nutritional requirements of humans (Turnbaugh et al., 2007).

Different factors are known to shape the gut microbiota compositions including age (Odamaki et al., 2016; Hill et al., 2017; Aleman and Valenzano, 2019), host genetics (Kovacs et al., 2011; Org et al., 2016; Elderman et al., 2018; Kim et al., 2020), drugs (Wilson and Nicholson, 2009; Maier et al., 2018; Vich Vila et al., 2020), body mass index (BMI) (Ley et al., 2005; Yun et al., 2017; Gao et al., 2018; Stanislawski et al., 2018; Bai et al., 2019), diet, mode of delivery (Salminen et al., 2004; Rutayisire et al., 2016; Akagawa et al., 2019; Reyman et al., 2019), and environmental factors (Li et al., 2014; Osadchiy et al., 2019) (**Figure 1**). In particular, dietary modification exert a large effect on the gut microbiota (Walker et al., 2011; Zoetendal et al., 2012; David et al., 2014; Carmody et al., 2015) and can produce a shift in several bacterial species within 24 h (Wu et al., 2011). Also, antibiotics affect microbiota composition by depleting resident microbiota and subsequent enrichment of certain antibiotic-resistant strains, leading to pathogenic effects (Morgun et al., 2015). Other non-antibiotic drugs, such as proton-pump inhibitors, but also several psychiatric drugs, are known to have an extensive impact on the human gut microbiota (Maier et al., 2018).

MICROBIOTA DYSBIOSIS IN DEPRESSION

Depression is a debilitating neuropsychiatric disorder that involves persistent low mood and loss of interest that can be long-lasting or recurrent, substantially decreasing the quality of life (Wittchen et al., 2011; Lim et al., 2012; Murray et al., 2013; Whiteford et al., 2013). Symptoms usually are a reduced interest or pleasure in previously pleasurable activities, loss of sexual desire, changes in appetite, weight loss or gain, sleep disorders and motor retardation, along with recurrent thoughts of guilt and death (McCarter, 2008). It affects approximately 4.4% of the world's population with an incidence rate above the rate of global population growth (Flux and Lowry, 2020). Despite the high prevalence rate of depression and the ongoing efforts to enhance the skills of healthcare providers, this mental disorder remains underdiagnosed and undertreated (Williams et al., 2017). The late diagnosis and treatment of depression are associated with a reduced treatment outcome, underscoring the importance of early intervention (Riedel et al., 2011).

The development of depression involves a complex interplay of biological, genetic, and environmental factors (Lopizzo et al., 2015). In addition to the strong association between gut microbiota and autism, schizophrenia and attention deficit hyperactivity disorder (for a review, see Eltokhi et al., 2020), accumulating shreds of evidence over the past 10 years support the hypothesis that gut microbiota may determine the initial risk and persistence of depression and contribute to treatment and resilience (for reviews, see Mangiola et al., 2016; Rogers et al., 2016; Flux and Lowry, 2020). The gut microbiota can signal to the CNS by way of neurohormones, vagal tonus, immune activation and metabolites that can alter eating behavior and mood (Martin et al., 2018). Moreover, healthy diets such as the Mediterranean one are suggested to reduce the risk of depression (Sanchez-Villegas et al., 2007; Skarupski et al., 2013; Pagliai et al., 2018; Konstantinos and Evangelia, 2019; Lassale et al., 2019) *via* modulation of the gut microbiota composition (De Filippis et al., 2016; Garcia-Mantrana et al., 2018; Krznaric et al., 2019; Nagpal et al., 2019). Confirming the role of gut microbiota in depression, a large epidemiological study revealed that the destabilization of the gut microbiota composition by antibiotics resulted in a 20–50% increased risk of depression (Lurie et al., 2015). Moreover, the underrepresentation of *Firmicutes* in the gut has been associated with depression (Huang et al., 2018), and 25.8% of individuals with inflammatory bowel disease (IBD) suffered from depression in the previous year (Lai and Cai, 2018).

Preclinical studies on rodents have investigated the link between gut microbiota and depression at a deeper level than clinical studies (Flux and Lowry, 2020). Studies mostly from the microbiota-devoid germ-free mice or mice treated with broad-spectrum antibiotics have shown that specific microbiota can impact brain physiology and behavior including deficiencies in learning, memory, recognition, and emotional behaviors (Gareau et al., 2011; Smith, 2015; Foster et al., 2017), accompanied by structural changes in the brain (Zhang et al., 2015; Principi and Esposito, 2016; Dinan and Cryan, 2017; Fung et al., 2017; Martin and Mayer, 2017). Different rodent models that showed high face validity to human depression have been used in microbiota research (Krishnan and Nestler, 2011). These models include olfactory bulbectomy (Harkin et al., 2003), social stress models (Toyoda, 2017), maternal separation (MS) models of early life adversity (Matthews and Robbins, 2003; Neumann et al., 2005; O'Mahony et al., 2009), repeated restraint stress models (Glavin et al., 1994; Bailey et al., 2010), chronic unpredictable mild stress (Duan et al., 2021; Zhang et al., 2021), and diet-induced

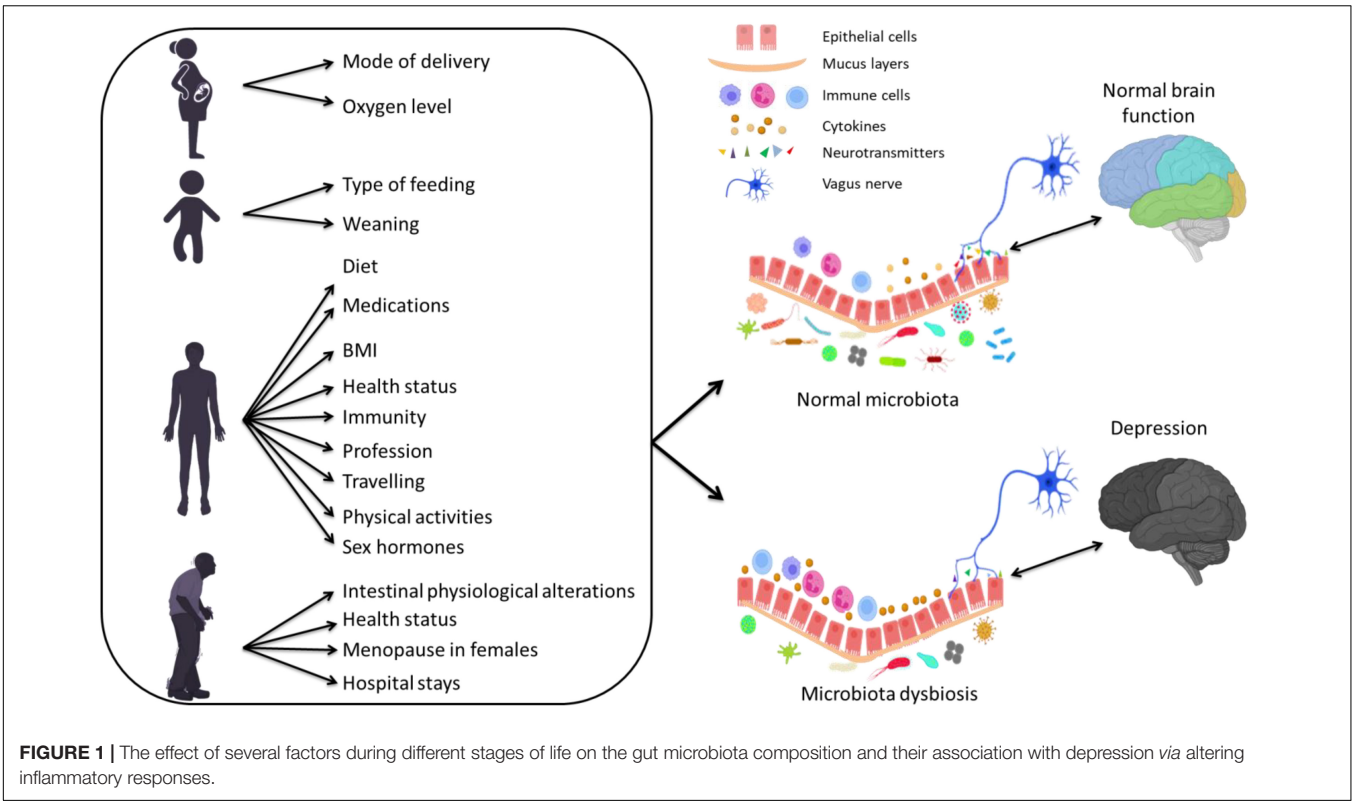

FIGURE 1 | The effect of several factors during different stages of life on the gut microbiota composition and their association with depression *via* altering inflammatory responses.

obesity (Bruce-Keller et al., 2015; Bridgewater et al., 2017; Agusti et al., 2018; Soto et al., 2018) (for a review, see Flux and Lowry, 2020). The depression-like behaviors in rodents are measured by several behavioral experiments including forced swim, tail-suspension, sucrose preference, splash and learned helplessness tests (Eltokhi et al., 2018). Confirming the link between gut microbiota and depression, stressed germ-free mice showed high circulating levels of depression-sustaining hormones such as ACTH and corticosterone (Sudo et al., 2004). Moreover, the transplantation of fecal matter from depressed patients into microbiota-depleted rats exhibited depressive-like behavior in the rats (Kelly et al., 2016).

Clinical evidence for the role of the microbiota in depression is provided by an alteration in the number of microbiota and their diversity in individuals with depression when compared to healthy controls (for a summary, see **Table 1**). A study of fecal samples from patients with major depressive disorder (MDD) documented increased counts of *Bacteroidales* and decreased counts of *Lachnospiraceae* (Naseribafrouei et al., 2014). The analysis of fecal matters from MDD patients revealed a negative, albeit weak, correlation between the abundance of *Faecalibacterium* and the severity of the depressive symptoms (Jiang et al., 2015), and a positive correlation between *Enterobacteriaceae* and *Alistipes* counts and depression (Jiang et al., 2015). In another clinical study, lower *Bifidobacterium* and/or *Lactobacillus* counts were more common in patients with MDD compared to healthy controls (Aizawa et al., 2016). Two other studies revealed a different abundance of bacterial families and taxa between patients with MDD and healthy controls (Chen Z. et al., 2018; Chung et al., 2019). Moreover, in a Chinese MDD cohort, alterations of microbiota composition were found in MDD patients with an overrepresentation of *Actinobacteria* and underrepresentation of *Bacteroidetes* (Zheng et al., 2016). Investigating a group suffering from treatment-resistant MDD revealed a link between microbiota neuroactive capacity and the quality of life and depression (Valles-Colomer et al., 2019). Similar gut microbiota dysbiosis between Irritable bowel syndrome (IBS), depression, and IBS/depression co-morbid patients confirms the close link between the gut microbiota composition and depression (Liu et al., 2016). Although several previous studies demonstrated that depression was linked to marked alterations in gut microbiota composition, contradicting results regarding the enrichment of certain microbiota phyla in individuals with depression were obtained (**Table 1**). This inconsistency may have resulted from differences in study design, sample sizes, demographic and clinical severity of patients, unmeasured confounding factors and/or the used statistical methods. Additionally, most of these studies had several limitations including small sample sizes and a lack of data on the dietary habits of the tested subjects, which hinders obtaining a solid conclusion about the suitability of the microbiota as a biomarker of depression. It is still unsure whether changes in the microbiota are a cause or a result of depression. As depression is associated with changes in dietary habits, sleep and stress, the gut microbiota dysbiosis may well be a consequence rather than a cause. On the other hand, the depressive phenotype was shown to be transmissible by fecal microbiota transplantation (FMT) from MDD patients to germ-free rodents, revealing increased

TABLE 1 | Clinical studies investigating a correlation between the human fecal microbiota and depression.

References	Sample	Sample size (patients/controls)	Mean age in years ± SD	Gender (males/females)	Changes in taxonomic composition in patients	Limitations/notes
Naseribafrouei et al., 2014	Fecal sample	55 Patients: 37 Controls: 18	Patients: 49.2 ± 13.9 Controls: 46.1 ± 13.9	Patients: (17/20) Controls: (7/11)	-High taxonomic level: ↑Bacteroidales ↓Lachnospiraceae -Low taxonomic level: ↑correlating OTUs of clades within the genus Alistipes and Oscillibacter	- A lack of data on the dietary habits of subjects - A small cohort with a risk of overseeing effects
Jiang et al., 2015	Fecal sample	76 Active-MDD: 29 Responded-MDD: 17 Controls: 30	Patients: Active-MDD: 25.3 ± 5.4 Responded-MDD: 27.1 ± 5.4 Controls: 26.8 ± 5.4	Patients: Active-MDD: (18/11) Responded-MDD: (9/8) Controls: (15/15)	-High taxonomic level: ↑Bacteroidete ↑Proteobacteria ↑Actinobacteria ↓Firmicutes -Low taxonomic level: ↑Enterobacteriaceae ↑Alistipes ↓Faecalibacterium	- A lack of data on the dietary habits of subjects - Possible effects of atypical antipsychotic medications - Further studies are required to evaluate the suitability of the microbiome as a biomarker.
Zheng et al., 2016	Fecal sample	121 Drug-naïve MDD: 39 Treated-MDD: 19 Controls: 63	Patients: 40.6 ± 11.7 Controls: 41.8 ± 12.3	Patients: (22/36) Controls: (23/40)	-High taxonomic level: ↑Actinobacteria ↓Bacteroidetes -Low taxonomic level: ↑OUTs assigned to the families Actinomycineae, Coriobacterineae, Lactobacillaceae, Streptococcaceae, Clostridiales incertae sedis XI (Parvimonas), Eubacteriaceae, Lachnospiraceae (Anaerostipes, Blautia, Dorea, Lachnospiracea incertae sedis), Ruminococcaceae (Clostridium IV) and Erysipelotrichaceae incertae sedis ↓OUTs assigned to the families Bacteroidaceae, Rikenellaceae (Alistipes), Lachnospiraceae (Coprococcus, Clostridium XIVa, Lachnospiraceae incertae sedis, Roseburia and Faecalibacterium), Acidaminococcaceae (Phascolarctobacterium), Veillonellaceae(Megamonas) and Sutterellaceae	- No examination of other neuropsychiatric disorders with similar clinical presentations to MDD - A possibility of site-specific and ethnic biases in microbial phenotypes
Aizawa et al., 2016	Fecal sample	100 Patients: 43 Controls: 57	Patients: 39.4 ± 10.0 Controls: 42.8 ± 12.7	Patients: (25/18) Controls: (22/35)	↓Bifidobacterium A tendency of ↓Lactobacillus	- Investigating only Bifidobacterium and Lactobacillus -Possible effects of antidepressant medications - Effects of diet were not fully taken into account in the analysis.

(Continued)

TABLE 1 | (Continued)

References	Sample	Sample size (patients/controls)	Mean age in years ± SD	Gender (males/females)	Changes in taxonomic composition in patients	Limitations/notes
Chen Z. et al., 2018	Fecal sample	20 Patients: 10 Controls: 10	Patients: 43.9 ± 13.8 Controls: 39.6 ± 9.0	Patients: (5/5) Controls: (5/5)	-High taxonomic level: ↑Firmicutes ↑Actinobacteria ↓Bacteroidetes ↓Proteobacteria -Low taxonomic level: ↑Lachnospiraceae ↑Actinomycetaceae ↑Nocardiaceae ↑Bifidobacteriaceae ↑Erysipelotrichaceae ↑Clostridiaceae ↑Ruminococcaceae ↑Porphyromonadaceae ↑Streptomycetaceae ↓Enterobacteriaceae ↓Sutterellaceae ↓Oscillospiraceae ↓Chitinophagaceae ↓Marinilabiliaceae ↓Rikenellaceae ↓Prevotellaceae	- A limited sample size - No detailed data on diet habits, alcohol intake, or residence - Possible effects of antidepressant medications
Chung et al., 2019	Fecal sample	73 Patients: 36 Controls: 37	Patients: 45.83 ± 14.08 Controls: 41.19 ± 12.73	Patients: (8/28) Controls: (14/23)	-High taxonomic level: ↑Actinobacteria ↑Firmicutes ↓Bacteroidetes ↓Proteobacteria -Low taxonomic level: ↑Peptostreptococcaceae ↑Porphyromonadaceae ↑Streptococcaceae ↑Bifidobacteriaceae ↑Lachnospiraceae ↓Prevotellaceae ↓Alcaligenaceae	- A cross-sectional study design with no causal inference between the microbiota alterations and depression - A moderate sample size that provided no stable results with cluster analysis to further discuss the impacts of dietary patterns on microbiota compositions - Possible effects of antidepressant medications -The dietary information was subjective to recall bias.

↑indicates an increase; ↓ indicates a decrease; MDD, Major depressive disorder; OTUs, Operational Taxonomic Units.

anxiety and depressive-like behavior in rodents (Kelly et al., 2016; Zheng et al., 2016). This strongly suggests that the alterations of the gut microbiota associated with depression may be a cause, rather than a consequence of the disorder.

Notably, several studies have shown that depression itself can affect the gut microbiota diversity *via* signals from the CNS to the gut environment, for example by changing secretion and motility in the stomach and gut. In an olfactory bulbectomy mouse model of depression, alteration of microbiota composition in the colon was suggested to be caused by increased activation of the stress response and alterations in colonic motility (Park et al., 2013). Moreover, diet disturbance in depression by the consumption of highly palatable foods is a major pathway from depression to gut microbiota dysbiosis (Rogers et al., 2016). Additionally, depression can reshape the gut microbiota composition by altering metabolic responses to food through hormones, inflammation, and autonomic alterations (Madison and Kiecolt-Glaser, 2019). For example, women suffering from depression had higher cortisol and fat oxidation levels (Kiecolt-Glaser et al., 2015), which can have a downstream effect on the gut microbiota (den Besten et al., 2013; Farzi et al., 2018). Other studies revealed that multiple classes of antidepressants also have anti-microbial properties against pathogenic bacteria (Macedo et al., 2017). For example, the antidepressant fluoxetine enriched the bacterial species associated with the regulation of BMI in mice (Lyte et al., 2019). The next-generation antidepressant ketamine plays a role in regulating the gut microbiota diversity (Yang et al., 2017) and showed increased *Lactobacillus*, *Turicibacter*, and *Sarcina* counts in the rat fecal microbiota and reduced opportunistic pathogens *Mucispirillum* and *Ruminococcus* (Getachew et al., 2018). To this end, the aforementioned studies suggest that the link between gut microbiota composition, antidepressants and depression is reciprocal.

THE EFFECT OF GUT MICROBIOTA ON LOCAL AND CIRCULATING INFLAMMATORY MARKERS AND ITS RELATION TO DEPRESSION

Depression has been associated with inflammation and its components such as inflammatory cytokines for more than 20 years (Ader and Cohen, 1985; Maes, 1995; Maes et al., 2012; Patel, 2013; Skaper et al., 2014; Miller and Raison, 2016; Leonard, 2018). Several gene variants are involved in both immune activation and depression (Barnes et al., 2017). Moreover, depression is known to be associated with polymorphisms in inflammation-related genes (Mikova et al., 2001; Kokai et al., 2002; Wong et al., 2008). Elevated levels of pro-inflammatory cytokines including Interleukin (IL)-1, IL-6, IL-8, and IL-12 were reported in individuals suffering from depression (Dowlati et al., 2010; Duivis et al., 2013; Lamers et al., 2013; Kim et al., 2016). Furthermore, IL-6, tumor necrosis factor-alpha (TNF-α), and IL-1β are implicated in the pathophysiology of depression (Brebner et al., 2000), and individuals with depression often have elevated circulating IL-1β, IL-6, and TNF with reduced levels of interferon-gamma (IFN-γ), IL-10, and IL-4 (Goldsmith et al., 2016). Longitudinal studies linked the high levels of pro-inflammatory cytokines with future risk for depression (van den Biggelaar et al., 2007; Gimeno et al., 2009). The pro-inflammatory cytokines have been connected to a pattern of sickness behaviors that include depressed mood, lethargy, heightened pain sensitivity, and sleep and appetite disturbances: all hallmarks of depression (Flux and Lowry, 2020). Moreover, non-specific inflammatory markers such as haptoglobin, fibrinogen, and C-reactive protein (CRP) are increased in depressed patients (Sluzewska et al., 1996).

Supporting the relationship between inflammation and depression, significant inflammatory activity in rodent models of depression has been identified (Song and Wang, 2011). Moreover, several antidepressants have been shown to reduce the endogenous production of pro-inflammatory cytokines along with a modification of immune reactivity in the CNS (Capuron et al., 2002; Nazimek et al., 2017; Gałecki et al., 2018). Tricyclic antidepressants inhibit the release of pro-inflammatory cytokines IL-6, IL-1β, and TNF-α (Xia et al., 1996). Additionally, the next-generation antidepressant ketamine has been shown to decrease depressive symptoms *via* a decrease in circulating IL-1β levels (Tan et al., 2017), a protein known to cause neuroinflammation and depressive behaviors (Dunn et al., 2005; Dunn, 2006; Swiergiel and Dunn, 2007; Ransohoff and Brown, 2012). Conversely, anti-inflammatory drugs have been shown to enhance recovery in patients with depression (Mendlewicz et al., 2006; Muller et al., 2006), and depressive symptoms are observed clinically with the administration of IFNs (Baranyi et al., 2013; Mahajan et al., 2014). IL-10 knockout mice displayed a decreased latency to immobility in a forced swim test as a measure of depression, which was rescued by the administration of IL-10 (Mesquita et al., 2008) that is known to inhibit pro-inflammatory cytokine production (Ledeboer et al., 2000). Recent evidence indicated that microbiota dysbiosis is associated with the development of several chronic inflammatory disorders such as IBD (Ni et al., 2017). Notably, several gut microbial taxa with differential abundance patterns common to immune-mediated inflammatory diseases were identified (Forbes et al., 2018). Several genera including *Lactobacillus*, *Bifidobacterium*, and *Faecalibacterium* have been shown to stimulate the anti-inflammatory cytokine including IL-10 (Sokol et al., 2008) and downregulate inflammatory cytokines (Llopis et al., 2009).

As the gut microbiota play a fundamental effect on the gut inflammatory and immune responses, it is highly likely that the role of gut microbiota dysbiosis in the pathophysiology of depression is induced by immune and inflammation responses (Slyepchenko et al., 2017). Evidence of increased bacterial translocation due to the disruption of tight junctions and barrier integrity of the GI tract has now surfaced in the pathogenesis of depression (Slyepchenko et al., 2017). The non-invasive bacterial translocation to the mesenteric lymph nodes, the lamina propria, and the peripheral blood results in immune activation and increased production of pro-inflammatory cytokines. Heightened IgA and IgM-mediated immune responses to lipopolysaccharide, a component of the cell walls of gram-negative bacteria, in MDD support the notion

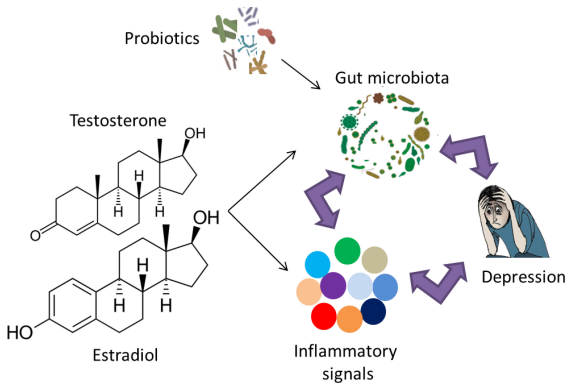

FIGURE 2 | The reciprocal link between gut microbiota, inflammation and depression. The role of probiotic supplementation in turning the gut microbiota composition into a healthier form may lead to normal brain function and alleviation of depressive symptoms *via* modulation of inflammatory responses. Examples of probiotic genera include *Lactobacillus*, *Bifidobacterium*, *Lactococcus*, *Propionibacterium*, *Bulgaricus*, and *Streptococcus*. Notably, sex hormones affect gut microbiota and/or inflammatory signals, which may play a role in the sex bias of depression.

of increased gut microbiota translocation due to a leaky gut (Maes et al., 2008).

Evidence from rodent experiments confirms the link between microbiota and depression *via* inflammatory markers. Socially stressed mice showing increased fecal Oscillospira and a decreased fecal Firmicutes/Bacteroidetes ratio developed depression-like symptoms (Zhang et al., 2017). These symptoms were rescued *via* an intravenous treatment with an anti-mouse IL-6 receptor antibody (MR16-1) that significantly decreased *Oscillospira* counts and attenuated the decrease in the fecal *Firmicutes/Bacteroidetes* ratio (Zhang et al., 2017). Genetic deletion or pharmacological inhibition of Caspase-1 that cleaves IL-1β and IL-18 into their mature isoforms exhibited reduced depression- and anxiety-like behaviors in a chronic restraint stress model, combined with an increase in *Akkermansia* species that is associated with decreased inflammation and a rebalancing of the gut microbiota (Alcocer-Gomez et al., 2014; Anhe et al., 2015; Yang et al., 2015). Recent work has targeted the effects of the inflammasome in studying the relationship between the immune system, gut microbiota and depression (Inserra et al., 2018). It was hypothesized that the increased NLRP3 signaling due to stress/depression can lead to an overrepresentation of pro-inflammatory bacterial clades within the gut microbiota (Inserra et al., 2018). This pathological change in the gut microbiota composition may even strengthen the stress/depression phenotype and increase the risk of other NLRP3-related co-morbid disorders. Notably, several pieces of evidence have shown that the link between microbiota, inflammation and depression is indeed reciprocal (**Figure 2**). Microbiota dysbiosis in inflammatory diseases such as IBS can lead to depression (Tribbick et al., 2015; Liu et al., 2016). Conversely, repeated stress and/or depression increases pro-inflammatory signaling (Rohleder, 2014), leading to microbiota dysbiosis and increased representation of pro-inflammatory bacterial clades (Rogers et al., 2016; Wong et al., 2016; Zheng et al., 2016).

INFLUENCE OF SEX HORMONES ON THE GUT MICROBIOTA COMPOSITION AND GENDER BIAS IN DEPRESSION

Depression is more frequent in women than men with a ratio of 2:1, which was reported globally and independent of race or ethnicity (Weissman and Klerman, 1977; Cyranowski et al., 2000; Andrade et al., 2003; Ford and Erlinger, 2004; Patten et al., 2006; Bromet et al., 2011; Salk et al., 2017). The finding of similar female: male prevalence ratios worldwide suggests that the differential risk is highly dependent on biological sex differences rather than race, culture or other potentially confounding social and economic factors (Albert, 2015). As the onset of depressive disorders in women peaks in their reproductive years, the increased prevalence of depression may be explained, in part, by sex hormones. Indeed, the female hormonal fluctuation during puberty, menstruation, pregnancy, and menopause is a trigger for depression (Albert, 2015). Estrogen and progesterone affect neurotransmitter, neuroendocrine, and circadian systems that have been implicated in mood disorders (Wharton et al., 2012). Androgens seem to have anxiolytic properties, whereas estrogen receptor activation has opposite consequences, with ERα having largely anxiogenic-like properties and ERβ serving to generate anxiolytic-like effects (Borrow and Handa, 2017). Furthermore, rates of depression in females correlate with the low levels of estrogen that occur throughout the life cycle (Albert et al., 2015). The risk of depression appears to increase during the perimenopausal transition (Cohen et al., 2006), with hormone replacement therapy being effective in the prevention of postmenopausal depression in women (Gordon and Girdler, 2014). In this light, a study has indicated that women who reported using an oral contraceptive showed reduced rates of MDD compared with non-users (Cheslack-Postava et al., 2015), suggesting a protective role of estrogen against depression. In contrast, other studies have shown depression and worsened mood as potential adverse effects of hormonal contraceptive use (Wiebe et al., 2011; Gingnell et al., 2013; Skovlund et al., 2016; de Wit et al., 2020). The heterogeneity in these findings may be explained by differences in study populations (de Wit et al., 2020).

Current evidence confirming the role of sex hormones on depression incidence relies mainly on rodent work. A recent study has explored the effect of treatment with a 5-α-reductase inhibitor that converts steroid hormones testosterone and progesterone into dihydrotestosterone and dihydroprogesterone, respectively on depression-like behavior in rats, as well as 1 month of treatment withdrawal (Diviccaro et al., 2019). The withdrawal from the 5-α-reductase inhibitor was associated with elevated depression-like symptoms, as measured by the forced swim test (Diviccaro et al., 2019). Interestingly, a change in sex hormone concentration is associated with an altered immune profile and a shift in inflammation responses (**Figure 2**; Kupelian et al., 2009; Casimir et al., 2010;

TABLE 2 | Clinical trials on probiotic supplementation in individuals with depression.

References	Sample size (INT/PL)	Mean age in years ± SD	Gender (males/females)	Study compound and duration	A change in INT group	Limitations/notes
Akkasheh et al., 2016	MDD: 40 INT: 20 PL: 20	INT: 38.30 ± 12.10 PL: 36.20 ± 8.20	INT: (3/17) PL: (3/17)	- The study was performed for 8 weeks. - INT received probiotic capsules daily and consisted of *Lactobacillus acidophilus* (2×10^9 CFU/g), *Lactobacillus casei* (2×10^9 CFU/g), and *Bifidobacterium bifidum* (2×10^9 CFU/g). - PL received capsules containing starch but no bacteria.	- ↓ BDI - ↓Serum insulin levels, homeostasis model assessment of insulin resistance, and serum hs-CRP concentrations - ↑Plasma total glutathione levels - No change in fasting plasma glucose, homeostatic model assessment of beta-cell function, quantitative insulin sensitivity check index, lipid profiles, or total antioxidant capacity levels	- No analysis of other biomarkers of inflammation or oxidative stress - A short intervention - Not knowing which strain in the probiotic supplements caused the treatment effect
Mohammadi et al., 2016	petrochemical workers: 70 INT 1: 25 INT 2: 25 PL: 20	INT 1: 33.20 ± 6.40 INT 2: 31.50 ± 5.80 PL: 33.10 ± 6.10	INT 1: (12/13) INT 2: (12/13) PL: (12/8)	- The study was performed for 6 weeks. - INT 1 received 100 g/day probiotic yogurt (*Lactobacillus acidophilus* LA5 and *Bifidobacterium lactis* BB12 with a total of min 1×10^7 CFU) + one placebo capsule. - INT 2 received one probiotic capsule daily (*Lactobacillus casei* 3×10^3, *Lactobacillus* acidophilus 3×10^7, *Lactobacillus rhamnosus* 7×10^9, *Lactobacillus bulgaricus* 5×10^8, *Bifidobacterium breve* 2×10^{10}, *Bifidobacterium longum* 1×10^9, *Streptococcus thermophilus* 3×10^8 CFU/g and 100 mg fructo-oligosaccharide with lactose as carrier substances) + 100 g/day conventional yogurt. - PL received 100 g/day conventional yogurt (*Streptococcus thermophilus* and *Lactobacillus bulgaricus*) + one placebo capsule (the same substance without bacteria).	- ↑GHQ in INT 1 and INT 2 - ↓DASS scores in INT 1 and INT 2 - No change of GHQ or DASS scores in PL	- A short intervention -No assessment of the rate that short-chain fatty acids were produced by probiotics in the gut

(Continued)

TABLE 2 | (Continued)

References	Sample size (INT/PL)	Mean age in years ± SD	Gender (males/females)	Study compound and duration	A change in INT group	Limitations/notes
Slykerman et al., 2017	Pregnant women of 14–16 weeks gestation: 423 INT: 212 PL: 211	INT: 33.50 ± 4.24 PL: 33.70 ± 4.44	Only females	- The study was performed until 6 months postpartum if breastfeeding. -INT received a daily *Lacticaseibacillus rhamnosus* HN001 at a dose of 6×10^9 CFU. -PL received a daily placebo (corn-derived maltodextrin).	- ↓Depression and anxiety scores in EPDS and STAI6 - ↓Clinically relevant anxiety on screening	- The EPDS and STAI6 are screening tools for postnatal depression and anxiety, but not diagnostic. -The information was collected retrospectively, and neither the EPDS nor the STAI6 has been validated using the questions phrased in the past tense.
Ghorbani et al., 2018	Individuals with moderate depression: 40 INT: 20 PL: 20	INT: 34.45 ± 3.95 PL: 35.50 ± 5.27	INT: (6/14) PL: (6/14)	- All Patients received fluoxetine (20 mg/d) for 4 weeks before and throughout the whole study. - The study was performed for 6 weeks. - INT received 2 capsules daily containing 500 mg probiotics (*Lactobacillus casei* 3×10^8 CFU/g, *Lactobacillus acidophilus* 2×10^8 CFU/g, *Lactobacillus bulgaricus* 2×10^9 CFU/g, *Lactobacillus rhamnosus* 3×10^8 CFU/g, *Bifidobacterium breve* 2×10^8 CFU/g, *Bifidobacterium longum,* 1×10^9 CFU/g, *Streptococcus thermophilus* 3×10^8 CFU/g) and 100 mg fructooligosaccharide as prebiotic. - PL received 2 placebo capsules daily containing 1,000 mg magnesium stearate.	- ↓HAM-D score at the endpoint of the intervention	- A short period of follow-up - A small number of participants
Majeed et al., 2018	MDD: 40 INT: 20 PL: 20	INT: 40.36 ± 10.28 PL: 43.88 ± 9.85	INT: (3/17) PL: (3/17)	- The study was performed for 90 days. - INT received a daily dose of 2×10^9 CFU *Bacillus coagulans* MTCC 5856 (600 mg) that contained also, microcrystalline cellulose, starch, sodium starch glycolate and magnesium stearate. -PL received placebo tablets that had the same ingredients except for *Bacillus coagulans* MTCC 5856.	- ↓HAM-D, MADRS, CES-D, IBS-QOL in INT - ↓CGI-I, CGI-S, Dementia – TFS, GI-DQ, mESS in INT - ↓ Serum myeloperoxidase in INT but not PL	- A short period of follow-up - A small number of participants

(Continued)

TABLE 2 | (Continued)

References	Sample size (INT/PL)	Mean age in years ± SD	Gender (males/females)	Study compound and duration	A change in INT group	Limitations/notes
Kazemi et al., 2019	MDD: 110 INT 1: 38 INT 2: 36 PL: 36	INT 1: 36.15 ± 7.85 INT 2: 37.35 ± 7.97 PL: 36.00 ± 8.47	INT 1: (11/27) INT 2: (9/27) PL: (12/24)	- The study was performed for 8 weeks. - INT 1 received probiotic product consisting of freeze-dried *Lactobacillus helveticus* R0052 and *Bifidobacterium longum* R0175 (CNCM strain I-3470) bacteria (10×10^9 CFU) per 5 g sachet + xylitol, maltodextrin, plum flavor and malic acid - INT 2 received a prebiotic product consisting of galactooligosaccharide and 0.2% Plum flavor - PL received a product consisting of xylitol, maltodextrin, plum flavor and malic acid.	- ↓BDI score in INT 1 compared to PL - ↓Kynurenine/tryptophan ratio compared to PL - ↑Tryptophan/isoleucine ratio compared to PL - No change of BDI score in INT 2 compared to PL - ↓Tryptophan/BCAAs ratio in INT 2 compared to PL	- 10 subjects from INT 1, 9 from INT 2 and 10 from PL dropped out before the trial completion - A lack of fecal microbiome analysis - The intervention was conducted at different times of the year - No control of changes in lifestyle, diet, vitamin D status, etc. - Different used antidepressant drugs
Wallace and Milev, 2021	MDD: 10 INT: 10	INT: 25.20 ± 7.00	INT: (3/7)	- The study was performed for 8 weeks. - INT received a probiotic supplement containing *Lactobacillus helveticus* R0052 and *Bifidobacterium longum* R0175 at a dose of 3×10^9 CFU once per day.	- ↓MADRS, QIDS-SR16 and SHAPS scores - ↓GAD-7 and STAI scores - ↑Sleep quality measured by PSQI	-A small number of participants - An open-label design and lack of placebo - A reduced generalizability of the results - The sample was disproportionately skewed toward young adult females.
Östlund-Lagerström et al., 2016	General older adults: 249 INT: 125 PL: 124	INT: 72.60 ± 5.80 PL: 72.00 ± 5.60	INT: (54/71) PL: (43/81)	-The study was performed for 12 weeks. -INT received a product consisting of a stick-pack containing freeze-dried *Lactobacillus reuteri* DSM 17938 (1×10^8 CFU/stick-pack), rhamnose, galactooligosaccharide and maltodextrin to a total weight of 1 g. -PL received a product consisting of maltodextrin.	- No change in GSRS, depression or anxiety scores - No change in the stress level (PSS scores) - No change in EQ-VAS or EQ-5D-index scores assessing the quality of life - No change in stool frequency	- A possibility that participants suffering from IBS were included in the study - An additional more fine-tuned instrument such as the ROME III symptom criteria, might have increased the sensitivity - The use of a low dose of *Lactobacillus reuteri* - The study was underpowered.
Romijn et al., 2017	Individuals with low mood: 79 INT: 40 PL: 39	INT: 35.80 ± 14.00 PL: 35.10 ± 14.50	INT: (8/32) PL: (9/30)	- The study was performed for 8 weeks. -INT received a product consisting of freeze-dried *Lactobacillus helveticus* R0052 and *Bifidobacterium longum* R0175 bacteria at a dosage of 3×10^9 CFU per 1.5 g sachet + xylitol, maltodextrin, plum flavor and malic acid. -PL received a product consisting of xylitol, maltodextrin, plum flavor and malic acid.	- No change in MADRS, CGI-S, CGI-I, QIDS-SR16, GAF, DASS - No difference in biomarker levels	- No measurement of BMI, body fat, dietary intake and physical activity -A lack of intestinal microbiome analysis -A small sample size - A short length of the intervention period

(Continued)

TABLE 2 | (Continued)

References	Sample size (INT/PL)	Mean age in years ± SD	Gender (males/females)	Study compound and duration	A change in INT group	Limitations/notes
Rudzki et al., 2019	MDD: 60 INT: 30 PL: 30	INT: 39.13 ± 9.96 PL: 38.90 ± 12.00	INT: (7/23) PL: (10/20)	- The study was performed for 8 weeks. -Both INT and PL received SSRI treatment during the whole study. - INT received 2 capsules daily with each containing 10×10^9 CFU of probiotic bacteria *Lactobacillus Plantarum* 299v. - PL received 2 capsules daily containing crystalline cellulose powder.	- No change in HAM-D 17, SCL-90 or PSS - Improvement of work speed in APT - Improvement of CVLT total recall -↓Kynurenine concentration -↑3HKYN:KYN ratio	-A small sample size - No measurements of intestinal permeability - No measurement of QUIN or vitamin B levels
Reininghaus et al., 2020	Inpatient MDD: 61 INT: 28 PL: 33	INT: 43.00 ± 14.31 PL: 40.11 ± 11.45	INT: (8/20) PL: (6/27)	- The study was performed for 4 weeks. -INT and PL received 125 mg D-Biotin. -INT received probiotics containing *Bifidobacterium bifidum* W23, *Bifidobacterium lactis* W51, *Bifidobacterium lactis* W52, *Lactobacillus acidophilus* W22, *Lacticaseibacillus casei* W56, *Lacticaseibacillus paracasei* W20, *Lactiplantibacillus plantarum* W62, *Lactobacillus salivarius* W24 and *Lactococcus lactis* W19 + 30 mg of common horsetail, 30 mg of fish collagen and 30 mg of keratin plus matrix -PL received a product containing 30 mg of common horsetail, 30 mg of fish collagen and 30 mg of keratin plus matrix.	- No difference between INT and PL in any of the psychiatric scales - No difference in intestinal barrier function -↑*Ruminococcus gauvreauii* in INT -↑Taxonomically related *Coprococcus*	- A short length of the intervention Period -The strong decrease in depression in both groups may have masked the difference between them - Changes in nutritional habits might have influenced the results. -A difference at baseline for smoking status between both groups - The high number of females may have skewed the results.

The clinical studies of Östlund-Lagerström et al. (2016), Romijn et al. (2017), Rudzki et al. (2019), Reininghaus et al. (2020) did not reveal a significant improvement in the depression phenotype. INT, Intervention; PL, Placebo; CFU, Colony-forming units, SSRI, Selective serotonin reuptake inhibitor; BDI, Beck Depression Inventory; GHQ, General health questionnaire; DASS, Depression anxiety and stress scale; EPDS, Edinburgh Postnatal Depression Scale; STAI6, State Trait Anxiety Inventory 6 item version; HAM-D, Hamilton rating scale for depression; MADRS, Montgomery–Asberg Depression Rating Scale; CES-D, Center for Epidemiological Studies Depression Scale; IBS-QOL, Irritable Bowel Syndrome Quality of Life Questionnaire; CGI-I, Clinical Global Impression-Improvement rating Scale; CGI-S, Clinical Global Impression Severity Rating Scale; Dementia – TFS, Dementia – Total frequency scoring; GI-DQ, Gastrointestinal Discomfort Questionnaire; mESS, Modified Epworth Sleepiness Scale; QIDS-SR16, Quick Inventory of Depressive Symptomatology; SHAPS, Snaith-Hamilton Pleasure Scale; GAD-7, Generalized Anxiety Disorder 7-item scale; STAI, State Trait Anxiety Inventory; PSQI, Pittsburgh Sleep Quality Index; GSRS, Gastrointestinal symptoms rating scale; PSS, Perceived stress scale; GAF, Global Assessment of Functioning; SCL-90, Symptom Checklist; APT, Attention and Perceptivity Test; CVLT, California Verbal Learning Test.

Karim et al., 2010; Maggio et al., 2011; Bobjer et al., 2013; Park and Lee, 2020; Grandys et al., 2021) (for reviews, see Monteiro et al., 2014; Au et al., 2016; Mohamad et al., 2018; Slavich and Sacher, 2019). The alteration of inflammatory responses due to sex hormones suggests their combined role in the pathophysiology of depression.

Although gut microbiota differed in males and females, castrated male mice showed similar microbiota composition to females, suggesting an influence of androgens on the gut microbiota composition (Markle et al., 2013; Yurkovetskiy et al., 2013). Moreover, testosterone treatment after gonadectomy rescued the alteration in the gut microbiota composition that was observed in the untreated males (Org et al., 2016). Several studies have shown a direct effect of estrogen on the gut microbiota composition (Flores et al., 2012; Cox-York et al., 2015; Chen and Madak-Erdogan, 2016; Org et al., 2016). Treatment with a 5-α-reductase inhibitor was associated with increased *Bacteroidetes* and *Prevotellaceae* counts, and the withdrawal was associated with a reduction in the family *Ruminococcaceae* and the genera *Oscillospira* and *Lachnospira* (Diviccaro et al., 2019). Interestingly, there seems to be a reciprocal interaction between gut microbiota and sex hormones leading to a change in the level of sex hormones because of differences in gut microbiota (Markle et al., 2013) and that gut microbiota regulate the production and/or utilization of testosterone and cause a difference in metabolism (Colldén et al., 2019).

Several studies have addressed the effects of sex on the gut microbiota in humans, which is suggested to be mediated, at least in part, by a difference in sex hormones levels (**Figure 2**; Mueller et al., 2006; Li et al., 2008; Ding and Schloss, 2014; Dominianni et al., 2015; Haro et al., 2016; Singh and Manning, 2016; Borgo et al., 2018; Gao et al., 2018; Sinha et al., 2019; Takagi et al., 2019) (for a recent review, see Kim et al., 2020). The sex differences in the gut microbiota composition mediated by sex hormones may exert adverse inflammatory and psychological effects related to depression and other neuropsychiatric disorders (Yurkovetskiy et al., 2013). For instance, adult women have reduced *Bacteroidetes* counts in their gut compared to age-matched men (Dominianni et al., 2015). Interestingly, the low levels of Bacteroidetes were previously observed in the fecal microbiota from patients diagnosed with clinical depression (Naseribafrouei et al., 2014). A study in a Chinese cohort revealed increased *Actinobacteria* levels in female MDD patients compared to female controls but reduced *Bacteroidetes* levels in male MDD patients compared to male controls (Chen J. J. et al., 2018).

In summary, the sex differences in the gut microbiota composition due to the effect of sex hormones may play a role in the sex bias of depression.

PROBIOTICS AS AN ADJUNCTIVE THERAPEUTIC OPTION FOR DEPRESSION

Given the strong association between the gut microbiota and the pathophysiology of depression, modulation of the gut microbiota composition can be a promising method for ameliorating the behavioral symptoms related to depression along with other neuropsychiatric disorders (Larroya-Garcia et al., 2019). One way for maintaining a healthy gut microbiota composition is mediated by the supplementation of probiotics; the consumable microbes intended to promote a healthy microbiota and can provide a benefit to the host when administered in adequate amounts (Butel, 2014) (**Figure 2**). The main bacterial genera used as probiotics in preclinical and clinical studies are the *Lactobacillus* and *Bifidobacterium* genera (Genedi et al., 2019). Studies involving animal models demonstrated that probiotics improved cognition, mood, anxiety, and stress (Sudo et al., 2004; Desbonnet et al., 2010; Bravo et al., 2011; Ait-Belgnaoui et al., 2014; Smith et al., 2014; Mohle et al., 2016; Bruce-Keller et al., 2018; Chunchai et al., 2018; Hadizadeh et al., 2019). Probiotics have also been studied in non-psychiatric individuals, and initial work showed improvements in cognitive function (Marotta et al., 2019) along with reducing constipation in different populations (Chmielewska and Szajewska, 2010; Miller and Ouwehand, 2013; Dimidi et al., 2014). Probiotic supplementation showed an enhancement in sleep, autonomic balance, and bowel habits and reduced stress and cortisol levels in Japanese medical students (Nishida et al., 2017). Moreover, healthy women who drank a probiotic-containing fermented milk product for 1 month showed lower brain activation when exposed to emotional stimuli (Tillisch et al., 2013). In a randomized controlled trial in healthy individuals, multispecies probiotics were able to reduce cognitive reactivity toward sad moods *via* a reduction in rumination and aggressive thoughts (Steenbergen et al., 2015). The *Lactobacillus helveticus* and *Bifidobacterium longum* probiotic mix given to healthy individuals for 1 month alleviated psychological distress compared to a control group, similar to the results seen in rats (Messaoudi et al., 2011). Moreover, the healthy individuals in the bottom third on the depressed/elated dimension reported improved mood after drinking probiotic-containing milk for 3 weeks (Benton et al., 2007).

The desire for a more effective treatment and a prevention of depression seems perpetually at the top of the list in terms of global health concerns to reduce the burden of this condition. The idea of treating depression with probiotics roots back to 1910 when Dr. George Porter Phillips reported that a gelatin-whey formula comprised of lactic-acid-producing bacteria decreased depressive symptoms in melancholic adults (Phillips, 1910). Preclinical studies and clinical trials have increasingly investigated the roles of probiotics in the treatment of depressive-like behaviors. In rodents, there is considerable evidence suggesting the effect of probiotics in decreasing the depression-like behaviors. *Lactobacillus rhamnosus* administration reduced stress-induced anxiety- and depressive-like behaviors in mice (Bravo et al., 2011). *Bifidobacterium longum* improved the depressive-like phenotype during the tail suspension test in a mouse model of heightened anxiety (Savignac et al., 2014). Likewise, daily *Lactobacillus helveticus NS8* treatment reduced anxiety- and depressive-like behavioral dysfunctions in adult specific-pathogen-free rats facing chronic restraint stress in comparison to a selective serotonin reuptake inhibitor (SSRI) treatment (Liang et al., 2015). In a chronic mild stress

model of depression, mice receiving a three-strain probiotic blend, *Lactobacillus helveticus*, *Lactobacillus plantarum*, and *Bifidobacterium longum*, displayed improved depression-like behavioral responses accompanied by a reduced TNF-α and interferon (IFN)-γ levels (Li et al., 2018). In another study, the administration of *Faecalibacterium prausnitzii via* oral gavage for 4 weeks in a chronic unpredictable mild stress model in rats resulted in decreased depression-like behaviors accompanied by increased IL-10 and decreased IL-6 and CRP levels (Hao et al., 2019). In another study, an administration of a probiotic formulation containing *Lactobacillus plantarum*, *Lactobacillus rhamnosus*, *Bifidobacterium lactis*, *Bifidobacterium breve*, and *Pediococcus pentosaceus* alleviated depressive-like behaviors in mice and decreased corticosterone level by restoring the gut microbiota composition (Liu et al., 2020). In Fischer and Long Evans rats subjected to maternal deprivation, a probiotic mixture composed of *Lactobacillus helveticus*, *Bifidobacterium longum*, *Lactococcus lactis*, and *Streptococcus thermophilus* reduced anxiety- and depression-like behaviors accompanied by a change in the levels of certain metabolites (Daugé et al., 2020).

Clinical studies revealed contradicting results regarding the efficiency of probiotics in decreasing depressive symptoms (for a summary, see **Table 2**). In an 8-week, randomized, double-blind, placebo-controlled clinical trial, a triple-strain probiotic mix, *Lactobacillus acidophilus*, *Lactobacillus casei*, and *Bifidobacterium bifidum*, resulted in improvements in depression scores in BDI in an MDD cohort (Akkasheh et al., 2016). Additionally, other beneficial metabolic effects were revealed including a significant reduction in inflammatory markers such as serum insulin, homeostasis model assessment of insulin resistance and serum hs-CRP (Akkasheh et al., 2016). Another 8-week, randomized, double-blind, placebo-controlled clinical trial examining the effect of a probiotic mix of *Lactobacillus helveticus* and *Bifidobacterium longum* on mild to moderate MDD reported a decrease in depression score in BDI (Kazemi et al., 2019). Interestingly, a randomized, placebo-controlled, double-blind study reported that daily *Lactobacillus rhamnosus* during pregnancy and into the post-partum period significantly decreased postnatal anxiety and depression scores (Slykerman et al., 2017). Another study testing the add-on effect of probiotic and prebiotic, the non-digestible plant-based carbohydrates that serve as nutrition for resident bacteria, on fluoxetine revealed a decrease in the score of hamilton rating scale for depression (HAM-D) compared to the placebo after 6 weeks of treatment (Ghorbani et al., 2018). One study provided petrochemical workers with either a probiotic capsule, probiotic yogurt, or conventional yogurt control, with both probiotic conditions resulting in a reduction of depressive symptoms on the general health questionnaire (GHQ) and depression anxiety and stress scale (DASS) scores as compared to control (Mohammadi et al., 2016). In another study, the efficacy of *Bacillus coagulans* administration on MDD in IBS patients was tested and revealed an improvement in HAM-D, Montgomery-Asberg Depression Rating Scale (MADRS), Center for Epidemiological Studies Depression Scale (CES-D) as well as reduced serum myeloperoxidase, an inflammatory biomarker (Majeed et al., 2018). In a recent open-label pilot study, a probiotic supplement containing *Lactobacillus helveticus* and *Bifidobacterium longum* administrated once per day for 8 weeks showed an improvement in affective clinical symptoms after 4 weeks, which was sustained till the end of the study (Wallace and Milev, 2021).

Other studies in the literature failed to show any improvement of depression scores in MADRS following 8 weeks of primary treatment with probiotics mix of *Lactobacillus helveticus* and *Bifidobacterium longum* (Romijn et al., 2017). Moreover, there was no change in psychological symptoms and the concentrations of CRP, IL-1β, IL-6, or TNF between baseline and the end of the study (Romijn et al., 2017). Worth notice is that individuals in this study were not taking any antidepressant medication at the time of the study, and their depressive history was entirely self-reported without a formal diagnostic interview (Romijn et al., 2017). In another study of individuals diagnosed with MDD, SSRI treatment supplemented with *Lactobacillus plantarum* did not exhibit any improvement in depressive symptoms and did not change the levels of circulating TNF, IL-6, or IL-1β, although there was an increase in cognitive functioning (Rudzki et al., 2019). In another study, the health properties of *Lactobacillus reuteri* DSM17938 were investigated in individuals older than 65 and revealed no improvement in digestive health, general wellbeing, stress, anxiety, or depression (Östlund-Lagerström et al., 2016). In a randomized clinical study in 2020, a combination of 9 bacterial species *Bifidobacterium bifidum* W23, *Bifidobacterium lactis* W51, *Bifidobacterium lactis* W52, *Lactobacillus acidophilus* W22, *Lactobacillus casei* W56, *Lactobacillus paracasei* W20, *Lactobacillus plantarum* W62, *Lactobacillus salivarius* W24, and *Lactobacillus lactis* W19 in addition to biotin yielded no improvement in psychiatric symptoms in patients with MDD (Reininghaus et al., 2020).

CONCLUSION

Gut microbiota were incorporated into neurobiological models of depression *via* an effect on immune, endocrine, and nervous system responses, allowing a more comprehensive model of depression (**Figure 2**). The strong association between microbiota dysbiosis and depression could pave the way for enhancing diagnostic accuracy and patient phenotyping for treatment selection. Moreover, it can advance the treatment and prevention of depression by modifying the gut microbiota composition and offer an important future strategy in psychiatry *via* nutritional interventions, prebiotic or probiotic supplementations. Although preclinical mechanistic experimental data indicated that the manipulation of the gut microbiota with probiotics may have antidepressant and anxiolytic effects, there is limited clinical evidence for the efficacy of probiotics in depression at present. Notably, several probiotic studies that failed to show an improvement in depression revealed also no change in pro-inflammatory markers. Given the reciprocal link

between microbiota, inflammation and depression discussed in this review, we believe that probiotics may partially exert their roles through a modification of the immune system. Generally, additional randomized clinical trials in patients with depression are necessary to fully evaluate their therapeutic potential on the clinical diagnosis and inflammatory biomarkers. Different factors should be kept into consideration to maximize the benefit of probiotic supplementation. The microbial diversity obtained by incorporating multiple strains of organisms is suggested to be more effective than using a single organism. Investigations at a finer taxonomic level coupled with multi-omic techniques such as transcriptomics, proteomics, and metabolomics are also needed to exclude confounding factors as much as possible. Since sex hormones can affect the inflammation biomarkers, with probiotics causing different inflammatory responses in female and male mice (Karunasena et al., 2014; Lee et al., 2017), sex should be taken into account in studies on gut microbiota, probiotics and depression.

AUTHOR CONTRIBUTIONS

AE conceptualized and wrote the first draft. IES edited and reviewed the final draft. Both authors contributed to the article and approved the submitted version.

FUNDING

AE is partially supported by a postdoc stipend from the Fritz Thyssen Foundation. IES has received funding from the Stanley Medical Foundation.

ACKNOWLEDGMENTS

AE sincerely appreciates the continuous support from Shaimaa Madbouly and Rolf Sprengel.

REFERENCES

Ader, R., and Cohen, N. (1985). High time for psychoimmunology. *Nature* 315, 103–104. doi: 10.1038/315103b0

Agusti, A., Moya-Pérez, A., Campillo, I., Montserrat-De La Paz, S., Cerrudo, V., et al. (2018). Bifidobacterium pseudocatenulatum CECT 7765 ameliorates neuroendocrine alterations associated with an exaggerated stress response and anhedonia in obese mice. *Mol. Neurobiol.* 55, 5337–5352. doi: 10.1007/s12035-017-0768-z

Ait-Belgnaoui, A., Colom, A., Braniste, V., Ramalho, L., Marrot, A., Cartier, C., et al. (2014). Probiotic gut effect prevents the chronic psychological stress-induced brain activity abnormality in mice. *Neurogastroenterol. Motil.* 26, 510–520. doi: 10.1111/nmo.12295

Aizawa, E., Tsuji, H., Asahara, T., Takahashi, T., Teraishi, T., Yoshida, S., et al. (2016). Possible association of Bifidobacterium and Lactobacillus in the gut microbiota of patients with major depressive disorder. *J. Affect. Disord.* 202, 254–257. doi: 10.1016/j.jad.2016.05.038

Akagawa, S., Tsuji, S., Onuma, C., Akagawa, Y., Yamaguchi, T., Yamagishi, M., et al. (2019). Effect of delivery mode and nutrition on gut microbiota in neonates. *Ann. Nutr. Metab.* 74, 132–139. doi: 10.1159/000496427

Akkasheh, G., Kashani-Poor, Z., Tajabadi-Ebrahimi, M., Jafari, P., Akbari, H., Taghizadeh, M., et al. (2016). Clinical and metabolic response to probiotic administration in patients with major depressive disorder: a randomized, double-blind, placebo-controlled trial. *Nutrition* 32, 315–320. doi: 10.1016/j.nut.2015.09.003

Albert, K., Pruessner, J., and Newhouse, P. (2015). Estradiol levels modulate brain activity and negative responses to psychosocial stress across the menstrual cycle. *Psychoneuroendocrinology* 59, 14–24. doi: 10.1016/j.psyneuen.2015.04.022

Albert, P. R. (2015). Why is depression more prevalent in women? *J. Psychiatry Neurosci.* 40, 219–221. doi: 10.1503/jpn.150205

Alcocer-Gomez, E., De Miguel, M., Casas-Barquero, N., Nunez-Vasco, J., Sanchez-Alcazar, J. A., Fernandez-Rodriguez, A., et al. (2014). NLRP3 inflammasome is activated in mononuclear blood cells from patients with major depressive disorder. *Brain Behav. Immun.* 36, 111–117. doi: 10.1016/j.bbi.2013.10.017

Aleman, F. D. D., and Valenzano, D. R. (2019). Microbiome evolution during host aging. *PLoS Pathog.* 15:e1007727. doi: 10.1371/journal.ppat.1007727

Andrade, L., Caraveo-Anduaga, J. J., Berglund, P., Bijl, R. V., De Graaf, R., Vollebergh, W., et al. (2003). The epidemiology of major depressive episodes: results from the International Consortium of Psychiatric Epidemiology (ICPE) Surveys. *Int. J. Methods Psychiatr. Res.* 12, 3–21. doi: 10.1002/mpr.138

Anhe, F. F., Roy, D., Pilon, G., Dudonne, S., Matamoros, S., Varin, T. V., et al. (2015). A polyphenol-rich cranberry extract protects from diet-induced obesity, insulin resistance and intestinal inflammation in association with increased Akkermansia spp. population in the gut microbiota of mice. *Gut* 64, 872–883. doi: 10.1136/gutjnl-2014-307142

Au, A., Feher, A., Mcphee, L., Jessa, A., Oh, S., and Einstein, G. (2016). Estrogens, inflammation and cognition. *Front. Neuroendocrinol.* 40, 87–100. doi: 10.1016/j.yfrne.2016.01.002

Bai, J., Hu, Y., and Bruner, D. W. (2019). Composition of gut microbiota and its association with body mass index and lifestyle factors in a cohort of 7-18 years old children from the American Gut Project. *Pediatr. Obes.* 14:e12480. doi: 10.1111/ijpo.12480

Bailey, M. T., Dowd, S. E., Parry, N. M. A., Galley, J. D., Schauer, D. B., and Lyte, M. (2010). Stressor exposure disrupts commensal microbial populations in the intestines and leads to increased colonization by Citrobacter rodentium. *Infect. Immun.* 78, 1509–1519. doi: 10.1128/IAI.00862-09

Baranyi, A., Meinitzer, A., Stepan, A., Putz-Bankuti, C., Breitenecker, R. J., Stauber, R., et al. (2013). A biopsychosocial model of interferon-alpha-induced depression in patients with chronic hepatitis C infection. *Psychother. Psychosom.* 82, 332–340. doi: 10.1159/000348587

Barnes, J., Mondelli, V., and Pariante, C. M. (2017). Genetic contributions of inflammation to depression. *Neuropsychopharmacology* 42, 81–98. doi: 10.1038/npp.2016.169

Baumler, A. J., and Sperandio, V. (2016). Interactions between the microbiota and pathogenic bacteria in the gut. *Nature* 535, 85–93. doi: 10.1038/nature18849

Benton, D., Williams, C., and Brown, A. (2007). Impact of consuming a milk drink containing a probiotic on mood and cognition. *Eur. J. Clin. Nutr.* 61, 355–361. doi: 10.1038/sj.ejcn.1602546

Bobjer, J., Katrinaki, M., Tsatsanis, C., Lundberg Giwercman, Y., and Giwercman, A. (2013). Negative association between testosterone concentration and inflammatory markers in young men: a nested cross-sectional study. *PLoS One* 8:e61466. doi: 10.1371/journal.pone.0061466

Borgo, F., Garbossa, S., Riva, A., Severgnini, M., Luigiano, C., Benetti, A., et al. (2018). Body mass index and sex affect diverse microbial niches within the gut. *Front. Microbiol.* 9:213. doi: 10.3389/fmicb.2018.00213

Borrow, A. P., and Handa, R. J. (2017). Estrogen receptors modulation of anxiety-like behavior. *Vitam. Horm.* 103, 27–52. doi: 10.1016/bs.vh.2016.08.004

Bravo, J. A., Forsythe, P., Chew, M. V., Escaravage, E., Savignac, H. M., Dinan, T. G., et al. (2011). Ingestion of Lactobacillus strain regulates emotional behavior and central GABA receptor expression in a mouse via the vagus nerve. *Proc. Natl. Acad. Sci. U.S.A.* 108, 16050. doi: 10.1073/pnas.1102999108

Brebner, K., Hayley, S., Zacharko, R., Merali, Z., and Anisman, H. (2000). Synergistic effects of interleukin-1beta, interleukin-6, and tumor necrosis factor-alpha: central monoamine, corticosterone, and behavioral variations. *Neuropsychopharmacology* 22, 566–580. doi: 10.1016/S0893-133X(99)00166-9

Bridgewater, L. C., Zhang, C., Wu, Y., Hu, W., Zhang, Q., Wang, J., et al. (2017). Gender-based differences in host behavior and gut microbiota composition

in response to high fat diet and stress in a mouse model. *Sci. Rep.* 7:10776. doi: 10.1038/s41598-017-11069-4

Bromet, E., Andrade, L. H., Hwang, I., Sampson, N. A., Alonso, J., De Girolamo, G., et al. (2011). Cross-national epidemiology of DSM-IV major depressive episode. *BMC Med.* 9:90. doi: 10.1186/1741-7015-9-90

Bruce-Keller, A. J., Salbaum, J. M., and Berthoud, H. R. (2018). Harnessing gut microbes for mental health: getting from here to there. *Biol. Psychiatry* 83, 214–223. doi: 10.1016/j.biopsych.2017.08.014

Bruce-Keller, A. J., Salbaum, J. M., Luo, M., Blanchard, E. I. V., Taylor, C. M., Welsh, D. A., et al. (2015). Obese-type gut microbiota induce neurobehavioral changes in the absence of obesity. *Biol. Psychiatry* 77, 607–615. doi: 10.1016/j.biopsych.2014.07.012

Butel, M. J. (2014). Probiotics, gut microbiota and health. *Med. Mal. Infect.* 44, 1–8. doi: 10.1016/j.medmal.2013.10.002

Cameron, E. A., and Sperandio, V. (2015). Frenemies: signaling and nutritional integration in pathogen-microbiota-host interactions. *Cell Host Microbe* 18, 275–284. doi: 10.1016/j.chom.2015.08.007

Capuron, L., Hauser, P., Hinze-Selch, D., Miller, A. H., and Neveu, P. J. (2002). Treatment of cytokine-induced depression. *Brain Behav. Immun.* 16, 575–580. doi: 10.1016/s0889-1591(02)00007-7

Carmody, R. N., Gerber, G. K., Luevano, J. M., Gatti, D. M., Somes, L., Svenson, K. L., et al. (2015). Diet dominates host genotype in shaping the murine gut microbiota. *Cell Host Microbe* 17, 72–84. doi: 10.1016/j.chom.2014.11.010

Casimir, G. J., Mulier, S., Hanssens, L., Zylberberg, K., and Duchateau, J. (2010). Gender differences in inflammatory markers in children. *Shock* 33, 258–262. doi: 10.1097/SHK.0b013e3181b2b36b

Chen, Z., Li, J., Gui, S., Zhou, C., Chen, J., Yang, C., et al. (2018). Comparative metaproteomics analysis shows altered fecal microbiota signatures in patients with major depressive disorder. *Neuroreport* 29, 417–425. doi: 10.1097/WNR.0000000000000985

Chen, J. J., Zheng, P., Liu, Y. Y., Zhong, X. G., Wang, H. Y., Guo, Y. J., et al. (2018). Sex differences in gut microbiota in patients with major depressive disorder. *Neuropsychiatr. Dis. Treat.* 14, 647–655. doi: 10.2147/NDT.S159322

Chen, K. L., and Madak-Erdogan, Z. (2016). Estrogen and microbiota crosstalk: Should we pay attention? *Trends Endocrinol. Metab.* 27, 752–755. doi: 10.1016/j.tem.2016.08.001

Cheslack-Postava, K., Keyes, K. M., Lowe, S. R., and Koenen, K. C. (2015). Oral contraceptive use and psychiatric disorders in a nationally representative sample of women. *Arch. Womens Ment. Health* 18, 103–111. doi: 10.1007/s00737-014-0453-4

Chmielewska, A., and Szajewska, H. (2010). Systematic review of randomised controlled trials: probiotics for functional constipation. *World J. Gastroenterol.* 16, 69–75. doi: 10.3748/wjg.v16.i1.69

Chunchai, T., Thunapong, W., Yasom, S., Wanchai, K., Eaimworawuthikul, S., Metzler, G., et al. (2018). Decreased microglial activation through gut-brain axis by prebiotics, probiotics, or synbiotics effectively restored cognitive function in obese-insulin resistant rats. *J. Neuroinflammation* 15:11. doi: 10.1186/s12974-018-1055-2

Chung, Y. E., Chen, H. C., Chou, H. L., Chen, I. M., Lee, M. S., Chuang, L. C., et al. (2019). Exploration of microbiota targets for major depressive disorder and mood related traits. *J. Psychiatr. Res.* 111, 74–82. doi: 10.1016/j.jpsychires.2019.01.016

Cohen, L. S., Soares, C. N., Vitonis, A. F., Otto, M. W., and Harlow, B. L. (2006). Risk for new onset of depression during the menopausal transition: the Harvard study of moods and cycles. *Arch. Gen. Psychiatry* 63, 385–390. doi: 10.1001/archpsyc.63.4.385

Colldén, H., Landin, A., Wallenius, V., Elebring, E., Fändriks, L., Nilsson, M. E., et al. (2019). The gut microbiota is a major regulator of androgen metabolism in intestinal contents. *Am. J. Physiol. Endocrinol. Metab.* 317, E1182–E1192. doi: 10.1152/ajpendo.00338.2019

Cox-York, K. A., Sheflin, A. M., Foster, M. T., Gentile, C. L., Kahl, A., Koch, L. G., et al. (2015). Ovariectomy results in differential shifts in gut microbiota in low versus high aerobic capacity rats. *Physiol. Rep.* 3:e12488. doi: 10.14814/phy2.12488

Cyranowski, J. M., Frank, E., Young, E., and Shear, M. K. (2000). Adolescent onset of the gender difference in lifetime rates of major depression: a theoretical model. *Arch. Gen. Psychiatry* 57, 21–27. doi: 10.1001/archpsyc.57.1.21

Daugé, V., Philippe, C., Mariadassou, M., Rué, O., Martin, J.-C., Rossignol, M.-N., et al. (2020). A probiotic mixture induces anxiolytic- and antidepressive-like effects in fischer and maternally deprived long evans rats. *Front. Behav. Neurosci.* 14:581296. doi: 10.3389/fnbeh.2020.581296

David, L. A., Maurice, C. F., Carmody, R. N., Gootenberg, D. B., Button, J. E., Wolfe, B. E., et al. (2014). Diet rapidly and reproducibly alters the human gut microbiome. *Nature* 505, 559–563. doi: 10.1038/nature12820

De Filippis, F., Pellegrini, N., Vannini, L., Jeffery, I. B., La Storia, A., Laghi, L., et al. (2016). High-level adherence to a Mediterranean diet beneficially impacts the gut microbiota and associated metabolome. *Gut* 65, 1812–1821. doi: 10.1136/gutjnl-2015-309957

de Wit, A. E., Booij, S. H., Giltay, E. J., Joffe, H., Schoevers, R. A., and Oldehinkel, A. J. (2020). Association of use of oral contraceptives with depressive symptoms among adolescents and young women. *JAMA Psychiatry* 77, 52–59. doi: 10.1001/jamapsychiatry.2019.2838

den Besten, G., Van Eunen, K., Groen, A. K., Venema, K., Reijngoud, D. J., and Bakker, B. M. (2013). The role of short-chain fatty acids in the interplay between diet, gut microbiota, and host energy metabolism. *J. Lipid Res.* 54, 2325–2340. doi: 10.1194/jlr.R036012

Desbonnet, L., Garrett, L., Clarke, G., Kiely, B., Cryan, J. F., and Dinan, T. G. (2010). Effects of the probiotic Bifidobacterium infantis in the maternal separation model of depression. *Neuroscience* 170, 1179–1188. doi: 10.1016/j.neuroscience.2010.08.005

Dimidi, E., Christodoulides, S., Fragkos, K. C., Scott, S. M., and Whelan, K. (2014). The effect of probiotics on functional constipation in adults: a systematic review and meta-analysis of randomized controlled trials. *Am. J. Clin. Nutr.* 100, 1075–1084. doi: 10.3945/ajcn.114.089151

Dinan, T. G., and Cryan, J. F. (2017). Gut instincts: microbiota as a key regulator of brain development, ageing and neurodegeneration. *J. Physiol.* 595, 489–503. doi: 10.1113/JP273106

Ding, T., and Schloss, P. D. (2014). Dynamics and associations of microbial community types across the human body. *Nature* 509, 357–360. doi: 10.1038/nature13178

Diviccaro, S., Giatti, S., Borgo, F., Barcella, M., Borghi, E., Trejo, J. L., et al. (2019). Treatment of male rats with finasteride, an inhibitor of 5alpha-reductase enzyme, induces long-lasting effects on depressive-like behavior, hippocampal neurogenesis, neuroinflammation and gut microbiota composition. *Psychoneuroendocrinology* 99, 206–215. doi: 10.1016/j.psyneuen.2018.09.021

Dominianni, C., Sinha, R., Goedert, J. J., Pei, Z., Yang, L., Hayes, R. B., et al. (2015). Sex, body mass index, and dietary fiber intake influence the human gut microbiome. *PLoS One* 10:e0124599. doi: 10.1371/journal.pone.0124599

Dowlati, Y., Herrmann, N., Swardfager, W., Liu, H., Sham, L., Reim, E. K., et al. (2010). A meta-analysis of cytokines in major depression. *Biol. Psychiatry* 67, 446–457. doi: 10.1016/j.biopsych.2009.09.033

Duan, J., Huang, Y., Tan, X., Chai, T., Wu, J., Zhang, H., et al. (2021). Characterization of gut microbiome in mice model of depression with divergent response to escitalopram treatment. *Transl. Psychiatry* 11:303. doi: 10.1038/s41398-021-01428-1

Duivis, H. E., Vogelzangs, N., Kupper, N., De Jonge, P., and Penninx, B. W. (2013). Differential association of somatic and cognitive symptoms of depression and anxiety with inflammation: findings from the Netherlands Study of Depression and Anxiety (NESDA). *Psychoneuroendocrinology* 38, 1573–1585. doi: 10.1016/j.psyneuen.2013.01.002

Dunn, A. J. (2006). Effects of cytokines and infections on brain neurochemistry. *Clin. Neurosci. Res.* 6, 52–68. doi: 10.1016/j.cnr.2006.04.002

Dunn, A. J., Swiergiel, A. H., and Beaurepaire, R. D. (2005). Cytokines as mediators of depression: What can we learn from animal studies? *Neurosci. Biobehav. Rev.* 29, 891–909. doi: 10.1016/j.neubiorev.2005.03.023

Elderman, M., Hugenholtz, F., Belzer, C., Boekschoten, M., Van Beek, A., De Haan, B., et al. (2018). Sex and strain dependent differences in mucosal immunology and microbiota composition in mice. *Biol. Sex Differ.* 9:26. doi: 10.1186/s13293-018-0186-6

Eltokhi, A., Janmaat, I. E., Genedi, M., Haarman, B. C. M., and Sommer, I. E. C. (2020). Dysregulation of synaptic pruning as a possible link between intestinal microbiota dysbiosis and neuropsychiatric disorders. *J. Neurosci. Res.* 98, 1335–1369. doi: 10.1002/jnr.24616

Eltokhi, A., Rappold, G., and Sprengel, R. (2018). Distinct phenotypes of *Shank2* mouse models reflect neuropsychiatric spectrum disorders of human patients with *SHANK2* Variants. *Front. Mol. Neurosci.* 11:240. doi: 10.3389/fnmol.2018.00240

Farzi, A., Fröhlich, E. E., and Holzer, P. (2018). Gut Microbiota and the neuroendocrine system. *Neurotherapeutics* 15, 5–22. doi: 10.1007/s13311-017-0600-5

Flores, R., Shi, J., Fuhrman, B., Xu, X., Veenstra, T. D., Gail, M. H., et al. (2012). Fecal microbial determinants of fecal and systemic estrogens and estrogen metabolites: a cross-sectional study. *J. Transl. Med.* 10:253. doi: 10.1186/1479-5876-10-253

Flux, M. C., and Lowry, C. A. (2020). Finding intestinal fortitude: integrating the microbiome into a holistic view of depression mechanisms, treatment, and resilience. *Neurobiol. Dis.* 135, 104578. doi: 10.1016/j.nbd.2019.104578

Forbes, J. D., Chen, C.-Y., Knox, N. C., Marrie, R.-A., El-Gabalawy, H., De Kievit, T., et al. (2018). A comparative study of the gut microbiota in immune-mediated inflammatory diseases—does a common dysbiosis exist? *Microbiome* 6:221. doi: 10.1186/s40168-018-0603-4

Ford, D. E., and Erlinger, T. P. (2004). Depression and C-reactive protein in US adults: data from the Third National Health and Nutrition Examination Survey. *Arch. Intern. Med.* 164, 1010–1014. doi: 10.1001/archinte.164.9.1010

Foster, J. A., Rinaman, L., and Cryan, J. F. (2017). Stress & the gut-brain axis: regulation by the microbiome. *Neurobiol. Stress* 7, 124–136.

Fung, T. C., Olson, C. A., and Hsiao, E. Y. (2017). Interactions between the microbiota, immune and nervous systems in health and disease. *Nat. Neurosci.* 20, 145–155. doi: 10.1038/nn.4476

Gałecki, P., Mossakowska-Wójcik, J., and Talarowska, M. (2018). The anti-inflammatory mechanism of antidepressants – SSRIs, SNRIs. *Prog. Neuropsychopharmacol. Biol. Psychiatry* 80, 291–294. doi: 10.1016/j.pnpbp.2017.03.016

Gao, X., Zhang, M., Xue, J., Huang, J., Zhuang, R., Zhou, X., et al. (2018). Body mass index differences in the gut microbiota are gender specific. *Front. Microbiol.* 9:1250. doi: 10.3389/fmicb.2018.01250

Garcia-Mantrana, I., Selma-Royo, M., Alcantara, C., and Collado, M. C. (2018). Shifts on gut microbiota associated to mediterranean diet adherence and specific dietary intakes on general adult population. *Front. Microbiol.* 9:890. doi: 10.3389/fmicb.2018.00890

Gareau, M. G., Wine, E., Rodrigues, D. M., Cho, J. H., Whary, M. T., Philpott, D. J., et al. (2011). Bacterial infection causes stress-induced memory dysfunction in mice. *Gut* 60, 307–317. doi: 10.1136/gut.2009.202515

Genedi, M., Janmaat, I. E., Haarman, B., and Sommer, I. E. C. (2019). Dysregulation of the gut-brain axis in schizophrenia and bipolar disorder: probiotic supplementation as a supportive treatment in psychiatric disorders. *Curr. Opin. Psychiatry* 32, 185–195. doi: 10.1097/YCO.0000000000000499

Gensollen, T., Iyer, S. S., Kasper, D. L., and Blumberg, R. S. (2016). How colonization by microbiota in early life shapes the immune system. *Science* 352, 539–544. doi: 10.1126/science.aad9378

Getachew, B., Aubee, J. I., Schottenfeld, R. S., Csoka, A. B., Thompson, K. M., and Tizabi, Y. (2018). Ketamine interactions with gut-microbiota in rats: relevance to its antidepressant and anti-inflammatory properties. *BMC Microbiol.* 18:222. doi: 10.1186/s12866-018-1373-7

Ghorbani, Z., Nazari, S., Etesam, F., Nourimajd, S., Ahmadpanah, M., and Razeghi Jahromi, S. (2018). The Effect of synbiotic as an adjuvant therapy to fluoxetine in moderate depression: a randomized multicenter trial. *Arch. Neurosci.* 5:e60507.

Gimeno, D., Kivimaki, M., Brunner, E. J., Elovainio, M., De Vogli, R., Steptoe, A., et al. (2009). Associations of C-reactive protein and interleukin-6 with cognitive symptoms of depression: 12-year follow-up of the Whitehall II study. *Psychol. Med.* 39, 413–423. doi: 10.1017/S0033291708003723

Gingnell, M., Engman, J., Frick, A., Moby, L., Wikström, J., Fredrikson, M., et al. (2013). Oral contraceptive use changes brain activity and mood in women with previous negative affect on the pill–a double-blinded, placebo-controlled randomized trial of a levonorgestrel-containing combined oral contraceptive. *Psychoneuroendocrinology* 38, 1133–1144. doi: 10.1016/j.psyneuen.2012.11.006

Glavin, G. B., Paré, W. P., Sandbak, T., Bakke, H.-K., and Murison, R. (1994). Restraint stress in biomedical research: An update. *Neurosci. Biobehav. Rev.* 18, 223–249. doi: 10.1016/0149-7634(94)90027-2

Goldsmith, D. R., Rapaport, M. H., and Miller, B. J. (2016). A meta-analysis of blood cytokine network alterations in psychiatric patients: comparisons between schizophrenia, bipolar disorder and depression. *Mol. Psychiatry* 21, 1696–1709. doi: 10.1038/mp.2016.3

Gordon, J. L., and Girdler, S. S. (2014). Hormone replacement therapy in the treatment of perimenopausal depression. *Curr. Psychiatry Rep.* 16:517. doi: 10.1007/s11920-014-0517-1

Grandys, M., Majerczak, J., Zapart-Bukowska, J., Duda, K., Kulpa, J. K., and Zoladz, J. A. (2021). Lowered serum testosterone concentration is associated with enhanced inflammation and worsened lipid profile in men. *Front. Endocrinol.* 12:735638. doi: 10.3389/fendo.2021.735638

Guinane, C. M., and Cotter, P. D. (2013). Role of the gut microbiota in health and chronic gastrointestinal disease: understanding a hidden metabolic organ. *Therap. Adv. Gastroenterol.* 6, 295–308. doi: 10.1177/1756283X13482996

Hadizadeh, M., Hamidi, G. A., and Salami, M. (2019). Probiotic supplementation improves the cognitive function and the anxiety-like behaviors in the stressed rats. *Iran. J. Basic Med. Sci.* 22, 506–514. doi: 10.22038/ijbms.2019.33956.8078

Hao, Z., Wang, W., Guo, R., and Liu, H. (2019). Faecalibacterium prausnitzii (ATCC 27766) has preventive and therapeutic effects on chronic unpredictable mild stress-induced depression-like and anxiety-like behavior in rats. *Psychoneuroendocrinology* 104, 132–142. doi: 10.1016/j.psyneuen.2019.02.025

Harkin, A., Kelly, J., and Leonard, B. (2003). A revew of the relevance and validity of olfactory bulbectomy as a model of depression. *Clin. Neurosci. Res.* 3, 253–262. doi: 10.1016/s1566-2772(03)00087-2

Haro, C., Rangel-Zuniga, O. A., Alcala-Diaz, J. F., Gomez-Delgado, F., Perez-Martinez, P., Delgado-Lista, J., et al. (2016). Intestinal Microbiota Is Influenced by Gender and Body Mass Index. *PLoS One* 11:e0154090. doi: 10.1371/journal.pone.0154090

Hill, C. J., Lynch, D. B., Murphy, K., Ulaszewska, M., Jeffery, I. B., O'shea, C. A., et al. (2017). Evolution of gut microbiota composition from birth to 24 weeks in the INFANTMET Cohort. *Microbiome* 5:4.

Huang, Y., Shi, X., Li, Z., Shen, Y., Shi, X., Wang, L., et al. (2018). Possible association of Firmicutes in the gut microbiota of patients with major depressive disorder. *Neuropsychiatr. Dis. Treat.* 14, 3329–3337. doi: 10.2147/NDT.S188340

Huttenhower, C., Gevers, D., Knight, R., Abubucker, S., Badger, J. H., Chinwalla, A. T., et al. (2012). Structure, function and diversity of the healthy human microbiome. *Nature* 486, 207–214. doi: 10.1038/nature11234

Inserra, A., Rogers, G. B., Licinio, J., and Wong, M.-L. (2018). The Microbiota-inflammasome hypothesis of major depression. *Bioessays* 40:1800027. doi: 10.1002/bies.201800027

Jiang, H., Ling, Z., Zhang, Y., Mao, H., Ma, Z., Yin, Y., et al. (2015). Altered fecal microbiota composition in patients with major depressive disorder. *Brain Behav. Immun.* 48, 186–194. doi: 10.1016/j.bbi.2015.03.016

Johansson, M. E., Sjövall, H., and Hansson, G. C. (2013). The gastrointestinal mucus system in health and disease. *Nat. Rev. Gastroenterol. Hepatol.* 10, 352–361. doi: 10.1038/nrgastro.2013.35

Karim, R., Stanczyk, F., Hodis, H., Cushman, M., Lobo, R., Hwang, J., et al. (2010). Associations between markers of inflammation and physiological and pharmacological levels of circulating sex hormones in postmenopausal women. *Menopause* 17, 785–790. doi: 10.1097/gme.0b013e3181cc50b2

Karunasena, E., Mcmahon, K. W., Chang, D., and Brashears, M. M. (2014). Host responses to the pathogen *Mycobacterium avium* subsp. paratuberculosis and beneficial microbes exhibit host sex specificity. *Appl. Environ. Microbiol.* 80, 4481–4490. doi: 10.1128/AEM.01229-14

Kazemi, A., Noorbala, A. A., Azam, K., Eskandari, M. H., and Djafarian, K. (2019). Effect of probiotic and prebiotic vs placebo on psychological outcomes in patients with major depressive disorder: a randomized clinical trial. *Clin. Nutr.* 38, 522–528. doi: 10.1016/j.clnu.2018.04.010

Kelly, J. R., Borre, Y., O' Brien, C., Patterson, E., El Aidy, S., Deane, J., et al. (2016). Transferring the blues: Depression-associated gut microbiota induces neurobehavioural changes in the rat. *J. Psychiatr. Res* .82, 109–118. doi: 10.1016/j.jpsychires.2016.07.019

Kiecolt-Glaser, J. K., Habash, D. L., Fagundes, C. P., Andridge, R., Peng, J., Malarkey, W. B., et al. (2015). Daily stressors, past depression, and metabolic responses to high-fat meals: a novel path to obesity. *Biol. Psychiatry* 77, 653–660. doi: 10.1016/j.biopsych.2014.05.018

Kim, Y. K., Na, K. S., Myint, A. M., and Leonard, B. E. (2016). The role of pro-inflammatory cytokines in neuroinflammation, neurogenesis and the neuroendocrine system in major depression. *Prog. Neuropsychopharmacol. Biol. Psychiatry* 64, 277–284. doi: 10.1016/j.pnpbp.2015.06.008

Kim, Y. S., Unno, T., Kim, B. Y., and Park, M. S. (2020). Sex differences in gut microbiota. *World J. Mens Health* 38, 48–60.

Kokai, M., Kashiwamura, S., Okamura, H., Ohara, K., and Morita, Y. (2002). Plasma interleukin-18 levels in patients with psychiatric disorders. *J. Immunother.* 25(Suppl. 1), S68–S71. doi: 10.1097/00002371-200203001-00011

Konstantinos, A., and Evangelia, M. (2019). Adherence to Mediterranean diet and risk of depression later in life. A cross sectional study in East Attica, Greece. *Glob. Psychiatry* 2, 201–209. doi: 10.2478/gp-2019-0012

Kovacs, A., Ben-Jacob, N., Tayem, H., Halperin, E., Iraqi, F. A., and Gophna, U. (2011). Genotype is a stronger determinant than sex of the mouse gut microbiota. *Microb. Ecol.* 61, 423–428. doi: 10.1007/s00248-010-9787-2

Krishnan, V., and Nestler, E. J. (2011). Animal models of depression: molecular perspectives. *Curr. Top. Behav. Neurosci.* 7, 121–147. doi: 10.1007/7854_2010_108

Krznaric, Z., Vranesic Bender, D., and Mestrovic, T. (2019). The Mediterranean diet and its association with selected gut bacteria. *Curr. Opin. Clin. Nutr. Metab. Care* 22, 401–406. doi: 10.1097/MCO.0000000000000587

Kupelian, V., Chiu, G., Araujo, A., Williams, R., Clark, R., and Mckinlay, J. (2009). Association of sex hormones and C-reactive protein levels in men. *Clin. Endocrinol.* 72, 527–533. doi: 10.1111/j.1365-2265.2009.03713.x

Lai, W., and Cai, S. (2018). Comment on "Prevalence of Anxiety and Depression in Patients with Inflammatory Bowel Disease". *Can. J. Gastroenterol. Hepatol.* 2018, 6747630–6747630. doi: 10.1155/2018/6747630

Lamers, F., Vogelzangs, N., Merikangas, K. R., De Jonge, P., Beekman, A. T., and Penninx, B. W. (2013). Evidence for a differential role of HPA-axis function, inflammation and metabolic syndrome in melancholic versus atypical depression. *Mol. Psychiatry* 18, 692–699. doi: 10.1038/mp.2012.144

Larroya-Garcia, A., Navas-Carrillo, D., and Orenes-Pinero, E. (2019). Impact of gut microbiota on neurological diseases: diet composition and novel treatments. *Crit. Rev. Food Sci. Nutr.* 59, 3102–3116. doi: 10.1080/10408398.2018.1484340

Lassale, C., Batty, G. D., Baghdadli, A., Jacka, F., Sánchez-Villegas, A., Kivimäki, M., et al. (2019). Healthy dietary indices and risk of depressive outcomes: a systematic review and meta-analysis of observational studies. *Mol. Psychiatry* 24, 965–986. doi: 10.1038/s41380-018-0237-8

LeBlanc, J. G., Milani, C., De Giori, G. S., Sesma, F., Van Sinderen, D., and Ventura, M. (2013). Bacteria as vitamin suppliers to their host: a gut microbiota perspective. *Curr. Opin. Biotechnol.* 24, 160–168. doi: 10.1016/j.copbio.2012.08.005

Ledeboer, A., Breve, J. J., Poole, S., Tilders, F. J., and Van Dam, A. M. (2000). Interleukin-10, interleukin-4, and transforming growth factor-beta differentially regulate lipopolysaccharide-induced production of pro-inflammatory cytokines and nitric oxide in co-cultures of rat astroglial and microglial cells. *Glia* 30, 134–142. doi: 10.1002/(sici)1098-1136(200004)30:2<134::aid-glia3>3.0.co;2-3

Lee, J. Y., Kim, N., Nam, R. H., Sohn, S. H., Lee, S. M., Choi, D., et al. (2017). Probiotics reduce repeated water avoidance stress-induced colonic microinflammation in Wistar rats in a sex-specific manner. *PLoS One* 12:e0188992. doi: 10.1371/journal.pone.0188992

Leonard, B. E. (2018). Inflammation and depression: a causal or coincidental link to the pathophysiology? *Acta Neuropsychiatr.* 30, 1–16. doi: 10.1017/neu.2016.69

Ley, R. E., Backhed, F., Turnbaugh, P., Lozupone, C. A., Knight, R. D., and Gordon, J. I. (2005). Obesity alters gut microbial ecology. *Proc. Natl. Acad. Sci. U.S.A.* 102, 11070–11075. doi: 10.1073/pnas.0504978102

Li, J., Jia, H., Cai, X., Zhong, H., Feng, Q., Sunagawa, S., et al. (2014). An integrated catalog of reference genes in the human gut microbiome. *Nat. Biotechnol.* 32, 834–841. doi: 10.1038/nbt.2942

Li, M., Wang, B., Zhang, M., Rantalainen, M., Wang, S., Zhou, H., et al. (2008). Symbiotic gut microbes modulate human metabolic phenotypes. *Proc. Natl. Acad. Sci. U.S.A.* 105, 2117–2122. doi: 10.1073/pnas.0712038105

Li, N., Wang, Q., Wang, Y., Sun, A., Lin, Y., Jin, Y., et al. (2018). Oral probiotics ameliorate the behavioral deficits induced by chronic mild stress in mice via the gut microbiota-inflammation axis. *Front. Behav. Neurosci.* 12:266. doi: 10.3389/fnbeh.2018.00266

Liang, S., Wang, T., Hu, X., Luo, J., Li, W., Wu, X., et al. (2015). Administration of Lactobacillus helveticus NS8 improves behavioral, cognitive, and biochemical aberrations caused by chronic restraint stress. *Neuroscience* 310, 561–577. doi: 10.1016/j.neuroscience.2015.09.033

Lim, S. S., Vos, T., Flaxman, A. D., Danaei, G., Shibuya, K., Adair-Rohani, H., et al. (2012). A comparative risk assessment of burden of disease and injury attributable to 67 risk factors and risk factor clusters in 21 regions, 1990-2010: a systematic analysis for the Global Burden of Disease Study 2010. *Lancet* 380, 2224–2260. doi: 10.1016/S0140-6736(12)61766-8

Liu, Q. F., Kim, H. M., Lim, S., Chung, M. J., Lim, C. Y., Koo, B. S., et al. (2020). Effect of probiotic administration on gut microbiota and depressive behaviors in mice. *Daru* 28, 181–189. doi: 10.1007/s40199-020-00329-w

Liu, Y., Zhang, L., Wang, X., Wang, Z., Zhang, J., Jiang, R., et al. (2016). Similar fecal microbiota signatures in patients with diarrhea-predominant irritable bowel syndrome and patients with depression. *Clin. Gastroenterol. Hepatol.* 14, 1602–1611.e5. doi: 10.1016/j.cgh.2016.05.033

Llopis, M., Antolin, M., Carol, M., Borruel, N., Casellas, F., Martinez, C., et al. (2009). *Lactobacillus casei* downregulates commensals' inflammatory signals in Crohn's disease mucosa. *Inflamm. Bowel Dis.* 15, 275–283. doi: 10.1002/ibd.20736

Lopizzo, N., Bocchio Chiavetto, L., Cattane, N., Plazzotta, G., Tarazi, F. I., Pariante, C. M., et al. (2015). Gene-environment interaction in major depression: focus on experience-dependent biological systems. *Front. Psychiatry* 6:68. doi: 10.3389/fpsyt.2015.00068

Lurie, I., Yang, Y. X., Haynes, K., Mamtani, R., and Boursi, B. (2015). Antibiotic exposure and the risk for depression, anxiety, or psychosis: a nested case-control study. *J. Clin. Psychiatry* 76, 1522–1528. doi: 10.4088/JCP.15m09961

Lyte, M., Daniels, K. M., and Schmitz-Esser, S. (2019). Fluoxetine-induced alteration of murine gut microbial community structure: evidence for a microbial endocrinology-based mechanism of action responsible for fluoxetine-induced side effects. *PeerJ* 7:e6199. doi: 10.7717/peerj.6199

Macedo, D., Filho, A. J. M. C., Soares, De Sousa, C. N., Quevedo, J., Barichello, T., et al. (2017). Antidepressants, antimicrobials or both? Gut microbiota dysbiosis in depression and possible implications of the antimicrobial effects of antidepressant drugs for antidepressant effectiveness. *J. Affect. Disord.* 208, 22–32. doi: 10.1016/j.jad.2016.09.012

Madison, A., and Kiecolt-Glaser, J. K. (2019). Stress, depression, diet, and the gut microbiota: human–bacteria interactions at the core of psychoneuroimmunology and nutrition. *Curr. Opin. Behav. Sci.* 28, 105–110. doi: 10.1016/j.cobeha.2019.01.011

Maes, M. (1995). Evidence for an immune response in major depression: a review and hypothesis. *Prog. Neuropsychopharmacol. Biol. Psychiatry* 19, 11–38. doi: 10.1016/0278-5846(94)00101-m

Maes, M., Berk, M., Goehler, L., Song, C., Anderson, G., Galecki, P., et al. (2012). Depression and sickness behavior are Janus-faced responses to shared inflammatory pathways. *BMC Med.* 10:66. doi: 10.1186/1741-7015-10-66

Maes, M., Kubera, M., and Leunis, J. C. (2008). The gut-brain barrier in major depression: intestinal mucosal dysfunction with an increased translocation of LPS from gram negative enterobacteria (leaky gut) plays a role in the inflammatory pathophysiology of depression. *Neuro Endocrinol. Lett.* 29, 117–124.

Maggio, M., Ceda, G. P., Lauretani, F., Bandinelli, S., Corsi, A. M., Giallauria, F., et al. (2011). SHBG, sex hormones, and inflammatory markers in older women. *J. Clin. Endocrinol. Metab.* 96, 1053–1059. doi: 10.1210/jc.2010-1902

Mahajan, S., Avasthi, A., Grover, S., and Chawla, Y. K. (2014). Incidence of depression in patients with chronic hepatitis C receiving combination therapy of pegylated interferon-alpha and ribavirin. *Psychother. Psychosom.* 83, 308–309. doi: 10.1159/000358527

Maier, L., Pruteanu, M., Kuhn, M., Zeller, G., Telzerow, A., Anderson, E. E., et al. (2018). Extensive impact of non-antibiotic drugs on human gut bacteria. *Nature* 555, 623–628. doi: 10.1038/nature25979

Majeed, M., Nagabhushanam, K., Arumugam, S., Majeed, S., and Ali, F. (2018). *Bacillus coagulans* MTCC 5856 for the management of major depression with irritable bowel syndrome: a randomised, double-blind, placebo controlled, multi-centre, pilot clinical study. *Food Nutr. Res.* 62:1218. doi: 10.29219/fnr.v62.1218

Mangiola, F., Ianiro, G., Franceschi, F., Fagiuoli, S., Gasbarrini, G., and Gasbarrini, A. (2016). Gut microbiota in autism and mood disorders. *World J. Gastroenterol.* 22, 361–368. doi: 10.3748/wjg.v22.i1.361

Markle, J. G., Frank, D. N., Mortin-Toth, S., Robertson, C. E., Feazel, L. M., Rolle-Kampczyk, U., et al. (2013). Sex differences in the gut microbiome drive

hormone-dependent regulation of autoimmunity. *Science* 339, 1084–1088. doi: 10.1126/science.1233521

Marotta, A., Sarno, E., Del Casale, A., Pane, M., Mogna, L., Amoruso, A., et al. (2019). Effects of probiotics on cognitive reactivity, mood, and sleep quality. *Front. Psychiatry* 10:164.doi: 10.3389/fpsyt.2019.00164

Martin, C. R., and Mayer, E. A. (2017). Gut-brain axis and behavior. *Nestle Nutr. Inst. Workshop Ser.* 88, 45–53.

Martin, C. R., Osadchiy, V., Kalani, A., and Mayer, E. A. (2018). The brain-gut-microbiome axis. *Cell. Mol. Gastroenterol. Hepatol.* 6, 133–148.

Matthews, K., and Robbins, T. W. (2003). Early experience as a determinant of adult behavioural responses to reward: the effects of repeated maternal separation in the rat. *Neurosci. Biobehav. Rev.* 27, 45–55. doi: 10.1016/s0149-7634(03)00008-3

McCarter, T. (2008). Depression overview. *Am. Health Drug Benefits* 1, 44–51.

Mendlewicz, J., Kriwin, P., Oswald, P., Souery, D., Alboni, S., and Brunello, N. (2006). Shortened onset of action of antidepressants in major depression using acetylsalicylic acid augmentation: a pilot open-label study. *Int. Clin. Psychopharmacol.* 21, 227–231. doi: 10.1097/00004850-200607000-00005

Mesquita, A. R., Correia-Neves, M., Roque, S., Castro, A. G., Vieira, P., Pedrosa, J., et al. (2008). IL-10 modulates depressive-like behavior. *J. Psychiatr. Res.* 43, 89–97. doi: 10.1016/j.jpsychires.2008.02.004

Messaoudi, M., Lalonde, R., Violle, N., Javelot, H., Desor, D., Nejdi, A., et al. (2011). Assessment of psychotropic-like properties of a probiotic formulation (Lactobacillus helveticus R0052 and Bifidobacterium longum R0175) in rats and human subjects. *Br. J. Nutr.* 105, 755–764. doi: 10.1017/S0007114510004319

Mikova, O., Yakimova, R., Bosmans, E., Kenis, G., and Maes, M. (2001). Increased serum tumor necrosis factor alpha concentrations in major depression and multiple sclerosis. *Eur. Neuropsychopharmacol.* 11, 203–208. doi: 10.1016/s0924-977x(01)00081-5

Miller, A. H., and Raison, C. L. (2016). The role of inflammation in depression: from evolutionary imperative to modern treatment target. *Nat. Rev. Immunol.* 16, 22–34. doi: 10.1038/nri.2015.5

Miller, L. E., and Ouwehand, A. C. (2013). Probiotic supplementation decreases intestinal transit time: meta-analysis of randomized controlled trials. *World J. Gastroenterol.* 19, 4718–4725. doi: 10.3748/wjg.v19.i29.4718

Mizrahi-Man, O., Davenport, E. R., and Gilad, Y. (2013). Taxonomic classification of bacterial 16S rRNA genes using short sequencing reads: evaluation of effective study designs. *PLoS One* 8:e53608. doi: 10.1371/journal.pone.0053608

Mohamad, N., Wong, S. K., Hasan, W., Jolly, J., Fozi, F., Ima-Nirwana, S., et al. (2018). The relationship between circulating testosterone and inflammatory cytokines in men. *Aging Male* 22, 1–12. doi: 10.1080/13685538.2018.1482487

Mohammadi, A. A., Jazayeri, S., Khosravi-Darani, K., Solati, Z., Mohammadpour, N., Asemi, Z., et al. (2016). The effects of probiotics on mental health and hypothalamic-pituitary-adrenal axis: a randomized, double-blind, placebo-controlled trial in petrochemical workers. *Nutr. Neurosci.* 19, 387–395. doi: 10.1179/1476830515y.0000000023

Mohle, L., Mattei, D., Heimesaat, M. M., Bereswill, S., Fischer, A., Alutis, M., et al. (2016). Ly6C(hi) monocytes provide a link between antibiotic-induced changes in gut microbiota and adult hippocampal neurogenesis. *Cell Rep.* 15, 1945–1956. doi: 10.1016/j.celrep.2016.04.074

Monteiro, R., Teixeira, D., and Calhau, C. (2014). Estrogen signaling in metabolic inflammation. *Mediators Inflamm.* 2014:615917. doi: 10.1155/2014/615917

Morgun, A., Dzutsev, A., Dong, X., Greer, R. L., Sexton, D. J., Ravel, J., et al. (2015). Uncovering effects of antibiotics on the host and microbiota using transkingdom gene networks. *Gut* 64, 1732–1743. doi: 10.1136/gutjnl-2014-308820

Mowat, A. M., and Agace, W. W. (2014). Regional specialization within the intestinal immune system. *Nat. Rev. Immunol.* 14, 667–685. doi: 10.1038/nri3738

Mueller, S., Saunier, K., Hanisch, C., Norin, E., Alm, L., Midtvedt, T., et al. (2006). Differences in fecal microbiota in different European study populations in relation to age, gender, and country: a cross-sectional study. *Appl. Environ. Microbiol.* 72, 1027–1033. doi: 10.1128/AEM.72.2.1027-1033.2006

Muller, N., Schwarz, M. J., Dehning, S., Douhe, A., Cerovecki, A., Goldstein-Muller, B., et al. (2006). The cyclooxygenase-2 inhibitor celecoxib has therapeutic effects in major depression: results of a double-blind, randomized, placebo controlled, add-on pilot study to reboxetine. *Mol. Psychiatry* 11, 680–684. doi: 10.1038/sj.mp.4001805

Murray, C. J., Atkinson, C., Bhalla, K., Birbeck, G., Burstein, R., Chou, D., et al. (2013). The state of US health, 1990-2010: burden of diseases, injuries, and risk factors. *JAMA* 310, 591–608. doi: 10.1001/jama.2013.13805

Nagpal, R., Shively, C., Register, T., Craft, S., and Yadav, H. (2019). Gut microbiome-Mediterranean diet interactions in improving host health. *F1000Res.* 8:699. doi: 10.12688/f1000research.18992.1

Naseribafrouei, A., Hestad, K., Avershina, E., Sekelja, M., Linlokken, A., Wilson, R., et al. (2014). Correlation between the human fecal microbiota and depression. *Neurogastroenterol. Motil.* 26, 1155–1162. doi: 10.1111/nmo.12378

Natividad, J. M., and Verdu, E. F. (2013). Modulation of intestinal barrier by intestinal microbiota: pathological and therapeutic implications. *Pharmacol. Res.* 69, 42–51. doi: 10.1016/j.phrs.2012.10.007

Nazimek, K., Strobel, S., Bryniarski, P., Kozlowski, M., Filipczak-Bryniarska, I., and Bryniarski, K. (2017). The role of macrophages in anti-inflammatory activity of antidepressant drugs. *Immunobiology* 222, 823–830. doi: 10.1016/j.imbio.2016.07.001

Neumann, I. D., Wigger, A., Krömer, S., Frank, E., Landgraf, R., and Bosch, O. J. (2005). Differential effects of periodic maternal separation on adult stress coping in a rat model of extremes in trait anxiety. *Neuroscience* 132, 867–877. doi: 10.1016/j.neuroscience.2005.01.034

Ni, J., Wu, G. D., Albenberg, L., and Tomov, V. T. (2017). Gut microbiota and IBD: causation or correlation? *Nat. Rev. Gastroenterol. Hepatol.* 14, 573–584. doi: 10.1038/nrgastro.2017.88

Nishida, K., Sawada, D., Kuwano, Y., Tanaka, H., Sugawara, T., Aoki, Y., et al. (2017). Daily administration of paraprobiotic Lactobacillus gasseri CP2305 ameliorates chronic stress-associated symptoms in Japanese medical students. *J. Funct. Foods* 36, 112–121. doi: 10.1016/j.jff.2017.06.031

Odamaki, T., Kato, K., Sugahara, H., Hashikura, N., Takahashi, S., Xiao, J.-Z., et al. (2016). Age-related changes in gut microbiota composition from newborn to centenarian: a cross-sectional study. *BMC Microbiol.* 16:90. doi: 10.1186/s12866-016-0708-5

O'Mahony, S. M., Marchesi, J. R., Scully, P., Codling, C., Ceolho, A.-M., Quigley, E. M. M., et al. (2009). Early life stress alters behavior, immunity, and microbiota in rats: implications for irritable bowel syndrome and psychiatric illnesses. *Biol. Psychiatry* 65, 263–267. doi: 10.1016/j.biopsych.2008.06.026

Org, E., Mehrabian, M., Parks, B. W., Shipkova, P., Liu, X., Drake, T. A., et al. (2016). Sex differences and hormonal effects on gut microbiota composition in mice. *Gut Microbes* 7, 313–322. doi: 10.1080/19490976.2016.1203502

Osadchiy, V., Martin, C. R., and Mayer, E. A. (2019). The gut-brain axis and the microbiome: mechanisms and clinical implications. *Clin. Gastroenterol. Hepatol.* 17, 322–332. doi: 10.1016/j.cgh.2018.10.002

Östlund-Lagerström, L., Kihlgren, A., Repsilber, D., Björkstén, B., Brummer, R. J., and Schoultz, I. (2016). Probiotic administration among free-living older adults: a double blinded, randomized, placebo-controlled clinical trial. *Nutr. J.* 15:80. doi: 10.1186/s12937-016-0198-1

Pacheco, A. R., and Sperandio, V. (2015). Enteric pathogens exploit the microbiota-generated nutritional environment of the gut. *Microbiol. Spectr.* 3:10.1128/microbiolspec.MBP-0001-2014. doi: 10.1128/microbiolspec.MBP-0001-2014

Pagliai, G., Sofi, F., Vannetti, F., Caiani, S., Pasquini, G., Molino Lova, R., et al. (2018). Mediterranean diet, food consumption and risk of late-life depression: the mugello study. *J. Nutr. Health Aging* 22, 569–574. doi: 10.1007/s12603-018-1019-3

Park, A. J., Collins, J., Blennerhassett, P. A., Ghia, J. E., Verdu, E. F., Bercik, P., et al. (2013). Altered colonic function and microbiota profile in a mouse model of chronic depression. *J. Neurogastroenterol. Motil.* 25, 733–e575. doi: 10.1111/nmo.12153

Park, J. M., and Lee, Y. J. (2020). Serum oestradiol levels are inversely associated with C-reactive protein levels in premenopausal women, but not postmenopausal women. *J. Int. Med. Res.* 48:300060520961228. doi: 10.1177/0300060520961228

Patel, A. (2013). Review: the role of inflammation in depression. *Psychiatr. Danub.* 25(Suppl. 2), S216–S223.

Patten, S. B., Wang, J. L., Williams, J. V., Currie, S., Beck, C. A., Maxwell, C. J., et al. (2006). Descriptive epidemiology of major depression in Canada. *Can. J. Psychiatry* 51, 84–90. doi: 10.1177/070674370605100204

Petersen, C., and Round, J. L. (2014). Defining dysbiosis and its influence on host immunity and disease. *Cell. Microbiol.* 16, 1024–1033. doi: 10.1111/cmi.12308

Phillips, J. G. P. (1910). The treatment of melancholia by the lactic acid Bacillus. *J. Ment. Sci.* 56, 422–430. doi: 10.1192/bjp.56.234.422

Poretsky, R., Rodriguez, R. L., Luo, C., Tsementzi, D., and Konstantinidis, K. T. (2014). Strengths and limitations of 16S rRNA gene amplicon sequencing in revealing temporal microbial community dynamics. *PLoS One* 9:e93827. doi: 10.1371/journal.pone.0093827

Principi, N., and Esposito, S. (2016). Gut microbiota and central nervous system development. *J. Infect.* 73, 536–546. doi: 10.1016/j.jinf.2016.09.010

Proctor, L. M., Creasy, H. H., Fettweis, J. M., Lloyd-Price, J., Mahurkar, A., Zhou, W., et al. (2019). The integrative human microbiome project. *Nature* 569, 641–648. doi: 10.1038/s41586-019-1238-8

Qin, J., Li, R., Raes, J., Arumugam, M., Burgdorf, K. S., Manichanh, C., et al. (2010). A human gut microbial gene catalogue established by metagenomic sequencing. *Nature* 464, 59–65. doi: 10.1038/nature08821

Rajilic-Stojanovic, M., and de Vos, W. M. (2014). The first 1000 cultured species of the human gastrointestinal microbiota. *FEMS Microbiol. Rev.* 38, 996–1047. doi: 10.1111/1574-6976.12075

Ransohoff, R. M., and Brown, M. A. (2012). Innate immunity in the central nervous system. *J. Clin. Invest.* 122, 1164–1171. doi: 10.1172/jci58644

Reininghaus, E. Z., Platzer, M., Kohlhammer-Dohr, A., Hamm, C., Mörkl, S., Bengesser, S. A., et al. (2020). PROVIT: supplementary probiotic treatment and vitamin B7 in Depression-A Randomized Controlled Trial. *Nutrients* 12:3422. doi: 10.3390/nu12113422

Reyman, M., Van Houten, M. A., Van Baarle, D., Bosch, A. A. T. M., Man, W. H., Chu, M. L. J. N., et al. (2019). Impact of delivery mode-associated gut microbiota dynamics on health in the first year of life. *Nat. Commun.* 10:4997.

Riedel, M., Moller, H. J., Obermeier, M., Adli, M., Bauer, M., Kronmuller, K., et al. (2011). Clinical predictors of response and remission in inpatients with depressive syndromes. *J. Affect. Disord.* 133, 137–149. doi: 10.1016/j.jad.2011.04.007

Rogers, G. B., Keating, D. J., Young, R. L., Wong, M. L., Licinio, J., and Wesselingh, S. (2016). From gut dysbiosis to altered brain function and mental illness: mechanisms and pathways. *Mol. Psychiatry* 21, 738–748. doi: 10.1038/mp.2016.50

Rohleder, N. (2014). Stimulation of systemic low-grade inflammation by psychosocial stress. *Psychosom. Med.* 76, 181–189. doi: 10.1097/PSY.0000000000000049

Romijn, A. R., Rucklidge, J. J., Kuijer, R. G., and Frampton, C. (2017). A double-blind, randomized, placebo-controlled trial of Lactobacillus helveticus and Bifidobacterium longum for the symptoms of depression. *Aust. N. Z. J. Psychiatry* 51, 810–821. doi: 10.1177/0004867416686694

Round, J. L., and Mazmanian, S. K. (2009). The gut microbiota shapes intestinal immune responses during health and disease. *Nat. Rev. Immunol.* 9, 313–323. doi: 10.1038/nri2515

Rowland, I., Gibson, G., Heinken, A., Scott, K., Swann, J., Thiele, I., et al. (2018). Gut microbiota functions: metabolism of nutrients and other food components. *Eur. J. Nutr.* 57, 1–24. doi: 10.1007/s00394-017-1445-8

Rudzki, L., Ostrowska, L., Pawlak, D., Malus, A., Pawlak, K., Waszkiewicz, N., et al. (2019). Probiotic Lactobacillus Plantarum 299v decreases kynurenine concentration and improves cognitive functions in patients with major depression: a double-blind, randomized, placebo controlled study. *Psychoneuroendocrinology* 100, 213–222. doi: 10.1016/j.psyneuen.2018.10.010

Rutayisire, E., Huang, K., Liu, Y., and Tao, F. (2016). The mode of delivery affects the diversity and colonization pattern of the gut microbiota during the first year of infants' life: a systematic review. *BMC Gastroenterol.* 16:86. doi: 10.1186/s12876-016-0498-0

Salk, R. H., Hyde, J. S., and Abramson, L. Y. (2017). Gender differences in depression in representative national samples: Meta-analyses of diagnoses and symptoms. *Psychol. Bull.* 143, 783–822. doi: 10.1037/bul0000102

Salminen, S., Gibson, G. R., Mccartney, A. L., and Isolauri, E. (2004). Influence of mode of delivery on gut microbiota composition in seven year old children. *Gut* 53, 1388–1389. doi: 10.1136/gut.2004.041640

Sanchez-Villegas, A., Henríquez, P., Bes-Rastrollo, M., and Doreste, J. (2007). Mediterranean diet and depression. *Public Health Nutr.* 9, 1104–1109.

Sassone-Corsi, M., and Raffatellu, M. (2015). No vacancy: how beneficial microbes cooperate with immunity to provide colonization resistance to pathogens. *J. Immunol.* 194, 4081–4087. doi: 10.4049/jimmunol.1403169

Savignac, H. M., Kiely, B., Dinan, T. G., and Cryan, J. F. (2014). Bifidobacteria exert strain-specific effects on stress-related behavior and physiology in BALB/c mice. *Neurogastroenterol. Motil.* 26, 1615–1627. doi: 10.1111/nmo.12427

Schroeder, B. O., and Backhed, F. (2016). Signals from the gut microbiota to distant organs in physiology and disease. *Nat. Med.* 22, 1079–1089. doi: 10.1038/nm.4185

Singh, P., and Manning, S. D. (2016). Impact of age and sex on the composition and abundance of the intestinal microbiota in individuals with and without enteric infections. *Ann. Epidemiol.* 26, 380–385. doi: 10.1016/j.annepidem.2016.03.007

Sinha, T., Vich Vila, A., Garmaeva, S., Jankipersadsing, S. A., Imhann, F., Collij, V., et al. (2019). Analysis of 1135 gut metagenomes identifies sex-specific resistome profiles. *Gut Microbes* 10, 358–366. doi: 10.1080/19490976.2018.1528822

Skaper, S. D., Facci, L., and Giusti, P. (2014). Neuroinflammation, microglia and mast cells in the pathophysiology of neurocognitive disorders: a review. *CNS Neurol. Disord. Drug Targets* 13, 1654–1666. doi: 10.2174/1871527313666141130224206

Skarupski, K. A., Tangney, C. C., Li, H., Evans, D. A., and Morris, M. C. (2013). Mediterranean diet and depressive symptoms among older adults over time. *J. Nutr. Health Aging* 17, 441–445. doi: 10.1007/s12603-012-0437-x

Skovlund, C. W., Mørch, L. S., Kessing, L. V., and Lidegaard, Ø. (2016). Association of hormonal contraception with depression. *JAMA Psychiatry* 73, 1154–1162. doi: 10.1001/jamapsychiatry.2016.2387

Slavich, G., and Sacher, J. (2019). Stress, sex hormones, inflammation, and major depressive disorder: extending Social Signal Transduction Theory of Depression to account for sex differences in mood disorders. *Psychopharmacology* 236, 1–17. doi: 10.1007/s00213-019-05326-9

Sluzewska, A., Rybakowski, J., Bosmans, E., Sobieska, M., Berghmans, R., Maes, M., et al. (1996). Indicators of immune activation in major depression. *Psychiatry Res.* 64, 161–167. doi: 10.1016/s0165-1781(96)02783-7

Slyepchenko, A., Maes, M., Jacka, F. N., Kohler, C. A., Barichello, T., Mcintyre, R. S., et al. (2017). Gut microbiota, bacterial translocation, and interactions with diet: pathophysiological links between major depressive disorder and non-communicable medical comorbidities. *Psychother. Psychosom.* 86, 31–46. doi: 10.1159/000448957

Slykerman, R. F., Hood, F., Wickens, K., Thompson, J. M. D., Barthow, C., Murphy, R., et al. (2017). Effect of *Lactobacillus rhamnosus* HN001 in Pregnancy on Postpartum Symptoms of Depression and Anxiety: a Randomised Double-blind Placebo-controlled Trial. *EBioMedicine* 24, 159–165. doi: 10.1016/j.ebiom.2017.09.013

Smith, C. J., Emge, J. R., Berzins, K., Lung, L., Khamishon, R., Shah, P., et al. (2014). Probiotics normalize the gut-brain-microbiota axis in immunodeficient mice. *Am. J. Physiol. Gastrointest. Liver Physiol.* 307, G793–G802. doi: 10.1152/ajpgi.00238.2014

Smith, P. A. (2015). The tantalizing links between gut microbes and the brain. *Nature* 526, 312–314. doi: 10.1038/526312a

Sokol, H., Pigneur, B., Watterlot, L., Lakhdari, O., Bermudez-Humaran, L. G., Gratadoux, J. J., et al. (2008). Faecalibacterium prausnitzii is an anti-inflammatory commensal bacterium identified by gut microbiota analysis of Crohn disease patients. *Proc. Natl. Acad. Sci. U.S.A.* 105, 16731–16736. doi: 10.1073/pnas.0804812105

Sommer, F., and Backhed, F. (2013). The gut microbiota–masters of host development and physiology. *Nat. Rev. Microbiol.* 11, 227–238. doi: 10.1038/nrmicro2974

Song, C., and Wang, H. (2011). Cytokines mediated inflammation and decreased neurogenesis in animal models of depression. *Prog. Neuropsychopharmacol. Biol. Psychiatry* 35, 760–768. doi: 10.1016/j.pnpbp.2010.06.020

Soto, M., Herzog, C., Pacheco, J. A., Fujisaka, S., Bullock, K., Clish, C. B., et al. (2018). Gut microbiota modulate neurobehavior through changes in brain insulin sensitivity and metabolism. *Mol. Psychiatry* 23, 2287–2301. doi: 10.1038/s41380-018-0086-5

Stanislawski, M. A., Dabelea, D., Wagner, B. D., Iszatt, N., Dahl, C., Sontag, M. K., et al. (2018). Gut Microbiota in the First 2 Years of Life and the Association with Body Mass Index at Age 12 in a Norwegian Birth Cohort. *mBio* 9:e01751-18. doi: 10.1128/mBio.01751-18

Steenbergen, L., Sellaro, R., Van Hemert, S., Bosch, J. A., and Colzato, L. S. (2015). A randomized controlled trial to test the effect of multispecies probiotics on cognitive reactivity to sad mood. *Brain Behav. Immun.* 48, 258–264. doi: 10.1016/j.bbi.2015.04.003

Sudo, N., Chida, Y., Aiba, Y., Sonoda, J., Oyama, N., Yu, X. N., et al. (2004). Postnatal microbial colonization programs the hypothalamic-pituitary-adrenal system for stress response in mice. *J. Physiol.* 558, 263–275. doi: 10.1113/jphysiol.2004.063388

Swiergiel, A. H., and Dunn, A. J. (2007). Effects of interleukin-1β and lipopolysaccharide on behavior of mice in the elevated plus-maze and open field tests. *Pharmacol. Biochem. Behav.* 86, 651–659. doi: 10.1016/j.pbb.2007.02.010

Takagi, T., Naito, Y., Inoue, R., Kashiwagi, S., Uchiyama, K., Mizushima, K., et al. (2019). Differences in gut microbiota associated with age, sex, and stool consistency in healthy Japanese subjects. *J. Gastroenterol.* 54, 53–63. doi: 10.1007/s00535-018-1488-5

Tan, S., Wang, Y., Chen, K., Long, Z., and Zou, J. (2017). Ketamine alleviates depressive-like behaviors via down-regulating inflammatory cytokines induced by chronic restraint stress in mice. *Biol. Pharm. Bull.* 40, 1260–1267. doi: 10.1248/bpb.b17-00131

Thursby, E., and Juge, N. (2017). Introduction to the human gut microbiota. *Biochem. J.* 474, 1823–1836. doi: 10.1042/bcj20160510

Tillisch, K., Labus, J., Kilpatrick, L., Jiang, Z., Stains, J., Ebrat, B., et al. (2013). Consumption of fermented milk product with probiotic modulates brain activity. *Gastroenterology* 144, 1394. doi: 10.1053/j.gastro.2013.02.043

Toyoda, A. (2017). Social defeat models in animal science: What we have learned from rodent models. *Anim. Sci. J.* 88, 944–952. doi: 10.1111/asj.12809

Tribbick, D., Salzberg, M., Ftanou, M., Connell, W. R., Macrae, F., Kamm, M. A., et al. (2015). Prevalence of mental health disorders in inflammatory bowel disease: an Australian outpatient cohort. *Clin. Exp. Gastroenterol.* 8, 197–204. doi: 10.2147/CEG.S77567

Turnbaugh, P. J., Ley, R. E., Hamady, M., Fraser-Liggett, C. M., Knight, R., and Gordon, J. I. (2007). The human microbiome project. *Nature* 449, 804–810.

Valles-Colomer, M., Falony, G., Darzi, Y., Tigchelaar, E. F., Wang, J., Tito, R. Y., et al. (2019). The neuroactive potential of the human gut microbiota in quality of life and depression. *Nat. Microbiol.* 4, 623–632. doi: 10.1038/s41564-018-0337-x

van den Biggelaar, A. H., Gussekloo, J., De Craen, A. J., Frolich, M., Stek, M. L., Van Der Mast, R. C., et al. (2007). Inflammation and interleukin-1 signaling network contribute to depressive symptoms but not cognitive decline in old age. *Exp. Gerontol.* 42, 693–701. doi: 10.1016/j.exger.2007.01.011

Vich Vila, A., Collij, V., Sanna, S., Sinha, T., Imhann, F., Bourgonje, A. R., et al. (2020). Impact of commonly used drugs on the composition and metabolic function of the gut microbiota. *Nat. Commun.* 11:362. doi: 10.1038/s41467-019-14177-z

Walker, A. W., Ince, J., Duncan, S. H., Webster, L. M., Holtrop, G., Ze, X., et al. (2011). Dominant and diet-responsive groups of bacteria within the human colonic microbiota. *ISME J.* 5, 220–230. doi: 10.1038/ismej.2010.118

Wallace, C. J. K., and Milev, R. V. (2021). The efficacy, safety, and tolerability of probiotics on depression: clinical results from an open-label pilot study. *Front. Psychiatry* 12:618279. doi: 10.3389/fpsyt.2021.618279

Weissman, M. M., and Klerman, G. L. (1977). Sex differences and the epidemiology of depression. *Arch. Gen. Psychiatry* 34, 98–111. doi: 10.1001/archpsyc.1977.01770130100011

Wharton, W., Gleason, C. E., Olson, S. R., Carlsson, C. M., and Asthana, S. (2012). Neurobiological underpinnings of the estrogen - mood relationship. *Curr. Psychiatry Rev.* 8, 247–256. doi: 10.2174/157340012800792957

Whiteford, H. A., Degenhardt, L., Rehm, J., Baxter, A. J., Ferrari, A. J., Erskine, H. E., et al. (2013). Global burden of disease attributable to mental and substance use disorders: findings from the Global Burden of Disease Study 2010. *Lancet* 382, 1575–1586. doi: 10.1016/s0140-6736(13)61611-6

Wiebe, E. R., Brotto, L. A., and Mackay, J. (2011). Characteristics of women who experience mood and sexual side effects with use of hormonal contraception. *J. Obstet. Gynaecol. Can.* 33, 1234–1240. doi: 10.1016/S1701-2163(16)35108-8

Williams, S., Chung, G., and Muennig, P. (2017). Undiagnosed depression: a community diagnosis. *SSM Popul. Health* 3, 633–638. doi: 10.1016/j.ssmph.2017.07.012

Wilson, I. D., and Nicholson, J. K. (2009). The role of gut microbiota in drug response. *Curr. Pharm. Des.* 15, 1519–1523. doi: 10.2174/138161209788168173

Wittchen, H. U., Jacobi, F., Rehm, J., Gustavsson, A., Svensson, M., Jonsson, B., et al. (2011). The size and burden of mental disorders and other disorders of the brain in Europe 2010. *Eur. Neuropsychopharmacol.* 21, 655–679. doi: 10.1016/j.euroneuro.2011.07.018

Wong, M. L., Dong, C., Maestre-Mesa, J., and Licinio, J. (2008). Polymorphisms in inflammation-related genes are associated with susceptibility to major depression and antidepressant response. *Mol. Psychiatry* 13, 800–812. doi: 10.1038/mp.2008.59

Wong, M. L., Inserra, A., Lewis, M. D., Mastronardi, C. A., Leong, L., Choo, J., et al. (2016). Inflammasome signaling affects anxiety- and depressive-like behavior and gut microbiome composition. *Mol. Psychiatry* 21, 797–805. doi: 10.1038/mp.2016.46

Wu, G. D., Chen, J., Hoffmann, C., Bittinger, K., Chen, Y.-Y., Keilbaugh, S. A., et al. (2011). Linking long-term dietary patterns with gut microbial enterotypes. *Science* 334, 105–108. doi: 10.1126/science.1208344

Xia, Z., Depierre, J. W., and Nassberger, L. (1996). Tricyclic antidepressants inhibit IL-6, IL-1 beta and TNF-alpha release in human blood monocytes and IL-2 and interferon-gamma in T cells. *Immunopharmacology* 34, 27–37. doi: 10.1016/0162-3109(96)00111-7

Yang, C., Qu, Y., Fujita, Y., Ren, Q., Ma, M., Dong, C., et al. (2017). Possible role of the gut microbiota–brain axis in the antidepressant effects of (R)-ketamine in a social defeat stress model. *Transl. Psychiatry* 7:1294. doi: 10.1038/s41398-017-0031-4

Yang, T., Santisteban, M. M., Rodriguez, V., Li, E., Ahmari, N., Carvajal, J. M., et al. (2015). Gut dysbiosis is linked to hypertension. *Hypertension* 65, 1331–1340. doi: 10.1161/hypertensionaha.115.05315

Yun, Y., Kim, H.-N., Kim, S. E., Heo, S. G., Chang, Y., Ryu, S., et al. (2017). Comparative analysis of gut microbiota associated with body mass index in a large Korean cohort. *BMC Microbiol.* 17:151. doi: 10.1186/s12866-017-1052-0

Yurkovetskiy, L., Burrows, M., Khan, A. A., Graham, L., Volchkov, P., Becker, L., et al. (2013). Gender bias in autoimmunity is influenced by microbiota. *Immunity* 39, 400–412. doi: 10.1016/j.immuni.2013.08.013

Zhang, J. C., Yao, W., Dong, C., Yang, C., Ren, Q., Ma, M., et al. (2017). Blockade of interleukin-6 receptor in the periphery promotes rapid and sustained antidepressant actions: a possible role of gut–microbiota–brain axis. *Transl. Psychiatry* 7:e1138. doi: 10.1038/tp.2017.112

Zhang, M., Li, A., Yang, Q., Li, J., Wang, L., Liu, X., et al. (2021). Beneficial Effect of Alkaloids From *Sophora alopecuroides* L. on CUMS-induced depression model mice via modulating gut microbiota. *Front. Cell. Infect. Microbiol.* 11:665159. doi: 10.3389/fcimb.2021.665159

Zhang, Y. J., Li, S., Gan, R. Y., Zhou, T., Xu, D. P., and Li, H. B. (2015). Impacts of gut bacteria on human health and diseases. *Int. J. Mol. Sci.* 16, 7493–7519. doi: 10.3390/ijms16047493

Zheng, P., Zeng, B., Zhou, C., Liu, M., Fang, Z., Xu, X., et al. (2016). Gut microbiome remodeling induces depressive-like behaviors through a pathway mediated by the host's metabolism. *Mol. Psychiatry* 21, 786–796. doi: 10.1038/mp.2016.44

Zoetendal, E. G., Raes, J., Van Den Bogert, B., Arumugam, M., Booijink, C. C., Troost, F. J., et al. (2012). The human small intestinal microbiota is driven by rapid uptake and conversion of simple carbohydrates. *ISME J.* 6, 1415–1426. doi: 10.1038/ismej.2011.212

Conflict of Interest: The authors declare that the research was conducted in the absence of any commercial or financial relationships that could be construed as a potential conflict of interest.

Publisher's Note: All claims expressed in this article are solely those of the authors and do not necessarily represent those of their affiliated organizations, or those of the publisher, the editors and the reviewers. Any product that may be evaluated in this article, or claim that may be made by its manufacturer, is not guaranteed or endorsed by the publisher.

frontiers | Frontiers in Neuroscience

ORIGINAL RESEARCH
published: 02 May 2022
doi: 10.3389/fnins.2022.819310

Neural Responses of Acupuncture for Treating Functional Dyspepsia: An fMRI Study

*Xiaohui Dong[1,2†], Tao Yin[1,2†], Siyi Yu[1,2†], Zhaoxuan He[1,2], Yuan Chen[3], Peihong Ma[1,2], Yuzhu Qu[1,2], Shuai Yin[4], Xiaoyan Liu[1,2], Tingting Zhang[1,2], Liuyang Huang[1,2], Jin Lu[1,2], Qiyong Gong[5] and Fang Zeng[2]**

[1] Acupuncture and Tuina School/The 3rd Teaching Hospital, Chengdu University of Traditional Chinese Medicine, Chengdu, China, [2] Acupuncture and Brain Science Center, Chengdu University of Traditional Chinese Medicine, Chengdu, China, [3] International Education School, Chengdu University of Traditional Chinese Medicine, Chengdu, China, [4] First Affiliated Hospital of Henan University of Traditional Chinese Medicine, Zhengzhou, China, [5] Department of Radiology, Huaxi MR Research Center, West China Hospital of Sichuan University, Chengdu, China

OPEN ACCESS

Edited by:
Chunhui Bao,
Shanghai University of Traditional Chinese Medicine, China

Reviewed by:
Jiliang Fang,
Guang'anmen Hospital, China Academy of Chinese Medical Sciences, China
Yang Hu,
Xidian University, China
Feng Han,
The Pennsylvania State University (PSU), United States

***Correspondence:**
Fang Zeng
zengfang@cdutcm.edu.cn

[†] These authors have contributed equally to this work

Specialty section:
This article was submitted to Gut-Brain Axis, a section of the journal Frontiers in Neuroscience

Received: 21 November 2021
Accepted: 15 February 2022
Published: 02 May 2022

Citation:
Dong X, Yin T, Yu S, He Z, Chen Y, Ma P, Qu Y, Yin S, Liu X, Zhang T, Huang L, Lu J, Gong Q and Zeng F (2022) Neural Responses of Acupuncture for Treating Functional Dyspepsia: An fMRI Study. Front. Neurosci. 16:819310. doi: 10.3389/fnins.2022.819310

Different acupoints exhibiting similar therapeutic effects are a common phenomenon in acupuncture clinical practice. However, the mechanism underlying this phenomenon remains unclear. This study aimed to investigate the similarities and differences in cerebral activities elicited through stimulation of CV12 and ST36, the two most commonly used acupoints, in the treatment of gastrointestinal diseases, so as to partly explore the mechanism of the different acupoints with similar effects. Thirty-eight eligible functional dyspepsia (FD) patients were randomly assigned into either group A (CV12 group) or group B (ST36 group). Each patient received five acupuncture treatments per week for 4 weeks. The Symptom Index of Dyspepsia (SID), Nepean Dyspepsia Symptom Index (NDSI), and Nepean Dyspepsia Life Quality Index (NDLQI) were used to assess treatment efficacy. Functional MRI (fMRI) scans were performed to detect cerebral activity changes at baseline and at the end of the treatment. The results demonstrated that (1) improvements in NDSI, SID, and NDLQI were found in both group A and group B ($p < 0.05$). However, there were no significant differences in the improvements of the SID, NDSI, and NDLQI scores between group A and group B ($p > 0.05$); (2) all FD patients showed significantly increased amplitude of low-frequency fluctuation (ALFF) in the left postcentral gyrus after acupuncture treatment, and the changes of ALFF in the left postcentral gyrus were significantly related to the improvements of SID scores ($r = 0.358$, $p = 0.041$); and (3) needling at CV12 significantly decreased the resting-state functional connectivity (rsFC) between the left postcentral gyrus and angular gyrus, caudate, middle frontal gyrus (MFG), and cerebellum, while needling at ST36 significantly increased the rsFC between the left postcentral gyrus with the precuneus, superior frontal gyrus (SFG), and MFG. The results indicated that CV12 and ST36 shared similar therapeutic effects for dyspepsia, with common modulation

on the activity of the postcentral gyrus in FD patients. However, the modulatory pattern on the functional connectivity of the postcentral gyrus was different. Namely, stimulation of CV12 primarily involved the postcentral gyrus–reward network, while stimulation of ST36 primarily involved the postcentral gyrus–default mode network circuitry.

Keywords: acupuncture, functional dyspepsia, default mode network, reward network, functional magnetic resonance imaging

INTRODUCTION

Functional dyspepsia (FD) is a common functional gastrointestinal disease (FGID) with clinical incidence ranging from 8 to 40% (Ghoshal et al., 2011; Mahadeva and Ford, 2016). The main clinical manifestations of FD are epigastric pain, epigastric burning, early satiety, and postprandial fullness, which cannot be attributed to organic and metabolic causes (Tack and Talley, 2013; Drossman, 2016). FD not only significantly affects the quality of life (QoL) of patients but also creates severe socioeconomic burden (Talley et al., 2006). Due to the complex etiology of FD, there is currently a lack of effective pharmaceuticals (Tack and Camilleri, 2018; Yamawaki et al., 2018; Tack et al., 2019), so non-pharmaceutical therapies are sought out by doctors and patients alike.

Acupuncture, as the most commonly used alternative and complementary treatment modality worldwide, has been accepted as an effective therapy for FD (Yang et al., 2020; Wang et al., 2021). A number of clinical studies have shown that acupuncture not only can relieve symptoms of dyspepsia but can also improve patient QoL and emotional states (Xu et al., 2006; Ma et al., 2012; Zeng et al., 2012; Yang et al., 2020). For example, our previous results indicated that genuine acupuncture can significantly improve QoL and symptoms of FD patients when compared to sham acupuncture and oral itopride (Ma et al., 2012). A data mining-based review found that more than 20 acupoints can be used for treating FD in clinical practice. Among them, *Zusanli* (ST36) and *Zhongwan* (CV12) are the most commonly used (Cao et al., 2016a,b). Despite the two points exhibiting treatment efficacy, their mechanisms in the treatment of FD remain to be further studied.

In the last decade, a number of neuroimaging studies have demonstrated that FD patients exhibit significant functional and structural alterations in multiple brain regions, including the frontal cortex, somatosensory cortex, postcentral gyrus, precuneus, and caudate tail (Zeng et al., 2009; Nan et al., 2014; Lee et al., 2016; Qi et al., 2020), and these abnormal functional activities can be regulated by acupuncture, to some degree (Zeng et al., 2012; Chen et al., 2021). For example, a previous functional MRI (fMRI) study found that acupuncture at *Weishu* (BL21) and *Zhongwan* (CV12) can modulate the disrupted functional connectivity (FC) between the insula and other brain regions in rat models of FD (Chen et al., 2021). Our previous studies also indicated that needling acupoints on the stomach meridian could significantly reduce abnormally high glucose metabolism in the homeostatic afferent network of FD patients and that this regulatory effect is different from needling sham acupoints and from needling acupoints not used for treating FD (Zeng et al., 2012, 2015). However, the question of whether different acupoints with similar therapeutic effects share similar influences on brain function in patients with FD has not been explored in previous studies.

Therefore, on the basis of verifying similar clinical effects of ST36 and CV12 in the treatment of FD, our study aimed to 1) observe the influence of acupuncture on brain functional activities of all FD patients using fMRI, and attempt to determine potential target brain areas related to acupuncture efficacy, and 2) investigate the effects of needling at ST36 and CV12 on FC of the target brain region, in order to explore the mechanism(s) governing similar effects exhibited by different acupoints.

MATERIALS AND METHODS

This was a randomized controlled neuroimaging trial. The FD patients were recruited from the campus of Chengdu University of Traditional Chinese Medicine (CDUTCM) and the Digestive Department of the Affiliated Hospital of CDUTCM between January 2016 and May 2018. All patients were diagnosed by clinicians in the Digestive Department of the Affiliated Hospital of CDUTCM.

This study was performed according to the principles of the Declaration of Helsinki (Version Edinburgh 2000). The study protocol was approved by the Ethics Committee of the Affiliated Hospital of CDUTCM (No. 2014KL-028) and registered at the Clinical Trial Registry (registration number: ChiCTR-IOR-15006402).

Participants

Patients were enrolled if they fulfilled all of the following inclusion criteria: (1) were aged 18 to 45 years; (2) were right-handed; (3) matched the Rome III diagnosis criteria for FD; (4) had not taken any gastrointestinal drugs or received acupuncture treatment for at least 15 days before entering the study; and (5) provided assigned informed consent. Patients were excluded if they (1) were pregnant or lactating; (2) had a history of head trauma with loss of consciousness or gastrointestinal surgery; (3) were currently taking drugs promoting gastrointestinal dynamics; (4) had any contraindications to acupuncture; or (5) had any MRI contraindications, such as pacemakers, fixed metal dentures, or severe claustrophobia.

After an initial 2-week baseline evaluation, 38 eligible patients were randomly assigned to two groups using a computer-generated randomization sequence. The randomization information was concealed from the researchers until the

completion of statistical analysis. Patients were blinded to the group assignment.

Acupuncture Intervention

The acupoint used for group A was *Zhongwan* (CV12), while the acupoint used for group B was *Zusanli* (ST 36). The locations of the acupoints are shown in **Figure 1**. Acupuncture treatment was administered by two licensed acupuncturists with more than 6 years of clinical experience and who had received specialized acupuncture training in the selection of acupoints and standard acupuncture operating procedures. Manual acupuncture treatment was administered using disposable sterile filiform needles (25–40 × 0.25 mm, Huatuo Medical Instrument Co., Ltd., Jiangsu, China). The acupuncture treatment protocol used is outlined in our previous study (Yin et al., 2017). All patients received five acupuncture treatments per week for 4 weeks.

Outcome Measurement

The Symptom Index of Dyspepsia (SID) and the Nepean dyspepsia index (NDI) were used to assess the efficacy of acupuncture for treating FD. The SID focused on the four chief symptoms of FD: postprandial fullness discomfort, early satiety, epigastric pain, and epigastric burning. Each symptom was graded as follows: asymptomatic (0 points), mild (1 point), moderate (2 points), or severe (3 points; Ma et al., 2012). The NDI is composed of the Nepean Dyspepsia Symptom Index (NDSI) and Nepean Dyspepsia Life Quality Index (NDLQI) (Talley et al., 1999). The NDSI evaluates the clinical symptoms of patients by measuring the frequency, intensity, and level of discomfort for 15 upper gastrointestinal symptoms. The NDLQI is an FD-specific questionnaire to assess patients' QoL from four dimensions, including interference (13 items), knowledge/control (7 items), eat/drink (3 items), and sleep/disturb (2 items). Furthermore, the Self-Rating Anxiety Scale (SAS) (Zung, 1971) and Self-Rating Depression Scale (SDS) (Zung et al., 1965) were used to evaluate the emotional states of patients. The SID, NDSI, NDLQI, SAS, and SDS were measured at baseline and the end of the treatment.

Functional MRI Scan

All patients received MRI scans at baseline and the end of the treatment. MRI data were acquired with a 3.0-T magnetic resonance scanner (Siemens, Munich, Germany) at Huaxi Magnetic Resonance Research Center, West China Hospital of Sichuan University, Chengdu, China. The scanning procedure contained a localizer, a high-resolution three-dimensional T1-weighted imaging (3D-T1WI), and a blood oxygenation level-dependent fMRI (BOLD-fMRI). According to previous studies, resting-state fMRI (rsfMRI) signals can vary when awake versus asleep, while the arousal level is closely related to rsfMRI signals at the sensorimotor region (Gu et al., 2019). Therefore, patients were told to maintain wakefulness during the scan to avoid the effect of falling asleep on brain activity in this study.

The scanning parameters were as follows: 3D-T1WI: repetition time (TR)/echo time (TE) = 1,900/2.26 ms; slice thickness = 1 mm; slices = 176; matrix size = 256 × 256; field of view (FOV) = 256 × 256 mm^2. BOLD-fMRI: TR/TE = 2,000/30 ms; flip angle = 90°; slice number = 30; matrix size = 64 × 64; FOV = 240 × 240 mm^2; slice thickness = 5 mm; total fMRI scans = 180, with the functional scan lasting 6 min.

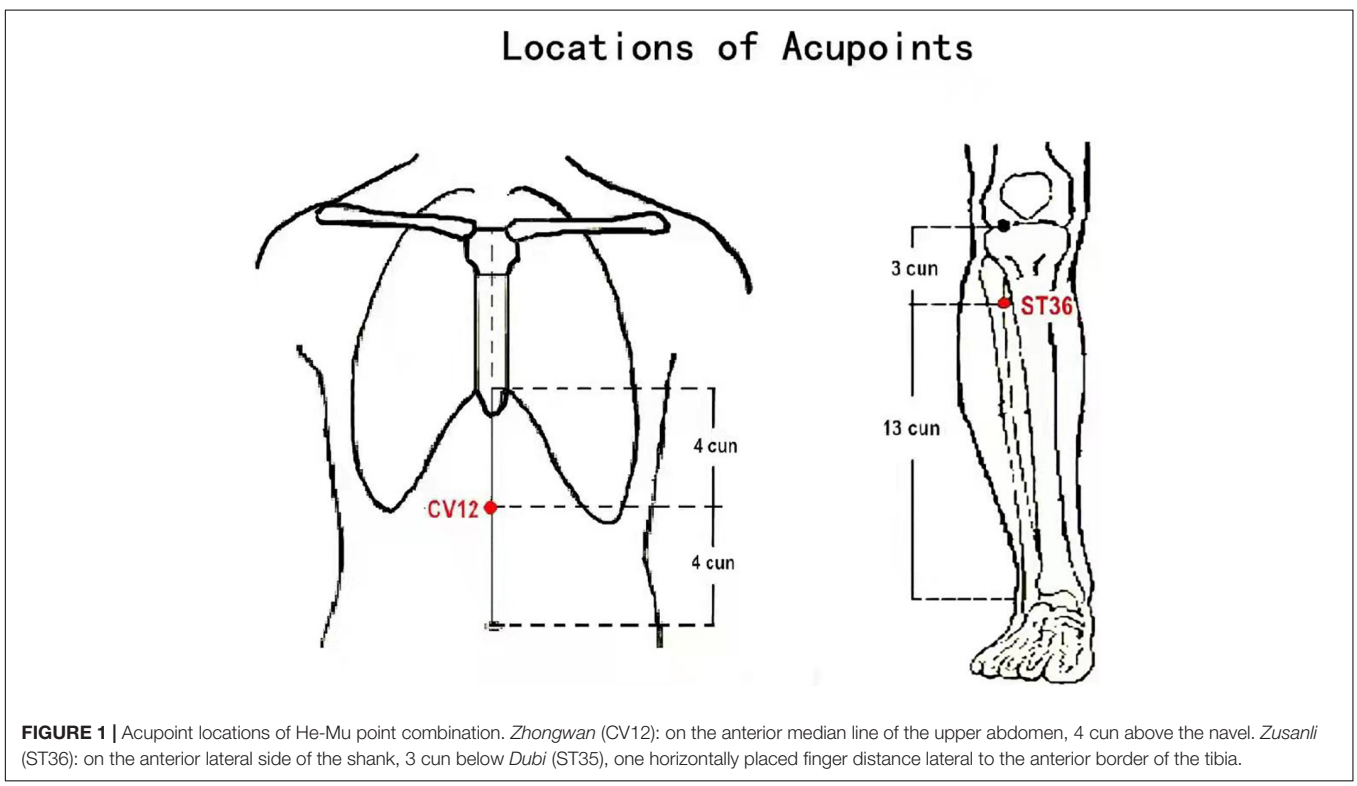

FIGURE 1 | Acupoint locations of He-Mu point combination. *Zhongwan* (CV12): on the anterior median line of the upper abdomen, 4 cun above the navel. *Zusanli* (ST36): on the anterior lateral side of the shank, 3 cun below *Dubi* (ST35), one horizontally placed finger distance lateral to the anterior border of the tibia.

Statistical Analysis

Clinical Data

Data analysis was performed using SPSS 22.0 statistic software package (IBM Corp, Somers, NY, United States). Independent-samples *t*-test, Mann–Whitney U-test, and chi-square tests were applied to compare the baseline demographic and clinical characteristics of FD patients. A paired *t*-test or Wilcoxon signed-rank test was applied to compare within-group differences, and analysis of covariance (ANCOVA) was applied for between-group analysis. Correlation analysis was performed using Pearson's correlation analysis. A p-value < 0.05 was considered statistically significant.

Functional MRI Data

Data Preprocessing

The functional BOLD data were preprocessed using Data Processing Assistant for Resting-State fMRI (DPARSF) software[1] in MATLAB (MathWorks, Inc., Natick, MA, United States). During the preprocessing phase, the first 10 timepoints were discarded to avoid instability in initial MRI signals, and slice-timing correction, head motion estimation, and realignment were performed. Then images were segmented and coregistered to each patients' high-resolution T1 scan and normalized to the standard Montreal Neurological Institute (MNI) template. After that, images were smoothed with a Gaussian kernel of 6-mm^3 full width at half maximum (FWHM) and band-pass filtered with a frequency window of 0.01–0.08 Hz. Patients with excessive head motion [with mean frame-wise displacement greater than 0.5 mm (Power et al., 2012)] were excluded from the analysis.

Amplitude of Low-Frequency Fluctuation and Functional Connectivity Analysis

After preprocessing, the amplitude of low-frequency fluctuation (ALFF) was first calculated using DPARSF. Paired *t*-test was used to assess the within-group differences of ALFF in all FD patients. Gaussian random field (GRF) correction was used, and voxel-level $p < 0.005$ and corrected cluster-level $p < 0.05$ were considered statistically significant. Next, correlation analysis of the ALFF change values and clinical improvement values of all FD patients was performed to obtain the brain areas associated with acupuncture efficacy. Finally, the regions that were most significantly correlated with clinical improvement value were selected as regions of interest (ROIs) for FC analysis. The paired *t*-test was performed to investigate the functional alterations of FD patients before and after acupuncture treatment in each group. GRF correction was made, and voxel-level $p < 0.05$ and corrected cluster-level $p < 0.05$ were considered statistically significant.

RESULTS

Five participants were excluded due to excessive head motion (mean framewise displacement > 0.5 mm) during imaging. Thirty-three FD patients (18 in group A and 15 in group B) were included in the final clinical data and fMRI data analysis.

[1]http://rfmri.org/DPARSF

The Baseline Characteristics of the Two Groups

The baseline characteristics of patients in the two groups are displayed in **Table 1**. As shown in **Table 1**, except for age, there was no significant difference in baseline characteristics between these two groups ($p > 0.05$; **Table 1**).

The Therapeutic Effects in the Two Groups

The within-group analyses showed that a significant increase in NDLQI scores and a significant decrease in SID scores, NDSI scores, SAS scores, and SDS scores were found in both group A and group B after acupuncture treatment ($p < 0.05$; **Table 2**).

The between-group analyses showed that there were no significant differences in the improvements of the SID scores, NDSI scores, NDLQI scores, SAS scores, and SDS scores between the two groups ($p > 0.05$; **Table 2**).

Cerebral Activity Changes Induced by Acupuncture Treatment in Both Groups

The Amplitude of Low-Frequency Fluctuation Changes in All Functional Dyspepsia Patients

After acupuncture treatment, significantly increased ALFF values in the left postcentral gyrus were found in all FD patients. Moreover, the ALFF value changes in the left postcentral gyrus were significantly related to the improvements of SID scores with age and gender as covariates ($r = 0.358$, $p = 0.041$, uncorrected) (**Figure 2**).

The Resting-State Functional Connectivity Changes of Postcentral Gyrus in the Two Groups

The left postcentral gyrus was selected as the ROI to investigate the FC changes of FD patients in group A and group B. Within-group comparisons demonstrated that there were significantly decreased resting-state FC (rsFC) between the left postcentral gyrus and angular gyrus, caudate, middle frontal gyrus (MFG), and cerebellum after treatment in group A. In addition, there were significantly increased rsFC between the left postcentral

TABLE 1 | The baseline characteristics in two groups.

Characteristic	Group A (n = 18)	Group B (n = 15)	Statistical value	p-Value
No. of women, n (%)	12 (66.67%)	13 (86.67%)	1.782	0.182
Age (years), mean ± SD	22.78 ± 1.63	21.20 ± 2.40	2.243	0.032*
BMI, mean ± SD	19.09 ± 1.48	19.70 ± 1.96	−1.030	0.311
Course of disease (M), mean ± SD	42.83 ± 26.15	33.60 ± 19.18	1.136	0.265
SID score, mean ± SD	3.89 ± 1.41	3.80 ± 1.42	−0.149	0.882
NDLQI score, mean ± SD	77.58 ± 8.41	74.60 ± 11.43	0.863	0.395
NDSI score, mean ± SD	45.67 ± 17.27	41.93 ± 14.07	0.671	0.507
SAS score, mean ± SD	40.32 ± 7.68	43.67 ± 9.77	−1.104	0.278
SDS score, mean ± SD	41.90 ± 9.11	45.18 ± 10.29	−0.971	0.339

*BMI, body mass index; NDLQI, the Nepean Dyspepsia Life Quality Index; NDSI, the Nepean Dyspepsia Symptom Index; SAS, Self-Rating Anxiety Scale; SDS, Self-Rating Depression Scale; SID, Symptom Index of Dyspepsia. *p < 0.05.*

TABLE 2 | Comparison of the therapeutic effects between group A and group B.

Items	Group A					Group B					*F*-value	*p*
	Pre	Pos	Pos–Pre	*Z*-value	*p*	Pre	Pos	Pos–Pre	*Z*-value	*p*		
SID score (mean ± SD)	3.89 ± 1.41	1.94 ± 0.54	−1.94 ± 1.47	−3.573	0.000**	3.80 ± 1.42	1.20 ± 1.08	−2.60 ± 1.45	−3.427	0.001*	1.416	0.243
NDLQI score (mean ± SD)	77.58 ± 8.41	89.93 ± 5.81	12.35 ± 8.32	−3.636	0.000**	74.60 ± 11.43	88.88 ± 11.56	14.28 ± 8.47	−3.408	0.001*	1.224	0.277
NDSI score (mean ± SD)	45.67 ± 17.27	20.17 ± 10.14	−25.50 ± 13.87	−3.724	0.000**	41.93 ± 14.07	14.00 ± 14.48	−27.93 ± 14.92	−3.352	0.001*	0.988	0.328
SAS score (mean ± SD)	40.32 ± 7.68	34.72 ± 7.13	−5.60 ± 9.86	−2.329	0.020*	43.67 ± 9.77	34.00 ± 8.77	−9.67 ± 6.28	−3.297	0.001*	0.894	0.352
SDS score (mean ± SD)	41.90 ± 9.11	36.04 ± 8.43	−5.86 ± 10.58	−2.509	0.012*	45.18 ± 10.29	34.67 ± 8.67	−10.52 ± 9.13	−3.109	0.002*	0.349	0.559

NDLQI, the Nepean Dyspepsia Life Quality Index; NDSI, the Nepean Dyspepsia Symptom Index; SAS, Self-Rating Anxiety Scale; SDS, Self-Rating Depression Scale; SID, Symptom Index of Dyspepsia.
*$p < 0.05$; **$p < 0.001$.*

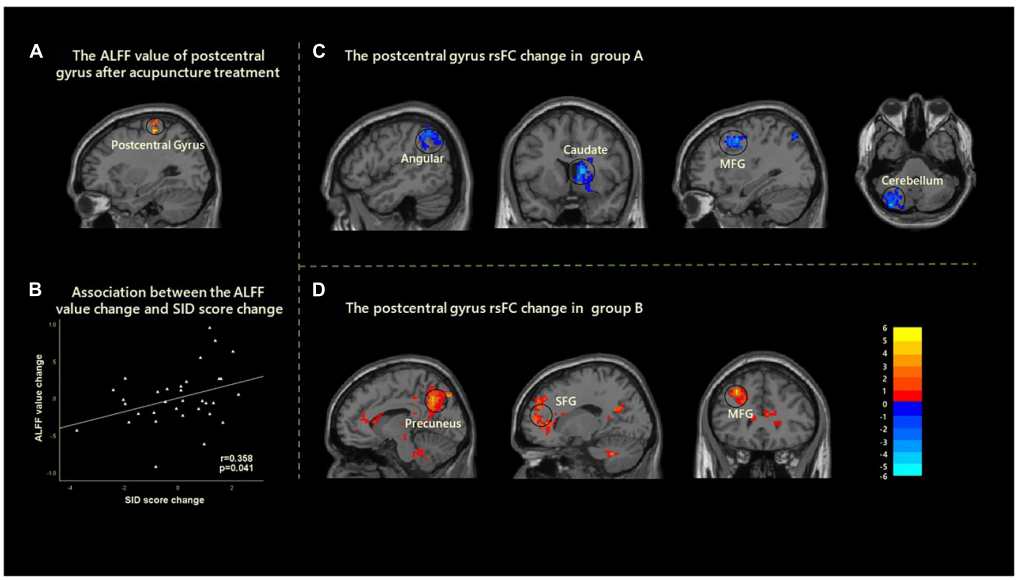

FIGURE 2 | Cerebral activity changes induced by the acupuncture stimulation in two groups. **(A)** A significantly increased ALFF was found in the left postcentral gyrus after acupuncture treatment. **(B)** Correlation analysis showed that the change of ALFF value in left postcentral gyrus and the improvement of SID were positively correlated with age and gender as covariates ($r = 0.358$, $p = 0.041$). **(C)** After acupuncture treatment, the decreased rsFC between the left postcentral gyrus with angular, caudate, MFG, and cerebellum were found in group A. **(D)** After acupuncture treatment, the increased rsFC between the left postcentral gyrus with precuneus, SFG, and MFG was found in group B. ALFF, amplitude of low-frequency fluctuation; rsFC, resting-state functional connectivity; MFG, middle frontal gyrus; SID, Symptom Index of Dyspepsia; SFG, superior frontal gyrus.

gyrus and precuneus, superior frontal gyrus (SFG), and MFG after treatment in group B (**Figure 2** and **Table 3**). However, there was no significant correlation between FC and clinical efficacy in group A and group B.

DISCUSSION

The current study focused on the potential central mechanism of different acupoints sharing similar therapeutic effects for FD. The results demonstrated that needling at both CV12 and ST36 could elicit activity changes in the postcentral gyrus response, although their response patterns were relatively different. Needling at ST36 mainly affected the postcentral gyrus–default mode network (DMN) circuitry, while needling at CV12 mainly aroused the postcentral gyrus–reward network (RN) circuitry.

The Similarities in Cerebral Responses Elicited by Acupuncture in Both Group A and Group B

In this study, the clinical observations indicated that needling at either CV12 or ST36 could significantly decrease SID

TABLE 3 | The differences of the left postcentral gyrus rsFC in each group.

ROI	Group	Cluster regions	L/R	Cluster sizes	Peak MNI			T
					x	*y*	*z*	
L_Postcentral Gyrus	Group A	Angular	R	280	49	−52	49	−3.74
		Caudate	R	274	15	9	12	−4.86
		Middle frontal gyrus	R	245	33	12	48	−4.42
		Cerebellum	L	338	−36	−81	−39	−5.51
	Group B	Precuneus	L	791	−10	−61	42	6.70
		Superior frontal gyrus	R	854	17	48	35	5.00
		Middle frontal gyrus	R	307	−30	30	42	6.37

rsFC, resting-state functional connectivity; MNI, Montreal Neurological Institute; ROI, region of interest.

scores, NDSI scores, SAS scores, and SDS scores and could increase NDLQI scores and that there were no significant differences in the improvements of variables mentioned above. The results indicated that both CV12 and ST36 were effective for improving symptoms, QoL, and emotional status of FD patients and that the therapeutic effects of both acupoints were similar. The current results were consistent with previous studies, which showed the effectiveness of both acupoints in the treatment of FD (Ma et al., 2012; Sun et al., 2021a). In addition, previous studies found that acupuncture treatment provided significant relief to gastrointestinal symptoms in comparison with FD patients awaiting acupuncture treatment (Chung et al., 2019). Therefore, performing acupuncture at CV12 and ST36 is a valuable treatment option for FD.

In addition to similar therapeutic effects, significantly increased ALFF values in the left postcentral gyrus were found in all FD patients (combined group A and group B) after acupuncture treatment. The postcentral gyrus of the parietal lobe corresponds to the primary sensory cortex, receiving various sensations from the body (Yu et al., 2019; DiGuiseppi and Tadi, 2021). Multiple neuroimaging studies had previously confirmed the involvement of the postcentral gyrus in the central pathology of FD patients. For instance, a H_2 (15) O-PET study found that FD patients demonstrated altered activity in the primary sensory cortex, including the postcentral gyrus, and that this altered activity corresponded to decreases in gastric distention (Van Oudenhove et al., 2010). Previous studies also found higher cerebral glucose metabolism in the postcentral gyrus in FD patients through 18 F-FDG PET-CT imaging (Zeng et al., 2011) and increased ALFF values in the postcentral gyrus through fMRI (Qi et al., 2020). These results indicated the role of the postcentral gyrus in the abnormal processing of gastrointestinal sensory signals. Furthermore, the participation of the postcentral gyrus in the integration of the regulatory effect of acupuncture on the gastrointestinal tract had been identified by several neuroimaging studies (Zeng et al., 2009; Zhou et al., 2013). Our previous studies indicated that acupuncture stimulation could decrease abnormally elevated glucose metabolism in the postcentral gyrus (Liu et al., 2012), and needling at ST36 could normalize the fMRI signals in the postcentral gyrus (Li et al., 2014). However, acupuncture does not always elicit brain responses in the postcentral gyrus, although brain responses have been observed in various acupuncture-related neuroimaging studies (Yan et al., 2005; Yang et al., 2014; Yeo et al., 2016; Zheng et al., 2018). This study indicated significant increases of ALFF values in the postcentral gyrus in all FD patients after acupuncture was performed, with increased ALFF values positively correlating with improvements in SID scores. The results indicated that the activity changes in the postcentral gyrus were related to acupuncture efficacy for FD.

The Differences in Postcentral Gyrus Responses Caused by Needling at ST36 Versus CV12

This study aimed to investigate similar effects shared by different acupoints by differentiating response modes of two acupoints on the postcentral gyrus through rsFC analysis, as all patients exhibited changes in the functional activity of the postcentral gyrus after acupuncture treatment, with changes significantly positively correlating with the curative effect of acupuncture.

The results showed that needling at ST36 resulted in significantly increased rsFC between the left postcentral gyrus with precuneus, SFG, and MFG. It is well known that the precuneus is an important hub within the DMN (Brewer et al., 2011; Utevsky et al., 2014), which regulates the affective and sensory process together with the medial prefrontal cortex (mPFC) and amygdala (Vanner et al., 2016). The precuneus is involved in episodic memory retrieval (Cavanna and Trimble, 2006; Sajonz et al., 2010), appetite control (Scharmuller et al., 2012; Tuulari et al., 2015), appraisal of food (Winter et al., 2017), and reappraisal of the benefits of eating food (Yokum and Stice, 2013). A variety of studies have identified the structural and functional abnormalities of the precuneus in FD patients (Zeng et al., 2011; Liu et al., 2013). For example, Lee et al. (2018) observed that higher rsFC between the insula and precuneus was negatively correlated with FD symptoms, food craving, and depression while in a state of hunger. Our previous study also showed that DMN in FD patients may indeed undergo dysfunctional changes, with changes in DMN found to be related to FD symptom severity (Liu et al., 2013). More importantly, a number of studies have reported that acupuncture can reverse the disrupted DMN to achieve therapeutic effects

in gastrointestinal disease (Bao et al., 2017; Sun et al., 2021a,b; Zhao et al., 2021). In these studies, needling at ST36 regulated the rsFC between the left postcentral gyrus with DMN. The results indicated that promoting self-regulation and adaptation *via* the DMN might be one of the functions achieved by needling ST36 for FD.

In contrast to ST36, CV12 elicited decreased rsFC values between the left postcentral gyrus and angular gyrus, caudate, MFG, and cerebellum in this study. The results indicated that needling at CV12 mainly regulated postcentral gyrus–RN circuitry in order to achieve treatment efficacy. The caudate nucleus and cerebellum, important components of the RN, play a crucial role in viscera activities (Allen et al., 1997; Ladabaum et al., 2001). Ladabaum et al. (2001) found significant activations of the bilateral caudate nucleus during proximal gastric dilation stimulation. Our previous results indicated increased gray matter volume in the right caudate (Liu et al., 2014), decreased gray matter density in the cerebellum (Zeng et al., 2013), and higher glycometabolism in the cerebellum (Zeng et al., 2011) in FD patients compared with healthy controls. In addition, higher glycometabolism in the cerebellum was decreased after acupuncture treatment (Zeng et al., 2015). These studies confirmed the structural and functional abnormalities in the caudate nucleus and cerebellum in FD patients, as well as the favorable regulatory effect of acupuncture on cerebellum activities. In fact, some researchers have found that the expectations of acupuncture efficacy may partly be based on the self-relevant phenomenon and self-referential introspection, which was often found to be related to activation of patient self-appraisal and RN (Pariente et al., 2005; Lundeberg et al., 2007).

In this study, performing acupuncture at ST36 and CV12 can affect the function of the postcentral gyrus, although the modes of influence are different. In addition, some studies focusing on peripheral nerve activity had found that the mechanisms of acupuncture at ST36 and CV12 to regulate gastrointestinal function were different. For example, one study had found that needling of the lower limb (ST36) caused gastrointestinal muscle contractions *via* the somatoparasympathetic pathway, while needling in the upper abdominal area (CV12) caused gastrointestinal muscle relaxation *via* the somatosympathetic pathway (Takahashi, 2006). Another study had indicated that electroacupuncture stimulation at the lower limb (ST36) but not in the abdomen (ST25) can promote the vagal–adrenal anti-inflammatory axis in mice (Liu et al., 2021). In summary, although acupoints in the different regions have similar therapeutic effects, the underlying mechanisms from central to peripheral were found to be relatively different.

LIMITATIONS

There were some limitations in this study. Firstly, the sample size was relatively small. Secondly, we observed the changes in clinical symptoms and functional activities of FD patients at baseline and the end of 4 weeks of acupuncture treatment, but its long-term efficacy remains unclear due to a lack of follow-up studies. In the future, further studies are needed to assess the long-term efficacy and investigate the potential mechanism of "different acupoints exhibiting similar effects."

CONCLUSION

In conclusion, acupuncture at ST36 and CV12 had similar therapeutic efficacy in the treatment of FD, and the realization of therapeutic effect may be related to the modulation of the activity of the postcentral gyrus. Meanwhile, the modulatory pattern was relatively different. Namely, ST36 mainly affected the rsFC between the postcentral gyrus and DMN, while the CV12 mainly affected the rsFC between the postcentral gyrus and RN.

DATA AVAILABILITY STATEMENT

The raw data supporting the conclusions of this article will be made available by the authors, without undue reservation.

ETHICS STATEMENT

The studies involving human participants were reviewed and approved by the Ethics Committee of the Affiliated Hospital of CDUTCM (approved number. 2014KL-028). The patients/participants provided their written informed consent to participate in this study.

AUTHOR CONTRIBUTIONS

FZ and QG: experimental design. ZH, PM, YQ, SYu, XL, TZ, LH, and JL: data collection. XD and TY: data analysis. XD: manuscript preparation. YC and SYi: manuscript revision. FZ: supervision. All authors contributed to the article and approved the submitted version.

FUNDING

This study was supported by grants from the National Natural Science Foundation of Outstanding Youth Fund in China (No. 81622052), the Ten Thousand Talent Program (W02020595), and the Youth Science and Technology Innovative Team of Sichuan Province (2019JDTD0011).

ACKNOWLEDGMENTS

We were grateful to Peiming Feng, Tingting Ma, and Jie Wu for the patient recruitment and Xueling Suo and Du Lei for MRI data acquisition and interpretation.

REFERENCES

Allen, G., Buxton, R. B., Wong, E. C., and Courchesne, E. (1997). Attentional activation of the cerebellum independent of motor involvement. *Science* 275, 1940–1943. doi: 10.1126/science.275.5308.1940

Bao, C., Wang, D., Liu, P., Shi, Y., Jin, X., Wu, L., et al. (2017). Effect of electro-acupuncture and moxibustion on brain connectivity in patients with Crohn's disease: a resting-state fMRI Study. *Front. Hum. Neurosci.* 11:559. doi: 10.3389/fnhum.2017.00559

Brewer, J. A., Worhunsky, P. D., Gray, J. R., Tang, Y. Y., Weber, J., and Kober, H. (2011). Meditation experience is associated with differences in default mode network activity and connectivity. *Proc. Natl. Acad. Sci. U.S.A.* 108, 20254–20259. doi: 10.1073/pnas.1112029108

Cao, F. L. T., Ha, L. J., Shan, C. X., Zhi, M. J., and Wang, F. C. (2016a). Analysis of compatibility laws for acupoint selection of acupuncture in treating diabetic gastroparasis. *Chin. J. Integr. Trad. West Med.* 36, 549–552.

Cao, F. L. T., Shan, C. X., Ha, L. J., Li, Y. Q., and Wang, F. C. (2016b). Study of the acupoint selection rules to treat diabetic gastroparesis with acupuncture based on the literature analysis. *Chin. J. Basic Med. Trad. Chin. Med.* 22, 110–214.

Cavanna, A. E., and Trimble, M. R. (2006). The precuneus: a review of its functional anatomy and behavioural correlates. *Brain* 129(Pt 3), 564–583. doi: 10.1093/brain/awl004

Chen, Y., Zhao, Y., Tan, R. Y., Zhang, P. Y., Long, T., Shi, Y., et al. (2021). The influence of stomach Back-Shu and Front-Mu points on insular functional connectivity in functional dyspepsia rat models. *Evid. Based Complement. Alternat. Med.* 2021:2771094. doi: 10.1155/2021/2771094

Chung, V. C., Wong, C. H., Wu, I. X., Ching, J. Y., Cheung, W. K., Yip, B. H., et al. (2019). Electroacupuncture plus on-demand gastrocaine for refractory functional dyspepsia: pragmatic randomized trial. *J. Gastroenterol. Hepatol.* 34, 2077–2085. doi: 10.1111/jgh.14737

DiGuiseppi, J., and Tadi, P. (2021). *Neuroanatomy, Postcentral Gyrus*. Treasure Island, FL: StatPearls.

Drossman, D. A. (2016). Functional gastrointestinal disorders: history, pathophysiology, clinical features and Rome IV. *Gastroenterology* 150, 1262–1279. doi: 10.1053/j.gastro.2016.02.032

Ghoshal, U. C., Singh, R., Chang, F. Y., Hou, X., Wong, B. C., Kachintorn, U., et al. (2011). Epidemiology of uninvestigated and functional dyspepsia in Asia: facts and fiction. *J. Neurogastroenterol. Motil.* 17, 235–244. doi: 10.5056/jnm.2011.17.3.235

Gu, Y., Han, F., and Liu, X. (2019). Arousal contributions to resting-state fMRI connectivity and dynamics. *Front. Neurosci.* 13:1190. doi: 10.3389/fnins.2019.01190

Ladabaum, U., Minoshima, S., Hasler, W. L., Cross, D., Chey, W. D., and Owyang, C. (2001). Gastric distention correlates with activation of multiple cortical and subcortical regions. *Gastroenterology* 120, 369–376. doi: 10.1053/gast.2001.21201

Lee, I. S., Kullmann, S., Scheffler, K., Preissl, H., and Enck, P. (2018). Fat label compared with fat content: gastrointestinal symptoms and brain activity in functional dyspepsia patients and healthy controls. *Am. J. Clin. Nutr.* 108, 127–135. doi: 10.1093/ajcn/nqy077

Lee, I. S., Wang, H., Chae, Y., Preissl, H., and Enck, P. (2016). Functional neuroimaging studies in functional dyspepsia patients: a systematic review. *Neurogastroenterol. Motil.* 28, 793–805. doi: 10.1111/nmo.12793

Li, Z., Zeng, F., Yang, Y., Chen, Y., Zhang, D., Sun, J., et al. (2014). Different cerebral responses to puncturing at ST36 among patients with functional dyspepsia and healthy subjects. *Forsch. Komplementmed.* 21, 99–104. doi: 10.1159/000360804

Liu, M. L., Liang, F. R., Zeng, F., Tang, Y., Lan, L., and Song, W. Z. (2012). Cortical-limbic regions modulate depression and anxiety factors in functional dyspepsia: a PET-CT study. *Ann. Nucl. Med.* 26, 35–40. doi: 10.1007/s12149-011-0537-4

Liu, P., Zeng, F., Yang, F., Wang, J., Liu, X., Wang, Q., et al. (2014). Altered structural covariance of the striatum in functional dyspepsia patients. *Neurogastroenterol. Motil.* 26, 1144–1154. doi: 10.1111/nmo.12372

Liu, P., Zeng, F., Zhou, G., Wang, J., Wen, H., von Deneen, K. M., et al. (2013). Alterations of the default mode network in functional dyspepsia patients: a resting-state fmri study. *Neurogastroenterol. Motil.* 25, e382–e388. doi: 10.1111/nmo.12131

Liu, S., Wang, Z., Su, Y., Qi, L., Yang, W., Fu, M., et al. (2021). A neuroanatomical basis for electroacupuncture to drive the vagal-adrenal axis. *Nature* 598, 641–645. doi: 10.1038/s41586-021-04001-4

Lundeberg, T., Lund, I., and Naslund, J. (2007). Acupuncture–self-appraisal and the reward system. *Acupunct. Med.* 25, 87–99. doi: 10.1136/aim.25.3.87

Ma, T. T., Yu, S. Y., Li, Y., Liang, F. R., Tian, X. P., Zheng, H., et al. (2012). Randomised clinical trial: an assessment of acupuncture on specific meridian or specific acupoint vs. sham acupuncture for treating functional dyspepsia. *Aliment. Pharmacol. Ther.* 35, 552–561. doi: 10.1111/j.1365-2036.2011.04979.x

Mahadeva, S., and Ford, A. C. (2016). Clinical and epidemiological differences in functional dyspepsia between the East and the West. *Neurogastroenterol. Motil.* 28, 167–174. doi: 10.1111/nmo.12657

Nan, J., Liu, J., Zhang, D., Yang, Y., Yan, X., Yin, Q., et al. (2014). Altered intrinsic regional activity and corresponding brain pathways reflect the symptom severity of functional dyspepsia. *Neurogastroenterol. Motil.* 26, 660–669. doi: 10.1111/nmo.12311

Pariente, J., White, P., Frackowiak, R. S., and Lewith, G. (2005). Expectancy and belief modulate the neuronal substrates of pain treated by acupuncture. *Neuroimage* 25, 1161–1167. doi: 10.1016/j.neuroimage.2005.01.016

Power, J. D., Barnes, K. A., Snyder, A. Z., Schlaggar, B. L., and Petersen, S. E. (2012). Spurious but systematic correlations in functional connectivity MRI networks arise from subject motion. *Neuroimage* 59, 2142–2154. doi: 10.1016/j.neuroimage.2011.10.018

Qi, R., Shi, Z., Weng, Y., Yang, Y., Zhou, Y., Surento, W., et al. (2020). Similarity and diversity of spontaneous brain activity in functional dyspepsia subtypes. *Acta Radiol.* 61, 927–935. doi: 10.1177/0284185119883391

Sajonz, B., Kahnt, T., Margulies, D. S., Park, S. Q., Wittmann, A., Stoy, M., et al. (2010). Delineating self-referential processing from episodic memory retrieval: common and dissociable networks. *Neuroimage* 50, 1606–1617. doi: 10.1016/j.neuroimage.2010.01.087

Scharmuller, W., Ubel, S., Ebner, F., and Schienle, A. (2012). Appetite regulation during food cue exposure: a comparison of normal-weight and obese women. *Neurosci. Lett.* 518, 106–110. doi: 10.1016/j.neulet.2012.04.063

Sun, R., He, Z., Ma, P., Yin, S., Yin, T., Liu, X., et al. (2021a). The participation of basolateral amygdala in the efficacy of acupuncture with deqi treating for functional dyspepsia. *Brain Imaging Behav.* 15, 216–230. doi: 10.1007/s11682-019-00249-7

Sun, R., Ma, P., He, Z., Yin, T., Qu, Z., Yin, S., et al. (2021b). Changed ACC-DMN functional connectivity after acupunture with deqi for functional dyspepsia treatment. *World J. Acupunct. Moxibustion* 31, 6–15.

Tack, J., and Camilleri, M. (2018). New developments in the treatment of gastroparesis and functional dyspepsia. *Curr. Opin. Pharmacol.* 43, 111–117. doi: 10.1016/j.coph.2018.08.015

Tack, J., and Talley, N. J. (2013). Functional dyspepsia–symptoms, definitions and validity of the Rome III criteria. *Nat. Rev. Gastroenterol. Hepatol.* 10, 134–141. doi: 10.1038/nrgastro.2013.14

Tack, J., Masuy, I., Van Den Houte, K., Wauters, L., Schol, J., Vanuytsel, T., et al. (2019). Drugs under development for the treatment of functional dyspepsia and related disorders. *Expert Opin. Investig. Drugs* 28, 871–889. doi: 10.1080/13543784.2019.1673365

Takahashi, T. (2006). Acupuncture for functional gastrointestinal disorders. *J. Gastroenterol.* 41, 408–417. doi: 10.1007/s00535-006-1773-6

Talley, N. J., Haque, M., Wyeth, J. W., Stace, N. H., Tytgat, G. N., Stanghellini, V., et al. (1999). Development of a new dyspepsia impact scale: the Nepean Dyspepsia index. *Aliment. Pharmacol. Ther.* 13, 225–235. doi: 10.1046/j.1365-2036.1999.00445.x

Talley, N. J., Locke, G. R. III, Lahr, B. D., Zinsmeister, A. R., Tougas, G., Ligozio, G., et al. (2006). Functional dyspepsia, delayed gastric emptying, and impaired quality of life. *Gut* 55, 933–939. doi: 10.1136/gut.2005.078634

Tuulari, J. J., Karlsson, H. K., Hirvonen, J., Salminen, P., Nuutila, P., and Nummenmaa, L. (2015). Neural circuits for cognitive appetite control in healthy and obese individuals: an fMRI study. *PLoS One* 10:e0116640. doi: 10.1371/journal.pone.0116640

Utevsky, A. V., Smith, D. V., and Huettel, S. A. (2014). Precuneus is a functional core of the default-mode network. *J. Neurosci.* 34, 932–940. doi: 10.1523/JNEUROSCI.4227-13.2014

Van Oudenhove, L., Vandenberghe, J., Dupont, P., Geeraerts, B., Vos, R., Dirix, S., et al. (2010). Abnormal regional brain activity during rest and (anticipated)

gastric distension in functional dyspepsia and the role of anxiety: a H(2)(15)O-PET study. *Am. J. Gastroenterol.* 105, 913–924. doi: 10.1038/ajg.2010.39

Vanner, S., Greenwood-Van Meerveld, B., Mawe, G., Shea-Donohue, T., Verdu, E. F., Wood, J., et al. (2016). Fundamentals of neurogastroenterology: basic science. *Gastroenterology* 150, 1280–1291. doi: 10.1053/j.gastro.2016.02.01

Wang, X. Y., Wang, H., Guan, Y. Y., Cai, R. L., and Shen, G. M. (2021). Acupuncture for functional gastrointestinal disorders: a systematic review and meta-analysis. *J. Gastroenterol. Hepatol.* 36, 3015–3026. doi: 10.1111/jgh.15645

Winter, S. R., Yokum, S., Stice, E., Osipowicz, K., and Lowe, M. R. (2017). Elevated reward response to receipt of palatable food predicts future weight variability in healthy-weight adolescents. *Am. J. Clin. Nutr.* 105, 781–789. doi: 10.3945/ajcn.116.141143

Xu, S., Hou, X., Zha, H., Gao, Z., Zhang, Y., and Chen, J. D. (2006). Electroacupuncture accelerates solid gastric emptying and improves dyspeptic symptoms in patients with functional dyspepsia. *Dig. Dis. Sci.* 51, 2154–2159. doi: 10.1007/s10620-006-9412-x

Yamawaki, H., Futagami, S., Wakabayashi, M., Sakasegawa, N., Agawa, S., Higuchi, K., et al. (2018). Management of functional dyspepsia: state of the art and emerging therapies. *Ther. Adv. Chronic. Dis.* 9, 23–32. doi: 10.1177/2040622317725479

Yan, B., Li, K., Xu, J., Wang, W., Li, K., Liu, H., et al. (2005). Acupoint-specific fMRI patterns in human brain. *Neurosci. Lett.* 383, 236–240. doi: 10.1016/j.neulet.2005.04.021

Yang, J. W., Wang, L. Q., Zou, X., Yan, S. Y., Wang, Y., Zhao, J. J., et al. (2020). Effect of acupuncture for postprandial distress syndrome: a randomized clinical trial. *Ann. Intern. Med.* 172, 777–785. doi: 10.7326/M19-2880

Yang, M., Yang, J., Zeng, F., Liu, P., Lai, Z., Deng, S., et al. (2014). Electroacupuncture stimulation at sub-specific acupoint and non-acupoint induced distinct brain glucose metabolism change in migraineurs: a PET-CT study. *J. Transl. Med.* 12:351. doi: 10.1186/s12967-014-0351-6

Yeo, S., van den Noort, M., Bosch, P., and Lim, S. (2016). Ipsilateral putamen and insula activation by both left and right GB34 acupuncture stimulation: an fMRI study on healthy participants. *Evid. Based Complement. Alternat. Med.* 2016:4173185. doi: 10.1155/2016/4173185

Yin, S., Chen, Y., Lei, D., Sun, R. R., Ma, T. T., Feng, P. M., et al. (2017). Cerebral mechanism of puncturing at He-Mu point combination for functional dyspepsia: study protocol for a randomized controlled parallel trial. *Neural Regen. Res.* 12, 831–840. doi: 10.4103/1673-5374.206655

Yokum, S., and Stice, E. (2013). Cognitive regulation of food craving: effects of three cognitive reappraisal strategies on neural response to palatable foods. *Int. J. Obes. (Lond.)* 37, 1565–1570. doi: 10.1038/ijo.2013.39

Yu, Y., Chen, L., Wang, Q., Hu, L., Ding, Q., Jia, X., et al. (2019). Altered amplitude of low-frequency fluctuations in inactive patients with nonneuropsychiatric systemic lupus erythematosus. *Neural Plast.* 2019:9408612. doi: 10.1155/2019/9408612

Zeng, F., Lan, L., Tang, Y., Liu, M., Liu, X., Song, W., et al. (2015). Cerebral responses to puncturing at different acupoints for treating meal-related functional dyspepsia. *Neurogastroenterol. Motil.* 27, 559–568. doi: 10.1111/nmo.12532

Zeng, F., Qin, W., Liang, F., Liu, J., Tang, Y., Liu, X., et al. (2011). Abnormal resting brain activity in patients with functional dyspepsia is related to symptom severity. *Gastroenterology* 141, 499–506. doi: 10.1053/j.gastro.2011.05.003

Zeng, F., Qin, W., Ma, T., Sun, J., Tang, Y., Yuan, K., et al. (2012). Influence of acupuncture treatment on cerebral activity in functional dyspepsia patients and its relationship with efficacy. *Am. J. Gastroenterol.* 107, 1236–1247. doi: 10.1038/ajg.2012.53

Zeng, F., Qin, W., Yang, Y., Zhang, D., Liu, J., Zhou, G., et al. (2013). Regional brain structural abnormality in meal-related functional dyspepsia patients: a voxel-based morphometry study. *PLoS One* 8:e68383. doi: 10.1371/journal.pone.0068383

Zeng, F., Song, W. Z., Liu, X. G., Xie, H. J., Tang, Y., Shan, B. C., et al. (2009). Brain areas involved in acupuncture treatment on functional dyspepsia patients: a PET-CT study. *Neurosci. Lett.* 456, 6–10. doi: 10.1016/j.neulet.2009.03.080

Zhao, T., Pei, L., Ning, H., Guo, J., Song, Y., Zhou, J., et al. (2021). Networks are associated with acupuncture treatment in patients with diarrhea-predominant irritable bowel syndrome: a resting-state imaging study. *Front. Hum. Neurosci.* 15:736512. doi: 10.3389/fnhum.2021.736512

Zheng, W., Su, Z., Liu, X., Zhang, H., Han, Y., Song, H., et al. (2018). Modulation of functional activity and connectivity by acupuncture in patients with Alzheimer disease as measured by resting-state fMRI. *PLoS One* 13:e0196933. doi: 10.1371/journal.pone.0196933

Zhou, S., Zeng, F., Liu, J., Zheng, H., Huang, W., Liu, T., et al. (2013). Influence of acupuncture stimulation on cerebral network in functional diarrhea. *Evid. Based Complement. Alternat. Med.* 2013:975769. doi: 10.1155/2013/975769

Zung, W. W. (1971). A rating instrument for anxiety disorders. *Psychosomatics* 12, 371–379. doi: 10.1016/S0033-3182(71)71479-0

Zung, W. W., Richards, C. B., and Short, M. J. (1965). Self-rating depression scale in an outpatient clinic. Further validation of the SDS. *Arch. Gen. Psychiatry* 13, 508–515. doi: 10.1001/archpsyc.1965.01730060026004

Conflict of Interest: The authors declare that the research was conducted in the absence of any commercial or financial relationships that could be construed as a potential conflict of interest.

Publisher's Note: All claims expressed in this article are solely those of the authors and do not necessarily represent those of their affiliated organizations, or those of the publisher, the editors and the reviewers. Any product that may be evaluated in this article, or claim that may be made by its manufacturer, is not guaranteed or endorsed by the publisher.

frontiers | Frontiers in Neuroscience

ORIGINAL RESEARCH
published: 03 May 2022
doi: 10.3389/fnins.2022.878541

Pyrroloquinoline Quinone Regulates Enteric Neurochemical Plasticity of Weaned Rats Challenged With Lipopolysaccharide

*Chenyu Shi[1], Song Xu[1], Caiyun Huang[2], Zijie Wang[1], Wenhui Wang[1], Dongxu Ming[1], Xindi Yin[3], Hu Liu[1] and Fenglai Wang[1]**

[1] State Key Lab of Animal Nutrition, College of Animal Science and Technology, China Agricultural University, Beijing, China, [2] College of Animal Science, Fujian Agriculture and Forestry University, Fuzhou, China, [3] Department of Nutrition and Health, China Agricultural University, Beijing, China

The enteric nervous system (ENS) is important for the intestinal barrier to defend and regulate inflammation in the intestine. The aim of this study was to investigate the effect of pyrroloquinoline quinone (PQQ) on regulating neuropeptide secretion by ENS neurons of rats challenged with lipopolysaccharide (LPS) to create enteritis. Thirty Sprague Dawley rats were divided into five groups, namely, basal (CTRL), basal plus LPS challenge (LPS), basal with 2.5 mg/kg b.w./day of PQQ plus challenge with LPS (PQQ 2.5), basal with 5.0 mg/kg b.w./day PQQ plus challenge with LPS (PQQ 5), and basal with 10.0 mg/kg b.w./day PQQ plus challenge with LPS (PQQ 10). After treatment with basal diet or PQQ for 14 days, rats were challenged with LPS except for the CTRL group. Rats were euthanized 6 h after the LPS challenge. Rats showed an increased average daily gain in PQQ treatment groups ($P < 0.05$). Compared with the LPS group, PQQ 5 and PQQ 10 rats showed increased villus height and villus height/crypt depth of jejunum ($P < 0.05$). In PQQ treatment groups, concentrations of IL-1β and TNF-α in serum and intestine of rats were decreased, and IL-10 concentration was increased in serum compared with the LPS group ($P < 0.05$). Compared with the LPS group, the concentration of neuropeptide Y (NPY), nerve growth factor (NGF), vasoactive intestinal peptide (VIP), substance P (SP), calcitonin gene-related peptide (CGRP), and brain-derived neurotropic factor (BDNF) in serum were decreased in PQQ treatment groups ($P < 0.05$). Compared with the LPS group, ileal mRNA levels of BDNF, NPY, and NGF were decreased in PQQ treatment groups ($P < 0.05$). Jejunal concentrations of SP, CGRP, VIP, BDNF, NPY, and NGF were decreased in PQQ treatment groups compared with the LPS group ($P < 0.05$). Compared with the LPS group, phosphor-protein kinase B (p-Akt)/Akt levels in jejunum and colon were decreased in PQQ treatment groups ($P < 0.05$). In conclusion, daily treatment with PQQ improved daily gain, jejunal morphology, immune responses. PQQ-regulated enteric neurochemical plasticity of ENS *via* the Akt signaling pathway of weaned rats suffering from enteritis.

Keywords: pyrroloquinoline quinone, enteric nervous system, neurochemical plasticity, Akt signaling pathway, enteritis rats

OPEN ACCESS

Edited by:
Chunhui Bao,
Shanghai University of Traditional Chinese Medicine, China

Reviewed by:
Katarzyna Palus,
University of Warmia and Mazury in Olsztyn, Poland
Yulan Liu,
Wuhan Polytechnic University, China

****Correspondence:***
Fenglai Wang
wangfl@cau.edu.cn

Specialty section:
This article was submitted to Gut-Brain Axis, a section of the journal Frontiers in Neuroscience

Received: *18 February 2022*
Accepted: *15 March 2022*
Published: *03 May 2022*

Citation:
Shi C, Xu S, Huang C, Wang Z, Wang W, Ming D, Yin X, Liu H and Wang F (2022) Pyrroloquinoline Quinone Regulates Enteric Neurochemical Plasticity of Weaned Rats Challenged With Lipopolysaccharide. Front. Neurosci. 16:878541. doi: 10.3389/fnins.2022.878541

INTRODUCTION

The intestine is the body organ with the largest membrane surface area that serves to absorb nutrients and sense, and recognize and defend against pathogens, antigens, toxins, and other detrimental secretions. The intestine accomplishes these diverse functions through coordinated effects of the enteroendocrine system, the enteric nervous system (ENS), the gut immune system, and the non-immune defense system of the intestine (Ferraris et al., 1989; De Giorgio, 2006). Intestinal nerve cells and glial cells in the ENS secrete neuropeptides and immune factors to pass signals between the ENS and the central nervous system (CNS). These signals influence mucosal secretions and gastrointestinal peristalsis and affect rhythms and hormone secretion in the CNS (Rao and Gershon, 2018; Boesmans et al., 2019). The ENS plays an important role in intestinal diseases, such as colitis, irritable bowel syndrome, and inflammatory bowel disease (Lasrado et al., 2017; Resnikoff et al., 2019; Jarret et al., 2020). The ENS, which includes submucosal nerve plexus, myenteric nerve plexus, and glial cells, usually is functional and structurally mature during the early life of mammals (Montedonico et al., 2006; Parathan et al., 2020). The capacity to regulate neuropeptides is called neurochemical plasticity. Enteric neuroplasticity is an adaption to intestinal contents and the intestinal microenvironment and is pronounced during early development in mammals (Moeser et al., 2017).

The phosphatidylinositol-3 kinase (PI3K)/protein kinase B (Akt) signaling pathway regulates the activity ofglycogen synthase kinase-3β (GSK-3β), Tau protein, and *N*-methyl-D-aspartame receptor (NMDA), which promotes the development of nerve cells and regeneration of synapses (Iqbal et al., 2016; Majewska and Szeliga, 2017; Falcon et al., 2019). The PI3K/Akt signaling pathway also plays an important regulatory role in intestinal neurological diseases by reducing the oxidative stress and apoptosis of nerve cells, improving the secretion of neurotropic factors, regulating survival and differentiation of nerve cells,and promoting the proliferation of intestinal nerve cells and glial cells (Ichihara et al., 2004; Du et al., 2009; Becker et al., 2013).

Pyrroloquinoline quinone (PQQ), a water-soluble quinone compound, was discovered as a redox cofactor of methanol dehydrogenase in pseudomonas TP1 and other Gram-negative bacteria (Duine et al., 1979; Duine, 1991). We demonstrated previously that dietary supplementation with PQQ could regulate intestinal morphology, mucosal barrier function, colonic microbiota, and antioxidant status to reduce diarrhea and improve the growth performance of weaned pigs (Yin et al., 2019; Huang et al., 2020, 2021; Ming et al., 2021). PQQ is a potent neuroprotective nutrient in the CNS and peripheral nerves, which can mitigate sciatic nerve injury, reduce neurotoxin-induced neurotoxicity, and promote neuronal cell regeneration (Liu et al., 2005; Hara et al., 2007; Shanan et al., 2019). PQQ treatment can ameliorate signs of memory impairment in aging mice and schizophrenic rats *via* reducing the expression of phosphorylation Akt and maintaining the GSK-3β level in the hippocampus (Zhou X. Q. et al., 2018; Zhou et al., 2020).

We hypothesized that PQQ treatment could influence the ENS and regulate enteric neuroplasticity to improve intestinal health. We tested this hypothesis in the enteritis rat model *via* developed challenging rats with lipopolysaccharide (LPS). We detected neuropeptides in serum and intestine and Akt signaling pathway expression in the intestine to determine if PQQ could regulate enteric neuroplasticity *via* the Akt signaling pathway.

MATERIALS AND METHODS

Animals and Experimental Treatment

All experimental protocols in this study were approved by the Animal Subjects Committee of China Agricultural University (Beijing, China) and carried out based on the National Research Council's Guide for the Care and Use of Laboratory Animals (AW01211202-1-2). Sprague Dawley male rats (n = 30, 21 days old) were purchased from SPF (Beijing) Biotechnology Co. Ltd., and were housed in a pathogen-free animal room with a 12/12 h light-dark cycle at 23°C. After 3 days of acclimatization, rats were divided randomly into 5 groups (n = 6 per treatment group), namely, (1) basal unchallenged (CTRL), (2) LPS challenged (LPS), (3) 2.5 mg/kg b.w./day low dose of PQQ and challenged with LPS (PQQ 2.5), (4) 5.0 mg/kg b.w./day medium dose of PQQ and challenged with LPS (PQQ 5), and (5) 10.0 mg/kg b.w./day high dose of PQQ and challenged with LPS (PQQ 10) (Lu et al., 2015). PQQ·Na_2 (purity, ≥98%; Changmao Biochemical Engineering Co. Ltd., Changzhou, China) dissolved in physiological saline was administrated intragastrically for 14 days. All rats were weighed every day and had free access to water and food. After the supplementation period, rats were injected with LPS [4 mg/kg b.w., isolated from *Escherichia coli* (serotype 055: B5) (Zani et al., 2008), purchased from Sigma, United States] except rats in the CTRL group on day 15. All rats were euthanized by intraperitoneal injection with pentobarbitone sodium (50 mg/kg b.w.) (Mohamed et al., 2020) at 6 h after the LPS dose.

Sample Collection

After euthanasia, serum samples were collected from the abdominal veins of rats and separated into serum and stored at −20°C for further analysis. Jejunal and colonic tissues (1 cm^2) were excised and stored in 4% paraformaldehyde solution (40% formaldehyde solution dissolved in phosphate-buffered saline (PBS)) for analysis of intestinal morphology. Notably, 2 cm segments from the middle of the jejunum, ileum, and colon were collected in freezing tubes which were frozen rapidly in liquid nitrogen and stored at −80°C for further analysis.

Jejunal Morphology

After fixation with 4% paraformaldehyde solution for 24 h, tissue samples were dehydrated and embedded in paraffin. Jejunal sections (5 μm) were stained with hematoxylin and eosin. Villus height (VH), crypt depth (CD), and villus height/crypt depth ratio (VCR) were viewed and evaluated using a microscope (Eclipse CI, Nikon) and imaging software (DS-U3, Nikon). Data

were collected from at least 10 well-oriented villi and crypts from 5 slides per sample.

Cytokines of Serum and Intestinal Segments

Cytokines, including interleukin (IL)-1β, IL-6, IL-10, and tumor necrosis factor (TNF)-α, were determined in serum, jejunum, ileum, and colon using enzyme-linked immunoassay (ELISA) kits (Beijing Kang Iia Hong Yuan Biological Technology Co., Ltd., Beijing, China) according to the manufacturer's instructions and quantified using a Multiskan Microplate Reader (Thermo Fisher Scientific, United States). Absorbance for kits was all set at 450 nm, and the minimal detections were 31.25 pg/ml for IL-1β and IL-6, 15.63 pg/ml for IL-10, and 9.38 pg/ml for TNF-α. The intra- and inter-assay coefficients of variation (CV) were $<$10% for each assay.

Quantitative Real-Time Polymerase Chain Reaction

Total RNA was extracted from the snap-frozen ileal tissue using RNAiso Plus (9109, TaKaRa Bio, Inc., Japan)/chloroform extraction. Complementary DNA (cDNA) was synthesized using the PrimeScript RT Reagent Kit with gDNA Eraser (RR047A, TaKaRa Bio, Inc., Japan). Quantitative real-time polymerase chain reaction PCR (RT-PCR) was conducted using the Roche Light Cycler® System (Roche, South San Francisco, CA, Canada). The primer sequences are shown in **Supplementary Table 1**. Target genes were detected by normalizing with β-actin and calculating using the $2^{-\Delta\Delta CT}$ method (Pfaffl et al., 2002).

Determination of the Concentration of Neuropeptides

Neuropeptides including neuropeptide Y (NPY), nerve growth factor (NGF), vasoactive intestinal peptide (VIP), substance P (SP), calcitonin gene-related peptide (CGRP), and brain-derived neurotropic factor (BDNF) were determined in serum using assay kits according to the manufacturer's instructions (**Supplementary Table 2**). These same neuropeptides were determined in the jejunum, ileum, and colon.

Immunohistochemistry

Fixed jejunum and colon tissues were embedded in paraffin and cut into sections (5 μm) followed by deparaffinization and rehydration. Tissue sections were placed in ethylenediaminetetraacetic acid (EDTA) antigen retrieval buffer (pH 8.0) to retrieve the antigen. Endogenous peroxidase activity was blocked with 3% H_2O_2 under dark conditions at room temperature and was then washed with PBS (PBS, pH 7.4). Bovine serum albumin (BSA, 5%) was added to tissues. Primary antibodies (**Supplementary Table 3**) diluted in PBS were incubated with tissue sections overnight at 4°. Tissue sections were covered with secondary antibodies for 50 min at room temperature, and positive expression for protein gene product 9.5 (PGP9.5), SP, CGRP, BDNF, NPY, and NGF was dyed brown with diaminobenzidine (DAB). Hematoxylin was used as a counterstain for nuclei dyed blue. Ganglia immunoreactive for neuropeptides was calculated in percentage in the total area of neurons.

Western Blot Assay

Jejunal and colonic tissues were ground in liquid nitrogen and lysed using radioimmunoprecipitation assay (RIPA) buffer with protease and phosphatase inhibitors. After sonication and centrifugation, protein concentration in the supernatant was quantified using a bicinchoninic acid (BCA) protein assay kit (02912E, CWbiotech, Beijing, China). Supernatant with 30 μg proteins from each sample was separated in sodium dodecyl sulfate (SDS) polyacrylamide gels and then transferred to polyvinylidene fluoride (PVDF) membranes (0.45 μm, Millipore, United States). Membranes were blocked and incubated with the primary antibodies of phosphatidylinositol 3-kinase (PI3K, #4257, Cell Signaling Technology, Danvers, MA, United States), protein kinase B (Akt, #9272, Cell Signaling Technology), phosphor-Akt (p-Akt, #9271, Cell Signaling Technology), and β-actin (#4970, Cell Signaling Technology) overnight at 4°C. The membranes were incubated with secondary antibodies (111-035-003, Jackson, United States) for 1 h at room temperature and reacted with electrochemiluminescence (ECL, WBKLS0500, Millipore, United States). The intensity of protein bands was analyzed using the ImageJ software.

Statistical Analysis

All data were analyzed with a one-way analysis of variance (ANOVA) using SAS (version 9.2, United States). Differences among mean values were evaluated using the Duncan's multiple range test. The individual rat was the experimental unit for traits of interest. Values are expressed as means and considered statistically different if $P \leq 0.05$. Figures were created using GraphPad Prism 9.

RESULTS

Average Daily Gain

Compared with CTRL and LPS groups, rats assigned to PQQ 5 and PQQ 10 groups expressed increased average daily gain (ADG) ($P < 0.05$, **Figure 1**). Rats assigned to the PQQ 5 group showed the greatest difference in ADG compared with both CTRL and LPS groups.

Jejunal Morphology

Rats challenged with LPS had non-distinct jejunal villus compared with the CTRL group (**Figure 2**). Rats in PQQ 2.5, PQQ 5, and PQQ 10 groups exhibited more complete and taller jejunal villus compared with the LPS group. Compared with the CTRL group, LPS treatment decreased jejunal VH and VCR in rats ($P < 0.05$, **Table 1**). Compared with the LPS group, PQQ 5 and PQQ 10 groups increased VH and VCR of the jejunum ($P < 0.05$). Neither LPS nor PQQ treatments affected CD.

Cytokines in Serum and Intestine

Compared with the CTRL group, concentrations of IL-1β, IL-6, and TNF-α increased, and IL-10 decreased in the serum of rats

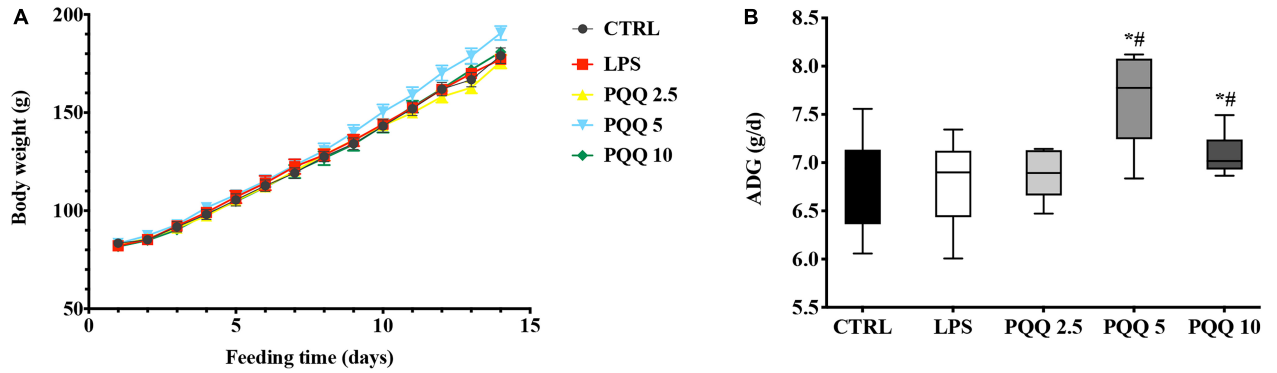

FIGURE 1 | Average daily gain of weaned rats (n = 6). **(A)** Body weight of rats was recorded with feeding time. **(B)** Average daily gain(ADG) of rats was evaluated by body weight. CTRL, control treatment; lipopolysaccharide (LPS), control and LPS treatment; pyrroloquinoline quinone (PQQ) 2.5, intragastric administration with 2.5 mg/kg b.w./day PQQ·Na_2 treatment; PQQ 5, intragastric administration with 5.0 mg/kg b.w./day PQQ·Na_2treatment; PQQ 10, intragastric administration with 10.0 mg/kg b.w./day PQQ·Na_2 treatment. *Means significant difference with the CTRL group ($P \leq 0.05$); #means significant difference with the LPS group ($P \leq 0.05$).

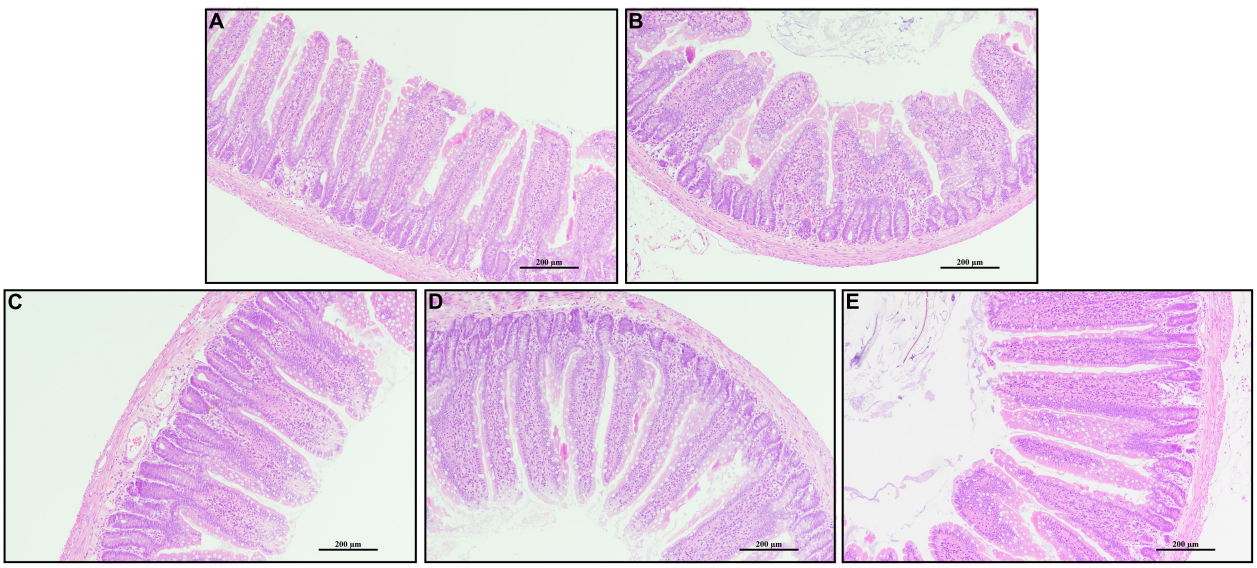

FIGURE 2 | Jejunal morphology by H and E stains. **(A)** Control treatment; **(B)** control and LPStreatment; **(C)** intragastric administration with 2.5 mg/kg b.w./day PQQ·Na_2 treatment; **(D)** intragastric administration with 5.0 mg/kg b.w./day PQQ·Na_2 treatment; and **(E)** intragastric administration with 10.0 mg/kg b.w./day PQQ·Na_2 treatment. Scale bars in pictures are 200 μm.

TABLE 1 | Jejunal villous morphology of weaned rats (n = 6).[1]

Items	Treatments					SEM	*P*-values
	CTRL	LPS	PQQ 2.5	PQQ 5	PQQ 10		
VH, μm	434.20	373.44*	389.78	472.57#	436.88#	10.99	0.02
CD, μm	113.79	120.79	121.82	122.60	112.33	2.52	0.60
VCR	3.86	3.12*	3.23*	3.92#	3.92#	0.11	0.03

[1]*CTRL, control treatment; LPS, control and LPS treatment; pyrroloquinoline quinone (PQQ) 2.5, intragastric administration with 2.5 mg/kg b.w./day PQQ·Na_2 treatment; PQQ 5, intragastric administration with 5.0 mg/kg b.w./day PQQ·Na_2 treatment; PQQ 10, intragastric administration with 10.0 mg/kg b.w./day PQQ·Na_2 treatment. VH, villus height; CD, crypt depth; VCR, villus height/crypt depth. *Means significant difference with the CTRL group ($P \leq 0.05$); #means significantdifference with the LPS group ($P \leq 0.05$).*

challenged with LPS ($P < 0.05$, **Figure 3**). Feeding PQQ at 2.5, 5.0, and 10.0 mg/kg b.w. to rats decreased ($P < 0.05$) concentrations of IL-1β and TNF-α, and increased concentration of IL-10 in serum compared with the LPS group. With a similar pattern, concentrations of IL-1β and TNF-α in jejunum, ileum, and colon were increased ($P < 0.05$) in the LPS group compared with the CTRL group. Concentrations of IL-1β and TNF-α in jejunum, ileum, and colon of rats were decreased ($P < 0.05$)compared with rats assigned to the LPS group.

Concentration of Neuropeptides in Serum

Compared with the CTRL group, concentrations of NPY, NGF, VIP, SP, and CGRP were increased ($P < 0.05$, **Figure 4**) in the serum of rats in the LPS group. There were no significant differences in BDNF between LPS and CTRL groups. Concentrations of NPY, NGF, VIP, SP, CGRP, and BDNF were decreased ($P < 0.05$) with PQQ intake compared with the LPS group. Feeding PQQ at 5.0 mg/kg b.w. decreased concentrations of NPY, NGF, VIP, and CGRP more than 2.5 or 10.0 mg/kg b.w. when compared with the LPS group.

mRNA Abundance of Neuropeptides in the Ileum

Compared with the CTRL group, mRNA concentrations for NPY and NGF were increased ($P < 0.05$, **Figure 5**) in the LPS group. Compared with the LPS group, mRNA concentrations for BDNF and NGF were decreased ($P < 0.05$) in PQQ 2.5, and mRNA concentration for NPY decreased ($P < 0.05$) in PQQ 5.

Concentration of Neuropeptides in Jejunum, Ileum and Colon

Compared with the CTRL group, concentrations of all detected neuropeptides were increased ($P < 0.05$, **Table 2**) in the jejunum and ileum of rats in the LPS group. Compared with the LPS group, concentrations of CGRP, VIP, NPY, and NGF were decreased ($P < 0.05$) in PQQ-fed groups in the jejunum, and SP and BDNF concentrations were decreased ($P < 0.05$) in PQQ 5 and PQQ 10 groups. In the ileum, concentrations of all neuropeptides measured were decreased ($P < 0.05$) in all PQQ-fed groups. In the colon, VIP concentration was increased, and BDNF concentration was decreased in the LPS group compared with the CTRL group ($P < 0.05$). Compared with the LPS group, colonic SP concentration was decreased ($P < 0.05$) in PQQ 10, CGRP concentration was increased ($P < 0.05$) in PQQ 5, VIP concentration was decreased ($P < 0.05$) in PQQ 2.5 and PQQ 5, BDNF concentration was increased ($P < 0.05$) in PQQ 5, NPY concentration was increased ($P < 0.05$) in PQQ 10, and NGF concentration was increased in PQQ 5.

Immunostaining of Neuropeptides in Jejunum and Colon

Compared with the CTRL group, the percentage of ganglia immunoreactive for PGP9.5 in the jejunum was decreased ($P < 0.05$, **Table 3**) in the LPS group and showed a lighter PGP9.5-positive area dyed with brown (**Figure 6**). Compared with the LPS group, the PGP9.5 immunoreactive percentage of ganglia in the jejunum of rats was increased ($P < 0.05$, **Table 3**) in the PQQ 5 group. Compared with the CTRL group, NGF-positive surface area in the jejunum was increased ($P < 0.05$, **Table 3**) and dyed darker (**Figure 6**) in the LPS group.

In the colon, SP-positive surface area increased ($P < 0.05$, **Table 3**) in the LPS group compared with the CTRL group. PQQ treatments decreased ($P < 0.05$, **Table 3**) SP-positive surface area in the colon compared with the LPS group. Colonic CGRP, NPY, and NGF were increased in the PQQ 5 group compared with the LPS group ($P < 0.05$, **Table 3**) and dyed darker (**Figure 7**) in the PQQ 5 group.

Activation of the Akt Pathway in Jejunum and Colon

Compared with the CTRL group, p-Akt/Akt was increased in LPS groups both in the jejunum and colon ofrats ($P < 0.05$, **Figures 8A,B**). Compared with the LPS group, p-Akt/Akt was decreased ($P < 0.05$, **Figure 8A**) in the jejunum of rats both in PQQ 2.5 and PQQ 5 groups. Additionally, p-Akt/Akt was decreased in the colon of rats in the PQQ 5 group compared with the LPS group ($P < 0.05$, **Figure 8B**). The abundance of PI3K was not affected by any treatments in both the jejunum and colon.

DISCUSSION

Pyrroloquinoline quinone is a natural antioxidant that has been used in the treatment of osteoporosis, muscle atrophy, radiation poisoning, and arthritis and promotes the growth of the organisms by regulating oxidation, repairing DNA damage, reducing apoptosis, and maintaining mitochondrial function (Kasahara and Kato, 2003; Huang et al., 2017; Wu et al., 2017; Xu et al., 2018; Geng et al., 2019; Jiang et al., 2019). We previously demonstrated that dietary PQQ could increase ADG and gain to feed ratio and reduce diarrhea incidence in weaned pigs (Yin et al., 2019; Huang et al., 2021; Ming et al., 2021). In this study, daily treatment with 5.0 mg/kg and 10.0 mg/kg PQQ increased ADG of rats compared with rats not supplemented with PQQ.

We developed the enteritis model by challenging rats with LPS and verified the existence of enteritis by evaluating jejunal morphology and cytokines in serum and intestine. LPS is a component of Gram-negative bacteria that can damage the intestinal barrier cause immune dysfunction, initiate apoptosis of intestine epithelial cells, and develop enteritis (Yoshioka et al., 2009; Li et al., 2018; Dong et al., 2020). In this study, rats challenged with LPS developed inflamed intestines as evidenced by damaged jejunal morphology, increased concentrations of IL-1β, IL-6, and TNF-α in serum and IL-1β and TNF-α in intestine, and decreased IL-10 in serum. These observations confirmed that rats challenged with LPS developed intestinal inflammation.

Intestinal morphology and immune function improved with PQQ supplementation of LPS-challenged rats. Intestinal damage reduces absorption and metabolism of nutrients and compromises the integrity of the intestinal barrier (Baumgart and Carding, 2007; Turner, 2009; Wang et al., 2015; Zhou et al., 2018). Intestinal morphology can be improved in weaned

TABLE 2 | Neuropeptide concentration in intestinal segments of weaned rats (n = 6).[1]

Items	Treatments					SEM	*P*-values
	CTRL	LPS	PQQ 2.5	PQQ 5	PQQ 10		
Jejunum							
SP (pg/mg)	5.98	8.10*	7.30*	6.28#	5.95#	0.32	< 0.01
CGRP (pg/mg)	8.53	11.02*	10.22*#	8.63#	8.68#	0.24	< 0.01
VIP (pg/mg)	56.56	82.00*	53.60#	65.55#	46.89#	4.47	< 0.01
BDNF (pg/mg)	9.84	14.80*	13.03*	10.61#	9.88#	0.92	0.01
NPY (ng/mg)	13.14	17.58*	10.96#	13.07#	10.32*#	0.77	< 0.01
NGF (pg/mg)	6.15	9.77*	7.24*#	6.33#	6.05#	0.17	< 0.01
Ileum							
SP (pg/mg)	4.96	7.82*	5.03#	5.07#	5.35*#	0.10	< 0.01
CGRP (pg/mg)	14.62	19.34*	15.63#	14.42#	15.87#	0.45	< 0.01
VIP (pg/mg)	31.44	44.58*	27.72*#	32.09#	34.42*#	0.98	< 0.01
BDNF (pg/mg)	27.69	42.70*	32.01*#	35.43*#	34.83*#	0.95	< 0.01
NPY (ng/mg)	6.62	8.53*	6.01*#	6.42#	7.31*#	0.20	< 0.01
NGF (pg/mg)	4.72	7.83*	5.00#	4.43#	5.99*#	0.19	< 0.01
Colon							
SP (pg/mg)	14.61	15.33	15.21	16.66	12.30*#	0.64	0.01
CGRP (pg/mg)	19.17	18.09	18.45	22.41*#	16.74	0.86	< 0.01
VIP (pg/mg)	71.69	103.69*	87.62*#	72.60#	100.42*	4.43	< 0.01
BDNF (pg/mg)	74.59	38.75*	39.55*	63.84#	50.57*	3.75	< 0.01
NPY (ng/mg)	15.3	13.86	15.55	13.28*	20.73*#	0.68	< 0.01
NGF (pg/mg)	12.98	11.85	11.11*	14.24#	11.88	0.68	0.03

[1]SP, substance P; CGRP, calcitonin gene-related peptide; VIP, vasoactive intestinal peptide; BDNF, brain-derived neurotropic factor; NPY, neuropeptide Y; NGF, nerve growth factor. CTRL, control treatment; lipopolysaccharide (LPS), control and LPS treatment; PQQ 2.5, intragastric administration with 2.5 mg/kg b.w./day PQQ·Na_2 treatment; PQQ 5, intragastric administration with 5.0 mg/kg b.w./day PQQ·Na_2 treatment; PQQ 10, intragastric administration with 10.0 mg/kg b.w./day PQQ·Na_2 treatment.

**Means significant difference with the CTRL group ($P \leq 0.05$); #means significantdifference with the LPS group ($P \leq 0.05$).*

TABLE 3 | Percentage of ganglia immunoreactive for neuropeptides in the total area by immunohistochemical staining (n = 6, %).[1]

Items	Treatments				SEM	*P*-values
	CTRL	LPS	PQQ 2.5	PQQ 5		
Jejunum						
PGP9.5	16.88	6.70*	10.79	16.80#	1.47	0.03
SP	0.30	0.43	0.29	0.26	0.03	0.26
CGRP	0.10	0.20	0.09	0.19	0.02	0.25
BDNF	0.49	0.37	0.38	0.32	0.03	0.23
NPY	0.30	0.45	0.59	0.28	0.06	0.26
NGF	2.83	4.11*	4.41*	4.00*	0.19	0.01
Colon						
PGP9.5	20.06	16.42	16.38	24.77	2.07	0.46
SP	0.06	0.14*	0.04#	0.07#	0.01	0.00
CGRP	0.09	0.08	0.10	0.18#	0.02	0.23
BDNF	0.77	0.40	0.42	0.52	0.08	0.42
NPY	0.44	0.36	0.28	0.61#	0.05	0.05
NGF	3.45	2.48	3.16	5.19#	0.41	0.13

[1]PGP9.5, protein gene product 9.5; CGRP, calcitonin gene-related peptide; NGF, nerve growth factor. CTRL, control treatment; LPS, control and LPS treatment; PQQ 2.5, intragastric administration with 2.5 mg/kg b.w./day PQQ·Na_2 treatment; PQQ 5, intragastric administration with 5.0 mg/kg b.w./day PQQ·Na_2 treatment; PQQ 10, intragastric administration with 10.0 mg/kg b.w./day PQQ·Na_2 treatment.

**Means significant difference with the CTRL group ($P \leq 0.05$); #means significantdifference with the LPS group ($P \leq 0.05$).*

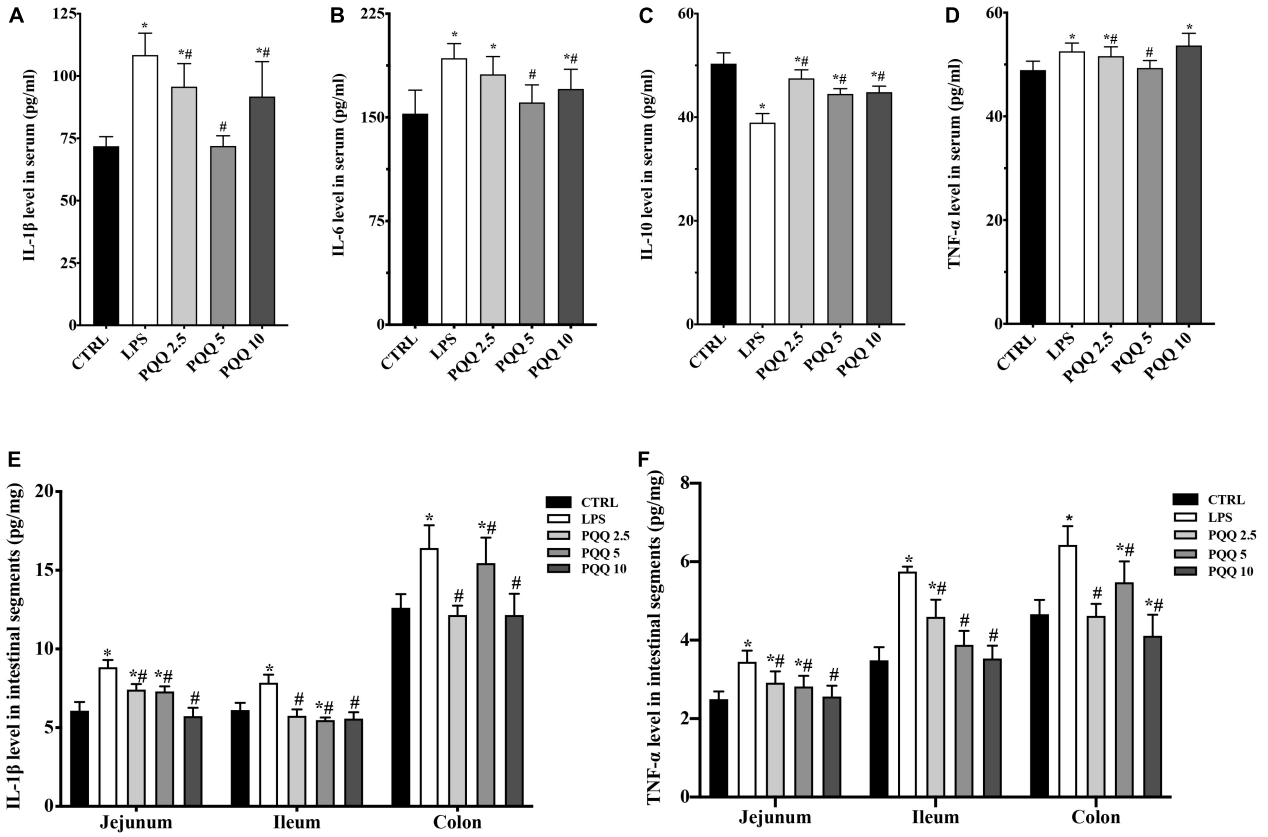

FIGURE 3 | Cytokine level in serum and intestinal segments of weaned rats. **(A)** IL-1β level in serum (n = 6); **(B)** IL-6 level in serum (n = 6); **(C)** IL-10 level in serum (n = 5); **(D)** TNF-α level in serum (n = 6); **(E)** IL-1β level in jejunum, ileum and colon (n = 6); and **(F)** TNF-α level in jejunum, ileum and colon (n = 6). CTRL, control treatment; LPS, control and LPS treatment; PQQ 2.5, intragastric administration with 2.5 mg/kg b.w./day PQQ·Na_2 treatment; PQQ 5, intragastric administration with 5.0 mg/kg b.w./day PQQ·Na_2 treatment; PQQ 10, intragastric administration with 10.0 mg/kg b.w./day PQQ·Na_2 treatment. *Means significant difference with the CTRL group ($P \leq 0.05$); #means significant difference with the LPS group ($P \leq 0.05$).

rats when they were supplemented with PQQ (Zhang et al., 2019). Our previous study showed that dietary supplementation with PQQ can increase intestinal VH and VCR in weaned pigs (Yin et al., 2019). In this study, PQQ treatment increased jejunal VH and VCR compared with rats challenged with LPS. PQQ has anti-inflammatory effects and can reduce arthritis by inhibiting the production of pro-inflammatory cytokines such as TNF-α and IL-6 (Harris et al., 2013; Liu et al., 2016). In our previous study, PQQ supplementation reduced gut inflammation which improved intestinal health and growth of weaned pigs (Yin et al., 2019; Huang et al., 2020). In this study, PQQ supplementation decreased concentrations of pro-inflammatory cytokines in serum and intestine and increased concentrations of the anti-inflammatory cytokine and IL-10 in serum, which confirmed that PQQ regulates immune responses.

Pyrroloquinoline quinone can regulate enteric nervous damage induced by LPS challenge. The ENS regulates intestinal secretions, peristalsis, and immunity through endocrine substances and neuropeptides secreted by myenteric neurons, submucosal neurons, and glial cells (Rao and Gershon, 2018; Boesmans et al., 2019). Normally, the neuropeptides are divided into inhibitory neurotransmitters and excitatory neurotransmitters to control intestinal relaxation and contraction, respectively (Rao and Gershon, 2018). When the intestine suffers pressure, mucosal damage, and inflammation, the ENS can release neuropeptides to regulate intestinal peristaltic and immune factors (Jakob et al., 2020). PGP 9.5 is a neuroendocrine marker and is reduced with intestinal inflammation and damage (Resnikoff et al., 2019; Heymans et al., 2020). In this study, the immunoreactive percentage of PGP9.5 in the jejunum was decreased by LPS treatment and increased by PQQ treatment, suggesting that PQQ reduced the damage of jejunal neurons caused by LPS.

Enteric neurochemical plasticity was regulated with PQQ treatment by regulating immunoreactive neurons and concentrations of neuropeptides. Neurochemical plasticity is the variable or modifiable changes of the nervous system elicited by adaptation to the environment. During the early development of rats, the ENS matures gradually and has the strongest neurochemical plasticity (Rząp et al., 2020). As the first isolated neuropeptide and known as the prototypic tachykinin (TK), SP stimulates systemic pain and vasodilation,

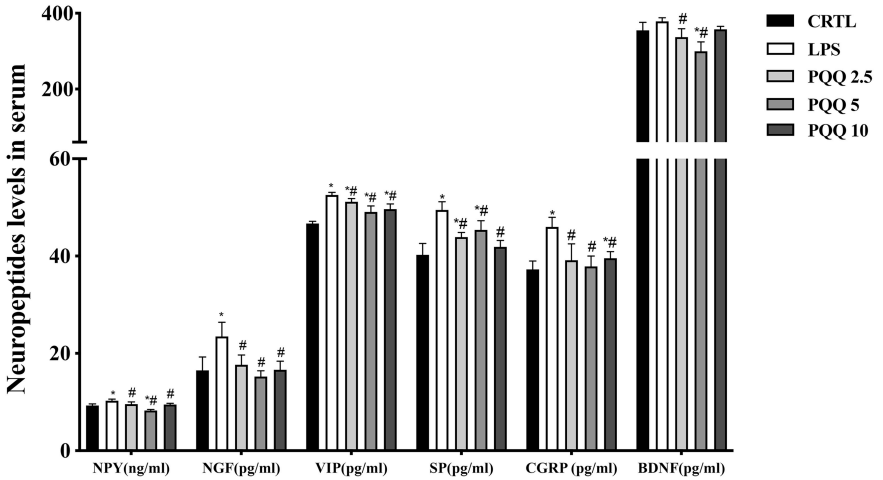

FIGURE 4 | Ileal neuropeptide mRNA expression levels of weaned rats (n = 6). SP, substance P; CGRP, calcitonin gene-related peptide; BDNF, brain-derived neurotropic factor; NPY, neuropeptide Y; NGF, nerve growth factor. CTRL, control treatment; LPS, control and LPS treatment; PQQ 2.5, intragastric administration with 2.5 mg/kg b.w./day PQQ·Na_2 treatment; PQQ 5, intragastric administration with 5.0 mg/kg b.w./day PQQ·Na_2 treatment; PQQ 10, intragastric administration with 10.0 mg/kg b.w./day PQQ·Na_2 treatment. *Means significant difference with the CTRL group ($P \leq 0.05$); #means significant difference with the LPS group ($P \leq 0.05$).

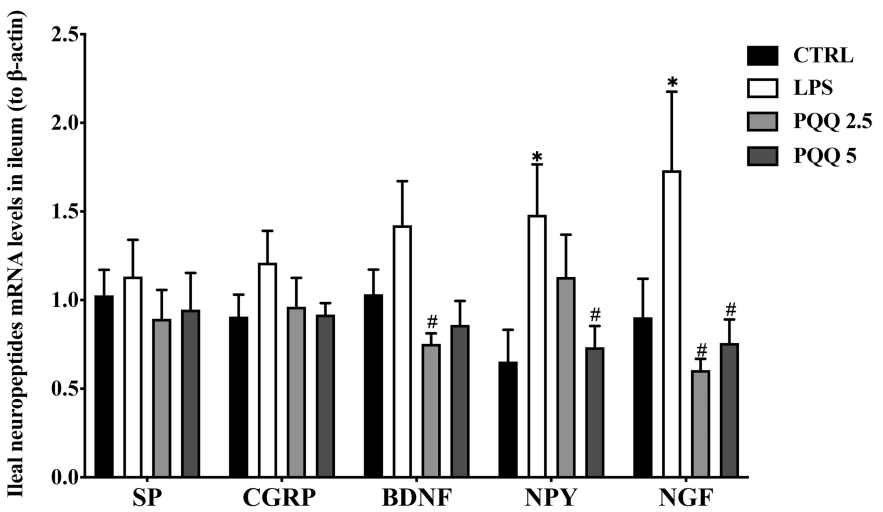

FIGURE 5 | Neuropeptide levels in serum of weaned rats. NPY, neuropeptide Y (n = 6); NGF, nerve growth factor (n = 5); VIP, vasoactive intestinal peptide (n = 6); SP, substance P (n = 5); CGRP, calcitonin gene-related peptide (n = 5); BDNF, brain-derived neurotropic factor (n = 5). CTRL, control treatment; LPS, control and LPS treatment; PQQ 2.5, intragastric administration with 2.5 mg/kg b.w./day PQQ·Na_2 treatment; PQQ 5, intragastric administration with 5.0 mg/kg b.w./day PQQ·Na_2 treatment; PQQ 10, intragastric administration with 10.0 mg/kg b.w./day PQQ·Na_2 treatment. *Means significant difference with the CTRL group ($P \leq 0.05$); #means significant difference with the LPS group ($P \leq 0.05$).

regulates immunity, promotes contraction as an excitatory neurotransmitter, and inhibits the secretion of digestive juices in the intestine (Euler and Gaddum, 1931; Holzer, 1998; Engel et al., 2012; Nässel et al., 2019). The concentration of SP is enhanced in the blood of rats suffering from colitis (Holzer, 1998). As a systemic vasodilator, CGRP simulates pain and regulates intestinal immunity similar to SP (Holzer, 1998; Engel et al., 2012; Lai et al., 2020). Sensory neurons in the gut of mice release CGRP to defend against *Salmonella* infection, and neurogenic inflammation challenged with LPS can promote CGRP release *via* activation of Toll-like receptor 4 (TLR4) in sensory neurons (Meseguer et al., 2014; Lai et al., 2020). As an inhibitory neurotransmitter and neuroprotective agent in the intestine, VIP is also an immunomodulator (Gonzalez-Rey and Delgado, 2005; Arciszewski et al., 2008). Rat myenteric neurons challenged with LPS increase the expression of VIP (Arciszewski et al., 2008). Except for promoting differentiation, development, and survival of neurons, BDNF regulates the sensitivity of the colon and rectum to constipation (Delafoy et al., 2006). It is synthesized by sensory neurons to mediate

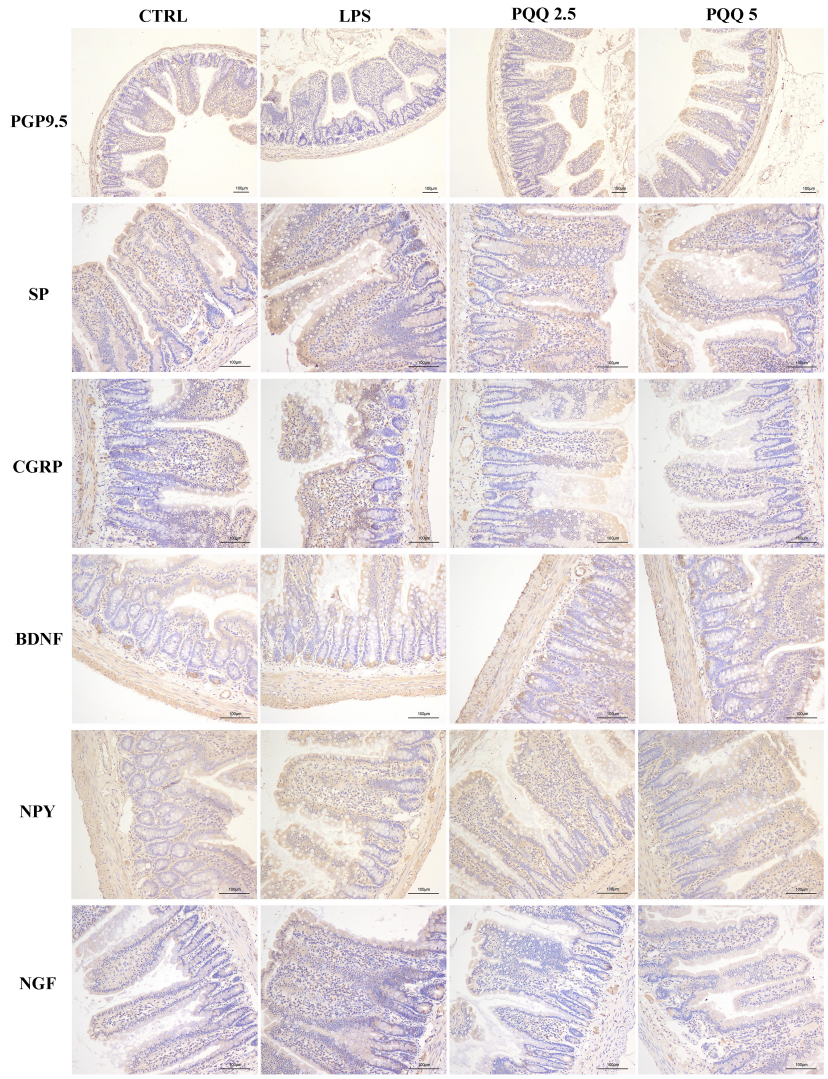

FIGURE 6 | Immunohistochemical staining of jejunal neurons (n = 6). PGP9.5, protein gene product 9.5; SP, substance P; CGRP, calcitonin gene-related peptide; BDNF, brain-derived neurotropic factor; NPY, neuropeptide Y; NGF, nerve growth factor. CTRL, control treatment; LPS, control and LPS treatment; PQQ 2.5, intragastric administration with 2.5 mg/kg b.w./day PQQ·Na_2 treatment; PQQ 5, intragastric administration with 5.0 mg/kg b.w./day PQQ·Na_2 treatment; PQQ 10, intragastric administration with 10.0 mg/kg b.w./day PQQ·Na_2 treatment. Scale bar = 100 μm.

inflammatory pain and regulate the sensitivity of visceral afferents in rats suffering from colitis (Matayoshi et al., 2005; Qiao et al., 2008). With systemic stress, NPY is released, regulates endocrine, behavior, stress, anxiety, appetite, and circadian rhythms, and functions in defecation and food intake (Adrian et al., 1983; Zhou et al., 2008). The level of NPY is increased in the hypothalamus and serum of mice suffering from colitis (Hassan et al., 2014; Reichmann et al., 2015). NGF is a nutrient protein for nerve cells and promotes the repair of damaged nerve fibers (Bilderback et al., 1999). At the site of inflammation, NGF concentration is increased, and cytokines promote the synthesis of NGF by neurons and other cells such as epithelial and endothelial cells (März et al., 1999; Minnone et al., 2017). In this study, concentrations of these neuropeptides were increased in serum and small intestine of rats in the LPS group. The increased levels were reduced with PQQ treatment. The optional PQQ dose approved to be 5.0 mg/kg b.w. The concentrations of IL-1β and TNF-α display a similar pattern to neuropeptides, suggesting that neuropeptides regulated immune factors concentrations. In the colon, SP and VIP concentrations showed the same trends as observed in the jejunum. This might be due to the main site of inflammation challenged with LPS. Additionally, P and VIP play the main role of immunomodulators in the nervous system. Treatments with PQQ increased concentrations of BDNF, NPY, and NGF in the colon which might be related to their neurotropic effects and the damage caused by the LPS challenge. These neuropeptides function in stress and neurotropic. When the intestine is

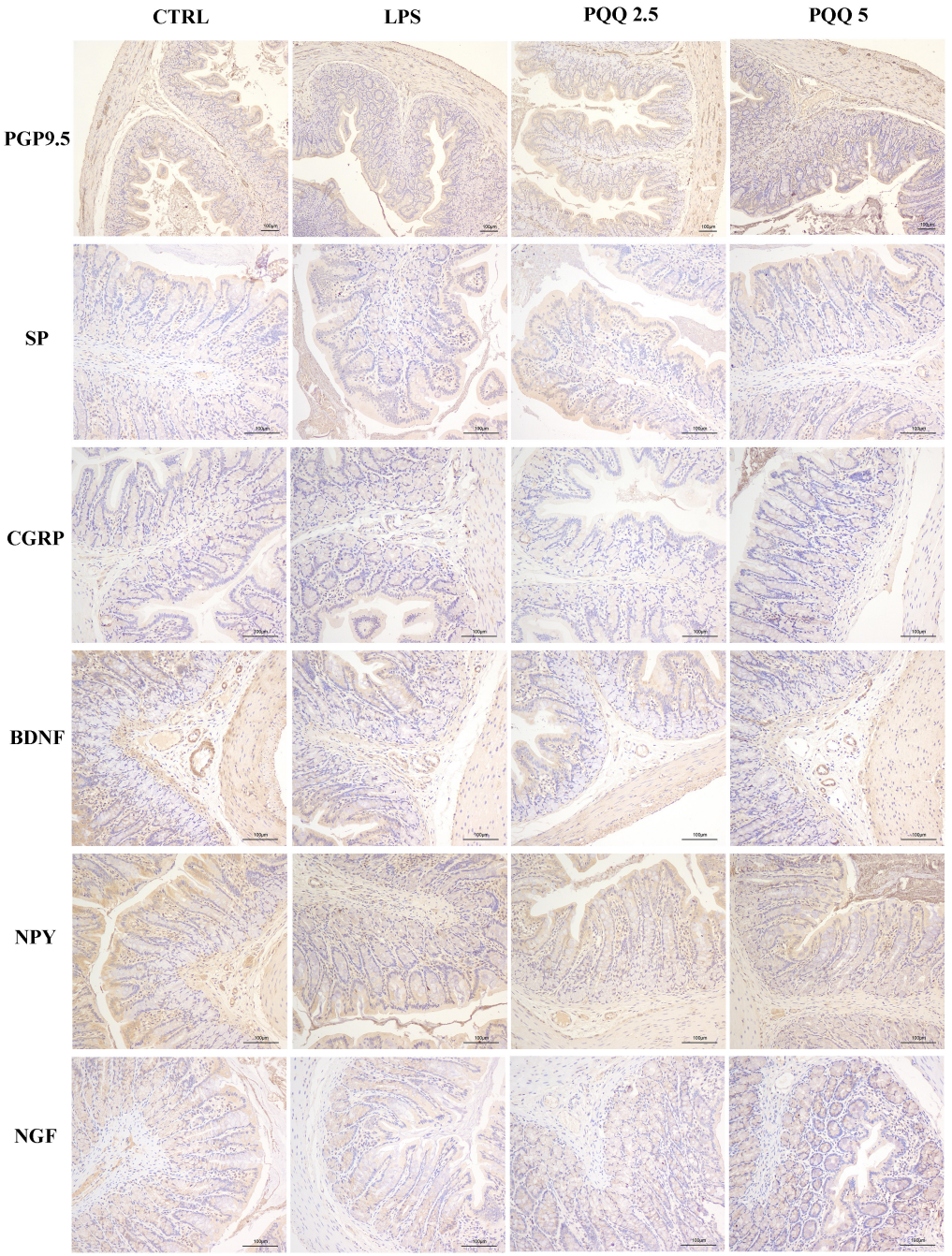

FIGURE 7 | Immunohistochemical staining of colonic neurons (n = 6). PGP9.5, protein gene product 9.5; SP, substance P; CGRP, calcitonin gene-related peptide; BDNF, brain-derived neurotropic factor; NPY, neuropeptide Y; NGF, nerve growth factor. CTRL, control treatment; LPS, control and LPS treatment; PQQ 2.5, intragastric administration with 2.5 mg/kg b.w./day PQQ·Na_2 treatment; PQQ 5, intragastric administration with 5.0 mg/kg b.w./day PQQ·Na_2 treatment; PQQ 10, intragastric administration with 10.0 mg/kg b.w./day PQQ·Na_2 treatment. Scale bar = 100 μm.

damaged, the neuropeptides secreted by the ENS aim to promote neuronal survival and maintain normal functions (Holzer, 1998; Arciszewski et al., 2008; Qiao et al., 2008). We deduced that PQQ played a different role in different pathological states, and we would investigate further. In conclusion, the results reported in this study suggest that PQQ influenced the release of neuropeptides which regulated the small intestine. We conclude that PQQ regulated enteric neurochemical plasticity of SP-, CGRP-, VIP-, BDNF-, NPY-, and NGF-immunoreactive neurons of weaned rats.

Expression of p-Akt decreased in jejunum and colon with PQQ supplementation. Akt can be phosphorylated by PI3K.

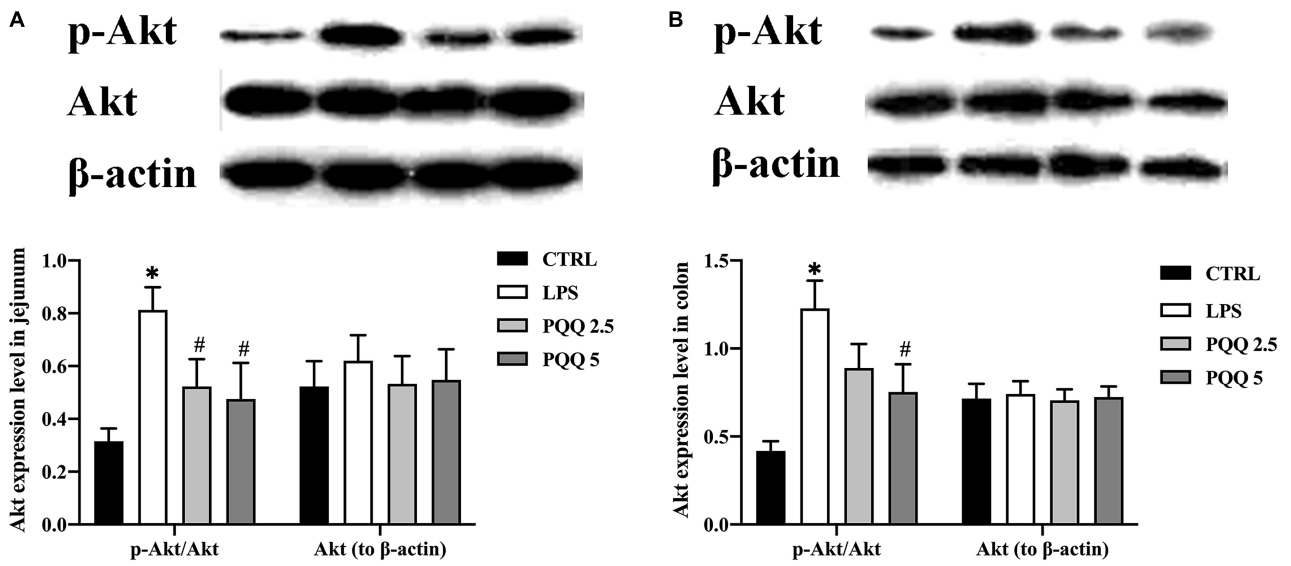

FIGURE 8 | Abundance of the Akt pathway in jejunal and colonic tissues of weaned rats (n = 6). **(A)** p-Akt, Akt, and PI3K abundances to β-actin in jejunum; **(B)** p-Akt, Akt, andPI3K abundances to β-actin in the colon. PI3K, phosphatidylinositol-3 kinase; Akt, protein kinase B; CTRL, control treatment; LPS, control and LPS treatment; PQQ 2.5, intragastric administration with 2.5 mg/kg b.w./day PQQ·Na_2 treatment; PQQ 5, intragastric administration with 5.0 mg/kg b.w./day PQQ·Na_2 treatment; PQQ 10, intragastric administration with 10.0 mg/kg b.w./day PQQ·Na_2 treatment. *Means significant difference with the CTRL group ($P \leq 0.05$); $^{\#}$means significant difference with the LPS group ($P \leq 0.05$).

Activated Akt can reduce and improve the activity of glycogen synthase kinase-3β (GSK-3β) by phosphorylation of Ser9 and Tyr216 sites, respectively (Majewska and Szeliga, 2017). GSK-3β is associated with cell survival and apoptosis, which can promote peripheral nerve regeneration, improve regrowth of synapses after peripheral nerve damage, and play a role in neurodegenerative diseases (Kitagishi et al., 2014; Huang et al., 2017). Activated GSK-3β can induce Tau perphosphate. Tau protein, a microtube-related protein, mainly acts on the far end of the axon, participates in axon transport, and interacts with the microtube protein, Tubulin, to stabilize the microtube and regulate NMDA receptor signaling pathways (Goedert et al., 1996; Iqbal et al., 2016; Falcon et al., 2019). By regulating GSK-3β and Tau protein, the PI3K/Akt signaling pathway affects a variety of CNS diseases, such as Alzheimer's disease, Parkinson's disease, and Huntington's disease (Kitagishi et al., 2014; Rai et al., 2019). PQQ inhibits apoptosis in the rat hippocampus by regulating the Akt/GSK-3β pathway (Zhou et al., 2020). In addition, PQQ can regulate memory *via* maintaining activation of GSK-3β while reducing the expression of p-AKT (Zhou X. Q. et al., 2018). In this study, PQQ reduced the magnitude of increased p-Akt in jejunum and colon of rats caused by LPS treatment which suggests that PQQ might regulate the secretory functions and structure of the ENS *via* the Akt signaling pathway.

In conclusion, based on ADG, jejunal morphology, immune responses, and enteric neuropeptide expression, we conclude that the intestinal health of weaned rats was damaged by the LPS challenge. Dietary PQQ supplementation reduced inflammatory injury and regulated neurochemical plasticity *via* the Akt signaling pathway in the intestine of rats suffering from enteritis.

DATA AVAILABILITY STATEMENT

The original contributions presented in the study are included in the article/**Supplementary Material**, further inquiries can be directed to the corresponding author.

ETHICS STATEMENT

The animal study was reviewed and approved by the Laboratory Animal Welfare and Animal Experimental Ethical Inspection Committee of China Agricultural University (AW01211202-1-2).

AUTHOR CONTRIBUTIONS

CS: conceptualization, data curation, formal analysis, investigation, methodology, and writing—original draft. SX, CH, ZW, WW, DM, XY, and HL: data curation and methodology. FW: conceptualization, writing – review, supervision, and funding acquisition. All authors have read and agreed to the published version of the manuscript.

FUNDING

This study was financially supported by the National Natural Science Foundation of China (Grant Nos. 32072772 and 31672459).

ACKNOWLEDGMENTS

We express our real thanks to Lee Johnston (University of Minnesota) and Bing Dong (China Agricultural University) for giving suggestions for revisions.

SUPPLEMENTARY MATERIAL

The Supplementary Material for this article can be found online at: https://www.frontiersin.org/articles/10.3389/fnins.2022.878541/full#supplementary-material

REFERENCES

Adrian, T. E., Allen, J. M., Bloom, S. R., Ghatei, M. A., Rossor, M. N., Roberts, G. W., et al. (1983). Neuropeptide Y distribution in human brain. *Nature* 306, 584–586. doi: 10.1038/306584a0

Arciszewski, M. B., Sand, E., and Ekblad, E. (2008). Vasoactive intestinal peptide rescues cultured rat myenteric neurons from lipopolysaccharide induced cell death. *Regul. Pept.* 146, 218–223. doi: 10.1016/j.regpep.2007.09.021

Baumgart, D. C., and Carding, S. R. (2007). Inflammatory bowel disease: cause and immunobiology. *Lancet* 369, 1627–1640. doi: 10.1016/S0140-6736(07)60750-8

Becker, L., Peterson, J., Kulkarni, S., and Pasricha, P. J. (2013). Ex vivo neurogenesis within enteric ganglia occurs in a PTEN dependent manner. *PLoS One* 8:e59452.

Bilderback, T. R., Gazula, V. R., Lisanti, M. P., and Dobrowsky, R. T. (1999). Caveolin interacts with Trk A and p75(NTR) and regulates neurotrophin signaling pathways. *J. Biol. Chem.* 274, 257–263. doi: 10.1074/jbc.274.1.257

Boesmans, W., Hao, M. M., Fung, C., Li, Z., Van den Haute, C., Tack, J., et al. (2019). Structurally defined signaling in neuro-glia units in the enteric nervous system. *Glia* 67, 1167–1178. doi: 10.1002/glia.23596

De Giorgio, R. (2006). The enteric nervous system, J. B. furness. Blackwell publishing, oxford (2006), (274 pp., price gbp 55.00, isbn 1-4051-3376-7). *Dig. Liver Dis.* 38:441. doi: 10.1016/j.dld.2006.03.010

Delafoy, L., Gelot, A., Ardid, D., Eschalier, A., Bertrand, C., Doherty, A. M., et al. (2006). Interactive involvement of brain derived neurotrophic factor, nerve growth factor, and calcitonin gene related peptide in colonic hypersensitivity in the rat. *Gut* 55, 940–945. doi: 10.1136/gut.2005.064063

Dong, N., Li, X., Xue, C., Zhang, L., Wang, C., Xu, X., et al. (2020). Astragalus polysaccharides alleviates LPS-induced inflammation via the NF-κB/MAPK signaling pathway. *J. Cell Physiol.* 235, 5525–5540. doi: 10.1002/jcp.29452

Du, F., Wang, L., Qian, W., and Liu, S. (2009). Loss of enteric neurons accompanied by decreased expression of GDNF and PI3K/Akt pathway in diabetic rats. *Neurogastroenterol. Motil.* 21, 1229–e1114.

Duine, J. A. (1991). Quinoproteins: enzymes containing the quinonoid cofactor pyrroloquinoline quinone, topaquinone or tryptophan-tryptophan quinone. *Eur. J. Biochem.* 200, 271–284. doi: 10.1111/j.1432-1033.1991.tb16183.x

Duine, J. A., Frank, J., and van Zeeland, J. K. (1979). Glucose dehydrogenase from *Acinetobacter calcoaceticus*: a 'quinoprotein'. *FEBS Lett.* 108, 443–446. doi: 10.1016/0014-5793(79)80584-0

Engel, M. A., Khalil, M., Siklosi, N., Mueller-Tribbensee, S. M., Neuhuber, W. L., Neurath, M. F., et al. (2012). Opposite effects of substance P and calcitonin gene-related peptide in oxazolone colitis. *Dig. Liver Dis.* 44, 24–29. doi: 10.1016/j.dld.2011.08.030

Falcon, B., Zivanov, J., Zhang, W., Murzin, A. G., Garringer, H. J., Vidal, R., et al. (2019). Novel tau filament fold in chronic traumatic encephalopathy encloses hydrophobic molecules. *Nature* 568, 420–423. doi: 10.1038/s41586-019-1026-5

Ferraris, R. P., Lee, P. P., and Diamond, J. M. (1989). Origin of regional and species differences in intestinal glucose uptake. *Am. J. Physiol.* 257(5 Pt 1), G689–G697. doi: 10.1152/ajpgi.1989.257.5.G689

Geng, Q., Gao, H., Yang, R., Guo, K., and Miao, D. (2019). Pyrroloquinoline quinone prevents estrogen deficiency-induced osteoporosis by inhibiting oxidative stress and osteocyte senescence. *Int. J. Biol. Sci.* 15, 58–68. doi: 10.7150/ijbs.25783

Goedert, M., Jakes, R., Spillantini, M. G., Hasegawa, M., Smith, M. J., and Crowther, R. A. (1996). Assembly of microtubule-associated protein tau into Alzheimer-like filaments induced by sulphated glycosaminoglycans. *Nature* 383, 550–553. doi: 10.1038/383550a0

Gonzalez-Rey, E., and Delgado, M. (2005). Role of vasoactive intestinal peptide in inflammation and autoimmunity. *Curr. Opin. Investig. Drugs* 6, 1116–1123.

Hara, H., Hiramatsu, H., and Adachi, T. (2007). Pyrroloquinoline quinone is a potent neuroprotective nutrient against 6-hydroxydopamine-induced neurotoxicity. *Neurochem. Res.* 32, 489–495. doi: 10.1007/s11064-006-9257-x

Harris, C. B., Chowanadisai, W., Mishchuk, D. O., Satre, M. A., Slupsky, C. M., and Rucker, R. B. (2013). Dietary pyrroloquinoline quinone (PQQ) alters indicators of inflammation and mitochondrial-related metabolism in human subjects. *J. Nutr. Biochem.* 24, 2076–2084. doi: 10.1016/j.jnutbio.2013.07.008

Hassan, A. M., Jain, P., Reichmann, F., Mayerhofer, R., Farzi, A., Schuligoi, R., et al. (2014). Repeated predictable stress causes resilience against colitis-induced behavioral changes in mice. *Front. Behav. Neurosci.* 8:386. doi: 10.3389/fnbeh.2014.00386

Heymans, C., de Lange, I. H., Hütten, M. C., Lenaerts, K., de Ruijter, N. J. E., Kessels, L., et al. (2020). Chronic intra-uterine ureaplasma parvum infection induces injury of the enteric nervous system in ovine fetuses. *Front. Immunol.* 11:189. doi: 10.3389/fimmu.2020.00189

Holzer, P. (1998). Implications of tachykinins and calcitonin gene-related peptide in inflammatory bowel disease. *Digestion* 59, 269–283. doi: 10.1159/000007504

Huang, C., Fan, Z., Han, D., Johnston, L. J., Ma, X., and Wang, F. (2021). Pyrroloquinoline quinone regulates the redox status in vitro and in vivo of weaned pigs via the Nrf2/HO-1 pathway. *J. Anim. Sci. Biotechnol.* 12:77. doi: 10.1186/s40104-021-00595-x

Huang, C., Ming, D., Wang, W., Wang, Z., Hu, Y., Ma, X., et al. (2020). Pyrroloquinoline quinone alleviates jejunal mucosal barrier function damage and regulates colonic microbiota in piglets challenged with enterotoxigenic *Escherichia coli*. *Front. Microbiol.* 11:1754. doi: 10.3389/fmicb.2020.01754

Huang, H., Liu, H., Yan, R., and Hu, M. (2017). PI3K/Akt and ERK/MAPK signaling promote different aspects of neuron survival and axonal regrowth following rat facial nerve axotomy. *Neurochem. Res.* 42, 3515–3524. doi: 10.1007/s11064-017-2399-1

Huang, Y., Chen, N., and Miao, D. (2017). Effect and mechanism of pyrroloquinoline quinone on anti-osteoporosis in Bmi-1 knockout mice-Anti-oxidant effect of pyrroloquinoline quinone. *Am. J. Transl. Res.* 9, 4361–4374.

Ichihara, M., Murakumo, Y., and Takahashi, M. (2004). RET and neuroendocrine tumors. *Cancer Lett.* 204, 197–211. doi: 10.1016/s0304-3835(03)00456-7

Iqbal, K., Liu, F., and Gong, C. X. (2016). Tau and neurodegenerative disease: the story so far. *Nat. Rev. Neurol.* 12, 15–27. doi: 10.1038/nrneurol.2015.225

Jakob, M. O., Murugan, S., and Klose, C. S. N. (2020). Neuro-immune circuits regulate immune responses in tissues and organ homeostasis. *Front. Immunol.* 11:308. doi: 10.3389/fimmu.2020.00308

Jarret, A., Jackson, R., Duizer, C., Healy, M. E., Zhao, J., Rone, J. M., et al. (2020). Enteric nervous system-derived il-18 orchestrates mucosal barrier immunity. *Cell* 180, 50–63.e12. doi: 10.1016/j.cell.2019.12.016

Jiang, C., Jiang, L., Li, Q., Liu, X., Zhang, T., Yang, G., et al. (2019). Pyrroloquinoline quinine ameliorates doxorubicin-induced autophagy-dependent apoptosis via lysosomal-mitochondrial axis in vascular endothelial cells. *Toxicology* 425, 152238. doi: 10.1016/j.tox.2019.152238

Kasahara, T., and Kato, T. (2003). Nutritional biochemistry: a new redox-cofactor vitamin for mammals. *Nature* 422:832. doi: 10.1038/422832a

Kitagishi, Y., Nakanishi, A., Ogura, Y., and Matsuda, S. (2014). Dietary regulation of PI3K/AKT/GSK-3β pathway in Alzheimer's disease. *Alzheimers Res. Ther.* 6:35. doi: 10.1186/alzrt265

Lai, N. Y., Musser, M. A., Pinho-Ribeiro, F. A., Baral, P., Jacobson, A., Ma, P., et al. (2020). Gut-innervating nociceptor neurons regulate peyer's patch microfold cells and SFB levels to mediate *Salmonella* host defense. *Cell* 180, 33–49.e22. doi: 10.1016/j.cell.2019.11.014

Lasrado, R., Boesmans, W., Kleinjung, J., Pin, C., Bell, D., Bhaw, L., et al. (2017). Lineage-dependent spatial and functional organization of the mammalian enteric nervous system. *Science* 356, 722–726. doi: 10.1126/science.aam7511

Li, L., Wan, G., Han, B., and Zhang, Z. (2018). Echinacoside alleviated LPS-induced cell apoptosis and inflammation in rat intestine epithelial cells by inhibiting the mTOR/STAT3 pathway. *Biomed. Pharmacother.* 104, 622–628. doi: 10.1016/j.biopha.2018.05.072

Liu, S., Li, H., Ou Yang, J., Peng, H., Wu, K., Liu, Y., et al. (2005). Enhanced rat sciatic nerve regeneration through silicon tubes filled with pyrroloquinoline quinone. *Microsurgery* 25, 329–337. doi: 10.1002/micr.20126

Liu, Z., Sun, C., Tao, R., Xu, X., Xu, L., Cheng, H., et al. (2016). Pyrroloquinoline quinone decelerates rheumatoid arthritis progression by inhibiting inflammatory responses and joint destruction via modulating NF-κB and MAPK pathways. *Inflammation* 39, 248–256. doi: 10.1007/s10753-015-0245-7

Lu, H., Shen, J., Song, X., Ge, J., Cai, R., Dai, A., et al. (2015). protective effect of pyrroloquinoline quinone (PQQ) in rat model of intracerebral hemorrhage. *Cell Mol. Neurobiol.* 35, 921–930. doi: 10.1007/s10571-015-0187-5

Majewska, E., and Szeliga, M. (2017). AKT/GSK3β signaling in glioblastoma. *Neurochem. Res.* 42, 918–924. doi: 10.1007/s11064-016-2044-4

März, P., Heese, K., Dimitriades-Schmutz, B., Rose-John, S., and Otten, U. (1999). Role of interleukin-6 and soluble IL-6 receptor in region-specific induction of astrocytic differentiation and neurotrophin expression. *Glia* 26, 191–200. doi: 10.1002/(sici)1098-1136(199905)26:3<191::aid-glia1>3.0.co;2-#

Matayoshi, S., Jiang, N., Katafuchi, T., Koga, K., Furue, H., Yasaka, T., et al. (2005). Actions of brain-derived neurotrophic factor on spinal nociceptive transmission during inflammation in the rat. *J. Physiol.* 569(Pt 2), 685–695. doi: 10.1113/jphysiol.2005.095331

Meseguer, V., Alpizar, Y. A., Luis, E., Tajada, S., Denlinger, B., Fajardo, O., et al. (2014). TRPA1 channels mediate acute neurogenic inflammation and pain produced by bacterial endotoxins. *Nat. Commun.* 5:3125. doi: 10.1038/ncomms4125

Ming, D., Huang, C., Wang, W., Wang, Z., Shi, C., Yin, X., et al. (2021). Effects of diet supplemented with excess pyrroloquinoline quinone disodium on growth performance, blood parameters and redox status in weaned pigs. *Animals (Basel)* 11:359. doi: 10.3390/ani11020359

Minnone, G., De Benedetti, F., and Bracci-Laudiero, L. (2017). NGF and its receptors in the regulation of inflammatory response. *Int. J. Mol. Sci.* 18:1028. doi: 10.3390/ijms18051028

Moeser, A. J., Pohl, C. S., and Rajput, M. (2017). Weaning stress and gastrointestinal barrier development: implications for lifelong gut health in pigs. *Anim. Nutr.* 3, 313–321. doi: 10.1016/j.aninu.2017.06.003

Mohamed, A. S., Hosney, M., Bassiony, H., Hassanein, S. S., Soliman, A. M., Fahmy, S. R., et al. (2020). Sodium pentobarbital dosages for exsanguination affect biochemical, molecular and histological measurements in rats. *Sci. Rep.* 10:378. doi: 10.1038/s41598-019-57252-7

Montedonico, S., Sri Paran, T., Pirker, M., Rolle, U., and Puri, P. (2006). Developmental changes in submucosal nitrergic neurons in the porcine distal colon. *J. Pediatr. Surg.* 41, 1029–1035. doi: 10.1016/j.jpedsurg.2005.12.063

Nässel, D. R., Zandawala, M., Kawada, T., and Satake, H. (2019). Tachykinins: neuropeptides that are ancient, diverse, widespread and functionally pleiotropic. *Front. Neurosci.* 13:1262. doi: 10.3389/fnins.2019.01262

Parathan, P., Wang, Y., Leembruggen, A. J., Bornstein, J. C., and Foong, J. P. (2020). The enteric nervous system undergoes significant chemical and synaptic maturation during adolescence in mice. *Dev. Biol.* 458, 75–87. doi: 10.1016/j.ydbio.2019.10.011

Pfaffl, M. W., Horgan, G. W., and Dempfle, L. (2002). Relative expression software tool (REST) for group-wise comparison and statistical analysis of relative expression results in real-time PCR. *Nucleic Acids Res.* 30:e36.

Qiao, L. Y., Gulick, M. A., Bowers, J., Kuemmerle, J. F., and Grider, J. R. (2008). Differential changes in brain-derived neurotrophic factor and extracellular signal-regulated kinase in rat primary afferent pathways with colitis. *Neurogastroenterol. Motil.* 20, 928–938.

Rai, S. N., Dilnashin, H., Birla, H., Singh, S. S., Zahra, W., Rathore, A. S., et al. (2019). The role of PI3K/Akt and ERK in neurodegenerative disorders. *Neurotox Res.* 35, 775–795. doi: 10.1007/s12640-019-0003-y

Rao, M., and Gershon, M. D. (2018). Enteric nervous system development: what could possibly go wrong? *Nat. Rev. Neurosci.* 19, 552–565. doi: 10.1038/s41583-018-0041-0

Reichmann, F., Hassan, A. M., Farzi, A., Jain, P., Schuligoi, R., and Holzer, P. (2015). Dextran sulfate sodium-induced colitis alters stress-associated behaviour and neuropeptide gene expression in the amygdala-hippocampus network of mice. *Sci. Rep.* 5:9970. doi: 10.1038/srep09970

Resnikoff, H., Metzger, J. M., Lopez, M., Bondarenko, V., Mejia, A., Simmons, H. A., et al. (2019). Colonic inflammation affects myenteric alpha-synuclein in nonhuman primates. *J. Inflamm. Res.* 12, 113–126. doi: 10.2147/jir.S196552

Rząp, D., Czajkowska, M., and Całka, J. (2020). Neurochemical plasticity of nNOS-, VIP- and CART-immunoreactive neurons following prolonged acetylsalicylic acid supplementation in the porcine jejunum. *Int. J. Mol. Sci.* 21:2157. doi: 10.3390/ijms21062157

Shanan, N., GhasemiGharagoz, A., Abdel-Kader, R., and Breitinger, H. G. (2019). The effect of pyrroloquinoline quinone and resveratrol on the survival and regeneration of cerebellar granular neurons. *Neurosci. Lett.* 694, 192–197. doi: 10.1016/j.neulet.2018.12.002

Turner, J. R. (2009). Intestinal mucosal barrier function in health and disease. *Nat. Rev. Immunol.* 9, 799–809. doi: 10.1038/nri2653

Euler, U. S. V., and Gaddum, J. H. (1931). An unidentified depressor substance in certain tissue extracts. *J. Physiol.* 72, 74–87. doi: 10.1113/jphysiol.1931.sp002763

Wang, B., Wu, G., Zhou, Z., Dai, Z., Sun, Y., Ji, Y., et al. (2015). Glutamine and intestinal barrier function. *Amino Acids* 47, 2143–2154. doi: 10.1007/s00726-014-1773-4

Wu, X., Li, J., Zhang, H., Wang, H., Yin, G., and Miao, D. (2017). Pyrroloquinoline quinone prevents testosterone deficiency-induced osteoporosis by stimulating osteoblastic bone formation and inhibiting osteoclastic bone resorption. *Am. J. Transl. Res.* 9, 1230–1242.

Xu, T., Yang, X., Wu, C., Qiu, J., Fang, Q., Wang, L., et al. (2018). Pyrroloquinoline quinone attenuates cachexia-induced muscle atrophy via suppression of reactive oxygen species. *J. Thoracic Dis.* 10, 2752–2759. doi: 10.21037/jtd.2018.04.112

Yin, X., Ming, D., Bai, L., Wu, F., Liu, H., Chen, Y., et al. (2019). Effects of pyrroloquinoline quinone supplementation on growth performance and small intestine characteristics in weaned pigs. *J. Anim. Sci.* 97, 246–256. doi: 10.1093/jas/sky387

Yoshioka, N., Taniguchi, Y., Yoshida, A., Nakata, K., Nishizawa, T., Inagawa, H., et al. (2009). Intestinal macrophages involved in the homeostasis of the intestine have the potential for responding to LPS. *Anticancer Res.* 29, 4861–4865.

Zani, A., Cordischi, L., Cananzi, M., De Coppi, P., Smith, V. V., Eaton, S., et al. (2008). Assessment of a neonatal rat model of necrotizing enterocolitis. *Eur. J. Pediatr. Surg.* 18, 423–426. doi: 10.1055/s-2008-1038951

Zhang, B., Yang, W., Zhang, H., He, S., Meng, Q., Chen, Z., et al. (2019). Effect of pyrroloquinoline quinone disodium in female rats during gestating and lactating on reproductive performance and the intestinal barrier functions in the progeny. *Br. J. Nutr.* 121, 818–830. doi: 10.1017/s0007114519000047

Zhou, W., Ramachandran, D., Mansouri, A., and Dailey, M. J.(2018). Glucose stimulates intestinal epithelial crypt proliferation by modulating cellular energy metabolism. *J. Cell Physiol.* 233, 3465–3475. doi: 10.1002/jcp.26199

Zhou, X. Q., Yao, Z. W., Peng, Y., Mao, S. S., Xu, D., Qin, X. F., et al. (2018). PQQ ameliorates D-galactose induced cognitive impairments by reducing glutamate neurotoxicity via the GSK-3beta/Akt signaling pathway in mouse. *Sci. Rep.* 8:8894. doi: 10.1038/s41598-018-26962-9

Zhou, X., Cai, G., Mao, S., Xu, D., Xu, X., Zhang, R., et al. (2020). Modulating NMDA receptors to treat MK-801-induced schizophrenic cognition deficit: effects of clozapine combining with PQQ treatment and possible mechanisms of action. *BMC Psychiatry* 20:106. doi: 10.1186/s12888-020-02509-z

Zhou, Z., Zhu, G., Hariri, A. R., Enoch, M. A., Scott, D., Sinha, R., et al. (2008). Genetic variation in human NPY expression affects stress response and emotion. *Nature* 452, 997–1001. doi: 10.1038/nature06858

Conflict of Interest: The authors declare that the research was conducted in the absence of any commercial or financial relationships that could be construed as a potential conflict of interest.

Publisher's Note: All claims expressed in this article are solely those of the authors and do not necessarily represent those of their affiliated organizations, or those of the publisher, the editors and the reviewers. Any product that may be evaluated in this article, or claim that may be made by its manufacturer, is not guaranteed or endorsed by the publisher.

frontiers | Frontiers in Neuroscience

ORIGINAL RESEARCH
published: 06 May 2022
doi: 10.3389/fnins.2022.843396

Contribution of Amygdala Histone Acetylation in Early Life Stress-Induced Visceral Hypersensitivity and Emotional Comorbidity

Le Guan[1†], Xi Shi[2†], Ying Tang[1†], Yan Yan[1], Liang Chen[1], Yu Chen[1], Guangcheng Gao[1], Chun Lin[1,3] and Aiqin Chen[1,2*]*

[1] Fujian Provincial Key Laboratory of Brain Aging and Neurodegenerative Diseases, School of Basic Medical Sciences, Pain Research Institute, Fujian Medical University, Fuzhou, China, [2] Department of Medical Oncology, The First Affiliated Hospital of Fujian Medical University, Fuzhou, China, [3] Department of Pediatrics, The First Affiliated Hospital of Fujian Medical University, Fuzhou, China

OPEN ACCESS

Edited by:
Jianhua Chen,
Shanghai Jiao Tong University, China

Reviewed by:
Tzer-Bin Lin,
Taipei Medical University, Taiwan
Tian Yuan,
Wake Forest School of Medicine, United States

***Correspondence:**
Chun Lin
chunlin77550@126.com
Aiqin Chen
aiqinchen3626@163.com

† These authors have contributed equally to this work

Specialty section:
This article was submitted to Gut-Brain Axis, a section of the journal Frontiers in Neuroscience

Received: *25 December 2021*
Accepted: *19 April 2022*
Published: *06 May 2022*

Citation:
Guan L, Shi X, Tang Y, Yan Y, Chen L, Chen Y, Gao G, Lin C and Chen A (2022) Contribution of Amygdala Histone Acetylation in Early Life Stress-Induced Visceral Hypersensitivity and Emotional Comorbidity. Front. Neurosci. 16:843396. doi: 10.3389/fnins.2022.843396

Patients with irritable bowel syndrome (IBS) experience not only enhanced visceral pain but also emotional comorbidities, such as anxiety and depression. Early life stress (ELS) is a high-risk for the development of IBS. Literatures have reported an important epigenetic modulation in sustaining extrinsic phenotypes. The amygdala is closely related to the regulation of visceral functions and emotional experiences. In this study, we hypothesized that ELS-induced reprogramming inappropriate adaptation of histone acetylation modification in the amygdala may result in visceral hypersensitivity and anxiety-like behaviors in ELS rats. To test this hypothesis, the model of ELS rats was established by neonatal colorectal dilatation (CRD). Visceral hypersensitivity was assessed based on the electromyography response of the abdominal external oblique muscle to CRD. Emotional comorbidities were examined using the elevated plus maze test, open field test, and sucrose preference test. Trichostatin A (TSA) and C646 were microinjected into the central amygdala (CeA) individually to investigate the effects of different levels of histone acetylation modification on visceral hypersensitivity and emotion. We found neonatal CRD resulted in visceral hypersensitivity and anxiety-like behaviors after adulthood. Inhibiting histone deacetylases (HDACs) in the CeA by TSA enhanced visceral sensitivity but did not affect anxiety-like behaviors, whereas inhibiting HAT by C646 attenuated visceral hypersensitivity in ELS rats. Interestingly, CeA treatment with TSA induced visceral sensitivity and anxiety-like behaviors in the control rats. Western blot showed that the expressions of acetylated 9 residue of Histone 3 (H3K9) and protein kinase C zeta type (PKMζ) were higher in the ELS rats compared to those of the controls. The administration of the PKMζ inhibitor ZIP into

the CeA attenuated visceral hypersensitivity of ELS rats. Furthermore, the expression of amygdala PKMζ was enhanced by TSA treatment in control rats. Finally, western blot and immunofluorescence results indicated the decrease of HDAC1 and HDAC2 expressions, but not HDAC3 expression, contributed to the enhancement of histone acetylation in ELS rats. Our results support our hypothesis that amygdala-enhanced histone acetylation induced by stress in early life results in visceral hypersensitivity and anxiety-like behaviors in ELS rats, and reversing the abnormal epigenetic mechanisms may be crucial to relieve chronic symptoms in ELS rats.

Keywords: amygdala, histone acetylation, histone deacetylase, protein kinase Mζ, early life stress (ELS)

INTRODUCTION

Patients with irritable bowel syndrome (IBS) experience not only enhanced visceral pain and abnormal bowel habits but also emotional comorbidities, such as anxiety and depression (Pimentel and Lembo, 2020). Visceral hypersensitivity and negative emotions of patients with IBS persist in a long-term and aggravate each other. Thus, the treatment for IBS in clinics is considered challenging (Vierck et al., 2014). However, whether visceral hypersensitivity of IBS shares the same molecular pathways with negative emotions or not remains unclear.

Patients with IBS are two to four times more likely to report a history of early life stress (ELS), such as abuse, poverty, or trauma, in the early stages than healthy controls (Bradford et al., 2012). ELS is a high-risk for the development of IBS. Literatures have reported an important epigenetic modulation in sustaining extrinsic phenotypes (Mitrousis et al., 2015; Louwies and Greenwood-Van Meerveld, 2020; Marcal et al., 2021). For example, histone acetylation modification can regulate gene expression and result in long-term abnormal behaviors (Graff and Tsai, 2013). Epigenetic modifications in the CeA serve as memories of adverse events that occurred during early life (Louwies and Greenwood-Van Meerveld, 2020). The level of histone acetylation is dependent on the activities of histone deacetylases (HDACs) and histone acetyltransferases (HATs) (Bahari-Javan et al., 2014). Studies have shown that HDAC inhibitors (HDACIs) could alleviate neuropathic pain (Khangura et al., 2019). HDACIs showed analgesic effects in animal models of inflammatory persistent pain (Mao et al., 2019). The upregulation of HDACs was also involved in chronic pain caused by bone cancer through the pathological activation of microglia and astrocytes in the spinal dorsal horn (Hu et al., 2017). On the other hand, C646, an inhibitor of HAT p300, attenuated mechanical allodynia and thermal hyperalgesia in the spinal cord (Mao et al., 2019). Furthermore, administration of the HAT inhibitor garcinol into central amygdala attenuated ELS-induced visceral hypersensitivity in adult female rats (Louwies and Greenwood-Van Meerveld, 2020). These studies have indicated that histone acetylation modification is correlated with chronic pain.

As an important part of the cortex–limbic network, the amygdala is closely related to the regulation of visceral functions, emotional experiences, and fear memories (Gauriau and Bernard, 2004; Chaloner and Greenwood-Van Meerveld, 2013; Lucassen et al., 2014; Cheng et al., 2019). The injection of HDAC inhibitor trichostatin A (TSA) into the lateral amygdala of rats enhanced H3 acetylation and auditory fear memory consolidation, whereas HAT inhibitor destroyed the consolidation and reconsolidation of Pavlovian fear conditioning ability (Maddox et al., 2013a). Microinjection of HDACIs into the central amygdala attenuated anxiety-like behaviors and hypersensitivity reactions caused by increased corticosteroid exposure (Tran et al., 2015). Above all, the amygdala is certainly involved in the regulation of pain and emotion, but little is known about the roles of histone acetylation modification in regulating visceral hypersensitivity and negative emotions of ELS rats. We previously found that the expression of protein kinase C zeta type (PKMζ) in the hippocampus of IBS rats increased (Chen et al., 2015; Tang et al., 2016). Zeta inhibitory peptide (ZIP), an inhibitor of PKMζ, could attenuate chronic visceral hypersensitivity in IBS rats (Chen et al., 2015; Tang et al., 2016). Studies have shown that amygdala PKMζ was involved in the regulation of stress and fear memory (McDonald and Mott, 2017; Zhou et al., 2018). However, elucidating the roles of amygdala PKMζ and the association between histone acetylation modification and PKMζ expression in ELS rats is required.

The primary aim of this study was to determine the roles of histone acetylation modification and HDAC1–3 in regulating visceral hypersensitivity and negative emotions of ELS rats. The secondary aim was to examine PKMζ expression and roles in the amygdala of ELS rats and to determine whether it is regulated by histone acetylation modification. This study could reveal novel underlying mechanism of IBS and provide new molecule targets for the treatment of IBS.

MATERIALS AND METHODS

Animal

Male Sprague–Dawley rats were purchased from the Laboratory Animal Center of Fujian Medical University. The approval number is SCXK (Fujian) 2012-0001. ELS rats were established by colorectal dilation (CRD) stimulation of 60 mmHg pressure for 1 min using a 2.5 mm × 20 mm human vascular reconstruction balloon (Chen et al., 2014; Fan et al., 2021). The stimulation was performed once a day from the 8th to the 14th day after birth. The pups were with dams until 21 days old. Control rats were fed normally under the same conditions (a 12-h

light/dark cycle with *ad libitum* access to food and water) without neonatal colorectal dilation. The animal procedures were approved by the Committee for Care and Use of Laboratory Animals of Fujian Medical University. Behavioral and molecular biological experiments were carried out at postnatal 8 weeks. Experiments were performed by researchers blinded to the treatment of animals.

Assessment of Visceral Hypersensitivity

Male rats (8 weeks old) were anesthetized with light isoflurane. Abdominal electromyography (EMG) response to CRD stimulation was measured to assess visceral hypersensitivity as previously described (Chen et al., 2014; Fan et al., 2021). CRD induces abdominal contractions, and this visceromotor response is used to assess visceral pain. EMG responses were measured with a system of RM6240BD (Chengdu, China). Two silver electrodes were inserted into the abdominal muscles to record EMG, which was induced by graded CRD of 40 or 60 mmHg for 10 s at intervals of 4 min. ΔEMG amplitude was determined as the following formula.

ΔEMG amplitude = (EMG amplitude of CRD-EMG amplitude of baseline) × 100%

/EMG amplitude of baseline.

Assessment of Anxiety-Like and Depression-Like Behaviors

The elevated plus-maze test (EPMT) was used to score anxiety-like behaviors in rats before and 24 h after the final drug treatment. A video camera was located above the EPM to record the behavior of each rat for 5 min (Yang et al., 2019). The video was then analyzed by an investigator who was blind to the treatment. Rats were placed in the experimental room for 30 min to adapt to the environment and were then placed in the center of the EPM facing an open arm. The percentage of time spent in the open arms and the number of open arm entries were used to quantify anxiety-like behaviors. Reduced open arm exploration and entries indicates higher level of anxiety.

The open field test (OFT) was used to assess locomotor and anxiety-like behaviors of rats (Liu et al., 2021). The open field was a large square arena with a side length of 100 cm and 40-cm-high walls in a dimly lit room. The activity of rats in the OFT was videotaped during a 5-min session and later tracked using an IR color dome camera (MODEL: TA-758RP, Shanghai Yishu Information Technology Co., Ltd., China) (Yang et al., 2019; Farazi et al., 2021). We measured the indicators including the total distance traveled, the distance and time spent in the center area, and the number of standings. Less center area exploration and standing activity indicates anxious emotion.

Sucrose preference test (SPT) was used to examine anhedonia in rats, which is the core manifestation of depression. The rats were single-housed in the cages and provided two bottles of water both containing 150 ml of 1% sucrose solution for the first 24 h. For the next 24 h, two bottles of water were supplied containing pure water and 1% sucrose solution, respectively. After the adaptive period, the rats were deprived of food and water for the next 24 h. Finally, each rat was free to access a bottle of 1% sucrose solution and a bottle of pure water at the same time, and sucrose preference was examined for 1 h (Zhang et al., 2021). The two bottles were repositioned midway during the test time to avoid position preference in drinking behaviors. The consumption of water and sucrose was measured by the weight difference of the water bottles before and after the test. Sucrose preference was calculated as sucrose intake/(sucrose intake + water intake) *100%.

Surgical Procedures

After isoflurane (Shandong Keyuan Pharmaceutical Co., Ltd., China) anesthesia, rats were fixed in a stereotaxic instrument (Narishige, Japan) for the stereotaxic implantation of a catheter. A small cut was made to expose the skull using aseptic techniques, and 1 mm holes were drilled −3.3 mm posterior and ± 4.8 mm lateral to the bregma. Bilateral catheters were lowered −7.5 mm from the dura.

Stereotaxic Implantation of Cannula for CeA Infusions

Implantation of cannula was carried out as previously described (Tran et al., 2015). A custom indwelling cannula, injector, and cannula cap were provided by Shenzhen RWD Life Science (RWD, Shenzhen, China). Each cannula (inside diameter: 0.34 mm; outer diameter: 0.48 mm), which extended 7.5 mm below the threaded pedestal, was placed flush to the skull at the same coordinates. A stainless steel screw was mounted triangularly to the two sides of the cannula and held to the skull with adhesive. The rats recovered without disturbance for 1 week. TSA [200 μmol/L (Wei et al., 2016); Meilunbio, Dalian, China], C646 [2 mmol/L (Maddox et al., 2013b); MedChem Express, China], PKMζ inhibitor ZIP [0.5 μmol/L (Chen et al., 2015); ab120993, Abcam] or vehicle (VEH) (0.1% dimethyl sulfoxide) was administered once. Isoflurane 2% was used to anesthetize rats through the anesthetic mask. Then the matched injector was placed into the cannula. We injected a total volume of 1 μl of TSA, C646, ZIP or VEH into each cannula at a rate of 0.05–0.1 μl min^{-1} for a total of 10–20 min using a microinjector (Shanghai Gaoge Industry and Trade Co., Ltd., China). The injector was kept in place for an additional 10 min to ensure complete diffusion of the solvent.

Verification of Cannula Placement

After the behavioral experiments, we microinjected bromophenol blue solution (5%) into the CeA and removed the brain for coronal section to examine the casing trajectory. The data with inaccurate location were excluded from the experimental statistics.

Nuclear Protein Extraction

Nuclear proteins were extracted from the tissue samples using the Nuclear and Cytoplasmic Protein Extraction Kit (P0027, Beyotime Biotechnology) according to the manufacturer's protocol. Protein quantification of the extraction product was performed using the Enhance BCA Protein Assay Kit system (P0012S, Beyotime Biotechnology). Following quantification, the samples were aliquoted and stored at −80°C for subsequent analysis.

Western Blot Assay

The proteins from the amygdala tissue samples were separated using 10–12% gradient polyacrylamide gel (P0012A, Beyotime Biotechnology), transferred to a polyvinylidene difluoride membrane electrophoretically, and probed with Histone H3 (acetylK9) (ab10812, Abcam, 1:500), HDAC1 (ab19845, Abcam, 1:1,000), HDAC2 (ab32117, Abcam, 1:2,000), HDAC3 (ab32369, Abcam, 1:7,000), and PKM zeta (ab59364, Abcam, 1:500), respectively. β-actin (AC004, ABclonal, 1:7,000), Histone H3 (ab1791, Abcam, 1:500), and GAPDH (MB001, Bioworld, 1:5,000) were used as the controls. Horseradish-peroxidase-conjugated secondary antibody (1:10,000) was used to incubate the membrane for 8 h. Protein bands were detected using an enhanced chemiluminescence kit (WBKLS0500, Immobilon, Millipore). Protein expression indicated by the intensity of protein bands was determined using Image J software.

Immunofluorescence Histochemical Staining

Animals were intracardially perfused with PBS and 4% paraformaldehyde. After fixation, dissected brains were cryoprotected in 20% sucrose overnight at 4°C and then in 30% sucrose at 4°C. Coronal sections of 20 μm were obtained using a cryostat and further processed for immunohistochemistry. Briefly, slices were incubated in blocking fluid (Beyotime) to permeabilize and block unspecific staining. Primary antibodies were incubated for 48 h at 22–24°C and secondary antibodies overnight at 4°C. Both primary and secondary antibodies were diluted in blocking fluid (Beyotime). Rabbit anti-HDAC1 (ab19845, Abcam, 1:1,000), anti-HDAC2 (ab32117, Abcam, 1:250), and anti-HDAC3 (ab32369, Abcam, 1:100) were used as primary antibodies. All secondary antibodies Alexa 488 (Invitrogen) was diluted 1:1,000. Immunofluorescence labeling of a specific protein was used to determine its localization with the cells. Immunofluorescence images were captured using laser scanning confocal microscope (FV3000, Olympus, Japan). Left or right CeA was imaged. Integrated optical density (IOD) of the specific protein was analyzed using the Image-Pro Plus 6.0 software (Media Cybernetics, United States). The relative concentration of the labeled protein was quantified by specific thresholding of the fluorescent region of interest and by measuring the IOD of the fluorescent signal.

Statistical Analysis

SPSS 17.0 software was used for data analysis. Data are presented as mean ± SEM. The data for EMG and behaviors were analyzed with one-way ANOVA and independent samples *t*-test. Western blotting and Immunofluorescent data were analyzed with one-way ANOVA and independent samples *t*-test. The administration of TSA, ZIP or C646 was compared using a paired-samples *t*-test. Statistical analysis was performed using GraphPad Prism 8.0. Immunofluorescent graphs were quantified by integrated optical density (IOD) with the Image-Pro Plus 6.0 software. $P < 0.05$ was considered statistically significant. If the distribution of data was non-normal or the variance was uneven, the non-parametric test (Mann–Whitney *U* test or Wilcoxon signed-rank test) was used.

RESULTS

Neonatal Colorectal Distension Resulted in Visceral Hypersensitivity and Anxiety-Like Behaviors in Adult Rats

Electromyography (EMG) amplitudes were significantly higher at 40 and 60 mmHg colorectal distension (CRD) pressure in ELS rats than in control rats (**Figures 1A,B**). Anxiety-like behaviors were examined using the elevated plus maze test (EPMT) and open field test (OFT) in rats. In the OFT, the distance, time spent in the center area, and the number of standings were lower in ELS rats than in control rats (**Figures 1D**, **F–H**), while the total distance did not change significantly (**Figure 1E**). Similar results were found in the experiments using the EPMT. Time spent in the open arms and entries into the open arms of ELS rats were significantly less than those of control rats (**Figures 1I–K**). Anhedonia was also measured using the sucrose preference test. However, there was no significant reduction in the sucrose preference ratio of ELS rats relative to that of control rats (**Figure 1C**). These results indicated that neonatal CRD resulted in visceral hypersensitivity and anxiety-like behaviors in adult rats.

The Effects of Central Amygdala Treatment of Trichostatin A or C646 on Visceral Hypersensitivity and Anxiety-Like Behaviors of Early Life Stress Rats

Chronic phenotypes can be sustained by epigenetic mechanisms, such as histone modifications. To clarify the contribution of histone acetylation to visceral hypersensitivity and anxiety-like behaviors of ELS rats, TSA and C646 were microinjected into the central amygdala (CeA) individually. Localization of drug placement and verification of the location accuracy of CeA were performed following bromophenol blue staining of microinjection. Those with inaccurate positioning were discarded.

Overall, significant effects of HDACI (TSA) infusion on EMG and open arms time of the EPMT in ELS rats were observed. DMSO had no effect on EMG and EPMT (**Figures 2A,D,G,J**). Treatment with TSA significantly enhanced visceral hypersensitivity at 3 h and 6 h in ELS rats (**Figures 2B,E**), whereas it was only at 6 h in control rats. The entries in the open arms of EPMT were not significantly changed by TSA treatment in control and IBS rats (**Figure 2H**). Interestingly, treatment with TSA resulted in a significant decrease in the time spent exploring the open arms of the EPMT (**Figure 2K**) only in control rats. Our results suggested that CeA treatment with TSA induced visceral hypersensitivity and anxiety-like behaviors in control rats and enhanced visceral hypersensitivity in ELS rats.

C646, a HAT inhibitor, was expected to have an opposite effect of TSA by increasing histone acetylation. Expectedly, the microinjection of C646 in the CeA attenuated visceral hypersensitivity of ELS rats when compared with control rats (**Figures 2C,F**). However, treatment of C646 did not affect

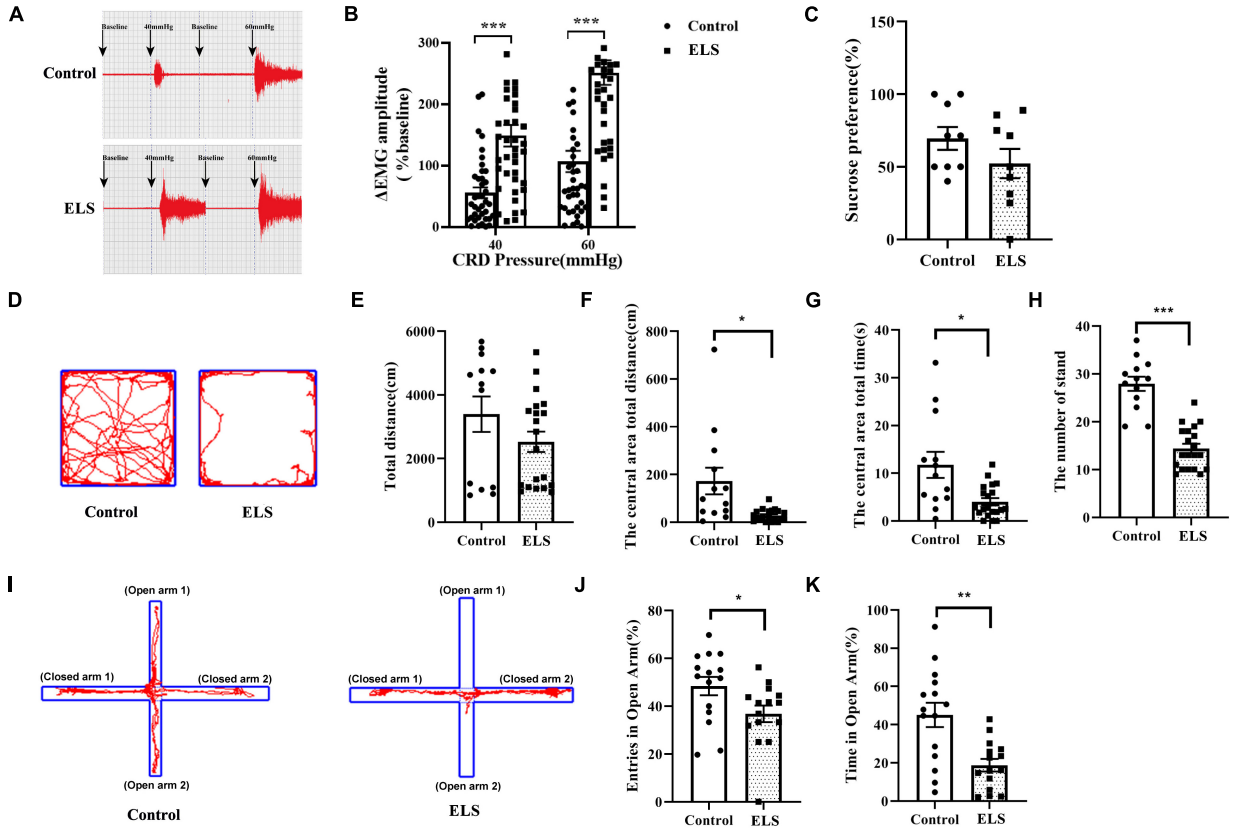

FIGURE 1 | Neonatal CRD resulted in visceral hypersensitivity and anxiety-like behaviors in adult rats. **(A,B)** Successful chronic visceral pain modeling with EMG assessment. The original typical traces of EMG **(A)**. Amplitude of ΔEMG in ELS rats, compared to that of controls, shown by quantification **(B)**. *N* = 40. One-way ANOVA and Mann–Whitney *U* test were performed. **(C)** Sucrose preference test used to detect depression-like behavior in rats. *N* = 9. Independent samples *t*-test was performed.**(D–H)** Anxiety-like behaviors were tested in the OFT. Original traces of OFT **(D)**. Quantification of the total distance **(E)**, the central area total distance **(F)**, the central area total time **(G)**, and the number of standings in OFT **(H)**. *N* = 13–20. Independent samples *t*-test was performed. **(I–K)** Anxiety-like behaviors were tested in the EPMT. Original trajectory representation diagram of EPMT **(I)**. Quantification of entries **(J)** and time **(K)** in the open arms. $^{*}p < 0.05$, $^{**}p < 0.01$, $^{***}p < 0.001$. *N* = 15. Independent samples *t*-test was performed **(J)**.One-way ANOVA and Mann–Whitney *U* test were performed **(K)**. N represents the number of rats per group.

anxiety-like behaviors of ELS rats in the experiment of the EPMT (**Figures 2I,L**).

The Involvement of Acetylated Lysine 9 Residue of Histone 3 (acH3K9) and Protein Kinase C Zeta Type in Early Life Stress Rats

Since our results indicated the contribution of histone acetylation to visceral sensitivity and anxiety-like behaviors of ELS rats, acH3K9 in the amygdala was assessed using western blot. acH3K9 expression was higher in ELS rats than in control rats (**Figure 3A**).

Our previous study showed that hippocampus PKMζ was involved in visceral sensitivity of ELS rats. In this study, we examined the expression of amygdala PKMζ using western blot, which was higher in ELS rats than in control rats (**Figure 3B**). The administration of PKMζ inhibitor ZIP into the CeA attenuated visceral hypersensitivity of ELS rats (**Figure 3G**). However, ZIP treatment didn't affect anxiety-like behaviors of ELS rats in the experiment of the EPMT (**Figures 3H–I**).

Protein expression is possibly regulated by histone acetylation. Amygdala PKMζ expression was assessed after TSA and C646 were microinjected into the CeA individually to alter the level of histone acetylation. TSA treatment increased amygdala PKMζ expression in control rats (**Figure 3C**), but not in ELS rats (**Figure 3D**). However, C646 treatment did not affect PKMζ expression in both control and ELS rats (**Figures 3E,F**).

Amygdala Histone Deacetylase 1–2 Expression Decreased in Early Life Stress Rats

To determine whether HDACs contributed to the elevation of histone acetylation in ELS rats, we examined the expression of nucleus HDAC1–3 in the amygdala. Amygdala nucleus HDAC1 and HDAC2 expressions decreased, whereas HDAC3 expression had no significant difference between ELS rats and control rats (**Figures 4A–C**). HDAC1–3 expression was further verified

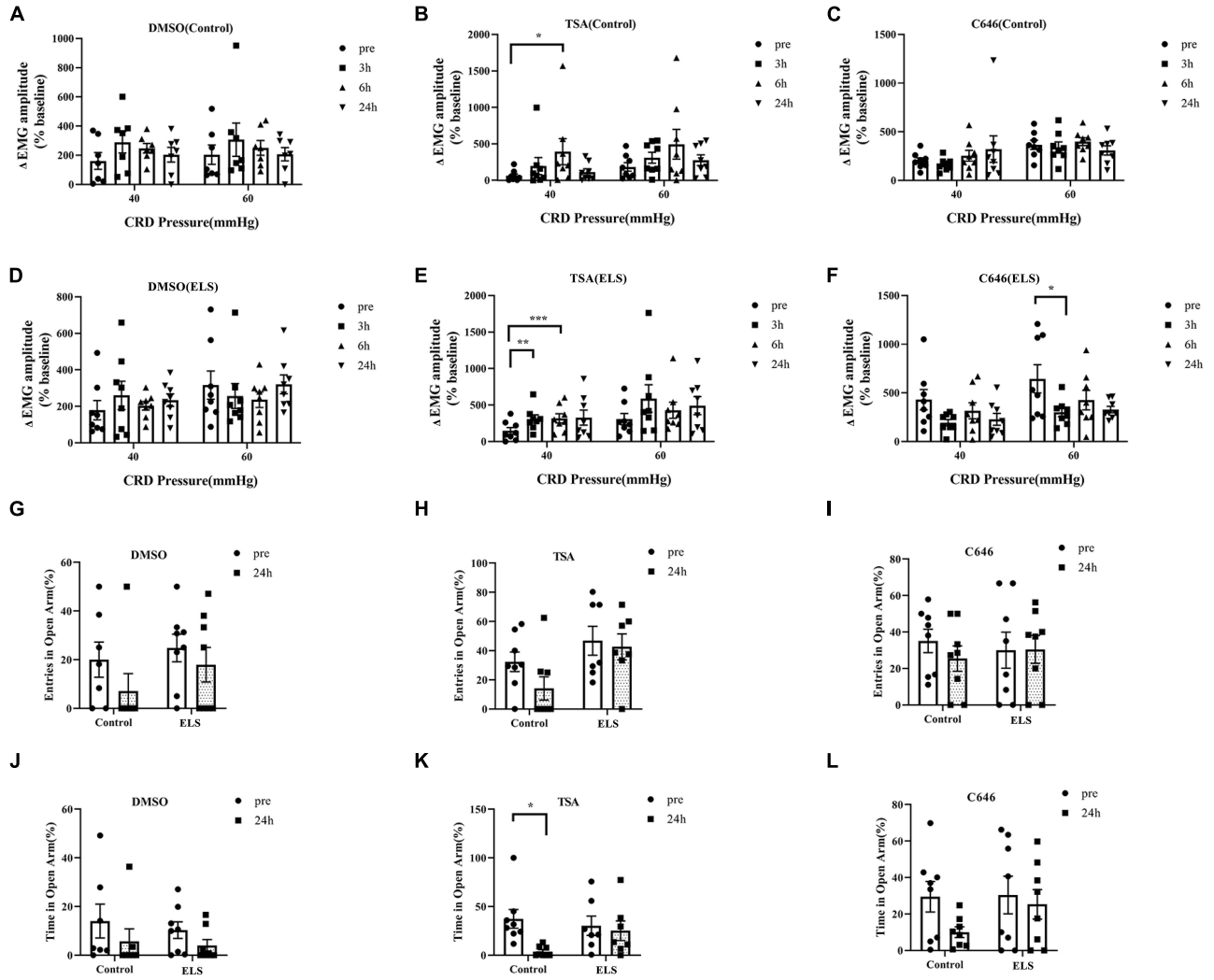

FIGURE 2 | Effects of TSA and C646 on pain and anxiety-like behaviors in rats. **(A–F)** Quantification of the amplitude of ΔEMG response to CRD (40, 60 mmHg) before and after microinjection of DMSO **(A)**, TSA **(B)**, C646 **(C)** in control rats and DMSO **(D)**, TSA **(E)**, C646 **(F)** in ELS rats. **(G–I)** Quantification of entries in the open arms before and after the microinjections of DMSO **(G)**, TSA **(H)**, and C646 **(I)** in rats. **(J–L)** Quantification of time in the open arms before and after the microinjections of DMSO **(J)**, TSA **(K)**, and C646 **(L)** in rats. $^{*}p < 0.05$, $^{**}p < 0.01$, $^{***}p < 0.001$. $N = 7–8$. A paired-samples *t*-test was performed **(A,G–J,L)**. A paired-samples *t*-test and Wilcoxon signed-rank test were performed **(B–F,K)**. N represents the number of rats per group.

using immunofluorescence (**Figure 5**). The results are consistent with those of western blot, indicating that the decrease of amygdala nucleus HDAC1 and HDAC2 expressions, but not HDAC3 expression, contributes to the enhancement of histone acetylation in ELS rats.

DISCUSSION

Our study indicated the important roles of histone acetylation modification in visceral hypersensitivity and negative emotion of ELS rats. We found that neonatal CRD resulted in visceral hypersensitivity and anxiety-like behaviors after adulthood. Inhibiting HDACs in the CeA enhanced visceral sensitivity but did not affect anxiety-like behaviors, whereas inhibiting HAT attenuated visceral hyperalgesia in ELS rats. Interestingly, CeA treatment with TSA induced visceral sensitivity and anxiety-like behaviors in control rats. Western blot showed that acH3k9 and PKMζ expressions were higher in ELS rats than in control rats. The administration of the PKMζ inhibitor ZIP into the CeA attenuated visceral hypersensitivity of ELS rats. Furthermore, amygdala PKMζ expression was enhanced by TSA treatment in control rats. Finally, western blot and immunofluorescence results indicated that the decrease of HDAC1 and HDAC2 expressions, but not HDAC3 expression, contributed to the enhancement of histone acetylation in ELS rats.

Irritable bowel syndrome is characterized by repeated abdominal pain in the absence of recognizable organic pathological changes, accompanied by abnormal defecation habit (Elsenbruch, 2014; Fadgyas-Stanculete et al., 2014;

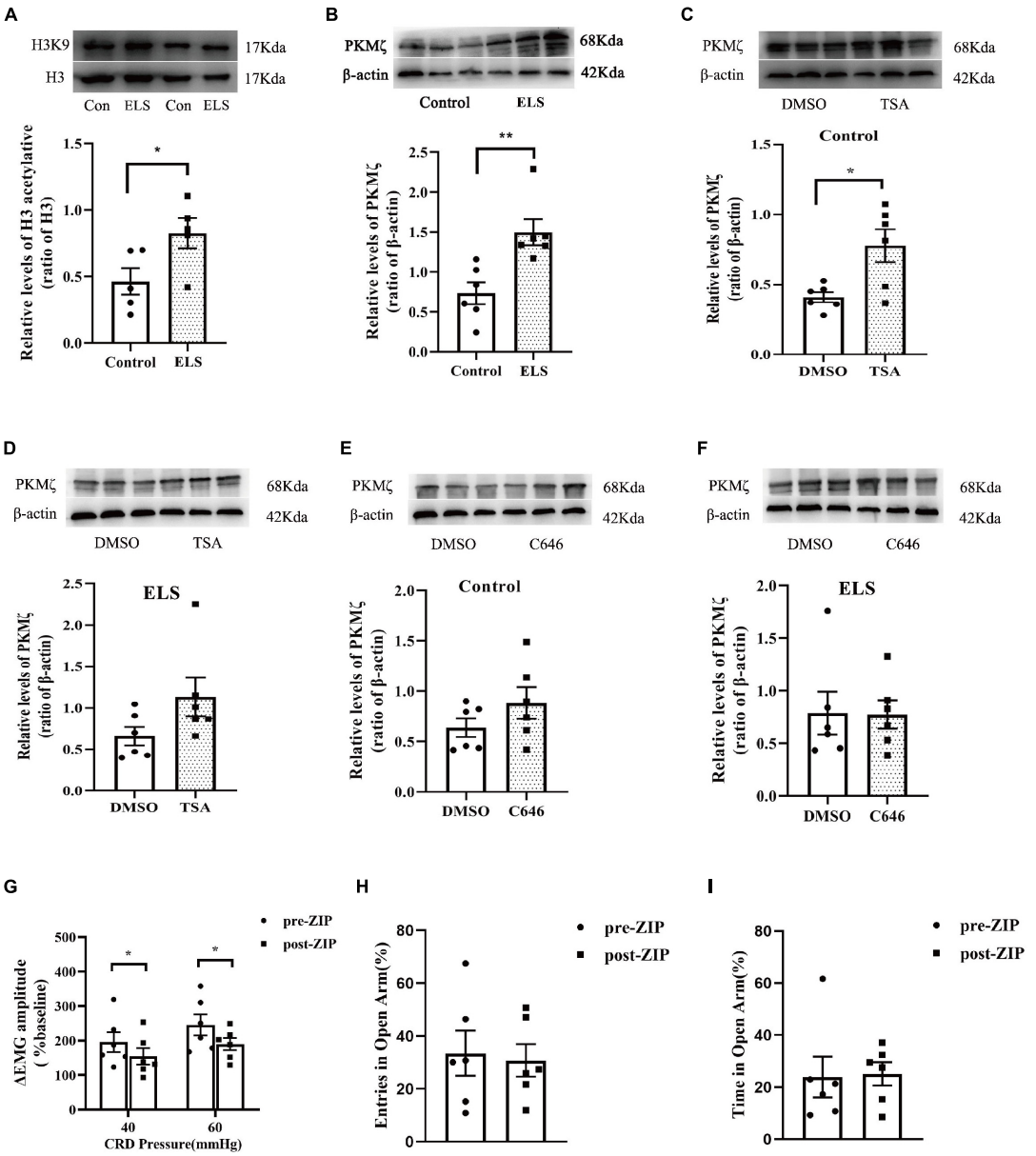

FIGURE 3 | The expression of acH3K9 and PKMζ in the amygdala of rats. And effects of ZIP on visceral hypersensitivity and anxiety-like behaviors in rats. Western blot showed that the expression of AcH3 **(A)** and PKMζ **(B)** increased in ELS rats compared to that in the controls. $N = 5$. **(C,D)** TSA treatment of CeA enhanced PKMζ expression in the control rats **(C)** but not in the ELS rats **(D)**. **(E,F)** C646 treatment of CeA did not affect PKMζ expression in both the control **(E)** and ELS rats **(F)**. ZIP (a PKMζ inhibitor) treatment of CeA attenuated visceral hypersensitivity **(G)** without affecting entries **(H)** and time **(I)** in the open arms of the EPMT in ELS rats. $^{*}p < 0.05$, $^{**}p < 0.01$. $N = 6$. Independent samples *t*-test was performed **(A,C–F)**. One-way ANOVA and Mann–Whitney *U* test were performed **(B)**. A paired-samples *t*-test and Wilcoxon signed-rank test were performed **(G–I)**. N represents the number of rats per group.

Meerveld and Johnson, 2018). Animal models of IBS were often established by recapitulating early-life stress, such as mother–infant separation (Moloney et al., 2015), unpredictable electrical stimulation (Louwies and Greenwood-Van Meerveld, 2020), and neonatal CRD (Chen et al., 2014; Gil et al., 2016; Fan et al., 2021). Our previous study indicated that neonatal CRD induced visceral hypersensitivity after adulthood (Chen et al., 2014; Fan et al., 2021). In this study, we focused not only on visceral pain but also on emotional comorbidity in ELS rats. We found that neonatal CRD resulted in visceral hypersensitivity and anxiety-like behaviors after adulthood in rats. Similar results were reported in IBS rats induced by neonatal maternal separation (Moloney et al., 2015). Functional brain imaging revealed that cognitive–emotional processes had an important influence on gastrointestinal sensation (Pellissier and Bonaz, 2017). Greenwood-Van Meerveld et al. reported that patients

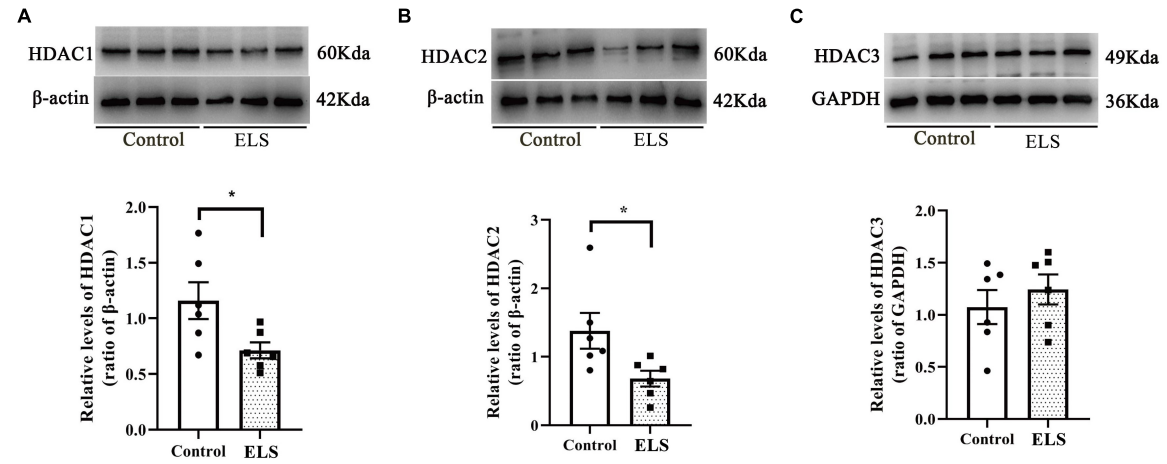

FIGURE 4 | The expression of HDAC1, HDAC2 and HDAC3 in the amygdala nucleus of rats. Western blot showed that the expression of HDAC1 **(A)** and HDAC2 **(B)** in the amygdala nucleus decreased significantly while HDAC3 **(C)** expression showed no significant difference in ELS rats compared to control rats $^{*}p < 0.05$. $N = 6$. Independent samples t-test was performed **(A–C)**. N represents the number of rats per group.

with IBS may experience aggravation of clinical symptoms under anxiety or stress (Greenwood-Van Meerveld et al., 2016; Pimentel and Lembo, 2020). The vicious circle of visceral hypersensitivity and negative emotions is considered challenging for the treatment of IBS. IBS patients show a hyperactive amygdala in brain imaging studies (Bonaz et al., 2002). A previous study showed that decreased CeA acH3K9 expression might lead to anxiety-like behaviors and hypersensitivity reactions caused by increased corticosteroid exposure (Tran et al., 2015). We also examined acH3K9 expression in the amygdala and found neonatal CRD caused increased acH3K9 in the amygdala of adult rats. The contradicting results may be caused by different methods of establishing animal models, which involved different pathophysiological mechanisms.

Since histone acetylation is involved in ELS rats, we hypothesized that modifying the acetylation level of histones might affect visceral hypersensitivity and anxiety-like behaviors of ELS rats. Therefore, we compared visceral pain reaction and emotions before and after HDAC inhibitor TSA and HAT inhibitor C646 were microinjected into the CeA individually. TSA is an effective, non-competitive, and reversible HDAC inhibitor that can increase the level of histone acetylation modification. TSA could enhance the acetylation of histones H3K9 and H4K8 (Zhang et al., 2019) in mice. In cultured cortical neurons, TSA treatment increased the expression of H3K9 and H3K18 (Borodinova et al., 2019). In contrast, C646 is a selective and competitive HAT p300 inhibitor that has little effect on other acetyltransferases. Previous studies reported that p300 preferentially acetylates histone H3K18/K27 instead of H3K9 (Lasko et al., 2017) and deletion of p300 specifically and dramatically reduced acetylations on H3K18 and H3K27 (Jin et al., 2011). In our study, CeA treatment with TSA induced visceral hypersensitivity and anxiety-like behaviors, whereas C646 did not affect visceral pain reaction and emotional behaviors in control rats. In ELS rats, visceral hypersensitivity was enhanced by TSA and alleviated by C646. Unexpectedly, anxiety-like behaviors of ELS rats were not significantly altered by either TSA or C646. In control rats, the level of CeA acH3K9 is low and TSA treatment might increase acH3K9 level which results in visceral hypersensitivity and anxiety-like behaviors. Though ELS rats showed high level of CeA acH3K9, it seems TSA treatment could further increase acH3K9 level to aggravate visceral pain. TSA could induce visceral hypersensitivity and anxiety-like behaviors in controls and enhance visceral hypersensitivity in ELS rats, suggesting the important role of histone acetylation in ELS. The results of C646 indicate p300 might participate in the process of visceral hypersensitivity but not anxiety-like behaviors of ELS rats. Since p300 preferentially acetylates histone H3K18/K27 (Jin et al., 2011; Lasko et al., 2017), it is reasonable for us to speculate that in addition to acH3K9, there are other sites of histone acetylation involved in ELS rats. Our results are consistent with the report that intrathecal injection of HAT inhibitors could reduce the visceral hypersensitivity by colorectal dilatation (Aguirre et al., 2017). In the chronic neuropathic pain model, the decrease of HDAC subtype sirtuin-1 (SIRT1) in the CeA increased H3K9, allowing animals to be at higher risk of emotional comorbidities, such as anxiety and depression. Moreover, this emotional comorbidity could be reversed by local overexpression of SIRT1 (Zhou et al., 2020). Although the type of chronic pain is different, emotional comorbidities seem to be involved with similar histone acetylation modification. However, literatures have reported that intrathecal injection of HDAC inhibitors could attenuate visceral hypersensitivity (Cao et al., 2015, 2016; Niederberger et al., 2017). Microinjection of HDACIs into the CeA attenuated anxiety-like behaviors and hypersensitivity reactions caused by increased corticosteroid exposure (Tran et al., 2015). Inconsistent results reported in literatures have suggested that the underlying mechanisms of chronic pain and emotional comorbidities vary based on the animal model and types of pain and tissue.

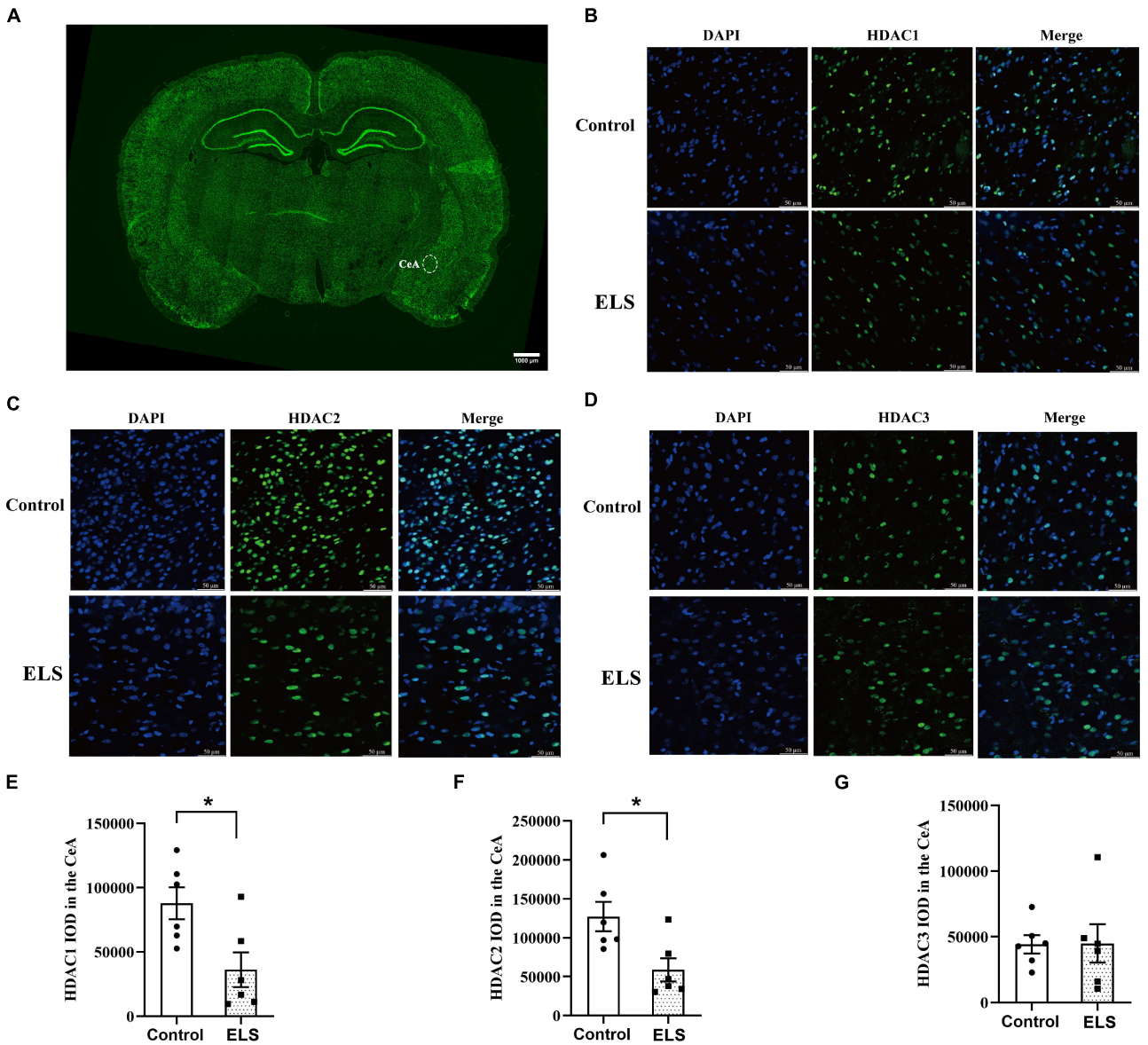

FIGURE 5 | The expression and localization of HDACs in CeA. **(A)** A representative picture of brain-slice immunofluorescence (HDAC2, green) from a control rat. The scale bar is 1,000 μm. Representative confocal immunofluorescent graphs of CeA HDAC1 **(B)**, HDAC2 **(C)**, and HDAC3 **(D)** reactivity in ELS rats and control rats. IOD value of CeA HDAC1 **(E)**, HDAC2 **(F)** and HDAC3 **(G)**. The localization of CeA HDAC1, HDAC2, and HDAC3 was mainly in the nucleus (blue). The expression of CeA HDAC1 (green) and HDAC2 (green) decreased significantly in ELS rats compared to that in control rats, whereas HDAC3 (green) did not show significant difference. The scale bar is 50 μm. $^*p < 0.05$. $N = 6$. Independent samples *t*-test was performed **(E–G)**. N represents the number of rats per group. IOD, integrated optical density.

Our previous studies found that the expression of PKMζ and PKMζ-dependent long-term potentiation were enhanced in the CA1 of IBS rats, and microinjection of ZIP in the hippocampus could alleviate visceral hypersensitivity (Chen et al., 2015; Tang et al., 2016), indicating that hippocampal PKMζ is involved in pain memory. However, PKMζ expression in the amygdala of IBS and the interface between histone acetylation and PKMζ are unclear. Therefore, we examined PKMζ expression and found that it was also significantly increased in the amygdala of ELS rats. Then we microinjected the PKMζ inhibitor ZIP into the CeA and found ZIP attenuated visceral hypersensitivity of ELS rats. However, ZIP treatment didn't affect anxiety-like behaviors of ELS rats in the experiment of the EPMT. Our finding indicated the increased PKMζ in CeA might contribute to visceral hypersensitivity but not emotional comorbidity of ELS rats. PKMζ seems a key molecule involved in the pain memory induced by early life stress. PKMζ inhibition could disrupt the expression of pain memory to attenuate visceral hypersensitivity of ELS rats. In contrast, PKMζ in the CeA is not likely associated with emotional comorbidity of ELS. The functional research of

the limbic brain showed that PKMζ inhibition in the basolateral amygdala, but not in the hippocampus, can disrupt fear memory (Kwapis et al., 2009). The role of PKMζ varies by brain areas and different emotional disorders. The current results might point toward two potentially different molecular mechanisms involved in the downstream of increased histone acetylation modification in CeA that modulate visceral hypersensitivity and emotional comorbidity of ELS rats. Histone acetylation and PKMζ in CeA are both involved in the visceral hypersensitivity of ELS rats. We examined if PKMζ is the molecular target of histone acetylation modification though enhanced histone acetylation in ELS rats is likely to regulate many genes. We found CeA treatment with TSA enhanced PKMζ expression, whereas C646 did not affect PKMζ expression, suggesting that PKMζ expression is possibly regulated by HDAC classes I and II, but not by p300. Memory research also found histone hyperacetylation enhanced PKMζ transcripts (Borodinova et al., 2019). However, more experiments need to be done to clarify the direct interaction of histone acetylation and PKMζ gene in ELS rats in the future.

A recent study found that the overexpression of neuron-specific HDAC2, but not that of HDAC1, reduced dendritic spine density, number of synapses, synaptic plasticity, and memory formation (Guan et al., 2009). On the contrary, HDAC2 deficiency resulted in an increase in the number of synapses and memory facilitation, similar to chronic treatment of HDAC in mice (Guan et al., 2009). The subtypes of HDAC plays different roles in synaptic plasticity and memory formation. Epigenetic modifications in the CeA serve as memories of adverse events that occurred during early life (Louwies and Greenwood-Van Meerveld, 2020). To clarify if high histone acetylation expression in ELS rats results from the decrease of HDAC expression, we examined HDAC1–3 expressions in the amygdala. It was found that HDAC1 and HDAC2 expressions decreased, whereas HDAC3 expression did not change significantly in the amygdala of ELS rats, indicating that the decreased HDAC1 and HDAC2 expression is responsible for the high level of histone acetylation in the amygdala of ELS rats. As a result, increased histone acetylation facilitated PKMζ expression in the CeA and caused visceral hypersensitivity in ELS rats. Recent literatures reported the existence of sexually dimorphic pain signaling in the spinal (Mapplebeck et al., 2018) and CeA (Louwies and Greenwood-Van Meerveld, 2020) of rats. Behavioral study showed estrous cycle and ELS are significant factors in visceral sensitivity (Moloney et al., 2016). In the future, it could be interesting to explore the sex difference in histone acetylation/PKMζ signaling in ELS rats induced by neonatal CRD.

In summary, we infer that neonatal CRD stimulation inhibited HDAC1 and HDAC2 expressions in the amygdala, which enhanced the level of histone acetylation in the amygdala of ELS rats. Modifying the levels of histone acetylation can affect visceral pain and anxiety-like behavior in rats. Moreover, PKMζ expression in the CeA was facilitated by increased histone acetylation, resulting in visceral hypersensitivity but not anxiety-like phenotype in ELS rats. Two potentially different molecular mechanisms might be involved in the downstream of increased histone acetylation modification in CeA that modulate visceral hypersensitivity and emotional comorbidity of ELS rats. Reprogramming inappropriate adaptations may result in sustaining extrinsic phenotypes, such as visceral hypersensitivity and anxiety-like behaviors in ELS rats. Since epigenetic programming is dynamic and revisable, reversing stress-induced abnormal epigenetic mechanisms may be crucial to relieve chronic symptoms in ELS rats.

CONCLUSION

Early life stress are induced by nociceptive stimulation in neonatal rats, which might induce inappropriate reprogramming by decreasing HDAC1 and HDAC2 expressions in the amygdala. Increased acH3K9 is involved in the phenotypes of visceral hypersensitivity and anxiety-like behaviors in ELS rats. Furthermore, enhancing amygdala histone acetylation facilitates the expression of synaptic plasticity-related protein PKMζ, which regulates visceral hypersensitivity of ELS rats. This study could provide new ideas for the treatment of IBS.

DATA AVAILABILITY STATEMENT

The raw data supporting the conclusions of this article will be made available by the authors, without undue reservation.

ETHICS STATEMENT

The animal study was reviewed and approved by the Committee for Care and Use of Laboratory Animals of Fujian Medical University.

AUTHOR CONTRIBUTIONS

LG: draft preparation, experiment design, *in vitro* experiments, and data analysis. XS and YT: behavioral experiments and data analysis. YY, LC, and GG: ELS model construct. YC: data analysis. CL and AC: experiment design, supervision, editing, and writing the manuscript. All authors contributed to the article and approved the submitted version.

FUNDING

This work was supported by Natural Science Foundation of Fujian Province (2020J01608 and 2021J01675), Fujian Science and Technology Innovation Joint Fund (2018Y9069), Educational Research Projects for Young and Middle-aged Teachers of Fujian Provincial Education Department (JAT190172).

ACKNOWLEDGMENTS

We would like to thank the Public Technology Service Center of Fujian Medical University (China) for providing technical support and experimental platforms.

REFERENCES

Aguirre, J. E., Winston, J. H., and Sarna, S. K. (2017). Neonatal immune challenge followed by adult immune challenge induces epigenetic-susceptibility to aggravated visceral hypersensitivity. *Neurogastroenterol. Motil.* 29:e13081. doi: 10.1111/nmo.13081

Bahari-Javan, S., Sananbenesi, F., and Fischer, A. (2014). Histone-acetylation: a link between Alzheimer's disease and post-traumatic stress disorder? *Front. Neurosci.* 8:160. doi: 10.3389/fnins.2014.00160

Bonaz, B., Baciu, M., Papillon, E., Bost, R., Gueddah, N., Le Bas, J. F., et al. (2002). Central processing of rectal pain in patients with irritable bowel syndrome: an fMRI study. *Am. J. Gastroenterol.* 97, 654–661. doi: 10.1111/j.1572-0241.2002.05545.x

Borodinova, A. A., Kuznetsova, M. A., Alekseeva, V. S., and Balaban, P. M. (2019). Histone acetylation determines transcription of atypical protein kinases in rat neurons. *Sci. Rep.* 9:4332. doi: 10.1038/s41598-019-40823-z

Bradford, K., Shih, W., Videlock, E. J., Presson, A. P., Naliboff, B. D., Mayer, E. A., et al. (2012). Association between early adverse life events and irritable bowel syndrome. *Clin. Gastroenterol. Hepatol.* 10, 385–90.e1–3. doi: 10.1016/j.cgh.2011.12.018

Cao, D. Y., Bai, G., Ji, Y., Karpowicz, J. M., and Traub, R. J. (2016). EXPRESS: histone hyperacetylation modulates spinal type II metabotropic glutamate receptor alleviating stress-induced visceral hypersensitivity in female rats. *Mol. Pain* 12:1744806916660722. doi: 10.1177/1744806916660722

Cao, D.-Y., Bai, G., Ji, Y., and Traub, R. J. (2015). Epigenetic upregulation of metabotropic glutamate receptor 2 in the spinal cord attenuates oestrogen-induced visceral hypersensitivity. *Gut* 64, 1913–1920. doi: 10.1136/gutjnl-2014-307748

Chaloner, A., and Greenwood-Van Meerveld, B. (2013). Early life adversity as a risk factor for visceral pain in later life: importance of sex differences. *Front. Neurosci.* 7:13. doi: 10.3389/fnins.2013.00013

Chen, A., Bao, C., Tang, Y., Luo, X., Guo, L., Liu, B., et al. (2015). Involvement of protein kinase zeta in the maintenance of hippocampal long-term potentiation in rats with chronic visceral hypersensitivity. *J. Neurophysiol.* 113, 3047–3055. doi: 10.1152/jn.00929.2014

Chen, Y., Chen, A. Q., Luo, X. Q., Guo, L. X., Tang, Y., Bao, C. J., et al. (2014). Hippocampal NR2B-containing NMDA receptors enhance long-term potentiation in rats with chronic visceral pain. *Brain Res.* 1570, 43–53. doi: 10.1016/j.brainres.2014.05.001

Cheng, W., Han, F., and Shi, Y. (2019). Neonatal isolation modulates glucocorticoid-receptor function and synaptic plasticity of hippocampal and amygdala neurons in a rat model of single prolonged stress. *J. Affect Disord.* 246, 682–694. doi: 10.1016/j.jad.2018.12.084

Elsenbruch, S. (2014). How positive and negative expectations shape the experience of visceral pain. *Handbook Exp. Pharmacol.* 225, 97–119. doi: 10.1007/978-3-662-44519-8_6

Fadgyas-Stanculete, M., Buga, A. M., Popa-Wagner, A., and Dumitrascu, D. L. (2014). The relationship between irritable bowel syndrome and psychiatric disorders: from molecular changes to clinical manifestations. *J. Mol. Psychiatry* 2:4. doi: 10.1186/2049-9256-2-4

Fan, F., Chen, Y., Chen, Z., Guan, L., Ye, Z., Tang, Y., et al. (2021). Blockade of BK channels attenuates chronic visceral hypersensitivity in an IBS-like rat model. *Mol. Pain* 17:17448069211040364. doi: 10.1177/17448069211040364

Farazi, N., Mahmoudi, J., Sadigh-Eteghad, S., Farajdokht, F., and Rasta, S. H. (2021). Synergistic effects of combined therapy with transcranial photobiomodulation and enriched environment on depressive- and anxiety-like behaviors in a mice model of noise stress. *Lasers Med. Sci.* 37, 1–11. doi: 10.1007/s10103-021-03370-6

Gauriau, C., and Bernard, J. F. (2004). A comparative reappraisal of projections from the superficial laminae of the dorsal horn in the rat: the forebrain. *J. Comp. Neurol.* 468, 24–56. doi: 10.1002/cne.10873

Gil, D. W., Wang, J., Gu, C., Donello, J. E., Cabrera, S., and Al-Chaer, E. D. (2016). Role of sympathetic nervous system in rat model of chronic visceral pain. *Neurogastroenterol. Motil.* 28, 423–431. doi: 10.1111/nmo.12742

Graff, J., and Tsai, L. H. (2013). Histone acetylation: molecular mnemonics on the chromatin. *Nat. Rev. Neurosci.* 14, 97–111. doi: 10.1038/nrn3427

Greenwood-Van Meerveld, B., Moloney, R. D., Johnson, A. C., and Vicario, M. (2016). Mechanisms of Stress-Induced Visceral Pain: Implications in Irritable Bowel Syndrome. *J. Neuroendocrinol.* 28, 1–10. doi: 10.1111/jne.12361

Guan, J. S., Haggarty, S. J., Giacometti, E., Dannenberg, J. H., Joseph, N., Gao, J., et al. (2009). HDAC2 negatively regulates memory formation and synaptic plasticity. *Nature* 459, 55–60. doi: 10.1038/nature07925

Hu, X. F., He, X. T., Zhou, K. X., Zhang, C., Zhao, W. J., Zhang, T., et al. (2017). The analgesic effects of triptolide in the bone cancer pain rats via inhibiting the upregulation of HDACs in spinal glial cells. *J. Neuroinflam.* 14:213. doi: 10.1186/s12974-017-0988-1

Jin, Q., Yu, L.-R., Wang, L., Zhang, Z., Kasper, L. H., Lee, J.-E., et al. (2011). Distinct roles of GCN5/PCAF-mediated H3K9ac and CBP/p300-mediated H3K18/27ac in nuclear receptor transactivation. *EMBO J.* 30, 249–262. doi: 10.1038/emboj.2010.318

Khangura, R. K., Sharma, J., Bali, A., Singh, N., and Jaggi, A. S. (2019). An integrated review on new targets in the treatment of neuropathic pain. *Korean J. Physiol. Pharmacol.* 23, 1–20. doi: 10.4196/kjpp.2019.23.1.1

Kwapis, J. L., Jarome, T. J., Lonergan, M. E., and Helmstetter, F. J. (2009). Protein kinase Mzeta maintains fear memory in the amygdala but not in the hippocampus. *Behav. Neurosci.* 123, 844–850. doi: 10.1037/a0016343

Lasko, L. M., Jakob, C. G., Edalji, R. P., Qiu, W., Montgomery, D., Digiammarino, E. L., et al. (2017). Discovery of a selective catalytic p300/CBP inhibitor that targets lineage-specific tumours. *Nature* 550, 128–132.

Liu, H., Huang, X., Xu, J., Mao, H., Li, Y., Ren, K., et al. (2021). Dissection of the relationship between anxiety and stereotyped self-grooming using the Shank3B mutant autistic model, acute stress model and chronic pain model. *Neurobiol. Stress* 15:100417. doi: 10.1016/j.ynstr.2021.100417

Louwies, T., and Greenwood-Van Meerveld, B. (2020). Sex differences in the epigenetic regulation of chronic visceral pain following unpredictable early life stress. *Neurogastroenterol. Motil.* 32:e13751. doi: 10.1111/nmo.13751

Lucassen, P. J., Pruessner, J., Sousa, N., Almeida, O. F., Van Dam, A. M., Rajkowska, G., et al. (2014). Neuropathology of stress. *Acta Neuropathol.* 127, 109–135.

Maddox, S. A., Watts, C. S., Doyere, V., and Schafe, G. E. (2013a). A naturally-occurring histone acetyltransferase inhibitor derived from Garcinia indica impairs newly acquired and reactivated fear memories. *PLoS One* 8:e54463. doi: 10.1371/journal.pone.0054463

Maddox, S. A., Watts, C. S., and Schafe, G. E. (2013b). p300/CBP histone acetyltransferase activity is required for newly acquired and reactivated fear memories in the lateral amygdala. *Learn Mem.* 20, 109–119. doi: 10.1101/lm.029157.112

Mao, Y., Zhou, J., Liu, X., Gu, E., Zhang, Z., and Tao, W. (2019). Comparison of Different Histone Deacetylase Inhibitors in Attenuating Inflammatory Pain in Rats. *Pain Res. Manag.* 2019:1648919.

Mapplebeck, J. C. S., Dalgarno, R., Tu, Y., Moriarty, O., Beggs, S., Kwok, C. H. T., et al. (2018). Microglial P2X4R-evoked pain hypersensitivity is sexually dimorphic in rats. *Pain* 159, 1752–1763. doi: 10.1097/j.pain.0000000000001265

Marcal, R., Llorente, L., Herrero, O., Planello, R., Guilherme, S., and Pacheco, M. (2021). Intergenerational Patterns of DNA Methylation in Procambarus clarkii Following Exposure to Genotoxicants: A Conjugation in Past Simple or Past Continuous? *Toxics* 9:271. doi: 10.3390/toxics9110271

McDonald, A. J., and Mott, D. D. (2017). Functional neuroanatomy of amygdalohippocampal interconnections and their role in learning and memory. *J. Neurosci. Res.* 95, 797–820. doi: 10.1002/jnr.23709

Meerveld, B. G., and Johnson, A. C. (2018). Mechanisms of Stress-induced Visceral Pain. *J. Neurogastroenterol. Motil.* 24, 7–18. doi: 10.5056/jnm17137

Mitrousis, N., Tropepe, V., and Hermanson, O. (2015). Post-Translational Modifications of Histones in Vertebrate Neurogenesis. *Front. Neurosci.* 9:483. doi: 10.3389/fnins.2015.00483

Moloney, R. D., Sajjad, J., Foley, T., Felice, V. D., Dinan, T. G., Cryan, J. F., et al. (2016). Estrous cycle influences excitatory amino acid transport and visceral pain sensitivity in the rat: effects of early-life stress. *Biol. Sex Differ.* 7:33. doi: 10.1186/s13293-016-0086-6

Moloney, R. D., Stilling, R. M., Dinan, T. G., and Cryan, J. F. (2015). Early-life stress-induced visceral hypersensitivity and anxiety behavior is reversed by histone deacetylase inhibition. *Neurogastroenterol. Motil.* 27, 1831–1836. doi: 10.1111/nmo.12675

Niederberger, E., Resch, E., Parnham, M. J., and Geisslinger, G. (2017). Drugging the pain epigenome. *Nat. Rev. Neurol.* 13, 434–447. doi: 10.1038/nrneurol.2017.68

Pellissier, S., and Bonaz, B. (2017). The Place of Stress and Emotions in the Irritable Bowel Syndrome. *Vitam. Horm.* 103, 327–354. doi: 10.1016/bs.vh.2016.09.005

Pimentel, M., and Lembo, A. (2020). Microbiome and Its Role in Irritable Bowel Syndrome. *Digest. Dis. Sci.* 65, 829–839. doi: 10.1007/s10620-020-06109-5

Tang, Y., Chen, A., Chen, Y., Guo, L., Dai, H., Huang, Y., et al. (2016). Zeta Inhibitory Peptide as a Novel Therapy to Control Chronic Visceral Hypersensitivity in a Rat Model. *PLoS One* 11:e0163324. doi: 10.1371/journal.pone.0163324

Tran, L., Schulkin, J., Ligon, C. O., and Greenwood-Van Meerveld, B. (2015). Epigenetic modulation of chronic anxiety and pain by histone deacetylation. *Mol. Psychiatry* 20, 1219–1231. doi: 10.1038/mp.2014.122

Vierck, C. J., Wong, F., King, C. D., Mauderli, A. P., Schmidt, S., and Riley, J. L. (2014). 3rd, Characteristics of sensitization associated with chronic pain conditions. *Clin. J. Pain* 30, 119–128. doi: 10.1097/AJP.0b013e318287aac7

Wei, L., Zhu, Y. M., Zhang, Y. X., Liang, F., Barry, D. M., Gao, H. Y., et al. (2016). Microinjection of histone deacetylase inhibitor into the ventrolateral orbital cortex potentiates morphine induced behavioral sensitization. *Brain Res.* 1646, 418–425. doi: 10.1016/j.brainres.2016.06.019

Yang, R., Sun, H., Wu, Y., Lu, G., Wang, Y., Li, Q., et al. (2019). Long-Lasting Sex-Specific Effects Based On Emotion- and Cognition-Related Behavioral Assessment of Adult Rats After Post-Traumatic Stress Disorder From Different Lengths of Maternal Separation. *Front. Psychiatry* 10:289. doi: 10.3389/fpsyt.2019.00289

Zhang, Y., Ren, L., Min, S., Lv, F., and Yu, J. (2021). Effects of N-Methyl-D-aspartate receptor (NMDAR) and Ca(2+)/calmodulin-dependent protein kinase IIalpha (CaMKIIalpha) on learning and memory impairment in depressed rats with different charge by modified electroconvulsive shock. *Ann. Transl. Med.* 9:1320. doi: 10.21037/atm-21-3690

Zhang, Y., Xie, H., Tang, W., Zeng, X., Lin, Y., Xu, L., et al. (2019). Trichostatin A, a Histone Deacetylase Inhibitor, Alleviates Eosinophilic Meningitis Induced by Angiostrongylus cantonensis Infection in Mice. *Front. Microbiol.* 10:2280. doi: 10.3389/fmicb.2019.02280

Zhou, C., Wu, Y., Ding, X., Shi, N., Cai, Y., and Pan, Z. Z. (2020). SIRT1 Decreases Emotional Pain Vulnerability with Associated CaMKIIα Deacetylation in Central Amygdala. *J. Neurosci.* 40, 2332–2342. doi: 10.1523/JNEUROSCI.1259-19.2020

Zhou, M., Liu, Z., Yu, J., Li, S., Tang, M., Zeng, L., et al. (2018). Quantitative Proteomic Analysis Reveals Synaptic Dysfunction in the Amygdala of Rats Susceptible to Chronic Mild Stress. *Neuroscience* 376, 24–39. doi: 10.1016/j.neuroscience.2018.02.010

Conflict of Interest: The authors declare that the research was conducted in the absence of any commercial or financial relationships that could be construed as a potential conflict of interest.

Publisher's Note: All claims expressed in this article are solely those of the authors and do not necessarily represent those of their affiliated organizations, or those of the publisher, the editors and the reviewers. Any product that may be evaluated in this article, or claim that may be made by its manufacturer, is not guaranteed or endorsed by the publisher.

frontiers | Frontiers in Neuroscience

ORIGINAL RESEARCH
published: 24 May 2022
doi: 10.3389/fnins.2022.889211

A Prebiotic Diet Alters the Fecal Microbiome and Improves Sleep in Response to Sleep Disruption in Rats

Samuel J. Bowers[1,2†], Keith C. Summa[1,3*†], Robert S. Thompson[4,5], Antonio González[6], Fernando Vargas[7], Christopher Olker[1,2], Peng Jiang[1,2], Christopher A. Lowry[4,5], Pieter C. Dorrestein[7,8], Rob Knight[6,8,9,10], Kenneth P. Wright Jr.[4,5,11], Monika Fleshner[4,5], Fred W. Turek[1,2,12,13] and Martha H. Vitaterna[1,2]*

[1] Center for Sleep and Circadian Biology, Northwestern University, Evanston, IL, United States, [2] Department of Neurobiology, Northwestern University Weinberg College of Arts and Sciences, Evanston, IL, United States, [3] Division of Gastroenterology & Hepatology, Department of Medicine, Northwestern University Feinberg School of Medicine, Chicago, IL, United States, [4] Department of Integrative Physiology, University of Colorado, Boulder, Boulder, CO, United States, [5] Center for Neuroscience, University of Colorado, Boulder, Boulder, CO, United States, [6] Department of Pediatrics, University of California San Diego School of Medicine, La Jolla, CA, United States, [7] Collaborative Mass Spectrometry Innovation Center, Skaggs School of Pharmacy & Pharmaceutical Sciences, University of California, San Diego, La Jolla, CA, United States, [8] Center for Microbiome Innovation, University of California, San Diego, La Jolla, CA, United States, [9] Department of Computer Science and Engineering, University of California, San Diego, La Jolla, CA, United States, [10] Department of Bioengineering, University of California, San Diego, La Jolla, CA, United States, [11] Sleep and Chronobiology Laboratory, University of Colorado, Boulder, Boulder, CO, United States, [12] The Ken & Ruth Davee Department of Neurology, Northwestern University Feinberg School of Medicine, Chicago, IL, United States, [13] Department of Psychiatry and Behavioral Sciences, Northwestern University Feinberg School of Medicine, Chicago, IL, United States

OPEN ACCESS

Edited by:
He Wang,
Fudan University, China

Reviewed by:
Shawn M. Talbott,
Amare Global, United States
Alessandro Silvani,
University of Bologna, Italy

***Correspondence:**
Samuel J. Bowers
samuel.bowers@northwestern.edu
Keith C. Summa
ksumma@northwestern.edu

† These authors have contributed equally to this work and share first authorship

Specialty section:
This article was submitted to Gut-Brain Axis, a section of the journal Frontiers in Neuroscience

Received: 03 March 2022
Accepted: 28 April 2022
Published: 24 May 2022

Citation:
Bowers SJ, Summa KC, Thompson RS, González A, Vargas F, Olker C, Jiang P, Lowry CA, Dorrestein PC, Knight R, Wright KP Jr, Fleshner M, Turek FW and Vitaterna MH (2022) A Prebiotic Diet Alters the Fecal Microbiome and Improves Sleep in Response to Sleep Disruption in Rats. Front. Neurosci. 16:889211. doi: 10.3389/fnins.2022.889211

Sleep disruption is a challenging and exceedingly common physiological state that contributes to a wide range of biochemical and molecular perturbations and has been linked to numerous adverse health outcomes. Modern society exerts significant pressure on the sleep/wake cycle *via* myriad factors, including exposure to electric light, psychological stressors, technological interconnection, jet travel, shift work, and widespread use of sleep-affecting compounds. Interestingly, recent research has identified a link between the microbiome and the regulation of sleep, suggesting that interventions targeting the microbiome may offer unique therapeutic approaches to challenges posed by sleep disruption. In this study, we test the hypothesis that administration of a prebiotic diet containing galactooligosaccharides (GOS) and polydextrose (PDX) in adult male rats improves sleep in response to repeated sleep disruption and during recovery sleep. We found that animals fed the GOS/PDX prebiotic diet for 4 weeks exhibit increased non-rapid eye movement (NREM) and rapid eye movement (REM) sleep during 5 days of sleep disruption and increased total sleep time during 24 h of recovery from sleep disruption compared to animals fed a control diet, despite similar baseline sleep characteristics. Further, the GOS/PDX prebiotic diet led to significant changes in the fecal microbiome. Consistent with previous reports, the prebiotic diet increased the relative abundance of the species *Parabacteroides distasonis*, which positively correlated with sleep parameters during recovery sleep. Taken together, these findings suggest that the GOS/PDX prebiotic diet may offer an approach to improve resilience to the physiologic challenge of sleep disruption, in part through impacts on the microbiome.

Keywords: sleep, sleep restriction, prebiotic, microbiome, microbiome-gut-brain axis

INTRODUCTION

Sleep disruption is a common problem in modern society. Sleep deprivation increases the risk of motor vehicle accidents (Barger et al., 2005; Bioulac et al., 2017), workplace injuries (Nakata, 2011), and medical errors (Trockel et al., 2020). Chronic sleep disruption has been associated with many adverse health consequences, including, but not limited to, increased rates of cardiovascular, metabolic, gastrointestinal, neurological, and psychiatric diseases (Kecklund and Axelsson, 2016; Liew and Aung, 2021). Many aspects of the modern environment contribute to sleep disruption: electric light, screen exposure, technological interconnection, societal and workplace expectations for near constant availability, jet travel, shift work, and widespread use of sleep-interfering chemicals such as caffeine (Grandner, 2017). Although lifestyle modifications may mitigate some of these factors, these are not often effective under all conditions nor are they widely adopted or sustainable over long periods of time. Furthermore, it seems unlikely that societal, environmental, and cultural factors contributing to insufficient sleep duration and poor sleep habits will reverse. Thus, interventions aimed at improving resilience to insufficient sleep may offer a viable strategy for mitigating adverse consequences.

Interestingly, recent work has demonstrated bidirectional connections between sleep and the microbiome in rodent models (Thompson et al., 2016, 2020; Bowers et al., 2020; Wang et al., 2022) and humans (Matenchuk et al., 2020). Considering the context of the large and growing bodies of literature linking adverse physiologic consequences and multiple diseases to sleep disruption (Kecklund and Axelsson, 2016; Liew and Aung, 2021) and to changes to the intestinal microbiome, or dysbiosis (Battson et al., 2018; Halverson and Alagiakrishnan, 2020; Meng et al., 2020), strategies targeting the structure and function of the microbiome are an exciting potential therapeutic opportunity (Wolter et al., 2021). One such approach is *via* dietary supplementation with prebiotics, which are compounds neither absorbed nor actively metabolized by human hosts but are selective substrates for intestinal bacteria thought to be beneficial (Manning and Gibson, 2004). Galactooligosaccharides (GOS) and polydextrose (PDX) are examples of prebiotics that have been shown to impact physiological processes in different model systems (Macfarlane et al., 2008; Do Carmo et al., 2016), including a recent report showing that GOS/PDX supplementation in rats accelerates recovery in response to environmental disruption of circadian rhythms (Thompson et al., 2021).

In this study, we test the hypothesis that dietary supplementation with the prebiotics GOS and PDX improves sleep in response to sleep deprivation and recovery sleep in adult male rats. We demonstrate that prebiotic diet supplementation led to changes in the structure and predicted function of the microbiome. The prebiotic diet did not impact baseline sleep, yet, surprisingly, promoted increased non-rapid eye movement (NREM) and rapid eye movement (REM) sleep during the sleep deprivation protocol as well as increased total sleep during recovery. These sleep changes were positively correlated with the relative abundance of the bacterium *Parabacteroides distasonis*, which we and others have previously shown to be increased by GOS/PDX supplementation and which may promote resilience in the setting of physiologic challenges such as chronic disruption of circadian rhythms (Thompson et al., 2021). An analysis of fecal bile acids demonstrated associations with *P. distasonis* and other bacteria impacted by the prebiotic diet, suggesting a potential mechanism by which the prebiotic diet may exert physiologic effects. These findings indicate that dietary interventions targeting the microbiome may provide resilience in the context of physiologically challenging environmental stimuli such as insufficient sleep.

Abbreviations: ANCOM, analysis of composition of microbiomes; BL, baseline; clr, centered log ratio; Con, control diet; EEG, electroencephalography; EMG, electromyography; GOS, galactooligosaccharides; LPS, lipopolysaccharide; NREM, non-rapid eye movement; OLM, object location memory; P, postnatal day; PC, principal coordinate; PCoA, principal coordinate analysis; PDX, polydextrose; PERMANOVA, permutational multivariate analysis of variance; Pre, prebiotic diet; REM, rapid eye movement; SD1-5, 24-h sleep disruption day 1-5; S1-5, 20-h sleep disruption window; ZT, Zeitgeber time.

MATERIALS AND METHODS

Animals and Experimental Design

Figure 1 presents a schematic of the experimental protocol. Twelve cohorts of eight 23-day old male Sprague Dawley rats (Envigo Laboratories, Madison, Wi, United States) were used for this experiment (N = 96). A total of 13 animals did not complete the experimental protocol and were thus eliminated from all analyses, for a total N = 83. No explicit power analysis was used, the sample size was selected to ensure an adequate number of biological replicates for the primary outcome measure: polysomnographic sleep recording (target of N = 10–12/experimental group). The experiment consisted of eight experimental groups in a 2 × 2 × 2 design (control diet *vs* prebiotic diet, *ad* libitum sleep *vs* sleep disruption, no social defeat *vs* social defeat). Rats were pair-housed until electroencephalographic (EEG) and electromyographic (EMG) implant surgery at 7 weeks of age, after which they were individually housed until the end of the experiment.

After placement of rats in cages on the day of arrival, diet groups (control diet *vs* prebiotic diet) were randomly assigned to the different cages. After EEG/EMG surgery, rats were assigned to further experimental groups (*ad* libitum sleep *vs* sleep disruption and no social defeat *vs* social defeat) randomly, with an effort to ensure prior cagemates were in different groups. Male Long Evans rats (Envigo Laboratories) were used as aggressors in the social defeat model (see below). All rats were maintained on a 12:12 light:dark cycle at room temperature (23 ± 2°C) with food and water available *ad* libitum throughout the experiment. All protocols were approved in advance by the Northwestern University Institutional Animal Care and Use Committee. Zeitgeber time (Zt) is defined as the number of hours after the onset of the light period (light onset = Zt0).

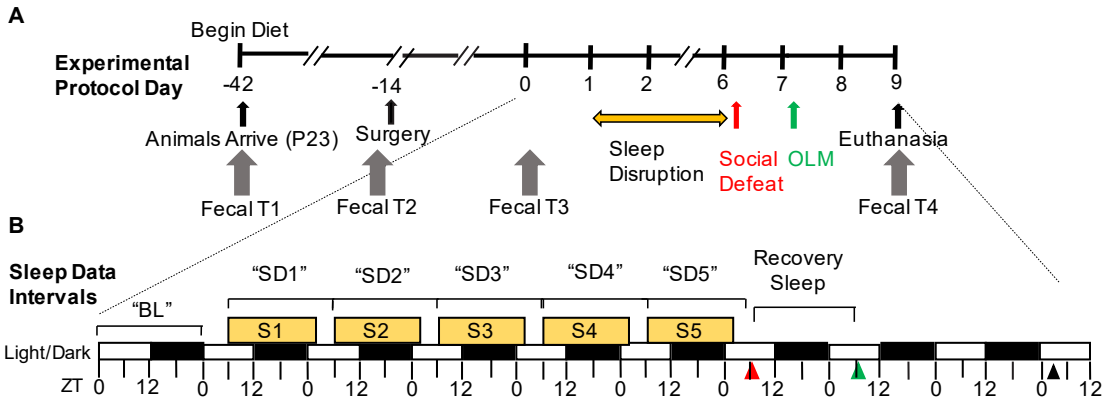

FIGURE 1 | Experimental timeline. **(A)** Overview of the experimental protocol. Experimental protocol days are depicted along the axis of the timeline. The yellow horizontal arrow denotes the sleep disruption portion of the protocol. The red and green arrows denote social defeat and object learning memory, respectively. Days of fecal sample collection are indicated with gray arrows. **(B)** Detail of indicated period that includes the sleep disruption protocol, social defeat stress (red arrowhead), object location memory (green arrowhead), and terminal sample collection (black arrowhead). Tick marks along the bottom of the timeline axis indicate Zeitgeber time (ZT) on that day, white/black rectangles indicate 12-h light/dark phases, and yellow rectangles indicate time periods of sleep disruption for the sleep-disrupted groups (ZT6-ZT2). EEG/EMG recording intervals, as used in the forthcoming figures, are indicated above the timeline. BL, baseline; OLM, object location memory; P, postnatal day; S, 20-h sleep disruption window; SD, 24-h sleep disruption day; ZT, Zeitgeber time.

Experimental Diets

Upon arrival to the facility, rats were started on *ad libitum* control or prebiotic diets as previously described (Thompson et al., 2021). The control diet was Envigo Teklad diet TD.110883 (Envigo Teklad, Madison, WI, United States). The prebiotic diet consisted of the control diet supplemented with galactooligosaccharides [GOS, 21.23 total g/kg (7.00 active g/kg); FrieslandCampina, Zwolle, Netherlands] and polydextrose (PDX, 7.69 total g/kg (7.00 active g/kg); Danisco, Terre Haute, IN, United States). The prebiotic diet was custom-made by Envigo Teklad (TD.110889). The control and prebiotic diets are isocaloric and contain similar macronutrient, vitamin, and mineral levels, as previously described (Thompson et al., 2016, 2021).

EEG/EMG Implantation Surgery

Four weeks after arrival, and 14 days prior to baseline sleep (i.e., on day −14), rats were implanted with electroencephalographic/electromyographic (EEG/EMG) sleep recording devices (Pinnacle Technologies, Lawrence, KS, United States). Surgical procedures were performed using a rat stereotaxic apparatus with standard aseptic techniques in a ventilated, specially equipped surgical suite. Anesthesia was induced by isoflurane gas. The EEG/EMG headmount consisted of a plastic 6-pin connector attached to four EEG electrodes and two EMG electrodes. Four stainless steel screws serving as two EEG leads and grounds were screwed into the skull with one lead located 5 mm anterior to bregma and 2 mm lateral to the central suture, another 1 mm anterior to bregma, 2 mm lateral to the central suture, and the other two at 1 mm anterior to lambda and 2.5 mm lateral to each side of the central suture. The exposed ends of two stainless steel Teflon-coated wires serving as EMG leads were then inserted into the nuchal muscles using a pair of forceps. The entire headmount was then sealed by dental acrylic and, at the front and the back of the implant, sutures were used to close the incision. Indirect heat support was provided until recovery from anesthetic by placing a heating pad underneath half of the cage the animals were returned to after surgery. Subcutaneous injection of analgesic meloxicam (2 mg/kg; Norbrook Laboratories, Northern Ireland) was given to the animals at the time of surgery and once more on the following day.

Sleep Recording and Analysis

After surgery, rats were moved into cylindrical sleep recording cages (Pinnacle Technologies) within individual acoustically-isolated and Faraday-shielded chambers. Two days before baseline sleep, the headmount was connected to the transmission tether. Cages had corncob bedding as well as food and water available *ad libitum*. Sleep was recorded for a 24-h baseline, then recordings were begun at the start of sleep restriction protocol (ZT6), in which rats were permitted 4 h of interrupted sleep opportunity per 24 h. At the end of the fifth 20-h sleep disruption session, rats were unplugged from their EEG/EMG tethers for social defeat (see below). Upon return to home cages, sleep recording resumed for 24 h (ZT7-ZT7) until rats were unplugged from their EEG/EMG tethers for evaluation in the object location memory (OLM) test. Data were collected using Pinnacle Acquisition software (Pinnacle Technologies), then scored as non-rapid eye movement sleep (NREM), rapid eye movement sleep (REM), or wake in 10 s epochs using machine learning-assisted sleep scoring program as described previously (Gao et al., 2016).

The initiation of a bout of NREM, REM, or wake was defined by the occurrence of two consecutive epochs of NREM, REM, or wake (respectively). A bout was terminated when two consecutive epochs failed to match the state of that bout. For example, a NREM sleep bout was initiated by two consecutive NREM epochs and was terminated when two consecutive non-NREM

epochs occurred. A brief arousal was defined as a single epoch of wake within a sleep bout. The delta power band was defined as 0.5–4 Hz, theta as 4–8 Hz, alpha as 8–11 Hz, sigma as 11–15 Hz, and beta as 15–30 Hz. Relative power was calculated as the raw power (μV^2) in a particular band divided by the total power in all bands.

Sleep Disruption Protocol

After baseline sleep recordings, half of the rats were tested in the sleep disruption protocol. Sleep disruption was achieved using a commercially available system integrated into the chambers (Pinnacle Technologies), which simulates the gentle handling technique *via* a rotating metal bar (22 cm in length) attached to a post at the center of the cage. For sleep disruption days, the rotation speed of the bar was set at seven rotations per minute with reversals of rotation direction (i.e., clockwise *vs.* counterclockwise) set to occur at semi-random intervals of 10 ± 10 s. The bar was programmed to rotate for 20 h per day (ZT6-ZT2) and was stationary for 4 h per day (ZT2-ZT6), for 5 days total. Experimenters visually inspected rats at regular intervals during the sleep disruption windows to ensure that the bar mechanism was functioning properly and that the sleep-disrupted rats were awake. Control animals were placed in identical cages with bars that remained stationary throughout the experiment.

Social Defeat Protocol

Male Long Evans rats were singly housed in large (44 cm × 24 cm × 21 cm) polycarbonate cages and screened for aggressive behavior before the experiment. Rats that began to injure their opponents by harmful bites during screening were not used for the social defeat procedure. On the day of the acute social defeat stress exposure, half of the experimental rats were introduced into the cage of an aggressor (testing done at ∼ZT6). As soon as the aggressor rat attacked and defeated the intruder rat, the intruder was covered with a 25 cm × 15 cm × 15 cm metal mesh cage while still inside the aggressor cage and left in place for 1 h. Control animals not receiving social defeat were unplugged from the recording tether and placed in a clean cage in a quiet room.

Object Location Memory Task

The object location memory (OLM) task is a hippocampal-dependent memory task (Murai et al., 2007) that is sensitive to stress exposure (Cazakoff et al., 2010; Howland and Cazakoff, 2010). All rats underwent testing in the OLM task the day after social defeat, beginning at ZT7. Rats were placed in a dimly lit (∼50 lux) 53 cm × 53 cm × 30 cm arena with no objects and allowed to explore for 5 min. Approximately 30–40 min later, they were returned to the chamber, this time containing two identical cylindrical objects (100 mL pyrex bottles with caps) on the same side of the arena. Rats were allowed to explore the arena for 5 min and after 90 min in their home cage were allowed to explore the arena again, with one object moved. Exploration of the moved object for longer than the non-moved object is considered evidence of successful acquisition of contextual memory (Murai et al., 2007). This is denoted by a "location index" expressed as a percentage of time [100 × (time exploring moved object/total time exploring either object)], with values significantly greater than 50% representing evidence of retained contextual memory (Ennaceur et al., 1997). In this experiment, location index was quantified during the 5 min of the testing session. LimeLight (Actimetrics, Wilmette, IL, United States) behavioral software was used to track the path of locomotor activity of each animal within the open field over time. De-identified video files were scored by two experimenters and average location indices were reported.

Fecal Sample Collection

Fecal samples were collected at four timepoints: (T1) the day of arrival; (T2) one to 2 days before surgery (4 weeks on diet); (T3) at baseline sleep (6 weeks on diet); and (T4) at the end of the experiment (see **Figure 1A**). Each collection occurred on days where clean cages were provided, so rats were placed into a clean chamber with fresh bedding and food and monitored closely until at least two fresh fecal pellets from each cage were collected. Only spontaneously voided pellets were collected. Samples were placed into individual 1.5 mL microfuge tubes, and frozen at −80°C until microbiome and metabolome analysis, at which point one sample from each animal (or two from each cage for timepoints T1 and T2) was cut in half. One half was used for fecal microbiome analysis and the other half was used for fecal metabolome analysis. At each collection timepoint, duplicate samples of bedding, water, food, and blank tubes were also collected.

Microbiome Analysis

To evaluate the impact of the prebiotic diet on the microbiome and to assess for correlations between our primary outcome of interest, the response to sleep disruption, and changes to the microbiome, 16S rRNA gene sequencing was used on a total of 334 fecal and 63 environmental samples. DNA was extracted from fecal samples and the V4 region of the 16S rRNA gene was amplified using the 515f/806rB primer pair with the barcode on the forward read (Apprill et al., 2015) and sequenced as previously described (Caporaso et al., 2012) using an Illumina MiSeq. Sequence data were processed using Deblur v1.1.0 (Amir et al., 2017), trimming to 150 nucleotides to create sub-operational-taxonomic-units (sOTUs). These were then inserted into the Greengenes 13_8 (Mcdonald et al., 2012) 99% reference tree using SATe-enabled Phylogenetic Placement (SEPP) (Mirarab et al., 2012). SEPP uses a simultaneous alignment and tree estimation strategy (Liu et al., 2009) to identify placements for sequence fragments within an existing phylogeny and alignment. Taxonomy was assigned using an implementation of the Ribosomal Database Project (RDP) classifier (Wang et al., 2007) as implemented in QIIME2 (Caporaso et al., 2010). Microbiome data were generally analyzed using the Qiita (Gonzalez et al., 2018) and Quantitative Insights Into Microbial Ecology 2 (QIIME2, version 2018.4) bioinformatics software packages (Caporaso et al., 2010; Bolyen et al., 2019).

Microbial diversity analysis was performed at a rarefied depth of 9,000 reads, resulting in the removal of 21 fecal samples that did not have 9,000 reads. Beta diversity, which measures

microbial similarity and dissimilarity between populations of samples, was assessed using weighted and unweighted UniFrac distance matrices as previously described (Lozupone et al., 2011). These matrices were used to generate principal coordinate analysis (PCoA) plots and to perform permutational multivariate analysis of variance (PERMANOVA) in QIIME2. Alpha diversity, which measures microbial taxonomic richness and evenness within a single sample, was calculated using scikit-bio 0.5.1 as implemented by QIIME2. Relative differential abundance was assessed at the OTU, genus, and species levels using analysis of the composition of microbiomes (ANCOM) (Mandal et al., 2015) as implemented in QIIME2. Count numbers of a taxon of interest were centered log ratio transformed in order to perform correlational analysis with physiological variables (Gloor et al., 2017).

PICRUSt2 Analysis of 16S rRNA Gene Data

We inferred the microbial gene content from the taxa abundance using the software package Phylogenetic Investigation of Communities by Reconstruction of Unobserved States (PICRUSt2[1]; v2.1.4-b) (Langille et al., 2013). This tool allows assessment of functional capacity of a microbiome using 16S rRNA gene sequencing data. To identify differentially abundant functional pathways and enzymes, DESeq2 (version 1.14.1) was performed using the Bioconductor R package in RStudio (version 1.2.1335, RStudio Inc.).

Metabolome Analysis

A total of 334 fecal and 63 environmental samples were processed for fecal metabolome analyses. A clean stainless-steel bead (Qiagen Catalog# 69989) and 1.5 mL chilled extraction solvent (50% MeOH) was added to each sample. The samples were then homogenized for five min at 25 Hz using a TissueLyser II system (Qiagen Catalog# 85300) and allowed to incubate for 20 min at −20°C. The fecal homogenates were then centrifuged at 14,000 rpm for 15 min at 4°C. 1.2 mL aliquots were then transferred into Nunc 2.0 mL DeepWell plate (Thermo Catalog# 278743) and frozen at −80 °C prior to lyophilization using a FreeZone 4.5 L Benchtop Freeze Dryer with Centrivap Concentrator (Labconco). Wells were resuspended with 200 μL of resuspension solvent (50% MeOH spiked with 2.0 μM sulfadimethoxine), vortexed for 30 s, and centrifuged at 2,000 rpm for 15 min at 4°C. 150 μL of the supernatant was transferred into a 96-well plate and maintained at 4°C prior to LC-MS analysis. A resuspension solvent QC and a six standard mix QC (50% MeOH spiked with 1.0 μM sulfamethazine, 1.0 μM sulfamethizole, 1.0 μM sulfachloropyridazine, 1.0 μM amitriptyline, and 1.0 μM coumarin 314) was run every 12th sample to assess sample background, carry over, chromatography behavior, peak picking, and plate effects.

Fecal extracts were analyzed using an ultra-high performance liquid chromatography system (Vanquish, Thermo) coupled to a hybrid quadrupole-Orbitrap mass spectrometer (Q-Exactive, Thermo) fitted with a HESI probe. Reverse phase chromatographic separation was achieved using a Kinetex C18 1.7 μm, 100 Å, 50 × 2.1 mm column (Phenomenex) held at 40 °C with a flow rate of 0.5 mL/min. 5.0 μL aliquots were injected per sample/QC. The mobile phase used was (A) 0.1% formic acid in water and (B) 0.1% formic acid in acetonitrile. The elution gradient was: 5.0% B for 1 min, increased to 100% B in the next 8 min, held at 100% B for 2 min, returned to 5.0% B in 0.5 min, equilibrated at 5.0% B for 2 min. Positive electrospray ionization parameters were: sheath gas flow rate of 52 (arb. units), aux gas flow rate of 14 (arb. units), sweep gas flow rate of 3 (arb. units), spray voltage of 3.5 kV, capillary temperature of 270 °C, S-Lens RF level of 50 (arb. units), and aux gas heater temperature of 435 °C. Negative electrospray ionization parameters were: sheath gas flow rate of 52 (arb. units), aux gas flow rate of 14 (arb. units), sweep gas flow rate of 3 (arb. units), spray voltage of 2.5 kV, capillary temperature of 270 °C, S-Lens RF level of 50 (arb. units), and aux gas heater temperature of 435 °C. MS data were acquired using a data dependent acquisition method with a resolution of 35,000 in MS^1 and 17,000 in MS^2. An MS^1 scan from 100–1,500 *m/z* was followed by an MS^2 scan, produced by collision induced disassociation, of the five most abundant ions from the prior MS^1 scan.

The orbitrap files (.raw) were exported to mzXML files using MSConvert (Chambers et al., 2012). Feature detection of the MS^1 data was performed using MZmine2 (Pluskal et al., 2010).

The resultant feature tables contained 12,570 features (fecal). Feature tables were also generated for samples of the control and prebiotic diets, containing 2,379 features. All these features were removed from the fecal feature table, resulting in a table of 10,229 non-dietary fecal metabolites. To annotate features with a metabolome standard initiative (MSI) level 1 level of confidence, mass and retention time were aligned and MS/MS fragmentation pattern was compared between features and 20 purified bile acid reference standards. Annotated features were normalized to an internal standard followed by a row sum (total bile acid ion count) normalization.

Statistical Analyses and Software

All graphs depict the mean ± SEM unless otherwise stated. Initial analysis of sleep data used in this study revealed that while 8/8 variables passed heteroscedasticity testing, only 4/8 passed multiple normality tests. Therefore, we elected to use either non-parametric testing or statistical approaches like mixed effects modeling that have been shown to be fairly robust in the setting of mild-moderate violations of assumptions (Schielzeth et al., 2020; Knief and Forstmeier, 2021). All PCoA plots (**Supplementary Figure 1**) were generated using the EMPeror visualization tool as implemented in QIIME2 (Vazquez-Baeza et al., 2013). Microbiome data processing and analysis, including microbiome PERMANOVA, were performed in QIIME2 as outlined above. Wilcoxon Rank-Sum tests and linear mixed effect modeling of metabolome data with Benjamini-Hochberg correction for multiple comparisons (**Table 1**), linear mixed effect modeling

[1]https://github.com/picrust/picrust2

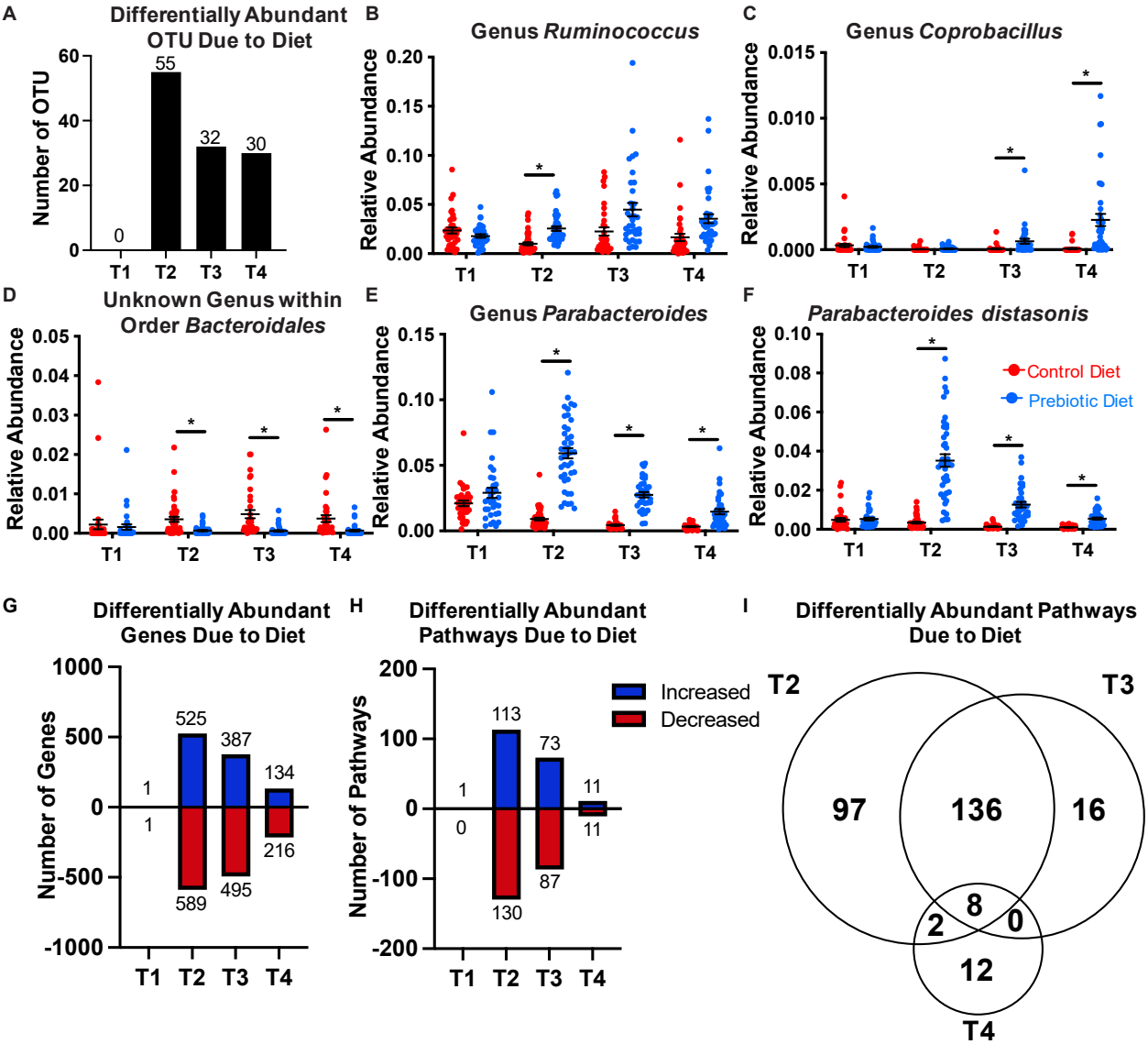

FIGURE 2 | The prebiotic diet results in significant changes in the relative abundance of several taxa. Fecal samples were collected on the day of arrival to the facility (T1), after 4 weeks on diet (T2), at baseline sleep (T3), and at the end of the experiment (T4). 16S rRNA gene microbiome sequencing and analyses were performed. ANCOM was performed at each timepoint to assess differentially abundant taxa due to diet. The number of OTUs that were differentially abundant at each timepoint is reported in panel **(A)**. **(B–E)** ANCOM was then performed at the genus level, revealing four genera that were differentially abundant at $\geq$1 timepoint. **(F)** ANCOM performed at the species level confirmed *Parabacteroides distasonis* was differentially abundant at T2-T4. PICRUSt2 was then performed to predict abundance of genes and metabolic pathways based on the 16S rRNA gene data. DESEq2 was performed at each timepoint to identify differentially abundant **(G)** genes, and **(H)** pathways due to diet. **(I)** A Venn diagram depicting the number of differentially abundant pathways present at each timepoint. Data are mean $\pm$SEM. Symbols: *differentially abundant at that timepoint *via* ANCOM. ANCOM, analysis of the composition of microbiomes; OTU, operational taxonomic unit. *n* = 33–45/group.

of body weight data (**Supplementary Figure 3**), DESeq2 analysis with Benjamini-Hochberg adjustment of PICRUSt2 data (**Supplementary Figure 2**), and microbe/metabolite Spearman correlation networking (**Figure 7**) were performed or generated in RStudio (version 1.2.1335, RStudio Inc., Boston, MA, United States). In order to account for the factorial design of the study and to allow interaction terms while also using a non-parametric test, aligned rank transform ANOVA (Conover and Iman, 1981; Wobbrock et al., 2011) was used in lieu of a regular 2-Way ANOVA to analyze post-sleep disruption sleep (**Figure 5**). Mixed-effects models with Bonferroni or Benjamini-Hochberg *post hoc* testing for alpha diversity data (**Supplementary Figure 1**), baseline sleep data (**Figure 3**), during sleep-disruption sleep data (**Figure 4**), as well as Spearman correlations of sleep/microbiome data (**Figure 6**), along with generation of all other graphs/figures, were performed using

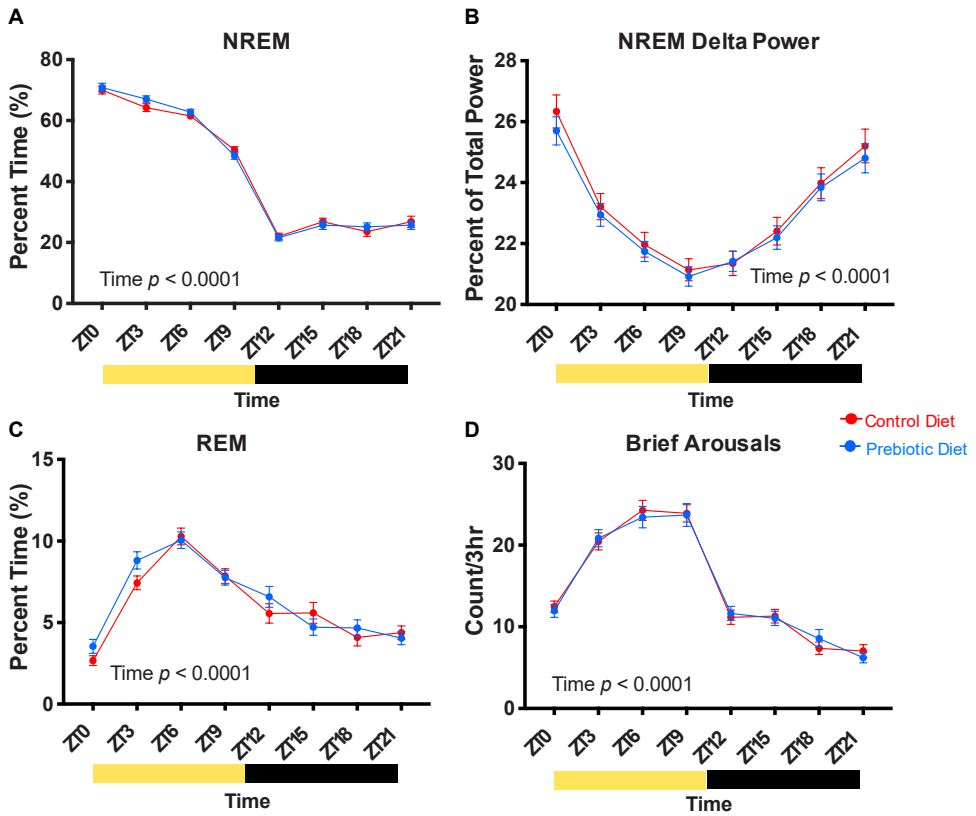

FIGURE 3 | The prebiotic diet does not impact baseline sleep. Two weeks after EEG/EMG surgery, after six total weeks on diet, 24 h of baseline sleep was recorded. **(A)** NREM sleep, **(B)** NREM EEG delta power, **(C)** REM sleep, and **(D)** brief arousals are reported in 3-h bins. Yellow bars below the x axes represent times where the lights were on, while black bars represent times the lights were off. Mixed effects modeling was performed to test for effects of time, diet, and any interactions. Data are mean ± SEM. n = 38–40/group. EEG, electroencephalogram; NREM, non-rapid eye movement; REM, rapid eye movement; ZT, Zeitgeber time.

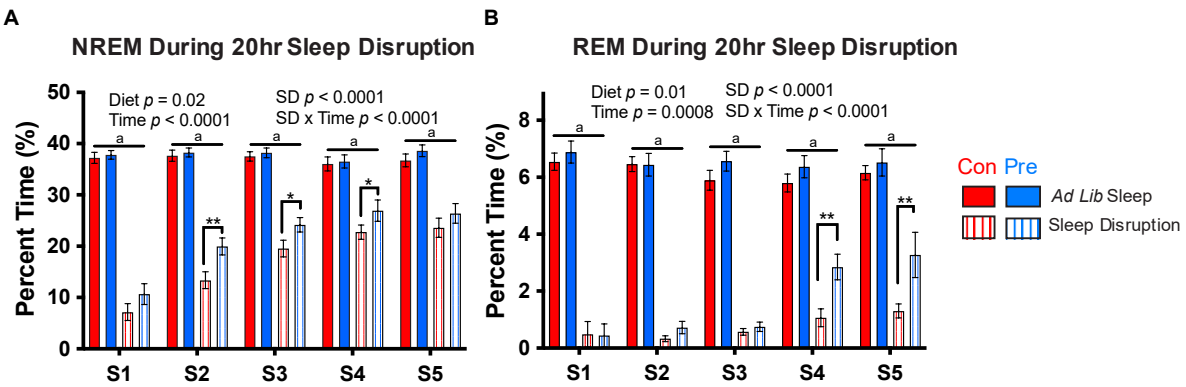

FIGURE 4 | The prebiotic diet increases sleep during the sleep disruption protocol. Rats were exposed to 5 days of sleep disruption achieved by a slowly rotating bar at the bottom of the cage for 20 h per day (ZT6-ZT2). Sleep was recorded throughout this protocol, and **(A)** NREM sleep and **(B)** REM sleep during the 20-h sleep disruption periods (S1-S5) are depicted above. Mixed-effect modeling testing for an effect of timepoint, diet, sleep disruption, and interactions was performed for each measure, and significant results are reported in the figure. Data are mean ± SEM. Symbols: $^{**}q < 0.01$, $^{*}q < 0.05$, Fisher's LSD test with Benjamini-Hochberg correction for multiple comparisons; $^{a}q < 0.001$ for all four within-timepoint pairwise comparisons between *ad lib* sleep groups and sleep disruption groups. Con, control diet; NREM, non-rapid eye movement sleep; REM, rapid eye movement sleep; Pre, prebiotic diet. n = 19–24/group.

GraphPad PRISM (version 9.2.0; GraphPad Inc., San Diego, CA, United States).

RESULTS

The Prebiotic Diet Alters the Structure and Function of the Fecal Microbiome

We first sought to characterize the effect of the prebiotic diet on the fecal microbiome over time. Rats arrived at postnatal day 23, at which time a baseline fecal sample was collected (timepoint T1). Samples were also collected at the start of the fourth week on diet (T2), the sixth week on diet (T3), and at the end of the experiment, corresponding to the seventh week on diet (T4, see **Figure 1**), and processed for 16S rRNA gene microbiome analysis. Unweighted and weighted UniFrac revealed significant differences in microbial community structure due to the diet at T2, T3, and T4 (**Supplementary Figures 1A,B**). This was accompanied by a reduction in alpha diversity in the prebiotic diet-fed rats compared to control diet-fed rats. Both Faith's phylogenetic diversity (**Supplementary Figure 1C**) and the total number of observed OTU (**Supplementary Figure 1D**) were reduced at T2 and T3 in the prebiotic diet group compared to control, but this difference was no longer present at T4. Furthermore, Pielou's evenness was not affected by diet condition throughout the experiment (**Supplementary Figure 1E**).

To characterize prebiotic diet-induced changes to the microbiome, we performed ANCOM at each timepoint to determine differentially abundant taxa. At the OTU level, ANCOM detected zero differentially abundant features at T1, 55 differentially abundant OTUs at T2, 32 differentially abundant OTUs at T3, and 30 differentially abundant OTUs at T4 (**Figure 2A**). Because 16S rRNA gene microbiome analysis is generally more reliable at accurate taxonomic prediction at the genus level than the species level (Gilbert et al., 2018; Knight et al., 2018), we then performed ANCOM on features that had taxonomic assignment at the genus level. We found four genera to be differentially abundant due to diet at one or more timepoints (**Figures 2B–E**).

Ruminococcus was increased at T2 in the prebiotic diet group, but not at the other timepoints (**Figure 2B**). The genus *Coprobacillus* was also increased due to the prebiotic diet, but only at T3 and T4 (**Figure 2C**). Conversely, an unknown genus within the order *Bacteroidales* was lower compared to control diet-fed rats at T2, T3, and T4 (**Figure 2D**). Interestingly, the genus *Parabacteroides* was greatly increased at all non-baseline timepoints, by a factor of 6.5 at T2, a factor of 7 at T3, and a factor of 5 at T4 (**Figure 2E**). Due to the particularly marked increase in genus *Parabacteroides* due to the diet, and the fact that there is a growing body of literature describing the role of a particular species within *Parabacteroides* (*Parabacteroides distasonis*) in host physiology (Lathrop et al., 2011; Dziarski et al., 2016; Valles-Colomer et al., 2019; Wang et al., 2019), we then performed ANCOM again at each timepoint at the species level to investigate whether *P. distasonis* was the driving factor behind the increase in genus *Parabacteroides*. Indeed, we found that *P. distasonis* was the dominant species within the genus, and that it was significantly increased at T2, T3, and T4 (**Figure 2F**). There were 26 OTUs that were assigned to *P. distasonis*, and the average confidence score of the assignments was 0.9755 (95% CI: 0.9459–1.005).

In order to assess whether the diet changed the function of the microbiome, we performed PICRUSt2 (Langille et al., 2013), which uses taxonomy based on 16S rRNA gene data to predict potential functional gene content of the microbiome based on reference sequences of each taxa. Then, we used DESEq2 to identify differentially abundant genes and pathways due to diet at each timepoint. We found that, using an FDR cutoff of 0.1, there were 1,114 differentially abundant genes (525 increased, 589 decreased) due to diet at T2, 882 differentially abundant genes (387 increased, 495 decreased) at T3, and 250 differentially abundant genes (134 increased, 216 decreased) at T4 (**Figure 2G**). Altered pathways followed a similar pattern, with 243 differentially abundant pathways (113 increased, 130 decreased) at T2, 160 differentially abundant pathways (73 increased, 87 decreased) at T3, and 22 differentially abundant pathways (11 increased, 11 decreased) at T4 (**Figure 2H**).

More than half of the differentially abundant pathways at T2 and T3 overlapped (144/257; **Figure 2I**). However, only 8 pathways were differentially abundant due to prebiotic diet at all three timepoints (**Figure 2I** and **Supplementary Figure 2**). The abundance of two pathways involved in lipopolysaccharide (LPS) synthesis were significantly increased with prebiotic diet, and two pathways relating to metabolism of exogenous molecules such as aromatic amines and nitrates were decreased due to prebiotic diet at all timepoints (**Supplementary Figure 2**). Furthermore, three pathways involved in sugar metabolism were altered at all time points due to the prebiotic diet (**Supplementary Figure 2**). Finally, abundance of a pathway involved in pyrimidine deoxyribonucleotides *de novo* biosynthesis was increased due to prebiotic diet at all three timepoints (**Supplementary Figure 2**). Together, these results indicate that the GOS/PDX prebiotic diet had a strong impact on the structure and function of fecal microbiome throughout the experiment, which was characterized by a 5–7-fold increase in the bacterium *P. distasonis*.

The Prebiotic Diet Does Not Alter Baseline Sleep

Baseline sleep was assessed using EEG/EMG recording before the sleep disruption protocol (see Methods, **Figure 1**). We did not observe an effect of 4 weeks exposure to the prebiotic diet on NREM sleep (**Figure 3A**), NREM EEG delta power (**Figure 3B**), REM sleep (**Figure 3C**), or brief arousals (a measure of sleep fragmentation, **Figure 3D**). These measures were significantly impacted by time of day, demonstrating the circadian rhythm of these sleep parameters.

The Prebiotic Diet Alters Sleep During and After Sleep Disruption

We measured sleep during the sleep disruption protocol to validate the efficacy of the motorized sleep disruption unit and to examine whether the prebiotic diet influenced the response to sleep restriction. As expected, we found that the sleep disruption

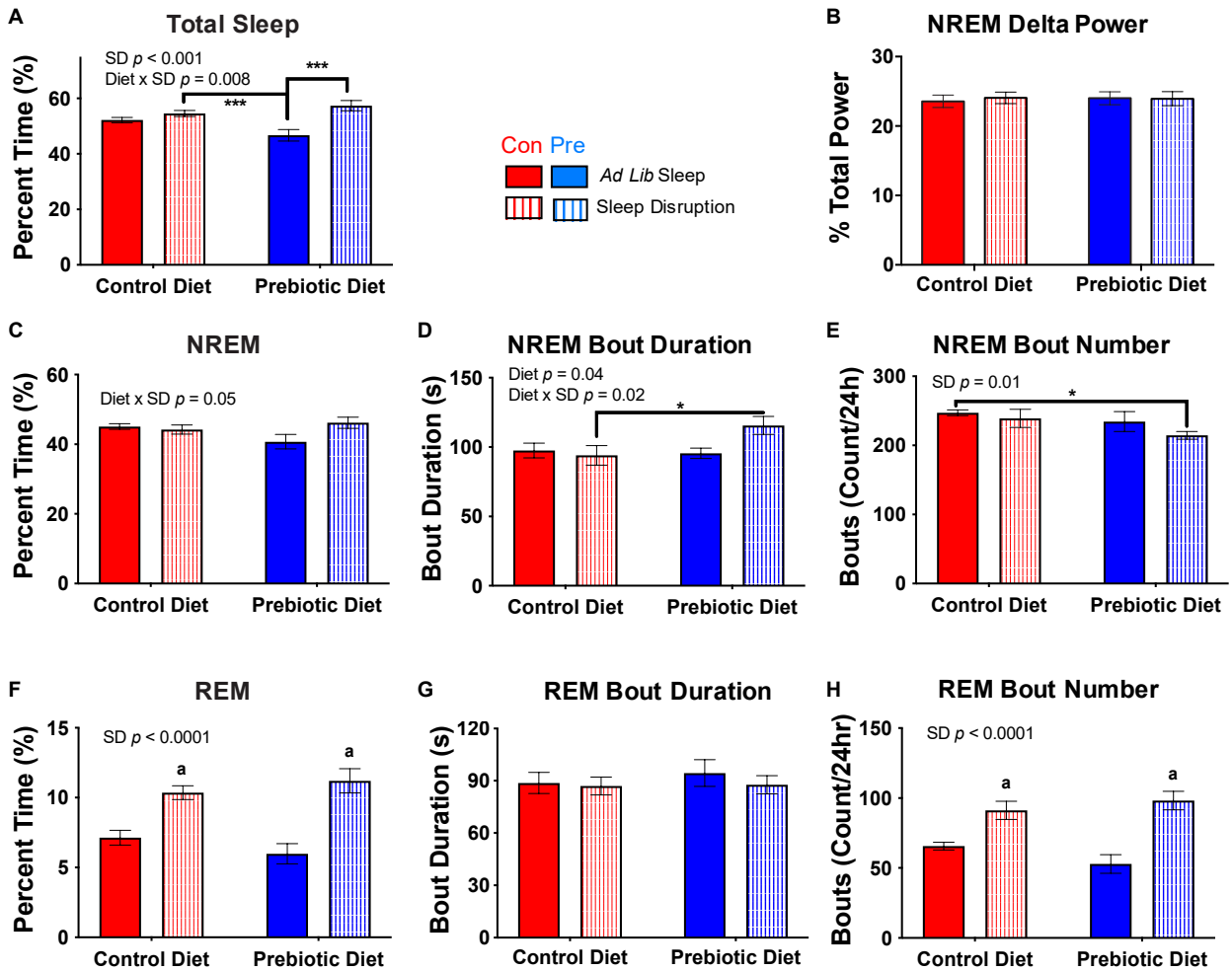

FIGURE 5 | The prebiotic diet improves recovery sleep post-sleep disruption. Twenty-four hours of *ad libitum* sleep was recorded after the completion of the 5-day sleep disruption protocol. **(A)** Total sleep, **(B)** NREM EEG delta power, **(C)** NREM sleep, **(D)** median NREM bout duration, **(E)** number of NREM bouts over 24 h, **(F)** REM sleep, **(G)** median REM bout duration, and **(H)** number of REM bouts over 24 h are depicted above for the control (*ad libitum* sleep throughout) and sleep-disrupted (with no social defeat) groups. Aligned rank transform ANOVA testing for an effect of diet, sleep disruption, and interaction was performed for each measure, and significant or near significant results are reported in the figure. Data are mean ± SEM. Symbols: ***$p < 0.001$, *$p < 0.05$, Bonferroni's *post hoc* test. [a] $p < 0.001$ vs both control diet, *ad libitum* sleep and prebiotic diet, *ad libitum* sleep groups, Bonferroni's *post hoc* test. Con, control diet; NREM, non-rapid eye movement sleep; Pre, prebiotic diet; REM, rapid eye movement sleep; SD, sleep disruption. n = 8–10/group.

protocol significantly reduced NREM sleep on all days of the sleep disruption protocol (**Figure 4A**), and nearly completely deprived rats of REM sleep, particularly on the first 3 days of the protocol (**Figure 4B**). The sleep disruption protocol appeared to become slightly less effective over time, as the amount of NREM and REM sleep obtained during the 20 h of sleep disruption increased over time in both groups (**Figure 4**). Interestingly, this process occurred more quickly in the prebiotic diet-fed rats: on days 2–4 of the sleep disruption protocol, rats in the prebiotic diet group obtained more NREM sleep during the 20-h sleep disruption period than in the control diet-fed rats (**Figure 4A**). The prebiotic diet-fed rats also obtained more REM sleep during the protocol than control diet-fed rats on days 4 and 5 (**Figure 4B**).

To assess the effect of the prebiotic diet on recovery from the 5-day sleep disruption protocol, we examined the first 24 h of recovery sleep, which began after completion of the 1-h acute social defeat stress exposure in the experimental groups or an equivalent amount of time in a clean cage in the control groups. Whereas there was no difference in total sleep due to sleep disruption in the control diet-fed rats, there was a significant increase in total sleep in the prebiotic diet-fed, sleep-disrupted rats compared to prebiotic diet-fed controls (**Figure 5A**). However, NREM delta power, a well-accepted measure of sleep intensity and sleep homeostatic drive (Meerlo et al., 2001; Kamphuis et al., 2015), was not changed in any group (**Figure 5B**). Examination of NREM sleep architecture revealed that the sleep deprived, prebiotic diet-fed rats had a trend for more NREM than non-sleep disrupted, prebiotic diet-fed rats (**Figure 5C**), and that this NREM sleep was more consolidated into longer bouts

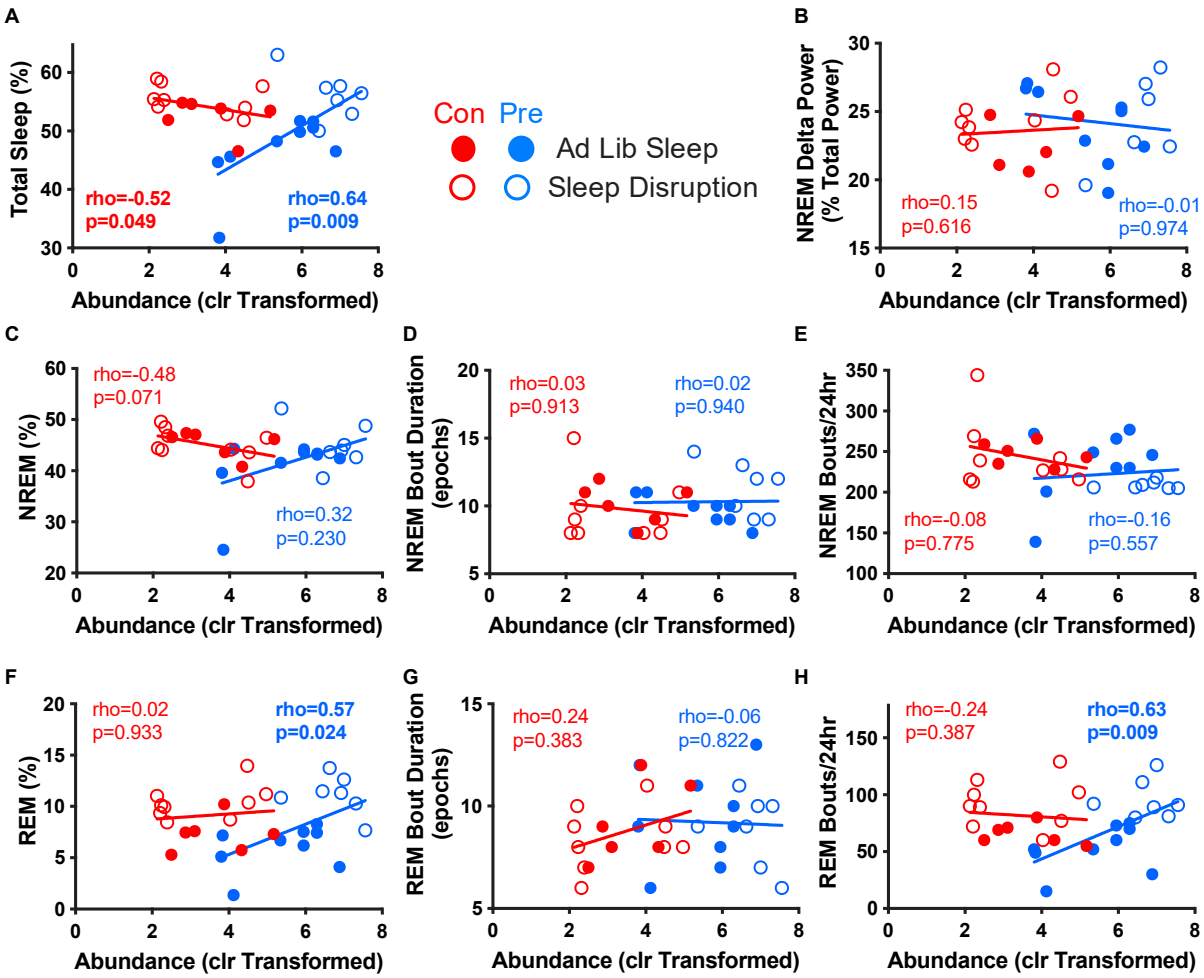

FIGURE 6 | *Parabacteroides distasonis* relative abundance is associated with multiple measures of post-sleep disruption recovery sleep. Spearman's rank-based correlation analysis between the centered log ratio transformed abundance of *P. distasonis* at the end of the experiment (T4) and various measures of recovery sleep post-sleep disruption was performed within diet group for control (no sleep disruption, no social defeat) and sleep disruption only groups. Results for **(A)** total sleep, **(B)** NREM delta power, **(C)** NREM percent, **(D)** median NREM bout duration, **(E)** NREM bouts per 24 h, **(F)** REM percent, **(G)**, median REM bout duration, and **(H)** REM bouts per 24 h are depicted above. Con, control diet; clr, centered log ratio; Pre, prebiotic diet; NREM, non-rapid-eye movement sleep, REM, rapid-eye movement sleep. *n* = 6–9/group.

(**Figures 5D,E**). REM sleep was significantly increased during recovery in both the control diet-fed and prebiotic diet-fed groups, and this increase was due to an increase in the number of bouts without an increase in median bout length (**Figures 5F–H**). Thus, the prebiotic diet increased total amount of recovery sleep as compared to non-sleep disrupted animals, and promoted consolidation of recovery NREM sleep after repeated sleep disruption.

We also sought to assess the physiological impact of the sleep disruption protocol. We regularly weighed the rats throughout the experiment and found no overall effect of diet or social defeat stress on body weight (**Supplementary Figure 3**). Though the sleep disruption protocol did not cause a reduction in body weight, it did reduce the rate of weight gain as indicated by an overall effect of sleep disruption on body weight, as well as a sleep disruption by time interaction (**Supplementary Figure 3**), consistent with prior studies demonstrating increased energy expenditure in the setting of sleep restriction (Mchill and Wright, 2017). The prebiotic diet did not ameliorate this effect. We investigated whether repeated sleep disruption impacted stress-induced changes in performance in the OLM task. At the end of the sleep disruption protocol, half of the rats were exposed to 1 h of social defeat stress, while the other half were transferred to a quiet room for 1 h (see Methods). Twenty-four hours later, all animals were subjected to an OLM task in which a location index significantly above 50% is considered to indicate recognition of the moved object and retained contextual memory (see Methods). In control diet-fed rats, groups exposed to the social defeat stressor did not achieve significantly greater than 50% location index, although the mean location index for these groups was overall similar to non-stressed groups (**Supplementary Figure 4**). In contrast, all prebiotic diet-fed

TABLE 1 | Fecal bile acids across the experiment.

	Effect of diet		Effect of diet		Effect of diet		Effect of sleep disruption		Effect of social defeat	
	T2		T3		T4					
Bile Acid	p_{adj}	**Fold Change**	p_{adj}	**Fold Change**	p_{adj}	**Fold Change**	p_{adj}	**Fold Change**	p_{adj}	**Fold Change**
Chenodeoxycholic	**0.047**	**−0.041**	0.787	0.008	0.727	0.027	**0.049**	**−0.081**	0.954	8.58E-05
Cholic	0.399	0.219	0.787	3.903	0.965	0.161	0.711	0.603	0.770	1.863
Deoxycholic	**0.047**	**−0.041**	0.787	0.008	0.727	0.027	**0.049**	**−0.081**	0.954	8.55E-05
Glycochenodeoxycholic	0.399	−0.076	0.787	0.358	0.619	0.911	0.711	−0.359	0.954	0.222
Glycocholic	0.399	0.668	0.787	0.442	0.965	−0.176	0.204	1.596	0.954	−0.101
Glycodeoxycholic	0.678	−0.012	0.787	0.128	0.619	0.601	0.578	−0.313	0.954	0.129
Glycohyocholic	0.908	0.271	0.787	2.434	0.965	0.180	0.862	0.150	0.960	0.002
Glycolithocholic	0.399	−0.512	0.787	0.178	0.965	0.122	0.711	0.770	0.770	2.245
Glycoursodeoxycholic	0.209	0.256	0.950	−0.112	0.965	−0.038	0.965	0.063	0.954	0.029
Lithocholic	**0.0004**	**−0.222**	0.787	0.130	0.965	0.041	0.197	0.197	0.954	−0.082
Muricholic	0.414	0.182	0.787	3.803	0.965	0.129	0.711	0.645	0.770	1.876
Muricholic_alpha	**0.0003**	**0.487**	0.787	−0.021	0.965	−0.074	0.711	0.113	0.954	0.056
Muricholic_beta	0.244	0.234	0.279	−0.387	0.213	−0.398	0.197	0.511	0.954	−0.106
Taurochenodeoxycholic	**0.010**	**2.739**	0.787	0.319	0.904	−0.216	0.981	0.017	0.954	0.063
Taurocholic	0.179	0.481	0.787	0.155	0.727	0.883	0.981	−0.044	0.954	0.690
Taurodeoxycholic	**0.010**	**3.12**	0.787	0.341	0.849	−0.240	0.981	0.035	0.954	0.140
Taurohyocholic	0.742	0.430	0.787	−0.073	0.213	−0.364	0.197	0.471	0.954	0.004
Taurohyodeoxycholic	0.069	1.408	0.787	−0.051	0.727	−0.187	0.197	0.385	0.954	−0.013
Taurolithocholic	0.908	0.130	0.682	3.060	0.965	−0.019	0.711	0.240	0.954	0.059
Ursodeoxycholic	0.177	−0.106	0.962	−0.020	0.965	0.067	0.981	−0.035	0.770	−0.104

Fecal samples were collected after 4 weeks on diet (T2), at baseline sleep (T3), and at the end of the experiment (T4), and untargeted LC/MS/MS metabolomics were performed.
Twenty fecal bile acids were identified using purified standards.
The effects of diet, sleep disruption, and social defeat were assessed using Wilcoxon Rank-Sum testing (T2, T3) or linear mixed effects modeling (T4).
Adjusted p values (Benjamini-Hochberg correction) and fold change compared to control conditions are displayed below. Significant adjusted p values and their affiliated fold changes are indicated in bold.

groups exhibited learning indices significantly greater than 50% (**Supplementary Figure 4**).

Relative Abundance of *Parabacteroides distasonis* Correlates With Recovery Sleep

We next evaluated whether any of these prebiotic diet-induced changes to sleep were associated with the observed changes in the fecal microbiome. We focused on *P. distasonis*, as this bacterium exhibited the most pronounced increase in relative abundance in response to the prebiotic diet (**Figure 2**), and which has been shown in prior studies to be beneficial to host physiology (Lathrop et al., 2011; Wang et al., 2019; Thompson et al., 2021). Mean-centered log ratio (clr) transformation was then performed to convert *P. distasonis* relative abundance data to a suitable form for correlational analysis with physiological data, as relative abundances are susceptible to spurious correlations because they are compositional, such that the relative abundances within a single sample sum to one. Using clr transformation has been shown to at least partially ameliorate this problem (Gloor et al., 2017). Using this approach, we found that the clr transformed abundance of *P. distasonis* at T4 correlated positively with total sleep during the first 24 h of recovery sleep after sleep disruption in prebiotic diet-fed rats but correlated negatively with recovery sleep in control diet-fed rats (**Figure 6A**). *P. distasonis* also positively correlated with REM sleep and the number of REM bouts during recovery sleep (**Figures 6F,H**) in prebiotic diet-fed rats, both of which were altered by sleep disruption but not by the prebiotic diet (see **Figure 5**). *P. distasonis* did not significantly correlate with NREM delta power (**Figure 6B**), NREM parameters (**Figures 6C–E**), or median REM bout duration (**Figure 6G**).

The Prebiotic Diet Alters the Fecal Bile Acid Pool

A proposed mechanism by which intestinal bacteria may influence host physiology is by generation of microbially-modified metabolites including those originating from dietary sources and host bile acids (Furusawa et al., 2013; De Vadder et al., 2014; Kuipers et al., 2014; Govindarajan et al., 2016; Stilling et al., 2016; Yanguas-Casas et al., 2017). Interestingly, a recent study of *P. distasonis* demonstrated that it exerts metabolic benefits in part *via* secondary bile acid production (Wang et al., 2019). We therefore evaluated the impact of the prebiotic diet on the fecal metabolome, and specifically on the bile acid pool, by performing untargeted LC/MS/MS mass spectrometry on fecal samples taken throughout the experimental protocol. We identified 20 different unconjugated and conjugated primary and secondary bile acids

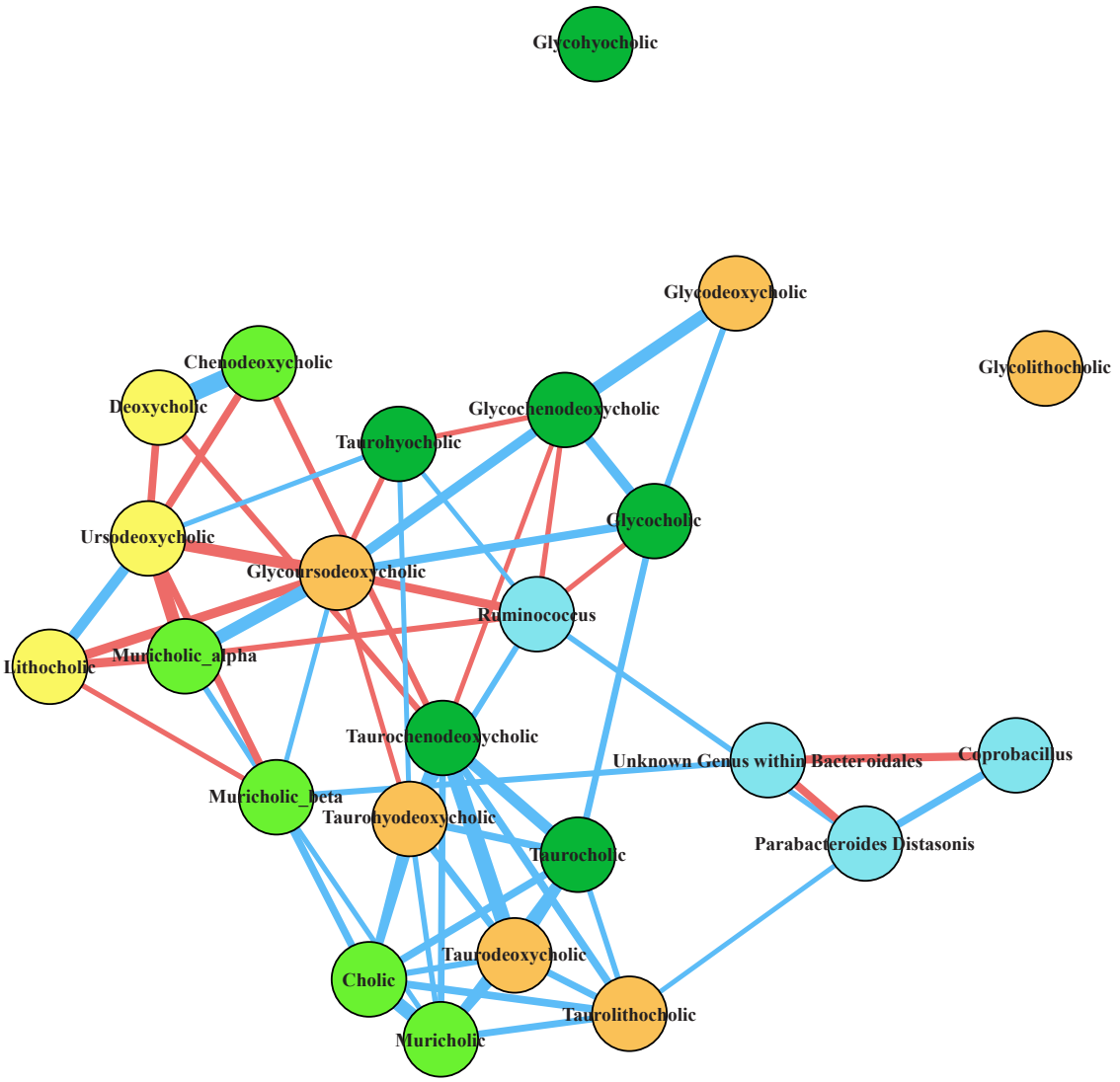

FIGURE 7 | Correlation network of taxa of interest and fecal bile acids at T3. Twenty bile acids were identified from untargeted LC/MS/MS mass spectrometry of fecal samples collected at the time of baseline sleep (T3). Pairwise Spearman's rank order correlations of bile acids and relative abundances of fecal bacteria of interest were performed across all animals, and correlations that were significant after correcting for multiple comparisons ($q < 0.05$) are depicted in the network diagram above. Nodes are colored as follows: light blue, bacteria; light green, primary bile acids; dark green, conjugated primary bile acids; yellow, secondary bile acids; orange, conjugated secondary bile acids. The thickness of the line between nodes correlates to the magnitude of Spearman's *rho*, blue lines indicate positive *rho* values, and red lines indicate negative *rho* values.

within the final feature tables using purified standards and investigated whether the diet altered levels of these bile acids at T2, T3, or T4 (**Table 1**). We found that at T2 (4 weeks on diet) there were six bile acids that were significantly altered due to diet after correcting for multiple comparisons. The primary bile acid muricholic acid was decreased, while another primary bile acid chenodeoxycholic acid was increased (**Table 1**). The conjugated primary bile acid taurochenodeoxycholic acid was also increased. Secondary bile acids deoxycholic acid and lithocholic acid were lower in the prebiotic diet group, and the conjugated secondary bile acid taurodeoxycholic acid was significantly increased in the prebiotic group. A number of these changes are consistent with our prior observations from independent experiments at a separate facility (Thompson et al., 2021). These diet effects were no longer present at T3 or T4 (**Table 1**). There was an overall effect of sleep disruption on the primary bile acid chenodeoxycholic acid and the secondary bile acid deoxycholic acid, but no other bile acids were affected by sleep disruption, and none of the 20 identified bile acids were impacted by social defeat stress exposure (**Table 1**).

To investigate whether the microbes we found to be most affected by the prebiotic diet were related to the fecal bile acid pool, we performed pairwise Spearman correlations of clr transformed abundances of *P. distasonsis, Ruminococcus, Coprobacillus,* and the unknown order within *Bacteroidales* (see **Figure 2**) with the normalized abundances of the 20 identified

bile acids at T3 (time of baseline sleep). The resultant network (**Figure 7**) of significant ($q < 0.05$) correlations revealed a tightly covarying network of primary and secondary bile acids, such that *P. distasonis*, *Ruminococcus,* and the unknown order within *Bacteroidales* all correlated with at least one bile acid, thus integrating the observed microbial changes with the detected alterations in the fecal bile acid pool.

DISCUSSION

In this study, we tested the hypothesis that dietary supplementation with the prebiotics GOS and PDX improves sleep in response to repeated sleep restriction in adult male rats. We demonstrate a significant impact on our primary outcome measure, demonstrating that the prebiotic diet leads to significant increases in sleep during both the sleep restriction and recovery sleep phases of the experimental protocol. In addition, as expected, the prebiotic diet exerts a significant and stable effect on the structure and predicted function of the microbiome (**Figure 2**). The impact on the microbiome is most prominent at time point 2 (T2), which occurred prior to the sleep restriction and acute stress exposure portions of the protocol and represents the effect of 4 weeks of the dietary intervention.

Alpha diversity was decreased in the animals exposed to the prebiotic diet, particularly at T2 and T3 (**Supplementary Figure 1**). Increases in diversity are generally thought beneficial as decreased diversity has been associated with adverse physiologic states such as stress exposure (Bharwani et al., 2016; Thompson et al., 2016) and diseases such as inflammatory bowel disease (Nishino et al., 2018), whereas increased diversity is presumed to represent a healthier and more resilient resident microbial ecosystem. However, quantification of taxonomic representation is agnostic to the physiological function of the taxa that are tallied. Thus, it is possible that despite an overall reduction in diversity, there is a relative increase in beneficial bacteria accompanied by a larger decrease in detrimental and/or neutral taxa, leading to a net positive physiologic status change despite a lower total number of taxa. For example, a large "bloom" of a beneficial species (such as *P. distasonis*, potentially) induced by the prebiotic diet may suppress other bacteria leading to an overall decrease in diversity. Recent published examples are compatible with this hypothesis that a net positive physiologic change can occur in the setting of decreased overall diversity: in a study comparing healthy individuals to patients with major depressive disorder, the healthy control subjects exhibited a decrease in alpha diversity compared to those with depression (Jiang et al., 2015); and in a study examining infants, individuals with a lower alpha diversity at 1 year of age had better performance on a validated learning scale at 2 years of age compared to those with greater alpha diversity at age 1 (Carlson et al., 2018).

Looking beyond the structural changes to the microbiome, further analysis demonstrates that multiple genes and pathways are significantly altered by the prebiotic diet (**Figure 2**). Of all pathways affected, a subset of eight are consistently changed in the same direction at each time point. These eight include pathways involved in LPS synthesis and the metabolism of carbohydrates and exogenous molecules (**Supplementary Figure 2**), suggesting that a major functional impact of the prebiotic diet is the regulation of lipopolysaccharide synthesis and of specific microbial metabolic pathways, which together may contribute to the observed microbial structural as well as the host physiologic changes induced by the prebiotic diet.

The largest dietary effects on the microbiome were seen at T2, prior to the sleep restriction and stress exposure components of the protocol, with overall lower numbers of differentially affected taxa, genes, and pathways at T3 and T4 (**Figure 2**). The reason for this pattern of changes is unclear, but may be related to an evolving microbial ecosystem in flux in response to prebiotic diet exposure. At T2, most notable among the many significant changes is the dramatic rise in *P. distasonis* relative abundance. We are aware of the limited resolution of taxonomic assignment using 16S rRNA gene analysis, but we are confident this taxonomic classification is accurate. Over time, the total number of significantly altered taxa, genes, and pathways may decrease as the microbial ecosystem moves toward a new "set point," perhaps explaining the fewer differential effects noted at T3 and T4. Future work may help better characterize the long-term complex microbial and metagenomic changes induced by the prebiotic diet, as well as the time course and dynamics of these changes.

The prebiotic diet does not impact baseline sleep (**Figure 3**) but does lead to significant increases in NREM and REM sleep during the sleep restriction protocol (**Figure 4**) and total sleep, NREM sleep, and NREM bout duration during the sleep recovery period (**Figure 5**). Thus, while the prebiotic diet did not impact sleep at baseline, it enabled rats to get more sleep *during* the sleep disruption protocol. Taken together, these results suggest that the prebiotic diet enables animals to better handle the physiologic challenge of experimental sleep restriction by improving their ability to obtain sleep during active sleep restriction as well as during the following recovery period.

The relative abundance of *P. distasonis* was found to positively correlate with several sleep parameters in prebiotic diet-fed rats, such as total sleep and REM sleep as well as total bouts of REM sleep (**Figure 6**). This suggests that *P. distasonis* may exert a particularly important role in mediating the sleep-promoting effects of the prebiotic diet. *Parabacteroides distasonis* is a commensal gram-negative bacterium that has previously been shown to exert immunomodulating properties in the intestine *via* induction of T_{regs} (Lathrop et al., 2011), ameliorate metabolic dysfunction in a genetic model of obesity and in mice fed a high-fat diet (Wang et al., 2019), help promote quicker re-entrainment in response to circadian rhythm disruption (Thompson et al., 2021), compensate for inadequate dietary protein intake in a mouse model of malnourishment (Martin et al., 2021), and contribute to resilience against metabolic, behavioral, and neurocognitive responses to chronic restraint stress (Deng et al., 2021).

In contrast to these beneficial effects associated with *P. distasonis*, other studies have found adverse consequences, such as increased susceptibility to dextran sodium sulfate-induced colitis in mice treated with *P. distasonis via* oral gavage

(Dziarski et al., 2016), exacerbation of disease phenotype in a mouse genetic model of amyotrophic lateral sclerosis when antibiotic-treated mice were supplemented with *P. distasonis* (Blacher et al., 2019), and depressive-like behavior in a genetically-induced mouse model of Crohn's disease-like ileitis (Gomez-Nguyen et al., 2021). These disparate findings suggest that the impact of *P. distasonis* may be context-dependent, strain-dependent, related to the underlying physiologic state of the host, and/or dependent on the way in which *P. distasonis* is augmented. For example, dietary prebiotic supplementation to increase relative abundance in otherwise healthy mice may yield different effects than those achieved by oral gavage or in the setting of an otherwise healthy intestine as opposed to an inflamed intestine or an intestine characterized by an altered microbial ecosystem depleted by antibiotic exposure.

There are multiple possible mechanisms by which changes to the intestinal microbiome may impact host physiologic processes, including physical host-microbe interactions, bile acid modification, production of metabolites, modulation of signaling pathways, and immune regulation (Lavelle and Sokol, 2020; Sipe et al., 2020; Agus et al., 2021). A particularly relevant possibility is that changes to bile acids induced by secondary microbial metabolism may then contribute to systemic physiologic effects in the host. Our analysis of fecal bile acids demonstrates consistent directional relationships between bacterial changes induced by the prebiotic diet and alterations in the fecal bile acid profiles, suggesting that, given the known functional capacity of the involved bacterial taxa, the metagenomic changes to the microbial ecosystem in response to the prebiotic diet are a reasonable explanation for the observed bile acid changes.

There are several limitations to our study that are important to consider. The study was performed on adult male rats, so the applicability to other model systems and to humans may be limited. Our experimental protocol incorporated exposures to dietary intervention, sleep restriction, and acute social defeat stress. Thus, the observed significant effects may be particular to the types of experimental manipulation and/or sequence of exposures, with different effects possible in other models or experimental contexts. Similarly, our outcome measurements related to the microbiome, fecal metabolome, and sleep, are limited to specific timepoints. These static "snapshots" of time during the protocol may not completely capture or characterize evolving physiologic processes related to the regulation of sleep and the gut microbial ecosystem that may not have yet reached equilibrium at the time of measurement or sample collection. The links between sleep parameters and changes to the microbiota and fecal metabolites described here are inherently correlational in nature, thus they are unable to reveal underlying causal relationships or mechanisms of action. Statistical techniques have been employed to infer information about the relationships described, but the analyses used here are ultimately limited, with the capability of identifying hypotheses and future experiments necessary to parse the biological mechanisms driving the observed effects.

Despite these limitations, our finding of a prebiotic diet capable of enhancing resilience to sleep disruption offers a unique opportunity to combat the common and adverse consequences of sleep deprivation by utilizing a dietary strategy to promote sleep *via* enhancement of the microbiome. Future work should delineate the causal relationships and underlying mechanisms driving the effects of the prebiotic diet on the microbiome, the fecal metabolome, and the regulation of sleep, in order to identify more precise therapeutic targets. In addition, further work should examine the role of prebiotic diet supplementation in other model systems and in other physiologically challenging states associated with insufficient or poor sleep, to investigate the replicability and generalizability of the prebiotic diet's sleep-promoting effects.

DATA AVAILABILITY STATEMENT

The datasets presented in this study can be found in online repositories. The names of the repository/repositories and accession number(s) can be found in the article/**Supplementary Material**.

ETHICS STATEMENT

The animal study was reviewed and approved by Northwestern University Institutional Animal Care and Use Committee.

AUTHOR CONTRIBUTIONS

SB and KS wrote the first draft of the manuscript and incorporated contributions from all co-authors into the final draft, which was approved by all authors prior to submission. SB, CO, PJ, AG, and FV carried out studies and collected data. SB, KS, RT, AG, FV, and PJ analyzed the data. SB, KS, RT, AG, FV, PJ, CL, PD, RK, KW, MF, FT, and MV interpreted the data. CL, PD, RK, KW, MF, FT, and MV designed the studies and obtained funding. All authors contributed to the article and approved the submitted version.

FUNDING

This study was funded by the Office of Naval Research (ONR) Multiple University Research Initiative (MURI) Grant N00014-15-1-2809.

ACKNOWLEDGMENTS

We would like to acknowledge Gail Ackermann for organizing and coordinating data processing and analysis, and Eun Joo Song for assistance with scoring sleep.

SUPPLEMENTARY MATERIAL

The Supplementary Material for this article can be found online at: https://www.frontiersin.org/articles/10.3389/fnins.2022.889211/full#supplementary-material

Supplementary Figure 1 | The Prebiotic Diet Causes Changes to Fecal Microbiome Beta and Alpha Diversity. Fecal samples were collected on the day of arrival to the facility (T1), after 4 weeks on diet (T2), at baseline sleep (T3), and at the end of the experiment (T4). 16S rRNA gene microbiome sequencing and analyses were performed. PERMANOVA testing for an effect of diet was performed at each timepoint, and PCoA depicting **(A)** unweighted UniFrac and **(B)** weighted UniFrac analysis of beta diversity, with one axis representing timepoint, are reported. Alpha diversity was measured at each timepoint using **(C)** Faith's phylogenetic diversity index, **(D)** the total number of OTU, and **(E)** Pielou evenness metric. Mixed-effect modeling testing for an effect of timepoint, diet, and interactions was performed for each dependent variable, and significant results are reported in the figure. Data are mean ± SEM. Symbols: **(A,B)** $^{***}p < 0.001$, $^{**}p < 0.01$, PERMANOVA; **(C–E)** $^{**}p < 0.01$, $^{*}p < 0.05$, Bonferroni *post hoc*. Abbreviations: OTU, operational taxonomic unit; PC, principal coordinate. n = 33–45/group.

Supplementary Figure 2 | Predicted Microbial Metabolic Pathways Altered by the Prebiotic Diet. Fecal samples were collected after 4 weeks on diet (T2), at baseline sleep (T3), and at the end of the experiment (T4). 16S rRNA gene microbiome sequencing and analyses were performed. PICRUSt2 was performed on the 16S rRNA gene microbiome data to predict genetic content. DESEq2 was then performed at each timepoint to identify predicted pathways that were differentially abundant due to diet. The above reports the pathway ID, description, fold change, and direction of change of the 8 pathways that were significantly altered by diet at T2, T3, and T4.

Supplementary Figure 3 | The Prebiotic Diet Does Not Prevent Sleep Disruption-Induced Changes in Body Weight. Animals were weighed throughout the experiment. Day 0 indicates the start of baseline sleep recording. Results of linear mixed effect modeling investigating overall effects and interactions with time are depicted above. Data represent mean ± SEM. n = 9–12/group.

Supplementary Figure 4 | The Prebiotic Diet Prevents Social Defeat-Induced Loss of Object Location Memory. Immediately after the end of the last sleep disruption period, half of the rats were exposed to 1 h of social defeat while the other half were exposed to a clean cage for an equivalent time period. Twenty-four hours later, object location memory was assessed in all rats. Location indices above 50% indicate retained contextual memory and learning. Data represent mean ± SEM. Symbols: $\hat{}p < 0.05$, one sample Wilcoxon Rank-Sum test vs. 50%. Abbreviations: Con, control diet; Pre, prebiotic diet. n = 9–12/group.

REFERENCES

Agus, A., Clement, K., and Sokol, H. (2021). Gut microbiota-derived metabolites as central regulators in metabolic disorders. *Gut* 70, 1174–1182. doi: 10.1136/gutjnl-2020-323071

Amir, A., Mcdonald, D., Navas-Molina, J. A., Kopylova, E., Morton, J. T., Zech Xu, Z., et al. (2017). Deblur rapidly resolves single-nucleotide community sequence patterns. *mSystems* 2:e00191-16. doi: 10.1128/mSystems.00191-16

Apprill, A., Mcnally, S., Parsons, R., and Weber, L. (2015). Minor revision to V4 region SSU rRNA 806R gene primer greatly increases detection of SAR11 bacterioplankton. *Aquat. Microb. Ecol.* 75, 129–137. doi: 10.3354/ame01753

Barger, L. K., Cade, B. E., Ayas, N. T., Cronin, J. W., Rosner, B., Speizer, F. E., et al. (2005). Extended work shifts and the risk of motor vehicle crashes among interns. *N. Engl. J. Med.* 352, 125–134. doi: 10.1056/NEJMoa041401

Battson, M. L., Lee, D. M., Weir, T. L., and Gentile, C. L. (2018). The gut microbiota as a novel regulator of cardiovascular function and disease. *J. Nutr. Biochem.* 56, 1–15. doi: 10.1016/j.jnutbio.2017.12.010

Bharwani, A., Mian, M. F., Foster, J. A., Surette, M. G., Bienenstock, J., and Forsythe, P. (2016). Structural & functional consequences of chronic psychosocial stress on the microbiome & host. *Psychoneuroendocrinology* 63, 217–227.

Bioulac, S., Micoulaud-Franchi, J. A., Arnaud, M., Sagaspe, P., Moore, N., Salvo, F., et al. (2017). Risk of motor vehicle accidents related to sleepiness at the wheel: a systematic review and meta-analysis. *Sleep* 40:zsx134.

Blacher, E., Bashiardes, S., Shapiro, H., Rothschild, D., Mor, U., Dori-Bachash, M., et al. (2019). Potential roles of gut microbiome and metabolites in modulating ALS in mice. *Nature* 572, 474–480. doi: 10.1038/s41586-019-1443-5

Bolyen, E., Rideout, J. R., Dillon, M. R., Bokulich, N. A., Abnet, C. C., Al-Ghalith, G. A., et al. (2019). Reproducible, interactive, scalable and extensible microbiome data science using QIIME 2. *Nat. Biotechnol.* 37, 852–857.

Bowers, S. J., Vargas, F., Gonzalez, A., He, S., Jiang, P., Dorrestein, P. C., et al. (2020). Repeated sleep disruption in mice leads to persistent shifts in the fecal microbiome and metabolome. *PLoS One* 15:e0229001. doi: 10.1371/journal.pone.0229001

Caporaso, J. G., Kuczynski, J., Stombaugh, J., Bittinger, K., Bushman, F. D., Costello, E. K., et al. (2010). QIIME allows analysis of high-throughput community sequencing data. *Nat. Methods* 7, 335–336. doi: 10.1038/nmeth.f.303

Caporaso, J. G., Lauber, C. L., Walters, W. A., Berg-Lyons, D., Huntley, J., Fierer, N., et al. (2012). Ultra-high-throughput microbial community analysis on the Illumina HiSeq and MiSeq platforms. *ISME J.* 6, 1621–1624. doi: 10.1038/ismej.2012.8

Carlson, A. L., Xia, K., Azcarate-Peril, M. A., Goldman, B. D., Ahn, M., Styner, M. A., et al. (2018). Infant gut microbiome associated with cognitive development. *Biol. Psychiatry* 83, 148–159. doi: 10.1016/j.biopsych.2017.06.021

Cazakoff, B. N., Johnson, K. J., and Howland, J. G. (2010). Converging effects of acute stress on spatial and recognition memory in rodents: a review of recent behavioural and pharmacological findings. *Prog. Neuropsychopharmacol. Biol. Psychiatry* 34, 733–741. doi: 10.1016/j.pnpbp.2010.04.002

Chambers, M. C., Maclean, B., Burke, R., Amodei, D., Ruderman, D. L., Neumann, S., et al. (2012). A cross-platform toolkit for mass spectrometry and proteomics. *Nat. Biotechnol.* 30, 918–920. doi: 10.1038/nbt.2377

Conover, W. J., and Iman, R. L. (1981). Rank transformations as a bridge between parametric and nonpaarametric statistics. *Am. Stat.* 35, 124–129. doi: 10.1063/1.3380661

De Vadder, F., Kovatcheva-Datchary, P., Goncalves, D., Vinera, J., Zitoun, C., Duchampt, A., et al. (2014). Microbiota-generated metabolites promote metabolic benefits via gut-brain neural circuits. *Cell* 156, 84–96. doi: 10.1016/j.cell.2013.12.016

Deng, Y., Zhou, M., Wang, J., Yao, J., Yu, J., Liu, W., et al. (2021). Involvement of the microbiota-gut-brain axis in chronic restraint stress: disturbances of the kynurenine metabolic pathway in both the gut and brain. *Gut Microbes* 13, 1–16. doi: 10.1080/19490976.2020.1869501

Do Carmo, M. M., Walker, J. C., Novello, D., Caselato, V. M., Sgarbieri, V. C., Ouwehand, A. C., et al. (2016). Polydextrose: physiological function, and effects on health. *Nutrients* 8:553. doi: 10.3390/nu8090553

Dziarski, R., Park, S. Y., Kashyap, D. R., Dowd, S. E., and Gupta, D. (2016). Pglyrp-regulated gut microflora *Prevotella falsenii*, *Parabacteroides distasonis* and *Bacteroides eggerthii* enhance and *Alistipes finegoldii* attenuates colitis in mice. *PLoS One* 11:e0146162. doi: 10.1371/journal.pone.0146162

Ennaceur, A., Neave, N., and Aggleton, J. P. (1997). Spontaneous object recognition and object location memory in rats: the effects of lesions in the cingulate cortices, the medial prefrontal cortex, the cingulum bundle and the fornix. *Exp. Brain Res.* 113, 509–519. doi: 10.1007/pl00005603

Furusawa, Y., Obata, Y., Fukuda, S., Endo, T. A., Nakato, G., Takahashi, D., et al. (2013). Commensal microbe-derived butyrate induces the differentiation of colonic regulatory T cells. *Nature* 504, 446–450. doi: 10.1038/nature12721

Gao, V., Turek, F., and Vitaterna, M. (2016). Multiple classifier systems for automatic sleep scoring in mice. *J. Neurosci. Methods* 264, 33–39. doi: 10.1016/j.jneumeth.2016.02.016

Gilbert, J. A., Blaser, M. J., Caporaso, J. G., Jansson, J. K., Lynch, S. V., and Knight, R. (2018). Current understanding of the human microbiome. *Nat. Med.* 24, 392–400. doi: 10.1038/nm.4517

Gloor, G. B., Macklaim, J. M., Pawlowsky-Glahn, V., and Egozcue, J. J. (2017). Microbiome datasets are compositional: and this is not optional. *Front. Microbiol.* 8:2224. doi: 10.3389/fmicb.2017.02224

Gomez-Nguyen, A., Basson, A. R., Dark-Fleury, L., Hsu, K., Osme, A., Menghini, P., et al. (2021). *Parabacteroides distasonis* induces depressive-like behavior in a mouse model of Crohn's disease. *Brain Behav. Immun.* 98, 245–250. doi: 10.1016/j.bbi.2021.08.218

Gonzalez, A., Navas-Molina, J. A., Kosciolek, T., Mcdonald, D., Vazquez-Baeza, Y., Ackermann, G., et al. (2018). Qiita: rapid, web-enabled microbiome meta-analysis. *Nat. Methods* 15, 796–798. doi: 10.1038/s41592-018-0141-9

Govindarajan, K., Macsharry, J., Casey, P. G., Shanahan, F., Joyce, S. A., and Gahan, C. G. (2016). Unconjugated bile acids influence expression of circadian genes: a potential mechanism for microbe-host crosstalk. *PLoS One* 11:e0167319. doi: 10.1371/journal.pone.0167319

Grandner, M. A. (2017). Sleep, health, and society. *Sleep Med. Clin.* 12, 1–22. doi: 10.1093/acprof:oso/9780199566594.003.0001

Halverson, T., and Alagiakrishnan, K. (2020). Gut microbes in neurocognitive and mental health disorders. *Ann. Med.* 52, 423–443. doi: 10.1080/07853890.2020.1808239

Howland, J. G., and Cazakoff, B. N. (2010). Effects of acute stress and GluN2B-containing NMDA receptor antagonism on object and object-place recognition memory. *Neurobiol. Learn. Mem.* 93, 261–267. doi: 10.1016/j.nlm.2009.10.006

Jiang, H., Ling, Z., Zhang, Y., Mao, H., Ma, Z., Yin, Y., et al. (2015). Altered fecal microbiota composition in patients with major depressive disorder. *Brain Behav. Immun.* 48, 186–194. doi: 10.1016/j.bbi.2015.03.016

Kamphuis, J., Lancel, M., Koolhaas, J. M., and Meerlo, P. (2015). Deep sleep after social stress: NREM sleep slow-wave activity is enhanced in both winners and losers of a conflict. *Brain Behav. Immun.* 47, 149–154. doi: 10.1016/j.bbi.2014.12.022

Kecklund, G., and Axelsson, J. (2016). Health consequences of shift work and insufficient sleep. *BMJ* 355:i5210. doi: 10.1136/bmj.i5210

Knief, U., and Forstmeier, W. (2021). Violating the normality assumption may be the lesser of two evils. *Behav. Res. Methods* 53, 2576–2590. doi: 10.3758/s13428-021-01587-5

Knight, R., Vrbanac, A., Taylor, B. C., Aksenov, A., Callewaert, C., Debelius, J., et al. (2018). Best practices for analysing microbiomes. *Nat. Rev. Microbiol.* 16, 410–422. doi: 10.1038/s41579-018-0029-9

Kuipers, F., Bloks, V. W., and Groen, A. K. (2014). Beyond intestinal soap–bile acids in metabolic control. *Nat. Rev. Endocrinol.* 10, 488–498. doi: 10.1038/nrendo.2014.60

Langille, M. G., Zaneveld, J., Caporaso, J. G., Mcdonald, D., Knights, D., Reyes, J. A., et al. (2013). Predictive functional profiling of microbial communities using 16S rRNA marker gene sequences. *Nat. Biotechnol.* 31, 814–821. doi: 10.1038/nbt.2676

Lathrop, S. K., Bloom, S. M., Rao, S. M., Nutsch, K., Lio, C. W., Santacruz, N., et al. (2011). Peripheral education of the immune system by colonic commensal microbiota. *Nature* 478, 250–254. doi: 10.1038/nature10434

Lavelle, A., and Sokol, H. (2020). Gut microbiota-derived metabolites as key actors in inflammatory bowel disease. *Nat. Rev. Gastroenterol. Hepatol.* 17, 223–237. doi: 10.1038/s41575-019-0258-z

Liew, S. C., and Aung, T. (2021). Sleep deprivation and its association with diseases-a review. *Sleep Med.* 77, 192–204. doi: 10.1016/j.sleep.2020.07.048

Liu, K., Raghavan, S., Nelesen, S., Linder, C. R., and Warnow, T. (2009). Rapid and accurate large-scale coestimation of sequence alignments and phylogenetic trees. *Science* 324, 1561–1564. doi: 10.1126/science.1171243

Lozupone, C., Lladser, M. E., Knights, D., Stombaugh, J., and Knight, R. (2011). UniFrac: an effective distance metric for microbial community comparison. *ISME J.* 5, 169–172. doi: 10.1038/ismej.2010.133

Macfarlane, G. T., Steed, H., and Macfarlane, S. (2008). Bacterial metabolism and health-related effects of galacto-oligosaccharides and other prebiotics. *J. Appl. Microbiol.* 104, 305–344. doi: 10.1111/j.1365-2672.2007.03520.x

Mandal, S., Van Treuren, W., White, R. A., Eggesbo, M., Knight, R., and Peddada, S. D. (2015). Analysis of composition of microbiomes: a novel method for studying microbial composition. *Microb. Ecol. Health Dis.* 26;27663. doi: 10.3402/mehd.v26.27663

Manning, T. S., and Gibson, G. R. (2004). Microbial-gut interactions in health and disease. *Prebiotics Best Pract. Res. Clin. Gastroenterol.* 18, 287–298.

Martin, A., Ecklu-Mensah, G., Ha, C. W. Y., Hendrick, G., Layman, D. K., Gilbert, J., et al. (2021). Gut microbiota mediate the FGF21 adaptive stress response to chronic dietary protein-restriction in mice. *Nat. Commun.* 12:3838. doi: 10.1038/s41467-021-24074-z

Matenchuk, B. A., Mandhane, P. J., and Kozyrskyj, A. L. (2020). Sleep, circadian rhythm, and gut microbiota. *Sleep Med. Rev.* 53:101340. doi: 10.1016/j.smrv.2020.101340

Mcdonald, D., Price, M. N., Goodrich, J., Nawrocki, E. P., Desantis, T. Z., Probst, A., et al. (2012). An improved Greengenes taxonomy with explicit ranks for ecological and evolutionary analyses of bacteria and archaea. *ISME J.* 6, 610–618. doi: 10.1038/ismej.2011.139

Mchill, A. W., and Wright, K. P. Jr. (2017). Role of sleep and circadian disruption on energy expenditure and in metabolic predisposition to human obesity and metabolic disease. *Obes. Rev.* 18(Suppl. 1), 15–24. doi: 10.1111/obr.12503

Meerlo, P., De Bruin, E. A., Strijkstra, A. M., and Daan, S. (2001). A social conflict increases EEG slow-wave activity during subsequent sleep. *Physiol. Behav.* 73, 331–335. doi: 10.1016/s0031-9384(01)00451-6

Meng, X., Zhang, G., Cao, H., Yu, D., Fang, X., De Vos, W. M., et al. (2020). Gut dysbacteriosis and intestinal disease: mechanism and treatment. *J. Appl. Microbiol.* 129, 787–805. doi: 10.1111/jam.14661

Mirarab, S., Nguyen, N., and Warnow, T. (2012). SEPP: SATe-enabled phylogenetic placement. *Pac. Symp. Biocomput.* 2012, 247–258. doi: 10.1142/9789814366496_0024

Murai, T., Okuda, S., Tanaka, T., and Ohta, H. (2007). Characteristics of object location memory in mice: behavioral and pharmacological studies. *Physiol. Behav.* 90, 116–124. doi: 10.1016/j.physbeh.2006.09.013

Nakata, A. (2011). Effects of long work hours and poor sleep characteristics on workplace injury among full-time male employees of small- and medium-scale businesses. *J. Sleep Res.* 20, 576–584. doi: 10.1111/j.1365-2869.2011.00910.x

Nishino, K., Nishida, A., Inoue, R., Kawada, Y., Ohno, M., Sakai, S., et al. (2018). Analysis of endoscopic brush samples identified mucosa-associated dysbiosis in inflammatory bowel disease. *J. Gastroenterol.* 53, 95–106. doi: 10.1007/s00535-017-1384-4

Pluskal, T., Castillo, S., Villar-Briones, A., and Oresic, M. (2010). MZmine 2: modular framework for processing, visualizing, and analyzing mass spectrometry-based molecular profile data. *BMC Bioinformatics* 11:395. doi: 10.1186/1471-2105-11-395

Schielzeth, H., Dingemanse, N. J., Nakagawa, S., Westneat, D. F., Allegue, H., Teplitsky, C., et al. (2020). Robustness of linear mixed-effects models to violations of distributional assumptions. *Methods Ecol. Evol.* 11, 1141–1152. doi: 10.1111/2041-210x.13434

Sipe, L. M., Chaib, M., Pingili, A. K., Pierre, J. F., and Makowski, L. (2020). Microbiome, bile acids, and obesity: how microbially modified metabolites shape anti-tumor immunity. *Immunol. Rev.* 295, 220–239. doi: 10.1111/imr.12856

Stilling, R. M., Van De Wouw, M., Clarke, G., Stanton, C., Dinan, T. G., and Cryan, J. F. (2016). The neuropharmacology of butyrate: the bread and butter of the microbiota-gut-brain axis? *Neurochem. Int.* 99, 110–132. doi: 10.1016/j.neuint.2016.06.011

Thompson, R. S., Gaffney, M., Hopkins, S., Kelley, T., Gonzalez, A., Bowers, S. J., et al. (2021). Ruminiclostridium 5, *Parabacteroides distasonis*, and bile acid profile are modulated by prebiotic diet and associate with facilitated sleep/clock realignment after chronic disruption of rhythms. *Brain Behav. Immun.* 97, 150–166. doi: 10.1016/j.bbi.2021.07.006

Thompson, R. S., Roller, R., Mika, A., Greenwood, B. N., Knight, R., Chichlowski, M., et al. (2016). Dietary prebiotics and bioactive milk fractions improve NREM sleep, enhance REM sleep rebound and attenuate the stress-induced decrease in diurnal temperature and gut microbial alpha diversity. *Front. Behav. Neurosci.* 10:240. doi: 10.3389/fnbeh.2016.00240

Thompson, R. S., Vargas, F., Dorrestein, P. C., Chichlowski, M., Berg, B. M., and Fleshner, M. (2020). Dietary prebiotics alter novel microbial dependent fecal metabolites that improve sleep. *Sci. Rep.* 10:3848. doi: 10.1038/s41598-020-60679-y

Trockel, M. T., Menon, N. K., Rowe, S. G., Stewart, M. T., Smith, R., Lu, M., et al. (2020). Assessment of physician sleep and wellness, burnout, and clinically significant medical errors. *JAMA Netw. Open* 3:e2028111. doi: 10.1001/jamanetworkopen.2020.28111

Valles-Colomer, M., Falony, G., Darzi, Y., Tigchelaar, E. F., Wang, J., Tito, R. Y., et al. (2019). The neuroactive potential of the human gut microbiota in quality of life and depression. *Nat. Microbiol.* 4, 623–632. doi: 10.1038/s41564-018-0337-x

Vazquez-Baeza, Y., Pirrung, M., Gonzalez, A., and Knight, R. (2013). EMPeror: a tool for visualizing high-throughput microbial community data. *Gigascience* 2:16. doi: 10.1186/2047-217X-2-16

Wang, K., Liao, M., Zhou, N., Bao, L., Ma, K., Zheng, Z., et al. (2019). *Parabacteroides distasonis* alleviates obesity and metabolic dysfunctions via production of succinate and secondary bile acids. *Cell Rep.* 26, 222.e5–235.e5. doi: 10.1016/j.celrep.2018.12.028

Wang, Q., Garrity, G. M., Tiedje, J. M., and Cole, J. R. (2007). Naive Bayesian classifier for rapid assignment of rRNA sequences into the new bacterial taxonomy. *Appl. Environ. Microbiol.* 73, 5261–5267. doi: 10.1128/AEM.00062-07

Wang, Z., Yuan, K., Ji, Y. B., Li, S. X., Shi, L., Wang, Z., et al. (2022). Alterations of the gut microbiota in response to total sleep deprivation and recovery sleep in rats. *Nat. Sci. Sleep* 14, 121–133. doi: 10.2147/NSS.S334985

Wobbrock, J. O., Findlater, L., Gergle, D., and Higgins, J. J. (2011). "The aligned rank transform for nonparametric factorial analyses using only anova procedures," in *Proceedings of the Conference on Human Factors in Computing Systems*, Vancouver, BC, 143–146.

Wolter, M., Grant, E. T., Boudaud, M., Steimle, A., Pereira, G. V., Martens, E. C., et al. (2021). Leveraging diet to engineer the gut microbiome. *Nat. Rev. Gastroenterol. Hepatol.* 18, 885–902. doi: 10.1038/s41575-021-00512-7

Yanguas-Casas, N., Barreda-Manso, M. A., Nieto-Sampedro, M., and Romero-Ramirez, L. (2017). TUDCA: an agonist of the bile acid receptor GPBAR1/TGR5 with anti-inflammatory effects in microglial cells. *J. Cell Physiol.* 232, 2231–2245. doi: 10.1002/jcp.25742

Conflict of Interest: KW reports research support/donated materials from DuPont Nutrition & Biosciences; Grain Processing Corporation; and Friesland Campina Innovation Centre. Financial relationships: consulting with or without receiving fees and/or serving on the advisory boards for Circadian Therapeutics, Ltd., Circadian Biotherapies, Inc., Philips Respironics, and the United States Army Medical Research and Materiel Command – Walter Reed Army Institute of Research.

The remaining authors declare that the research was conducted in the absence of any commercial or financial relationships that could be construed as a potential conflict of interest.

Publisher's Note: All claims expressed in this article are solely those of the authors and do not necessarily represent those of their affiliated organizations, or those of the publisher, the editors and the reviewers. Any product that may be evaluated in this article, or claim that may be made by its manufacturer, is not guaranteed or endorsed by the publisher.

frontiers | Frontiers in Neuroscience

ORIGINAL RESEARCH
published: 07 July 2022
doi: 10.3389/fnins.2022.912442

Sleep Deficiency Is Associated With Exacerbation of Symptoms and Impairment of Anorectal and Autonomic Functions in Patients With Functional Constipation

Jie Liu[1†], Wei Wang[1†], Jiashuang Tian[1†], Chaolan Lv[2], Yuhan Fu[3], Ronnie Fass[3], Gengqing Song[3] and Yue Yu[1,2]**

[1] Department of Gastroenterology, Affiliated Anhui Provincial Hospital, Anhui Medical University, Hefei, China, [2] Division of Life Sciences and Medicine, Department of Gastroenterology, The First Affiliated Hospital of University of Science and Technology of China (USTC), University of Science and Technology of China, Hefei, China, [3] Division of Gastroenterology and Hepatology, MetroHealth Medical Center, Case Western Reserve University, Cleveland, OH, United States

OPEN ACCESS

Edited by:
Jianhua Chen,
Shanghai Jiao Tong University, China

Reviewed by:
Ji-Hong Chen,
McMaster University, Canada
Leonel Rodriguez,
Yale University, United States

***Correspondence:**
Yue Yu
yuyuemd@ustc.edu.cn
Gengqing Song
gsong@metrohealth.org

[†] *These authors have contributed equally to this work*

Specialty section:
This article was submitted to Gut-Brain Axis, a section of the journal Frontiers in Neuroscience

Received: *04 April 2022*
Accepted: *07 June 2022*
Published: *07 July 2022*

Citation:
Liu J, Wang W, Tian J, Lv C, Fu Y, Fass R, Song G and Yu Y (2022) Sleep Deficiency Is Associated With Exacerbation of Symptoms and Impairment of Anorectal and Autonomic Functions in Patients With Functional Constipation. Front. Neurosci. 16:912442. doi: 10.3389/fnins.2022.912442

Objective: Sleep deficiency (SD) is commonly seen in patients with functional constipation (FC). Our aim was to determine whether the presence of SD would influence symptoms, anorectal motility, sensation, and autonomic function in FC patients.

Materials and Methods: A total of 85 FC patients with SD and 193 FC patients without SD underwent high-resolution anorectal manometry. SD was assessed by using the Pittsburgh Sleep Quality Index (PSQI) score. Participants were required to fill in the entire questionnaires, including Patients' Constipation-symptoms, State-Trait Anxiety Inventory, and Hamilton Depression Scale. Autonomic dysfunction was studied by recording the heart rate variability. Multiple logistic regression was performed to explore the potential risk factors for anorectal function.

Results: Functional constipation patients with SD had a higher total score of constipation symptom ($P < 0.001$), in comparison with those without SD. FC patients with SD demonstrated significantly lower threshold volume for first sensation ($P < 0.001$) and urge ($P < 0.001$), as compared to those without SD. The PSQI score positively correlated with constipation symptom total score ($P < 0.001$), and negatively correlated with threshold volume for first sensation ($P < 0.001$) and urge ($P < 0.001$). FC patients with SD had a reduced vagal activity ($P = 0.016$) and a higher sympathetic activity as compared to those without SD ($P = 0.003$). Multivariate logistic regression revealed that SD, anxiety and depression were independent risk factors for anorectal function, with SD exhibiting the highest degree of association with first sensation (OR: 4.235).

Conclusion: Sleep deficiency is associated with worse constipation related symptoms, altered anorectal function and perception, and impaired autonomic function in FC patients.

Keywords: constipation, autonomic dysfunction, anorectal function, anxiety, depression, sleep deficiency

INTRODUCTION

Sleep deficiency (SD) is defined as subjects not getting enough sleep and/or sleeping at an inappropriate time of day (Hyun et al., 2019; Orr et al., 2020). SD is frequently associated with disorders of gut-brain interaction (DGBI), such as irritable bowel syndrome (IBS), functional dyspepsia, and chronic constipation (Orr et al., 2020). SD is related to various gastrointestinal symptoms, including abdominal pain, acid reflux, abdominal distension, and belching (Hyun et al., 2019). Previous studies have shown that lack of sleep is associated with an increased risk of multiple gastrointestinal complaints and decreased quality of life (Jiang et al., 2017; Orr et al., 2020). For example, DGBI is associated with excessive daytime sleepiness in a study involving 3600 Chinese patients (Wu et al., 2017). Moreover, SD is directly related to gastrointestinal dysfunction and symptoms (Chen et al., 2011; Schurman et al., 2012). IBS patients with SD are found to have anorectal dysfunction (Chen et al., 2011).

Although SD has been associated with DGBI, the relationship of SD with anorectal function remains unclear due to conflicting data in the literature. Several studies have indicated that SD affects gastrointestinal motility in patients with DGBI. Park et al. (2020) reported lower melatonin concentrations in sleep-deprived mice compared to the control group. Furthermore, the metagenomic analysis of microbiota indicated an abundance of colitogenic microbiota in sleep-deprived mice. Therefore, the authors concluded that intestinal dysbiosis could be influenced by sleep deprivation, resulting in increased colitogenic microbiota, which could aggravate colonic dysfunction. Haase et al. (2015) found that basal colonic activity was suppressed during both deep sleep and light sleep compared to nocturnal wake periods *via* 3D-Transit system. Besides, suppressed basal colonic activity was detected during both deep sleep ($P < 0.05$) and light sleep ($P < 0.05$) when compared with nocturnal wake periods. However, Liu et al. (2010, 2011) showed that SD did not affect anorectal function in healthy subjects.

Sleep deprivation is closely related to autonomic dysfunction (Tobaldini et al., 2017). It has been shown that autonomic dysfunction is closely associated with the development of functional constipation and enhancement of parasympathetic activity could significantly improve symptoms of functional constipation (FC) (Chen et al., 2018, 2021). Furthermore, pro-inflammatory cytokines are released in the setting of acute sleep deprivation, which might result in recurrent symptoms in patients with inflammatory bowel disease and IBS (Axelsson et al., 2013). SD is also linked to anorectal dysfunction and creates some degree of rectal hyperalgesia in patients with IBS (Chen et al., 2011). The interaction between SD and altered anorectal function may be multi-factorial and needs further investigation.

Recent studies showed that patients with FC had significantly lower sleep quality compared with patients with IBS (Chen et al., 2020). However, the relationship between SD and its impact on anorectal function remains largely unknown in patients with FC. The aim of this study was to investigate the impact of patient-reported SD on symptoms, anorectal function, and rectal sensitivity in patients with FC.

MATERIALS AND METHODS

Patients

Patients who met the Rome IV diagnostic criteria (Drossman, 2016) for FC were recruited into the study at the Gastrointestinal Motility Center, Department of Gastroenterology, the First Affiliated Hospital of University of Science and Technology of China (USTC), from November 2016 to January 2020. The exclusion criteria were: severe cardiac and pulmonary diseases, diabetes, chronic kidney disease, and other chronic gastrointestinal disorders such as inflammatory bowel disease, peptic ulcer disease, and cancer. Meanwhile, patients reporting a chief complaint of abdominal pain were ruled out given that abdominal pain inherently distinguishes FC with IBS-C (Ruffle et al., 2021). Our study excluded patients taking pain modulators and patients with severe mental diseases, such as patients with depression scores higher than 24, suggesting severe depression. In particular, patients who were taking chronic opioids and non-sleep aid medications that could potentially affect sleep quality were excluded. These non-sleep aid medications include the following: (i) antiasthmatic medications, such as aminophylline, doxofylline, and ephedrine; (ii) antidepressants, such as paroxetine, fluoxetine, and imipramine; (iii) antibiotics, such as penicillin, macrolides, quinolones, and (iv) glucocorticoid.

A total of 326 FC patients were eligible for the study. Twelve patients were excluded from the study due to incomplete data. Thirty-six patients were also excluded based on the exclusion criteria (14 patients who took medications that affect sleep quality, 15 patients with diabetes, 4 patients with IBD, and 3 patients with colorectal cancer). Finally, a total of 278 FC patients (114 males and 164 females) were included in this study (**Figure 1**).

The study was approved by the Ethics Committee of Anhui Provincial Hospital (Registration No: 2022-RE-143). The study protocol was registered in the Chinese Clinical Trial Registry (No. ChiCTR-2000037449). Written informed consent was obtained from all participants before their enrollment into the study.

Experimental Protocol

This is a cross-sectional cohort study, and patients with FC were divided into two groups based on the Pittsburgh Sleep Quality Index (PSQI) scores: FC patients with SD ($n = 85$) (PSQI scores ≥ 5) and FC patients without SD ($n = 193$) (PSQI scores < 5).

All participants were required to fill in the entire questionnaires, including PSQI, Patients' Constipation-symptoms (PAC-SYM), State-Trait Anxiety Inventory (STAI), and Hamilton Depression Scale (HAMD). All FC patients underwent high resolution anorectal manometry (HRAM) and received electrocardiogram (ECG) recording for heart rate variability analysis.

Measurements

High Resolution Anorectal Manometry

All FC patients underwent HRAM (MedKinetic, Ningbo, China), and the process of HRAM was described in our previous research

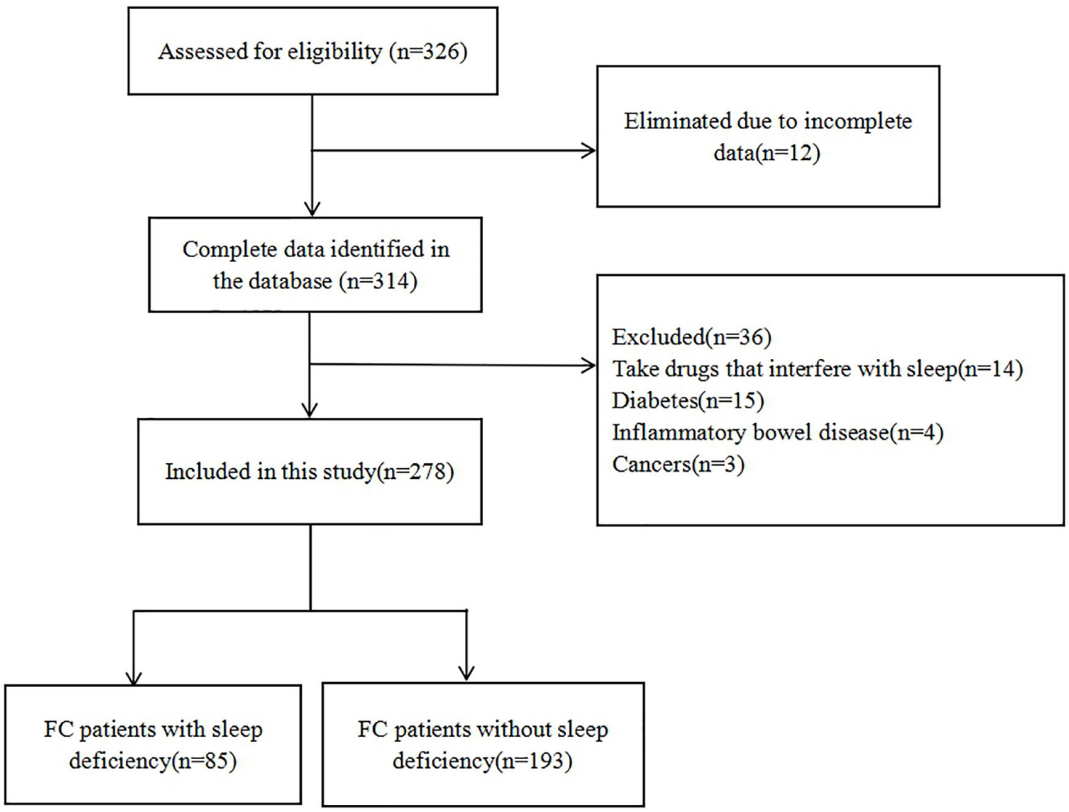

FIGURE 1 | Flow chart of FC patient recruitment in this study.

(Liu et al., 2020). Each patient received 1–2 doses of glycerin enema for bowel preparation 30–60 min prior to the HRAM test. Rectal enema is the preoperative preparation for anorectal manometry, in order to avoid the residue of stool in anorectal, which affects the acquisition of dynamic parameters. A water-perfused anorectal manometric catheter was used to measure the anal sphincter pressure at a 1-cm interval. The device employs the technology of proprietary pressure transduction, which allows every pressure-sensor element to sense pressure over a 2.5-mm length in each of the twelve sectors that are dispersed radially. Patients were placed in the left lateral position and the catheter was inserted into the rectum after lubrication. Manometry parameters, including average resting pressures, maximum and sustained squeeze pressures, were analyzed by the manometry software (Manometryapp, MedKinetic, Ningbo, China). The pressure of the anal sphincter was examined during voluntary effort, while the study participants were asked to squeeze the anus for as long as possible to record squeeze pressures.

The threshold volume for rectoanal inhibitory reflexes (RAIR) was examined through inflation of the balloon in a stepwise manner to 10 ml, beginning at 10 ml until we observed relation of the anal sphincter at a lower distension volume. The sensation test was examined by the rectal balloon distended at a 10 ml interval until the participant indicated the first sensation. After that, we increased the volume of the balloon in progressive 10-ml increments so that the participant felt the sensations of the urge and the maximum urge to defecate. The results for inducing these sensations were depended on the subjects' report subjectively, and the threshold volumes for this sensory test were documented. Rectal compliance of every subject was calculated from the slope of the volume-pressure curve, which was automatically analyzed by the manometry software (Manometryapp, MedKinetic, Ningbo, China) (Lee and Bharucha, 2016).

Questionnaires

The PSQI as a tool for diagnosing SD was employed to assess the quality of sleep in the past month. The PSQI is split into seven dimensions, namely, subjective sleep quality, daytime dysfunction, sleep latency, use of sleep medication, sleep duration, SD, and habitual sleep efficiency. Each dimension is scored on a four-point Likert scale (0–3, from none to the most profound effect). A total score of 5 or more suggests "SD." The PSQI has shown a specificity of 86.5 and 89.6% sensitivity using this cutoff point (Chen et al., 2011; Liu et al., 2011).

The PAC-SYM questionnaire was used in the psychometric assessment of patients with chronic constipation. This questionnaire evaluated the severity of symptoms in patients with FC. The survey included 12 items divided into 3 symptom subscales, including rectal (3 items), stool (5 items), and abdominal (3 items). The rectal domain collected information about pain, burning, tearing, or bleeding during bowel movements. The abdominal domain evaluated discomfort,

bloating, pain, and stomach cramps. The stool domain was categorized as hard, small, incomplete, straining, and difficult bowel movement. The items of this scale were scored through five-point Likert scales, ranging from 0 to 4. In this case, 0 represented the absence of symptoms, while 4 indicated very severe symptoms. A low average score showed a low symptom burden (Frank et al., 1999).

The STAI was adopted for assessing the levels of anxiety (Guillén-Riquelme and Buela-Casal, 2014). STAI is a 20-item instrument scored on a four-point Likert-type scale (1–4, from not at all to very much). Healthy subjects without anxiety have total scores < 40 (Vigneau and Cormier, 2008). HAMD was adopted for assessing the levels of depression. HAMD is a 17-item instrument and uses a 5-point Likert scale (0–4, from no symptom to severe symptoms). A global HAMA score of >7 indicates "depression" (Lu et al., 2020).

Assessment of Autonomic Functions

The functions of the autonomic nervous system of the subjects were measured with spectral analysis of HRV (heart rate variability), as described in our previous research. The HRV analysis software V.1.2.0.0 (Cardiotrak Holter system; Hangzhou Baihui Electrocardiograms, China) was employed to analyze each subject's HRV data, whereas HRV signals were provided by using an electrocardiogram (ECG) recording (ct-082, Hangzhou Baihui Electrocardiograms, China). Calculation of the power in every frequency sub-band was employed to determine the power spectral analysis. In general, parasympathetic or vagal activities are represented by the band of high frequency (0.15–0.50 Hz, HF), while the power in the band of low frequency (0.04–0.15 Hz, LF) primarily represents sympathetic activity. Furtherly, the HF/(HF + LF) ratio was used to represent parasympathetic activity. Meanwhile, the Baevsky Index or Sympathetic Index (SI) was calculated to represent sympathetic tone according to the formula $SI = \frac{AMo \times 100\%}{2\text{Mo} \times \text{MxDMn}}$. The most frequent RR interval was transformed into the mode (Mo), which is expressed in seconds (Ali et al., 2021). A 50 ms bin width was used for calculating the amplitude of mode (AMo), which is expressed as a percentage of the total number of intervals measured. MxDMn represented the variability as the difference between longest (Mx) and shortest (Mn) RR interval values, expressed in seconds. The SI is expressed as s^{-2}.

Statistical Analysis

All the statistical analyses were implemented in the SPSS V.16.0 software. Continuous variables are given as mean ± standard deviation. Statistical comparisons were investigated using normality testing, followed by paired *t*-test. Pearson's correlation coefficient were used to assess the relationship among PSQI, anorectal function and constipation symptoms. Moreover, a multivariate logistic regression analysis was employed, including anorectal function as the dependent variables and all those variables with statistically significant differences in the bivariate analysis as independent variables. Anxiety and depression were considered as potential confounding factors. $P < 0.05$ signified statistical significance.

RESULTS

Overall Study Population

Finally, a total of 278 FC patients who underwent HRAM were enrolled for this study, including 85 FC patients with SD (accounting for 30.58% in FC) and 193 FC patients without SD. All patients tolerated the procedures without any adverse effects. No remarkable differences were reported between the groups regarding age, BMI, as well as, gender and there was no difference in duration of constipation between the FC subgroups ($t = 1.548$, $P = 0.123$) (**Table 1**).

Constipation Symptom and Anxiety/Depression Score

Functional constipation patients with SD had a higher PAC-SYM score than group FC patients without SD (15.720 ± 1.493 vs. 12.750 ± 1.339, $P < 0.001$) (**Table 2**). Specifically, FC patients with SD had a higher abdominal symptom score (4.670 ± 1.084 vs. 4.340 ± 0.876, $P = 0.008$) and higher rectal symptom score (4.890 ± 0.926 vs. 4.560 ± 0.882, $P = 0.005$) compared with FC patients without SD. However, there was no difference in defecation symptoms score between the two groups (4.550 ± 0.838 vs. 4.410 ± 0.886, $P = 0.207$). Meanwhile, there was also no significant difference in the anxiety and depression scores between FC patients with SD and those without SD ($P = 0.411$ and $P = 0.451$, respectively) (**Table 2**).

Anorectal Function

When compared to FC patients without SD, FC patients with SD had a significantly lower threshold volume for the first sensation (22.00 ± 3.87 vs. 24.48 ± 3.85, $P < 0.001$), the urge to defecate (106.71 ± 9.92 vs. 114.97 ± 9.08, $P < 0.001$), and maximal defecation (123.18 ± 10.69 vs. 141.63 ± 11.50, $P < 0.001$). Conversely, FC patients with SD had a significantly higher threshold volume for the RAIR (17.46 ± 4.15 vs. 16.12 ± 4.84, $P = 0.019$). FC patients with SD had lower anal sphincter pressure for maximal squeeze than that of FC patients without SD (143.14 ± 14.12 vs. 151.03 ± 11.87, $P < 0.001$). However, there was no difference in length of anal sphincter and compliance between FC patients with SD and those without SD ($P = 0.800$ and $P = 0.685$, respectively) (**Table 3**).

Multivariate Logistic Regression Analysis

Results of the logistic regression are shown in **Table 4**. In summary, In summary, among all the potential factors included in the model, SD (OR: 4.235) and anxiety (OR: 1.743) showed a statistically significant influence on the first sensation, while SD (OR: 2.496) showed an influence on the urge to defecate. In addition, SD (OR: 3.147) and depression (OR: 3.024) showed a significant influence on maximal defecation, while SD (OR: 2.145) showed a statistically significant influence on RAIR.

Correlations Between Pittsburgh Sleep Quality Index and Other Parameters

Pittsburgh sleep quality index significantly correlated with total score of PAC-SYM ($r = 0.686$, $P < 0.001$), as well as abdominal

TABLE 1 | Characteristics of the FC population (*N* = 278).

Variables	FC patients with SD (*n* = 85)	FC patients without SD (*n* = 193)	χ^2/t	*P*
Gender				
Male (*n*)	38	76	0.692	0.405
Female (*n*)	47	117		
Age (years; mean ± SE)	47.39 ± 9.58	46.64 ± 10.09	0.576	0.565
BMI (kg/m^2; mean ± SE)	24.34 ± 4.29	23.61 ± 3.91	1.397	0.164
Duration of constipation (months; mean ± SE)	34.92 ± 7.71	33.25 ± 8.42	1.548	0.123

Data are expressed as mean ± standard deviation.
FC, functional constipation; SD, sleep deficiency; BMI, body mass index.
No statistically significant difference was noted in age, gender, BMI among the two groups.

and rectal subscores ($r = 0.194$; $P = 0.001$ and $r = 0.156$; $P = 0.009$, respectively), but there was no correlation between PSQI and defecation symptoms ($r = -0.041$, $P = 0.501$). PSQI negatively correlated with the threshold volume for the first sensation ($r = -0.330$; $P < 0.001$), urge to defecate ($r = -0.366$; $P < 0.001$), maximal defecation ($r = -0.671$; $P < 0.001$), and RAIR ($r = 0.323$; $P < 0.001$) in patients with FC. PSQI also negatively correlated with maximal squeeze ($r = -0.233$; $P = 0.001$) despite the lack of correlation between PSQI and resting and sustained squeeze in FC patients ($r = 0.054$; $P = 0.366$ and $r = -0.074$; $P = 0.219$, respectively) (**Table 5**). The scatter plot between PSQI and PAC-SYM score was shown in **Figure 2**.

Mechanisms Involving Autonomic Functions

Functional constipation patients with SD had a significantly lower parasympathetic activity when compared to that of FC patients without SD [HF/(HF + LF) ratio, 0.42 ± 0.05 vs. 0.46 ± 0.04, $P = 0.016$] (**Figure 3A**). Meanwhile, FC patients with SD had a higher sympathetic activity than that of FC patients without SD (SI, 37.48 ± 7.75 vs. 34.88 ± 6.09, $P = 0.003$) (**Figure 3B**).

DISCUSSION

In this study, we investigated the influence of SD on symptoms, anorectal motility, sensation in FC patients by a validated sleep questionnaire (PSQI) and HRAM, and explored potential mechanisms using spectral analysis of HRV. We found that FC patients with SD had more severe constipation symptoms (especially abdominal and rectal symptoms) than those without SD. Meanwhile, FC patients with SD had a significantly lower sensory threshold for anorectal balloon distension and a lower anal sphincter pressure for the maximal squeeze. Notably, we also showed that SD increased sympathetic activity while simultaneously suppressed parasympathetic activity. Results from multivariate logistic regression analysis shown that SD was significant independent risk factors for anorectal function with first sensation exhibiting the highest degree of association, while anxiety was independent risk factors for first sensation and depression was independent risk factors for maximal defecation.

Although the relationship between SD and DGBI is incompletely understood, latest studies indicated that there were close associations of SD with lower gastrointestinal symptoms. In a cross-sectional internet-based survey for Japanese population, Yamamoto et al. (2021) tested the relationship between chronic constipation and sleep and the authors demonstrated that subjects with constipation and poor sleep experienced severe symptoms and had poor quality of life, which is consistent with our findings. Jiang et al. (2017) investigated 126 patients with chronic constipation and reported that patients with sleep disorders had worse constipation symptoms evaluated by the

TABLE 2 | Constipation symptom, anxiety, and depression in FC patients with or without SD.

	FC with SD	FC without SD	*t*	*P*
PAC-SYM				
Abdominal symptoms	4.67 ± 1.08	4.34 ± 0.88	2.673	0.008
Rectal symptoms	4.89 ± 0.93	4.56 ± 0.88	2.824	0.005
Defecation symptoms	4.55 ± 0.84	4.41 ± 0.89	1.266	0.207
Total score	15.72 ± 1.49	12.75 ± 1.34	16.424	<0.001
STAI total score	37.18 ± 9.16	36.17 ± 9.48	0.823	0.411
HAMD total score	6.18 ± 2.08	5.99 ± 1.92	0.754	0.451

Data are expressed as mean ± standard deviation.
FC, functional constipation; SD, sleep deficiency; PAC-SYM, patient assessment of constipation symptoms; STAI, State-Trait Anxiety Inventory; HAMD, Hamilton Depression Scale.

TABLE 3 | Anorectal function in FC patients with or without SD.

	FC with SD	FC without SD	*t*	*P*
Threshold volume, ml				
First sensation	22.00 ± 3.87	24.48 ± 3.85	4.94	<0.001
Urge	106.71 ± 9.92	114.97 ± 9.08	6.80	<0.001
Maximal	123.18 ± 10.69	141.63 ± 11.50	12.59	<0.001
RAIR	17.46 ± 4.15	16.12 ± 4.84	2.36	0.019
Anal sphincter pressure, mm Hg				
Resting	56.06 ± 5.52	55.67 ± 5.47	0.54	0.590
Maximal	143.14 ± 14.12	151.03 ± 11.87	4.81	<0.001
Sustained squeeze	197.34 ± 7.99	201.53 ± 7.82	0.083	0.934
Length of anal sphincter, cm	2.25 ± 0.29	2.23 ± 0.33	0.254	0.800
Compliance, ml/mm Hg	6.18 ± 0.67	6.15 ± 0.63	0.406	0.685

Data are expressed as mean ± standard deviation.
FC, functional constipation; SD, sleep deficiency; RAIR, rectoanal inhibitory reflexes.

TABLE 4 | Multivariate logistic regression analysis about the potential factors of anorectal function for FC patients.

Potential factors	First sensation			Urge			Maximal			RAIR		
	OR	95%CI	*P*	OR	95%CI	*P*	OR	95%CI	*P*	OR	95%CI	*P*
Age	0.953	0.691–1.453	0.162	0.867	0.603–1.215	0.174	0.783	0.596–1.269	0.246	0.961	0.711–1.608	0.144
Gender	1.023	0.768–1.957	0.092	1.105	0.794–2.013	0.084	0.983	0.631–1.857	0.272	1.314	0.823–1.965	0.063
SD	4.235	2.018–7.869	**0.001**	2.496	1.836–3.871	**0.018**	3.147	1.981–4.746	**0.005**	2.145	1.768–2.939	**0.041**
Anxiety	1.743	1.106–2.459	**0.015**	0.768	0.987–1.416	0.496	1.006	0.536–1.896	0.355	0.793	1.018–2.153	0.403
Depression	1.412	0.926–2.728	0.052	1.245	0.871–2.669	0.073	3.024	1.168–6.739	**0.003**	1.306	1.002–2.781	0.064

OR, odds ratio; CI, confidence interval; RAIR, rectoanal inhibitory reflexes; FC, functional constipation; SD, sleep deficiency. The bold values indicate P < 0.050.

constipation scoring system (CSS) scale, compared to those without sleep disorders (P = 0.031). Latest study evaluated the sleep quality in patients with FC and constipation-predominant IBS (IBS-C), and the results showed that FC patients had worse sleeping quality than IBS-C patients (Chen et al., 2020). In this study, we found that FC patients with SD patients were characterized by more severe abdominal and rectal symptoms than those without SD. However, no remarkable differences were reported between the groups regarding defecation symptoms, which may be because included patients already had severe defecation alterations for a long-term course based on Rome IV criteria. Meanwhile, our study showed that the PSQI significantly correlated with the abdominal (P = 0.001) and rectal symptoms (P = 0.009) in FC patients with SD.

While the influence of sleep dysfunction on anorectal function and motility was investigated in previous studies for IBS patients, the impact of SD on anorectal functions and motility in FC has been scarcely studied. To our best knowledge, it is the first study to determine whether the presence of SD would influence symptoms, anorectal motility, sensation, and autonomic function in patients with FC. By application of HRAM, we observed that FC patients with SD had a lower threshold volume for the first sensation, maximal defecation, urge to defecate, and a significant increase in the threshold volume for RAIR when compared to FC patients without SD, which is similar to previous findings (Chen et al., 2011; González Cañete et al., 2014). FC patients with SD had a lower threshold volume for the first sensation, maximal defecation, urge to defecate when compared to FC patients without SD. What is more, FC patients with SD had a significant decrease in the maximal squeeze pressure, which may due to autonomic dysfunction (Iino et al., 2004). Meanwhile, our study showed that the PSQI significantly correlated with the perception threshold to anorectal balloon distension in FC patients with SD.

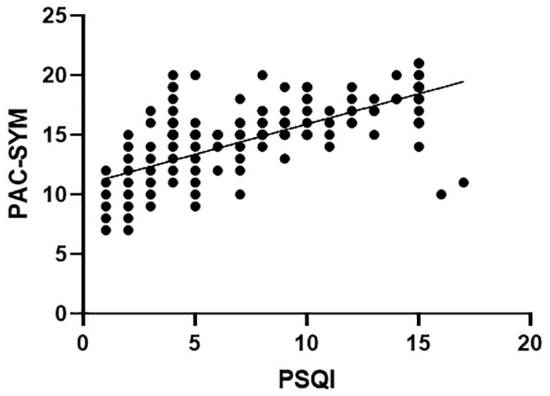

FIGURE 2 | Sleep quality scores (PSQI) significantly correlated with constipation symptom scores (PAC-SYM) in FC patients (Pearson Coefficient = 0.686, P < 0.001).

TABLE 5 | Correlations between PSQI and constipation symptom as well as anorectal function in FC patients.

	FC	
	r	*P*
Threshold volume, ml		
First sensation	–0.330	<0.001
Urge	–0.366	<0.001
Maximal	–0.671	<0.001
RAIR	0.323	<0.001
Anal sphincter pressure, mm Hg		
Resting	0.054	0.366
Maximal	–0.233	0.001
Sustained squeeze	–0.074	0.219
Length of anal sphincter, cm	0.048	0.422
Compliance, ml/mm Hg	0.040	0.509
PAC-SYM		
Abdominal symptoms	0.194	0.001
Rectal symptoms	0.156	0.009
Defecation symptoms	–0.041	0.501
Total score	0.686	<0.001

Data are expressed as Pearson's correlation coefficient with p values in parentheses.
PSQI, Pittsburgh Sleep Quality Index; FC, functional constipation; RAIR, rectoanal inhibitory reflexes; PAC-SYM, patient assessment of constipation symptoms.

The PSQI serves as a major tool to evaluate sleep quality during the past month. Previous studies have shown that the PSQI score correlates with some mental health diagnoses, including anxiety, stress, depression, and psychotic disorders (Zhao et al., 2018). Anxiety as well as other psychological indicators might influence the relationship of the perception of SD with visceral hypersensitivity (Meerveld and Johnson, 2018). Thus, it might be controversial that if the poor quality of sleep combined with anxiety and/or other psychological comorbidities but not SD itself influences rectal sensitivity as noted in this research. However, no difference in STAI and HAMD scores was observed between FC patients with and without SD. Besides, multivariate logistic regression analysis was

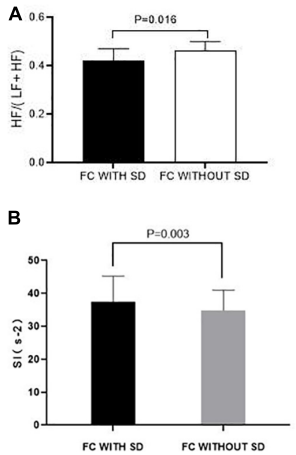

FIGURE 3 | Effects of SD on autonomic function in FC patients. **(A)** Parasympathetic activity represented as the ratio of HF/(LF + HF) in FC patients with SD was significantly lower than that of FC patients without SD ($P < 0.050$). **(B)** Sympathetic activity represented as the Baevsky Index or Sympathetic Index (SI) in FC patients with SD was significantly higher than that of FC patients with SD ($P < 0.050$).

applied, to elucidate the association among anorectal function, SD, anxiety and depression. Results showed that SD, anxiety and depression were significant independent risk factors for anorectal function, with SD exhibiting the highest degree of association with first sensation (OR: 4.235). Therefore, it is more likely that poor sleep quality most significantly affects anorectal function in FC patients, although other comorbidities, consisting of stress and negative events, might influence rectal sensitivity (Parker et al., 2019).

It is known that autonomic dysfunction plays an important role in the pathogenesis of FC (Mazur et al., 2012). In the current study, HRV analysis was used to represent the autonomic cardiac function, which can be explored as a substitute for autonomic nerve function. Furtherly, this approach has been previously employed to demonstrate that a sympathetic to parasympathetic post-prandial ratio decreases with an increase in vagal activity (Bruinstroop et al., 2013). What is more, alterations in cardiac autonomic functions triggered by meal opine it can be a surrogate for gastrointestinal autonomic function (Wang X. et al., 2019). It has been reported that poor sleep will lead to sympathetic activation. Wang S. et al. (2019) reported that poor sleep would increase the LF/HF ratio and make LF higher, reflecting increased sympathetic activity and decreased parasympathetic activity. Carter et al. (2018) reported that individuals with chronic insomnia exhibit increased sympathetic neural as well as cardiovascular reactivity to stress, augmented sympathetic neural outflow, and blunted baroreflex sensitivity relative to good-sleeper individuals. Of note, Liu et al. (2018) documented that an escalation in sympathetic nerve activity is associated with constipation. Meanwhile, our previous study showed that the imbalance between sympathetic and parasympathetic nerves plays a vital role in constipation symptoms (Liu et al., 2020). Notably, the current study showed that sleep disorders will influence the balance between parasympathetic and sympathetic nerves thus remarkably increasing sympathetic activities, which is similar outcomes to previous research (Carter et al., 2018; Wang S. et al., 2019).

On the other hand, visceral hypersensitivity has been reported by the incidence of functional gastrointestinal conditions, e.g., non-cardiac chest pain, IBS, as well as heartburn (Simrén et al., 2018). Visceral hypersensitivity is linked to insufficient sleep, while SD could promote visceral perception conversely. Moreover, the interrelation between visceral hypersensitivity and SD has been regarded as an etiological event of chronic hyperalgesia syndromes (Lee, 2006). Although previous study have shown that sleep disorders cannot result in anorectal motility changes in healthy people (Liu et al., 2011), Whitehead et al. (1990) found that patients with IBS have high chances of reporting the first rectal pain sensation at lower pressures compared to healthy individuals. To date, there is no report on the relationship between constipation and visceral hypersensitivity. In the current study, we found that FC patients were recognized by a lower sensory threshold to anorectal balloon distension. We believe that SD is associated with impairment of anorectal functions in FC patients and this change may be related to autonomic nerve function and visceral hypersensitivity. However, it is worth mentioning that the data regarding volume differences between the groups presented in our study were small statistical changes. This may suggest our patients with FC plus SD were likely associated with more severe anorectal hypersensitivity by their ability to differentiate a small balloon volume changes. SD may play a role in the pathogenesis of visceral hypersensitivity in patients with FC. Fass et al. (2000) demonstrated that the visceral sensitivity of functional bowel disorder patients can be aggravated by sleep maintenance disorders. Consequently, SD may be involved in the mechanism behind these changes. Visceral hypersensitivity is linked to insufficient sleep, whereas SD could promote visceral perception. Moreover, the interrelation between visceral hypersensitivity and SD has been considered an etiological event of chronic hyperalgesia syndromes (Lee, 2006). Notably, the gut microbiota is another potential mechanism that affects the rectal sensitivity in patients with FC. Previous studies reported a decrease in beneficial bacteria such as Lactobacillus, an increase in harmful bacteria, and a reduction in species richness in FC patients (Wang and Yao, 2021). Colonic functions could be modulated by gut microbiota *via* the metabolites of bacterial fermentation, which could trigger the release of gut hormones. Subsequently, colonic sensation, secretion, and motility could be impacted by these gut hormones (Ohkusa et al., 2019; Ding et al., 2021). Overall, the relationship between SD and altered anorectal function in FC may be multi-factorial, and the underlying mechanism needs further investigation.

A systematic review put forward a new model of communication between DGBI and sleep microbial metabolites, including the serotonergic system, the vagus nerve, and immune reactions (Sen et al., 2021). Non-rapid eye movement (NREM) sleep was decreased by serotonin depletion in the brain during the inactive phase and was increased during the active phase in rats (Nakamaru-Ogiso et al., 2012). This

suggests that serotonin might play an important role in communicating gut microbiome and sleep regulation in the brain. Meanwhile, vagotomized mice did not display sleep deprivation-associated inflammation, which demonstrated the role of the vagus nerve in crosstalk between the gut microbiota and sleep (Zhang et al., 2021). Regional homogeneity (ReHo) and resting-state functional magnetic resonance imaging scans were performed by Feng et al. (2022) revealing the relationships among ReHo values in the left fusiform gyrus, the relative abundance of Lactobacilli, and depression scores in chronic insomnia patients. In addition, some bacterial genera related to the ReHo values of the right triangular inferior frontal gyrus were also found; and the relative abundance of genus Coprobacter was correlated with the ReHo values of the left angular gyrus. These findings revealed complex relationships between DGBI and chronic insomnia. Schoch et al. (2022) reported a link between sleep habits and gut microbiota. They found that daytime sleep is related to bacterial diversity, while nighttime sleep fragmentation and variability are linked with bacterial maturity and enterotype. In addition, they proposed a sleep-brain-gut link, suggesting that sleep neurophysiology is related to bacterial diversity and enterotype. Another study has demonstrated that indigenous spore-forming microbes from the gut microbiota produced metabolites that promoted host 5-HT biosynthesis in the gastrointestinal tract and impacted gut motility (Yano et al., 2015). It is well known that 5-HT regulated gut motility and alterations in 5-HT signaling might contribute to FC.

LIMITATIONS

There were some potential limitations in the present study. Firstly, although patients with serious mental diseases were excluded, patients with mild depression were included. Sleep issues may be related to or exacerbated by mental diseases and impact our results. Secondly, the healthy control group can be used as the baseline control, improving the comparison of the parameters of the water perfusion manometry system, such as the sensory test of FC patients with/without SD. However, it is difficult and ethically challenging perform a manometric examination in healthy people. Thirdly, the sensory test's value was determined subjectively by the patients' report, which might be disturbed by the patient's status at the time of examination. Besides, HRAM with water perfused was used in the current study, while most recent studies are performed using solid state catheters. Previous studies reported no differences at rest between the two types of catheters, but solid-state catheters offer greater sensitivity to rapid pressure changes compared to water perfusion (Liem et al., 2012; Rasijeff et al., 2017). Thus, using a water-perfused HRAM catheter may lead to different results. Finally, another limitation includes the fact that other objective measures of colonic function (such as transit studies, etc.) were not included in the assessment of FC patients, and the patients did not undergo a formal mental health assessment before participating in the study. Although patients with serious mental diseases were excluded, sleep issues may be related or exacerbated by the mental diseases which can in turn impact our results.

CONCLUSION

In summary, the present study verifies the previous concept of the relationship of subjective disturbances of sleep with gastrointestinal symptoms. We established that individuals with FC with SD are remarkably sensitive to rectal distention discomfort, and they exhibit evidence of changed anorectal function and severe constipation symptoms. The potential mechanisms may be related to autonomic nervous function and visceral hypersensitivity. However, it remains to be investigated if the mechanism(s) of SD affecting constipation, such as the central nervous system's dysfunctions, affects intestinal function.

DATA AVAILABILITY STATEMENT

This datasets presented in this study can be found in online repositories. The names of the repository/repositories and accession number(s) can be found in the article/supplementary material.

ETHICS STATEMENT

The study was approved by the Ethics Committee of Anhui Provincial Hospital (Registration No: 2022-RE-143). The study protocol was registered in the Chinese Clinical Trial Registry (No. ChiCTR-2000037449). Written informed consent was obtained from all participants before their enrollment into the study. Written informed consent was obtained from the individual(s) for the publication of any potentially identifiable images or data included in this article.

AUTHOR CONTRIBUTIONS

YY and GS planned the study. JL, WW, JT, CL, and YY performed HRAM. JL and CL collected and interpreted the data. JL drafted the manuscript. YY, GS, YF, and RF revised the manuscript critically. All authors read and approved the final manuscript.

FUNDING

This study was supported by External Science and Technology Cooperation Planning Projects of Anhui Province of China (No. 1604b0602021).

ACKNOWLEDGMENTS

We appreciate all subjects who participated in this research.

REFERENCES

Ali, M. K., Liu, L., Chen, J. H., and Huizinga, J. D. (2021). Optimizing Autonomic Function Analysis *via* Heart Rate Variability Associated With Motor Activity of the Human Colon. *Front. Physiol.* 12:619722. doi: 10.3389/fphys.2021.619722

Axelsson, J., Rehman, J. U., Akerstedt, T., Ekman, R., Miller, G. E., Höglund, C. O., et al. (2013). Effects of sustained sleep restriction on mitogen-stimulated cytokines, chemokines and T helper 1/ T helper 2 balance in humans. *PLoS One* 8:e82291. doi: 10.1371/journal.pone.0082291

Bruinstroop, E., la Fleur, S. E., Ackermans, M. T., Foppen, E., Wortel, J., Kooijman, S., et al. (2013). The autonomic nervous system regulates postprandial hepatic lipid metabolism. *Am. J. Physiol. Endocrinol. Metab.* 304, E1089–E1096. doi: 10.1152/ajpendo.00614.2012

Carter, J. R., Grimaldi, D., Fonkoue, I. T., Medalie, L., Mokhlesi, B., and Cauter, E. V. (2018). Assessment of sympathetic neural activity in chronic insomnia: evidence for elevated cardiovascular risk. *Sleep* 41:zsy048. doi: 10.1093/sleep/zsy048

Chen, C. L., Liu, T. T., Yi, C. H., and Orr, W. C. (2011). Evidence for altered anorectal function in irritable bowel syndrome patients with sleep disturbance. *Digestion* 84, 247–251. doi: 10.1159/000330847

Chen, H. D., Bair, M. J., Chang, W. C., Hsu, C. S., Wong, M. W., Hung, J. S., et al. (2020). Similarities and differences between IBS-C and FC with regards to symptomatology, sleep quality and psychological attributes. *J. Formos. Med. Assoc.* 119, 75–80. doi: 10.1016/j.jfma.2019.02.017

Chen, J., Ni, M., and Yin, J. (2018). Electroacupuncture treatments for gut motility disorders. *Neurogastroenterol. Motil.* 30:e13393. doi: 10.1111/nmo.13393

Chen, Q. Y., Li, N., and Jiang, J. (2021). Relationship between functional constipation and brain-gut-microbiota axis. *Zhonghua Wei Chang Wai Ke Za Zhi* 24, 1048–1053. doi: 10.3760/cma.j.cn441530-20210921-00377

Ding, W., You, Z., Chen, Q., Yang, L., Doheny, J., Zhou, X., et al. (2021). Gut Microbiota Influences Neuropathic Pain Through Modulating Proinflammatory and Anti-inflammatory T Cells. *Anesth. Analg.* 132, 1146–1155. doi: 10.1213/ANE.0000000000005155

Drossman, D. A. (2016). Functional gastrointestinal disorders: history, pathophysiology, clinical features and rome IV. *Gastroenterology* [Epub ahead of print]. doi: 10.1053/j.gastro.2016.02.032

Fass, R., Fullerton, S., Tung, S., and Mayer, E. A. (2000). Sleep disturbances in clinic patients with functional bowel disorders. *Am. J. Gastroenterol.* 95, 1195–2000. doi: 10.1111/j.1572-0241.2000.02009.x

Feng, Y., Fu, S., Li, C., Ma, X., Wu, Y., Chen, F., et al. (2022). Interaction of Gut Microbiota and Brain Function in Patients With Chronic Insomnia: a Regional Homogeneity Study. *Front. Neurosci.* 15:804843. doi: 10.3389/fnins.2021.804843

Frank, L., Kleinman, L., Farup, C., Taylor, L., and Miner, P. Jr. (1999). Psychometric validation of a constipation symptom assessment questionnaire. *Scand. J. Gastroenterol.* 34, 870–877. doi: 10.1080/003655299750025327

González Cañete, N., Peña D'ardaillon, F., Candia Johns, P., and Durán Agüero, S. (2014). Relationship between sleep and constipation in the elderly Chileans. *Nutr. Hosp.* 31, 357–362. doi: 10.3305/nh.2015.31.1.7976

Guillén-Riquelme, A., and Buela-Casal, G. (2014). Meta-analysis of group comparison and meta-analysis of reliability generalization of the State-Trait Anxiety Inventory Questionnaire (STAI). *Rev. Esp. Salud Publica* 88, 101–112. doi: 10.4321/S1135-57272014000100007

Haase, A. M., Fallet, S., Otto, M., Scott, S. M., Schlageter, V., and Krogh, K. (2015). Gastrointestinal motility during sleep assessed by tracking of telemetric capsules combined with polysomnography - a pilot study. *Clin. Exp. Gastroenterol.* 8, 327–332. doi: 10.2147/CEG.S91964

Hyun, M. K., Baek, Y., and Lee, S. (2019). Association between digestive symptoms and sleep disturbance: a cross-sectional community-based study. *BMC Gastroenterol.* 19:34. doi: 10.1186/s12876-019-0945-9

Iino, S., Taguchi, K., Maekawa, S., and Nojyo, Y. (2004). Motor, sensory and autonomic nerve terminals containing NAP-22 immunoreactivity in the rat muscle. *Brain Res.* 1002, 142–150. doi: 10.1016/j.brainres.2004.01.007

Jiang, Y., Tang, Y. R., Xie, C., Yu, T., Xiong, W. J., and Lin, L. (2017). Influence of sleep disorders on somatic symptoms, mental health, and quality of life in patients with chronic constipation. *Medicine* 96:e6093. doi: 10.1097/MD.0000000000006093

Lee, O. Y. (2006). Psychosocial factors and visceral hypersensitivity in irritable bowel syndrome. *Korean J. Gastroenterol.* 47, 111–119.

Lee, T. H., and Bharucha, A. E. (2016). How to Perform and Interpret a High-resolution Anorectal Manometry Test. *J. Neurogastroenterol. Motil.* 22, 46–59. doi: 10.5056/jnm15168

Liem, O., Burgers, R. E., Connor, F. L., Benninga, M. A., Reddy, S. N., Mousa, H. M., et al. (2012). Solid-state vs water-perfused catheters to measure colonic high-amplitude propagating contractions. *Neurogastroenterol. Motil.* 24, 345–e167. doi: 10.1111/j.1365-2982.2011.01870.x

Liu, J., Chen, H., Wu, D., Wei, R., Lv, C., Dong, J., et al. (2020). Ameliorating Effects of Transcutaneous Electrical Acustimulation at Neiguan (PC6) and Zusanli (ST36) Acupoints Combined with Adaptive Biofeedback Training on Functional Outlet Obstruction Constipation. *Evid. Based Complement. Alternat. Med.* 2020:8798974. doi: 10.1155/2020/8798974

Liu, T. T., Yi, C. H., Chen, C. L., and Orr, W. C. (2010). Does sleep dysfunction affect anorectal motility in healthy adults? *Scand. J. Gastroenterol.* 45, 1262–1263. doi: 10.3109/00365521.2010.501526

Liu, T. T., Yi, C. H., Chen, C. L., and Orr, W. C. (2011). Impact of sleep dysfunction on anorectal motility in healthy humans. *J. Neurogastroenterol. Motil.* 17, 180–184. doi: 10.5056/jnm.2011.17.2.180

Liu, Z., Ge, Y., Xu, F., Xu, Y., Liu, Y., Xia, F., et al. (2018). Preventive effects of transcutaneous electrical acustimulation on ischemic stroke-induced constipation mediated *via* the autonomic pathway. *Am. J. Physiol. Gastrointest. Liver Physiol.* 315, G293–G301. doi: 10.1152/ajpgi.00049.2018

Lu, J., Shi, L., Huang, D., Fan, W., Li, X., Zhu, L., et al. (2020). Depression and Structural Factors Are Associated With Symptoms in Patients of Irritable Bowel Syndrome With Diarrhea. *J. Neurogastroenterol. Motil.* 26, 505–513. doi: 10.5056/jnm19166

Mazur, M., Furgała, A., Jabłoński, K., Mach, T., and Thor, P. (2012). Autonomic nervous system activity in constipation-predominant irritable bowel syndrome patients. *Med. Sci. Monit.* 18, CR493–CR499. doi: 10.12659/msm.883269

Meerveld, B. G., and Johnson, A. C. (2018). Mechanisms of Stress-induced Visceral Pain. *J. Neurogastroenterol. Motil.* 24, 7–18. doi: 10.5056/jnm17137

Nakamaru-Ogiso, E., Miyamoto, H., Hamada, K., Tsukada, K., and Takai, K. (2012). Novel biochemical manipulation of brain serotonin reveals a role of serotonin in the circadian rhythm of sleep-wake cycles. *Eur. J. Neurosci.* 35, 1762–1770. doi: 10.1111/j.1460-9568.2012.08077.x

Ohkusa, T., Koido, S., Nishikawa, Y., and Sato, N. (2019). Gut Microbiota and Chronic Constipation: a Review and Update. *Front. Med.* 6:19. doi: 10.3389/fmed.2019.00019

Orr, W. C., Fass, R., Sundaram, S. S., and Scheimann, A. O. (2020). The effect of sleep on gastrointestinal functioning in common digestive diseases. *Lancet. Gastroenterol. Hepatol.* 5, 616–624. doi: 10.1016/S2468-1253(19)30412-1

Park, Y. S., Kim, S. H., Park, J. W., Kho, Y., Seok, P. R., Shin, J. H., et al. (2020). Melatonin in the colon modulates intestinal microbiota in response to stress and sleep deprivation. *Intest. Res.* 18, 325–336. doi: 10.5217/ir.2019.00093

Parker, C. H., Naliboff, B. D., Shih, W., Presson, A. P., Videlock, E. J., Mayer, E. A., et al. (2019). Negative Events During Adulthood Are Associated With Symptom Severity and Altered Stress Response in Patients With Irritable Bowel Syndrome. *Clin. Gastroenterol. Hepatol.* 17, 2245–2252. doi: 10.1016/j.cgh.2018.12.029

Rasijeff, A., Withers, M., Burke, J. M., Jackson, W., and Scott, S. M. (2017). High-resolution anorectal manometry: a comparison of solid-state and water-perfused catheters. *Neurogastroenterol. Motil.* 29:e13124. doi: 10.1111/nmo.13124

Ruffle, J. K., Tinkler, L., Emmett, C., Ford, A. C., Nachev, P., Aziz, Q., et al. (2021). Constipation Predominant Irritable Bowel Syndrome and Functional Constipation Are Not Discrete Disorders: a Machine Learning Approach. *Am. J. Gastroenterol.* 116, 142–151. doi: 10.14309/ajg.0000000000000816

Schoch, S. F., Castro-Mejía, J. L., Krych, L., Leng, B., Kot, W., Kohler, M., et al. (2022). From Alpha Diversity to Zzz: interactions among sleep, the brain, and gut microbiota in the first year of life. *Prog. Neurobiol.* 209:102208. doi: 10.1016/j.pneurobio.2021.102208

Schurman, J. V., Friesen, C. A., Dai, H., Danda, C. E., Hyman, P. E., and Cocjin, J. T. (2012). Sleep problems and functional disability in children with functional gastrointestinal disorders: an examination of the potential mediating effects of physical and emotional symptoms. *BMC Gastroenterol.* 12:142. doi: 10.1186/1471-230X-12-142

Sen, P., Molinero-Perez, A., O'Riordan, K. J., McCafferty, C. P., O'Halloran, K. D., and Cryan, J. F. (2021). Microbiota and sleep: awakening the gut feeling. *Trends Mol. Med.* 27, 935–945. doi: 10.1016/j.molmed.2021.07.004

Simrén, M., Törnblom, H., Palsson, O. S., van Tilburg, M., Van Oudenhove, L., Tack, J., et al. (2018). Visceral hypersensitivity is associated with GI symptom severity in functional GI disorders: consistent findings from five different patient cohorts. *Gut* 67, 255–262. doi: 10.1136/gutjnl-2016-312361

Tobaldini, E., Costantino, G., Solbiati, M., Cogliati, C., Kara, T., Nobili, L., et al. (2017). Sleep, sleep deprivation, autonomic nervous system and cardiovascular diseases. *Neurosci. Biobehav. Rev.* 74, 321–329. doi: 10.1016/j.neubiorev.2016.07.004

Vigneau, F., and Cormier, S. (2008). The factor structure of the State-Trait Anxiety Inventory: an alternative view. *J. Pers. Assess.* 90, 280–285. doi: 10.1080/00223890701885027

Wang, J. K., and Yao, S. K. (2021). Roles of Gut Microbiota and Metabolites in Pathogenesis of Functional Constipation. *Evid. Based Complement. Alternat. Med.* 2021:5560310. doi: 10.1155/2021/5560310

Wang, S., Gao, H., Ru, Z., Zou, Y., Li, Y., Cao, W., et al. (2019). Poor Sleep Quality Associated With High Risk Of Ventricular Tachycardia After Acute Myocardial Infarction. *Nat. Sci. Sleep* 11, 281–289. doi: 10.2147/NSS.S222359

Wang, X., Yang, B., Yin, J., Wei, W., and Chen, J. (2019). Electroacupuncture *via* chronically implanted electrodes improves gastrointestinal motility by balancing sympathovagal activities in a rat model of constipation. *Am. J. Physiol. Gastrointest. Liver Physiol.* 316, G797–G805. doi: 10.1152/ajpgi.00018.2018

Whitehead, W. E., Holtkotter, B., Enck, P., Hoelzl, R., Holmes, K. D., Anthony, J., et al. (1990). Tolerance for rectosigmoid distention in irritable bowel syndrome. *Gastroenterology* 98, 1187–1192. doi: 10.1016/0016-5085(90)90332-u

Wu, S., Chen, S., Zhao, Y., Ma, X., Wang, R., and He, J. (2017). Association Between Excessive Daytime Sleepiness and Functional Gastrointestinal Disorders: a Population-based Study in China. *J. Neurogastroenterol. Motil.* 23, 298–305. doi: 10.5056/jnm16056

Yamamoto, S., Kawamura, Y., Yamamoto, K., Yamaguchi, Y., Tamura, Y., Izawa, S., et al. (2021). Internet Survey of Japanese Patients With Chronic Constipation: focus on Correlations Between Sleep Quality. *J. Neurogastroenterol. Motil.* 27, 602–611. doi: 10.5056/jnm20135

Yano, J. M., Yu, K., Donaldson, G. P., Shastri, G. G., Ann, P., Ma, L., et al. (2015). Indigenous bacteria from the gut microbiota regulate host serotonin biosynthesis. *Cell* 161, 264–276. doi: 10.1016/j.cell.2015.02.047

Zhang, Y., Xie, B., Chen, X., Zhang, J., and Yuan, S. (2021). A key role of gut microbiota-vagus nerve/spleen axis in sleep deprivation-mediated aggravation of systemic inflammation after LPS administration. *Life Sci* 265:118736. doi: 10.1016/j.lfs.2020.118736

Zhao, W., Jin, H., Xu, M., Wang, D., Liu, Y., Tang, Y., et al. (2018). Sleep Quality of Functional Gastrointestinal Disorder Patients in Class-Three Hospitals: a Cross-Sectional Study in Tianjin. China. *Biomed. Res. Int.* 2018:3619748. doi: 10.1155/2018/3619748

Conflict of Interest: The authors declare that the research was conducted in the absence of any commercial or financial relationships that could be construed as a potential conflict of interest.

Publisher's Note: All claims expressed in this article are solely those of the authors and do not necessarily represent those of their affiliated organizations, or those of the publisher, the editors and the reviewers. Any product that may be evaluated in this article, or claim that may be made by its manufacturer, is not guaranteed or endorsed by the publisher.

frontiers | Frontiers in Neuroscience

SYSTEMATIC REVIEW
published: 14 July 2022
doi: 10.3389/fnins.2022.933290

Chinese Herbal Medicine for Functional Dyspepsia With Psychological Disorders: A Systematic Review and Meta-Analysis

Xiaoying Luo[1†], Lin Wang[1†], Shuangshuang Fang[1], Xiangli Qing[2], Tianyuan Jiang[1,3], Yang Yang[1], Xiaolan Su[1] and Wei Wei[1*]*

[1] Department of Gastroenterology, Wangjing Hospital, China Academy of Chinese Medical Sciences, Beijing, China, [2] Graduate School of Chengdu University of Traditional Chinese Medicine, Chengdu, China, [3] Graduate School of Beijing University of Chinese Medicine, Beijing, China

OPEN ACCESS

Edited by:
He Wang,
Fudan University, China

Reviewed by:
Cheng Lu,
Institute of Basic Research in Clinical Medicine, China Academy of Chinese Medical Sciences, China
Jun Shi,
Shanghai University of Traditional Chinese Medicine, China

***Correspondence:**
Wei Wei
sxxtyy@sina.com
Xiaolan Su
suxiaolan1982@126.com

[†] These authors have contributed equally to this work and share first authorship

Specialty section:
This article was submitted to Gut-Brain Axis, a section of the journal Frontiers in Neuroscience

Received: 30 April 2022
Accepted: 06 June 2022
Published: 14 July 2022

Citation:
Luo X, Wang L, Fang S, Qing X, Jiang T, Yang Y, Su X and Wei W (2022) Chinese Herbal Medicine for Functional Dyspepsia With Psychological Disorders: A Systematic Review and Meta-Analysis. Front. Neurosci. 16:933290. doi: 10.3389/fnins.2022.933290

Background and Aims: Functional dyspepsia (FD) is closely associated with gut–brain interaction disorder (DGBI), characterized by the interaction of gastrointestinal symptoms and central nervous system dysregulation. Chinese herbal medicine (CHM) has a good concurrent effect in the treatment of FD, especially for patients with concurrent psychological disorders. A meta-analysis was designed to evaluate the efficacy and safety of CHMs in the treatment of FD.

Methods: The PubMed, Embase, Cochrane Library, Web of Science, Chinese Biological Medical Database (CBM), Wanfang Data, China National Knowledge Infrastructure (CNKI), and China Science and Technology Journal Database (VIP) were searched to collect randomized controlled trials of FD treated with CHM. The retrieval time limit is from the establishment of the database till 11 April 2022. Two researchers independently searched databases, screened documents, extracted data, and evaluated the risk of bias of included studies. RevMan 5.4 software was used for meta-analysis.

Results: A total of 11 studies including 951 patients were included. The study was divided into two parts. The first part included 5 clinical trials, including 471 patients. The experimental group was treated only with CHM and the control group was only treated with placebo. The results of first part showed that the total effective rate of CHM in the treatment of FD was higher than that in the placebo group (84.5 vs. 49.4%) [relative risk (RR) = 1.76; 95% confidence interval (CI) (1.13, 2.75); $P = 0.01$]. In addition, CHM treatment could reduce the total symptom score [standardized mean difference (SMD) = −10.05; 95% CI (−13.50, −6.59); $Z = 5.70$; $P < 0.0001$] and depression score [SMD = −7.68; 95% CI (−14.43, −0.94); $Z = 2.23$; $P = 0.03$]. The second part included 6 clinical trials, including 480 patients. The experimental group was only treated with CHM and the control group was treated with prokinetic agents combined with flupentixol melitracen (deanxit). The results of second part showed that the total effective rate of CHM in the treatment of FD was higher than that of the control

group (92.6 vs. 78.8%) [RR = 1.17; 95% CI (1.09, 1.26), $P < 0.0001$]. In addition, CHM treatment could reduce HAMA score [mean difference (MD) = −3.19; 95% CI (−3.79, −2.59); $Z = 10.40$; $P < 0.00001$], HAMD score [MD = −4.32; 95% CI (−6.04, −2.61); $Z = 4.94$; $P < 0.00001$], and gastric emptying rate [MD = 12.62; 95% CI (5.84, 19.40); $Z = 3.65$; $P = 0.0003$]. The results of the two parts of the meta-analysis showed no serious adverse reactions, and there was no significant difference in the adverse reactions between the experimental group and the control group [MD = 1.14; 95% CI (0.53, 2.42); $Z = 0.33$; $P = 0.74$]; [MD = 0.14; 95% CI (0.01, 2.67); $Z = 1.30$; $P = 0.19$].

Conclusion: The current evidence shows that CHM treatment has great potential and safety in alleviating the symptoms of FD and improving the psychological disorders of anxiety and depression in patients with FD. Limited by the quantity and quality of the included studies and other biases, the above conclusions need more high-quality studies to be verified.

Systematic Review Registration: https://www.crd.york.ac.uk/PROSPERO/, identifier [CRD42022311129].

Keywords: Chinese herbal medicine, functional dyspepsia (FD), psychological disorder, metaanalysis, effectiveness

INTRODUCTION

Functional dyspepsia (FD) is a common digestive system disease. In 2016, the Rome Committee defined functional gastrointestinal diseases, including FD, as abnormal brain–intestinal interactions (Drossman and Hasler, 2016). The prevalence of FD is about 16% in the general population and up to 18–45% in China (Ge, 2017; Ford et al., 2020). Characteristic symptoms of FD include epigastric pain, epigastric burning, postprandial fullness, or early satiety that persists for at least 6 months. Although the disease does not have obvious organic lesions, the symptoms are persistent and difficult to heal, and easy to repeat, which seriously affects the quality of life and physical and mental health of patients (Ge, 2017).

The pathophysiological mechanism of FD is complex, and its pathogenesis is the result of the combined effects of multiple factors such as gastrointestinal motility disorder, visceral hypersensitivity, intestinal flora imbalance, dysfunction of the gut–brain axis, and mental and emotional factors (Ford et al., 2020). FD is a typical physical and mental disease of the digestive system with a co-morbidity rate of up to 49.3% with psychological disorders (Chen, 2016; Xiong, 2016). With the accelerated pace of life and work, the relationship between FD and psychological factors has been extensively studied. Studies have shown that (Zhu et al., 2015; Zhang, 2018) abnormal emotional factors can lead to brain–gut axis dysfunction, visceral hypersensitivity, and gastrointestinal inflammation and immunity, causing or promoting the occurrence of FD.

The current treatment modalities for FD mainly include pharmacotherapy, lifestyle modification, and psychotherapy (Ford et al., 2020). Clinical medications are generally used for symptomatic treatment, such as acid inhibitors and prokinetics, but these drugs often do not provide complete relief of symptoms. Central neuromodulators have an important role in refractory functional gastrointestinal disease and are especially suitable for patients with combined psychological disorders, but they have many side effects and adverse reactions, and their symptoms tend to worsen after patients stop the antidepressant treatment, so there are many limitations in clinical application. Psychotherapy generally needs to be administered in conjunction with a specialist clinic, and patients who are unable or unwilling to receive treatment are unlikely to benefit. Moreover, a Chinese research study showed that more than 90% of patients with psychological disorders seen in gastroenterology departments were unwilling to receive psychotherapy (Feng et al., 2021). FD is prone to recurring clinically and the treatment effect is not good, which is a considerable burden for individuals and society (Drossman, 2021). Therefore, the search for an effective treatment is a critical issue that needs to be urgently addressed (Ford et al., 2021).

Given the limitations of clinical treatment methods, Chinese herbal medicine (CHM) has shown evident advantages in the treatment of FD. A previous randomized controlled trial (RCT)-based meta-analysis by our team showed that Chinese medicine compounds are more effective than placebo in treating FD due to the improved indigestion symptoms, CMS, gastric emptying rate, and the quality of life of patients with FD (Xiaoying et al., 2021). In recent years, an increasing number of scholars have paid attention to the therapeutic effect of CHM on FD with psychological disorders. Therefore, this study is based on randomized clinical trials. Based on previous studies, the literature has been updated, and more attention has been paid to the improvement of clinical symptoms in FD patients with psychological disorders. The clinical efficacy and safety of CHM in treating FD with psychological disorders were systematically evaluated with the aim of drawing a higher level of evidence and a more objective and a comprehensive evaluation conclusion to guide clinical treatment.

DATA AND METHODS

Literature Search

The meta-analysis was conducted according to the Preferred Reporting Items for Systematic Reviews and Meta-Analysis Statement (PRISMA). We searched eight databases including PubMed, Embase, Cochrane Library, Web of Science, China National Knowledge Infrastructure (CNKI), Chinese Biological Medical Database (CBM), Wanfang, and China Science Journal Database (VIP). The retrieval time is from the establishment time of each database to 11 April 2022. The conference papers and dissertations of related clinical trials were simultaneously retrieved in CNKI and Wanfang data resource systems.

The following search terms were used: (functional dyspepsia OR postprandial distress syndrome OR epigastric pain syndrome) AND (psychological disorders OR anxiety OR depression) AND (Traditional Chinese Medicine OR Chinese Medicine OR Chinese Traditional Medicine OR Herbal Medicine OR formula OR Decoction OR recipe OR prescription OR tablet OR capsule OR granule) AND (random).

Study Selection

Inclusion Criteria

Study Type

Clinical RCTs published in Chinese or English.

Research Objects

The participants were patients with FD over the age of 18 who met the diagnostic criteria of Rome II, Rome III, or Rome IV and at least have 1 psychological disorder (Talley et al., 1999; Tack et al., 2006; Stanghellini et al., 2016). Patients with severe organic or mental diseases were excluded from the study.

Intervention Measures

①Treatment group: only oral CHM treatment and does not involve the addition and subtraction of drug taste and dosage; there is no limit to the form of CHM (decoction, granules, capsules, etc.), and the course of medication should not be less than 2 weeks.

②Control group: the first part is only oral placebo control. The placebo should conform to the shape, nature, and taste of CHM similar to that of the treatment group, and the course of treatment is the same as that of the treatment group. The second part is the combination of prokinetics + deanxit.

Curative Effect Evaluation Index

Main outcome evaluation index:

①The total effective rate with the extractable dichotomous variable data. A patient-reported assessment is preferred if the study involved both investigator-reported and patient-reported results.

②The scores of the scale reflecting psychological disorders such as HAMD, HAMA, SDS, SAS, and so on.

Secondary outcome evaluation indexes: total symptom score, gastric emptying rate, and adverse reactions.

If the main outcome evaluation index does not meet the above requirements, the outcome evaluation index, including TCM syndrome efficacy or gastric emptying rate can also be included; studies reporting different outcome indicators from the same clinical trial were combined and included.

Exclusion Criteria

(1) Non-English and Chinese literature; (2) the original information is not published publicly; (3) interventions are interfered by other treatments; (4) unable to get the full text or the data is incomplete; and (5) repeated published literature.

Data Extraction

Two researchers independently read the title, abstract, and full text of the literature and screened and included the literature according to the standard of arrangement. In the case of objection, the third party intervened to evaluate it. The extracted data included literature title, author, publication date, research source, sample size, western medicine diagnostic criteria, intervention measures, course of treatment and follow-up time, outcome evaluation index and results, and adverse reaction events.

The Quality Evaluation of Included Literature

Two researchers independently conducted the quality evaluation, and a third investigator evaluated the objections. This evaluation was performed according to the Cochrane ROB Tool in terms of: generation of random sequence, concealment of allocation, blind method, incomplete outcome data, selective reporting, and other biases, and the results were exported *via* Review Manager V 5.4.

Statistical Analysis

We used Rev Man 5.4 for merge-effect analysis. Two classification variables were analyzed by relative risk (RR), and the numerical variables were analyzed by mean difference (MD) or standardized mean difference (SMD), all of which were expressed by 95% confidence intervals (CIs).

The heterogeneity among statistics of multiple identical studies was tested by tests for heterogeneity and evaluated using the X^2 test combined with I^2 statistics. If $P > 0.10$ and $I^2 < 50\%$, the heterogeneity was considered acceptable (Higgins et al., 2003). If the included research has homogeneity, the fixed effects model is used, and if there is heterogeneity, a random-effect model (Dersimonian and Laird, 1986) is used. It was considered to be statistically significant when $P < 0.05$.

RESULTS

Retrieval Results

A total of 185 studies were obtained through preliminary search, including 140 in CNKI, 1 in Wanfang, 13 in PubMed, 3 in VIP, 25 in Cochrane, and 3 in Web of Science. First, we removed 14 duplicate documents. Second, 152 articles were excluded by reading the literature titles and abstracts, and 8 articles were

excluded by reading the full text. Finally, 11 studies were included in the meta-analysis (Zhao and Gan, 2005; Han and Wang, 2011; Lu and Chen, 2011; Du et al., 2014; Xi et al., 2014; Zhang, 2014; Zhang et al., 2016, 2017a,b,c; Zhu and Gu, 2017; Li et al., 2018; Tominaga et al., 2018; Chen et al., 2020). Among them, there are five studies (Zhao and Gan, 2005; Du et al., 2014; Zhu and Gu, 2017; Tominaga et al., 2018; Chen et al., 2020) on CHM vs. placebo and six studies (Han and Wang, 2011; Lu and Chen, 2011; Xi et al., 2014; Zhang, 2014; Zhang et al., 2016, 2017a,b,c; Li et al., 2018) on CHM vs. prokinetics + deanxit (**Figure 1**).

Basic Characteristics of Included Studies

A total of 11 RCTs were selected. Among them, there are five studies on CHM vs. placebo, one (Tominaga et al., 2018) from Japan and the rest (Zhao and Gan, 2005; Du et al., 2014; Zhu and Gu, 2017; Chen et al., 2020) from China. Four (Zhao and Gan, 2005; Du et al., 2014; Tominaga et al., 2018; Chen et al., 2020) of all studies were published in English and one (Zhu and Gu, 2017) in Chinese.

There are six studies of CHM vs. prokinetics + deanxit, all from China and published in Chinese. The 951 participants in the 11 RCTs were divided into the following 2-part studies, and the number of participants in each study ranged from 43 to 118. Of the 11 studies involved, 2 (Tominaga et al., 2018; Chen et al., 2020) were multicenter studies, and the number of participating research centers ranged from 9 to 56. The basic information of the 11 studies included in the analysis is shown in **Table 1**. The specific drug composition of Chinese medicine compounds involved in the study is shown in **Table 2**.

Risk of Bias Assessment

All the inclusion trials were randomized, but some of them did not describe the specific randomization method, hence the evaluation was "unclear." Some of these inclusion trials did not describe blindness. Among them, trials that neither described randomization method nor blindness were considered high risk, and the others were evaluated as "unclear." Complete details of the bias risk assessment are shown in **Figures 2**, **3**.

Meta Results

Total Effective Rate

Chinese Herbal Medicine vs. Placebo Group

Among the five studies included, three studies (Zhao and Gan, 2005; Du et al., 2014; Tominaga et al., 2018) reported the total effective rate. There were a total of 341 cases, of which 181 cases were in the Chinese medicine compound treatment group. Of these, 153 cases were reported effective (84.5%). Of the 160 cases in the placebo control group, of which 79 cases were effective (49.4%).

The heterogeneity test showed high heterogeneity ($P = 0.006$, $I^2 = 80\%$); therefore, a randomized effect model was adopted. The results showed that the therapeutic effect of CHM was significantly better than that of placebo on the overall symptom improvement [RR = 1.76; 95% confidence interval (CI) (1.13, 2.75), $P = 0.01$] (**Figure 4**).

Chinese Herbal Medicine vs. Western Medicine Group

Six studies (Han and Wang, 2011; Lu and Chen, 2011; Xi et al., 2014; Zhang, 2014; Zhang et al., 2016, 2017a,b,c; Li et al., 2018) all reported the total clinical effective rate. Totaling 480 cases, 244 cases were in the Chinese medicine compound treatment group. Of these, 226 cases were effective (92.6%), and of the 236 cases in the control group, 186 cases were effective (78.8%).

The comprehensive analysis showed low heterogeneity ($I^2 = 0$, $P = 0.98$), and a fixed-effects model was used. The comprehensive results showed that the effective rate of the CHM was significantly better than that of the control group, and the difference was statistically significant [RR = 1.17; 95% CI (1.09, 1.26), $P < 0.0001$] (**Figure 5**).

Total Symptom Score

Chinese Herbal Medicine vs. Placebo Group

A total of 4 studies (Zhao and Gan, 2005; Zhu and Gu, 2017; Tominaga et al., 2018; Chen et al., 2020), including 381 participants compared total symptom scores. The comprehensive analysis showed high heterogeneity ($I^2 = 98\%$), and a random-effects model was used. The comprehensive results showed that the CHM could effectively reduce the total symptom score [SMD = −10.05; 95% CI (−13.50, −6.59); $Z = 5.70$; $P < 0.00001$] (**Figure 6**).

Depression Scale

Chinese Herbal Medicine vs. Placebo Group

Three studies (Zhao and Gan, 2005; Du et al., 2014; Tominaga et al., 2018) including 341 investigators compared post-treatment depression scores. The heterogeneity test showed high heterogeneity ($P < 0.00001$, $I^2 = 99\%$); therefore, a randomized effect model was adopted. Two of the studies used the HAMD score (Zhao and Gan, 2005; Du et al., 2014) and one (Tominaga et al., 2018) study used the HADS score. The comprehensive results showed that the CHM could effectively reduce the depression score [SMD = −7.68; 95% CI (−14.43, −0.94); $Z = 2.23$; $P = 0.03$] (**Figure 7**).

Two other studies also evaluated depression improvement. According to Chen et al.'s (2020) results, the JX pill group had a greater improvement in the HAMD total score from baseline to 4 weeks than the placebo group, but the difference was not significant [mean between-group difference, −0.7 points (95% CI, −1.8 to −0.3); $P = 0.093$]. Zhu and Gu (2017) showed that compared with the placebo group, the effective rate of the CHM group was significantly increased (68.75 vs. 37.50%, $P < 0.05$). The cure rates of the CHM group were significantly higher than those of the placebo group (27.08% vs. 0, $P < 0.05$).

Chinese Herbal Medicine vs. Western Medicine Group

Six studies (Han and Wang, 2011; Lu and Chen, 2011; Xi et al., 2014; Zhang, 2014; Zhang et al., 2016, 2017a,b,c; Li et al., 2018) including 480 investigators compared HAMD scores after treatment. The comprehensive analysis showed high heterogeneity ($I^2 = 98\%$), and a random-effects model was used. The comprehensive results showed that the CHM could

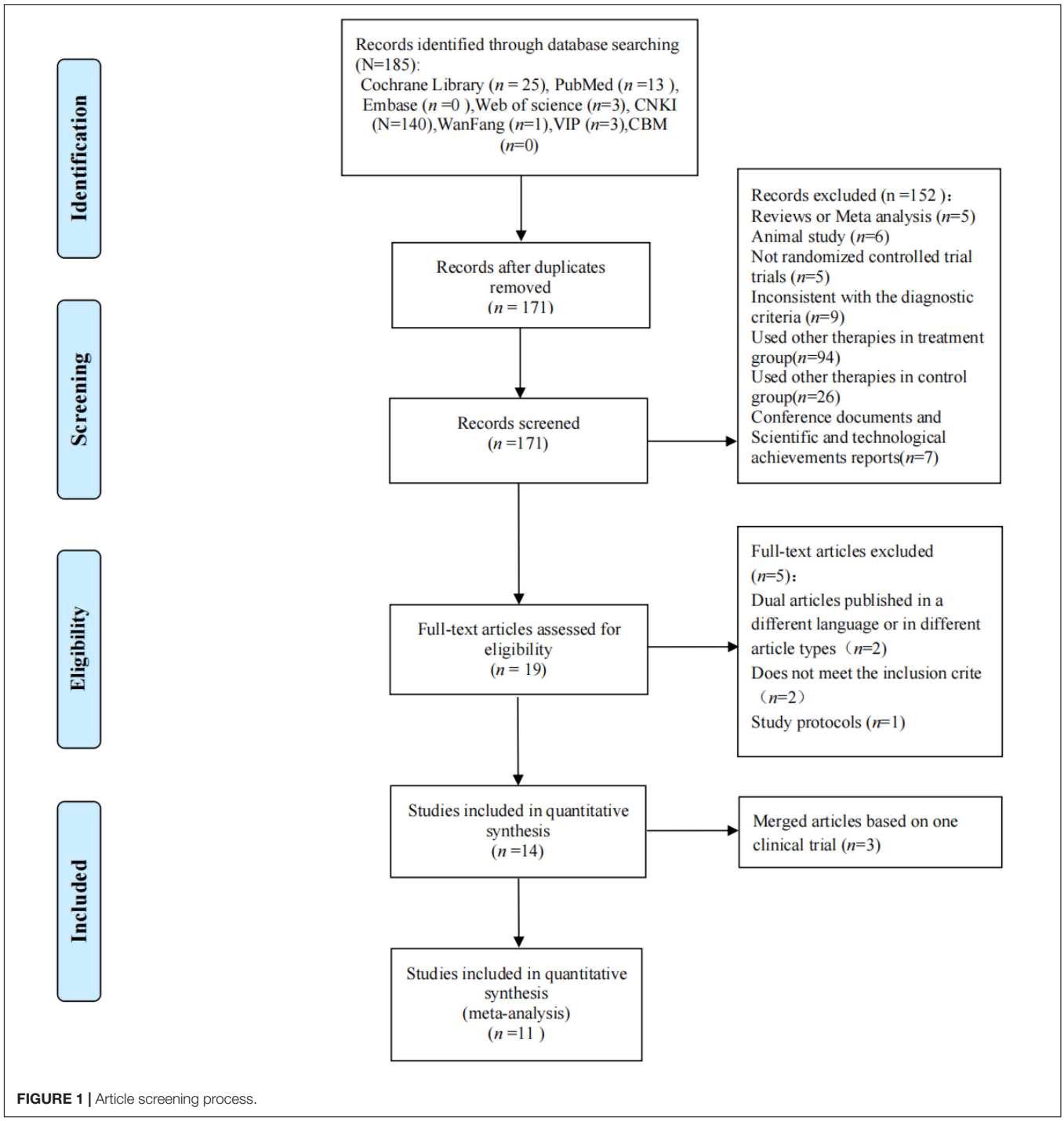

FIGURE 1 | Article screening process.

effectively reduce the HAMD score [MD = −4.32; 95% CI (−6.04, −2.61); $Z = 4.94$; $P < 0.00001$] (**Figure 8**).

HAMA Score

Chinese Herbal Medicine vs. Placebo Group

Only Chen et al. (2020) evaluated anxiety. The results showed that JX pill had a greater improvement in the HAMA scores from baseline to 4 weeks than the placebo group, but the difference was not significant [mean between-group difference, −0.3 points (95% CI, −1.3 to −0.7); $P = 0.446$].

Chinese Herbal Medicine vs. Western Medicine Group

Three studies (Lu and Chen, 2011; Zhang et al., 2016, 2017a,b,c; Li et al., 2018) including 254 investigators compared HAMA scores after treatment. The comprehensive analysis showed high heterogeneity (I^2 = 80%), and a random-effects model was used. The comprehensive results showed that the CHM could

TABLE 1 | Basic characteristics of included articles.

References	Language	Country	Diagnostic criteria	Psychological disorders	Number of research centers	Sample size (T:C)	Sex ratio (male: female)	Durations	Follow-up	Outcomes	Adverse events (T:C)
CHM vs. placebo											
Zhao and Gan, 2005	English	China	Rome III	HAMD > 20; HAMA > 14	1	43 (30:13)	43 (16:27)	8 weeks	NR	①②③④	0
Du et al., 2014	English	China	Rome III	Depression	1	180 (90:90)	NR	8 weeks	6 months	①③⑤	0
Tominaga et al., 2018	English	Japan	Rome III	HADS < 10	56	118 (61:57)	125 (36:89)	8 weeks	NR	①②③	4 (3:1)
Chen et al., 2020	English	China	Rome III	HAMD > 20; HAMA > 14	9	141 (70:71)	141 (107:3)	4 weeks	4 weeks	②③④	4 (3:1)
Zhu and Gu's (2017)	Chinese	China	Rome III	Mild to moderate depression on the HAMD-17	1	80 (48:32)	80 (37:43)	6 weeks	NR	②③	15 (8:7)
CHM vs. mosapride/domperidone + deanxit											
Han and Wang, 2011	Chinese	China	Rome III	HAMD ≥ 17	1	60 (30:30)	60 (20:40)	4 weeks	NR	①③	NR
Lu and Chen, 2011	Chinese	China	Rome III	HAMA > 7; HAMD > 7	1	55 (31:24)	55 (19:36)	4 weeks	NR	①③④	NR
Xi et al., 2014	Chinese	China	Rome III	HAMD ≥ 8	1	96 (48:48)	96 (39:57)	30 days	6 months	①③⑤	0
Zhang, 2014	Chinese	China	Rome III	HAMD ≥ 7	1	70 (35:35)	70 (29:41)	30 days	3 months	①③⑤	3 (0:3)
Zhang et al., 2016, 2017a,b,c	Chinese	China	Rome III	HAMD > 20; HAMA > 14	1	119 (60:59)	119 (49:70)	4 weeks	NR	①③④	Incomplete information
Li et al., 2018	Chinese	China	Rome III	HAMD ≥ 20; HAMA ≥ 14	1	80 (40:40)	80 (34:46)	4 weeks	NR	①③④⑤	0

T, treatment group; C, control group; NR, not report. ① Total efficiency, ② total symptom score, ③ depression scale, ④ HAMA score, and ⑤ gastric emptying rate.

effectively reduce the HAMA score [MD = −3.19; 95% CI (−3.79, −2.59); $Z = 10.40$; $P < 0.00001$] (**Figure 9**).

Gastric Emptying Rate

Chinese Herbal Medicine vs. Western Medicine Group

Three studies (Xi et al., 2014; Zhang, 2014; Li et al., 2018) involving six articles reported the gastric emptying rate. All studies used radioimaging. The heterogeneity test showed high heterogeneity ($P < 0.00001$, $I^2 = 97\%$); thus, the randomized effect model was adopted. The combined results showed that the Chinese herbal formula could effectively reduce the gastric emptying rate [MD = 12.62; 95% CI (5.84, 19.40); $Z = 3.65$; $P = 0.0003$] (**Figure 10**).

Adverse Reactions

Chinese Herbal Medicine vs. Placebo Group

All 5 studies reported drug safety evaluations and included a total of 561 patients. In Zhu and Gu's (2017) study, eight cases of adverse reactions occurred in the GHM group, including three cases of dry mouth, two cases of dizziness, one case of loss of appetite, one case of nausea, and one case of gastrointestinal discomfort. There were seven cases of adverse reactions in the placebo group, including nausea two cases, one case of insomnia, one case of fatigue, three cases of constipation. In Chen et al.'s (2020), one participant in the CHM group reported slight diarrhea, one participant reported mild constipation, and one participant had abnormal liver function (ALT, 108.7 U/L; AST, 63.7 U/L); no specific adverse reactions were reported in the placebo group. The comprehensive results showed that the incidence of adverse reactions was 4.68% in the CHM group and 3.44% in the placebo group, with no significant difference between the two groups [MD = 1.14; 95% CI (0.53, 2.42); $Z = 0.33$; $P = 0.74$] (**Figure 11**).

Chinese Herbal Medicine vs. Western Medicine Group

Out of the six studies (Xi et al., 2014; Zhang, 2014; Zhang et al., 2016, 2017a,b,c; Li et al., 2018), four conducted drug safety evaluation. Among them Zhang et al. (2016, 2017a,b,c) mentioned only in the abstract that there were no adverse reactions in either group during the study period. Li et al. (2018) conducted a 6-month follow-up, and the result was that there were no serious adverse reactions in both groups. During Zhang (2014) treatment, two patients in the control group had mild dizziness, one patient had dry mouth and slight bitterness, and no adverse reactions occurred in the treatment group. During the Xi et al. (2014) study, no adverse reactions occurred in both groups. None of the reported adverse reactions affected the course of treatment. The comprehensive results showed that there was no significant difference in the occurrence of adverse reactions between the two groups [MD = 0.14; 95% CI (0.01, 2.67); $Z = 1.30$; $P = 0.19$] (**Figure 12**).

DISCUSSION

Our study suggests that herbal treatment of FD with psychological disorders has great potential to improve

TABLE 2 | Composition of Chinese medicine compounds.

References	Chinese herbal medicine	Control group	Chinese herbal formula
CHM vs. placebo			
Zhao and Gan, 2005	Xinwei decoction (1 dose, TID)	Placebo (1 dose, TID)	Chaihu (Radix Bupleuri) 10 g, Xiangfu (Rhizoma Cyperi) 10 g, Hehuanhua (Flos Albiziae) 30 g, Meiguihua (Flos Rosae Rugosae) 20 g, Taizishen (Radix Pseudostellariae) 15 g, Quangualou (Fructus Trichosanthis) 15 g, Baizhu (Rhizoma Atractylodis Macrocephalae) 10 g, Zhishi (Fructus Aurantii Immaturus) 10 g, Sharen (Fructus Amomi) 10 g, Yujin (Radix Curcumae) 12 g, Fushen (Sclaerotium Poriae Circum Radicem Pini) 15 g, Baihe (Bulbus Lilii) 15 g, Xiangyuan (Fructus Citri) 10 g, parched Maiya (Fructus Hordei Germinatus) 10 g, parched Guya (Fructus Oryzae Germinatus) 10 g, Qiancaogen (Radix Rubiae) 12 g, and Xuchangqing (Radix Cynanchi Paniculati) 15 g
Du et al., 2014	Xiaoyao pill (3 g, BID)	Placebo (3 g, BID)	Chai Hu (radix bupleuri), Dang Gui (*Angelica sinensis*), Bai Shao (radix paeoniae alba), Chao Bai Zhu (roasted rhizoma atractylodis macrocephalae), Fu Ling (*Wolfiporia extensa*), Zhi Gan Cao (radix glycyrrhizae), Bo He (mint), and Sheng Jiang (rhizoma zinjiberis recens)
Tominaga et al., 2018	Rikkunshito (7.5 g, TID)	Placebo (7.5 g, TID)	NR
Chen et al., 2020	Formulation of Jiawei Xiaoyao (6 g, BID)	Placebo (6 g, BID)	NR
Zhu and Gu's (2017)	Morinda officinalis oligose capsule (1 pill, BID)	Placebo (1 pill, BID)	NR
CHM vs. mosapride/domperidone + deanxit group			
Li et al., 2018	Danzhi Xiaoyao San and Simo Soup and Simo decoction (1 dose, BID)	Mosapride citrate tablets (5 mg, TID); deanxit (1 pill, BID)	Muxiang (AUCKLANDIAE RADIX) 10 g, Wuyao (LINDERAE RADIX) 10 g, Zhiqiao (AURANTII FRUCTUS) 10 g, Binglang (ARECAE SEMEN) 10 g, Mudanpi (MOUTAN CORTEX) 10 g, Zhizi (GARDENIAE FRUCTUS) 10 g, Chaihu (BUPLEURI RADIX) 10 g, Fuling (PORIA) 10 g, Danggui (ANGELICAE SINENSIS RADIX) 10 g, Baishao (PAEONIAE RADIX ALBA) 15 g, Baizhu (RHIZOMA ATRACTYLODIS) 10 g, Gancao (GLYCYRRHIZAE RADIX ET RHIZOMA) 5 g
Xi et al., 2014	Modified Sini Powder (1 dose, BID)	Domperidone maleate tablets (12.72 mg, TID); deanxit (1 pill, BID)	Fushen (PORIA) 20 g, Chaihu (BUPLEURI RADIX) 12 g, Zhishi (AURANTII FRUCTUS IMMATURUS) 12 g, Baizhu (RHIZOMA ATRACTYLODIS) 10 g, Baishao (PAEONIAE RADIX ALBA) 10 g, Chenpi (CITRI RETICULATAE PERICARPIUM) 12 g, Dafupi (ARECAE PERICARPIUM) 20 g, Shichangpu (ACORI TATARINOWII RHIZOMA) 10 g, Yujin (CURCUMAE RADIX) 12 g, Gancao (GLYCYRRHIZAE RADIX ET RHIZOMA) 6 g
Zhang, 2014	Recipe of soothing the liver and regulating the stomach (200 ml, BID)	Domperidone maleate tablets (12.72 mg, TID); deanxit (1 pill, BID)	Fushen (PORIA) 20 g, Chaihu (BUPLEURI RADIX) 12 g, Baizhu (RHIZOMA ATRACTYLODIS) 18 g, Zhishi (AURANTII FRUCTUS IMMATURUS) 12 g, Dafupi (ARECAE PERICARPIUM) 20 g, Chenpi (CITRI RETICULATAE PERICARPIUM) 12 g, Baishao (PAEONIAE RADIX ALBA) 10 g, Yujin (CURCUMAE RADIX) 12 g, Shichangpu (ACORI TATARINOWII RHIZOMA) 10 g, Gancao (GLYCYRRHIZAE RADIX ET RHIZOMA) 6 g
Zhang et al., 2016; Zhang et al., 2017a,b,c	Shugan Jianpi Anshen recipe (100 ml, BID)	Domperidone tablets (10 mg, TID); deanxit (10 mg, BID)	Chaihu (BUPLEURI RADIX) 10 g, Shichangpu (ACORI TATARINOWII RHIZOMA) 10 g, Ezhu (CURCUMAE RHIZOMA) 10 g, Huanglian (COPTIDIS RHIZOMA) 10 g, Houpo (MAGNOLIAE OFFICINALIS CORTEX) 12 g, Zhiqiao (AURANTII FRUCTUS) 10 g, Yujin (CURCUMAE RADIX) 12 g, Qingbanxia (PINELLIAE RHIZOMA PRAEPARATUM CUM ALUMINE) 15 g, Baishao (PAEONIAE RADIX ALBA) 10 g, Baizhu (RHIZOMA ATRACTYLODIS) 15 g, Fuling (PORIA) 15 g, Baihe (LILII BULBUS) 15 g, Shanzha (CRATAEGI FRUCTUS) 15 g, Maiya (HORDEI FRUCTUS GERMINATUS) 15 g, Shenqu (MEDICATED LEAVEN) 15 g, Hehuanpi (ALBIZIAE CORTEX) 20 g
Han and Wang, 2011	Modified Sini Powder (1 dose, BID)	Domperidone tablets (10 mg, TID); deanxit (10.5 mg, QD)	Chaihu (BUPLEURI RADIX) 6 g, Zhiqiao (AURANTII FRUCTUS) 10 g, Baishao (PAEONIAE RADIX ALBA) 12 g, Zhigancao (GLYCYRRHIZAE RADIX ET RHIZOMA PRAEPARATA CUM MELLE) 6 g, Lianqiao (FORSYTHIAE FRUCTUS) 10 g, Hehuanpi (ALBIZIAE CORTEX) 12 g, Xiangfu (CYPERI RHIZOMA) 6 g, Muxiang (AUCKLANDIAE RADIX) 6 g, Qingbanxia (PINELLIAE RHIZOMA PRAEPARATUM CUM ALUMINE) 9 g

NR, no report.

both dyspeptic symptoms and anxiety/depressive states with good clinical safety. To our knowledge, no other study has done a systematic review and meta-analysis of any treatment for FD with psychological disorders. Psychological factors are not only important in the development of the FD, but also have an important impact on the prognosis and quality of life of patients. Studies have confirmed (Lin et al., 2019; Esterita et al., 2021) that FD is significantly associated with depression and anxiety disorders. The improvement of anxiety and sleep

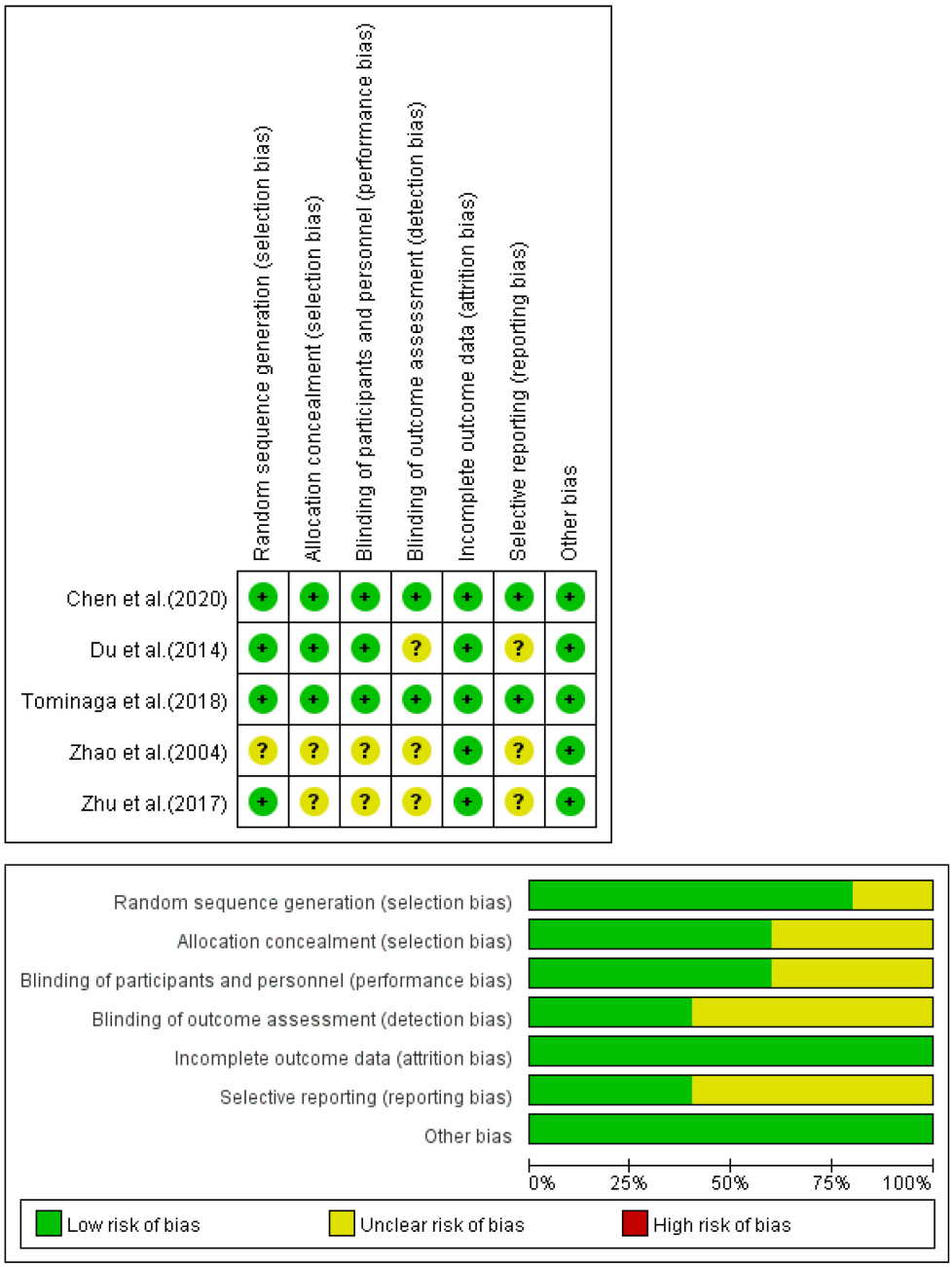

FIGURE 2 | Assessment of the risk of bias of CHM vs. placebo.

disorders contributes to sustained remission of FD symptoms over a period of 3–6 months (Singh et al., 2021). Clinical consideration of psychological factors may contribute to better management of FD.

Previous meta-analyses have shown that CHM is significantly better than placebo in improving global symptoms of dyspepsia (Yu et al., 2016; Ho et al., 2022). Our study on the efficacy of CHM vs. placebo in the treatment of FD with psychological disorders showed better results than placebo in terms of total effective rate, total syndrome score, and depression scale. However, there was a high heterogeneity of the findings in all these aspects. This may be related to the inconsistency of the scales of assessment used in these aspects in the included studies.

Our study further compared the efficacy of CHM with that of positive medicine in the treatment of FD with psychological disorders. The results showed that CHM was more beneficial in the total effective rate, depression scale, HAMA score, and gastric emptying rate compared to the mosapride/dopantelone + deanxit group. Currently, pharmacologic treatment is the main

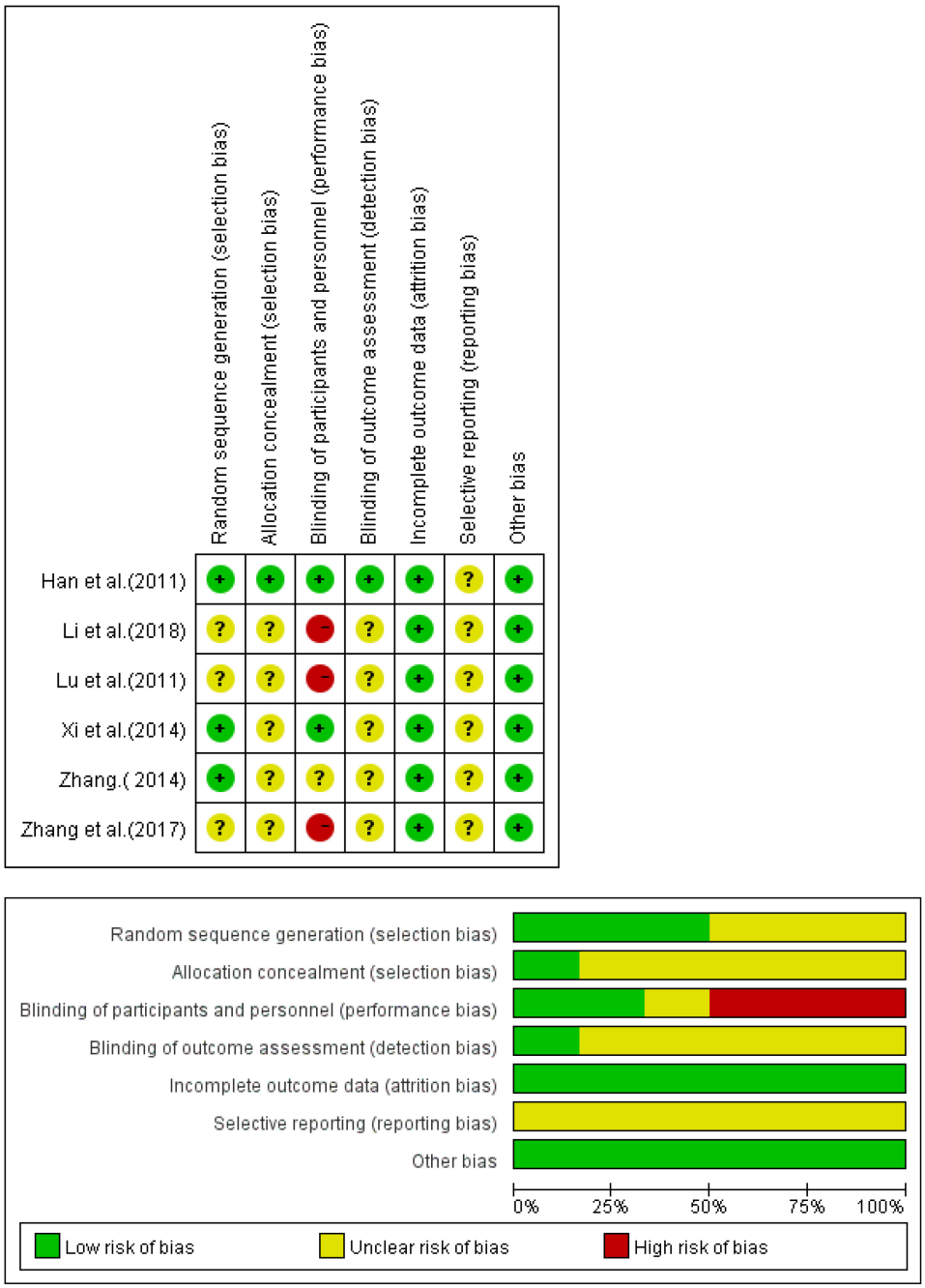

FIGURE 3 | Assessment of the risk of bias of CHM vs. western medicine group.

treatment for FD, and for patients with psychological disorders, psychotropic treatments are generally selected. However, due to the complexity of the FD mechanism, the heterogeneity of the resulting symptoms, and the fact that the same symptoms may be caused by different etiologies, there is no uniform therapeutic drug in clinical practice. This is the reason why the selection of effective control drugs was more difficult in our study. During the screening of the literature, it was found that researchers chose a wide variety of control drugs, including those using only prokinetics or acid inhibitors or psychotropic drugs, as well as multiple drug combinations. The combination of prokinetics with deanxit was the most studied, so we used this as a control group.

One meta-analysis study found that there was no significant difference in the therapeutic effect of the prokinetics domperidone and mosapride in FD, so we combined the studies of domperidone + deanxit with mosapride + deanxit for analysis (Yang et al., 2017). In China, deanxit and fluoxetine were

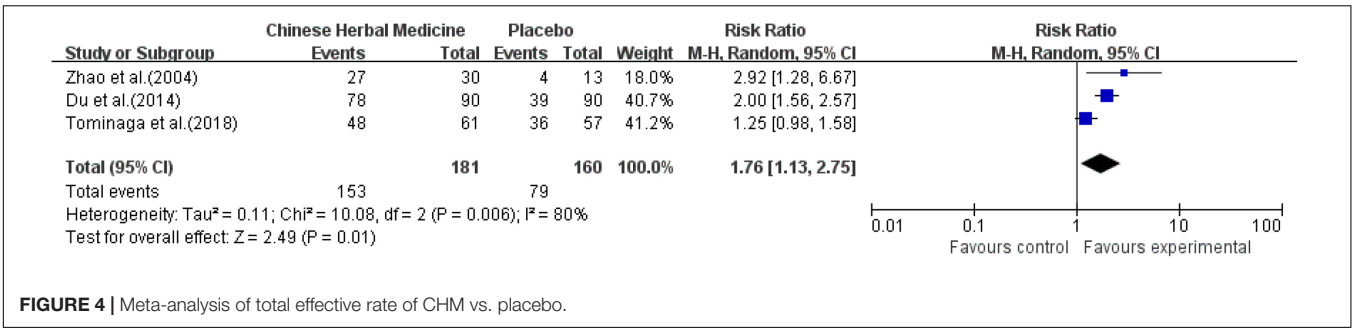

FIGURE 4 | Meta-analysis of total effective rate of CHM vs. placebo.

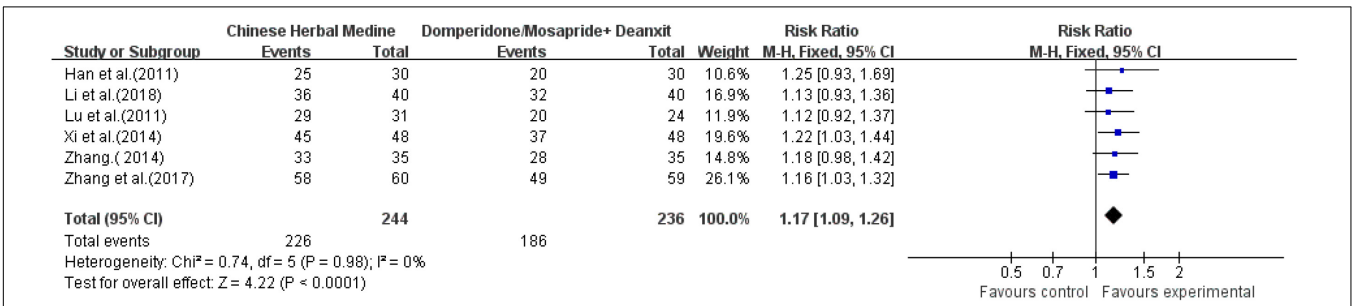

FIGURE 5 | Meta-analysis of total effective rate of CHM vs. western medicine group.

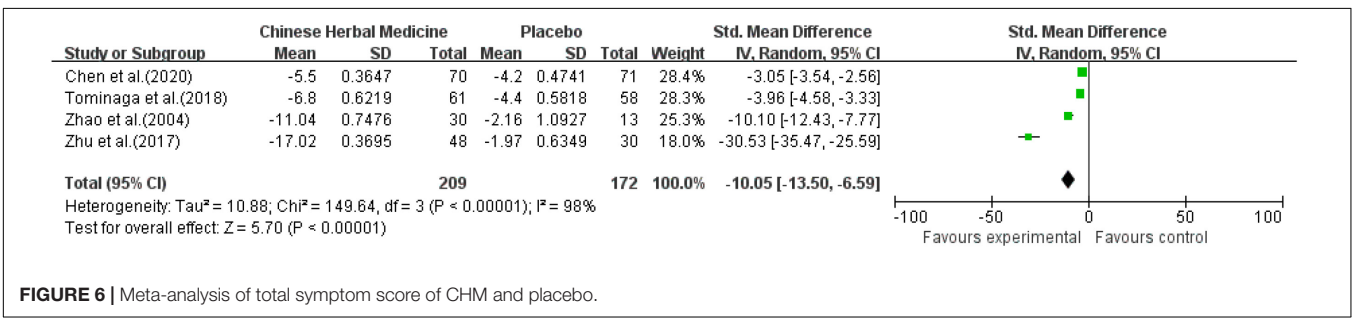

FIGURE 6 | Meta-analysis of total symptom score of CHM and placebo.

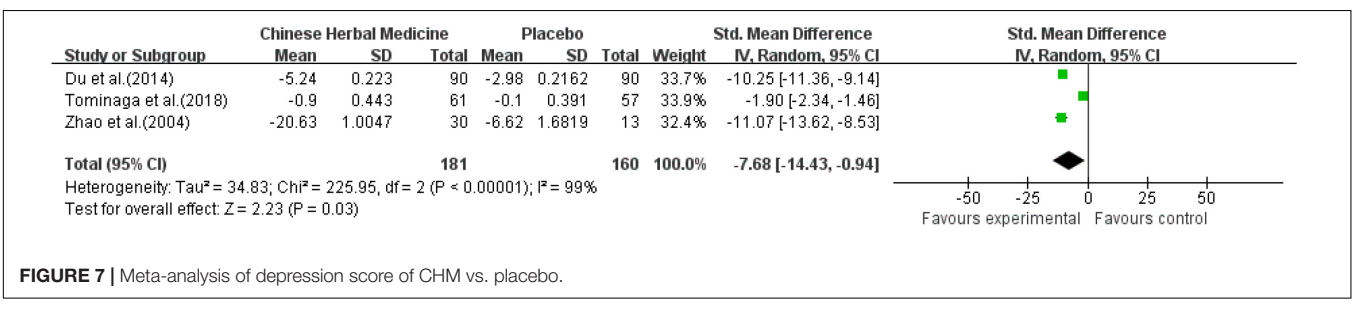

FIGURE 7 | Meta-analysis of depression score of CHM vs. placebo.

the most common anti-depressant drugs used for FD based on a study in 2019 (Luo et al., 2019). The efficacy of flupenthixol melitracen on overall FD symptoms and on depression and anxiety in patients with chronic somatic diseases has been demonstrated (Hashash et al., 2008; Wang et al., 2015). Some studies have shown that CHM is more effective than prokinetics in relieving global dyspeptic symptoms (Chu et al., 2018; Ho et al., 2021). Our study provides a stronger foundation for the effectiveness of CHM in treating FD with psychological disorders by comparing it with positive western medicine. However, there was high heterogeneity in HAMA, HAMD scores, and gastric emptying rate among the studies. The studies included different levels of psychological disorders, so the baseline HAMA and HAMD scores were inconsistent across studies. In addition, differences in Chinese herbal prescriptions may have led to differences in the degree of efficacy. The write-up of reasons may explain the high heterogeneity of HAMA and HAMD scores. Xi et al. (2014) did not introduce the test method of gastric emptying rate, and the high heterogeneity of gastric emptying rate still cannot be clearly explained.

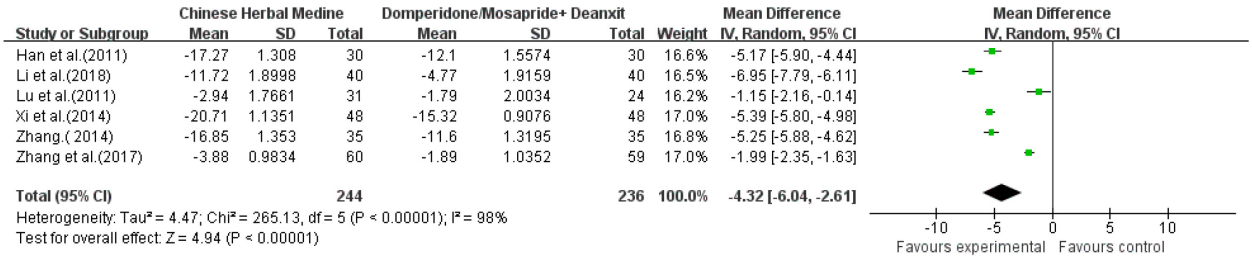

FIGURE 8 | Meta-analysis of HAMD score of CHM vs. western medicine group.

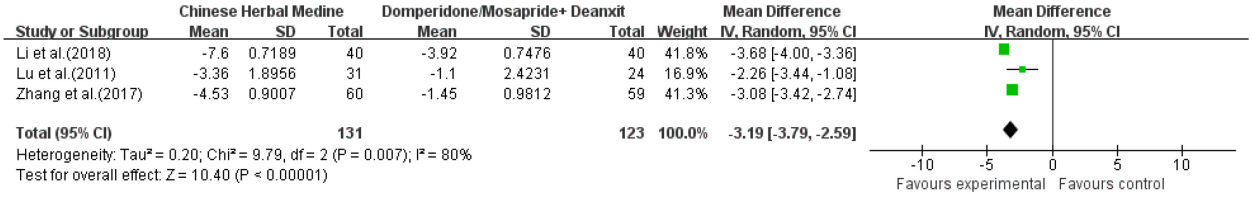

FIGURE 9 | Meta-analysis of HAMA score of CHM vs. western medicine group.

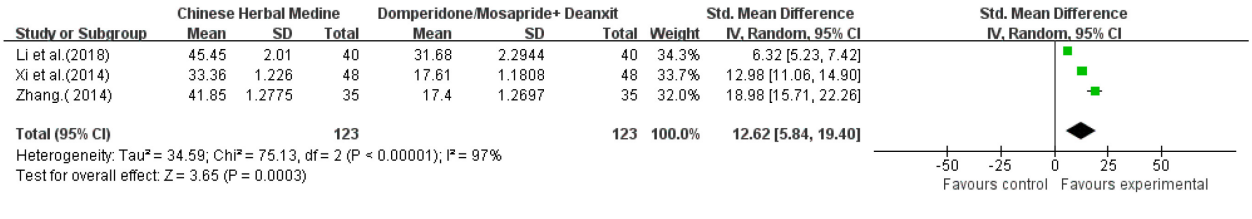

FIGURE 10 | Meta-analysis of gastric emptying rate of CHM vs. western medicine group.

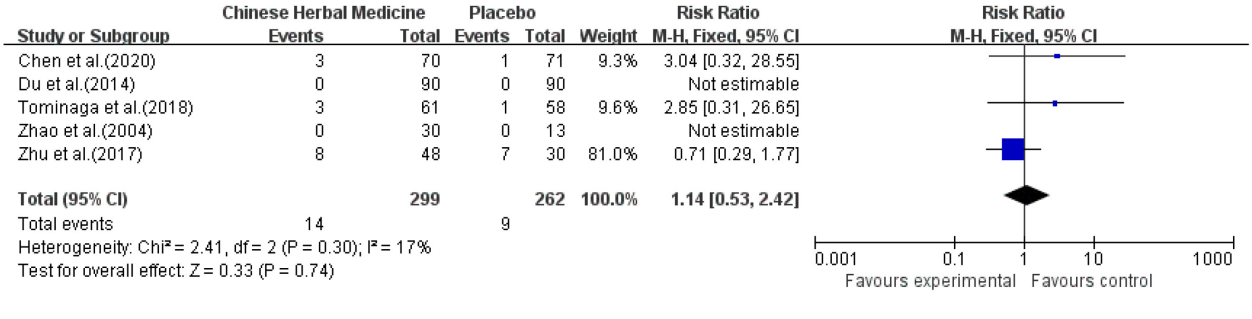

FIGURE 11 | Meta-analysis of adverse reactions of CHM and placebo.

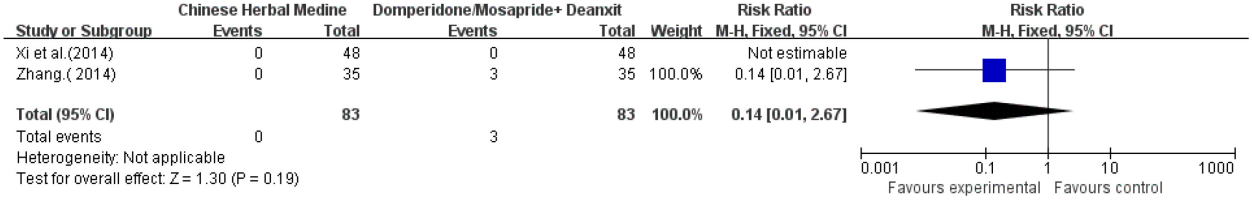

FIGURE 12 | Meta-analysis of adverse reactions of CHM vs. western medicine group.

Furthermore, none of the medical treatments are proven to alter the long-term natural history of FD (Ford et al., 2020). But four inclusion trials (Du et al., 2014; Xi et al., 2014; Zhang, 2014; Chen et al., 2020) reported better follow-up results of CHM in our study. Du followed up for 6 months, and there were five cases of recurrence in the placebo group. Chen conducted a 4-week follow-up and found that six patients in the placebo group relapsed and six patients in the CHM group had no recurrence. Xi conducted a 6-month follow-up, six cases recurred in the western medicine group and no cases recurred in the CHM group. Zhang conducted a 3-month follow-up and found that HAMD and gastric emptying were better improved in Zhang, who conducted a 3-month follow-up and found that HAMD and gastric emptying were better improved in the CHM group.

In this meta-analysis, adverse reactions were not mentioned in 2 of the 11 studies (Han and Wang, 2011; Lu and Chen, 2011). In the remaining studies, no serious adverse reactions were found in the CHM group for FD with psychological disorders. A meta-analysis result of Ford et al. (2017) showed that the total numbers of adverse events, and the adverse events leading to withdrawal in the psychotropic drugs group were significantly more common than those in the placebo group. In our study, there was no significant difference in the incidence of adverse reactions compared with the placebo or western medicine groups. It may be related to the good safety of deanxit applied within 2 weeks (Luo et al., 2019). Previous clinical studies of CHM for the treatment of FD have also shown a high level of safety (Yu et al., 2016; Chu et al., 2018; Gwee et al., 2021; Ho et al., 2021, 2022).

In conclusion, this study collected clinical data from RCTs and evaluated systematically and objectively the clinical efficacy and safety of CHM for FD with psychological disorders treatment using evidence-based medicine. It provides evidence for the efficacy and safety of CHM in the treatment of FD with psychological disorders and suggests that CHM has great potential in the clinical application of this disease. Also, in agreement with Gwee et al. (2021), an attractive aspect of herbal medicine is the prospect of targeting multiple pathophysiological mechanisms simultaneously. In-depth mechanistic studies should be followed up.

LIMITATIONS

In this study, there are still some deficiencies. Most of the included studies were completed in China, and the statistical results have certain regional characteristics. The number of included studies and subjects was small, and there were differences in the prescriptions and dosage forms of the included CHM. Due to the different prescriptions of the herbal treatment group, all 11 studies were not combined for analysis but were divided into two parts according to the difference of the control group (placebo group, prokinetics + deanxit group). This approach, while attempting to avoid higher heterogeneity, results in no more than six items in each part, which hinders funnel plot analysis and publication bias detection.

DATA AVAILABILITY STATEMENT

The raw data supporting the conclusions of this article will be made available by the authors, without undue reservation.

AUTHOR CONTRIBUTIONS

WW was responsible for the design and conception of this study. XL and LW conducted the statistical analysis, graph drawing, and manuscript writing. SF, XQ, TJ, XS, and YY were responsible for searching databases, screening documents, extracting data, and evaluating methodological quality. All authors critically revised the manuscript.

FUNDING

This study was supported by the National Natural Science Foundation of China: International (Regional) Cooperation and Exchange Project (81820108033).

ACKNOWLEDGMENTS

Thank you to everyone involved for their important help.

REFERENCES

Chen, G., Feng, P., Wang, S., Ding, X., Xiong, J., Wu, J., et al. (2020). An Herbal Formulation of Jiawei Xiaoyao for the Treatment of Functional Dyspepsia: A Multicenter, Randomized, Placebo-Controlled, Clinical Trial. *Clin. Transl. Gastroenterol.* 11:e00241. doi: 10.14309/ctg.0000000000000241

Chen, Y. L. (2016). The psychosomatics viewpoint of chronic gastrointestinal disease. *Chin. J. Diagn. Electron.* 4, 168–172.

Chu, M. H. K., Wu, I. X. Y., Ho, R. S. T., Wong, C. H. L., Zhang, A. L., Zhang, Y., et al. (2018). Chinese herbal medicine for functional dyspepsia: systematic review of systematic reviews. *Therap. Adv. Gastroenterol.* 11:1756284818785573. doi: 10.1177/1756284818785573

Dersimonian, R., and Laird, N. (1986). Meta-analysis in clinical trials. *Control. Clin. Trials* 7, 177–188. doi: 10.1016/0197-2456(86)90046-2

Drossman, D. A. (2021). Worldwide prevalence and burden of functional gastrotestinal disorders,results of Rome Foundation global study. *Gastroenterology* 160, 99–114.e3. doi: 10.1053/j.gastro.2020.04.014

Drossman, D. A., and Hasler, Wl (2016). Rome IV-functional GI disorders:disorders of gut-brain interaction. *Gastroenterology* 150, 1257–1261. doi: 10.1053/j.gastro.2016.03.035

Du, H. G., Ming, L., Chen, S. J., and Li, C. D. (2014). Xiaoyao pill for treatment of functional dyspepsia in perimenopausal women with depression. *World J. Gastroenterol.* 20, 16739–16744. doi: 10.3748/wjg.v20.i44.16739

Esterita, T., Dewi, S., Suryatenggara, F. G., and Glenardi, G. (2021). Association of Functional Dyspepsia with Depression and Anxiety: A Systematic Review. *J. Gastrointestin. Liver Dis.* 30, 259–266. doi: 10.15403/jgld-3325

Feng, L., Li, Z., Gu, X., Jiang, J., and Liu, X. (2021). Psychosomatic Disorders in Patients with Gastrointestinal Diseases: Single-Center Cross-Sectional Study

of 1186 Inpatients. *Gastroenterol. Res. Pract.* 2021:6637084. doi: 10.1155/2021/6637084

Ford, A. C., Luthra, P., Tack, J., Boeckxstaens, G. E., Moayyedi, P., and Talley, N. J. (2017). Efficacy of psychotropic drugs in functional dyspepsia: systematic review and meta-analysis. *Gut* 66, 411–420. doi: 10.1136/gutjnl-2015-310721

Ford, A. C., Mahadeva, S., Carbone, M. F., Lacy, B. E., and Talley, N. J. (2020). Functional dyspepsia. *Lancet* 396, 1689–1702. doi: 10.1016/S0140-6736(20)30469-4

Ford, A. C., Moayyedi, P., Black, C. J., Yuan, Y., Veettil, S. K., Mahadeva, S., et al. (2021). Systematic review and network meta-analysis:effectiveness of drugs for functional dysspepsia. *Aliment. Pharmacol. Ther.* 53, 8–21. doi: 10.1111/apt.16072

Ge, J. B. (2017). *Practical Internal Medicine. 15th Edition*. Beijing: People's Health Publishing House, 1530.

Gwee, K. A., Holtmann, G., Tack, J., Suzuki, H., Liu, J., Xiao, Y., et al. (2021). Herbal medicines in functional dyspepsia-Untapped opportunities not without risks. *Neurogastroenterol. Motil.* 33:e14044. doi: 10.1111/nmo.14044

Han, Y., and Wang, H. (2011). Observation on the curative effect of 30 cases of functional dyspepsia with depression with modified Sini powder. *J. Trad. Chin. Med.* 30, 457–458.

Hashash, J. G., Abdul-Baki, H., Azar, C., Elhajj, I. I., El Zahabi, L., Chaar, H. F., et al. (2008). Clinical trial: a randomized controlled cross-over study of flupenthixol + melitracen in functional dyspepsia. *Aliment. Pharmacol. Ther.* 27, 1148–1155. doi: 10.1111/j.1365-2036.2008.03677

Higgins, J. P., Thompson, S. G., Deeks, J. J., and Altman, D. G. (2003). Measuring inconsistency in meta-analyses. *Br. Med. J.* 327, 557–560. doi: 10.1136/bmj.327.7414.557

Ho, L. C., Wu, H. T., Hung, H. C., Chou, H. W., Cheng, K. P., Lin, C. H., et al. (2021). Chinese herbal medicine for functional dyspepsia: a network meta-analysis of prokinetic-controlled randomised trials. *Chin. Med.* 16:140. doi: 10.1186/s13020-021-00556-6

Ho, L. C., Wu, H. T., Hung, H. C., Chou, H. W., Cheng, K. P., Lin, C. H., et al. (2022). Herbal medicine for functional dyspepsia: Network meta-analysis of placebo-controlled randomised trials. *J. Ethnopharmacol.* 283:114665. doi: 10.1016/j.jep.2021.114665

Li, X., Yu, B., and Danzhi, X. (2018). San and Simo Decoction in the treatment of 40 cases of functional dyspepsia with anxiety and depression. *J. Guangxi Univ. Chin. Med.* 21, 21–24.

Lin, S., Gao, T., Sun, C., Jia, M., Liu, C., and Ma, A. (2019). The association between functional dyspepsia and depression: a meta-analysis of observational studies. *Eur. J. Gastroenterol. Hepatol.* 31, 911–918. doi: 10.1097/MEG.0000000000001451

Lu, H., and Chen, J. (2011). Effect of the method of regulating Qi for reducing turbid on functional dyspepsia with anxiety and depression. *Hebei. J. TCM* 33, 986–988.

Luo, L., Du, L., Shen, J., Cen, M., and Dai, N. (2019). Benefit of small dose antidepressants for functional dyspepsia: Experience from a tertiary center in eastern China. *Medicine* 98:e17501. doi: 10.1097/MD.0000000000017501

Singh, P., Ballou, S., Rangan, V., Katon, J., Hassan, R., Iturrino, J., et al. (2021). Clinical and Psychological Factors Predict Outcome in Patients With Functional Dyspepsia: A Prospective Study. *Clin. Gastroenterol. Hepatol.* 20, 1251–1258.e1. doi: 10.1016/j.cgh.2021.07.043

Stanghellini, V., Chan, F. K., Hasler, W. L., Malagelada, J. R., Suzuki, H., Tack, J., et al. (2016). Gastroduodenal disorders. *Gastroenterology* 150, 1380–1392. doi: 10.1053/j.gastro.2016.02.011

Tack, J., Talley, N. J., Camilleri, M., Holtmann, G., Hu, P., Malagelada, J. R., et al. (2006). Functional gastroduodenal disorders. *Gastroenterology* 130, 1466–1479. doi: 10.1053/j.gastro.2005.11.059

Talley, N. J., Stanghellini, V., Heading, R. C., Koch, K. L., Malagelada, J. R., and Tytgat, G. N. (1999). Functional gastroduodenal disorders. *Gut* 45, 37–42. doi: 10.1136/gut.45.2008.ii37

Tominaga, K., Sakata, Y., Kusunoki, H., Odaka, T., Sakurai, K., Kawamura, O., et al. (2018). Rikkunshito simultaneously improves dyspepsia correlated with anxiety in patients with functional dyspepsia: A randomized clinical trial (the DREAM study). *Neurogastroenterol. Motil.* 30:e13319. doi: 10.1111/nmo.13319

Wang, L., Zhong, Z., Hu, J., Rong, X., Liu, J., Xiao, S., et al. (2015). Sertraline plus deanxit to treat patients with depression and anxiety in chronic somatic diseases: a randomized controlled trial. *BMC Psychiatr.* 15:84. doi: 10.1186/s12888-015-0449-2

Xi, Y., Dang, Z., Zhang, L., Niu, X., Wang, Y., Xu, X., et al. (2014). Clinical study on intervening effects on functional dyspepsia plus depression treated with Jiawei Sinisan. *Chin. J. Exp. Trad. Med. Formul.* 20, 202–204.

Xiaoying, L., Yang, Y., Xinyong, M., Gengqing, S., Qian, L., Tianyuan, J., et al. (2021). Treatment of functional dyspepsia with traditional Chinese medicine: a meta-analysis of a randomized, double-blind, placebo-controlled trial (English). *Digit. Chin. Med.* 4, 273–289.

Xiong, N. (2016). *Research on Psychosocial Behavioral Characteristics of Patients With Functional Gastrointestinal Disease*. Beijing: Peking Union Medical College.

Yang, Y. J., Bang, C. S., Baik, G. H., Park, T. Y., Shin, S. P., Suk, K. T., et al. (2017). Prokinetics for the treatment of functional dyspepsia: Bayesian network meta-analysis. *BMC Gastroenterol.* 17:83. doi: 10.1186/s12876-017-0639-0

Yu, G., Jiajie, Z., Xiaolan, S., Jianqin, Y., Yijie, L., Qingguo, W., et al. (2016). Efficacy of Chinese herbal medicine in functional dyspepsia: A meta-analysis of randomized, double-blind,placebo-controlled trials. *J. Trad. Chin. Med. Sci.* 3, 147–156.

Zhang, L. (2014). *Description of Adjusting Liver and Harmonizing Stomach on Functional Dyspepsia and Depressive State of Intervention Treatment and Research*. Henan: Henan University of Traditional Chinese Medicine.

Zhang, Y., Wang, S., Han, X., Liu, X., Zhang, M., Gao, W., et al. (2017a). Clinical observation of 60 cases of functional dyspepsia with anxiety and depression treated by self-made Shugan Jianpi Anshen prescription. *J. Gansu Univ. Chin. Med.* 34, 77–80.

Zhang, Y., Wang, S., Han, X., Liu, X., Zhang, M., Gao, W., et al. (2017b). Observation on the curative effect of Shugan Jianpi Anshen Fang on functional dyspepsia patients with anxiety and depression. *World Latest Med. Inf.* 17, 66–67.

Zhang, Y., Wang, S., Han, X., Liu, X., and Gao, W. (2017c). The effect of soothing liver and invigorating spleen calming therapy on gastrointestinal hormones in patients with functional dyspepsia accompanied with anxiety and depression. *Chin. Health Stand. Manage.* 8, 108–110.

Zhang, Y., Wang, S., Liu, X., Zhang, M., Gao, W., Han, X., et al. (2016). Effect of liver-soothing spleen-invigorating and spiritcalming prescription on MTL and SP in patients of functional dyspepsia with anxiety-depression. *Chin. Med. Mod. Dis. Educ. China* 14, 51–53.

Zhang, Y. F. (2018). *The Relevant Research Phychological Factors and Variation of IL-1β and Intestinal Flora in Patient With Functional Dyspepsia*. Zhangjiakou: Hebei North University.

Zhao, L., and Gan, A. P. (2005). Clinical and psychological assessment on xinwei decoction for treating functional dyspepsia accompanied with depression and anxiety. *Am. J. Chin. Med.* 33, 249–257. doi: 10.1142/S0192415X05002801

Zhu, L., Hong, X., Fang, X., Shi, L., Xiong, N., Wang, Z., et al. (2015). A clinical study of functional dyspepsia and mental disorder co-morbidity. *Chin. J. Intern. Med.* 54, 525–529.

Zhu, Q., and Gu, S. (2017). Efficacy and mechanism of Morinda Officinalis Oligose Capsule in treatment of functional dyspepsia accompanied by mild - to - moderate depression. *Mod. Med. Health* 33, 1010–1012.

Conflict of Interest: The authors declare that the research was conducted in the absence of any commercial or financial relationships that could be construed as a potential conflict of interest.

Publisher's Note: All claims expressed in this article are solely those of the authors and do not necessarily represent those of their affiliated organizations, or those of the publisher, the editors and the reviewers. Any product that may be evaluated in this article, or claim that may be made by its manufacturer, is not guaranteed or endorsed by the publisher.

frontiers | Frontiers in Neuroscience

SYSTEMATIC REVIEW
published: 15 July 2022
doi: 10.3389/fnins.2022.918701

Effects and Mechanisms of Acupuncture on Diarrhea-Predominant Irritable Bowel Syndrome: A Systematic Review

Gezhi Zhang[1,2], Tao Zhang[1,2], Zeng Cao[1,2], Zijing Tao[1,2], Tianhao Wan[1], Mengxi Yao[1,2], Xiaolan Su[1,2] and Wei Wei[1,2]**

[1] Department of Gastroenterology, Wangjing Hospital, China Academy of Chinese Medical Sciences, Beijing, China,
[2] Beijing Key Laboratory of Functional Gastrointestinal Disorders Diagnosis and Treatment of Traditional Chinese Medicine, Beijing, China

Background: Irritable bowel syndrome (IBS) is a common disorder of gut-brain interaction with challenging treatment. According to evidence-based studies, acupuncture is likely to be a promising therapy and subservient adjunct for IBS. Mechanism study of acupuncture based on related clinical trials of high quality, nevertheless, is still vacant.

Aim: This study aims to assess the results and qualities of current clinical evidence and conclude the relevant pathophysiological mechanisms and therapeutic effects of acupuncture on IBS with diarrhea (IBS-D).

Methods: Literature from four databases, namely, PubMed, Cochrane Library, EMBASE, and Web of Science, was systematically searched to obtain eligible randomized controlled trials (RCTs), which contained mechanism research of acupuncture treatment in IBS-D patients. Two independent reviewers completed data extraction and quality evaluation using the RevMan 5.4.1 software.

Results: Ten trials that covered 19 items related to mechanism research were included in this review. Acupuncture was reported to improve IBS-D symptoms and quality of life, with positive effects in regulating brain-gut peptides, cerebral activities, neuroendocrine functions, psychological state, and inflammatory GI and hypersensitive intestinal tracts.

Conclusion: Acupuncture has potential influence on pathophysiology alterations such as regulating brain-gut peptides, altering cerebral connectivity and activity, promoting neuroendocrine functions and mental state, and mitigating inflammation as well as hypersensitivity of bowels in IBS-D patients, but further studies of high quality are still necessary.

Systematic Review Registration: [https://www.crd.york.ac.uk/PROSPERO], identifier [CRD42022320331].

Keywords: brain-gut disorders, microbiota-gut-brain axis (MGB axis), acupuncture therapy, electroacupuncture therapy, transcutaneous electrical acustimulation, systematic review, diarrhea-predominant irritable bowel syndrome (IBS-D)

OPEN ACCESS

Edited by:
Jianhua Chen,
Shanghai Jiao Tong University, China

Reviewed by:
Yu Wang,
China Academy of Chinese Medical Sciences, China
Xuliang Shi,
Hebei University of Chinese Medicine, China

****Correspondence:***
Xiaolan Su
suxiaolan1982@126.com
Wei Wei
sxxtyy@sina.com

Specialty section:
This article was submitted to Gut-Brain Axis, a section of the journal Frontiers in Neuroscience

Received: *12 April 2022*
Accepted: *20 June 2022*
Published: *15 July 2022*

Citation:
Zhang G, Zhang T, Cao Z, Tao Z, Wan T, Yao M, Su X and Wei W (2022) Effects and Mechanisms of Acupuncture on Diarrhea-Predominant Irritable Bowel Syndrome: A Systematic Review. Front. Neurosci. 16:918701. doi: 10.3389/fnins.2022.918701

INTRODUCTION

Irritable bowel syndrome (IBS) is a functional gastrointestinal (GI) disorder, or disorder of gut-brain interaction, affecting almost 9.2% of the general population (Oka et al., 2020). Without organic abnormalities, its clinical manifestations are characterized by abdominal pain or flatulence, accompanied by alteration in stool frequency or form (Mearin et al., 2016). IBS is divided into four subtypes according to Rome IV criteria (Drossman and Hasler, 2016), namely, IBS with constipation (IBS-C), IBS with diarrhea (IBS-D), IBS with a mixed pattern of constipation and diarrhea (IBS-M), and unclassified IBS, among which IBS-D is the most prevalent.

The pathogenesis of IBS-D is considered to be associated with genetic and environmental factors, but the particular mechanisms still remain unclear. IBS-D is regarded as a multifactorial disease, and stress was thought as the main cause of IBS-D (Labus et al., 2019); but with more and deeper investigations in recent years, the pathophysiology of IBS-D has been ascribed to multiple possibilities such as inflammatory GI, visceral hypersensitivity, genetic susceptibility, abnormal brain-gut interactions, and altered gut microbiota (Tang et al., 2021), rather than the simple response of the body to stress (Yaklai et al., 2021). Böhmelt et al. (2005) concluded that symptoms of IBS-D were related to the central dysfunction of viscerosomatic pathway led by the activation of immune-brain communication *via* vagal afferent fibers and the hypothalamic-pituitary-adrenal axis (HPA) (Böhmelt et al., 2005). To be more specific, the role of inflammatory cytokines imbalance cannot be ignored in IBS-D. Kumar et al. (2022) concluded that there seems to be a trend existing in the condition of increased levels of TNF-α and IL-6 and decreased level of IL-10. Besides, IL-10 is advocated as a potent cytokine target of anti-inflammatory therapy, especially in IBS-D. Visceral hypersensitivity induced by stress, reflected in the visceral pain threshold ordinarily, is also a reliable symbol (Nozu and Okumura, 2022). Present studies have demonstrated that genetic differences could be associated with IBS-D risk and symptoms (abdominal pain, sleep disturbance, and fatigue) (Zhao T. et al., 2022). Functional neuroimaging aids in the detection of brain alterations in IBS-D patients, and it is speculated that various functional disorders could have a shared pathophysiology (Nisticò et al., 2022). Referring to the microbiota-gut-brain axis, impaired intestinal mast cells led by the imbalance of intestinal flora excrete inflammatory mediators, and then, neurotransmitters are released, thus inducing aberrant intestinal motility and sensitivity (Chen et al., 2022). Thus, its complicacy on pathophysiological mechanisms resulted in restricted treatment methods, insufficient efficacy, and huge financial burdens.

As a common ailment with significant impact, IBS-D affects patients' health as well as the quality of life (QOL), and the management of it mostly concentrates on symptomatic relief. Conventional remedies include pharmacological therapies (such as antibiotics, antagonists of serotonin 5-HT3 receptors, and antidepressants), dietary and lifestyle interventions, fecal microbiota transplantation (FMT), and other non-pharmacological approaches (Bonetto et al., 2021). However, most of these methods are always accompanied by some deficiencies or controversies. For instance, possible side effects of 5-HT3 antagonists are ischemic colitis and constipation (Adriani et al., 2018); another case in point is that the FMT was proved to have obvious clinical benefits in 8 single-arm trails but showed no superiority to placebo in 5 RCTs according to a meta-analysis (Myneedu et al., 2019). According to statistics from the United States, nearly two-thirds of IBS-D patients gave unsatisfactory comments on their current therapies (Zhang et al., 2022), the reason being the lack of efficacy or concomitant side effects. Despite the urgent demand for curative effect, the treatment of IBS-D is still challenging. Recently, a considerable part of patients tended to seek for complementary and interactive therapies, including acupuncture, moxibustion, traditional Chinese herbal medicines, and cognitive behavioral therapy. Although psychological interventions such as cognitive behavioral therapy or meditation have not shown obvious side effects, they are hard to be applied in long-term therapy for their specificity of manipulation.

Acupuncture, as one of the most popular complementary and alternative therapies, has been employed as an effective treatment for a great deal of common and tricky diseases. Originated in China, acupuncture has been successfully introduced into other countries. Data from the World Health Organization (WHO) showed that more than half of its member countries (103/194) had included acupuncture as a common treatment in their healthcare systems (Zhuang et al., 2013); 29 countries including Japan, Korea, the United States, and Canada had also approved legislation on acupuncture (Zhang et al., 2022). In the theoretical system of Traditional Chinese Medicine (TCM), acupuncture is defined as a therapeutic approach that regulates Qi (a TCM team that can be simply understood as a kind of energy) and blood through stimulating specific points (acupoints) in bodies. Modern relevant studies have found that its possible biological mechanisms are related to the microbiota-gut-brain (MGB) axis involving multiple factors such as neurotransmitters, immune regulation, oxidative stress, and intestinal flora (Zhang et al., 2022). Therefore, acupuncture has been applied to improve the imbalance of GMB in many diseases such as gastritis, colitis, obesity, and hypertension (Zheng et al., 2016; Wei et al., 2019). According to evidence-based studies (Huang et al., 2021; Zhao Y. et al., 2022), acupuncture is likely to be a promising therapy and subservient adjunct for IBS-D through modulating gut-brain axis and gut microbiome, but relevant evidence has not been systematically summarized until now. On the one hand, acupuncture was proved to exert more favorable effects than other interventions (pharmacological treatments) (Manheimer et al., 2012). On the other hand, acupuncture was compared with sham acupuncture but did not show a significant advantage in therapeutic efficacy (Lowe et al., 2017). Moreover, acupoints selection and parameters of acupuncture differ from each other in diverse studies, making it difficult to evaluate the authentic effects of acupuncture on IBS-D. Due to the low-quality evidence provided by systematic reviews and meta-analyses, the conclusion that acupuncture has exact beneficial effects for IBS-D still needs further confirmation.

On this account, to better understand the pathophysiological mechanisms and therapeutic effects of acupuncture on IBS-D in clinical studies, this study made efforts to summarize and assess concerning trials as comprehensively as possible. Based on diverse manipulations, the three most common types of acupuncture employed clinically, namely, manual acupuncture (MA), electroacupuncture (EA), and transcutaneous electrical acustimulation (TEA; Chen et al., 2018), are chosen in this article.

MATERIALS AND METHODS

Protocol and Registration

The protocol of this systematic review was registered in the International Prospective Register of Systematic Reviews (PROSPERO),[1] and the registration number is CRD42022320331.

Selection Criteria

Study Designs

Randomized controlled trials (RCTs) published in peer-reviewed journals, with no restrictions on published date or language, were included.

Participants

Adults who were diagnosed with IBS-D under Rome I∼IV Criteria were included. There were no restrictions on gender or race.

Interventions

Trials that applied acupuncture therapy (mainly include MA, EA, and TEA; exclude acupoint moxibustion, acupoint embedding, and acupoint injection) in IBS-D patients were included. There were no limitations on the number of acupoints or the duration of treatment.

Comparators

Trials that compared sham acupuncture, moxibustion, medication, and no interventions with the experimental group were included (sham acupuncture and moxibustion should operate on the same acupoints as the experimental group).

Main Outcomes

Trials that conducted measurements containing mechanism research (serology such as inflammatory cytokines, visceral sensitivity, cerebral imaging, electroencephalogram, and questionnaires of mental status) on acupuncture were included.

Search Strategy

A comprehensive search on relevant literature, the publication date of which was from inception to 20 March 2022, was accomplished in four databases, namely, PubMed, Cochrane Library, EMBASE, and Web of Science. Medical Subject Headings (MeSH) and entry terms of keywords were accessed from each database and then combined. The full search strategies of four databases were attached in the **Supplementary Material**.

[1]https://www.crd.york.ac.uk/PROSPERO

Study Selection and Data Extraction

Two researchers estimated the qualification of studies independently through browsing titles, abstracts, and full texts in proper order under the selection criteria above. Two researchers extracted data from included studies and checked the accuracy. Detailed information of extracted data is as follows: the first author, year of publication, study design, participant characteristics (including total number, gender, group allocation, and diagnostic standard), interventions (acupoints selection, duration, and frequency of treatment), main outcomes, and mechanism research. Any disagreement was resolved by discussion until consensus was reached or by consulting a third reviewer.

Quality Assessment

Two researchers assessed the methodological quality and risk bias (random sequence generation, allocation concealment, blinding method, incomplete outcome data, selective reporting, and other bias) of all included studies using the RevMan 5.4.1 software (Cochrane Collaboration, Oxford, United Kingdom) based on *Cochrane Handbook for Systematic Reviews*. Any disagreement was resolved by discussion until consensus was reached or by consulting a third researcher.

RESULTS

Study Selection

The process of study selection based on PRISMA is shown in **Figure 1**. In total, 390 potential documents were retrieved from four databases, and of them, 180 documents remained after duplicate removal, which were to be examined through titles and abstracts soon afterward. Subsequently, 14 RCTs appeared to satisfy the included criteria and were carefully scanned with full texts. Two independent reviewers decided on the final 10 trials (Schneider et al., 2007; Chu et al., 2012; Wu et al., 2013; Zhan et al., 2014; Li, 2015; Zhao et al., 2015; Zhenzhong et al., 2015; Guo et al., 2021; Hu et al., 2021; Sun et al., 2021) to be included until consensus was reached.

Study Characteristics

Characteristics of ten included studies are shown in **Table 1**. Publication date of the ultimate 10 studies in this review ranged from 2007 to 2022, and a total of 665 participants were involved while the exact number of each study varied from 30 to 231. The percentage of females in these participants was 51.4–82.4%, unknown in two trials (Zhao et al., 2015; Zhenzhong et al., 2015). The intervention methods in experimental groups were all acupuncture, including MA, EA, and TEA. Three of them (Schneider et al., 2007; Chu et al., 2012; Hu et al., 2021) took sham acupuncture as contrast, compared to four (Wu et al., 2013; Zhan et al., 2014; Li, 2015; Guo et al., 2021) using medication treatment and two (Zhao et al., 2015; Zhenzhong et al., 2015) with moxibustion. Nine studies (Schneider et al., 2007; Wu et al., 2013; Zhan et al., 2014; Li, 2015; Zhao et al., 2015; Zhenzhong et al., 2015; Guo et al., 2021; Hu et al., 2021; Sun

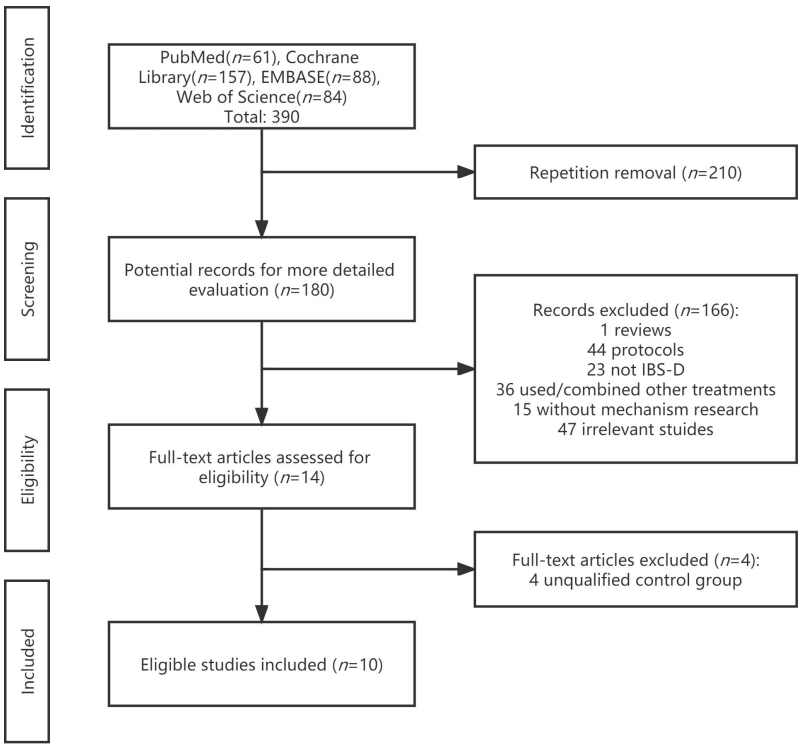

FIGURE 1 | Process of study selection based on PRISMA.

et al., 2021) adopted certain gastrointestinal symptom scales to reflect the acupuncture efficacy in IBS-D (see **Figure 2A**), and quality of life scales (QOL) were put to use in four trials (Schneider et al., 2007; Guo et al., 2021; Hu et al., 2021; Sun et al., 2021) (see **Figure 2B**). As for mechanism research, 19 items in aggregate from manifold categories (inflammatory cytokines, genetic polymorphism, mental status, visceral sensation, stress hormones, neurotransmitters and their receptors, autonomic functions and brain activation) were investigated in studies (see **Figure 2C**). Detailed information of study characteristics was shown in **Table 2**.

Clinical Effects

Gastrointestinal Symptoms and Quality of Life

Nine studies indicated decreased GI symptom scores after the acupuncture treatment based on multiple methods and symptom scales (**Figure 2A**), making it difficult to evaluate these results in a synthetic way. Four of these trials reported improvements in QOL under acupuncture treatment, and the IBS-QOL was the most selected scale to measure GI symptoms in IBS-D among the studies (**Figure 2B**).

Pathophysiology

Inflammatory Cytokines

Five inflammatory cytokines were tested in two trials (Wu et al., 2013; Hu et al., 2021), including interleukin 10 (IL-10), IL-6, IL-4, IL-2, and interferon-γ (INF-γ). All the items were assessed from the blood samples using corresponding commercial kits. In the study by Hu et al. (2021), IL-10 and IL-6 were not significantly changed after TEA treatment. The other trial (Wu et al., 2013) took INF-γ, IL-2, IL-4, and IL-10 as targets and demonstrated that IL-4 and IL-10 levels were obviously increased, while no significant alteration was observed in INF-γ and IL-2 levels.

Visceral Sensation

Two studies conducted rectum distension and recorded the maximum tolerable thresholds pressure during the trial (Chu et al., 2012; Zhao et al., 2015). Zhao et al. (2015) put a plastic balloon in patients' rectum and progressively injected gas into it, while Chu et al. (2012) accomplished that with a computer-driven barostat. Their results were quite different. The former proved that significant increase in maximum pain perception thresholds was observed after EA treatment, but the latter indicated no obvious change.

Mental Status

Depression and anxiety were two main objects to appraise mental status. Two studies evaluated depression and anxiety state with *Hamilton Depression Rating Scale* (HAMD) and/or *Hamilton Anxiety Rating Scale* (HAMA), reporting improvement in psychological condition after MA and EA.

Stress Hormones

Measurement of salivary cortisol was processed by radioimmune assay in one study (Schneider et al., 2007). After acupuncture treatment, the cortisol concentrations showed significant reduction at all assessment points.

TABLE 1 | Characteristics of included studies of acupuncture vs. sham acupuncture, medication, and moxibustion in treating Diarrhea-Predominant Irritable Bowel Syndrome.

References	Design	Participants	Interventions	Main outcomes	Mechanism research
Hu et al., 2021	Parallel	*n*: 37 (F 19); Age (mean): TEA (44.4 ± 13.4), CONT (45.4 ± 11.7); Groups (*n*): TEA (21), CONT (16); Diagnosis: Rome IV	EXP: TEA (LI4, ST36); CONT: Sham TEA (LI4, ST36, no current delivered); Duration and frequency: EXP&CONT: 30 min, twice per d, for 1 month	Decreased VAS scores in TEA and greater than SA ($P < 0.05$); improved IBS-QOL scores in TEA not in SA; decreased IBS-SSS scores in both TEA and SA	Inflammatory cytokines (Serum; IL-10 and IL-6); Neurotransmitters (Serum, NE); GI hormones (Serum, PP)
Guo et al., 2021	Parallel	*n*: 231 (F 103); Age (mean): MA (46 ± 12), CONT (44 ± 13); Groups (*n*): MA (154), CONT (77); Diagnosis: Rome III	EXP: MA (GV20, GV29, ST25, ST36, ST37, SP6, LR3); CONT: Oral pinaverium bromide tablets; Duration and frequency: EXP: 30 min, once every other d, for 6 wk; CONT: 50 mg, tid, for 6 wk	Decreased IBS-SSS scores in MA and greater than CONT ($P < 0.01$); improved IBS-QOL in MA and greater than CONT ($P < 0.01$)	Genetic polymorphism (5-HTTLPR)
Sun et al., 2021	Parallel	*n*: 73 (F 39); Age (mean): MA + EA (39 ± 10), EA (41 ± 10); Groups (*n*): MA + EA (36), EA (37); Diagnosis: Rome IV	EXP: MA (GV20, GV24, GB13); CONT: MA + EA (CV4, CV12, ST25, BL25, ST36, ST37, LI4, LR3); Duration and frequency: EXP&CONT: 30 min, once per d, 6 times per wk, for 4 consecutive wk	Decreased IBS-SSS scores in MA + EA and greater than EA ($P < 0.05$); improved IBS-QOL in MA + EA and greater than EA ($P < 0.05$)	Mental status (HAMD)
Li, 2015	Parallel	n: 60 (F 33); Age (mean): MA (32), CONT (34); Groups (*n*): MA (30), CONT (30); Diagnosis: Rome III	EXP: MA (CV6, CV12, ST25, ST36, ST37, ST39, SP6, SP7, SP9); CONT: Oral pinaverium bromide tablets; Duration and frequency: EXP: 25 min, once per d, 5 times per wk, for 4 wk; CONT: 50mg, tid, for 4 wk	Decreased symptom scores in MA and greater than CONT ($P < 0.05$) (symptom scores without identified source)	Neurotransmitters (Serum; VIP and 5-HT)
Zhenzhong et al., 2015	Parallel	*n*: 41 (F NA); Age (mean): EA (39 ± 5), Mox (39 ± 8); Groups (*n*): EA (19), Mox (22); Diagnosis: Rome III	EXP: EA (ST36, ST37); CONT: Moxibustion (ST36, ST37); Duration and frequency: EXP&CONT: 30 min, once per d, 6 times per wk, for 4 consecutive wk	Decreased VAS scores in both EA and Mox; decreased BSFS scores in Mox and greater than EA ($P < 0.001$)	Neurotransmitters (Colon tissue; SP and VIP)
Zhao et al., 2015	Parallel	*n*: 62 (F NA); Age (mean): EA (42.75 ± 10.22), Mox (39.53 ± 8.91); Groups (*n*): EA (32), Mox (30); Diagnosis: Rome III	EXP: EA (ST25, ST37); CONT: Moxibustion (ST25, ST37); Duration and frequency: EXP&CONT: 30 min, once per d, 6 times per wk, for 4 consecutive wk	Decreased VAS scores in both EA and Mox; decreased BSFS scores in Mox not in EA; decreased HAMD and HAMA scores in both EA and Mox ($P < 0.05$ or $P < 0.01$)	Mental status (HAMD and HAMA); Neurotransmitters (Sigmoid tissue; 5-HT, 5-HT3R and 5-HT4R); Brain activation (fMRI)
Zhan et al., 2014	Parallel	*n*: 57 (F 36); Age (mean): MA (42 ± 14), CONT (37 ± 13); Groups (*n*): MA (29), CONT (28); Diagnosis: Rome III	EXP: MA (GV20, GV29, LR3, ST25, ST36, ST37, SP6); CONT: Oral live combined bifidobacterium and lactobacillus tablets/pinaverium bromide tablets; Duration and frequency: EXP: 30 min, once per d, 5 times per wk, for 4 wk; CONT: 2 g, tid/50 mg, tid, for 4 wk	Decreased Rome III IBS symptom scores in MA and greater than CONT ($P < 0.01$); significantly higher PR in MA than CONT ($P < 0.05$)	Neurotransmitters (Serum; 5-HT)
Wu et al., 2013	Parallel	*n*: 40 (F 22); Age (mean): MA (41 ± 13), CONT (39 ± 13); Groups (*n*): MA (21), CONT (19); Diagnosis: Rome III	EXP: MA (GV20, GV29, LR3, ST25, ST36, ST37, SP6); CONT: Oral live combined bifidobacterium and lactobacillus tablets/pinaverium bromide tablets; Duration and frequency: EXP: 30 min, once per d, 5 times per wk, for 4 wk; CONT: 2 g, bid/50 mg, tid, for 4 wk	Decreased symptom scores in MA and greater than CONT ($P < 0.05$) (symptom scores without identified source); significantly higher PR in MA than CONT ($P < 0.05$)	Inflammatory cytokines (Serum; IFN-γ, IL-2, IL-4, IL-10 and IFN-γ/IL-4)
Chu et al., 2012	Parallel	*n*: 30 (F 15); Age (mean): EA (42.3 ± 12.2), SA (44.2 ± 14.5); Groups (*n*): MA (15), CONT (15); Diagnosis: Rome III	EXP: EA (ST36, ST37, SP6); CONT: Sham EA (ST36, ST37, SP6; touch but not penetrate into acupoints); Duration: EXP&CONT: 15 and 30 min, once during fMRI	–	Brain activation (fMRI)
Schneider et al., 2007	Parallel	*n*: 34 (F 28); Age (mean): MA (46.23 ± 15.00), SA (41.80 ± 14.51); Groups (*n*): MA (19), CONT (15); Diagnosis: Rome II	EXP: MA (LR3, ST21, ST25, ST36, SP6, HT7, GV20, RN12); CONT: Sham MA (LR3, ST21, ST25, ST36, SP6, HT7, GV20, RN12; 2 cm adjacent to acupoints); Duration and frequency: EXP&CONT: twice a wk, for 5 wk	Decreased FDDQL global scores and SF-36 pain scales in both MA and SA	Stress hormones (salivary cortisol); Autonomic functions (ECG)

BSFS, Bristol Stool Form Scale; CONT, control group; EA, electroacupuncture; ECG, electrocardiogram; EXP, experimental group; F, female; FDDQL, functional digestive diseases quality of life; fMRI, functional magnetic resonance imaging; HAMA, Hamilton Anxiety Rating Scale; HAMD, Hamilton Depression Rating Scale; IBS-QOL, IBS quality of life; IBS-SSS, IBS severity scoring system; IFN-γ, interferon γ; IL, interleukin; MA, manual acupuncture; Mox, moxibustion; NE, norepinephrine; PP, pancreatic polypeptide; PR, proportion of responders; SA, sham acupuncture/TEA; SF-36, 36-Item Short Form Survey; SP, substance P; TEA, transcutaneous electrical acustimulation; VAS, visual analog scale; VIP, vasoactive intestinal peptide; 5-HT, 5-hydroxytryptamine; 5-HT3R, serotonin receptor 3; 5-HT4R, serotonin receptor 4; 5-HTTLPR, serotonin transporter.

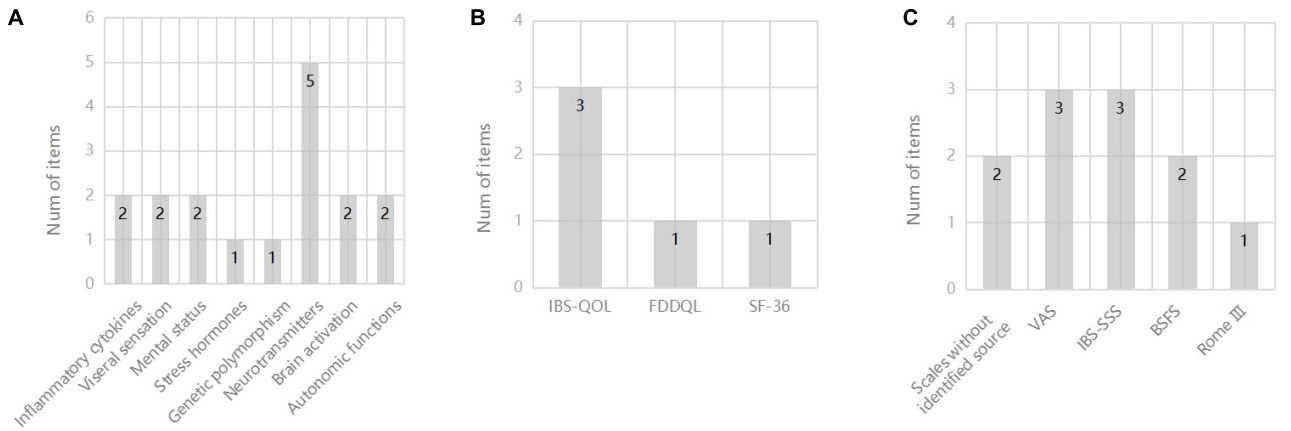

FIGURE 2 | (A) Number of items for different scales of IBS-D symptoms; **(B)** Number of items for different scales of QOL; **(C)** Number of items for different mechanism research. BSFS, Bristol Stool Form Scale; FDDQL, functional digestive diseases quality of life; IBS-QOL, IBS quality of life; IBS-SSS, IBS severity scoring system; SF-36, 36-Item Short Form Survey; VAS, visual analog scale.

Genetic Polymorphism

The serotonin transporter polymorphism (5-HTTLPR) genotypes were determined by means of DNA amplification with polymerase chain reaction (PCR) in one study (Guo et al., 2021). The results indicated that there could be a correlation between clinical efficacy of acupuncture and 5-HTTLPR polymorphism, and the efficacy is more obvious in patients with LS and SS genotypes.

Mechanisms

Neurotransmitters and Their Receptors

Six neurotransmitters were tested in five of the ten trials (Zhan et al., 2014; Li, 2015; Zhao et al., 2015; Zhenzhong et al., 2015; Hu et al., 2021), including norepinephrine (NE), vasoactive intestinal peptide (VIP), substance P (SP), 5-hydroxytryptamine (5-HT), and serotonin receptor 3 and receptor 4 (5-HT3R/5-HT4R). Enzyme-linked immunosorbent assay (ELISA) and immunohistochemical (IHC) staining were applied as testing methods in studies, from which MA/EA was reported to decrease VIP, SP, 5-HT, and its receptors levels, but NE levels alteration was not significant after TEA.

Brain Activation

By means of functional magnetic resonance imaging (fMRI), one study observed decreased activated voxel values in the functional brain areas of the prefrontal cortex (PFC, the senior center of feeling pain) under stimulation with colorectal distension (CRD) after EA treatment (Zhao et al., 2015). In addition, another study, treated with EA as well, reported a significantly higher activation in the right insula, pulvinar, and medial nucleus of the thalamus under fMRI (Chu et al., 2012).

Autonomic Functions

The NE and pancreatic polypeptide (PP) were assessed in one study using a reagent test kit (Hu et al., 2021), to reflect the sympathetic activity and vagal activity. After TEA treatment, however, NE and PP levels did not vary significantly. Besides, one more trial showed an acupuncture-induced decrease in heart rate response through electrocardiogram (ECG) during orthostatic stress (Schneider et al., 2007), which indicated an increase in parasympathetic tone.

Methodological Quality

The risk of bias graph and summary of assessment on methodological quality about included studies were displayed in **Figure 3**. All studies showed a low risk in selection bias (random sequence generation). The risk of selection bias (allocation concealment), detection bias (blinding of outcome assessment), attrition bias (incomplete outcome data), and reporting bias (selective reporting) was unclear in most trials due to the lack of detailed illustrations or experiment protocols previously. A proportion of studies manifested a high risk in performance bias (blinding of participants and personnel), owing to the non-acupuncture control groups such as oral medicine and moxibustion.

DISCUSSION

In view of the sophisticated and multifactorial pathophysiology, general symptomatic treatment like pharmacotherapy is incapable to appease the momentous requirement for care in IBS-D patients (De Ponti, 2013). It has been calculated that 30–50% of patients with IBS-D take complementary and alternative medicine (CAM) therapies to relieve their symptoms (Nguyen, 2018), and clinical evidence supporting the utilization of acupuncture is demonstrating that CAM interventions like this present improvement in IBS-D overall symptoms and QOL indeed (Grundmann and Yoon, 2014). Acupuncture has been widely used in the treatment of GI dysfunctions such as IBS-D, inflammatory bowel disease, and functional dyspepsia. As the most classical method, MA is commonly applied in various modes, which might exert quite different impacts on

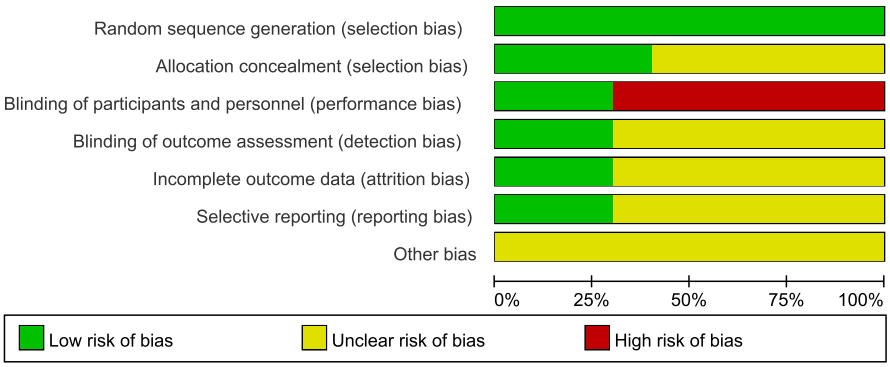

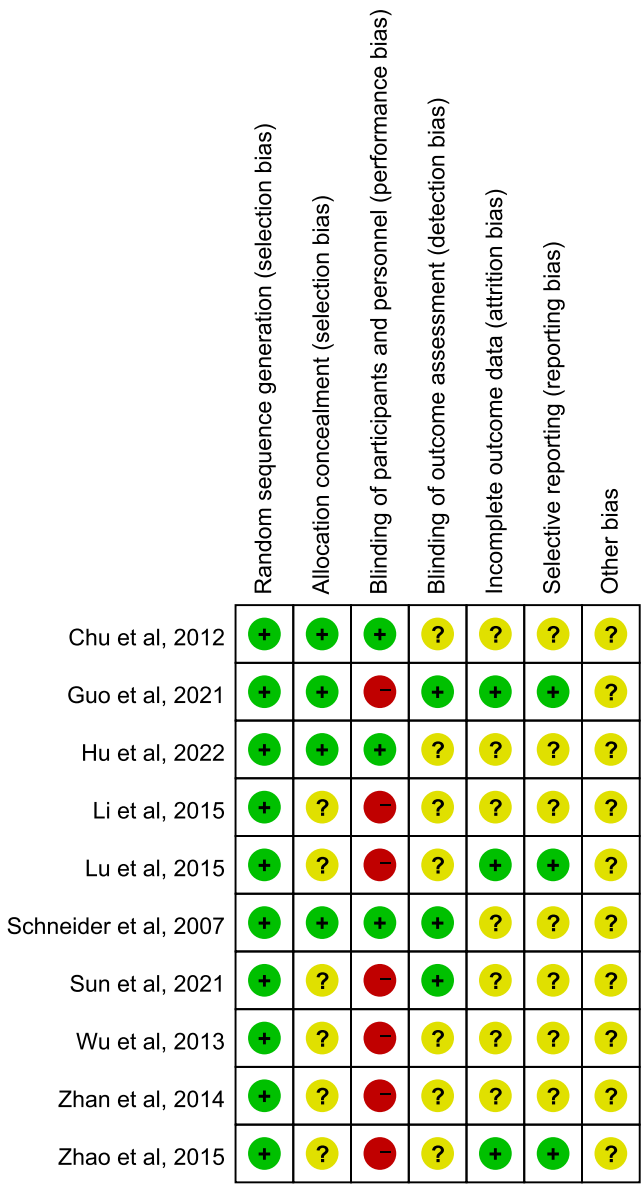

FIGURE 3 | Risk of bias graph and summary of included studies.

TABLE 2 | Mechanism research of included studies.

Reference	Detecting items	Research methods and techniques	Main results
Brain-gut peptides (neurotransmitters and GI hormones)			
Hu et al., 2021	Serum NE and PP levels	Corresponding commercial kits	No significant alteration in NE and PP levels with TEA nor with sham TEA
Li, 2015	Serum VIP and 5-HT levels	ELISA	Decreased serum VIP and 5-HT levels in MA and greater than CONT ($P < 0.05$)
Zhenzhong et al., 2015	Colon tissue SP and VIP levels	Immunohistochemical staining	Decreased SP and VIP expression in both EA and Mox
Zhao et al., 2015	Sigmoid tissue 5-HT, 5-HT3R and 5-HT4R levels	Immunohistochemical staining	Decreased 5-HT3R and 5-HT4R expression in both EA and Mox; decreased 5-HT expression in Mox and greater than EA ($P < 0.05$)
Zhan et al., 2014	Serum 5-HT levels	ELISA	Decreased serum 5-HT levels in both MA and CONT
Cerebral activities			
Zhao et al., 2015	Brain activation	fMRI	Decreased voxel values of PFC in EA
Chu et al., 2012	Brain activation	fMRI	Significantly higher activation at right insula, pulvinar and medial nucleus of the thalamus was observed in EA compared to SA
Neuroendocrine functions			
Hu et al., 2021	Serum NE and PP levels	Corresponding commercial kits	No significant alteration in NE and PP levels with TEA nor with sham TEA
Schneider et al., 2007	Salivary cortisol levels Heart rate and blood pressure	Radioimmune assay ECG	Decreased cortisol concentrations in MA not in SA Parasympathetically decreased heart rate response in MA not in SA during orthostasis
Mental status			
Sun et al., 2021	Depression	HAMD	Decreased HAMD scores in MA + EA and greater than EA ($P < 0.05$)
Zhao et al., 2015	Depression and anxiety	HAMD and HAMA	Decreased HAMD and HAMA scores in both EA and Mox ($P < 0.05$ or $P < 0.01$)
Inflammation and hypersensitivity of the bowels			
Hu et al., 2021	Serum IL-10 and IL-6 levels	Corresponding commercial kits	No significant alteration in IL-10 and IL-6 levels with TEA nor with sham TEA
Wu et al., 2013	Serum IFN-γ, IL-2, IL-4, IL-10 and IFN-γ/IL-4	Not mentioned	Improved serum IL-4 and IL-10 in MA and greater than CONT ($P < 0.05$); decreased serum IFN-γ/IL-4 in MA and greater than CONT ($P < 0.01$)
Zhao et al., 2015	Rectal sensory thresholds	VAS	Significant increases in the urgent defecation perception thresholds and maximum pain perception thresholds were observed in both EA and Mox groups after treatment ($P < 0.05$ or $P < 0.01$)
Chu et al., 2012	Rectal sensation	Likert scale	A significant correlation ($P < 0.005$) between subjective rectal pain rating and brain activation was observed in hypothalamus, bilateral thalami and bilateral insula
Genetic polymorphism			
Guo et al., 2021	5-HTTLPR	Genetic polymorphism	SS genotypes take over a higher proportion in IBS-D patients; curative effect of acupuncture was better in LS and SS genotypes than LL and the same genotype in CONT

CONT, control group; EA, electroacupuncture; ECG, electrocardiogram; ELISA, enzyme-linked immunosorbent assay; fMRI, functional magnetic resonance imaging; HAMA, Hamilton Anxiety Rating Scale; HAMD, Hamilton Depression Rating Scale; IFN-γ, interferon γ; IL, interleukin; MA, manual acupuncture; LS, SS, and LL, three genotypes in 5-HTTLPR; Mox, moxibustion; NE, norepinephrine; PFC, prefrontal cortex (the senior center of feeling pain); PP, pancreatic polypeptide; SA, sham acupuncture/TEA; SP, substance P; TEA, transcutaneous electrical acustimulation; VAS, visual analog scale; VIP, vasoactive intestinal peptide; 5-HT, 5-hydroxytryptamine; 5-HT3R, serotonin receptor 3; 5-HT4R, serotonin receptor 4; 5-HTTLPR, serotonin transporter.

one disease (Guo Y. et al., 2020). Compared with the uncertain factitiousness of MA, EA seems to be a more reliable approach due to the additional neuromodulation conducted by machines. It is approved that electrical stimulation from EA improves nausea and vomiting, encelialgia, delayed gastric emptying, and myoelectric activity (Sarosiek et al., 2017). TEA replaces the needles of EA with self-adhesive electrodes laid on acupoints (Qu et al., 2017) and becomes a more accepted treatment for its convenience and economy (Chen et al., 2018). Acupoints have been emphasized as crucial elements for the effects of acupuncture, and by stimulating the specific acupoints, the required efficacy can be achieved. Several studies have reviewed and concluded the most commonly used acupoints for IBS-D, including ST25, ST36, CV12, LR3, SP6, GV20, etc. (Zhu et al., 2018; Yan et al., 2019; Su et al., 2021; Zhang et al., 2022). Acupuncture has been approved to realize the symptom relief and the quality-of-life improvement in mild and moderate IBS-D according to a Delphi expert consensus (Su et al., 2021). Mechanism study of acupuncture based on IBS-related clinical trials of high quality, nevertheless, is still insufficient. The primary aim of this review is to summarize and reveal the underlying mechanisms of acupuncture treating IBS-D based on the studies published at present.

We combined RCTs with mechanism studies of acupuncture in remedying IBS-D patients in this systematic review and concluded the extant indications that were likely to provide

conceivable explanations for the curative effects of acupuncture by evidence-based evaluation. In this review, we found that a majority of RCTs laid their emphasis on brain-gut peptides, cerebral activities, neuroendocrine functions, psychological state, and inflammatory GI and hypersensitive intestinal tracts to clarify potential mechanisms of acupuncture. All ten studies pointed out that acupuncture therapies, such as MA, EA, and TEA, were of certain benefit in relieving IBS-D symptoms, and four studies reported improvement in the QOL of IBS, which was in accordance with a previous investigation (Guo J. et al., 2020) in the rough.

The IBS-D is defined as a disorder of gut-brain interaction since Rome IV came out (Drossman et al., 2018). In pace with further studies, it is also labeled as a disturbance of MGB axis (Hillestad et al., 2022), which consists of gut microbiota, intestinal epithelial barrier, neurotransmitters, enteric nervous system (ENS), central nervous system (CNS), autonomic nervous system, and hypothalamic-pituitary-adrenal (HPA) axis, participating in the bidirectional communication between gut and brain (Gros et al., 2021). At present, the available proof has attested the important role of brain-gut peptides (including neurotransmitters and GI hormones) in regulating the MGB axis on IBS-D pathophysiology, in consideration that many physiological manifestations such as GI motility abnormalities, visceral paresthesias, central disorders, and psychosocial factors (anxiety and depression) are associated with them (Mayer et al., 2019; Chen et al., 2022). Serotonin (also called 5-hydroxytriptamin, 5-HT) that serves as a critical neurotransmitter in the body and as a paracrine messenger in GI (Mittal et al., 2017) is reported to control neurological functions and modulate GI secretion, peristalsis, and absorption plus visceral hyperalgesia (Spohn and Mawe, 2017). Serotonin receptors are widely believed to play a part in anxiety and depression performances, among which the inhibition of 5-HT3R and the activation of 5-HT4R could realize anti-depressant effects (Żmudzka et al., 2018). In addition, 5-HT3R intervenes in the gut-brain communication, modulating gut motility and visceral pain signaling (Breit et al., 2018); both 5-HT3R and 5-HT4R mediate gastric accommodation (Gros et al., 2021). Imbalance in norepinephrine (NE) along with serotonin levels influences the comorbidity between emotional distress to a great extent (Chávez-Castillo et al., 2019), but relevant studies on investigating the function of NE are limited (Barandouzi et al., 2022). Intestinal NE can enhance the growth of *Escherichia coli* (*E. coli*) and promote intestinal motility to form biofilm and virulence of *E. coli* (Jubelin et al., 2018). As one of the main mediators of stress, which could be a risk factor for IBS-D, a high NE level is correlated with anxiety disorders (Gros et al., 2021). In terms of alteration in GI motility, vasoactive intestinal peptide (VIP) and substance P (SP) are bound to be mentioned, which also involve pathological reactions such as abdominal pain or discomfort, abnormal defecation, and visceral hypersensitivity (Bednarska et al., 2017). As a GI hormone, pancreatic polypeptide (PP) is deemed as a marker to evaluate vagal efferent activity (Simonian et al., 2005), and studies showed that the PP level dropped in the TEA group (Song et al., 2018). In this review, four studies demonstrated a reduction in 5-HT, 5-HT3R, 5-HT4R, VIP, and SP levels after MA/EA treatment (Zhan et al., 2014; Li, 2015; Zhao et al., 2015; Zhenzhong et al., 2015). Hu et al. (2021) found that NE levels were not changed significantly with TEA; however, the potential autonomic mechanism of it should not be ignored because factors like differences in manipulation (selection of stimulation parameters and acupoints), experimental conditions, or patient population could probably affect autonomic functions. Furthermore, TEA-induced reduction of NE showed a borderline negative correlation with improvement in abdominal pain, suggesting that over-dynamic sympathetic nerve might exert a limited function on abdominal pain.

To help understand the pathophysiological mechanisms of IBS-D, functional magnetic resonance imaging (fMRI) has been applied in a large proportion of studies, which put their emphasis on structural and functional brain connectivity (Kano et al., 2020). Some studies based on psychological abnormalities in IBS-D patients indicated a correlation between GI symptoms, severity of mentation and unusual activation of certain cerebral regions (Drossman et al., 2003) (enhanced or decreased activation in the ACC, IC and PFC (Silverman et al., 1997)). One study in this review showed decreased activation of PFC after EA treatment (Zhao et al., 2015); another study formulated that acupuncture might exert potential influence on the modulation of 5-HT pathway in insula and mood *via* ascending pathway in the higher cortical center (pulvinar and medical nucleus of the thalamus) to process pain in IBS-D (Chu et al., 2012). As for autonomic functions, NE and PP levels, which were used to reflect sympathetic activity and vagal activity, respectively, in a study (Hu et al., 2021), did not change significantly with TEA; another study showed decreased heart rate response and increased parasympathetic tone through ECG with MA. In addition, there was a significant relation between the decrease in heart rate response and increase in pain-related QOL (SF-36) in MA (Hu et al., 2021). An early trial displayed an augmented parasympathetic tone accompanied by the palpable abatement of salivary cortisol and alleviation of pain in response to acupuncture treatment, which coincides with the overactive axis in IBS-D patients (Posserud et al., 2004).

Anxiety and depression are thought to exist in 30–50% of patients with chronic GI symptoms (Lee et al., 2017) and are associated with the brain-gut axis, suggesting that more emphasis should be attached to the inspection and management of neuropsychiatric symptoms (Dao et al., 2021). Empirical evidence declares that such psychosomatic symptoms lead to a double acceleration in the morbidity of GI symptoms as well (Takajo et al., 2019). Two studies applied Hamilton Depression Rating Scale (HAMD) and/or Hamilton Anxiety Rating Scale (HAMA) to estimate the mental status of IBS-D patients and reported a pronounced decrease in scores after MA and/or EA (Zhao et al., 2015; Sun et al., 2021).

Two studies tried to validate the anti-inflammatory effect of TEA and MA through detecting cytokines. One trial assessed the serum levels of IL-6 and IL-10, which were pro-inflammatory and anti-inflammatory cytokines, respectively, and showed that

TEA treatment did not significantly change neither IL-6 nor IL-10 levels in comparison with sham TEA (Hu et al., 2021). The other trial took peripheral Th1 cytokine INF-γ and IL-2, Th2 cytokines IL-4 and IL-10 as targets and demonstrated that anti-inflammatory cytokines (IL-4, IL-10) levels were obviously elevated under acupuncture treatment, while no significant alteration was observed in pro-inflammatory cytokines (INF-γ and IL-2), verifying the upregulation effect of acupuncture on Th2 cytokines level and the recovery on imbalanced Th1/Th2 (Wu et al., 2013). It has been speculated by a previous researcher (Zhang et al., 2018) that TEA might activate peripheral nerves and deliver a signal to the center where the cerebrum processes signals and exports a stronger vagal efferent semaphore, and subsequently, the gut releases acetylcholine to make the secretion of inflammatory cytokines back to a balance. Abdominal pain and distension are typical characteristics of visceral hypersensitivity; another two studies measured the sensibility of bowels *via* proctectasia. One of them performed enhanced urgent defecation perception thresholds and maximum pain perception thresholds with EA (Zhao et al., 2015); the other study showed no distinct difference in pain tolerance, the possible reason of which was attributed to a single session of EA by the author (Chu et al., 2012). In the light of numerous findings, IBS-D has a bearing on increased irritability of esthesioneure in the gut. EA regulates intestinal motility, intestinal microflora (Song et al., 2020), visceral receptor sensitivity, and brain-gut axis (Chen et al., 2019), so as to mitigate the hypersensitive condition in irritable bowels (Hu et al., 2021).

The differential transcriptional activity caused by polymorphism in the promoter region of the gene coding 5-HTT (5-HTTLPR) was speculated to affect complicated symptoms and diseases including IBS-D and affective disorders (Goldman et al., 2010). Previous scholars have proved that 5-HTTLPR polymorphism affects the activity of serotonin reuptake transporter (SERT) and closely relates to the pathogenesis as well as symptom burdens of IBS-D (Jia et al., 2019; Zhao T. et al., 2022). One study in this review determined the 5-HTTLPR genotypes of patients before acupuncture therapy, and they were classified into three types, namely, LL, LS, and SS (L stands for long and S stands for short). The results indicated the correlation between the curative effect of MA and 5-HTTLPR polymorphism, and it was more evident in LS and SS crowds.

Limitations and Expectations

Several limitations in this review are as follows: (1) Heterogenicities among the included trials. In view of the diverse designs (acupoints protocols), outcomes, evaluation methods, and mechanisms in these studies, it is difficult to merge the cognate data for further meta-analysis. (2) Inadequate high-quality methodological studies. Critical clues such as allocation concealment and blinding of outcome assessment remain unavailable, which is possibly leading to untrustworthy results and conclusions, especially under the undefined placebo effects of acupuncture. Additionally, most included trials were performed in one country (Zhuang et al., 2013; Zheng et al., 2016; Adriani et al., 2018; Myneedu et al., 2019; Wei et al., 2019; Huang et al., 2021; Zhang et al., 2022; Zhao Y. et al., 2022), accompanied by equivocal reporting bias. (3) Ignorance of the impacts of other diseases. Most included studies focus on intestinal tract symptoms to find out the mechanism of acupuncture, thus neglecting the other factors. (4) Insufficient types of outcome evaluation methods. For instance, there is no study among these trials that utilize intestinal flora or food sensitivities as endpoints to assess the effects of acupuncture. To ameliorate these deficiencies, future studies should make more efforts in experimental design and multi-area investigation. Mechanism studies about acupuncture should lay more emphasis on the MGB axis so as to keep abreast of the latest cognition and consensus on pathophysiology in IBS-D.

CONCLUSION

In conclusion, this systematic review demonstrated the qualities and results of relevant RCTs, indicating that acupuncture therapies (MA, EA, and TEA) might improve the IBS-D symptoms through regulating brain-gut peptides, altering cerebral connectivity and activity, promoting neuroendocrine functions and mental state, and mitigating inflammation as well as hypersensitivity of bowels. In consideration that most current studies only fix their attention on one or a few focal points, the chain of evidence about mechanisms of acupuncture on IBS-D patients seems to be quite scattered. This review tried to summarize and integrate existing evidence through available RCTs, hoping to provide acupuncturists and researchers with some reliable information about the mechanisms of acupuncture on IBS-D.

DATA AVAILABILITY STATEMENT

The original contributions presented in this study are included in the article/**Supplementary Material**, further inquiries can be directed to the corresponding authors.

AUTHOR CONTRIBUTIONS

XS designed the review protocol. GZ conducted the literature research and drafted the manuscript. GZ and TZ contributed to the data extraction. ZC and ZT contributed to the quality assessment. TW and MY contributed to the methodological guidance. XS and WW contributed to the critical revision of the manuscript. All authors contributed to the article and approved the submitted version.

FUNDING

This article is supported by funds as follows: (1) National Natural Science Foundation of China (NSFC) Projects of International Cooperation (NO.81820108033); (2) The General Program of NSFC (NO.81573806); and (3) National Key Technology Research and Development Program during the "12th Five-Year Plan" of the Ministry of Science and Technology (MOST)

of the People's Republic of China (NO.2013BAI02B00). As the main channels for supporting basic research in China, the NSFC series and MOST are oriented to the whole country, focusing on funding researchers in colleges, universities and institutions with eligible research condition and strength.

SUPPLEMENTARY MATERIAL

The Supplementary Material for this article can be found online at: https://www.frontiersin.org/articles/10.3389/fnins.2022.918701/full#supplementary-material

REFERENCES

Adriani, A., Ribaldone, D. G., Astegiano, M., Durazzo, M., Saracco, G. M., and Pellicano, R. (2018). Irritable bowel syndrome: the clinical approach. *Panminerva Med.* 60, 213–222. doi: 10.23736/S0031-0808.18.03541-3

Barandouzi, Z. A., Lee, J., Del Carmen Rosas, M., Chen, J., Henderson, W. A., Starkweather, A. R., et al. (2022). Associations of neurotransmitters and the gut microbiome with emotional distress in mixed type of irritable bowel syndrome. *Sci. Rep.* 12:1648. doi: 10.1038/s41598-022-05756-0

Bednarska, O., Walter, S. A., Casado-Bedmar, M., Ström, M., Salvo-Romero, E., Vicario, M., et al. (2017). Vasoactive Intestinal Polypeptide and Mast Cells Regulate Increased Passage of Colonic Bacteria in Patients With Irritable Bowel Syndrome. *Gastroenterology* 153, 948–960.e3. doi: 10.1053/j.gastro.2017.06.051

Böhmelt, A. H., Nater, U. M., Franke, S., Hellhammer, D. H., and Ehlert, U. (2005). Basal and stimulated hypothalamic-pituitary-adrenal axis activity in patients with functional gastrointestinal disorders and healthy controls. *Psychosom. Med.* 67, 288–294. doi: 10.1097/01.psy.0000157064.72831.ba

Bonetto, S., Fagoonee, S., Battaglia, E., Grassini, M., Saracco, G. M., and Pellicano, R. (2021). Recent advances in the treatment of irritable bowel syndrome. *Pol. Arch. Intern. Med.* 131, 709–715. doi: 10.20452/pamw.16067

Breit, S., Kupferberg, A., Rogler, G., and Hasler, G. (2018). Vagus Nerve as Modulator of the Brain-Gut Axis in Psychiatric and Inflammatory Disorders. *Front. Psychiatry* 9:44. doi: 10.3389/fpsyt.2018.00044

Chávez-Castillo, M., Núñez, V., Nava, M., Ortega, Á, Rojas, M., Bermúdez, V., et al. (2019). Depression as a Neuroendocrine Disorder: emerging Neuropsychopharmacological Approaches beyond Monoamines. *Adv. Pharmacol. Sci.* 2019:7943481. doi: 10.1155/2019/7943481

Chen, J. D. Z., Ni, M., and Yin, J. (2018). Electroacupuncture treatments for gut motility disorders. *Neurogastroenterol. Motil.* 30:e13393. doi: 10.1111/nmo.13393

Chen, M., Ruan, G., Chen, L., Ying, S., Li, G., Xu, F., et al. (2022). Neurotransmitter and Intestinal Interactions: focus on the Microbiota-Gut-Brain Axis in Irritable Bowel Syndrome. *Front. Endocrinol.* 13:817100. doi: 10.3389/fendo.2022.817100

Chen, Y., Zhao, Y., Luo, D. N., Zheng, H., Li, Y., and Zhou, S. Y. (2019). Electroacupuncture Regulates Disorders of Gut-Brain Interaction by Decreasing Corticotropin-Releasing Factor in a Rat Model of IBS. *Gastroenterol. Res. Pract.* 2019:1759842. doi: 10.1155/2019/1759842

Chu, W. C., Wu, J. C., Yew, D. T., Zhang, L., Shi, L., Yeung, D. K., et al. (2012). Does acupuncture therapy alter activation of neural pathway for pain perception in irritable bowel syndrome?: a comparative study of true and sham acupuncture using functional magnetic resonance imaging. *J. Neurogastroenterol. Motil.* 18, 305–316. doi: 10.5056/jnm.2012.18.3.305

Dao, V. H., Hoang, L. B., Trinh, T. O., Tran, T. T. T., and Dao, V. L. (2021). Psychobiotics for Patients with Chronic Gastrointestinal Disorders Having Anxiety or Depression Symptoms. *J. Multidiscip. Healthc.* 14, 1395–1402. doi: 10.2147/JMDH.S312316

De Ponti, F. (2013). Drug development for the irritable bowel syndrome: current challenges and future perspectives. *Front. Pharmacol.* 4:7. doi: 10.3389/fphar.2013.00007

Drossman, D. A., and Hasler, W. L. (2016). Rome IV-Functional GI Disorders: disorders of Gut-Brain Interaction. *Gastroenterology* 150, 1257–1261. doi: 10.1053/j.gastro.2016.03.035

Drossman, D. A., Ringel, Y., Vogt, B. A., Leserman, J., Lin, W., Smith, J. K., et al. (2003). Alterations of brain activity associated with resolution of emotional distress and pain in a case of severe irritable bowel syndrome. *Gastroenterology* 124, 754–761. doi: 10.1053/gast.2003.50103

Drossman, D. A., Tack, J., Ford, A. C., Szigethy, E., Törnblom, H., and Van Oudenhove, L. (2018). Neuromodulators for Functional Gastrointestinal Disorders (Disorders of Gut-Brain Interaction): a Rome Foundation Working Team Report. *Gastroenterology* 154, 1140–1171.e1. doi: 10.1053/j.gastro.2017.11.279

Goldman, N., Glei, D. A., Lin, Y. H., and Weinstein, M. (2010). The serotonin transporter polymorphism (5-HTTLPR): allelic variation and links with depressive symptoms. *Depress Anxiety* 27, 260–269. doi: 10.1002/da.20660

Gros, M., Gros, B., Mesonero, J. E., and Latorre, E. (2021). Neurotransmitter Dysfunction in Irritable Bowel Syndrome: emerging Approaches for Management. *J. Clin. Med.* 10:3429. doi: 10.3390/jcm10153429

Grundmann, O., and Yoon, S. L. (2014). Complementary and alternative medicines in irritable bowel syndrome: an integrative view. *World J. Gastroenterol.* 20, 346–362. doi: 10.3748/wjg.v20.i2.346

Guo, J., Sun, J. H., Chen, L., Geng, H., Wu, X. L., Song, Y. F., et al. (2021). Correlation between curative effect and 5-HTTLPR polymorphism in treatment of diarrhea-predominant irritable bowel syndrome with acupuncture for regulating shen and strengthening spleen. *Zhongguo Zhen Jiu* 41, 365–370. doi: 10.13703/j.0255-2930.20200313-k0002

Guo, J., Xing, X., Wu, J., Zhang, H., Yun, Y., Qin, Z., et al. (2020). Acupuncture for Adults with Diarrhea-Predominant Irritable Bowel Syndrome or Functional Diarrhea: a Systematic Review and Meta-Analysis. *Neural Plast.* 2020:8892184. doi: 10.1155/2020/8892184

Guo, Y., Wei, W., and Chen, J. D. (2020). Effects and mechanisms of acupuncture and electroacupuncture for functional dyspepsia: a systematic review. *World J. Gastroenterol.* 26, 2440–2457. doi: 10.3748/wjg.v26.i19.2440

Hillestad, E. M. R., van der Meeren, A., Nagaraja, B. H., Bjørsvik, B. R., Haleem, N., Benitez-Paez, A., et al. (2022). Gut bless you: the microbiota-gut-brain axis in irritable bowel syndrome. *World J. Gastroenterol.* 28, 412–431. doi: 10.3748/wjg.v28.i4.412

Hu, P., Sun, K., Li, H., Qi, X., Gong, J., Zhang, Y., et al. (2021). Transcutaneous Electrical Acustimulation Improved the Quality of Life in Patients With Diarrhea-Irritable Bowel Syndrome. *Neuromodulation* [Epub ahead of print]. doi: 10.1016/j.neurom.2021.10.009

Huang, J., Lu, M., Zheng, Y., Ma, J., Ma, X., Wang, Y., et al. (2021). Quality of Evidence Supporting the Role of Acupuncture for the Treatment of Irritable Bowel Syndrome. *Pain Res. Manag.* 2021:2752246. doi: 10.1155/2021/2752246

Jia, Z., Wang, L., Yu, B., Li, Q., and Dong, X. (2019). Association between polymorphisms in the serotonin transporter gene-linked polymorphic region and risk for irritable bowel syndrome in China: evidence based on a meta-analysis. *J. Int. Med. Res.* 47, 2810–2818. doi: 10.1177/0300060519859144

Jubelin, G., Desvaux, M., Schüller, S., Etienne-Mesmin, L., Muniesa, M., and Blanquet-Diot, S. (2018). Modulation of Enterohaemorrhagic *Escherichia coli* Survival and Virulence in the Human Gastrointestinal Tract. *Microorganisms* 6:115. doi: 10.3390/microorganisms6040115

Kano, M., Grinsvall, C., Ran, Q., Dupont, P., Morishita, J., Muratsubaki, T., et al. (2020). Resting state functional connectivity of the pain matrix and default mode network in irritable bowel syndrome: a graph theoretical analysis. *Sci. Rep.* 10:11015. doi: 10.1038/s41598-020-67048-9

Kumar, S., Singh, P., and Kumar, A. (2022). Targeted therapy of irritable bowel syndrome with anti-inflammatory cytokines. *Clin. J. Gastroenterol.* 15, 1–10. doi: 10.1007/s12328-021-01555-8

Labus, J. S., Osadchiy, V., Hsiao, E. Y., Tap, J., Derrien, M., Gupta, A., et al. (2019). Evidence for an association of gut microbial Clostridia with brain functional connectivity and gastrointestinal sensorimotor function in patients with irritable bowel syndrome, based on tripartite network analysis. *Microbiome* 7:45. doi: 10.1186/s40168-019-0656-z

Lee, C., Doo, E., Choi, J. M., Jang, S. H., Ryu, H. S., Lee, J. Y., et al. (2017). Brain-Gut Axis Research Group of Korean Society of Neurogastroenterology and Motility. The Increased Level of Depression and Anxiety in Irritable Bowel Syndrome Patients Compared with Healthy Controls: systematic Review and Meta-analysis. *J. Neurogastroenterol. Motil.* 23, 349–362. doi: 10.5056/jnm16220

Li, Y. C. (2015). Clinical Study of Ascending-descending Acupuncture Method Regulation of the Spleen and Stomach for Treatment of Spleen Deficiency-type Diarrhea in Irritable Bowel Syndrome. *Shang. J. Acupunct. Moxibustion* 34, 25–27. doi: 10.13460/j.issn.1005-0957.2015.01.0025

Lowe, C., Aiken, A., Day, A. G., Depew, W., and Vanner, S. J. (2017). Sham acupuncture is as efficacious as true acupuncture for the treatment of IBS: a randomized placebo controlled trial. *Neurogastroenterol. Motil.* 29:e13040. doi: 10.1111/nmo.13040

Manheimer, E., Cheng, K., Wieland, L. S., Min, L. S., Shen, X., Berman, B. M., et al. (2012). Acupuncture for treatment of irritable bowel syndrome. *Cochrane Database Syst. Rev.* 5:CD005111. doi: 10.1002/14651858.CD005111.pub3

Mayer, E. A., Labus, J., Aziz, Q., Tracey, I., Kilpatrick, L., Elsenbruch, S., et al. (2019). Role of brain imaging in disorders of brain-gut interaction: a Rome Working Team Report. *Gut* 68, 1701–1715. doi: 10.1136/gutjnl-2019-318308

Mearin, F., Lacy, B. E., Chang, L., Chey, W. D., Lembo, A. J., Simren, M., et al. (2016). Bowel Disorders. *Gastroenterology* [Epub ahead of print]. doi: 10.1053/j.gastro.2016.02.031

Mittal, R., Debs, L. H., Patel, A. P., Nguyen, D., Patel, K., O'Connor, G., et al. (2017). Neurotransmitters: the Critical Modulators Regulating Gut-Brain Axis. *J. Cell. Physiol.* 232, 2359–2372. doi: 10.1002/jcp.25518

Myneedu, K., Deoker, A., Schmulson, M. J., and Bashashati, M. (2019). Fecal microbiota transplantation in irritable bowel syndrome: a systematic review and meta-analysis. *United European Gastroenterol. J.* 7, 1033–1041. doi: 10.1177/2050640619866990

Nguyen, L. (2018). Complementary and Alternative Medicine for the Management of Irritable Bowel Syndrome. *Gastroenterol. Hepatol.* 14, 536–538.

Nisticò, V., Rossi, R. E., D'Arrigo, A. M., Priori, A., Gambini, O., and Demartini, B. (2022). Functional Neuroimaging in Irritable Bowel Syndrome: a Systematic Review Highlights Common Brain Alterations With Functional Movement Disorders. *J. Neurogastroenterol. Motil.* 28, 185–203. doi: 10.5056/jnm21079

Nozu, T., and Okumura, T. (2022). Pathophysiological Commonality Between Irritable Bowel Syndrome and Metabolic Syndrome: role of Corticotropin-releasing Factor-Toll-like Receptor 4-Proinflammatory Cytokine Signaling. *J. Neurogastroenterol. Motil.* 28, 173–184. doi: 10.5056/jnm21002

Oka, P., Parr, H., Barberio, B., Black, C. J., Savarino, E. V., and Ford, A. C. (2020). Global prevalence of irritable bowel syndrome according to Rome III or IV criteria: a systematic review and meta-analysis. *Lancet Gastroenterol. Hepatol.* 5, 908–917. doi: 10.1016/S2468-1253(20)30217-X

Posserud, I., Agerforz, P., Ekman, R., Björnsson, E. S., Abrahamsson, H., and Simrén, M. (2004). Altered visceral perceptual and neuroendocrine response in patients with irritable bowel syndrome during mental stress. *Gut* 53, 1102–1108. doi: 10.1136/gut.2003.017962

Qu, F., Li, R., Sun, W., Lin, G., Zhang, R., Yang, J., et al. (2017). Use of electroacupuncture and transcutaneous electrical acupoint stimulation in reproductive medicine: a group consensus. *J. Zhejiang Univ. Sci. B* 18, 186–193. doi: 10.1631/jzus.B1600437

Sarosiek, I., Song, G., Sun, Y., Sandoval, H., Sands, S., Chen, J., et al. (2017). Central and Peripheral Effects of Transcutaneous Acupuncture Treatment for Nausea in Patients with Diabetic Gastroparesis. *J. Neurogastroenterol. Motil.* 23, 245–253. doi: 10.5056/jnm16097

Schneider, A., Weiland, C., Enck, P., Joos, S., Streitberger, K., Maser-Gluth, C., et al. (2007). Neuroendocrinological effects of acupuncture treatment in patients with irritable bowel syndrome. *Complement. Ther. Med.* 15, 255–263. doi: 10.1016/j.ctim.2006.12.002

Silverman, D. H., Munakata, J. A., Ennes, H., Mandelkern, M. A., Hoh, C. K., and Mayer, E. A. (1997). Regional cerebral activity in normal and pathological perception of visceral pain. *Gastroenterology.* 112, 64–72. doi: 10.1016/s0016-5085(97)70220-8

Simonian, H. P., Kresge, K. M., Boden, G. H., and Parkman, H. P. (2005). Differential effects of sham feeding and meal ingestion on ghrelin and pancreatic polypeptide levels: evidence for vagal efferent stimulation mediating ghrelin release. *Neurogastroenterol Motil.* 17, 348–354. doi: 10.1111/j.1365-2982.2004.00634.x

Song, G., Sun, Y., Bashashati, M., Quezada, A., Sigaroodi, S., Sarosiek, I., et al. (2018). Efficacy of needleless transcutaneous electroacupuncture in synchronization with breathing for symptomatic idiopathic gastroparesis: a blinded and controlled acute treatment trial. *Neurogastroenterol Motil.* 30, e13361. doi: 10.1111/nmo.13361

Song, Y. F., Pei, L. X., Chen, L., Geng, H., Yuan, M. Q., Xu, W. L., et al. (2020). Electroacupuncture Relieves Irritable Bowel Syndrome by Regulating IL-18 and Gut Microbial Dysbiosis in a Trinitrobenzene Sulfonic Acid-Induced Post-Inflammatory Animal Model. *Am J Chin Med.* 48, 77–90. doi: 10.1142/S0192415X20500044

Spohn, S. N., and Mawe, G. M. (2017). Non-conventional features of peripheral serotonin signalling - the gut and beyond. *Nat Rev Gastroenterol Hepatol.* 14, 412–420. doi: 10.1038/nrgastro.2017.51

Su, X. T., Wang, L. Q., Zhang, N., Li, J. L., Qi, L. Y., Wang, Y., et al. (2021). Standardizing and optimizing acupuncture treatment for irritable bowel syndrome: a Delphi expert consensus study. *Integr Med Res.* 10, 100728. doi: 10.1016/j.imr.2021.100728

Sun, Y. Z., Wang, S. L., and Yu, T. Y. (2021). [Tiaoshen acupuncture method combined with electroacupuncture for diarrhea-type irritable bowel syndrome : a randomized controlled trial]. *Zhongguo Zhen Jiu.* 41, 13–16. doi: 10.13703/j.0255-2930.20191220-k0001

Takajo, T., Tomita, K., Tsuchihashi, H., Enomoto, S., Tanichi, M., Toda, H., et al. (2019). Depression Promotes the Onset of Irritable Bowel Syndrome through Unique Dysbiosis in Rats. *Gut Liver.* 13, 325–332. doi: 10.5009/gnl18296

Tang, H. Y., Jiang, A. J., Wang, X. Y., Wang, H., Guan, Y. Y., Li, F., et al. (2021). Uncovering the pathophysiology of irritable bowel syndrome by exploring the gut-brain axis: a narrative review. *Ann Transl Med.* 9, 1187. doi: 10.21037/atm-21-2779

Wei, D., Xie, L., Zhuang, Z., Zhao, N., Huang, B., Tang, Y., et al. (2019). Gut Microbiota: a New Strategy to Study the Mechanism of Electroacupuncture and Moxibustion in Treating Ulcerative Colitis. *Evid Based Complement Alternat Med.* 2019, 9730176. doi: 10.1155/2019/9730176

Wu, X. L., Wang, Y. L., Sun, J. H., Shu, Y. Y., Pei, L. X., Zhou, J. L., et al. (2013). [Clinical observation on acupuncture for diarrhea-predominant irritable bowel syndrome patients in syndrome of liver-stagnation and spleen-deficiency and its impact on Th1/Th2]. *Zhongguo Zhen Jiu.* 33, 1057–1060. doi: 10.13703/j.0255-2930.2013.12.003

Yaklai, K., Pattanakuhar, S., Chattipakorn, N., and Chattipakorn, S. C. (2021). The Role of Acupuncture on the Gut-Brain-Microbiota Axis in Irritable Bowel Syndrome. *Am J Chin Med.* 49, 285–314. doi: 10.1142/S0192415X21500154

Yan, J., Miao, Z. W., Lu, J., Ge, F., Yu, L. H., Shang, W. B., et al. (2019). Acupuncture plus Chinese Herbal Medicine for Irritable Bowel Syndrome with Diarrhea: a Systematic Review and Meta-Analysis. *Evid Based Complement Alternat Med.* 2019, 7680963. doi: 10.1155/2019/7680963

Zhan, D. W., Sun, J. H., Luo, K. T., Xu, L. Z., Zhou, J. L., Pei, L. X., et al. (2014). [Effects and efficacy observation of acupuncture on serum 5-HT in patients with diarrhea-predominant irritable bowel syndrome]. *Zhongguo Zhen Jiu.* 34, 135–138. doi: 10.13703/j.0255-2930.2014.02.009

Zhang, B., Shi, H., Cao, S., Xie, L., Ren, P., Wang, J., et al. (2022). Revealing the magic of acupuncture based on biological mechanisms: a literature review. *Biosci Trends.* 16, 73–90. doi: 10.5582/bst.2022.01039

Zhang, B., Xu, F., Hu, P., Zhang, M., Tong, K., Ma, G., et al. (2018). Needleless Transcutaneous Electrical Acustimulation: a Pilot Study Evaluating Improvement in Post-Operative Recovery. *Am J Gastroenterol.* 113, 1026–1035. doi: 10.1038/s41395-018-0156-y

Zhao, J. M., Lu, J. H., Yin, X. J., Chen, X. K., Chen, Y. H., Tang, W. J., et al. (2015). Comparison of electroacupuncture and moxibustion on brain-gut function in patients with diarrhea-predominant irritable bowel syndrome: a randomized controlled trial. *Chin J Integr Med.* 21, 855–865.

Zhao, T., Zhang, Y., Lee, J., Starkweather, A. R., Young, E. E., and Cong, X. (2022). The Associations of Single Nucleotide Polymorphisms with Risk and Symptoms of Irritable Bowel Syndrome. *J Pers Med.* 12, 142. doi: 10.3390/jpm12020142

Zhao, Y., Jiang, H. L., Shi, Y., Zhang, W., Zhang, L. X., Hou, Y. J., et al. (2022). Electroacupuncture Alleviates Visceral Hypersensitivity in IBS-D Rats by Inhibiting EGCs Activity through Regulating BDNF/TrkB Signaling Pathway. *Evid Based Complement Alternat Med.* 2022, 2497430. doi: 10.1155/2022/2497430

Zheng, Y., Zhang, J., Wang, Y., Wang, Y., Lan, Y., Qu, S., et al. (2016). Acupuncture Decreases Blood Pressure Related to Hypothalamus Functional Connectivity with Frontal Lobe, Cerebellum, and Insula: a Study of Instantaneous and Short-Term Acupuncture Treatment in Essential Hypertension. *Evid Based Complement Alternat Med.* 2016, 6908710. doi: 10.1155/2016/6908710

Zhenzhong, L., Xiaojun, Y., Weijun, T., Yuehua, C., Jie, S., Jimeng, Z., et al. (2015). Comparative effect of electroacupuncture and moxibustion on the expression

of substance P and vasoactive intestinal peptide in patients with irritable bowel syndrome. *J Tradit Chin Med.* 35, 402–410. doi: 10.1016/s0254-6272(15)30116-3

Zhu, L., Ma, Y., Ye, S., and Shu, Z. (2018). Acupuncture for Diarrhoea-Predominant Irritable Bowel Syndrome: a Network Meta-Analysis. *Evid Based Complement Alternat Med.* 2018, 2890465. doi: 10.1155/2018/2890465

Zhuang, Y., Xing, J. J., Li, J., Zeng, B. Y., and Liang, F. R. (2013). History of acupuncture research. *Int Rev Neurobiol.* 111, 1–23. doi: 10.1016/B978-0-12-411545-3.00001-8

Żmudzka, E., Sałaciak, K., Sapa, J., and Pytka, K. (2018). Serotonin receptors in depression and anxiety: insights from animal studies. *Life Sci.* 210, 106–124. doi: 10.1016/j.lfs.2018.08.050

Conflict of Interest: The authors declare that the research was conducted in the absence of any commercial or financial relationships that could be construed as a potential conflict of interest.

The reviewer YW declared a shared affiliation with the authors at the time of review.

Publisher's Note: All claims expressed in this article are solely those of the authors and do not necessarily represent those of their affiliated organizations, or those of the publisher, the editors and the reviewers. Any product that may be evaluated in this article, or claim that may be made by its manufacturer, is not guaranteed or endorsed by the publisher.

frontiers | Frontiers in Neuroscience

TYPE Original Research
PUBLISHED 05 August 2022
DOI 10.3389/fnins.2022.931161

OPEN ACCESS

EDITED BY
Xiaoming Jin,
Indiana University–Purdue University Indianapolis, United States

REVIEWED BY
Jinhui Liu,
Nanjing Medical University, China
Chelsea Hutch,
University of Michigan, United States

*CORRESPONDENCE
Qing Shu
shuqingj@whu.edu.cn

†These authors have contributed equally to this work and share first authorship

SPECIALTY SECTION
This article was submitted to Gut-Brain Axis, a section of the journal Frontiers in Neuroscience

RECEIVED 28 April 2022
ACCEPTED 07 July 2022
PUBLISHED 05 August 2022

CITATION
Shao Y, Tian J, Yang Y, Hu Y, Zhu Y and Shu Q (2022) Identification of key genes and pathways revealing the central regulatory mechanism of brain-derived glucagon-like peptide-1 on obesity using bioinformatics analysis. *Front. Neurosci.* 16:931161. doi: 10.3389/fnins.2022.931161

Identification of key genes and pathways revealing the central regulatory mechanism of brain-derived glucagon-like peptide-1 on obesity using bioinformatics analysis

Yuwei Shao[1†], Jun Tian[1†], Yanan Yang[2], Yan Hu[1], Ye Zhu[3] and Qing Shu[1*]

[1]Department of Rehabilitation, Zhongnan Hospital of Wuhan University, Wuhan, China, [2]Department of Traditional Chinese Medicine, China Resources Wugang General Hospital, Wuhan, China, [3]College of Health Sciences, Wuhan Sports University, Wuhan, China

Objective: Central glucagon-like peptide-1 (GLP-1) is a target in treating obesity due to its effect on suppressing appetite, but the possible downstream key genes that GLP-1 regulated have not been studied in depth. This study intends to screen out the downstream feeding regulation genes of central GLP-1 neurons through bioinformatics analysis and verify them by chemical genetics, which may provide insights for future research.

Materials and methods: GSE135862 genetic expression profiles were extracted from the Gene Expression Omnibus (GEO) database. The gene ontology (GO) and Kyoto Encyclopedia of Genes and Genomes pathway (KEGG) enrichment analyses were carried out. STRING database and Cytoscape software were used to map the protein-protein interaction (PPI) network of the differentially expressed genes (DEGs). After bioinformatics analysis, we applied chemogenetic methods to modulate the activities of GLP-1 neurons in the nucleus tractus solitarius (NTS) and observed the alterations of screened differential genes and their protein expressions in the hypothalamus under different excitatory conditions of GLP-1 neurons.

Results: A total of 49 DEGs were discovered, including 38 downregulated genes and 11 upregulated genes. The two genes with the highest expression scores were *biglycan* (*Bgn*) and *mitogen-activated protein kinase activated protein kinase 3* (*Mapkapk3*). The results of GO analysis showed that there were 10 molecular functions of differential genes. Differential genes were mainly localized in seven regions around the cells, and enriched in 10 biology processes. The results of the KEGG signaling pathway enrichment analysis showed that differential genes played an important role in seven pathways. The top 15 genes selected according to the Cytoscape software included *Bgn* and *Mapkapk3*. Chemogenetic activation of GLP-1 in NTS induced a decrease in food intake and body mass, while chemogenetic inhibition

induced the opposite effect. The gene and protein expression of GLP-1 were upregulated in NTS when activated by chemogenetics. In addition, the expression of Bgn was upregulated and that of Mapkapk3 was downregulated in the hypothalamus.

Conclusion: Our data showed that GLP-1 could modulate the protein expression of Bgn and Mapkapk3. Our findings elucidated the regulatory network in GLP-1 to obesity and might provide a novel diagnostic and therapeutic target for obesity.

KEYWORDS

glucagon-like peptide-1 (GLP-1), appetite, obesity, bioinformatics, chemical genetics

Introduction

Over the past 40 years, the prevalence of obesity has increased substantially worldwide. The prevalence in children increased from less than 1% in 1975 to 6 to 8% in 2016, in adult males increased from 3 to 11%, and in adult females increased from 6 to 15% during the same period (Jaacks et al., 2019). China has the highest number of obese people in the world, with about 46% of adults and 15% of children suffering from obesity or being overweight (Wang et al., 2019). As one of the most important risk factors for diabetes, cardiovascular disease, cancer, osteoarthritis, movement disorders, and sleep apnea, obesity seriously affects human health (Seidell and Halberstadt, 2015). One of the most effective solutions to obesity is to control appetite and reduce caloric intake (Bray and Siri-Tarino, 2016). Various therapies have shown efficacy to treat obesity, including pharmacotherapy (Narayanaswami and Dwoskin, 2017), operation therapy (Nudel and Sanchez, 2019), and even traditional Chinese medicine (TCM) (Santos et al., 2020; Ni et al., 2021).

Appetite is regulated by a complex system of central and peripheral signals that interact to modulate an individual's response to nutrition. Peripheral regulation includes satiety signaling and adiposity signaling, whereas central regulation is accomplished by a variety of factors, including the neuropeptidergic, monoaminergic, and endocannabinoid systems. Satiety signals mainly include cholecystokinin (CCK), GLP-1, and casein tyrosine (Valassi et al., 2008).

Glucagon-like peptide 1 is an intestinal hormone that is released in response to food intake. It can enhance the stimulation of insulin synthesis and secretion by glucose while inhibiting the secretion of glucagon and delaying gastric emptying (D'Alessio, 2016). GLP-1 exerts an inhibitory effect on food intake *via* its receptor GLP-1R, which is widely distributed in the brain, gastrointestinal tract, and pancreas (Fakhry et al., 2017). In clinical practice, medication and surgery are widely used. The mechanisms of these interventions in treating obesity are all related to the regulation of GLP-1 (Albaugh et al., 2019; Luo et al., 2020). Some non-pharmaceutical TCM therapies, such as acupuncture, have also shown the potential to affect metabolism by modulating GLP-1 (Firouzjaei et al., 2016). GLP-1 is well-known to medical workers as an important hormone in appetite regulatory pathways, but little is known about how they act in the central nervous system and peripheral nervous system to produce enhanced satiety and inhibit appetite mechanisms. At present, high-throughput gene chip technology and bioinformatics analysis have been widely used in the pathogenesis of diseases, molecular diagnosis, and other aspects (Huang et al., 2018). New scientific and technological methods represented by genomics approaches provide a large amount of research data for mechanistic studies of appetite regulation. Therefore, in this study, we used high-throughput sequencing data from public platforms to decipher the central regulatory mechanism of GLP-1R agonist (GLP1-RA) administration through a bioinformatics approach. Overall, this study advances our understanding of the central mechanisms that synergize the inhibitory effects of appetite and body weight to treat obesity and provides a basis for further research.

Abbreviations: GLP-1, glucagon-like peptide 1; GEO, gene expression omnibus; GO, gene ontology; KEGG, Kyoto encyclopedia of genes and genomes pathway; PPI, protein-protein interaction; DEGs, differentially expressed genes; NTS, nucleus tractus solitarius; Bgn, biglycan; Mapkapk3, mitogen-activated protein kinase activated protein kinase 3; TCM, traditional Chinese medicine; CCK, cholecystokinin; GLP1-RA, GLP-1 receptor agonist; RIP-Seq, RNA co-immunoprecipitation combined with high-throughput sequencing; DVC, dorsal vagal complex; MBH, medial basal hypothalamus; logFC, log value of gene fold change; BP, biological process; MF, molecular function; CC, cellular component; FDR, false discovery rate; MCC, maximal clique centrality; rAAV, adeno-associated virus; cre, cyclization recombination enzyme; CNO, clozapine-N-oxide; WB, Western blotting; RT-qPCR, reverse transcription-quantitative polymerase chain reaction; cDNA, complementary DNA; IF, immunofluorescence; IOD, integrated optical density; AP, posterior area; ECM, extracellular matrix; Erk1/2, extracellular signal-regulated kinase; JNK, c-Jun N-terminal kinase.

Materials and methods

Gene chip data acquisition

The high-throughput dataset GSE135862 related to the mechanisms of appetite regulation by GLP-1/CCK was retrieved and downloaded from GEO, a comprehensive database of gene expression. The chip contains a total of 48 samples. All of the studies were conducted in 9- to 10-week-old C57/Bl6 male mice, which were maintained on standard chow and fasted for 6 h before treatment administration. Multiple variables such as injection of drugs, injection sites, and group settings were included in the experimental conditions. Mice were randomized into treatment groups and received an IP injection of saline, AC710222, exenatide, AC3174, AC170222, or a combination of these drugs twice daily for 5 days. The injection sites were the dorsal vagal complex (DVC) and the medial basal hypothalamus (MBH), respectively. The experimental content is RIP-Seq (RNA co-immunoprecipitation combined with high-throughput sequencing). The purpose of this study was to investigate the pathway of GLP-1 in the brain. In this study, we selected the groups injected with GLP1-RA AC3174 and the blank control group for data comparison and analysis.

Screening of differentially expressed genes

Samples injected with drug as saline were set as the control group and samples injected with drug as GLP1-RA were set as the intervention group using $P < 0.05$, log value of gene fold change (logFC) <-1, or logFC > 1 as the criterion (Zhang et al., 2019). The GSE135862 dataset was analyzed by the R language DESeq2 package to screen differentially expressed genes between different groups of the dataset and find out differentially expressed genes that may be involved in the regulation of appetite by GLP-1R.

Gene ontology and Kyoto encyclopedia of genes and genomes pathway enrichment analysis of differentially expressed genes

Gene ontology is a commonly used analytical method whose main function is to annotate genes or their products and identify the characteristic biological characteristics of high-throughput genomic or transcriptome data. GO annotates and classifies genes according to Biological Process (BP), Molecular Function (MF), and Cellular Component (CC). The KEGG database is available for querying pathway information and signaling pathway retrieval, and so on. The main goal of the KEGG database is to endow genes and genomes with functional significance at the molecular level and higher levels, which establish links between genes in the genome and advanced functions of cells and organisms (Kanehisa et al., 2016, 2017). This study used the DAVID (version: 6.8)[1] database for integrative analysis. Using Fisher Exact or EASE Score statistical methods, GO items were screened with $P < 0.05$, false discovery rate (FDR) <1, and KEGG items with $P < 0.05$ (Sherman et al., 2007).

Analysis of differentially expressed gene protein interaction network

STRING (version: 11.5)[2] is an online analysis tool that can be used to present and evaluate interactions between proteins (Szklarczyk et al., 2019). The magnitude of the likelihood of a protein is evaluated by scoring its mutual-action network. In this study, the analyzed differential genes were input into the STRING analysis tool to find potential links between them. The screening condition for constructing the interaction network of differentially gene-encoded proteins was the threshold of interaction likelihood. The STRING database export results were then imported into Cytoscape 3.9.1 software for visual analysis. The cytoHubba plugin in the software was used to find out the top 15 hub genes scored according to the Maximal Clique Centrality (MCC) and Degree scoring methods, respectively (Hu and Chan, 2013).

Preparation of recombinant adeno-associated virus

Promoter sequences of GLP-1 protein were determined by searching the gene database and published relevant literature (Rasouli et al., 2011; Shi et al., 2017). Customized recombinant adeno-associated virus (rAAV), which included GLP-1 promoter and cyclization recombination enzyme (cre) applied in this experiment, was provided by Wuhan BrainVTA Technology Co., Ltd. The sequences of the other three rAAVs are as follows: rAAV-Efla-DIO-EGFP-WPRE-pA (rAAV-GFP), rAAV-hSyn-DIO-hM3D (Gq) -mCherry-WPRE-pA (rAAV-HM3D), and rAAV-hSyn-DIO-hM4D (Gi) -mCherry-WPRE-pA (rAAV-HM4D), which were purchased from commercial companies (BrainVTA Co., Ltd, Wuhan, China).

1 https://david.ncifcrf.gov/
2 https://cn.string-db.org/

Animals and intervention

We acquired 15 male Sprague–Dawley rats, aged 6 weeks, and weighing 180 to 200 g from Beijing Vital River Laboratory Animal Technology Co., Ltd. (Beijing, China, No. 11400700298971). All rats were placed in a controlled environment at 22 ± 2°C and 50 ± 10% relative humidity with a 12-h light/12-h dark cycle in the Experimental Animal Center, Zhongnan Hospital of Wuhan University, with standard food and water provided *ad libitum* for the duration of the study. The study protocol was authorized by the Institutional Animal Care and Use Committee of Wuhan University, Wuhan City, Hubei Province, China (AUP Number: WP2020-08085).

After 1 week of adaptive feeding, all rats were numbered according to body weight, and 15 rats were divided into the GLP-1 group (n = 5), HM3D group (n = 5), and HM4D group (n = 5) by stratified randomization. Stereotactic injection of NTS was performed according to validated parameters (AP: Lambda-3.2 mm, ML: ± 0.5–0.7 mm, DV: 9.6 mm, and oblique angle backward 24°) for injection (Shu et al., 2020). Rats in each group were injected with rAAV as follows: rats in the GLP-1 group were injected with rAAV-GLP-1 and rAAV-GFP into NTS with 260 nl of each rAAV; rats in the HM3D group were injected with rAAV-GLP-1 and rAAV-3D into NTS, 260 nl of each rAAV; and rats in HM4D group were injected with rAAV-GLP-1 and rAAV-4D, 260 nl of each rAAV. The chronological order of injection was based on the body weight of the rats, and the rats whose body weight first reached about 400 g were injected first, and finally, the NTS virus injection was completed in all rats at about 5 days. All rats were observed for 1 week after the completion of the injection, with the supplement of food and water *ad libitum* during the observation period. Specific rAAV gene sequence and combinatorial strategy were shown in **Figure 1**. Three weeks after rAAV injection in all rats, the exogenous gene carried by rAAV was expressed in target neurons. We collected the baseline data of all rats (body mass, lee's index, and 24 h food intake) 3 weeks after the injection of the last rat, and assigned this day as day 0. Rats in all three groups received four times intraperitoneal injections of Clozapine-N-oxide (CNO) at a dose of 1 mg/kg on the 1st, 3rd, 6th, and 9th day of the experiment (Gomez et al., 2017).

Behavior test

After collecting the baseline data on day 0 of the experiment, we intraperitoneally injected CNO into all rats on the 1st day and recorded the cumulative food intake at 0.5, 1, 2, and 24 h after injection to evaluate the short-term feeding behavior of rats after regulating neuronal excitability. Subsequently, we recorded the cumulative 24 h food intake after the rats received CNO injection and body weight on the 3rd, 6th, and 9th days of the experiment, which aims to observe the long-term feeding behavior and body weight changes of rats after multiple regulations of neuronal excitability.

Western blotting

All rats were anesthetized and sacrificed by cervical dislocation after 9 days of treatment. Thirty minutes before sacrifice, rats in HM3D and HM4D groups were in intraperitoneal injection with CNO to activate or inhibit GLP-1 neurons. We froze the tissue of NTS and hypothalamus in liquid nitrogen after stripping them from the rat brains and stored them at −80°C. NTS tissue was detected with GLP-1 antibody, while hypothalamus tissue was detected with Bgn antibody and Mapkapk3 antibody applying a standard WB protocol. The primary antibody concentrations were as follows: GLP-1 (1:1000, AF0166, Affinity, Japan), Bgn (1:1000, 16409-1-AP, Proteintech, China), and Mapkapk3 (1:1000, 15424-1-AP, China). We used the housekeeping protein β-actin (1:1000; Proteintech, China) for normalization. We performed WB in triplicate for all target proteins. Protein expression was calculated based on the target protein and β-actin ratios of optical density, which we analyzed using the BandScan software.

Reverse transcription-quantitative polymerase chain reaction

We isolated total RNA of rat NTS and hypothalamus stored at −80°C with an AZfresh total RNA extraction kit (15596-026, Ambion, United States) and determined RNA concentrations at an absorbance ratio of 260/280 nm. We then reverse transcribed an aliquot (1 μg) of extracted RNA into first-strain complementary DNA (cDNA) using a ReverTra Ace qPCR RT kit (R223-01, VAZYME). We quantified gene expression of GLP-1 of NTS, Bgn, and Mapkapk3 of the hypothalamus by using an SYBR Green real-time PCR Master Mix Plus (Q111-02; VAZYME) and standard protocol. Measurements were conducted in triplicate under standard reaction conditions, and normalization was ensured to β-actin. We obtained primaries from the Biofavor Technology Company (Wuhan, China). All temperature circulation and gene amplification were processed in a CFX96 Touch real-time PCR detection system (Bio-Rad). All RT-PCR assays and primer sequences are shown in **Table 1**.

Immunofluorescence staining

Rats were anesthetized with isoflurane and received transcardial perfusion with saline and 5% paraformaldehyde. Rat brains were immersion in 5% paraformaldehyde for 72 h for perfusion fixation followed by dehydration in 25% sucrose solution. The coronal plane where the NTS and hypothalamus

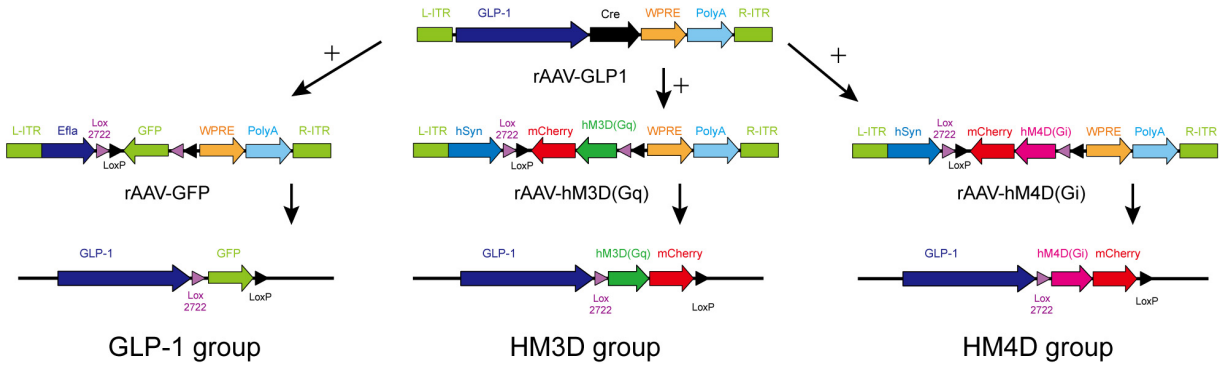

FIGURE 1
Gene sequence and combinatorial strategy of rAAVs.

are located was selected for the frozen section. The frozen sections in the NTS area with a thickness of 10 μm were selected. After thawing by natural gradient, 10% donkey serum or goat serum was used for blocking. After repairing with sodium citrate antigen retrieval solution, which leads the virus fluorescence to be destroyed, the three groups of brain slices were incubated with c-fos primary antibody. In GLP-1 group, GLP-1 neurons were labeled with anti-GFP (1:2000, ab5450, Abcam, United States) + green fluorescent secondary antibody (1:500, Alexa Fluor® 488 Donkey Anti-Goat, ab150129, Abcam, United States), and activated neurons were labeled with anti-cfos (#2250S, Cell Signaling Technology, United States) + red fluorescent secondary antibody (1:500, SA00013-8, CoraLite594 Donkey Anti-Rabbit, Proteintech, China). In HM3D and HM4D groups, GLP-1 neurons were labeled with anti-DsRed (632496, TAKARA, Japan) + red fluorescent secondary antibody (1:800, SA00013-4, CoraLite594 Goat Anti-Rabbit, Proteintech, China) and activated neurons were labeled with anti-cfos (1:2000, ab208942, Abcam, United States) + green fluorescent secondary antibody (1:200, SA00013-1, CoraLite488 Goat Anti-Mouse, Proteintech, China). The co-expression of GLP-1 neurons and cfos in the neuron cells indicated that GLP-1 neurons were activated. The activated GLP-1 neurons in the NTS area of each group were counted and statistically analyzed. The protein expression of differential genes in the hypothalamus of rats in each group was demonstrated by immunofluorescence single labeling. The tissue of the hypothalamus was prepared into frozen slices with a thickness of 20 μm, cubed with anti-Bgn (1:100, 16409-1-AP, Proteintech, China) or anti-Mapkapk3 (1:200, 15424-1-AP, Proteintech, China), and labeled with a green fluorescent (1:500, SA00013-2, CoraLite488 Goat Anti-Rabbit, Proteintech, China). Nuclei were stained with DAPI and observed under a fluorescence microscope. The expression of Bgn and Mapkapk3 in the hypothalamus was analyzed by the imagepro plus 6.0 software with integrated optical density (IOD) for fluorescence intensity analysis.

Statistical analysis

SPSS 25.0 software package was used for statistical analysis. The results were expressed as mean ± standard deviation ($x \pm s$). One-way analysis of variance was used for comparison between groups within the same time period. If there was an overall difference, multiple comparisons with the Tukey's method were used. Repeated measures analysis of variance was used to compare different time points within the same group, and if there were differences, multiple comparisons with the Tukey's method were used. $P < 0.05$ was considered significant.

Results

Differentially expressed gene analysis results

Based on the screening criteria of $P < 0.05$, $|\log FC| > 1$, 49 related differentially expressed genes were analyzed in the GSE135862 dataset. Among them, there were 11 upregulated differentially expressed genes and 38 downregulated differentially expressed genes. According to the expression

TABLE 1 Real-time PCR primer sequences.

Gene	Primer	Sequence (5′-3′)	PCR Products
β-actin	Forward	CACGATGGAGGGGCCGGACTCATC	241 bp
	Reverse	TAAAGACCTCTATGCCAACACAGT	
Rat GLP-1	Forward	TCGTGGCTGGATTGTTT	142 bp
	Reverse	TGGCGTTTGTCTTCGTT	
Bgn	Forward	GAGAACAGTGGCTTTGAACC	178 bp
	Reverse	GCTTGGAGTAGCGAAGTAGAT	
Mapkapk3	Forward	GTGCTGGGTCTGGGTGTGA	350 bp
	Reverse	CGGTGGGCAATGTTCTGG	

fold of the differential genes, the related genes with the largest differential fold were selected, which then upregulated *Bgn* and down-regulated *Mapkapk3*, respectively. A specific heatmap can be seen in Figure 2.

Gene ontology and Kyoto encyclopedia of genes and genomes pathway enrichment analysis results of differentially expressed genes

The results of GO analysis showed that the molecular functions of differential genes mainly included pseudouridine synthase activity, BMP receptor binding, xylosyltransferase activity, proton antiporter activity (sodium, monovalent cation, potassium), calcium-dependent protein kinase activity, low-density lipoprotein particle receptor activity, transferase activity, and transferring glycosyl and pentosyl groups; differential genes were mainly localized in seven regions around the cells, which were catenin complex, organelle membrane contact site, nuclear outer membrane, varicosity, mitochondria-associated ER membrane, nuclear lamina, and transport vesicle and extracellular matrix; and the biological pathways in which differential genes were involved included apoptotic process involved in development, extracellular structure organization, activation of MAPKK activity, apoptotic process involved in morphogenesis, positive regulation of coagulation, positive regulation of hemostasis, positive regulation of blood coagulation, regulation of apoptotic process involved in development, cell junction maintenance, and regulation of apoptotic process involved in morphogenesis. The results of

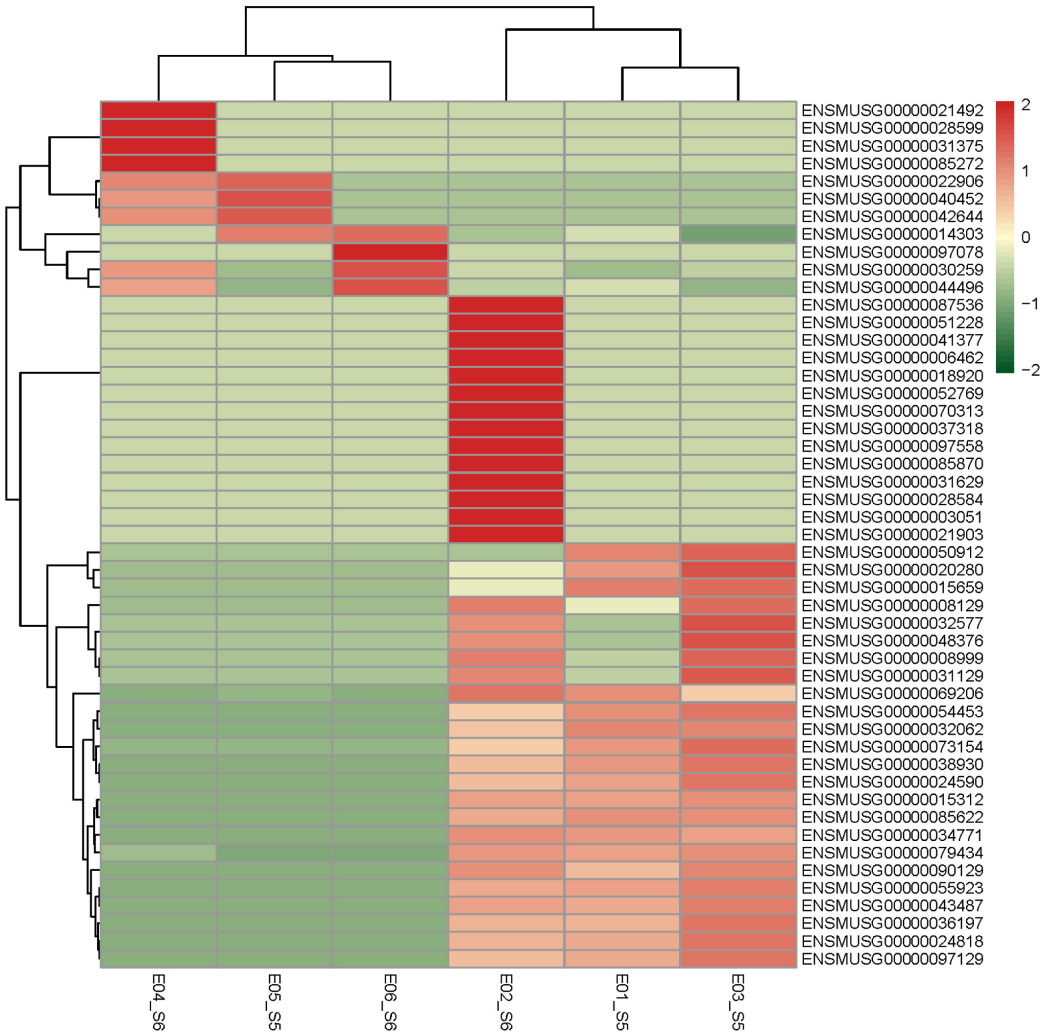

FIGURE 2
Heatmap of DEGs. Red areas represent highly expressed genes and green areas represent lowly expressed genes. DEGs, differentially expressed genes.

KEGG signaling pathway enrichment analysis showed that differential genes played an important role in platelet activation pathway, complement and coagulation cascades pathway, other glycan degradation pathway, other type of O-glycan biosynthesis pathway, cellular senescence pathway, cytokine-cytokine receptor interaction pathway, and apoptosis pathway. Specific results can be seen in Figure 3.

Protein-protein interaction networks and important genes of differentially expressed genes

The PPI network of DEGs and its modules are shown in Figure 4. With the STRING database, 46 of 49 DEGs were mapped onto a PPI network. There are 46 nodes and 66 edges (Figure 4A). After the PPI network is imported into Cytoscape, the key nodes and subnetworks in the PPI network are predicted and explored by several topological algorithms using the cytoHubba plugin. The top 15 genes selected according to the MCC and degree method were *F12*, *Gadd45b*, *Cdh12*, *Nyx*, *Mapkapk3*, *Bgn*, *Tnf*, *Lmnb1*, *Tnfrsf1b*, *F2r*, *Bmpr1a*, *Acvr1*, *Bmp7*, *Nog*, and *F2* (Figures 4B,C).

Different glucagon-like peptide 1 neuronal excitability modulates appetite-related behavior

As shown in Figures 5A–C, there was no significant difference in body weight, Lee's index, and 24-h food intake among the three groups before intervention ($P > 0.05$). After the first time of CNO injection, the feeding behavior of the three groups of rats showed significant differences (Figure 5D).

FIGURE 3
Gene ontology and KEGG enrichment analysis. **(A)** GO enrichment result of DEGs; **(B)** the results of KEGG signaling pathway enrichment analysis; The *x*-axis label represents *P*-value and the number of genes and the *y*-axis label represents GO and KEGG terms, different colors represent different classification. DEGs, differentially expressed genes; GO, gene ontology; KEGG, Kyoto Encyclopedia of Genes and Genomes pathway.

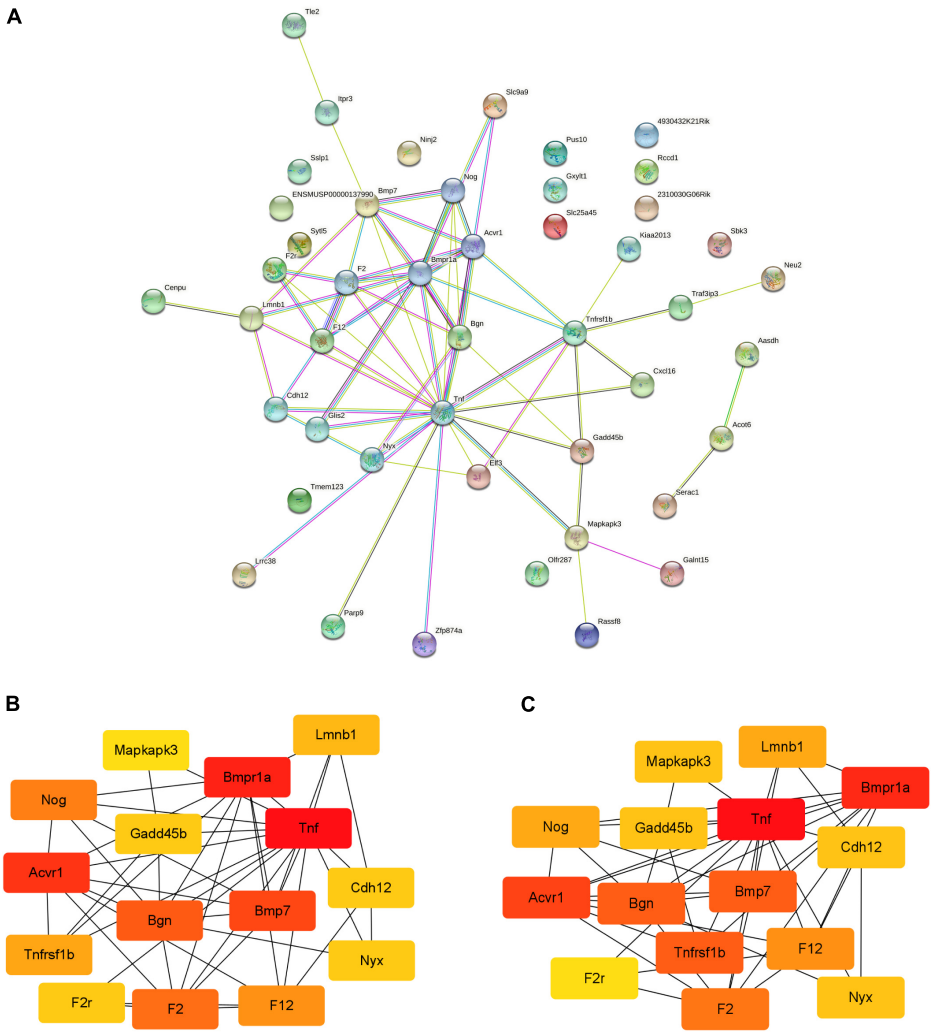

FIGURE 4
The PPI networks of DEGs and modules. **(A)** PPI network analyzed by STRING database; **(B,C)** the top 15 genes selected according to the MCC and degree method. PPI, protein-protein interaction; DEGs, differentially expressed genes; MCC, maximal clique centrality.

Compared with the GLP-1 group, rats in the HM3D group showed a significant reduction in food intake from 1 h after CNO injection ($P < 0.05$), and the cumulative food intake was significantly lower than that in the GLP-1 group at 1 h, 2 h, and 24 h after CNO injection ($P < 0.05$ or $P < 0.01$). Compared with the GLP-1 group, the HM4D group showed a significant increase in food intake only at 1 h after CNO injection ($P < 0.01$); compared with the HM3D group, the food intake of the HM4D group increased significantly at 1, 2, and 24 h after injection ($P < 0.05$ or $P < 0.01$). There was no statistical difference in the 24-h food intake before CNO injection among the groups of rats, which showed the highest food intake in the HM4D group and the lowest food intake in the HM3D group on days 3, 6, and 9 of injection (Figure 5E). The body weights of rats in the three groups showed different trends during the experiment. Rats in the GLP-1 group did not show significant variation in body weights after CNO injection. The body weights of rats in the HM3D group were lower than the baseline since the 6th day after CNO injection ($P < 0.05$), and the body weights of rats in the HM4D group increased since the 3rd day after CNO injection. However, we did not observe significant differences in body weight among the three groups of rats at each time point (Figure 5F).

Chemical genetics technology can activate or inhibit glucagon-like peptide 1 neurons in the nucleus tractus solitarius

As shown in Figures 6A,B,C, both the protein and gene expression of GLP-1 in NTS were upregulated in the HM3D

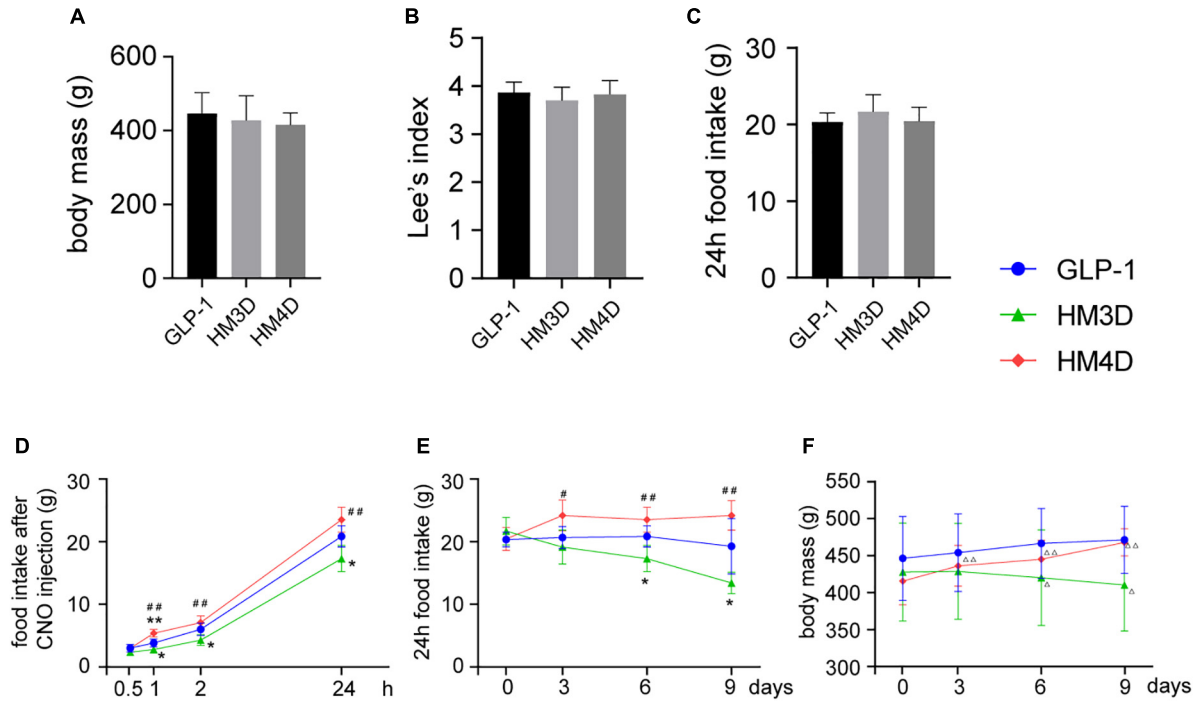

FIGURE 5
Appetite-related behavioral changes in each group. **(A–C)** Baseline of body mass, lee's index, and 24 h food intake of rats in each group, which were collected at day 0; **(D)** cumulative food intake of rats in each group at different time points after the first CNO injection; **(E)** changes in 24 h food intake of rats in each group after CNO injection during the intervention period; **(F)** changes in body mass of rats in each group during the intervention period; vs. GLP-1 group, $^{*}P < 0.05$, $^{**}P < 0.01$; vs. HM3D group, $^{\#}P < 0.05$, $^{\#\#}P < 0.01$; vs. day 0, $^{\triangle}P < 0.05$, $^{\triangle\triangle}P < 0.01$. CNO, Clozapine-N-oxide.

group, while in the HM4D group were downregulated. As shown in Figures 6D,F, the GLP-1 neurons in the NTS region of the three groups of rats were successfully labeled with GFP or DsRed primary antibody, and the GLP-1 neurons expressed different amounts of c-fos. The number of activated GLP-1 neurons in the HM3D group was significantly higher than that in the GLP-1 group and the HM4D group ($P < 0.05$); the number of activated neurons in the GLP-1 group was higher than that in the HM4D group ($P < 0.05$) (Figure 6E). The results indicated that CNO injection could effectively activate or inhibit GLP-1 neurons in NTS.

Different excitatory properties of glucagon-like peptide 1 neurons regulate the protein and gene expression of biglycan and mitogen-activated protein kinase activated protein kinase 3 in the hypothalamus

As shown in Figures 7A,B, the activation of GLP-1 neurons upregulated the gene and protein expression of Bgn in the hypothalamus ($P < 0.01$); while suppressing it induced the opposite effect ($P < 0.01$). On the contrary, activated GLP-1 neurons can downregulate the gene and protein expression of Mapkapk3 in the hypothalamus ($P < 0.01$), while suppressing GLP-1 can activate Mapkapk3 ($P < 0.01$) (Figures 7C,D). Observing the fluorescence images of the hypothalamus, it was found that both Bgn and Mapkapk3 proteins were widely expressed in the hypothalamus without obvious cell specificity (Figure 7E). By analyzing the fluorescence intensity, we found that the expression of Bgn increased after activation of GLP-1, while Mapkapk3 decreased (Figure 7F), which was consistent with the results of WB and qPCR.

Discussion

Glucagon-like peptide 1, a peptide hormone from the intestinal tract, plays a central role in the coordination of postprandial glucose homeostasis (Gribble and Reimann, 2021). Intake and digestion of carbohydrates, fats, proteins, and bile acids are the main physiological stimuli that promote GLP-1 secretion (Gribble and Reimann, 2019). GLP-1 biosynthesis and release are performed by enteroendocrine cells of the intestine, L cells (Song et al., 2019). L cells are more distributed

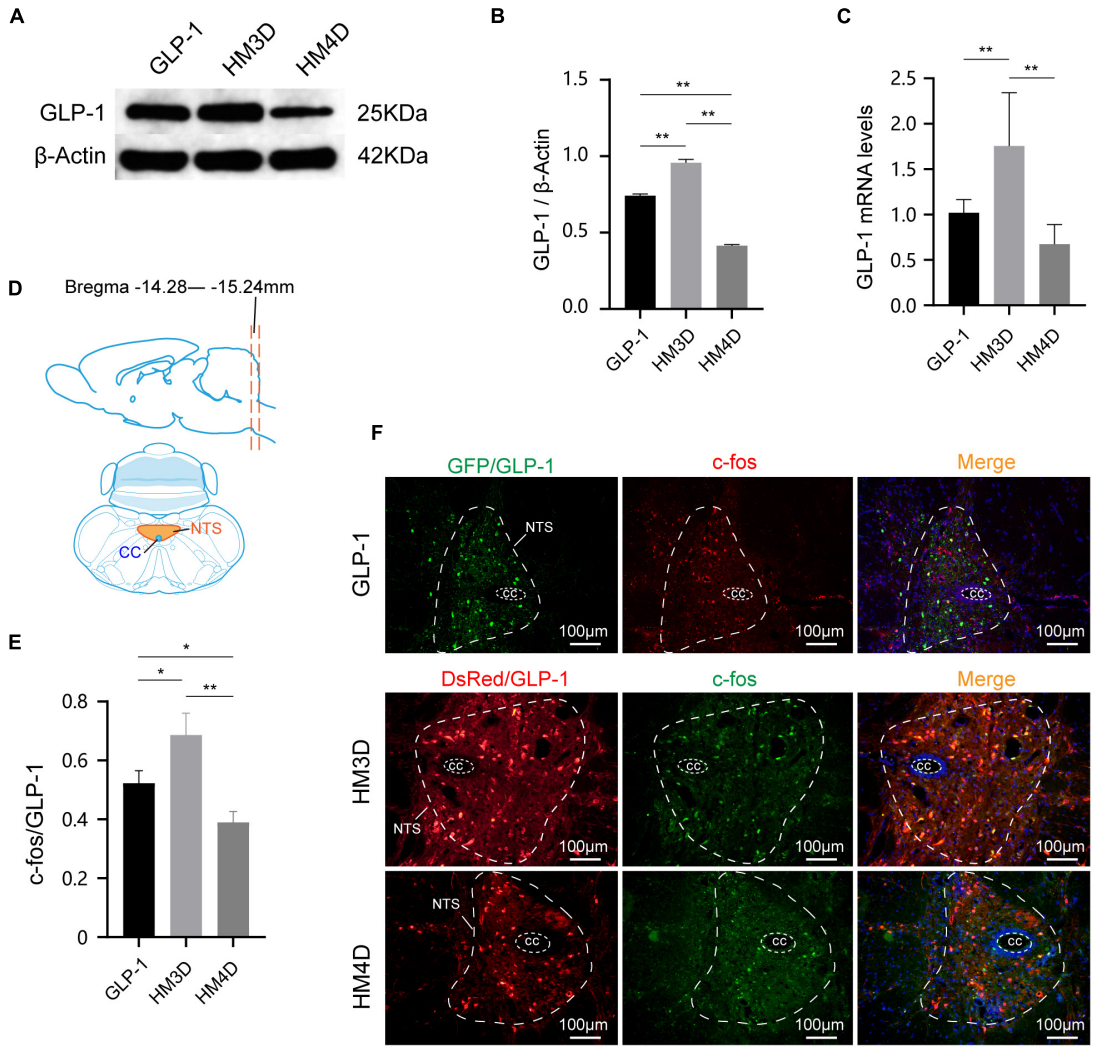

FIGURE 6
Comparison of protein and gene expression of GLP-1 in NTS. **(A,B)** WB and protein expression of GLP-1in NTS; **(C)** gene expression of GLP-1 in NTS; **(D)** the slice range and localization pattern of the coronal plane where the NTS is located; **(E)** comparison of activation numbers of GLP-1 neurons in NTS; **(F)** representative figures of activated GLP-1 neurons in the NTS of rats in each group; $^{*}P < 0.05$, $^{**}P < 0.01$. WB, Western blotting; GLP-1, glucagon-like peptide 1; cc, central canal; NTS, nucleus of the solitary tract.

in the jejunum, ileum, and colon (Sjolund et al., 1983). Therefore, the stimulation of L cells occurs downstream of food digestion, which is closely related to the local rate of nutrient absorption of the intestine and can control gastric emptying and intestinal tract creeping through feedback regulation (Gribble and Reimann, 2021). Therefore, its main functions include not only stimulating insulin secretion and inhibiting glucagon secretion but also regulating gastrointestinal motility, and working together in many ways to maintain blood glucose homeostasis. In addition to being secreted by the intestine, GLP-1 also exists in neurons of NTS, which release GLP-1 in the central nervous system, including the project to the feeding centers in the hypothalamus (Llewellyn-Smith et al., 2011). GLP-1-mediated neural circuits are the core mechanism by which GLP-1 neurons in NTS exert their appetite-suppressing effects (Cheng et al., 2020). Therefore, it is also a physiological regulator of appetite and food intake (Holst, 2007).

Glucagon-like peptide 1 exerts its physiological function by binding to a dedicated G-protein-coupled receptor, GLP-1R, expressed in a variety of cell types (Thorens, 1992). Numerous attempts have been made to identify alternative GLP-1R or subtypes, but at present only a single GLP-1R has been identified, whether expressed in the brain, the stomach, or the pancreas (Wei and Mojsov, 1995). In addition to being expressed in the gastrointestinal tract, pancreas, and brain, studies have shown that GLP-1R can be also detected in the vagal afferent nerves, scattered atrial cardiomyocytes, vascular smooth muscle, lung, and some immune cells (Pyke

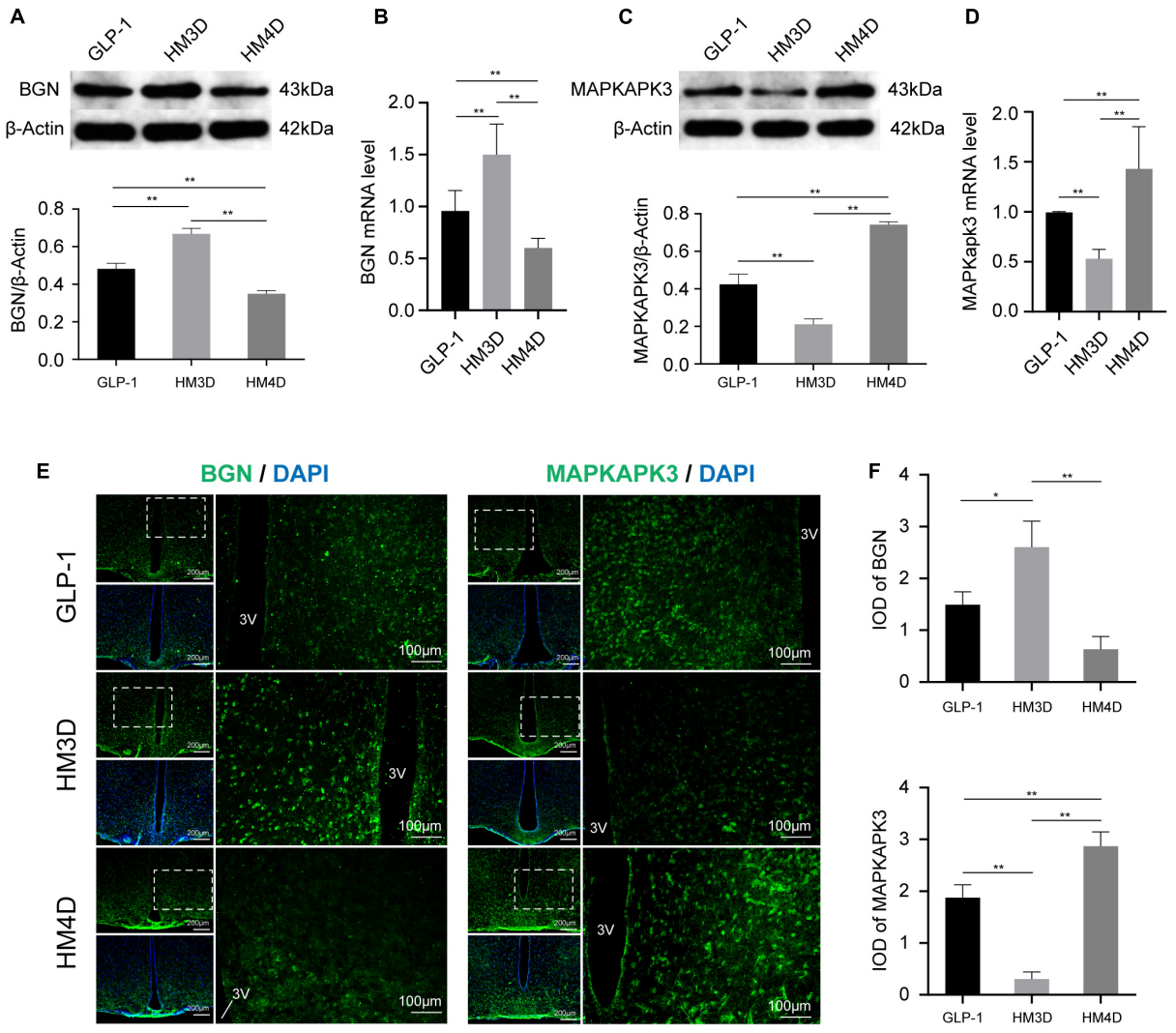

FIGURE 7
Comparison of protein and gene expression of Bgn and Mapkapk3 in the hypothalamus. **(A)** WB and protein expression of Bgn in hypothalamus; **(B)** gene expression of Bgn in hypothalamus; **(C)** WB and protein expression of Mapkapk3 in hypothalamus; **(D)** gene expression of Mapkapk3 in hypothalamus; **(E)** representative figures of Bgn and Mapkapk3 in hypothalamus of rats in each group; **(F)** comparison of IOD of Bgn and Mapkapk3 in hypothalamus; $^{*}P < 0.05$, $^{**}P < 0.01$. 3V, the 3rd ventricle. WB, Western blotting; Bgn, biglycan; Mapkapk3, mitogen-activated protein kinase activated protein kinase 3; IOD, integrated optical density.

et al., 2014; Richards et al., 2014; He et al., 2019). The lateral hypothalamic GLP-1R has been identified as an indispensable element of normal food reinforcement, food intake, and body weight regulation (Lopez-Ferreras et al., 2018). As mentioned earlier, GLP-1R-expressing vagal afferent cells have been found to form fibers within the intestinal villi adjacent to enteroendocrine cells. Therefore, it is generally believed that GLP-1R is a chemosensory neuron of the vagal afferents nerve, which helps the vagal afferents nerve receive nutrient detection information in a paracrine manner by binding to GLP-1 released locally by enteroendocrine cells (Krieger et al., 2016; Grill, 2020). Meanwhile, the activity of GLP-1R in vagal afferents also encodes the feeling of distention in the gastrointestinal tract through the inner ganglia of myenteric plexus intramuscular array detection in gastric and intestinal smooth muscle layers (Williams et al., 2016; Bai et al., 2019). Thus, the vagal afferents of the intestine receive gastrointestinal stimulation through both chemoreceptors and mechanoreceptors to generate neural signals toward the corresponding nuclei of the brainstem, such as those in the NTS and posterior area (AP), then to the hypothalamus, which releases GLP-1 and activates the receptor. However, the current link of this endogenous peripheral GLP-1 indirectly interacting with the central GLP-1 system (*via* the vagal and/or endocrine pathways) remains controversial, and the necessary intestine-brain circuit has not been empirically confirmed (Brierley

et al., 2021). Therefore, further research in this field should be conducted in the future.

Glucagon-like peptide 1 forms the basis for a variety of current drugs for the treatment of type 2 diabetes and obesity, as well as new agents currently being developed. GLP1-RAs are used clinically to treat T2DM and promote weight loss in people with obesity (Knudsen and Lau, 2019). Although the identity of the GLP-1R-expressing target cells underlying appetite suppression remains under discussion, powerful evidence indicates that GLP1-RAs exert their effects by targeting GLP-1R in the brainstem and/or hypothalamus (Knudsen and Lau, 2019). The mechanism of action of GLP-1 and its receptor in the brain is still unclear, which has caused some difficulties in the optimization of drug development and obesity treatment. Therefore, this study aimed to investigate the differential genes in the brain after GLP1-RAs treatment. After bioinformatics analysis, we found two significantly different genes, Bgn of upregulated genes and Mapkapk3 of downregulated genes.

Biglycan, a class I small leucine-rich proteoglycans, is a key component of the extracellular matrix (ECM) that participates in scaffolding the collagen fibrils and mediates cell signaling. Dysregulation of Bgn expression can result in a wide range of clinical conditions such as metabolic disorder, inflammatory disorder, musculoskeletal defects, and malignancies (Appunni et al., 2021). ECM disorganization is a pivotal step in metabolic disorders like obesity which involves accommodating the expanding adipose tissue mass (Kim et al., 2016). The ECM in these states releases non-fibrillar proteoglycans such as Bgn, which take part in receptor-mediated interactions to regulate inflammation and organ-specific metabolic disturbances. The ECM plays a role in regulating neurite outgrowth, and neural function and plasticity as well as metabolic diseases (Dityatev et al., 2010). Also, ECM remodeling is crucial for regulating the morphogenesis of the intestine (Bonnans et al., 2014). In this study, GO analysis also found differential genes enriched in ECM. KEGG analysis showed that differential genes play an important role in other types of glycans degradation and biosynthesis pathway. So, the upregulation of Bgn expression in this study may indicate increased ECM remodeling, and as previously mentioned, changes in intestinal mechanical signaling can regulate gastrointestinal motility and food intake.

Mitogen-activated protein kinase activated protein kinase 3 is a member of the Mapk signaling pathway family (Wei et al., 2015). The Mapk family is significant in various cellular processes such as apoptosis, oxidative stress, differentiation, inflammatory response, and proliferation, and includes three members: extracellular signal-regulated kinase (Erk1/2), p38, and c-Jun N-terminal kinase (JNK) (Miloso et al., 2008). p38 Mapk is the best-characterized kinase upstream of Mapkapk3 (Freshney et al., 1994). Studies have shown that p38Mapk can promote β-cell exhaustion in the pancreas, and β-cells can express GLP-1R (Manieri and Sabio, 2015). At the same time, p38 can also regulate the secretion of insulin, and the insulin level in p38-deficient mice is increased. Then, in this study, Mapkapk3 is a downstream factor of p38, and the downregulation of Mapkapk3 may inhibit the p38 Mapk pathway, thereby promoting insulin secretion and increasing the expression of GLP-1R. Studies have shown that the silencing of *Bgn* gene can upregulate p38Mapk (Appunni et al., 2021). In the verification of bioinformatics analysis results, we found that the expression of Bgn mRNA was upregulated and the expression of Mapkapk3 mRNA was downregulated when the GLP-1 neurons were activated, which implied the inhibitory effect of BGN in regulating the p38 pathway from another perspective.

Conclusion

In summary, we screened out the key differential genes that affect feeding behavior after GLP-1R activation through bioinformatics analysis. Bgn and Mapkapk3 were found to be more associated with changes in feeding behavior. Changes in Bgn and Mapkapk3 in the hypothalamus were also detected after activating or inhibiting GLP-1 neurons in the NTS by chemogenetic treatment, which were consistent with the results of bioinformatics analysis. It shows that Bgn and Mapkapk3 may be important downstream cytokines of GLP-1 in regulating appetite, which were worthy of further research in the future.

Data availability statement

The raw data supporting the conclusions of this article will be made available by the authors, without undue reservation.

Ethics statement

The animal study was reviewed and approved by the Institutional Animal Care and Use Committee of Wuhan University.

Author contributions

QS, JT, and YY designed the study protocol and obtained the funding. YS and YH were responsible for the bioinformatics analysis part, animal experimentation, and basic experiment parts. QS was responsible for data analysis. QS, JT, and YS drafted this manuscript. All authors have read and approved the final manuscript, adhere to the trial authorship guidelines, and agreed to publication.

Funding

This work was supported by the Natural Science Foundation of China under grant number (81804180); the Traditional Chinese Medicine Research Project of Hubei Provincial Health Commission (No. ZY2021M031); and the Joint Fund of Hubei Provincial Health Commission under Grant Number (WJ2019H163).

Acknowledgments

We thank all the medical workers in the Department of Rehabilitation Medicine, Zhongnan Hospital of Wuhan University, for their support and assistance in this study.

Conflict of interest

The authors declare that the research was conducted in the absence of any commercial or financial relationships that could be construed as a potential conflict of interest.

Publisher's note

References

Albaugh, V. L., Banan, B., Antoun, J., Xiong, Y., Guo, Y., Ping, J., et al. (2019). Role of Bile Acids and GLP-1 in Mediating the Metabolic Improvements of Bariatric Surgery. *Gastroenterology* 104:e1044. doi: 10.1053/j.gastro.2018.11.017

Appunni, S., Rubens, M., Ramamoorthy, V., Anand, V., Khandelwal, M., and Sharma, A. (2021). Biglycan: an emerging small leucine-rich proteoglycan (SLRP) marker and its clinicopathological significance. *Mol. Cell Biochem.* 476, 3935–3950. doi: 10.1007/s11010-021-04216-z

Bai, L., Mesgarzadeh, S., Ramesh, K. S., Huey, E. L., Liu, Y., Gray, L. A., et al. (2019). Genetic Identification of Vagal Sensory Neurons That Control Feeding. *Cell* 112:e1123. doi: 10.1016/j.cell.2019.10.031

Bonnans, C., Chou, J., and Werb, Z. (2014). Remodelling the extracellular matrix in development and disease. *Nat. Rev. Mol. Cell Biol.* 15, 786–801. doi: 10.1038/nrm3904

Bray, G. A., and Siri-Tarino, P. W. (2016). The Role of Macronutrient Content in the Diet for Weight Management. *Endocrinol. Metab. Clin. North Am.* 45, 581–604. doi: 10.1016/j.ecl.2016.04.009

Brierley, D. I., Holt, M. K., Singh, A., de Araujo, A., McDougle, M., Vergara, M., et al. (2021). Central and peripheral GLP-1 systems independently suppress eating. *Nat. Metab.* 3, 258–273. doi: 10.1038/s42255-021-00344-4

Cheng, W., Ndoka, E., Hutch, C., Roelofs, K., MacKinnon, A., Khoury, B., et al. (2020). Leptin receptor-expressing nucleus tractus solitarius neurons suppress food intake independently of GLP1 in mice. *JCI Insight* 5:e134359. doi: 10.1172/jci.insight.134359

D'Alessio, D. (2016). Is GLP-1 a hormone: whether and When? *J. Diabetes Investig.* 7, 50–55. doi: 10.1111/jdi.12466

Dityatev, A., Schachner, M., and Sonderegger, P. (2010). The dual role of the extracellular matrix in synaptic plasticity and homeostasis. *Nat. Rev. Neurosci.* 11, 735–746. doi: 10.1038/nrn2898

Fakhry, J., Wang, J., Martins, P., Fothergill, L. J., Hunne, B., Prieur, P., et al. (2017). Distribution and characterisation of CCK containing enteroendocrine cells of the mouse small and large intestine. *Cell Tissue Res.* 369, 245–253. doi: 10.1007/s00441-017-2612-1

Firouzjaei, A., Li, G. C., Wang, N., Liu, W. X., and Zhu, B. M. (2016). Comparative evaluation of the therapeutic effect of metformin monotherapy with metformin and acupuncture combined therapy on weight loss and insulin sensitivity in diabetic patients. *Nutr Diabetes* 6, e209. doi: 10.1038/nutd.2016.16

Freshney, N. W., Rawlinson, L., Guesdon, F., Jones, E., Cowley, S., Hsuan, J., et al. (1994). Interleukin-1 activates a novel protein kinase cascade that results in the phosphorylation of Hsp27. *Cell* 78, 1039–1049. doi: 10.1016/0092-8674(94)90278-x

Gomez, J. L., Bonaventura, J., Lesniak, W., Mathews, W. B., Sysa-Shah, P., Rodriguez, L. A., et al. (2017). Chemogenetics revealed: dREADD occupancy and activation via converted clozapine. *Science* 357, 503–507. doi: 10.1126/science.aan2475

Gribble, F. M., and Reimann, F. (2019). Function and mechanisms of enteroendocrine cells and gut hormones in metabolism. *Nat. Rev. Endocrinol.* 15, 226–237. doi: 10.1038/s41574-019-0168-8

Gribble, F. M., and Reimann, F. (2021). Metabolic Messengers: glucagon-like peptide 1. *Nat. Metab.* 3, 142–148. doi: 10.1038/s42255-020-00327-x

Grill, H. J. (2020). A Role for GLP-1 in Treating Hyperphagia and Obesity. *Endocrinology* 161:bqaa093. doi: 10.1210/endocr/bqaa093

He, S., Kahles, F., Rattik, S., Nairz, M., McAlpine, C. S., Anzai, A., et al. (2019). Gut intraepithelial T cells calibrate metabolism and accelerate cardiovascular disease. *Nature* 566, 115–119. doi: 10.1038/s41586-018-0849-9

Holst, J. J. (2007). The physiology of glucagon-like peptide 1. *Physiol. Rev.* 87, 1409–1439. doi: 10.1152/physrev.00034.2006

Hu, A. L., and Chan, K. C. (2013). Utilizing both topological and attribute information for protein complex identification in PPI networks. *IEEE/ACM Trans. Comput. Biol. Bioinform.* 10, 780–792. doi: 10.1109/TCBB.2013.37

Huang, X., Liu, S., Wu, L., Jiang, M., and Hou, Y. (2018). High Throughput Single Cell RNA Sequencing. *Bioinform. Anal. Appl. Adv. Exp. Med. Biol.* 1068, 33–43. doi: 10.1007/978-981-13-0502-3_4

Jaacks, L. M., Vandevijvere, S., Pan, A., McGowan, C. J., Wallace, C., Imamura, F., et al. (2019). The obesity transition: stages of the global epidemic. *Lancet Diabetes Endocrinol.* 7, 231–240. doi: 10.1016/S2213-8587(19)30026-9

Kanehisa, M., Furumichi, M., Tanabe, M., Sato, Y., and Morishima, K. (2017). KEGG: new perspectives on genomes, pathways, diseases and drugs. *Nucleic Acids Res.* 45, D353–D361. doi: 10.1093/nar/gkw1092

Kanehisa, M., Sato, Y., Kawashima, M., Furumichi, M., and Tanabe, M. (2016). KEGG as a reference resource for gene and protein annotation. *Nucleic Acids Res.* 44, D457–D462. doi: 10.1093/nar/gkv1070

Kim, J., Lee, S. K., Shin, J. M., Jeoun, U. W., Jang, Y. J., Park, H. S., et al. (2016). Enhanced biglycan gene expression in the adipose tissues of obese women and its association with obesity-related genes and metabolic parameters. *Sci. Rep.* 6:30609. doi: 10.1038/srep30609

Knudsen, L. B., and Lau, J. (2019). The Discovery and Development of Liraglutide and Semaglutide. *Front. Endocrinol.* 10:155. doi: 10.3389/fendo.2019.00155

Krieger, J. P., Arnold, M., Pettersen, K. G., Lossel, P., Langhans, W., and Lee, S. J. (2016). Knockdown of GLP-1 Receptors in Vagal Afferents Affects Normal Food Intake and Glycemia. *Diabetes* 65, 34–43. doi: 10.2337/db15-0973

Llewellyn-Smith, I. J., Reimann, F., Gribble, F. M., and Trapp, S. (2011). Preproglucagon neurons project widely to autonomic control areas in the mouse brain. *Neuroscience* 180, 111–121. doi: 10.1016/j.neuroscience.2011.02.023

Lopez-Ferreras, L., Richard, J. E., Noble, E. E., Eerola, K., Anderberg, R. H., Olandersson, K., et al. (2018). Lateral hypothalamic GLP-1 receptors are critical

for the control of food reinforcement, ingestive behavior and body weight. *Mol. Psychiatr.* 23, 1157–1168. doi: 10.1038/mp.2017.187

Luo, S., Gill, H., Feltis, B., Hung, A., Nguyen, L. T., and Lenon, G. B. (2020). The Effects of a Weight-Loss Herbal Formula RCM-107 and Its Eight Individual Ingredients on Glucagon-Like Peptide-1 Secretion-An In Vitro and In Silico Study. *Int. J. Mol. Sci.* 21:2854. doi: 10.3390/ijms21082854

Manieri, E., and Sabio, G. (2015). Stress kinases in the modulation of metabolism and energy balance. *J. Mol. Endocrinol.* 55, R11–R22. doi: 10.1530/JME-15-0146

Miloso, M., Scuteri, A., Foudah, D., and Tredici, G. (2008). MAPKs as mediators of cell fate determination: an approach to neurodegenerative diseases. *Curr. Med. Chem.* 15, 538–548. doi: 10.2174/092986708783769731

Narayanaswami, V., and Dwoskin, L. P. (2017). Obesity: current and potential pharmacotherapeutics and targets. *Pharmacol. Ther.* 170, 116–147. doi: 10.1016/j.pharmthera.2016.10.015

Ni, W., Wang, P., Chen, H., Liu, Y., Zhang, W., Qiu, L., et al. (2021). Obesity complicated with insulin resistance treated with the electroacupuncture at the combination of back-shu and front-mu points. *World J. Acupunct.* 32, 213–217.

Nudel, J., and Sanchez, V. M. (2019). Surgical management of obesity. *Metabolism* 92, 206–216. doi: 10.1016/j.metabol.2018.12.002

Pyke, C., Heller, R. S., Kirk, R. K., Orskov, C., Reedtz-Runge, S., Kaastrup, P., et al. (2014). GLP-1 receptor localization in monkey and human tissue: novel distribution revealed with extensively validated monoclonal antibody. *Endocrinology* 155, 1280–1290. doi: 10.1210/en.2013-1934

Rasouli, M., Ahmad, Z., Omar, A. R., and Allaudin, Z. N. (2011). Engineering an L-cell line that expresses insulin under the control of the glucagon-like peptide-1 promoter for diabetes treatment. *BMC Biotechnol.* 11:99. doi: 10.1186/1472-6750-11-99

Richards, P., Parker, H. E., Adriaenssens, A. E., Hodgson, J. M., Cork, S. C., Trapp, S., et al. (2014). Identification and characterization of GLP-1 receptor-expressing cells using a new transgenic mouse model. *Diabetes* 63, 1224–1233. doi: 10.2337/db13-1440

Santos, R. V., Rodrigues, J. M., and Jesus, M. I. (2020). Review on the effects obesity treatment with acupuncture and phytoacupuncture. *World J. Acupunct. Moxibustion* 30, 223–228.

Seidell, J. C., and Halberstadt, J. (2015). The global burden of obesity and the challenges of prevention. *Ann. Nutr. Metab.* 66(Suppl. 2), 7–12. doi: 10.1159/000375143

Sherman, B. T., Huang, da, W., Tan, Q., Guo, Y., Bour, S., et al. (2007). DAVID Knowledgebase: a gene-centered database integrating heterogeneous gene annotation resources to facilitate high-throughput gene functional analysis. *BMC Bioinform.* 8:426. doi: 10.1186/1471-2105-8-426

Shi, X., Chacko, S., Li, F., Li, D., Burrin, D., Chan, L., et al. (2017). Acute activation of GLP-1-expressing neurons promotes glucose homeostasis and insulin sensitivity. *Mol. Metab.* 6, 1350–1359. doi: 10.1016/j.molmet.2017.08.009

Shu, Q., Shao, Y., Tian, J., and Yang, Y. (2020). Preliminary investigation of localization of solitary nucleus microinjection in rats. *Acta Lab. Anim. Sci. Sin.* 28, 429–435.

Sjolund, K., Sanden, G., Hakanson, R., and Sundler, F. (1983). Endocrine cells in human intestine: an immunocytochemical study. *Gastroenterology* 85, 1120–1130.

Song, Y., Koehler, J. A., Baggio, L. L., Powers, A. C., Sandoval, D. A., and Drucker, D. J. (2019). Gut-Proglucagon-Derived Peptides Are Essential for Regulating Glucose Homeostasis in Mice. *Cell Metab* 97:e973. doi: 10.1016/j.cmet.2019.08.009

Szklarczyk, D., Gable, A. L., Lyon, D., Junge, A., Wyder, S., Huerta-Cepas, J., et al. (2019). STRING v11: protein-protein association networks with increased coverage, supporting functional discovery in genome-wide experimental datasets. *Nucleic Acids Res.* 47, D607–D613. doi: 10.1093/nar/gky1131

Thorens, B. (1992). Expression cloning of the pancreatic beta cell receptor for the gluco-incretin hormone glucagon-like peptide 1. *Proc. Natl. Acad. Sci. U.S.A* 89, 8641–8645. doi: 10.1073/pnas.89.18.8641

Valassi, E., Scacchi, M., and Cavagnini, F. (2008). Neuroendocrine control of food intake. *Nutr. Metab. Cardiovasc. Dis.* 18, 158–168. doi: 10.1016/j.numecd.2007.06.004

Wang, Y., Xue, H., Sun, M., Zhu, X., Zhao, L., and Yang, Y. (2019). Prevention and control of obesity in China. *Lancet Glob. Health* 7:e1166–e1167. doi: 10.1016/S2214-109X(19)30276-1

Wei, Y., An, Z., Zou, Z., Sumpter, R., Su, M., Zang, X., et al. (2015). The stress-responsive kinases MAPKAPK2/MAPKAPK3 activate starvation-induced autophagy through Beclin 1 phosphorylation. *Elife* 4:e05289. doi: 10.7554/eLife.05289

Wei, Y., and Mojsov, S. (1995). Tissue-specific expression of the human receptor for glucagon-like peptide-I: brain, heart and pancreatic forms have the same deduced amino acid sequences. *FEBS Lett.* 358, 219–224. doi: 10.1016/0014-5793(94)01430-9

Williams, E. K., Chang, R. B., Strochlic, D. E., Umans, B. D., Lowell, B. B., and Liberles, S. D. (2016). Sensory Neurons that Detect Stretch and Nutrients in the Digestive System. *Cell* 166, 209–221. doi: 10.1016/j.cell.2016.05.011

Zhang, Y., Zheng, Y., Fu, Y., and Wang, C. (2019). Identification of biomarkers, pathways and potential therapeutic agents for white adipocyte insulin resistance using bioinformatics analysis. *Adipocyte* 8, 318–329. doi: 10.1080/21623945.2019.1649578

frontiers | Frontiers in Neuroscience

TYPE Original Research
PUBLISHED 15 September 2022
DOI 10.3389/fnins.2022.939915

OPEN ACCESS

EDITED BY
Chunhui Bao,
Shanghai University of Traditional Chinese Medicine, China

REVIEWED BY
Jesus Miguel Pradillo,
Complutense University of Madrid, Spain
Weijun Peng,
Second Xiangya Hospital of Central South University, China
Mingsan Miao,
Henan University of Traditional Chinese Medicine, China

*CORRESPONDENCE
Baiyan Liu
liubaiyan9657@163.com

†These authors share first authorship

SPECIALTY SECTION
This article was submitted to Gut-Brain Axis, a section of the journal Frontiers in Neuroscience

RECEIVED 09 May 2022
ACCEPTED 22 August 2022
PUBLISHED 15 September 2022

CITATION
Chen B, Yi J, Xu Y, Wen H, Tian F, Liu Y, Xiao L, Li L and Liu B (2022) Apolipoprotein E knockout may affect cognitive function in D-galactose-induced aging mice through the gut microbiota–brain axis. *Front. Neurosci.* 16:939915. doi: 10.3389/fnins.2022.939915

Apolipoprotein E knockout may affect cognitive function in D-galactose-induced aging mice through the gut microbiota–brain axis

Bowei Chen[1†], Jian Yi[1†], Yaqian Xu[1], Huiqiao Wen[1], Fengming Tian[1], Yingfei Liu[1], Lan Xiao[2], Lisong Li[3] and Baiyan Liu[4*]

[1]The First Affiliated Hospital, Hunan University of Chinese Medicine, Changsha, China, [2]College of Pharmacy, Hunan University of Chinese Medicine, Changsha, China, [3]College of Information Science and Engineering, Hunan University of Chinese Medicine, Changsha, China, [4]Hunan Academy of Chinese Medicine, Changsha, China

The gut microbiota plays an important role in central nervous system (CNS) disorders. Apolipoprotein E (ApoE) can affect the composition of the gut microbiota and is closely related to the CNS. However, the mechanism by which ApoE affects cognitive dysfunction through the gut microbiota–brain axis has thus far not been investigated. In this study, we used wild-type mice and ApoE knockout ($ApoE^{-/-}$) mice to replicate the aging model and examined the effects of ApoE deletion on cognitive function, hippocampal ultrastructure, synaptophysin (SYP) and postsynaptic density 95 (PSD-95) in aging mice. We also explored whether ApoE deletion affects the gut microbiota and the metabolite profile of the hippocampus in aging mice and finally examined the effect of ApoE deletion on lipids and oxidative stress in aging mice. The results showed that the deletion of ApoE aggravated cognitive dysfunction, hippocampal synaptic ultrastructural damage and dysregulation of SYP and PSD-95 expression in aging mice. Furthermore, ApoE deletion reduced gut microbial makeup in aging mice. Further studies showed that ApoE deletion altered the hippocampal metabolic profile and aggravated dyslipidemia and oxidative stress in aging mice. In brief, our findings suggest that loss of ApoE alters the composition of the gut microbiota, which in turn may affect cognitive function in aging mice through the gut microbiota–brain axis.

KEYWORDS

apolipoprotein E, aging, cognitive function, gut microbiota, metabolomics, oxidative stress

Introduction

Aging is a process in which the functions of various tissues and organs in the body gradually degenerate. With the intensification of population aging, aging has become a serious social problem (Joe and Ringman, 2019). Brain aging-induced cognitive and memory decline is one of the early symptoms of aging patients, and changes in hippocampal structure and function are closely related to learning and memory impairments (Kodali et al., 2021; Kokudai et al., 2021). At present, effectively delaying brain aging, maintaining the normal function of the hippocampus, and preventing cognitive dysfunction have become research hotspots in medicine.

Recently, increasing clinical and experimental evidence has suggested that the gut microbiota plays a crucial role in central nervous system (CNS) diseases through the gut microbiota-brain axis (Chakrabarti et al., 2022; Mou et al., 2022). The cognitive dysfunction associated with aging has been reported to be associated with intestinal microbiome disturbances (Pw and Jeffery, 2015; Mangiola et al., 2018). For example, medical studies in the elderly population have found higher *Firmicutes*/*Bacteroidetes* ratios in the gut microbiome of demented subjects than in non-demented controls (Saji et al., 2019). The gut microbiota is considered an invisible organ that mediates bidirectional signaling between the gut-brain axis (Doifode et al., 2021). Unfortunately, the relevant mechanisms between gut microbiota and brain aging have not been fully elucidated. Therefore, in-depth studies are warranted to elucidate the potential link between the gut microbiota-brain axis and cognitive impairment induced by brain aging.

Apolipoprotein E (ApoE) is the main plasma apolipoprotein, and it regulates lipid metabolism and maintains cholesterol balance. It also participates in the normal growth and development and damage repair of the CNS (Aires et al., 2021). Studies have shown that ApoE is the most abundantly expressed apolipoprotein in the brain and is responsible for regulating a large part of brain lipid metabolism, especially the transfer of cholesterol and phospholipids from glial cells to neurons (Hudry et al., 2019). Furthermore, loss of ApoE disrupts the blood–brain barrier in aging mice (Mulder et al., 2001) and leads to cognitive impairment (Zerbi et al., 2014) and cerebrovascular dysfunction (Bell et al., 2012). Recent studies have also found that ApoE deficiency alters the composition of the gut microbiome (Gan et al., 2022; Zajac et al., 2022). However, the mechanism by which ApoE affects lipid metabolism and cognitive impairment through the gut microbiota brain axis has not been investigated to date.

The gut microbiota is both a participant and a regulator of metabolic processes (Wang et al., 2017). Metabolomics can be used to effectively screen biomarkers and deeply analyze the molecular mechanisms of host health or disease (Rowland et al., 2018). To this end, we used ApoE knockout ($ApoE^{-/-}$) mice as study subjects to explore whether ApoE is involved in postaging cognitive dysfunction through the gut microbiota-brain axis. We explored the effect of ApoE deletion on cognitive function and gut microbes in D-galactose-induced aging mice. We also used a metabolomic approach to confirm whether the absence of ApoE affects the metabolite profile of the aging mouse hippocampus. In addition, we examined the effect of ApoE deletion on blood lipids and oxidative stress in aging mice. We hope to reveal the mechanism by which ApoE affects cognitive dysfunction in aged mice through the gut microbiota-brain axis.

Materials and methods

Animals

Twenty 10-week-old male SPF $ApoE^{-/-}$ mice were purchased from Gempharmatech Co., Ltd. (Nanjing, China), with a body weight of 25 ± 5 g [serial number: T001458, genetic background: C57BL/6 J, genotype: (ApoE) KO/KO, and license number: CXK (SU) 2018-0008]. Forty 10-week-old male SPF wild-type C57BL/6J mice, with a body weight 20 ± 2 g, were also used. Bedding materials and feed were provided by Hunan Laike Jingda Co., Ltd. (Changsha, China). The animals had free distilled drinking water, and the housing conditions were as follows: temperature of 20–25°C, humidity of 40–55%, natural light, normal feeding, and bedding replacement every other day.

Main reagents and instruments

D-galactose (V900922) was purchased from Sigma–Aldrich (Shanghai, China), anti-synaptophysin (SYP) antibody (ab32127) and anti-postsynaptic density 95 (PSD-95) antibody (ab238135) were purchased from Abcam (Cambridge, United Kingdom), and a superoxide dismutase (SOD) detection kit (20190412), a glutathione peroxidase (GSH-PX) detection kit (20190309), and a malondialdehyde (MDA) detection kit (20190315) were purchased from Jiancheng Co., Ltd. (Nanjing, China).

Vectra3 tissue section analysis system (Marlborough, United States), Illumina NovaSeq 6,000 sequencing system (Santiago, United States), Thermo Dionex U3000 UHPLC (Waltham, United States), Agilent 7890B-5977B GC–MS (Santa Clara, United States), Enspire multifunctional microplate reader (Waltham, United States), Waters ACQUITY UPLC HSS T3 (100 mm × 2.1 mm, 1.8 μm) chromatographic column (Framingham, United States).

Design of animal experiments

Forty wild-type mice were randomly divided into two groups [the control group and the model group (n = 20)], after

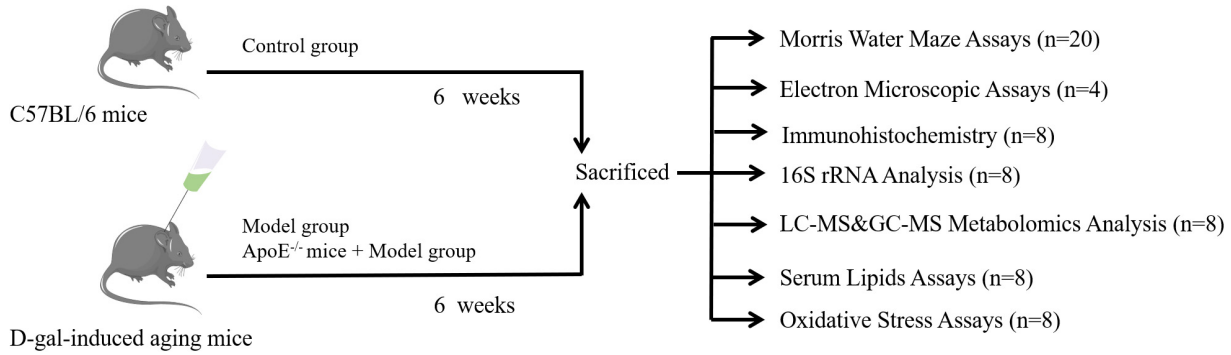

FIGURE 1
Experimental design.

adaptive feeding, and the other 20 ApoE$^{-/-}$ mice were set as the ApoE group. Except for the control group, the other groups were injected subcutaneously with 100 mg·kg^{-1} of D-galactose on the back of the neck once a day for 6 consecutive weeks, and the blank group was injected with the same amount of normal saline. The subcutaneous injection of D-galactose is a commonly used method to replicate aging models (Azman and Zakaria, 2019; Huang et al., 2020). After the Y maze and Morris water maze (MWM) in the 6th week, all mice were anesthetized by intraperitoneal injection of 1% sodium pentobarbital, the eyeballs were removed, blood was collected, and then the serum was obtained by centrifugation. Eight mice were randomly selected from each group for analysis of the gut microbiome, metabolomics, blood lipids and oxidative stress, and the remaining 12 were subjected to transmission electron microscopy analysis and immunohistochemical detection. As shown in **Figure 1**. This experimental protocol was approved by the Ethics Committee of the First Affiliated Hospital of Hunan University of Traditional Chinese Medicine (ZYFY20210710).

Y–maze test

According to the details in Reference (Suryavanshi et al., 2014), the memory ability of brief learning in mice was evaluated using the Y-maze test. The Y-maze consists of 3 arms radially oriented outward in 3 equal parts, and a single arm is 30 cm in length, 8 cm in width, and 15 cm in height with an angle between arms of 120. The Y maze was placed in a quiet room, and at the midpoint of the Y-maze at the beginning of the experiment, the movements of the mice were recorded over 8 min, and only consecutive entries into 3 different arms were counted as 1 correct alternating exploration, after which the mice were returned to their cages. After each assay was finished, a 75% ethanol wipe was used to eliminate mouse odor. The alternation rate was calculated as follows: alternation rate = number of correct alternations/(total alternations-2) × 100%.

Morris water maze test

According to the details in Hui et al. (2017), the MWM was used to test the long-term working memory ability of the mice. The MWM used a black round stainless steel pool (depth 60 cm, diameter 150 cm), and the top of the pool was connected to a video detection system. The platform was fixed in the second quadrant, tap water was injected into the pool, the water level was 1–2 cm higher than the platform, and the water temperature was controlled at 22–24°C. The mice were put into the water with their heads facing the pool wall, the water entry points were randomly selected, and the detection time was 60 s. The time when the mouse found the underwater platform was recorded. If it was found within 60 s, the animal was allowed to stay on the platform for 10 s to rest. If the platform was not found, the animal was guided to the platform and stayed for 10 s. Each animal was trained three times a day, with an interval of 15–20 min between each training session for 5 consecutive days. On the 6th day, the platform was removed, the animals were placed into the water from the opposite side of the original platform quadrant, and the latency and number of times the animals crossed the original platform quadrant within 60 s were recorded.

Detection of synaptic ultrastructure in the hippocampus

Specimens that had been placed in the transmission electron microscope (TEM) for 48 h were postfixed in 1% osmic acid at room temperature for 2 h, dehydrated stepwise through an ethanol gradient, and again dehydrated in acetone. After embedding in an embedding machine, the tissues were cut into 60–80-nm ultrathin sections, double stained with uranyl acetate and lead citrate, and dried overnight at room temperature. Synapses with clearly observed presynaptic and postsynaptic membranes and synaptic vesicles were selected

and photographed through TEM. Five synapses were randomly selected from each mouse, and a total of 20 synapses were selected from each mouse group, and structural parameters of synaptic interfaces were calculated using Image-Pro Plus 6.0 software (Jones and Devon, 1978; Güldner and Ingham, 1980).

Immunohistochemical detection

The expression levels of SYP and PSD-95 were determined by immunohistochemistry. The detection procedure was similar to that described in a previous study (Chen et al., 2022): the sections were dewaxed, antigen retrieval and blocked sequentially. SYP (1:100) and PSD-95 (1:100) primary antibodies were added and incubated overnight at 4°C, and then incubated with the corresponding secondary antibodies for 1 h at room temperature. Routine DAB staining was followed by counterstaining with hematoxylin and mounting of the slides. A smart tissue section imaging system was used for whole slide scanning, and images of the dentate gyrus (DG), CA1, and CA3 regions were collected from the hippocampus region. Densitometry was calculated using Image-Pro Plus 6.0 software.

Gut microbiota analysis

The genomic DNA of mouse cecal contents was extracted using a DNA extraction kit, and then the concentration of DNA was detected by agarose gel electrophoresis and a NanoDrop2000. Using genomic DNA as a template, primers 343F and 798R were used to amplify the V3-V4 region by PCR. After purification and quantification, a sequencing library was constructed. The following sequences were used: V3–V4 forward primer, 343F TACGGRAGGCAGCAGCAG; reverse primer, 798R AGGGTATCTAATCCT.

Using the QIIME 2 analysis process, DADA2 was used to denoise the raw data, cluster with 100% similarity, remove and correct low-quality sequences, identify and dechimerize algorithms, etc. The representative sequences of amplicon sequence variants (ASVs) were aligned with the template sequences in the SILVA-132-99 database to obtain the flora information of all ASVs at the levels of microbial phylum, class, order, family, genus, and species classification.

Metabolomics analysis

LC–MS analysis

The hippocampal tissue was removed from the −80°C refrigerator and thawed at 4°C. Then, 30 mg of tissue sample was accurately weighed, 20 μL of internal standard and 600 μL of methanol-water (V:V = 4:1) were added, and the samples were placed in a grinder and ground. Ultrasonic extraction was performed in an ice-water bath for 10 min. After standing at −20°C for 2 h and centrifuging for 10 min (13,000 rpm, 4°C), 150 μL of the supernatant was aspirated with a syringe, filtered through a 0.22-μm filter, and transferred to a sample vial until LC–MS analysis.

The chromatographic column was an ACQUITY UPLC HSS T3 (100 mm × 2.1 mm, 1.8 μm), and the mobile phases were A-water (containing 0.1% formic acid) and B-acetonitrile (containing 0.1% formic acid). The gradient elution program was 0–4 min, 5% B; 4–9 min, 30% B; 8–10 min, 50% B; 10–14 min, 80% B; 14–15 min, 100% B, and 15–16 min, 5% B. The following chromatographic conditions were used: flow rate, 0.35 mL·min^{-1}; injection volume, 2 μL; column temperature, 45°C. The following were the mass spectrometry conditions: the ion source was electrospray ionization (ESI); the positive and negative ion scanning modes were used for measurement, with spray voltages of 3,800 and −3,000 V, respectively; the capillary temperature was 320°C; the aux gas heater temperature was 350°C; the sheath gas flow rate was 35 Arb; the aux gas flow rate was 8 Arb; the full MS resolution was 70,000; and the mass range was 100–1 200 m/z. To ensure the stability of the entire analysis system, quality control (QC) samples were used for method verification in this experiment. The QC samples were obtained by mixing 10 μL of each normal sample. One QC sample was injected between every 10 samples to assess the stability of the mass spectrometry system.

GC-MS analysis

Similar to the above method, 30 mg of hippocampal tissue was accurately weighed, and 20 μL of internal standard and 600 μL of methanol-water (V:V = 4:1) were sequentially added. Then, the sample was placed in a grinder and ground. Next, 120 μL of chloroform was added, and the sample was vortexed for 2 min and then sonicated in an ice-water bath for 10 min. After standing at −20°C for 30 min, the samples were centrifuged for 10 min (13,000 rpm, 4°C), and 150 μL of the supernatant was removed and placed into a glass derivatization bottle. After evaporating the sample with a centrifugal concentrator desiccator, 80 μL of methoxyamine hydrochloride in pyridine (15 mg/mL) was added to a glass derivatized vial. After vortexing for 2 min, the oximation reaction was performed in a shaking incubator at 37°C for 90 min. After removing the sample, 50 μL of bis (trimethylsilyl) trifluoroacetamide (BSTFA) (containing 1% chlorotrimethylsilane); containing 1% trimethylchlorosilane (TMCS) derivatization reagent and 20 μL of n-hexane were added to 10 μL of 10 internal standards, vortexed for 2 min, and reacted at 70°C for 60 min. Finally, the sample was placed at room temperature for 30 min for GC–MS metabolomic analysis.

The chromatographic conditions were as follows: Column, DB-5MS capillary column (30 m × 0.25 mm × 0.25 μm, Agilent J&W Scientific, Folsom, CA, United States); inlet temperature, 260°C; carrier gas, helium, at a volume flow of 1 mL·min-1;

injection volume, 1 μL, splitless injection; and solvent delay, 6.2 min. The program temperature was as follows: the initial temperature of the column oven was 60°C and kept for 0.5 min; the temperature increased to 125°C at 8°C/min; the temperature was heated to 210°C at 8°C/min; and finally, the temperature was heated to 305°C at 20°C/min and kept for 5 min. The mass spectrometry conditions were as follows: ion source temperature, 230°C; quadrupole temperature, 150°C; and electron energy, 70 eV. The scanning mode was full scan mode (SCAN), and the mass scanning range was m/z 50–500. Both the LC–MS and GC–MS analyses were performed by OE Biotech Co., Ltd. (Shanghai, China).

Blood lipid detection

One hundred microliters of serum and distilled water were diluted and mixed at 1:1 and then sent to the Laboratory Department of the First Affiliated Hospital of Hunan University of Chinese Medicine. A Beckman Coulter AU680 automatic biochemical analyzer was used to detect the total cholesterol (TC), triglyceride (TG) and low-density lipoprotein (LDL) levels.

Oxidative stress detection

After rinsing the hippocampal tissue with precooled normal saline, sterile ophthalmic scissors were used to cut the tissue into pieces, and normal saline was added according to the ratio of m (tissue): V (normal saline) = 1 g:9 mL using an automatic homogenizer. The homogenate was made into a 10% homogenate by mass fraction and centrifuged at 1,000 g (4°C) for 15 min, and the supernatant was diluted with an appropriate amount of normal saline to a suitable concentration range. The instructions of the kit were strictly followed to detect SOD and GSH-Px activity and the MDA content in serum and brain tissue.

Statistical analysis

GraphPad Prism 8.0.2 statistical analysis software was used for statistical analysis of the data. Measurement data are expressed as the mean plus or minus standard error ($\bar{x} \pm s$). One-way analysis of variance (ANOVA) was used for data comparison among multiple groups in the experiment, and the LSD test was used for multiple comparisons. $P < 0.05$ was considered statistically significant.

In the 16S rRNA analysis, Usearch software was used to dechimerize and cluster the data to obtain operational taxonomic units (OTUs) for alpha diversity and beta diversity analyses. Linear discriminant analysis (LDA) was used to estimate the communities or species that had significantly different effects on sample partitioning.

In the metabolomic analysis, partial least squares discriminant analysis (PLS-DA) combined with variable importance of projection (VIP) > 1 and $P < 0.05$ was used to screen differential metabolites. Metabolic pathway enrichment analysis was performed using the Kyoto Encyclopedia of Genes and Genomes (KEGG) database.[1]

Results

Apolipoprotein E deletion aggravates cognitive dysfunction in aging mice

In the Y-maze test, compared with the control group, the alternation rate in the model group was significantly decreased ($P < 0.01$), and the alternation rate was further decreased in the ApoE group ($P < 0.05$, **Figure 2A**). In the navigation test, with an increase in the training time and the number of training sessions, the time for mice in each group to find the platform tended to shorten. Compared with the control group, the escape latency of mice in the model group was significantly prolonged ($P < 0.01$), and the latency of the ApoE group was further prolonged compared with that of the model group ($P < 0.01$, **Figure 2B**). The results of the space exploration test showed that compared with the control group, the model group spent less time in the target quadrant ($P < 0.01$), and the number of platform crossings was significantly reduced ($P < 0.01$). Compared with that of the model group, there was no significant change in the number of platform crossings in the ApoE group ($P > 0.05$), but the time spent in the target quadrant was significantly increased ($P < 0.01$), as shown in **Figures 2C–E**. These results suggest that deletion of ApoE aggravates D-galactose injection-induced cognitive impairment.

Apolipoprotein E deletion aggravates hippocampal synaptic ultrastructural damage in aging mice

TEM was used to assess hippocampal synaptic ultrastructure. The synaptic structure of the hippocampal neurons in the control group was complete, and the presynaptic membrane, synaptic cleft, postsynaptic membrane and postsynaptic dense material were clearly visible. Compared with the control group, the synaptic structure of the model group was blurred, the postsynaptic dense material was sparse, and the boundary between the anterior and posterior

1 https://www.kegg.jp/

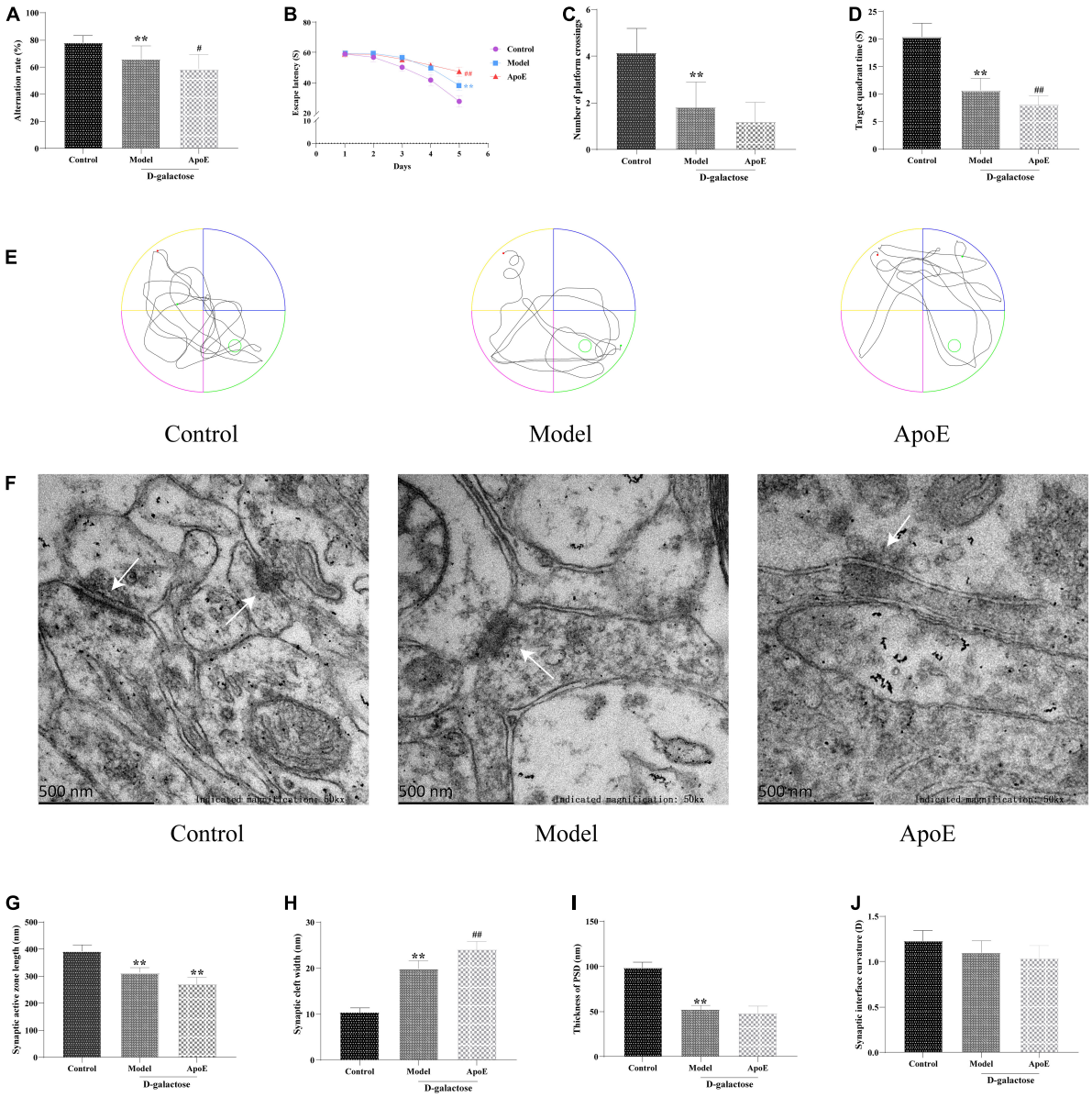

FIGURE 2
Effects of ApoE on cognitive function and hippocampal synaptic ultrastructure in aging mice. **(A)** Y-maze test, $n = 20$. **(B)** Navigation test, $n = 20$. **(C)** Platform crossing, $n = 20$. **(D)** Target quadrant time, $n = 20$. **(E)** MWM representative figures. **(F)** Ultrastructure of hippocampal synapses. **(G)** Synaptic active zone length, $n = 4$ (Five synapses were randomly selected from each mouse). **(H)** Synaptic cleft width, $n = 4$ (Five synapses were randomly selected from each mouse). **(I)** Thickness of PSD, $n = 4$ (Five synapses were randomly selected from each mouse). **(J)** Synaptic interface curvature, $n = 4$ (Five synapses were randomly selected from each mouse). $^{**}p < 0.01$ vs. Control group, $^{\#\#}p < 0.01$, $^{\#}p < 0.05$ vs. Model group.

membranes was unclear. Compared with that of the model group, the synaptic structure of the ApoE group was blurred, and a large number of vesicles accumulated around these structures, as shown in Figure 2F. In addition, compared with the control group, we observed that the length of the synaptic active zone and the thickness of the postsynaptic density were significantly decreased ($P < 0.01$), and the width of the synaptic cleft was significantly increased ($P < 0.01$) in the model group. Compared with the model group, the length of the synaptic active zone further decreased ($P < 0.01$) and the width of the synaptic cleft further increased ($P < 0.01$) in the ApoE group, but the curvature of the synaptic interface did not alter (Figures 2F–J). This result suggested that the deletion of ApoE aggravated the damage to the hippocampal synaptic structure induced by D-galactose injection.

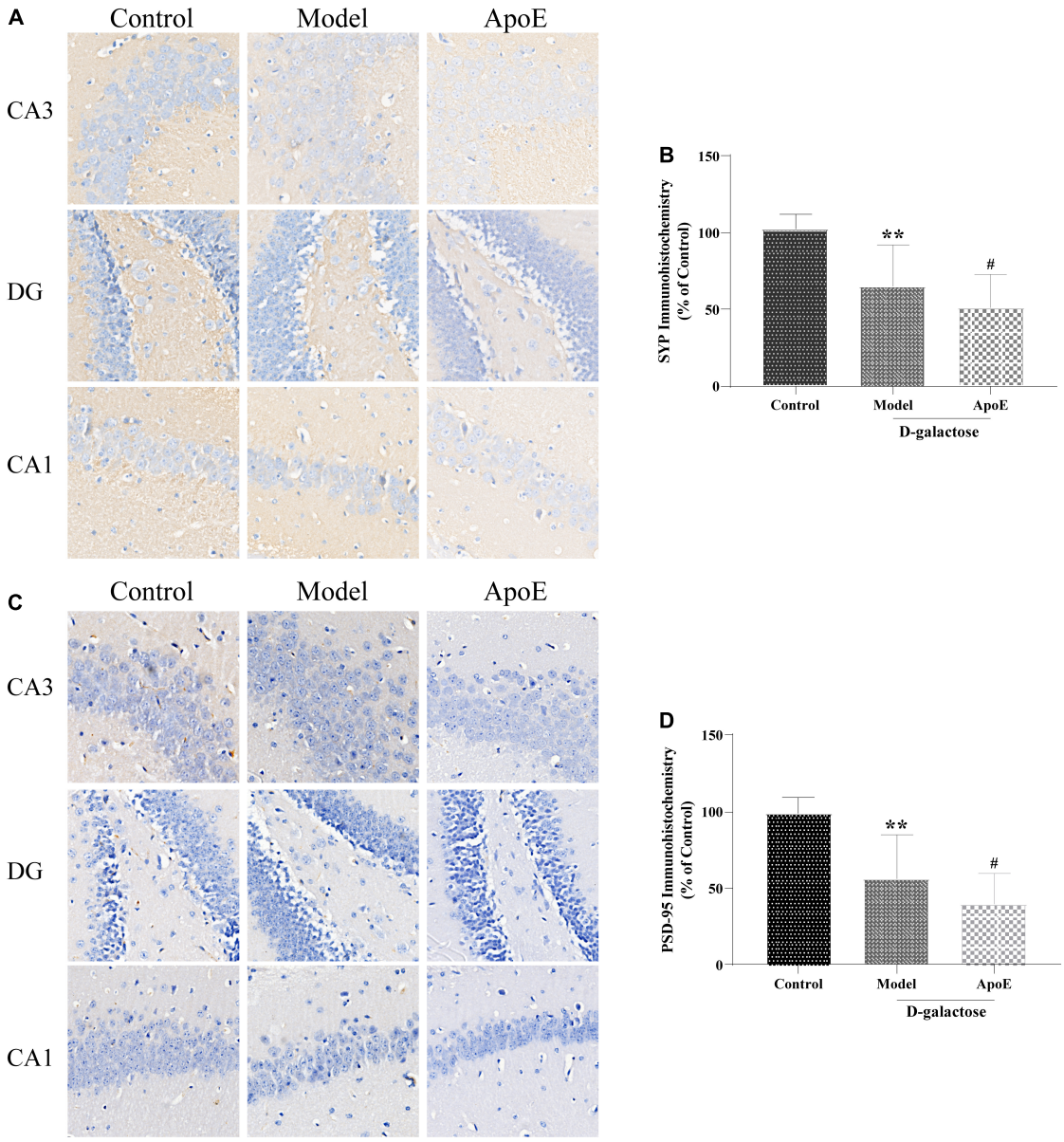

FIGURE 3
ApoE Deletion aggravates the dysregulation of SYP and PSD-95 expression in the hippocampus of aging mice. **(A)** Immunohistochemistry staining for SYP in different hippocampal regions. **(B)** Quantification of SYP intensity, $n = 8$. **(C)** Immunohistochemistry staining for PSD-95 in different hippocampal regions. **(D)** Quantification of PSD-95 intensity, $n = 8$. $^{**}p < 0.01$ vs. Control group, $^{\#}p < 0.05$ vs. Model group.

Apolipoprotein E deletion aggravates the dysregulation of synaptophysin and PSD-95 expression in the hippocampus of aging mice

Compared with the control group, the expression of SYP and PSD-95 in the hippocampus of the model group was significantly reduced ($P < 0.01$). Compared with the model group, hippocampal SYP and PSD-95 expression were further reduced in the ApoE group ($P < 0.05$). These results suggest that the ApoE deletion aggravates the dysregulation of SYP and PSD-95 expression in the hippocampus induced by D-galactose injection, as shown in Figure 3.

Deletion of apolipoprotein E affects the gut microbial composition of aging mice

We used the Chao1 index, observed species index and Shannon index to assess the alpha diversity of the gut

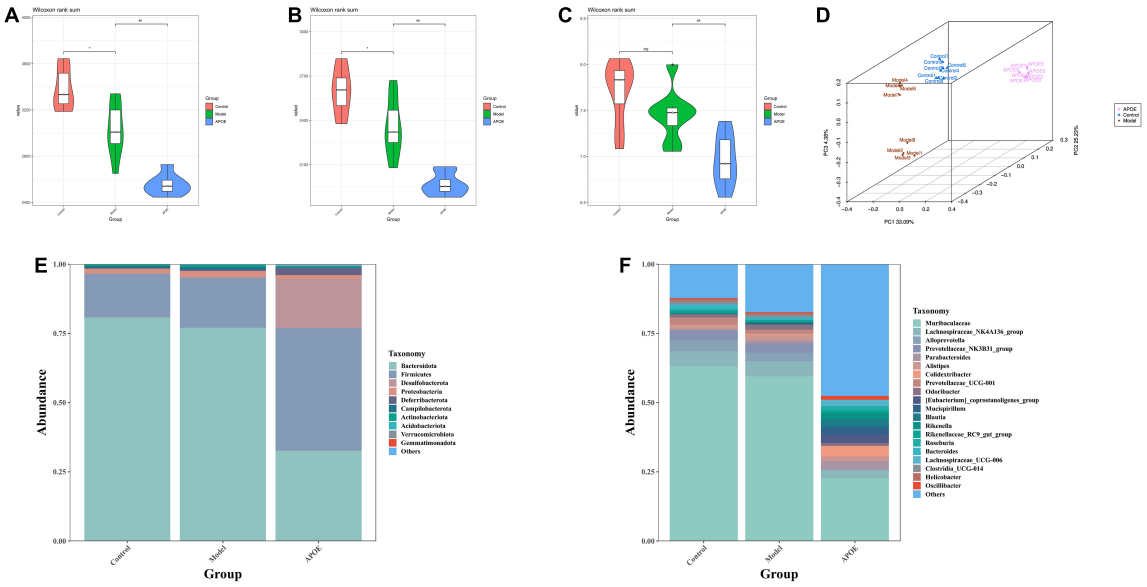

FIGURE 4
Deletion of ApoE affects the gut microbial composition of aging mice. **(A)** Chao 1 index, $n = 8$. **(B)** Observed species index, $n = 8$. **(C)** Shannon index, $n = 8$. **(D)** PCoA analysis. **(E)** Relative abundance of gut microbiota (phylum level). **(F)** Relative abundance of gut microbiota (genus level). $^{*}P < 0.05$ vs. Control group, $^{\#\#}p < 0.01$ vs. Model group.

microbes. We found that the microbiota number and diversity were reduced in the model group compared with the control group ($P < 0.05$). The ApoE group was found to have a further decrease in the number and diversity of microbiota relative to the model group ($P < 0.01$), as shown in Figures 4A–C. In addition, beta diversity analysis was utilized to assess the differences between microbial communities. Principal coordinates analysis (PCoA) based on weighted UniFrac distance showed significantly different gut microbial compositions and structures in each group, as shown in Figure 4D. To understand the impact of ApoE deletion on the gut microbiota, we further analyzed the taxonomic levels of the gut microbiota between the different groups. At the phylum level, compared with the control group, the model group showed that the relative abundance of *Bacteroidota* decreased, the abundance of *Firmicutes* increased, and the ratio of *Bacteroidetes*/*Firmicutes* decreased significantly. Compared with the model group, the ApoE group mice showed decreased relative abundances of *Bacteroidota* and *Desulfobacterota* and increased abundances of *Firmicutes* and *Desulfobacterota*, and the ratio of *Bacteroidetes*/*Firmicutes* decreased significantly, as shown in Figure 4E. At the genus level, compared with the control group, the relative abundance of *Muribaculaceae* decreased and *Parabacteroides* increased in the model group. Compared to the model group, *Muribaculaceae*, *Lachnospiraceae_NK4A136_group* and *Alloprevotella* were significantly decreased in ApoE mice, and the abundances of *Parabacteroides*, *Colidextribacter*, *Mucispirillum*, *Bacteroidesk*, and *Clostridia_UCG-014* were increased, as shown in Figure 4F.

Linear discriminant analysis effect size (LEfSe) was applied to identify key microbiota that were differentially represented in ApoE$^{-/-}$ mice. We found that the dominant bacterial groups in the control group were *Bacteroidota* at the phylum level, *Bacteroidia* at the class level, *Bacteroidales* at the order level, *Muribaculaceae* and *Prevotellaceae* at the family level. The dominant bacteria in the model group may be Ruminococcaceae at the family level. The dominant flora of the ApoE group were *Firmicutes* at the phylum level, *Clostridia* at the class level, and *Desulfovibrionaceae Lachnospiraceae* and *Rikenellaceae* at the family level, as shown in Figures 5A,B.

Furthermore, to determine whether taxonomic changes in gut microbes affect their function, functional prediction of representative sequences of gut microbes was performed by PICRUSt2. Compared with the model group, the ApoE group had significant differences in energy metabolism, lipid metabolism, amino acid metabolism, and nervous system pathways, as shown in Figure 5C.

Deletion of apolipoprotein E alters the metabolic profile of the hippocampus of aging mice

The metabolite effects of ApoE on the hippocampal tissue of aging mice were first analyzed by LC–MS. We detected a total of 8,251 species peaks, of which 2,872 metabolites were identified. PLS-DA was used to distinguish the overall differences in metabolic profiles between groups. As shown

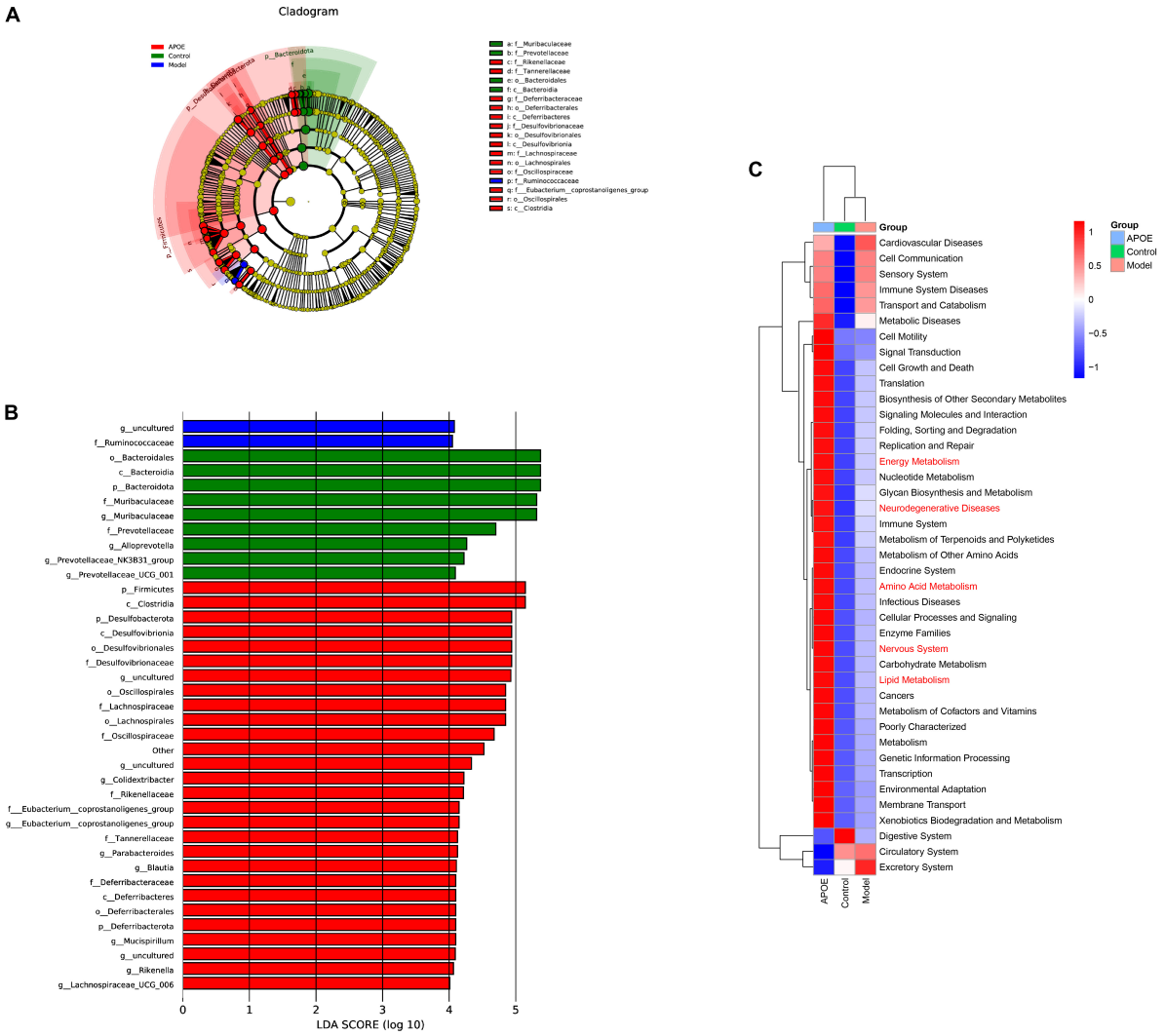

FIGURE 5
LEfSe and PICRUSt2 analysis. **(A)** Cladogram of LEfSe analysis. **(B)** LDA of LEfSe analysis. **(C)** PICRUSt2 analysis.

in Figures 6A,B, the differences between the groups were significant. According to the VIP $>$ 1 and $p < 0.05$ criteria, the differential metabolites between the different groups were determined, there were 47 differential metabolites between the model group and the control group, and 32 differential metabolites were found between the ApoE group and the model group (Supplementary Table 1).

Subsequently, we analyzed the metabolite effects of ApoE on the hippocampal tissue of aging mice by GC–MS. GC–MS is efficient at detecting compounds with strong volatility, small molecular weight, and low polarity and can be used as a complement to LC–MS for thermally stable compounds. We identified a total of 668 metabolites by GC–MS. PLS-DA was used to discriminate the overall differences in metabolic profiles between the groups, as shown in Figures 6C,D, and the differences between the groups were significant. Differential metabolites between groups were determined according to VIP $>$ 1 and $p < 0.05$. There were 53 differential metabolites between the model group and the control group, and 42 differential metabolites were found between the ApoE group and the model group (Supplementary Table 2).

By integrating the data of the dual-platform metabolome, we found a total of 100 differential metabolites between the model group and the control group and a total of 74 differential metabolites between the ApoE group and the model group, as shown in Figures 6E,F. Subsequently, we analyzed the metabolic pathways involved in the above 74 metabolites based on the KEGG database. Finally, we found that pyrimidine metabolism, alanine, aspartate, and glutamate metabolism, galactose metabolism and glycerophospholipid metabolism were the main metabolic pathways, as shown in Figure 6G. Notably, we found that alanine, aspartate and glutamate

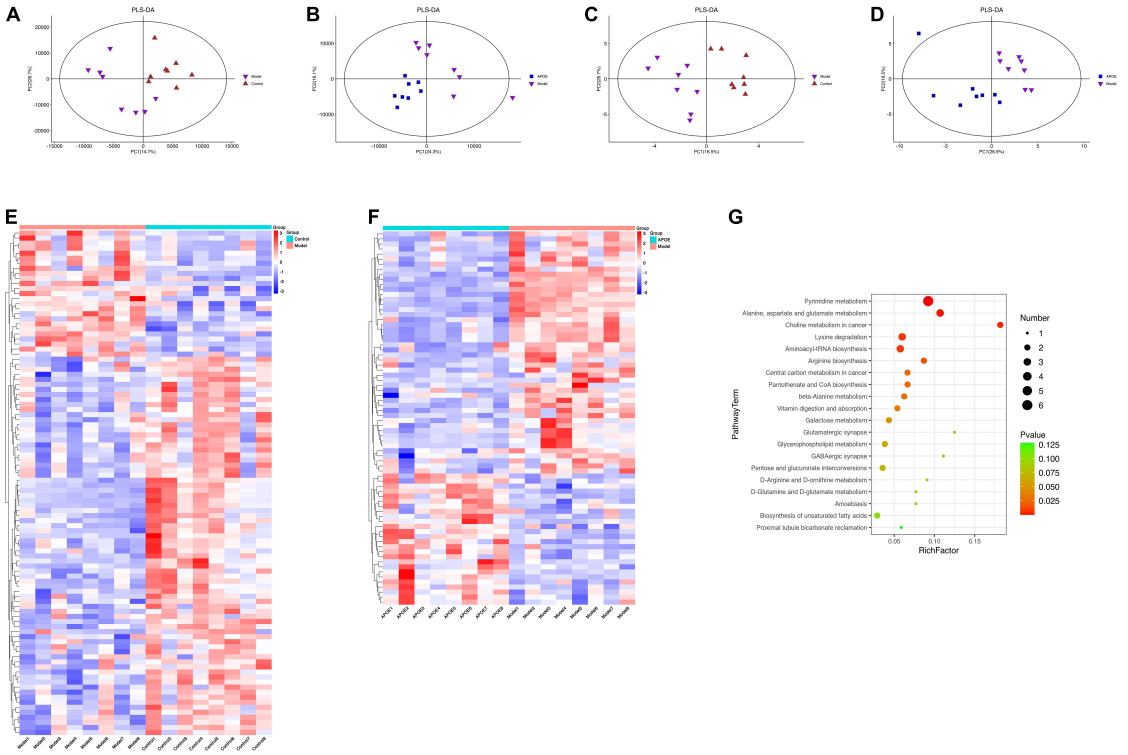

FIGURE 6
Deletion of ApoE alters the metabolic profile of the hippocampus of aging mice. **(A)** PLS-DA of LC-MS about model group vs. control group. **(B)** PLS-DA of LC-MS about ApoE group vs. model group. **(C)** PLS-DA of GC-MS about model group vs. control group. **(D)** PLS-DA of GC-MS about ApoE group vs. model group. **(E)** Differentially abundant metabolites about model group vs. control group. **(F)** Differentially abundant metabolites about ApoE group vs. model group. **(G)** Analysis of metabolic pathway enrichment.

metabolism and glycerophospholipid metabolism, which were significantly enriched by metabolomics, were quite similar to the metabolic pathways such as amino acid metabolism and lipid metabolism predicted by PICRUSt in the 16S analysis. This result suggests that there may be some connection between gut microbes and hippocampal metabolites.

Deletion of apolipoprotein E alters blood lipids and oxidative stress levels in aging mice

The enrichment analysis of the above 16 S and differential metabolites in the hippocampus suggested that ApoE deletion might contribute to cognitive impairment in aging mice by affecting lipid metabolism. Therefore, we investigated the effect of ApoE deletion on serum lipids in aging mice. As shown in Figures 7A–C, compared with those of the control group, the concentrations of TC, TG and LDL in the model group were significantly increased ($p < 0.01$). Compared to those of the model group, the levels of TC, TG and LDL in the ApoE group were further increased ($p < 0.01$), suggesting that the absence of ApoE aggravated dyslipidemia in aging mice.

In addition, lipid metabolism disorders often lead to lipid peroxidation, and oxidative stress is an important factor in cellular aging (Mecocci et al., 2018; Zarrouk et al., 2020). We further examined the effect of ApoE deletion on the activities of T-SOD and GSH-Px and the MDA content in the serum and brain tissue of aging mice. As shown in Figures 7D–I, compared with those of the control group, the MDA content in the serum and brain tissue of the mice in the model group was significantly increased ($P < 0.01$), and the activities of T-SOD and GSH-Px were significantly decreased ($P < 0.01$). In comparison with that in the model group, the MDA content in the ApoE group was further increased ($P < 0.01$), and the SOD and GSH-Px activities were further decreased ($P < 0.05$ or $P < 0.01$). This result suggested that ApoE aggravated oxidative stress in aging mice.

Discussion

At present, studies have confirmed that ApoE is related to atherosclerosis (AS), Alzheimer's disease (AD) and other vascular diseases and CNS dysfunction. Within the CNS, ApoE is synthesized and secreted by astrocytes and is involved in

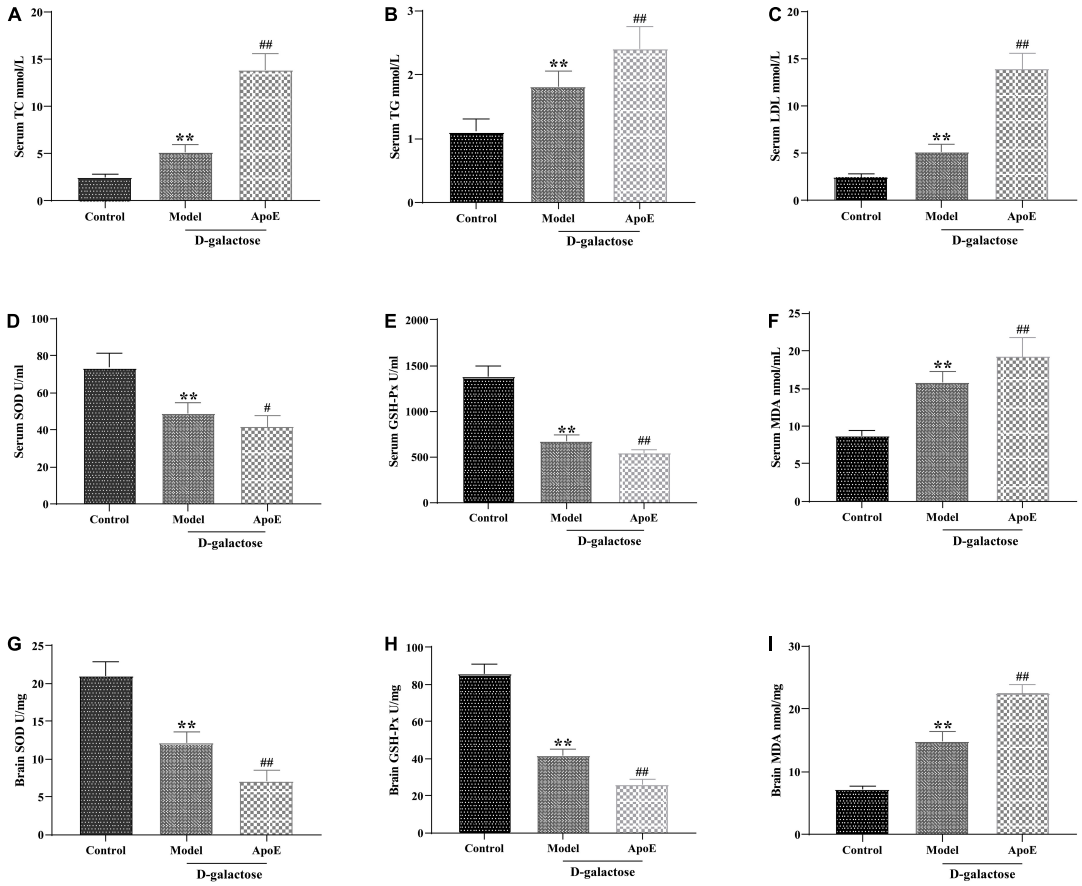

FIGURE 7
Deletion of ApoE alters blood lipids and oxidative stress levels in rapidly aging mice. **(A)** TC, $n = 8$. **(B)** TG, $n = 8$. **(C)** LDL, $n = 8$. **(D)** SOD in serum, $n = 8$. **(E)** GSH-Px in serum, $n = 8$. **(F)** MDA in serum, $n = 8$. **(G)** SOD in brain tissue, $n = 8$. **(H)** GSH-Px in brain tissue, $n = 8$. **(I)** MDA in brain tissue, $n = 8$. $^{**}p < 0.01$ vs. Control group. $^{\#}p < 0.05$, $^{\#\#}p < 0.01$ vs. Model group.

maintaining the homeostasis of cholesterol and phospholipids, regulating the mobilization and redistribution of cholesterol and phospholipids during neural membrane remodeling, and thus in regulating the maintenance of synaptic plasticity as well as repair processes when neuronal cells are damaged (Cantuti-Castelvetri et al., 2018). Therefore, ApoE$^{-/-}$ mice are not only used in the study of atherosclerosis but are also used as a new animal model in the study of the mechanism of cognitive impairment (Watson et al., 2021). In this study, we found that loss of ApoE aggravated cognitive dysfunction and hippocampal synaptic ultrastructural damage in aging mice, aggravated the dysregulation of hippocampal SYP and PSD-95 protein expression, and altered the gut microbiome composition and the metabolic profile of hippocampal tissue. It was also found that the absence of ApoE aggravated lipid metabolism disorders and oxidative stress in aging mice. Our findings further elucidate the potential of ApoE as a therapeutic target for improving cognitive impairment in aging.

The gut microbiota is considered to be the host's "second genome" and plays an important role in maintaining body homeostasis and in the development of cognitive dysfunction (Li et al., 2019; Liu et al., 2021b). *Bacteria* have recently been identified in the brains of AD patients, suggesting that the microbiota may be a contributing factor to related neuroinflammation (Emery et al., 2017). Probiotics can modulate gut microbiota dysbiosis and microbiota–gut–brain axis deficits to improve cognitive dysfunction in aged mice (Yang et al., 2020; Liu et al., 2021c). In the present study, Chao1 index and observed species index of α diversity for evaluating intestinal microorganisms in aging mice were significantly decreased, and the correlation index was further decreased after ApoE knockout, suggesting that ApoE knockout reduced gut microbial diversity in aging mice. In addition, at the phylum level, the ratio of *Bacteroidetes*/*Firmicutes* in ApoE$^{-/-}$ mice was significantly decreased. The *Bacteroidetes*/*Firmicutes* ratio is often used to reflect the health of the gut microbiota (Mariat et al., 2009), Recent studies have shown that in amnesic mice, the *Bacteroidetes*/*Firmicutes* ratio was significantly reduced, and restoration of the *Bacteroidetes*/*Firmicutes* ratio reversed memory deficits (Zhao et al., 2022). At the genus

level, *Muribaculaceae*, *Lachnospiraceae_NK4A136_group*, *Parabacteroides,* and *Alloprevotella* were significantly decreased in ApoE group mice, and the abundance of *Parabacteroides* was increased. Studies have found that a high abundance of *Muribaculaceae* is closely related to longevity (Sibai et al., 2020); the high abundance of *Lachnospiraceae_NK4A136_group* can improve inflammation and oxidative stress in aging mice (Sheng et al., 2022). *Alloprevotella* is a beneficial bacterium that is closely related to lipid metabolism in aging mice (Wu et al., 2022), and increasing the abundance of *Alloprevotella* can improve the memory function of mice (Liu et al., 2021a). In contrast, *Parabacteroide*s can be used as an independent risk factor for mild cognitive impairment in the elderly (Khine et al., 2020), and a high abundance of *Parabacteroides* can exacerbate neurodegeneration (Blacher et al., 2019). LEfSe analysis found that at the phylum level, the dominant flora was likely *Firmicutes* in ApoE$^{-/-}$ mice. *Firmicute*s are mostly gram-positive bacteria and are significantly increased in the gut of aging mice (Kim et al., 2016). Finally, through PICRUSt2 analysis, we found that energy metabolism, lipid metabolism, amino acid metabolism, and nervous system may be the main metabolic pathways of the differential flora. Based on the above studies, we speculated that ApoE might regulate the ratio of *Bacteroidetes*/*Firmicutes* to affect lipid metabolism and oxidative stress to improve age-related cognitive dysfunction, but the mechanism remains to be further investigated.

A link between metabolic biomarkers and the gut microbiota has been demonstrated, with important consequences for the host (Luo et al., 2020). In this study, the endogenous metabolites in the hippocampus of ApoE$^{-/-}$ aging mice were systematically analyzed based on LC–MS and GC–MS metabolomics platforms. The ApoE group was significantly separated from the model group, suggesting significant changes in hippocampal metabolites. Seventy-four differentially expressed metabolites were identified as potential metabolic markers affected by ApoE. KEGG enrichment analysis found that pyrimidine metabolism; alanine, aspartate and glutamate metabolism; galactose metabolism; and glycerophospholipid metabolism were the main metabolic pathways. At present, the role of pyrimidine metabolism in the aging process remains to be further defined. In addition, some scholars have studied the metabolic changes in the levels of glutamate groups (glutamic acid, gamma-aminobutyric acid, glutamine, aspartic acid and alanine) in the rat brain, and the results show that the changes in the levels of these amino acids are related to aging (Rajeswari and Radha, 1984). Glycerophospholipids are amphiphilic molecules that play important roles in functions such as nerve cell membranes, receptors, transporters, ion channels, and reservoirs for lipid mediators. At the same age, the level of glycerophospholipids in the brains of AD patients is lower than that of the control group (Kim et al., 2014). These alterations in glycerophospholipids lead to changes in cell membrane permeability and ionic homeostasis, which also contribute to oxidative stress and neurodegenerative changes (Sagy-Bross et al., 2015).

It is worth noting that the enrichment analysis of the gut microbes and differential metabolites in the hippocampus suggests that ApoE may affect cognitive dysfunction in aging mice by regulating lipid metabolism. Lipids are one of the basic components of neuronal cell membranes and are closely related to the normal metabolism and abnormal accumulation of Aβ (Ehehalt et al., 2003). Many studies have shown that lipid metabolism plays an important role in the process of aging and gradual cognitive dysfunction (Johnson and Stolzing, 2019; Wei et al., 2020; Mutlu et al., 2021). In this study, we found that the serum concentrations of TC, TG, and LDL were significantly increased in aging mice, while ApoE deletion aggravated dyslipidemia in aging mice. Clinical studies have shown that higher serum concentrations of TC and LDL-C and a higher LDL-C/HDL-C ratio are positively correlated with cognitive decline (An et al., 2019). ApoE plays a crucial role in lipid metabolism (Aires et al., 2021). Another study of 1,065 individuals aged 56–105 found that centenarians had the highest ApoE plasma concentrations (Muenchhoff et al., 2017). The above studies suggest that ApoE may affect the cognitive function of aging mice by regulating lipid metabolism. Disorders of lipid metabolism are often accompanied by oxidative stress (Zarrouk et al., 2020), and oxidative stress is an important risk factor for aging and cognitive dysfunction (Mecocci et al., 2018). Abnormal oxidative stress can cause lipid peroxidation, leading to apoptosis and tissue damage, which is a major risk factor for various neurodegenerative diseases (Vatner et al., 2020). This study showed that the MDA content in the serum and hippocampus of aging mice was significantly increased, the activities of T-SOD and GSH-Px were significantly decreased, and ApoE knockout exacerbated oxidative stress in aging mice. Recently, the gut microbiota–brain axis has gained extensive attention as a channel for communication and physiological regulation. The activity of the gut microbiome may promote abnormal lipid deposition and oxidation reactions, which can damage the brain (Shao et al., 2020). This study speculated that ApoE knockout affected gut microbiota diversity in aging mice, aggravated disordered lipid metabolism and oxidative stress and exacerbated cognitive dysfunction in aging mice.

Notably, this study has some limitations. We did not use germ-free mice or fecal transplantation and could not determine exactly which flora are associated with the effects of ApoE. Second, there are several ApoE alleles (ApoE2, ApoE3, and ApoE4) in humans, and this study did not explore the effect of the corresponding alleles on aging. Additionally, the findings still need to be clinically validated and warrant further investigation. Moreover, we did not determine whether aging and ApoE deletion lead to altered lipid metabolism in the gut. We will continue this research in future work.

Conclusion

In summary, this study demonstrated that ApoE deficiency aggravated cognitive function and hippocampal synaptic ultrastructural damage in aging mice, aggravated the dysregulation of hippocampal SYP and PSD-95 protein expression, affected the gut microbial composition and hippocampal metabolic profile in aging mice, and aggravated dyslipidemia and oxidative stress in aging mice. This study helps us to further reveal the underlying mechanism by which ApoE improves aging-related cognitive dysfunction through the gut microbiota–brain axis, which is worthy of further research.

Data availability statement

The datasets presented in this study can be found in online repositories. The names of the repository/repositories and accession number (s) can be found in the article/**Supplementary material**.

Ethics statement

This animal study was reviewed and approved by the Ethics Committee of the First Affiliated Hospital of Hunan University of Traditional Chinese Medicine.

Author contributions

BC and JY: draft preparation, *in vitro* experiments, and writing the manuscript. YX: behavioral experiments and data analysis. HW, FT, and YL: model construct. LL and LX: data analysis. BL: experiment design and supervision. All authors contributed to the article and approved the submitted version.

Funding

This work was supported by the Hunan Provincial Department of Education Open Platform Fund (20K096), Hunan Provincial Traditional Chinese Medicine Research Project (2020098), Changsha Natural Science Foundation (kq2014223), and Hunan University of Chinese Medicine Double First-Class Discipline Open Fund (2022ZYX15).

Conflict of interest

The authors declare that the research was conducted in the absence of any commercial or financial relationships that could be construed as a potential conflict of interest.

Publisher's note

All claims expressed in this article are solely those of the authors and do not necessarily represent those of their affiliated organizations, or those of the publisher, the editors and the reviewers. Any product that may be evaluated in this article, or claim that may be made by its manufacturer, is not guaranteed or endorsed by the publisher.

Supplementary material

The Supplementary Material for this article can be found online at: https://www.frontiersin.org/articles/10.3389/fnins.2022.939915/full#supplementary-material

SUPPLEMENTARY TABLE 1
Differential metabolites identified by LC-MS.

SUPPLEMENTARY TABLE 2
Differential metabolites identified by GC-MS.

References

Aires, R., Porto, M., de Assis, L. M., Pereira, P., Carvalho, G., Côco, L., et al. (2021). DNA damage and aging on hematopoietic stem cells: Impact of oxidative stress in ApoE/ mice. *Exp. Gerontol.* 156:111607. doi: 10.1016/j.exger.2021.111607

An, Y., Zhang, X., Wang, Y., Wang, Y., Liu, W., Wang, T., et al. (2019). Longitudinal and nonlinear relations of dietary and Serum cholesterol in midlife with cognitive decline: Results from EMCOA study. *Mol. Neurodegener.* 14:51. doi: 10.1186/s13024-019-0353-1

Azman, K., and Zakaria, R. (2019). D-Galactose-induced accelerated aging model: An overview. *Biogerontology* 20, 763–782. doi: 10.1007/s10522-019-09837-y

Bell, R., Winkler, E., Singh, I., Sagare, A., Deane, R., Wu, Z., et al. (2012). Apolipoprotein E controls cerebrovascular integrity via cyclophilin a. *Nature* 485, 512–516. doi: 10.1038/nature11087

Blacher, E., Bashiardes, S., Shapiro, H., Rothschild, D., Mor, U., Dori-Bachash, M., et al. (2019). Potential roles of gut microbiome and metabolites in modulating ALS in mice. *Nature* 572, 474–480. doi: 10.1038/s41586-019-1443-5

Cantuti-Castelvetri, L., Fitzner, D., Bosch-Queralt, M., Weil, M., Su, M., Sen, P., et al. (2018). Defective cholesterol clearance limits remyelination in the aged central nervous system. *Science* 359, 684–688. doi: 10.1126/science.aan4183

Chakrabarti, A., Geurts, L., Hoyles, L., Iozzo, P., Kraneveld, A., La Fata, G., et al. (2022). The microbiota-gut-brain axis: Pathways to better brain health. Perspectives on what we know, what we need to investigate and how to put knowledge into practice. *Cell. Mol. Life Sci.* 79:80. doi: 10.1007/s00018-021-04060-w

Chen, B., Yi, J., Xu, Y., Zheng, P., Tang, R., and Liu, B. (2022). Construction of a circRNA-miRNA-mRNA network revealed the potential mechanism of Buyang

Huanwu Decoction in the treatment of cerebral ischemia. *Biomed. Pharmacother.* 145:112445. doi: 10.1016/j.biopha.2021.112445

Doifode, T., Giridharan, V., Generoso, J., Bhatti, G., Collodel, A., Schulz, P., et al. (2021). The impact of the microbiota-gut-brain axis on Alzheimer's disease pathophysiology. *Pharmacol. Res.* 164:105314. doi: 10.1016/j.phrs.2020.105314

Ehehalt, R., Keller, P., Haass, C., Thiele, C., and Simons, K. (2003). Amyloidogenic processing of the Alzheimer beta-amyloid precursor protein depends on lipid rafts. *J. Cell Biol.* 160, 113–123. doi: 10.1083/jcb.200207113

Emery, D. C., Shoemark, D. K., Batstone, T. E., Waterfall, C. M., Coghill, J. A., Cerajewska, T. L., et al. (2017). 16S rRNA next generation sequencing analysis shows bacteria in alzheimer's Post-Mortem brain. *Front. Aging Neurosci.* 9:195. doi: 10.3389/fnagi.2017.00195

Gan, G., Lu, B., Zhang, R., Luo, Y., Chen, S., Lei, H., et al. (2022). Chronic apical periodontitis exacerbates atherosclerosis in apolipoprotein E-deficient mice and leads to changes in the diversity of gut microbiota. *Int. Endod. J.* 55, 152–163. doi: 10.1111/iej.13655

Güldner, F., and Ingham, C. (1980). Increase in postsynaptic density material in optic target neurons of the rat suprachiasmatic nucleus after bilateral enucleation. *Neurosci. Lett.* 17, 27–31. doi: 10.1016/0304-3940(80)90056-7

Huang, J., Hou, B., Zhang, S., Wang, M., Lu, X., Wang, Q., et al. (2020). The protective effect of Adiponectin-Transfected endothelial progenitor cells on cognitive function in D-Galactose-Induced aging rats. *Neural Plast.* 2020:1273198. doi: 10.1155/2020/1273198

Hudry, E., Klickstein, J., Cannavo, C., Jackson, R., Muzikansky, A., Gandhi, S., et al. (2019). Opposing Roles of apolipoprotein E in aging and neurodegeneration. *Life Sci. Alliance* 2:e201900325. doi: 10.26508/lsa.201900325

Hui, S., Yang, Y., Peng, W., Sheng, C., Gong, W., Chen, S., et al. (2017). Protective effects of *Bushen Tiansui* decoction on hippocampal synapses in a rat model of Alzheimer's disease. *Neural Regen. Res.* 12, 1680–1686. doi: 10.4103/1673-5374.217347

Joe, E., and Ringman, J. (2019). Cognitive symptoms of Alzheimer's disease: Clinical management and prevention. *BMJ* 367:l6217. doi: 10.1136/bmj.l6217

Johnson, A., and Stolzing, A. (2019). The role of lipid metabolism in aging, lifespan regulation, and age-related disease. *Aging Cell* 18:e13048. doi: 10.1111/acel.13048

Jones, D., and Devon, R. (1978). An ultrastructural study into the effects of pentobarbitone on synaptic organization. *Brain Res.* 147, 47–63. doi: 10.1016/0006-8993(78)90771-0

Khine, W., Voong, M., Ng, T., Feng, L., Rane, G., Kumar, A., et al. (2020). Mental awareness improved mild cognitive impairment and modulated gut microbiome. *Aging* 12, 24371–24393. doi: 10.18632/aging.202277

Kim, K., Jeong, J., Yoo, S., and Kim, D. (2016). Gut microbiota lipopolysaccharide accelerates inflamm-aging in mice. *BMC Microbiol.* 16:9. doi: 10.1186/s12866-016-0625-7

Kim, S., Cheon, H., Song, J., Yun, S., Park, S., and Jeon, J. (2014). Aging-related changes in mouse serum glycerophospholipid profiles. *Osong Public Health Res. Perspect.* 5, 345–350. doi: 10.1016/j.phrp.2014.10.002

Kodali, M., Attaluri, S., Madhu, L., Shuai, B., Upadhya, R., Gonzalez, J., et al. (2021). Metformin treatment in late middle age improves cognitive function with alleviation of microglial activation and enhancement of autophagy in the hippocampus. *Aging Cell* 20:e13277. doi: 10.1111/acel.13277

Kokudai, Y., Honma, M., Masaoka, Y., Yoshida, M., Sugiyama, H., Yoshikawa, A., et al. (2021). Cascade process mediated by left hippocampus and left superior frontal gyrus affects relationship between aging and cognitive dysfunction. *BMC Neurosci.* 22:75. doi: 10.1186/s12868-021-00680-x

Li, B., He, Y., Ma, J., Huang, P., Du, J., Cao, L., et al. (2019). Mild cognitive impairment has similar alterations as Alzheimer's disease in gut microbiota. *Alzheimers Dement.* 15, 1357–1366. doi: 10.1016/j.jalz.2019.07.002

Liu, X., Tang, S., Zhong, H., Tong, X., Jie, Z., Ding, Q., et al. (2021b). A genome-wide association study for gut metagenome in Chinese adults illuminates complex diseases. *Cell Discov.* 7:9. doi: 10.1038/s41421-020-00239-w

Liu, X., Zhao, Y., Zhu, H., Wu, M., Zheng, Y., Yang, M., et al. (2021c). Taxifolin retards the D-galactose-induced aging process through inhibiting Nrf2-mediated oxidative stress and regulating the gut microbiota in mice. *Food Funct.* 12, 12142–12158.

Liu, C., Cheng, Y., Guo, Y., and Qian, H. (2021a). Magnesium-L-threonate alleviate colonic inflammation and memory impairment in chronic-plus-binge alcohol feeding mice. *Brain Res. Bull.* 174, 184–193. doi: 10.1016/j.brainresbull.2021.06.009

Luo, D., Chen, K., Li, J., Fang, Z., Pang, H., Yin, Y., et al. (2020). Gut microbiota combined with metabolomics reveals the metabolic profile of the normal aging process and the anti-aging effect of FuFang Zhenshu TiaoZhi(FTZ) in mice. *Biomed. Pharmacother.* 121:109550. doi: 10.1016/j.biopha.2019.109550

Mangiola, F., Nicoletti, A., Gasbarrini, A., and Ponziani, F. (2018). Gut microbiota and aging. *Eur. Rev. Med. Pharmacol.* 22, 7404–7413. doi: 10.26355/eurrev_201811_16280

Mariat, D., Firmesse, O., Levenez, F., Guimarães, V., Sokol, H., Doré, J., et al. (2009). The Firmicutes/Bacteroidetes ratio of the human microbiota changes with age. *BMC Microbiol.* 9:123. doi: 10.1186/1471-2180-9-123

Mecocci, P., Boccardi, V., Cecchetti, R., Bastiani, P., Scamosci, M., Ruggiero, C., et al. (2018). A long journey into aging, brain aging, and alzheimer's disease following the oxidative stress tracks. *J. Alzheimers Dis.* 62, 1319–1335. doi: 10.3233/JAD-170732

Mou, Y., Du, Y., Zhou, L., Yue, J., Hu, X., Liu, Y., et al. (2022). Gut microbiota interact with the brain through systemic chronic inflammation: Implications on neuroinflammation, neurodegeneration, and aging. *Front. Immunol.* 13:796288. doi: 10.3389/fimmu.2022.796288

Muenchhoff, J., Song, F., Poljak, A., Crawford, J., Mather, K., Kochan, N., et al. (2017). Plasma apolipoproteins and physical and cognitive health in very old individuals. *Neurobiol. Aging* 55, 49–60. doi: 10.1016/j.neurobiolaging.2017.02.017

Mulder, M., Blokland, A., van den Berg, D. J., Schulten, H., Bakker, A., Terwel, D., et al. (2001). Apolipoprotein E protects against neuropathology induced by a high-fat diet and maintains the integrity of the blood-brain barrier during aging. *Lab. Invest.* 81, 953–960. doi: 10.1038/labinvest.3780307

Mutlu, A., Duffy, J., and Wang, M. (2021). Lipid metabolism and lipid signals in aging and longevity. *Dev. Cell* 56, 1394–1407. doi: 10.1016/j.devcel.2021.03.034

Pw, O., and Jeffery, I. (2015). Gut microbiota and aging. *Science* 350, 1214–1215. doi: 10.1126/science.aac8469

Rajeswari, T. S., and Radha, E. (1984). Metabolism of the glutamate group of amino acids in rat brain as a function of age. *Mech. Ageing Dev.* 24, 139–149. doi: 10.1016/0047-6374(84)90066-6

Rowland, I., Gibson, G., Heinken, A., Scott, K., Swann, J., Thiele, I., et al. (2018). Gut microbiota functions: Metabolism of nutrients and other food components. *Eur. J. Nutr.* 57, 1–24. doi: 10.1007/s00394-017-1445-8

Sagy-Bross, C., Kasianov, K., Solomonov, Y., Braiman, A., Friedman, A., Hadad, N., et al. (2015). The role of cytosolic phospholipase A2 α in amyloid precursor protein induction by amyloid beta1-42 : Implication for neurodegeneration. *J. Neurochem.* 132, 559–571. doi: 10.1111/jnc.13012

Saji, N., Murotani, K., Hisada, T., Tsuduki, T., Sugimoto, T., Kimura, A., et al. (2019). The relationship between the gut microbiome and mild cognitive impairment in patients without dementia: A cross-sectional study conducted in Japan. *Sci. Rep.* 9:19227. doi: 10.1038/s41598-019-55851-y

Shao, A., Lin, S., Wang, L., Tu, S., Lenahan, C., and Zhang, J. (2020). Oxidative stress at the crossroads of aging, stroke and depression. *Aging Dis.* 11, 1537–1566. doi: 10.14336/AD.2020.0225

Sheng, S., Yang, J., Xu, Y., Kong, X., Wang, J., and Wang, Y. (2022). Alleviation effects of grape seed proanthocyanidin extract on inflammation and oxidative stress in a D-galactose-induced aging mouse model by modulating the gut microbiota. *Food Funct.* 13, 1348–1359. doi: 10.1039/d1fo03396d

Sibai, M., Altuntaş, E., Yıldırım, B., Öztürk, G., Yıldırım, S., and Demircan, T. (2020). Spalax leucodonMicrobiome and longevity: High abundance of Longevity-Linked muribaculaceae in the gut of the Long-Living rodent. *OMICS* 24, 592–601. doi: 10.1089/omi.2020.0116

Suryavanshi, P., Ugale, R., Yilmazer-Hanke, D., Stairs, D., and Dravid, S. (2014). GluN2C/GluN2D subunit-selective NMDA receptor potentiator CIQ reverses MK-801-induced impairment in prepulse inhibition and working memory in Y-maze test in mice. *Br. J. Pharmacol.* 171, 799–809. doi: 10.1111/bph.12518

Vatner, S., Zhang, J., Oydanich, M., Berkman, T., Naftalovich, R., and Vatner, D. (2020). Healthful aging mediated by inhibition of oxidative stress. *Ageing Res. Rev.* 64:101194. doi: 10.1016/j.arr.2020.101194

Wang, Y., Kuang, Z., Yu, X., Ruhn, K., Kubo, M., and Hooper, L. (2017). The intestinal microbiota regulates body composition through NFIL and the circadian clock. *Science* 357, 912–916. doi: 10.1126/science.aan0677

Watson, Y., Nelson, B., Kluesner, J., Tanzy, C., Ramesh, S., Patel, Z., et al. (2021). Aggregate trends of apolipoprotein e on cognition in transgenic alzheimer's disease mice. *J. Alzheimers Dis.* 83, 435–450. doi: 10.3233/JAD-210492

Wei, S., Gao, L., Jiang, Y., Shang, S., Chen, C., Dang, L., et al. (2020). The apolipoprotein e ε4 Allele-Dependent relationship between serum lipid levels

and cognitive function: A Population-Based cross-sectional study. *Front. Aging Neurosci.* 12:44. doi: 10.3389/fnagi.2020.00044

Wu, L., Liu, X., Hu, R., Chen, Y., Xiao, M., Liu, B., et al. (2022). Agrocybe cylindraceaPrebiotic crude polysaccharides combined with GG postpone aging-related oxidative stress in mice. *Food Funct.* 13, 1218–1231. doi: 10.1039/d1fo02079j

Yang, X., Yu, D., Li, X., Li, H., and Du, J. (2020). Probiotics modulate the microbiota–gut–brain axis and improve memory deficits in aged SAMP8 mice. *Acta Pharm. Sin. B* 10, 475–487.

Zajac, D., Green, S., Johnson, L., and Estus, S. (2022). APOE genetics influence murine gut microbiome. *Sci. Rep.* 12:1906. doi: 10.1038/s41598-022-05763-1

Zarrouk, A., Hammouda, S., Ghzaiel, I., Hammami, S., Khamlaoui, W., Ahmed, S., et al. (2020). Association between oxidative stress and altered cholesterol metabolism in alzheimer's disease patients. *Curr. Alzheimer Res.* 17, 823–834. doi: 10.2174/1567205017666201203123046

Zerbi, V., Wiesmann, M., Emmerzaal, T., Jansen, D., Van Beek, M., Mutsaers, M., et al. (2014). Resting-state functional connectivity changes in aging apoE4 and apoE-KO mice. *J. Neurosci.* 34, 13963–13975. doi: 10.1523/JNEUROSCI.0684-14.2014

Zhao, T., Zhong, S., Xu, J., Jiao, W., Liu, W., Huang, L., et al. (2022). PAYCS alleviates Scopolamine-Induced memory deficits in mice by reducing oxidative and inflammatory stress and modulation of gut Microbiota-Fecal Metabolites-Brain neurotransmitter axis. *J. Agr. Food Chem.* 70, 2864–2875. doi: 10.1021/acs.jafc.1c06726

frontiers | Frontiers in Neuroscience

TYPE Original Research
PUBLISHED 16 September 2022
DOI 10.3389/fnins.2022.884543

OPEN ACCESS

EDITED BY
He Wang,
Fudan University, China

REVIEWED BY
Yaping Pan,
China Medical University, China
Sudarshana Borah,
Dibrugarh University, India

*CORRESPONDENCE
Yan Li
feifeiliyan@163.com

SPECIALTY SECTION
This article was submitted to Gut-Brain Axis, a section of the journal Frontiers in Neuroscience

RECEIVED 26 February 2022
ACCEPTED 28 July 2022
PUBLISHED 16 September 2022

CITATION
Yan C, Diao Q, Zhao Y, Zhang C, He X, Huang R and Li Y (2022) *Fusobacterium nucleatum* infection-induced neurodegeneration and abnormal gut microbiota composition in Alzheimer's disease-like rats. *Front. Neurosci.* 16:884543. doi: 10.3389/fnins.2022.884543

Fusobacterium nucleatum infection-induced neurodegeneration and abnormal gut microbiota composition in Alzheimer's disease-like rats

Caixia Yan[1], Qilin Diao[1], Yuxi Zhao[1], Cheng Zhang[1], Xiaoya He[1], Ruijie Huang[1,2] and Yan Li[1]*

[1]State Key Laboratory of Oral Diseases, West China Hospital of Stomatology, National Clinical Research Center for Oral Diseases, Sichuan University, Chengdu, China, [2]Department of Pediatric Dentistry, State Key Laboratory of Oral Diseases, West China Hospital of Stomatology, National Clinical Research Center for Oral Diseases, Sichuan University, Chengdu, China

Objective: To explore whether *Fusobacterium nucleatum* could lead to behavioral and pathological changes in Alzheimer's disease (AD)-like model rat and whether they could affect the gut microbiota.

Methods: The cognitive ability and alveolar bone loss of Sprague-Dawley (SD) rats were tested by Morris water maze and Micro-CT, respectively. HE staining and immunohistochemistry were used to analyze the pathological changes and Aβ1–42 in brains. Western blot was applied to detect the expression of p-Tau 181 in the brain. Limulus amebocyte lysate assay and PCR were performed to determine serum LPS level and whether *F. nucleatum* accessed the brain, respectively. The gut microbiota was analyzed by the 16S rRNA gene sequence.

Results: Oral infection with *F. nucleatum* could induce increased alveolar bone loss and learning impairment in AD-like rats. Additionally, *F. nucleatum* exposure increased the Aβ1–42 expression by about one-fourth ($P < 0.05$), p-Tau181 by about one-third ($P < 0.05$), and serum LPS ($P < 0.05$) in AD-like rats. Moreover, *F. nucleatum* could change the gut microflora composition in AD-like rats, accompanied by a significant increase in the abundance of *Streptococcus* and *Prevotella*.

Conclusion: Oral infection with *F. nucleatum* could contribute to abnormalities in cognitive ability and pathological change in the brain of AD-like rats, which may be related to abnormal gut microbiota composition.

KEYWORDS

periodontitis, Alzheimer's disease, *Fusobacterium nucleatum*, Aβ, gut microbiota

Introduction

Alzheimer's disease (AD) is a multifactorial neurodegenerative disease, which affects cognitive function and memory, is characterized by amyloid β (Aβ, formed by activities of β and γ secretase) and neurofibrillary tangles (NFTs, composed of over-phosphorylated tau protein), but its pathogenesis is not yet clear (Blennow and Zetterberg, 2018; Weller and Budson, 2018). Most studies supported that inflammatory response plays an important role in the pathogenesis of AD by promoting Aβ deposition and leading to neuron loss and cognitive dysfunction (Long and Holtzman, 2019). Recently, more researchers were involved in the relationship between periodontitis and AD. Epidemiological studies had shown that people with periodontitis were at increased risk for AD, while people with AD were more prone to periodontitis, tooth loss, and mucosal lesions due to cognitive decline and impaired oral health (Chen C.K. et al., 2017).

Periodontitis is a chronic inflammatory disease caused by pathogenic bacteria in subgingival biofilm, and its pathogenesis is related to aberrant host immune response and destruction of periodontal tissues (Socransky and Haffajee, 2002; Sczepanik et al., 2020). Although periodontitis is not fatal, periodontal pathogens could travel through the systemic circulation to various organs, leading to the development of some life-threatening diseases. Studies had found that the presence and severity of periodontitis are associated with the development of systemic diseases, such as AD (Matsushita et al., 2020), and *Porphyromonas gingivalis* (*P. gingivalis*), a frequently studied periodontal pathogen, has been reported to increase the risk of AD, symptoms associated with AD were relieved after anti-*P. gingivalis*-toxin treatment (Dominy et al., 2019).

Fusobacterium nucleatum (*F. nucleatum*, *F.n*), another important periodontal pathogen, could mediate its interpolymerization with other bacteria and adhesion to various host cells (Fardini et al., 2011; Li et al., 2021). Current studies confirmed that *F. nucleatum* plays an important role in the occurrence and development of colorectal cancer and chemotherapeutic resistance, and could also be isolated from septicemia-related infections, pelvic inflammatory disease, abscesses of the brain and other organs (Han et al., 2003; Gregory et al., 2015; Brennan and Garrett, 2019). In line with these data, Sparks Stein and coworkers demonstrated that antibody levels to *F. nucleatum* and *P. intermedia*, at baseline, significantly increased as compared to the controls and correlated with a declined cognitive function in AD patients (Sparks Stein et al., 2012). In recent years, studies have found that gut microbiota might play an important role in neurological diseases. Animal studies using germ-free mice had shown that mice lacking the microbes have abnormal brain development, learning and memory deficits, and anxiety-like behaviors, suggesting that gut microbiota played a key role in early brain development and adult neurogenesis (Desbonnet et al., 2014; Grover and Kashyap, 2014). The gut–brain axis is a communication pathway between the center neuro system and the enteric nervous system (Kowalski and Mulak, 2019). It is suggested that AD patients have different gut microbiota from non-AD people, and this abnormal gut microbiota may be involved in the deposition of the brain Aβ (Seo et al., 2019). Therefore, further studies on the gut microbiota of AD patients can help us better understand the etiology of the disease. In our study, *F. nucleatum* was orally infected D-galactose/$AlCl_3$ induced AD-like rats, and we found that *F. nucleatum* changed the gut microbiota and played a pathogenic role in AD.

Materials and methods

Animals

Thirteen 5-week-old Sprague-Dawley (SD) male rats (130–150 g) purchased from the Dashuo company were housed in plastic cages in a temperature-controlled (25°C) colony room at a 12/12 h light/dark cycle. Food and water were available *ad libitum*. All animal procedures in this study were approved by the Ethics Committee of West China Hospital of Sichuan University (WCHSIRB-D-2021-009) and conformed to the ARRIVE (Animal Research: Reporting of *in vivo* Experiments) guidelines for preclinical studies. All efforts were made to minimize the number of animals used.

Alzheimer's disease-like and periodontitis rat model

After 1 week of environment acclimation, the rats were randomly divided into three groups, AD + ligation + non (AD, $n = 4$), AD + ligation + *F. nucleatum* (AD + *F.n*, $n = 5$), and blank (Con, $n = 4$). The rats were subcutaneously injected in the neck and back with D-galactose and $AlCl_3$ (120 mg/kg/day and 10 mg/kg/day, 0.1–0.5 ml) or PBS every day from the 6th week to the 22nd week to establish an AD-like model (as shown in **Figure 1A**). Rats were ligated with a 5–0 silk suture around the bilateral maxillary second molars (M2) for experimental periodontitis in the 16th week. *F. nucleatum* ATCC 25586 was anaerobically grown and resuspended to a concentration of 1×10^9 CFU/mL in 4% carboxymethyl cellulose (CMC), and was smeared on the silk suture (0.2 ml) every other day from the 16th week to the 22nd week (Chukkapalli et al., 2014). The Con group received 0.2 ml of PBS in 4% CMC.

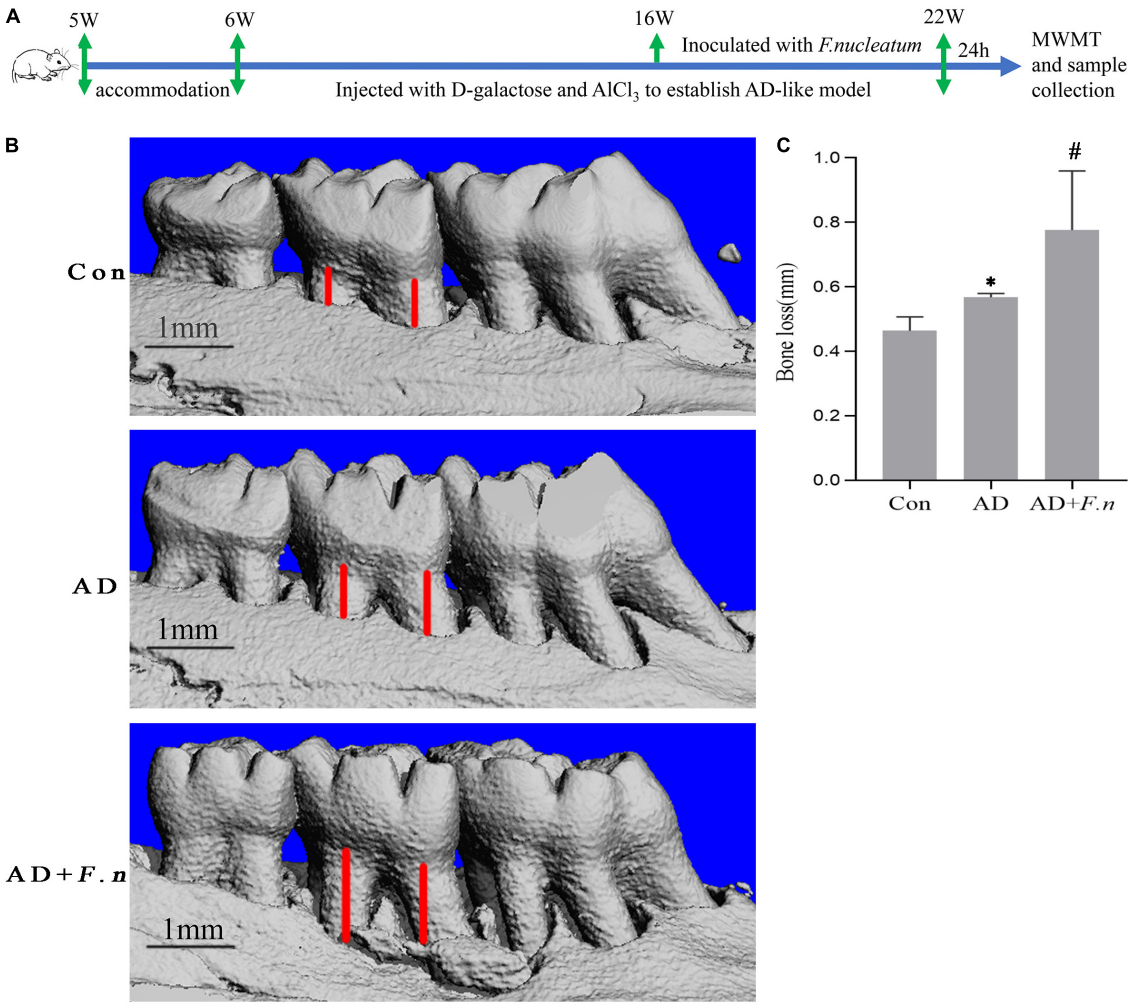

FIGURE 1
Micro-CT showed alveolar bone loss in each group (n = 4–5). **(A)** Flow chart. **(B)** Three-dimensional view of bone resorption. **(C)** Alveolar bone loss in each group. Data presented as mean ± SEM. *P < 0.05 vs. Con group, #P < 0.05 vs. AD group, indicates statistically significant differences.

Morris water maze test

The Morris water maze test (MWMT, MT-200, Chengdu Taimeng Technology Co., Ltd.) was performed in the 23rd week to study the spatial learning and memory abilities of rats. Morris water maze test (MWMT) was carried out as described by Bhuvanendran et al. (2019) with few modifications. The water pool was a circular white pool with a diameter of 200 cm and a depth of 60 cm filled with non-toxic white paint opaque water and the temperature was held constant at 23 ± 1°C. The pool was separated into four equal quadrants, and an invisible platform was submerged 1 cm under the water surface in the center of the first quadrant and was considered the target quadrant. During the training days, the location of the platform remained the same and the rats were given tests for successive 4 days. In each trial, a rat was released in a quadrant and allowed to swim freely for 90 s to find the invisible platform and stay on it for 15 s. If the rats could not find the located platform in 90 s, it was gently guided to the platform, and allowed to stay there for 15 s. The time taken to reach the platform (escape latency) was recorded and the practice was repeated for four different starting quadrants of the trial per day. A probe trial test was performed on the 5th day without the platform to evaluate the memory consolidation rate. The rats were allowed to swim freely for 90 s, and count the number of times the mouse crossed the area where the platform had been placed.

Specimen collection

Animals were sacrificed one day after the probe trial test. First, fresh feces of rats were collected for quick freezing. The

rats were deeply anesthetized with an intraperitoneal injection of 2.5% tribromoethanol. After the collection of blood, the rats were sacrificed and the brain was collected. One cerebral hemisphere was immediately stored at −80°C until further analysis and the other half fixed in 4% paraformaldehyde for 24 h, then were processed and embedded in paraffin. Bilateral maxillary bones were removed and fixed in 4% paraformaldehyde for 24 h.

Micro-computed tomography

To evaluate morphological changes in the alveolar bone, the maxillary bone was scanned by Micro-CT (Jia et al., 2019). Fixed maxillary bones of each group were randomly selected and scanned with a Micro-CT (μCT50; SCANCO) at the voxel resolution of 10 μm. Three-dimensional reconstruction and data analysis were performed by Scanco Evaluation. To calculate bone loss, the distance between the cementoenamel junction and alveolar bone crest (CEJ-ABC distance) was measured for two predetermined maxillary sites on palatal sides of M2.

Hematoxylin-eosin staining

The histological changes in the sections of brain tissues from the different groups were observed using HE staining (Chen S. et al., 2017). After being preserved in 10% formalin solution for 24 h, brains were embedded in paraffin and 5 μm sections were sliced. The samples were then dewaxed and rehydrated, subsequently stained with hematoxylin and eosin, and examined under standard light microscopy for a general histopathology examination. The images were captured by a camera (Nikon, 90i, Tokyo, Japan).

Immunohistochemistry

The immunohistochemical staining was performed as described by Shin et al. (2019) with slight modifications (Shin et al., 2019). After being fixed in 4% paraformaldehyde for 24 h, the brains were embedded in paraffin and then cut at a thickness of 5 μm. The sections for staining were deparaffinized and washed. Following, they were heated in 0.01 M sodium citrate buffer (pH 6.0) for antigen retrieval. Endogenous peroxide activity was quenched with 3% hydrogen peroxide. Sections were incubated with primary antibodies against Aβ1–42 (Abcam, ab10148, 1:200) overnight at 4°C, followed by anti-rabbit IgG (ZSGB-BIO, PV-9001). Then sections were incubated with horseradish enzyme labeled streptomycin working solution at room temperature for 30 min. Finally, color was developed with 3,3′-diaminobenzidine (ZSGB-BIO, ZLI-9018), and then it was counterstained with hematoxylin. After gradient dehydration with alcohol, the slices were sealed with neutral resin. The images were captured. And 6 visual fields per slices were being counted in a blind manner.

Western blotting

The supernatant of brain protein was mixed with sample buffer and boiled. Protein from boiled samples was separated by 10% sodium dodecyl sulfate (SDS)-polyacrylamide gel electrophoresis and transferred to PVDF membranes. Then, the membranes were blocked in PBS–0.1% Tween 20 containing 5% milk and incubated with rabbit monoclonal IgG antibodies against GAPDH (1:1,000, Signalway Antibody, United States), Tau (phosphoThr181, 1:500, Signalway Antibody, United States), and mouse monoclonal IgG antibodies Tau (Tau46, 1:500, CST, United States) overnight at 4°C. The membranes were then incubated with goat anti-rabbit or rabbit anti-mouse IgG antibodies (1:5,000, Signalway Antibody, United States). The protein was visualized with Enhanced ECL Reagent Kit (Beijing Bio Excellence Biotechnology Co., Ltd., China). Images were captured by using a gel imaging system (Bio-Rad, United States).

Limulus amebocyte lysate assay

Serum was isolated by centrifuging the blood after clotting at 4,000 rpm for 10 min. The serum level of LPS was measured with Tachypleus Amebocyte Lysate (EC64405, Xiamen Limulus Reagent Biotechnology Co., Ltd., xiamen, China) according to the manufacturer's protocol.

Brain genomic DNA isolation and polymerase chain reaction

To confirm the spread of periodontal pathogens from the mouth to the brain of AD-like rats, genomic DNA was isolated from the brains of all groups following the manufacturer's protocol (DNeasy Blood and Tissue Kit, Qiagen, Germany) (Wang et al., 2015). DNA amplification was performed using a PCR amplification kit (Sangon Biotech Co., Ltd., Shanghai, China) according to the manufacturer's instructions. Briefly, the PCR mixture contained 12.5 μl Taq PCR Master, 0.5 μl (10 μg/ml) DNA samples, 1 μl forward primer, 1 μl reverse primer, and 1 μl sterilized ddH2O. The primers used for amplification were as follows:

5′-GGCCACAAGGGGACTGAGACA-3′ (forward) and 5′-TTTAGCCGTCACTTCTTCTGTTGG-3′ (reverse) (Sangon Biotech Co., Ltd., Shanghai, China) and its reliability is verified. The reaction temperature was 94°C for 4 min, followed by 40 cycles of 94°C for 30 s, 60°C for 30 s, 72°C for 10 s, and then 72°C for 10 min. DNA amplification products were electrophoresed in a 2.0% agarose gel electrophoresis under 120 V for 20 min with *F. nucleatum* ATCC 25586 DNA as the positive group (183 bp) and a blank reaction system as the negative group.

Fecal DNA extraction and 16S rRNA gene sequencing

DNA from 13 fecal samples of Con, AD, and AD + *F.n* groups were extracted using a Qiagen stool DNA extraction kit (Qiagen, Germany) according to the instructions. Eleven DNA samples (3 in Con, 3 in AD, 5 in AD + *F.n*), with ratios of 1.8–2.0 (for A260/280 nm) and >1.8 (for A260/A230 nm), were used for downstream experiments (Wang et al., 2016). For the analysis of the composition of the gut microbiota, the V3 and V4 regions of the 16S rRNA gene were amplified using universal primers 338F and 806R. The sequencing was performed on the Illumina Miseq platform following the usual operating procedures of Personal Biotechnology Co., Ltd. (Shanghai, China). The DNA fragments were paired-end sequenced with the Illumina platform. The obtained sequences were denoise, quality controlled, dereplication, etc. to obtain high-quality sequences. The cluster_size module was used to cluster high quality sequences at a 97% similarity level, and the Operational taxonomic unit amplicon sequence variants (ASVs) tables were obtained. Finally, the singletons ASVs (ASVs detected in only 1 sample) and their representative sequences were removed from the ASV table. Calculated the length distribution of the high-quality sequences contained in the sample, and the obtained sequences were annotated with the Greengenes database. α diversity indices were determined using the Simpson index for diversity and the Chao1 index for species richness. β diversity can be demonstrated by Principal coordinate analysis (PCoA) and the Bray-Curtis distance was used to denote the β diversity distance (Li et al., 2019).

Statistical analysis

All data were statistically analyzed by GraphPad Prism 6.0. Data were expressed as mean ± SEM. Morris's water maze was analyzed with repeated measurements ANOVA. Comparisons between the three groups were evaluated by ANOVA or Kruskal-Wallis Test. Differences with $P < 0.05$ were considered statistically significant.

Results

Fusobacterium nucleatum increased alveolar bone loss

Micro-CT showed that the AD and AD + *F.n* groups had significantly more alveolar bone loss than the Con group, indicating the successful induction of periodontitis. Furthermore, alveolar bone loss in the AD + *F.n* group in rats infected with *F. nucleatum* for 6 weeks was increased compared with those of rats in the AD group (**Figures 1B,C**). These results suggested that oral infection with *F. nucleatum* induced more alveolar bone loss in AD-like periodontitis rats.

Fusobacterium nucleatum damaged the cognitive ability of rats in Morris water maze test

To clarify whether *F. nucleatum* could induce cognitive impairment, we tested the learning ability of rats by MWMT. As shown in **Figure 2A**, the escape latency of the AD and AD + *F.n* groups were significantly increased from day 2 to day 4 when compared with the Con group ($P < 0.05$), indicating successful induction of the AD-like rat model through D-galactose and $AlCl_3$ injection. In addition, when compared with the AD group, the escape latency of the AD + *F.n* group was significantly increased, in particular, there was an average increase of about 20 s on the fourth day ($P < 0.05$). These data indicated that chronic *F. nucleatum* oral infection could damage the learning ability further of AD-like with periodontitis rats.

In the space exploration experiment, we found that the track of rats in the Con group was mainly concentrated in and around the target quadrant (the first quadrant), while rats in the AD and AD + *F.n* groups moved disorderly or presented marginal movement, and rarely enter the target quadrant (**Figure 2C**). Moreover, the AD and AD + *F.n* groups had a significantly decreased number of times cross the platform than the Con group. These data also indicate the successful construction of the AD-like rat model. However, we didn't find any evidence that *F. nucleatum* aggravated memory ability in rats as the AD + *F.n* group had a similar number of times cross the platform with the AD group (**Figure 2B**).

Fusobacterium nucleatum could induce the expression of Aβ1–42 and p-Tau181

To clarify whether *F. nucleatum* could induce neurodegeneration, the neuronal morphology in the cortex (Cotx) and hippocampus (Hipp) of rats by HE were first

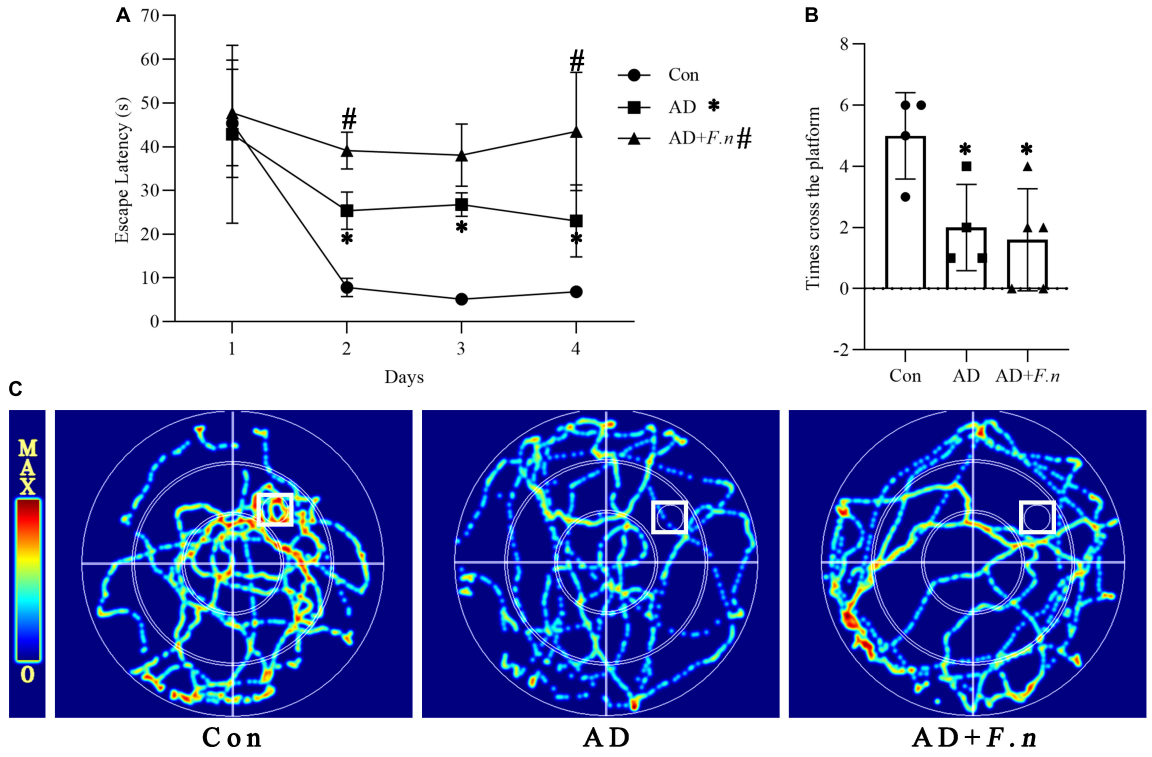

FIGURE 2
Morris water maze test (MWMT) showed the cognitive ability of rats in each group. **(A)** Escape latency. **(B)** The number of times cross the platform. **(C)** Heat map of rat movement track. Data presented as mean ± SEM. n = 4–5 in each group, *$P < 0.05$ vs. Con group, #$P < 0.05$ vs. AD group, indicates statistically significant differences.

investigated. We found that neurons in Cotx and Hipp of rats in the Con group were neatly arranged and compact, without significant cell vacuolation and necrosis (Figure 3A). Neuronal degeneration and karyopyknosis in brain tissue were observed in AD and AD + *F.n* groups, and cells in the hippocampus were loosely organized and vacuolation.

The Aβ1–42 expression in Cotx and Hipp of rats was examined by IHC. And the number of positive Aβ1–42 cells in brain tissue of AD and AD + *F.n* groups significantly increased (Figures 3B,C, $P < 0.05$). Compared with the AD group, the expression of Aβ1–42 in the AD + *F.n* group was significantly increased by about one-fourth ($P < 0.05$). These data indicated that chronic *F. nucleatum* oral infection could trigger neurodegeneration and Aβ1–42 express in the Cotx and Hipp of AD-like rats.

The expression of p-Tau181 and Tau protein in the brain of rats were detected by WB, as shown in Figures 3D,E. Compared with the Con group, the level of p-Tau181 in the AD group and AD + *F.n* group was significantly increased ($P < 0.05$). In addition, when compared with the AD group, the relative expression of p-Tau181 in AD + *F.n* group was significantly increased by about one-third ($P < 0.05$). These data indicated oral infection with *F. nucleatum* could induce phosphorylated tau increased in the brain of AD-like periodontitis rats.

No *Fusobacterium nucleatum* was detected in the brain of rats following oral application of *Fusobacterium nucleatum*

We next explored the possible mechanisms by which *F. nucleatum*-caused cognitive impairment, neurodegeneration, and Aβ1–42 expression. PCR was used to examine whether *F. nucleatum* entered the brain first. None of the brain tissue lysates demonstrated DNA from *F. nucleatum* in the non-infected and infected groups (data not shown).

Serum LPS increased after *Fusobacterium nucleatum* infection

Serum LPS of rats in each group was detected by LAL assay (as shown in Figure 4). Compared with the Con group, serum LPS of the AD group was significantly increased, suggesting the AD-like model could induce an increase in serum LPS levels, which may be related to systemic inflammation. Moreover, the AD + *F.n* group also had a significantly increased LPS level when compared with the AD group. These data suggested

10.3389/fnins.2022.884543

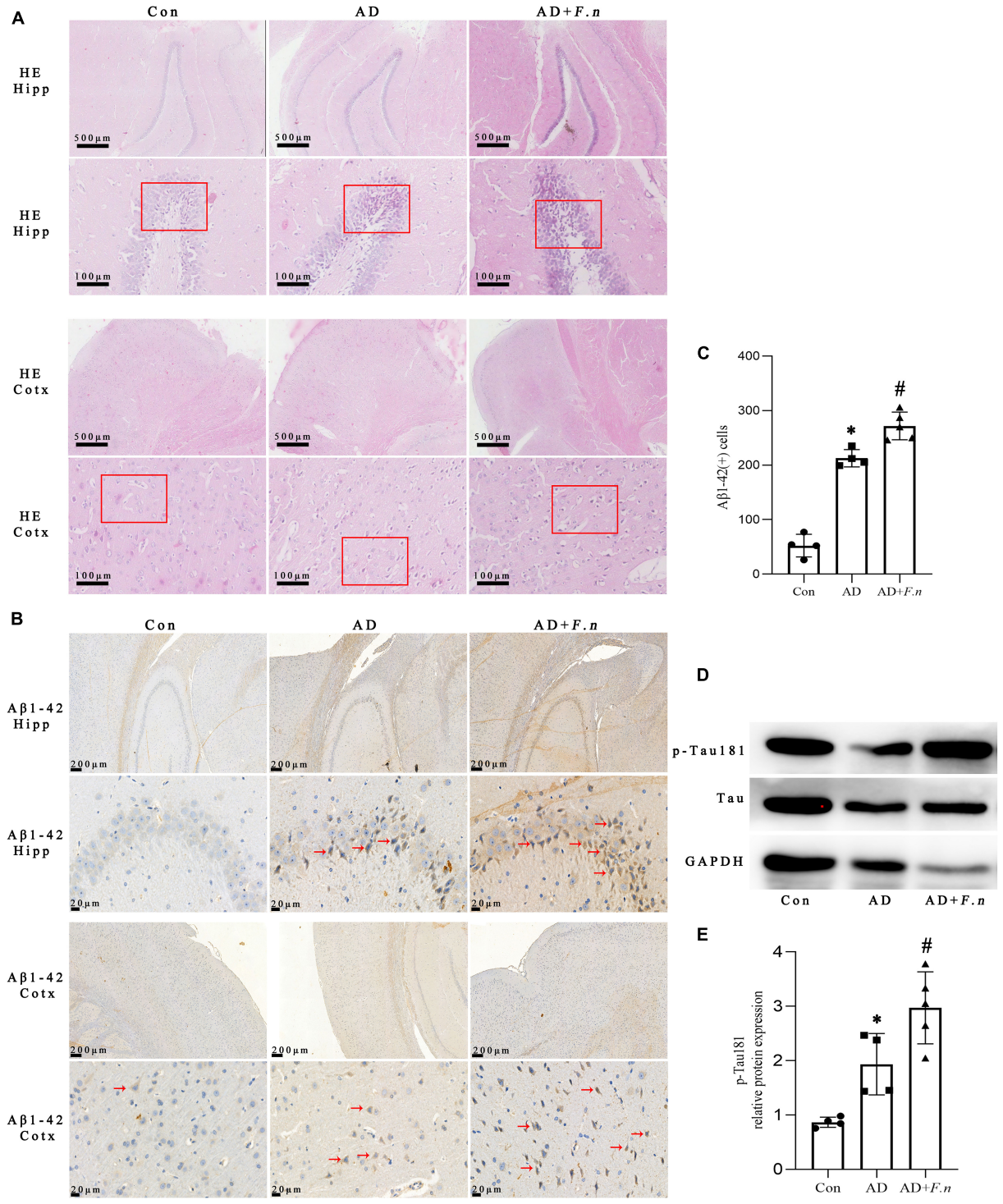

FIGURE 3

HE and IHC showed histopathological changes, and WB showed tau hyperphosphorylation in each group. **(A)** HE showed cell morphology and arrangement. **(B)** IHC showed the expression of Aβ1–42 cells. **(C)** The number of Aβ1–42 cells in the brain. **(D)** WB showed the expression of p-Tau181 in the brain. **(E)** Quantitative analysis of the blots. Data presented as mean ± SEM. $n = 4–5$ in each group, $^{*}P < 0.05$ vs. Con group, $\#P < 0.05$ vs. AD group, indicates statistically significant differences.

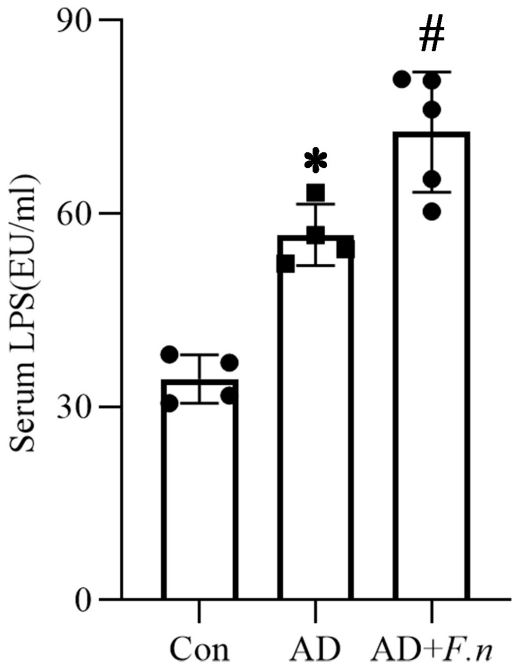

FIGURE 4
Serum LPS. Limulus amebocyte lysate (LAL) assay detected the serum LPS in three groups, *$P < 0.05$ vs. Con group, #$P < 0.05$ vs. AD group, indicates statistically significant differences.

that *F. nucleatum* oral infection could trigger chronic systemic inflammation, we inferred that *F. nucleatum* might trigger neuropathy by inducing the release of LPS and the resulting inflammatory response in the circulatory system.

Fusobacterium nucleatum could change the gut microbiota diversity of Alzheimer's disease-like rats

A total of 866,530 high-quality sequences were captured from 11 fecal samples, with an average of 78,775 sequences per sample, and average length of 426 bp. The gut microflora of all samples was classified into 29 phyla, 89 classes, 158 orders, 280 families, 470 genera, and 5,763 ASVs.

α-diversity index of gut microflora was evaluated according to the observed species, Simpson, and Chao1 indices. As shown in Figure 5A, there was no significant difference in the three parameters among the three groups ($P > 0.05$). Regarding gut microflora structure, the dissimilarity tests showed that it was different between the AD group and the Con group to some extent ($P < 0.1$), but the AD group was similar to the AD + *F.n* group ($P > 0.05$; as shown in Table 1). The rarefaction analysis revealed that the sequence depth was almost sufficient to recover the diversity of this community (Figure 5B). Venn figure showed that there were, respectively, 1,573, 2,789, and 3,082 ASVs in Con, AD, and AD + *F.n* groups. Among them, AD and AD + *F.n* overlapped the most ASVs, 407. Only 187 ASVs were shared by three groups (Figure 5C).

Fusobacterium nucleatum could change the gut microbiota composition and metabolism of Alzheimer's disease-like rats

At the level of phylum (Figure 6A), the top five phylum were *Firmicutes*, *Proteobacteria*, *Actinobacteria*, *Bacteroidetes,* and *TM7*. The relative abundance in the top five phylum had no significant differences between groups. According to hierarchical clustering analysis, the samples from the Con group (A1–3) clustered together and were well separated from the AD group (B1–3). Moreover, the AD + *F.n* group (C1–5) had a relatively nearer distance to AD (B1–3) compared to Con, which meant their community was more similar to each other. Although some genera were common to all samples, such as *Aerococcus*, the variability in genera distribution among different samples was noticeable (Figure 6B). Then, the structure and predominant taxa from the phylum to genus level of the gut microbial community in each group was evaluated by the linear discriminant analysis effect size (LEfSe) test and displayed in Figure 6C. Marked taxa from AD was *g_Coprococcus*, and most specific taxa were from AD + *F.n* group in phylum and genus were *p_Tenericutes* and *g_Prevotella*.

At the genus level, *Psychrobacter*, *Enterococcus,* and *Aerococcus* accounted for 50% of the community in the Con group, while in the AD group *Aerococcus* constituted 81.98%, AD + *F.n* group consists of the genera of *Aerococcus* and *Streptococcus* for 50% of the community. For the top 20 genera (Figure 6D), a variance analysis was performed and found that *Psychrobacter*, *Streptococcus*, *Lactococcus*, *Staphylococcus*, *Jeotgalicoccus,* and *Prevotella* have a differential expression. When compared with the AD group, the relative abundance of *Streptococcus* and *Prevotella* in the AD + *F.n* group was significantly increased.

PICRUSt2 was used to predict metabolic pathway in MetaCyc and found that some pathways were significantly increased or decreased in the AD + *F.n* group compared to the AD group (Figure 6E). Furthermore, pathways related to neurotransmitter degradation were significantly changed in the gut microbiome of *F. nucleatum*-treated rats compared with AD. ORNARGDEG-PWY, ARGDEG-PWY, THREOCAT-PWY, PWY-7456, and PWY-6572 involved in the degradation of L-arginine, L-ornithine, putrescine, 4-aminobutanoate, L-threonine, mannan, and chondroitin sulfate were significantly increased, while CRNFORCAT-PWY involved in the creatinine degradation decreased.

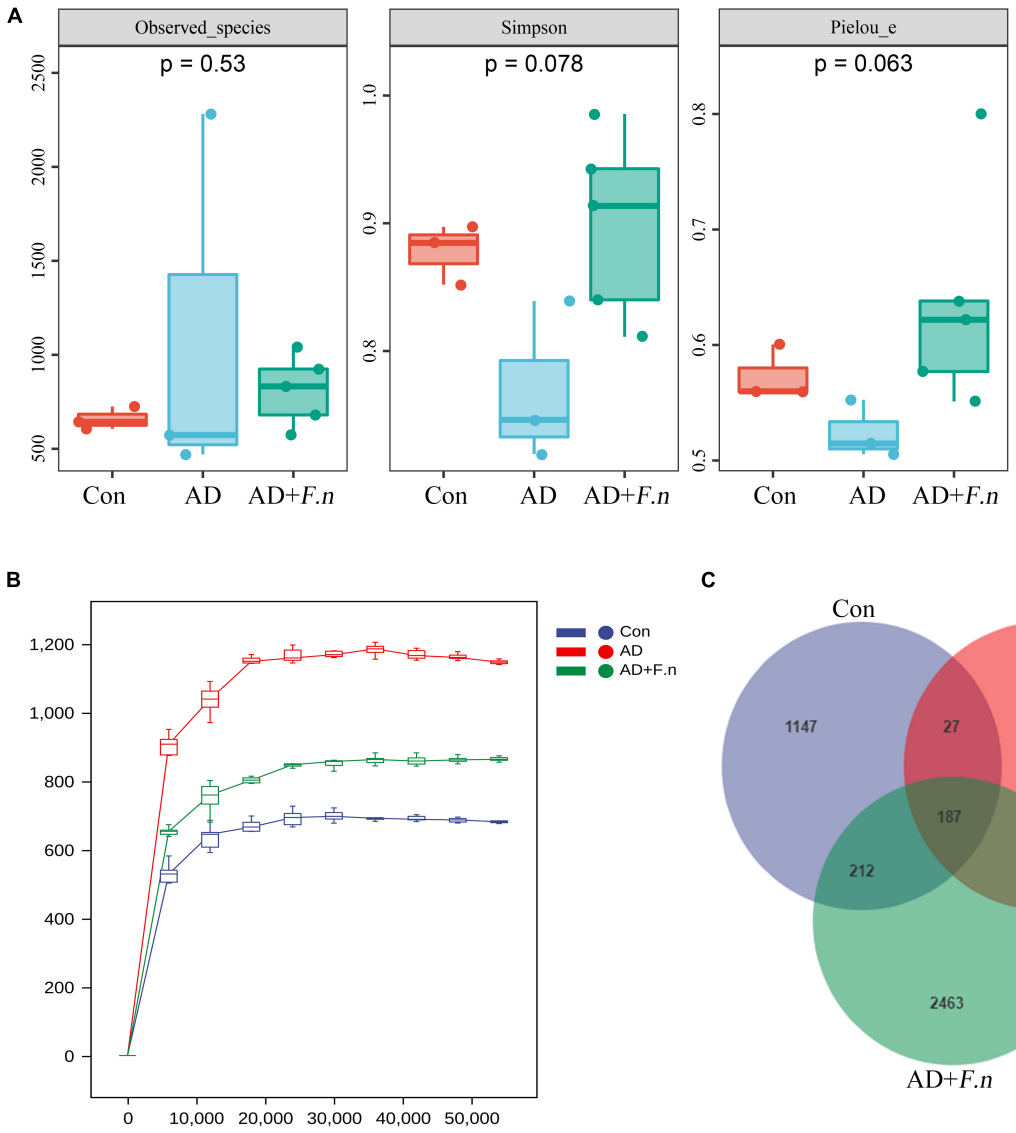

FIGURE 5
Gut microbiota diversity. **(A)** α diversity. **(B)** Rarefaction curves. **(C)** Venn diagram showing the unique shared ASVs in three groups.

TABLE 1 Comparison of the overall microbial community structure using ANOSIM.

Group 1	Group 2	*P*
Con	AD	0.087
AD	AD + *F.n*	0.463

Discussion

Periodontitis can cause inflammatory mediators to enter the blood circulation and further aggravate the development of some systemic diseases (Loos and Van Dyke, 2020). It is widely believed that Aβ deposition and phosphorylated tau may be associated with the local and surrounding inflammatory environment, especially when stimulated by gram-negative bacteria, which can accelerate Aβ accumulation and over-phosphorylated tau expression (Dioguardi et al., 2020; Tetz et al., 2020). This study has shown that periodontitis and its causative bacteria may also be associated with AD. Among them, the most studied is the relationship between *P. gingivalis* infection and AD. In this study, we demonstrated that periodontitis, caused by *F. nucleatum* infection, could exacerbate the pathological features of AD in an AD-like rat model.

D-galactose (D-gal) injected rodent models can recapitulate many features of AD, including cognitive deficits, neuronal degeneration, and apoptosis, and have been extensively applied

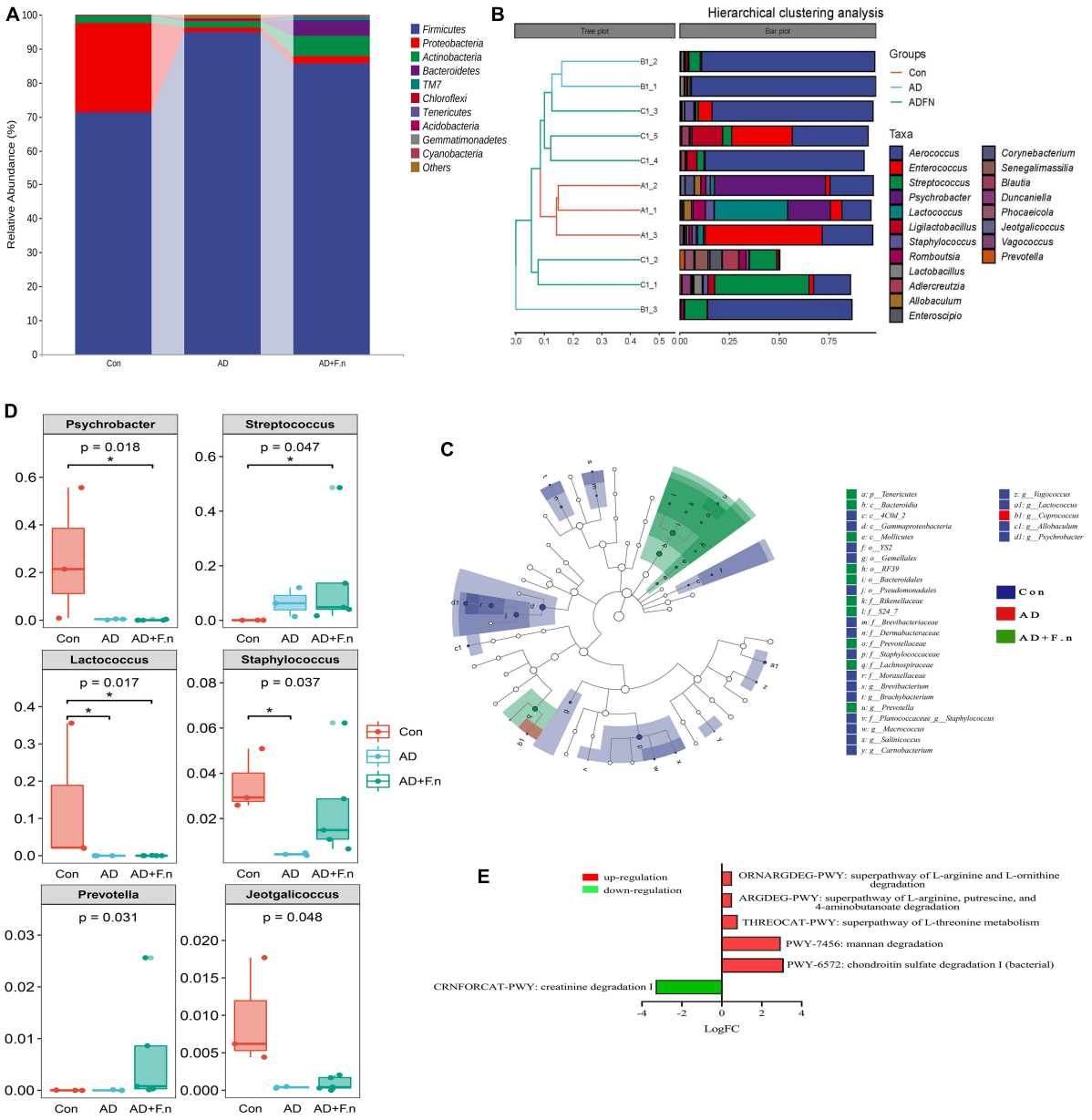

FIGURE 6
Gut microbiota composition and metabolism. **(A)** Classification and abundance of fecal bacteria at the phylum level (top 10) in each group. **(B)** Taxonomic classification and hierarchical clustering analysis of the bacterial communities at the genus levels from three groups (top 20). **(C)** The enriched taxa in the feces of rats were displayed in cladograms. **(D)** Significant difference in relative abundances of top 20 bacteria at the genus level in three groups. **(E)** Predicting metabolic pathways in MetaCyc, $*P < 0.05$.

in study (Chiroma et al., 2018). Aluminum chloride ($AlCl_3$) can damage the membrane structure, induce neuronal fiber degeneration, inhibit nerve conduction, and lead to the unbalanced activity of α and β secretases (Sumathi et al., 2015). Treating rodents with D-gal + $AlCl_3$ can result in impaired cognitive function and successfully build an AD-like model (Liaquat et al., 2017). In this experiment, rats after D-gal + $AlCl_3$ treatment showed impaired spatial learning and memory ability, indicating that we successfully established an AD-like disease model in rats. It has been well established that *P. gingivalis* has a negative effect on cognitive function in animals with AD. For example, one study conducted behavioral tests and demonstrated that elderly C57BL/6J mice infected with *P. gingivalis* showed significant spatial learning and memory impairment compared with uninfected control mice (Ding et al., 2018). Furthermore, oral administration of *P. gingivalis*-LPS also can cause learning and memory impairments in C57BL/6 mice (Zhang et al., 2018). This study not only verified the

established connection between *F. nucleatum* and AD but also found that oral infection of *F. nucleatum* can aggravate the learning disability of AD-like rats.

Periodontal infections serve as a significant risk factor affecting cognitive ability as demonstrated in a prospective observational clinical study in which cognitive decline is reported in AD patients with active chronic periodontitis compared to AD patients without active chronic periodontitis (Chen C.K. et al., 2017). Our results showed that oral infection with *F. nucleatum* can significantly increase the accumulation of Aβ and phosphorylated tau181 expression. Similarly, oral infection of wild-type mice with *P. gingivalis* for 22 weeks also resulted in a significant increase formation of Aβ, and the expression of p-Tau396 (Ilievski et al., 2018). It is reported that the LPS of gram-negative bacteria can act on the human immune system, inhibit the body's immune defense, and then trigger inflammation (Morris et al., 2014). *In vivo* studies have also demonstrated that bacterial components, such as LPS and bacterial DNA, can lead to increased accumulation of Aβ and phosphorylated tau (Tetz et al., 2020). Some researchers conducted oral infection of *P. gingivalis* in 8-week-old wild C57BL/6 mice for 22 weeks and found that the Aβ plaque and surrounding LPS in the brain were significantly increased (Ilievski et al., 2018). In addition, LPS can co-locate with Aβ around the cerebrovascular area in patients with AD (Zhao et al., 2017). Regarding the ectopic detection rate of periodontal bacteria, different studies have different results. Animal experiments showed that orally infected with *P. gingivalis* for 3 weeks through pulp in wild type, and *P. gingivalis* was not detected in the brain (Foschi et al., 2006). Poole et al. showed that no bacterial DNA was found in the brain tissues after 12 and 24 weeks of oral infection of *Treponema denticola*, a periodontal pathogen (Poole et al., 2015). The present study did not detect *F. nucleatum* in the brain of rats, and the differences in these results may be related to the type of bacteria, the mouse model, and the time and route of infection.

In this study of gut microbiota diversity, we have found no significant difference in α- and β-diversity after D-gal + $AlCl_3$ or *F. nucleatum* treatment. Bauerl et al. (2018) analyzed the gut microbiota of APP/PS1 transgenic AD mice and found that the α diversity of APP/PS1 mice aged 24 months and 6 months was lower than that of wild-type mice of the same age, and the gut microbiota structure of the two groups was significantly different. However, Bonfili et al. (2017) and Peng et al. (2018) found that there was no significant difference in α diversity between aging mice and 3 × Tg-AD mice and control mice, while β diversity showed a significant difference in gut microflora structure compared with control mice. The reason why our study is inconsistent with the above results may be associated with the animal species, AD model, and age.

Then, we found that after oral infection with *F. nucleatum*, the abundance of *Streptococcus* and *Prevotella* in the gut tract of AD-like rats was significantly increased. Clinical studies found that the abundance of *Streptococcus* is increased in the gut tract of patients with Parkinson's disease, which can produce neurotoxins, such as streptomycin, streptomycin, and streptomycin, leading to permanent nerve damage (Li et al., 2017). In addition, *Streptococcus* is enriched in the gut microbiota of patients with colorectal cancer and has been associated with an increased risk of diseases, such as sepsis and endocarditis (Spigelblatt et al., 1985; Wang et al., 2012; Sutej et al., 2020). As for *Prevotella*, it is reported that the gut microbiota of patients newly diagnosed with AD was dysregulated, in which the abundance of *Prevotella*, which can promote inflammation, was significantly increased (Guo et al., 2021). In animal experiments, 16S rRNA gene sequencing analysis of gut microbiota of AD mice with accelerated aging also showed that the abundance of *Prevotella* was significantly increased (Peng et al., 2018). Among other neurological diseases, the abundance of *Prevotella* has been reported to correlate with the severity of Parkinson's disease (Scheperjans et al., 2015). In addition, the successful colonization of *Prevotella* in the gut tract of mice can induce the production and accumulation of Th17 cells in the colon, and also increase the expression of Th17-related cytokines (interleukin 6/1β) in serum (Huang et al., 2020). Moreover, we found that *Lactococcus* and *Jeotgalicoccus* have a decreased relative abundance in the AD group. *Lactococcus* can convert glutamate into gamma-aminobutyric acid, a major inhibitory neurotransmitter, and abnormalities in this signaling pathway are associated with cognitive disorders, including AD (Gonzalez-Burgos et al., 2011). Moreover, another study reported that *Lactococcus lactis* can use as a treatment to restore the disturbed intestinal microbiota of Parkinson's mice to the normal level, thus reducing neuroinflammation (Fang et al., 2020). *Jeotgalicoccus* can promote the fermentation of resistant starch and cellulose in the colon, and produce short-chain fatty acids (such as acetic acid, propionic acid, and butyric acid), in which butyric acid could reduce inflammation by reducing LPS translocation and inhibits the growth of facultative anaerobic bacteria to maintain the health of gut (Ege, 2017; Yang et al., 2017).

Next, we determined the predicted function of gut microbiota using the PICRUSt software, and we found through a MetaCyc pathway analysis that some enriched metabolites in *F. nucleatum* infection AD-like rats are related to amino acid and their derivatives metabolism (L-arginine degradation, L-threonine metabolism, L-ornithine, putrescine, 4-aminobutanoate degradation, and creatinine degradation) and carbohydrate metabolism (chondroitin sulfate degradation and mannan degradation) pathways. Studies have shown that changes in serum amino acid metabolism are associated with some systemic metabolic diseases (Newgard et al., 2009), for example, branched-chain amino acids contribute to the development of obesity-related insulin resistance, and aromatic amino acids (such as phenylalanine, tryptophan, and tyrosine) have also been confirmed to be involved in the pathogenesis

of diabetes and cardiovascular diseases (Wang et al., 2011; Magnusson et al., 2013).

In this study, we chose co-injection of D-gal and $AlCl_3$ to construct an animal model of AD, and found the chronic oral application of *F. nucleatum* can result in spatial learning impairment, neurodegeneration, Aβ formation with increased serum LPS, and increased abundance of *Streptococcus* and *Prevotella* in the gut tract. Whether this neuropathology is directly caused by serum LPS or gut microbiota is not clear and needs to be determined in future studies. The importance of our study is the demonstration that D-gal + $AlCl_3$ induced AD-like rats can result in the accumulation of Aβ and phosphorylated tau181, increased serum LPS and abundance of *Streptococcus* and *Prevotella*, following chronic oral application of *F. nucleatum*.

In this study, using the AlCl3 + D-galactose induced AD-like rat model with periodontitis, we explored the possibility of *F. nucleatum* altering neurodegeneration and the Aβ1–42 formation in the brain. We also provide new evidence that the neuropathological features were greatly influenced by *F. nucleatum* infection and the consequential gut microbiota change. Our study strengthened the relationship between *F. nucleatum* and AD. The experimental basis supports the possibility of targeting microbial etiology for the treatment of AD.

Data availability statement

The datasets presented in this study can be found in online repositories. The names of the repository/repositories and accession number(s) can be found below: https://ngdc.cncb.ac.cn/search/?dbId=&q=CRA004727.

Ethics statement

The animal study was reviewed and approved by the Ethics Committees of the West China Hospital of Sichuan University (WCHSIRB-D-2021-009).

Author contributions

CY wrote the manuscript and contributed to the data analysis. QD and YZ contributed to the manuscript writing. RH and YL conducted the study. CZ and XH contributed to data management and analysis. YL designed the study and analyzed the imaging data. All authors contributed to and approved the final manuscript.

Funding

This study was supported by the National Natural Science Foundation of China (Grant no. 81771085), and the Key Project of the Science and Technology Department of Sichuan Province (Grant no. 2020YFSY0008).

Acknowledgments

We appreciated Shuzhen Li and Changqing Lu for their help in this study.

Conflict of interest

The authors declare that the research was conducted in the absence of any commercial or financial relationships that could be construed as a potential conflict of interest.

Publisher's note

References

Bauerl, C., Collado, M. C., Diaz Cuevas, A., Vina, J., and Perez Martinez, G. (2018). Shifts in gut microbiota composition in an APP/PSS1 transgenic mouse model of Alzheimer's disease during lifespan. *Lett. Appl. Microbiol.* 66, 464–471. doi: 10.1111/lam.12882

Bhuvanendran, S., Bakar, S. N. S., Kumari, Y., Othman, I., Shaikh, M. F., and Hassan, Z. (2019). Embelin improves the spatial memory and hippocampal long-term potentiation in a rat model of chronic cerebral hypoperfusion. *Sci. Rep.* 9:14507. doi: 10.1038/s41598-019-50954-y

Blennow, K., and Zetterberg, H. (2018). Biomarkers for Alzheimer's disease: Current status and prospects for the future. *J. Int. Med.* 284, 643–663. doi: 10.1111/joim.12816

Bonfili, L., Cecarini, V., Berardi, S., Scarpona, S., Suchodolski, J. S., Nasuti, C., et al. (2017). Microbiota modulation counteracts Alzheimer's disease progression influencing neuronal proteolysis and gut hormones plasma levels. *Sci. Rep.* 7:2426. doi: 10.1038/s41598-017-02587-2

Brennan, C. A., and Garrett, W. S. (2019). *Fusobacterium nucleatum* – symbiont, opportunist and oncobacterium. *Nat. Rev. Microbiol.* 17, 156–166. doi: 10.1038/s41579-018-0129-6

Chen, C. K., Wu, Y. T., and Chang, Y. C. (2017). Association between chronic periodontitis and the risk of Alzheimer's disease: A retrospective, population-based, matched-cohort study. *Alzheimers Res. Ther.* 9:56. doi: 10.1186/s13195-017-0282-6

Chen, S., Dong, Z. P., Cheng, M., Zhao, Y. Q., Wang, M. Y., Sai, N., et al. (2017). Homocysteine exaggerates microglia activation and neuroinflammation through microglia localized STAT3 overactivation following ischemic stroke. *J. Neuroinflammation* 14:187. doi: 10.1186/s12974-017-0963-x

Chiroma, S. M., Mohd Moklas, M. A., Mat Taib, C. N., Baharuldin, M. T. H., and Amon, Z. (2018). d-galactose and aluminium chloride induced rat model with cognitive impairments. *Biomed. Pharmacother.* 103, 1602–1608. doi: 10.1016/j.biopha.2018.04.152

Chukkapalli, S. S., Rivera, M. F., Velsko, I. M., Lee, J. Y., Chen, H., Zheng, D. H., et al. (2014). Invasion of oral and aortic tissues by oral spirochete *Treponema denticola* in ApoE(-/-) mice causally links periodontal disease and atherosclerosis. *Infect. Immunity* 82, 1959–1967. doi: 10.1128/Iai.01511-14

Desbonnet, L., Clarke, G., Shanahan, F., Dinan, T. G., and Cryan, J. F. (2014). Microbiota is essential for social development in the mouse. *Mol. Psychiatry* 19, 146–148. doi: 10.1038/mp.2013.65

Ding, Y., Ren, J., Yu, H., Yu, W., and Zhou, Y. (2018). Porphyromonas gingivalis, a periodontitis causing bacterium, induces memory impairment and age-dependent neuroinflammation in mice. *Immun. Ageing* 15:6. doi: 10.1186/s12979-017-0110-7

Dioguardi, M., Crincoli, V., Laino, L., Alovisi, M., Sovereto, D., Mastrangelo, F., et al. (2020). The role of periodontitis and periodontal bacteria in the onset and progression of Alzheimer's Disease: A systematic review. *J. Clin. Med.* 9:495. doi: 10.3390/jcm9020495

Dominy, S. S., Lynch, C., Ermini, F., Benedyk, M., Marczyk, A., Konradi, A., et al. (2019). Porphyromonas gingivalis in Alzheimer's disease brains: Evidence for disease causation and treatment with small-molecule inhibitors. *Sci. Adv.* 5:eaau3333. doi: 10.1126/sciadv.aau3333

Ege, M. J. (2017). The hygiene hypothesis in the age of the microbiome. *Ann. Am. Thorac. Soc.* 14(Suppl_5), S348–S353. doi: 10.1513/AnnalsATS.201702-139AW

Fang, X., Zhou, X., Miao, Y., Han, Y., Wei, J., and Chen, T. (2020). Therapeutic effect of GLP-1 engineered strain on mice model of Alzheimer's disease and Parkinson's disease. *AMB Express* 10:80. doi: 10.1186/s13568-020-01014-6

Fardini, Y., Wang, X., Temoin, S., Nithianantham, S., Lee, D., Shoham, M., et al. (2011). *Fusobacterium nucleatum* adhesin FadA binds vascular endothelial cadherin and alters endothelial integrity. *Mol. Microbiol.* 82, 1468–1480. doi: 10.1111/j.1365-2958.2011.07905.x

Foschi, F., Izard, J., Sasaki, H., Sambri, V., Prati, C., Muller, R., et al. (2006). *Treponema denticola* in disseminating endodontic infections. *J Dent Res* 85, 761–765. doi: 10.1177/154405910608500814

Gonzalez-Burgos, G., Fish, K. N., and Lewis, D. A. (2011). GABA neuron alterations, cortical circuit dysfunction and cognitive deficits in schizophrenia. *Neural Plast.* 2011:723184. doi: 10.1155/2011/723184

Gregory, S. W., Boyce, T. G., Larson, A. N., Patel, R., and Jackson, M. A. (2015). *Fusobacterium nucleatum* osteomyelitis in 3 previously healthy children: A case series and review of the literature. *J. Pediatric Infect. Dis. Soc.* 4, e155–e159. doi: 10.1093/jpids/piv052

Grover, M., and Kashyap, P. C. (2014). Germ-free mice as a model to study effect of gut microbiota on host physiology. *Neurogastroenterol. Mot.* 26, 745–748. doi: 10.1111/nmo.12366

Guo, M., Peng, J., Huang, X., Xiao, L., Huang, F., and Zuo, Z. (2021). Gut microbiome features of Chinese patients newly diagnosed with Alzheimer's disease or mild cognitive impairment. *J. Alzheimers Dis.* 80, 299–310. doi: 10.3233/JAD-201040

Han, X. Y., Weinberg, J. S., Prabhu, S. S., Hassenbusch, S. J., Fuller, G. N., Tarrand, J. J., et al. (2003). Fusobacterial brain abscess: A review of five cases and an analysis of possible pathogenesis. *J. Neurosurg.* 99, 693–700. doi: 10.3171/jns.2003.99.4.0693

Huang, Y., Tang, J., Cai, Z., Zhou, K., Chang, L., Bai, Y., et al. (2020). Prevotella induces the production of Th17 cells in the colon of mice. *J. Immunol. Res.* 2020:9607328. doi: 10.1155/2020/9607328

Ilievski, V., Zuchowska, P. K., Green, S. J., Toth, P. T., Ragozzino, M. E., Le, K., et al. (2018). Chronic oral application of a periodontal pathogen results in brain inflammation, neurodegeneration and amyloid beta production in wild type mice. *PLoS One* 13:e0204941. doi: 10.1371/journal.pone.0204941

Jia, X., Jia, L., Mo, L., Yuan, S., Zheng, X., He, J., et al. (2019). Berberine ameliorates periodontal bone loss by regulating gut microbiota. *J. Dent. Res.* 98, 107–116. doi: 10.1177/0022034518797275

Kowalski, K., and Mulak, A. (2019). Brain-gut-microbiota axis in Alzheimer's disease. *J. Neurogastroenterol. Mot.* 25, 48–60. doi: 10.5056/jnm18087

Li, Q., Wang, H., Tan, L., Zhang, S., Lin, L., Tang, X., et al. (2021). Oral Pathogen *Fusobacterium nucleatum* coaggregates with *Pseudomonas aeruginosa* to modulate the inflammatory cytotoxicity of pulmonary epithelial cells. *Front. Cell Infect. Microbiol.* 11:643913. doi: 10.3389/fcimb.2021.643913

Li, W., Wu, X., Hu, X., Wang, T., Liang, S., Duan, Y., et al. (2017). Structural changes of gut microbiota in Parkinson's disease and its correlation with clinical features. *Sci. China Life Sci.* 60, 1223–1233. doi: 10.1007/s11427-016-9001-4

Li, Y., Wang, K., Zhang, B., Tu, Q., Yao, Y., Cui, B., et al. (2019). Salivary mycobiome dysbiosis and its potential impact on bacteriome shifts and host immunity in oral lichen planus. *Int. J. Oral. Sci.* 11:13. doi: 10.1038/s41368-019-0045-2

Liaquat, L., Ahmad, S., Sadir, S., Batool, Z., Khaliq, S., Tabassum, S., et al. (2017). Development of AD like symptoms following co-administration of AlCl3 and D-gal in rats: A neurochemical, biochemical and behavioural study. *Pak. J. Pharm. Sci.* 30(2(Suppl.)), 647–653.

Long, J. M., and Holtzman, D. M. (2019). Alzheimer disease: An update on pathobiology and treatment strategies. *Cell* 179, 312–339. doi: 10.1016/j.cell.2019.09.001

Loos, B. G., and Van Dyke, T. E. (2020). The role of inflammation and genetics in periodontal disease. *Periodontol. 2000* 83, 26–39. doi: 10.1111/prd.12297

Magnusson, M., Lewis, G. D., Ericson, U., Orho-Melander, M., Hedblad, B., Engstrom, G., et al. (2013). A diabetes-predictive amino acid score and future cardiovascular disease. *Eur. Heart J.* 34, 1982–1989. doi: 10.1093/eurheartj/ehs424

Matsushita, K., Yamada-Furukawa, M., Kurosawa, M., and Shikama, Y. (2020). Periodontal disease and periodontal disease-related bacteria involved in the pathogenesis of Alzheimer's disease. *J. Inflamm. Res.* 13, 275–283. doi: 10.2147/JIR.S255309

Morris, M. C., Gilliam, E. A., and Li, L. (2014). Innate immune programing by endotoxin and its pathological consequences. *Front. Immunol.* 5:680. doi: 10.3389/fimmu.2014.00680

Newgard, C. B., An, J., Bain, J. R., Muehlbauer, M. J., Stevens, R. D., Lien, L. F., et al. (2009). A branched-chain amino acid-related metabolic signature that differentiates obese and lean humans and contributes to insulin resistance (vol 9, pg 311, 2009). *Cell Metabolism* 9, 565–566. doi: 10.1016/j.cmet.2009.05.001

Peng, W. J., Yi, P. J., Yang, J. J., Xu, P. P., Wang, Y., Zhang, Z. Y., et al. (2018). Association of gut microbiota composition and function with a senescence-accelerated mouse model of Alzheimer's disease using 16S rRNA gene and metagenomic sequencing analysis. *Aging* 10, 4054–4065. doi: 10.18632/aging.101693

Poole, S., Singhrao, S. K., Chukkapalli, S., Rivera, M., Velsko, I., Kesavalu, L., et al. (2015). Active Invasion of *Porphyromonas gingivalis* and infection-induced complement activation in ApoE(-/-) mice brains. *J. Alzheimers Dis.* 43, 67–80. doi: 10.3233/Jad-140315

Scheperjans, F., Aho, V., Pereira, P. A., Koskinen, K., Paulin, L., Pekkonen, E., et al. (2015). Gut microbiota are related to Parkinson's disease and clinical phenotype. *Mov. Disord.* 30, 350–358. doi: 10.1002/mds.26069

Sczepanik, F. S. C., Grossi, M. L., Casati, M., Goldberg, M., Glogauer, M., Fine, N., et al. (2020). Periodontitis is an inflammatory disease of oxidative stress: We should treat it that way. *Periodontol. 2000* 84, 45–68. doi: 10.1111/prd.12342

Seo, D. O., Boros, B. D., and Holtzman, D. M. (2019). The microbiome: A target for Alzheimer disease? *Cell Res.* 29, 779–780. doi: 10.1038/s41422-019-0227-7

Shin, J., Kong, C., Lee, J., Choi, B. Y., Sim, J., Koh, C. S., et al. (2019). Focused ultrasound-induced blood-brain barrier opening improves adult hippocampal neurogenesis and cognitive function in a cholinergic degeneration dementia rat model. *Alzheimers Res. Ther.* 11:110. doi: 10.1186/s13195-019-0569-x

Socransky, S. S., and Haffajee, A. D. (2002). Dental biofilms: Difficult therapeutic targets. *Periodontology* 28, 12–55. doi: 10.1034/j.1600-0757.2002.280102.x

Sparks Stein, P., Steffen, M. J., Smith, C., Jicha, G., Ebersole, J. L., Abner, E., et al. (2012). Serum antibodies to periodontal pathogens are a risk factor for Alzheimer's disease. *Alzheimers Dement.* 8, 196–203. doi: 10.1016/j.jalz.2011.04.006

Spigelblatt, L., Saintonge, J., Chicoine, R., and Laverdiere, M. (1985). Changing pattern of neonatal streptococcal septicemia. *Pediatr. Infect. Dis. J.* 4, 56–58. doi: 10.1097/00006454-198501000-00014

Sumathi, T., Shobana, C., Thangarajeswari, M., and Usha, R. (2015). Protective effect of L-Theanine against aluminium induced neurotoxicity in cerebral cortex, hippocampus and cerebellum of rat brain – histopathological, and biochemical approach. *Drug Chem. Toxicol.* 38, 22–31. doi: 10.3109/01480545.2014.900068

Sutej, I., Peros, K., Trkulja, V., Rudez, I., Baric, D., Alajbeg, I., et al. (2020). The epidemiological and clinical features of odontogenic infective endocarditis. *Eur. J. Clin. Microbiol. Infect. Dis.* 39, 637–645. doi: 10.1007/s10096-019-03766-x

Tetz, G., Pinho, M., Pritzkow, S., Mendez, N., Soto, C., and Tetz, V. (2020). Bacterial DNA promotes Tau aggregation. *Sci. Rep.* 10:2369. doi: 10.1038/s41598-020-59364-x

Wang, K., Lu, W. X., Tu, Q. C., Ge, Y. C., He, J. Z., Zhou, Y., et al. (2016). Preliminary analysis of salivary microbiome and their potential roles in oral lichen planus. *Sci. Rep.* 6:22943. doi: 10.1038/srep22943

Wang, K., Miao, T. Y., Lu, W. X., He, J. Z., Cui, B. M., Li, J. Y., et al. (2015). Analysis of oral microbial community and Th17-associated cytokines in saliva of patients with oral lichen planus. *Microbiol. Immunol.* 59, 105–113. doi: 10.1111/1348-0421.12232

Wang, T. J., Larson, M. G., Vasan, R. S., Cheng, S., Rhee, E. P., McCabe, E., et al. (2011). Metabolite profiles and the risk of developing diabetes. *Nat. Med.* 17, 448–453. doi: 10.1038/nm.2307

Wang, T. T., Cai, G. X., Qiu, Y. P., Fei, N., Zhang, M. H., Pang, X. Y., et al. (2012). Structural segregation of gut microbiota between colorectal cancer patients and healthy volunteers. *ISME J.* 6, 320–329. doi: 10.1038/ismej.2011.109

Weller, J., and Budson, A. (2018). Current understanding of Alzheimer's disease diagnosis and treatment. *F1000Res* 7:F1000FacultyRev–1161. doi: 10.12688/f1000research.14506.1

Yang, Y., Chen, G., Yang, Q., Ye, J., Cai, X., Tsering, P., et al. (2017). Gut microbiota drives the attenuation of dextran sulphate sodium-induced colitis by Huangqin decoction. *Oncotarget* 8, 48863–48874. doi: 10.18632/oncotarget.16458

Zhang, J., Yu, C., Zhang, X., Chen, H., Dong, J., Lu, W., et al. (2018). *Porphyromonas gingivalis* lipopolysaccharide induces cognitive dysfunction, mediated by neuronal inflammation via activation of the TLR4 signaling pathway in C57BL/6 mice. *J. Neuroinflammation* 15:37. doi: 10.1186/s12974-017-1052-x

Zhao, Y., Cong, L., Jaber, V., and Lukiw, W. J. (2017). Microbiome-derived lipopolysaccharide enriched in the perinuclear region of Alzheimer's disease brain. *Front Immunol* 8:1064. doi: 10.3389/fimmu.2017.01064

frontiers | Frontiers in Neuroscience

TYPE Original Research
PUBLISHED 06 October 2022
DOI 10.3389/fnins.2022.993132

OPEN ACCESS

EDITED BY
Chunhui Bao,
Shanghai University of Traditional Chinese Medicine, China

REVIEWED BY
Masaaki Tanichi,
Ground Self Defense Forces Japan, Japan
Shengtao Zhu,
Capital Medical University, China

*CORRESPONDENCE
Akiyoshi Saitoh
akiyoshi_saitoh@rs.tus.ac.jp

SPECIALTY SECTION
This article was submitted to Gut-Brain Axis, a section of the journal Frontiers in Neuroscience

RECEIVED 13 July 2022
ACCEPTED 06 September 2022
PUBLISHED 06 October 2022

CITATION
Yoshioka T, Ohashi M, Matsumoto K, Omata T, Hamano T, Yamazaki M, Kimiki S, Okano K, Kobayashi R, Yamada D, Hada N, Kato S and Saitoh A (2022) Repeated psychological stress, chronic vicarious social defeat stress, evokes irritable bowel syndrome-like symptoms in mice.
Front. Neurosci. 16:993132.
doi: 10.3389/fnins.2022.993132

Repeated psychological stress, chronic vicarious social defeat stress, evokes irritable bowel syndrome-like symptoms in mice

Toshinori Yoshioka[1], Misaki Ohashi[1], Kenjiro Matsumoto[2], Tomoki Omata[1], Takumi Hamano[1], Mayuna Yamazaki[1], Sayaka Kimiki[1], Kotaro Okano[1], Riho Kobayashi[1], Daisuke Yamada[1], Noriyasu Hada[3], Shinichi Kato[2] and Akiyoshi Saitoh[1]*

[1]Laboratory of Pharmacology, Faculty of Pharmaceutical Sciences, Tokyo University of Science, Noda, Japan, [2]Division of Pathological Sciences, Department of Pharmacology and Experimental Therapeutics, Kyoto Pharmaceutical University, Kyoto, Japan, [3]Laboratory of Pharmacognosy, Faculty of Pharmaceutical Sciences, Tokyo University of Science, Noda, Japan

Increasing evidence has demonstrated that emotional states and intestinal conditions are inter-connected in so-called "brain–gut interactions." Indeed, many psychiatric disorders are accompanied by gastrointestinal symptoms, such as the irritable bowel syndrome (IBS). However, the functional connection remains elusive, partly because there are few useful experimental animal models. Here, we focused on a highly validated animal model of stress-induced psychiatric disorders, such as depression, known as the chronic vicarious social defeat stress (cVSDS) model mice, which we prepared using exposure to repeated psychological stress, thereafter examining their intestinal conditions. In the charcoal meal test and the capsaicin-induced hyperalgesia test, cVSDS model mice showed a significantly higher intestinal transit ratio and increased visceral pain-related behaviors, respectively. These changes persisted over one month after the stress session. On the other hand, the pathological evaluations of the histological and inflammatory scores of naive and cVSDS model mice did not differ. Furthermore, keishikashakuyakuto—a kampo medicine clinically used for the treatment of IBS—normalized the intestinal motility change in cVSDS model mice. Our results indicate that cVSDS model mice present IBS-like symptoms such as chronic intestinal peristaltic changes and abdominal hyperalgesia without organic lesion. We therefore propose the cVSDS paradigm as a novel animal model of IBS with wide validity, elucidating the correlation between depressive states and intestinal abnormalities.

KEYWORDS

gut-brain axis, social defeat stress, psychological stress, intestinal abnormality, irritable bowel syndrome, animal model

Introduction

Irritable bowel syndrome (IBS) is a disorder chronically presenting gastrointestinal symptoms derived from the small and large intestines, even with no primary organic, systemic, or metabolic illness. According to ROME IV, IBS is categorized by stool consistency into four subtypes—IBS with constipation (IBS-C), IBS with diarrhea (IBS-D), mixed IBS (IBS-M), and unclassified IBS—and is generally characterized by the symptoms of chronic abnormal intestinal movement and abdominal pain without organic pathological changes (Lacy et al., 2016; Bai et al., 2017). However, the detailed pathophysiological conditions and underlying mechanism of IBS remain unclear, and effective treatment has not been established (Adriani et al., 2018).

Accumulating evidence has asserted a deep anatomical and functional brain and gut association—the "gut–brain axis" (Rhee et al., 2009; Mayer, 2011; Cryan and Dinan, 2012). Notably, many IBS patients have concurrent psychiatric disorders, such as depression, anxiety, and posttraumatic stress disorder (PTSD) (Palsson and Drossman, 2005; Ng et al., 2019). Correspondingly, for example, the representative symptoms of depression include not only depressed mood, anxiety, and anhedonia but also abdominalgia, constipation, and diarrhea (Ballou et al., 2019). Especially in digestive symptoms, in major depressive disorder (MDD) patients' brain–gut interactions have adverse influences (Liang et al., 2018; Du et al., 2020). Emotional states and gut dysfunctions are thus considered to be highly associated.

One of the difficulties in elucidating the pathophysiology of IBS is the paucity of useful animal models. Recently, the chronic social defeat stress (cSDS) and chronic vicarious social defeat stress (cVSDS) models have been regarded as widely valid animal models of MDD and PTSD that also presents anxiety- and anhedonia-like phenotypes (Kudryavtseva et al., 1991; Rygula et al., 2005, 2006; Warren et al., 2013; Iñiguez et al., 2019). Notably, we previously reported the induction by the juvenile cSDS paradigm in mice of IBS-like symptoms in their adulthood (Matsumoto et al., 2021). While cSDS model mice (hereinafter referred to as "physical stress (PS) mice," as in previous reports) are submitted to repeated physical attacks from the other mouse, cVSDS model mice ["emotional stress (ES) mice"] receive emotional stress only through witnessing PS mice (Sial et al., 2016). Recently, we found that chronic psychological stress of cVSDS significantly diminished the cell survival rate in the dentate gyrus of the hippocampus, which is closely related to the pathophysiological condition of depressive disorders (Yoshioka et al., 2022).

Here, we focused on the cVSDS paradigm and evaluated the impact of ESs on intestinal conditions. We further assessed the potential of the paradigm as a novel animal model of IBS.

Materials and methods

Animals

We obtained male C57BL/6J mice, aged 5–6 weeks, and "aggressor" CD-1 retired breeder mice from Sankyo Labo Service Corporation Inc. (Tokyo, Japan), and acclimatized them to the breeding room for about 7 days before the experiments. We housed the mice under controlled air temperature and pressure and 12-h light/dark cycles (lights on between 08:00 and 20:00) with *ad libitum* food and water. We housed C57BL/6J mice 4–6 mice per cage (225 × 338 × 140 mm), and CD-1 mice, singly. We conducted all experiments in accordance with the guidelines of the animal welfare committees at the Tokyo University of Science (Approval Nos. Y19032, Y20020, Y21002, and Y22014).

Chronic social defeat stress and chronic vicarious social defeat stress paradigms

We performed the procedure for cSDS and cVSDS conditioning as previously reported with minor modifications (Sial et al., 2016; Yoshioka et al., 2022). Briefly, we divided mice randomly into three groups (naive; PS; ESs). We housed the "aggressor" CD-1 mice individually in their home cages and used them for experiments followed by a 3-day screening. During a defeat session, we placed an ES mouse on one side of the home cage of an "aggressive" CD-1 mouse separated by a perforated acryl divider, and then exposed a PS mouse to the CD-1 mouse. We performed this procedure for 10 min per day around 18:00–19:00 and repeated it over ten consecutive days. Each day we subjected each PS and each ES mouse to a different CD-1 mouse. After each session, we housed the PS mice with the CD-1 mice, separating each pair by the divider, and housed the ES mice singly until the next session; we housed the naive mice 4–6 in a cage for 10 days.

Social interaction test

On day 11 counted from the first defeat session, we conducted a SIT to evaluate stress condition (Golden et al., 2011). We placed a mouse in the interaction field (450 mm × 450 mm) with a wire-mesh cage at one end. We tracked the movements of the mouse for 2.5 min before placing an unfamiliar "aggressor" CD-1 target mouse in the wire-mesh cage, and tracked the movements for another 2.5 min. We then auto-measured the time spent in the interaction zone (area around the wire-mesh cage, 140 mm × 240 mm) using SCANET-40 (Melquest Ltd., Toyama, Japan).

Plasma corticosterone quantification

We collected a three-drop blood sample from the submandibular vein of mice with a 25-gauge needle. Immediately thereafter, we centrifuged the blood samples for 10 min at 2 000 × *g* at 4°C, and aliquoted the supernatant for the enzyme-linked immunosorbent assay, storing it at -20°C until use. We measured corticosterone levels with a Corticosterone ELISA Kit (Enzo Life Sciences Inc., Farmingdale, NY, USA) according to the manufacturer's protocol.

Charcoal meal test

We deprived mice of food for 14–16 h before the test. Following another single cSDS or cVSDS exposure for 10 min, we orally administrated 10 mL/kg of vermilion Indian ink, sacrificed the mice 10 min thereafter by dislocating the cervical vertebra, and immediately extracted the duodenum and small intestine (from the end of the pylorus to the origin of cecum). We calculated the intestinal transit ratio as the charcoal transport distance divided by the total intestine length.

Defecation frequency and stool water content

We conducted stool evaluation according to a previous report (Li et al., 2006). In brief, we placed each mouse in a clean cage for 1 h and collected fecal pellets in a sealed sample tube each time when the animals defecated. After counting the number of pellets and weighing the wet stool, we dried the stool overnight at 65°C and weighed the dry stool as well. The stool water content was calculated as the difference between the wet and dry stool weights divided by the wet stool weight.

Capsaicin-induced hyperalgesia test

We performed this test with minor modifications to that of a previous report (Eijkelkamp et al., 2007). In brief, we, respectively, habituated mice in an acryl cylinder (diameter, 115 mm; height, 180 mm) for 1 h. We then administered 0.1 mL of capsaicin-containing reagent (0.1% wt/vol in 4% Tween80/0.9% NaCl; FUJIFILM Wako Pure Chemical, Osaka, Japan) intrarectally, and counted the number of visceral pain-related behaviors for 15 min. We defined the behavioral evaluation criteria as follows: licking (of the lower abdomen), squashing (of the abdomen against the floor), and jumping (vertically). We also counted immobility when the mice stopped all behaviors apart from respiration movement for more than 3 sec per 5 sec duration.

Pathological evaluation

We extracted the small and large intestines from the mice, washed them with phosphate buffered saline, fixed them in a neutral buffered 10% formalin solution at 4°C, embedded them into paraffin, sectioned them at a thickness of 4 μm, and stained them with hematoxylin and eosin using a standard protocol. We carried out the histological scoring based on previous reports (Theiss et al., 2009; Matsumoto et al., 2018).

Intestinal permeability

We evaluated intestinal permeability as described previously (Matsumoto et al., 2021). In brief, we collected blood from the submandibular vein of mice 1 h after the oral administration of 200 μL of FITC-dextran (MW 4000) solution (50 mg/mL; Merck KGaA, Darmstadt, Germany). Immediately thereafter, we centrifuged the blood samples for 10 min at 2000 × *g* and 4°C and aliquoted the supernatant. We measured the plasma FITC concentration as fluorescence intensity using ALVO MX (PerkinElmer, Waltham, MA, USA).

Drug treatment

We prepared keishikashakuyakuto with hot water extraction and obtained it as a freeze-dried mixture of Cinnamon Bark (lot. 6G28M) 4: Peony Root (lot. 8E24M) 6: Jujube (lot. 8E01M) 4: Glycyrrhiza (lot. 8C27) 2: Ginger (lot. 8E15M) 1. We purchased all cut crude ingredients from Daikoshoyaku Co., Ltd. (Aichi, Japan). We dissolved the drug in 0.1% methylcellulose, and 30 min before the test, we orally administered mice the drug at a dose of 1 g/kg.

Statistical analysis

We determined the sample size by referring to previous reports (Eijkelkamp et al., 2007; Warren et al., 2013; Matsumoto et al., 2021; Yoshioka et al., 2022). Data were acquired from at least two divided experiments. Investigators were blinded to animal groups and/or drug administration information during testing. All data are presented as means ± standard error of the mean (s.e.m.). We performed the analysis using GraphPad Prism7 (GraphPad Software Inc., San Diego, CA, USA). We analyzed the data from two groups using the Student's *t*-test. We analyzed the data from the remaining groups using one-way or two-way analysis of variance (ANOVA), followed by the *post hoc* Bonferroni's test. We defined statistical significance as $^{*}p < 0.05$, $^{**}p < 0.01$.

Results

Preparation of physical stress and emotional stress mice

To assess the influence of cSDS and cVSDS on the physiological and behavioral responses, we designed an experimental plan indicated in Figure 1A. In evaluating stress condition, our results indicated that cVSDS, but not cSDS, significantly impaired body weight gain of mice compared to naive mice (one-way ANOVA; $F_{(2,\ 73)} = 7.332$, $p < 0.01$; Figure 1B). In the SIT, cSDS, but not cVSDS, significantly reduced the time spent in the interaction zone in the presence of an unfamiliar CD-1 target mouse (two-way ANOVA; between-group main effect: $F_{(2,\ 124)} = 7.720$, $p < 0.01$; within-group main effect: $F_{(1,\ 124)} = 11.94$, $p < 0.01$; interaction effects: $F_{(2,\ 124)} = 2.888$, non-significant; Figure 1C). On the other hand, plasma corticosterone level was increased in both paradigms (one-way ANOVA; $F_{(2,\ 16)} = 8.969$, $p < 0.01$; Figure 1D). These results closely resemble those of previous reports (Warren et al., 2013; Yoshioka et al., 2022).

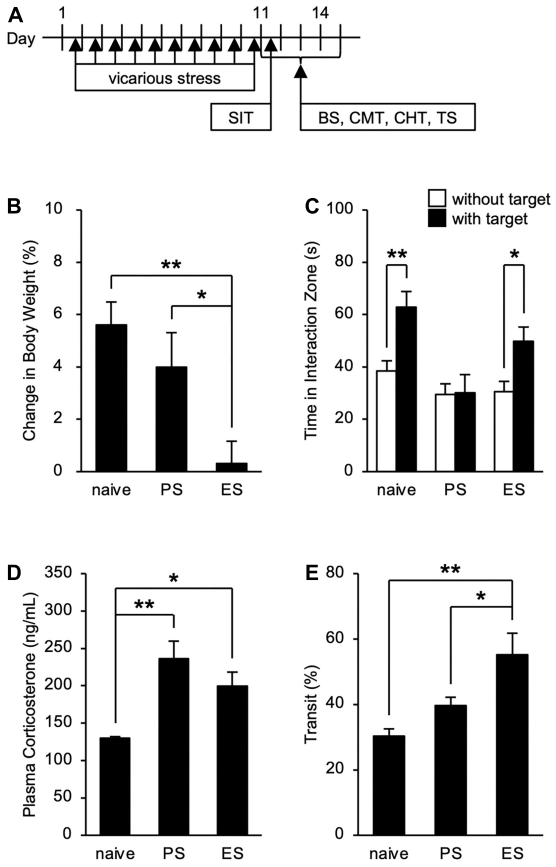

FIGURE 1
Effects of chronic social defeat stress (cSDS) and chronic vicarious social defeat stress (cVSDS) on the physiological and behavioral responses of mice. **(A)** Schematic representations of experimental designs. SIT: social interaction test; BS: blood sampling; CMT: charcoal meal test; CHT: capsaicin-induced hyperalgesia test; TS: tissue sampling. **(B)** Effect of cSDS and cVSDS on body weight gain. Data are presented as means ± s.e.m., and analyzed using one-way factorial ANOVA, followed by Bonferroni's *post hoc* test. $*p < 0.05$, $**p < 0.01$. naive, $n = 24$; PS, $n = 24$; ES, $n = 28$. **(C)** Time spent in the interaction zone in the social interaction test. Data are presented as means ± s.e.m., and analyzed using two-way factorial ANOVA, followed by Bonferroni's *post hoc* test. $*p < 0.05$, $**p < 0.01$. naive, $n = 20$; PS, $n = 22$; ES, $n = 23$. **(D)** Plasma corticosterone quantification. Data are presented as means ± s.e.m., and analyzed using one-way factorial ANOVA, followed by Bonferroni's *post hoc* test. $*p < 0.05$, $**p < 0.01$. naive, $n = 6$; PS, $n = 6$; ES, $n = 7$. **(E)** Intestinal transit ratio in the charcoal meal test. Data are presented as means ± s.e.m., and analyzed using one-way factorial ANOVA, followed by Bonferroni's *post hoc* test. $*p < 0.05$, $**p < 0.01$. naive, $n = 12$; PS, $n = 15$; ES, $n = 15$.

Chronic vicarious social defeat stress, but not chronic social defeat stress, increases intestinal peristalsis

We next investigated the impact of cSDS and cVSDS on intestinal peristalsis. After the 10-day stress loading, the charcoal transit ratio in ES mice, but not PS mice, was significantly elevated compared to that of naive mice in the CMT (one-way ANOVA; $F_{(2,\ 39)} = 7.719$, $p < 0.01$; Figure 1E), indicating that cVSDS, but not cSDS, influenced intestinal peristalsis. However, in the SIT, while a single VSDS exposure did not affect the time spent in the interaction zone in the absence or presence of an unfamiliar CD-1 target mouse (two-way ANOVA; between-group main effect: $F_{(1,\ 28)} = 0.001874$, non-significant; within-group main effect: $F_{(1,\ 28)} = 1.926$, non-significant; interaction effects: $F_{(1,\ 28)} = 0.2629$, non-significant; Supplementary Figure 1A), the charcoal transit ratio was decreased (Student's *t*-test: $p = 0.0454$; Supplementary Figure 1B). In addition, ES mice showed a gradual increase in the defecation frequency, total stool weight, and stool water content during the stress session (two-way ANOVA; main effect of stress: $F_{(1,\ 22)} = 4.842$, $p = 0.0386$, $F_{(1,\ 22)} = 6.520$, $p = 0.0181$, $F_{(1,\ 22)} = 11.77$, $p < 0.01$, respectively; main effect of time: $F_{(4,\ 88)} = 0.4411$, non-significant, $F_{(4,\ 88)} = 1.264$, non-significant, $F_{(4,\ 88)} = 11.16$, $p < 0.01$, respectively; interaction effects: $F_{(4,\ 88)} = 2.203$, non-significant, $F_{(4,\ 88)} = 1.614$, non-significant, $F_{(4,\ 88)} = 15.94$, $p < 0.01$, respectively; Figure 2), suggesting that cVSDS evokes diarrhea-like symptoms in mice.

Chronic vicarious social defeat stress evokes abdominal hyperalgesia

To examine the visceral pain in ES mice, we performed the CHT. cVSDS provoked an increase in licking counts (two-way ANOVA; main effect of stress: $F_{(1,\ 28)} = 23.57$, $p < 0.01$; main

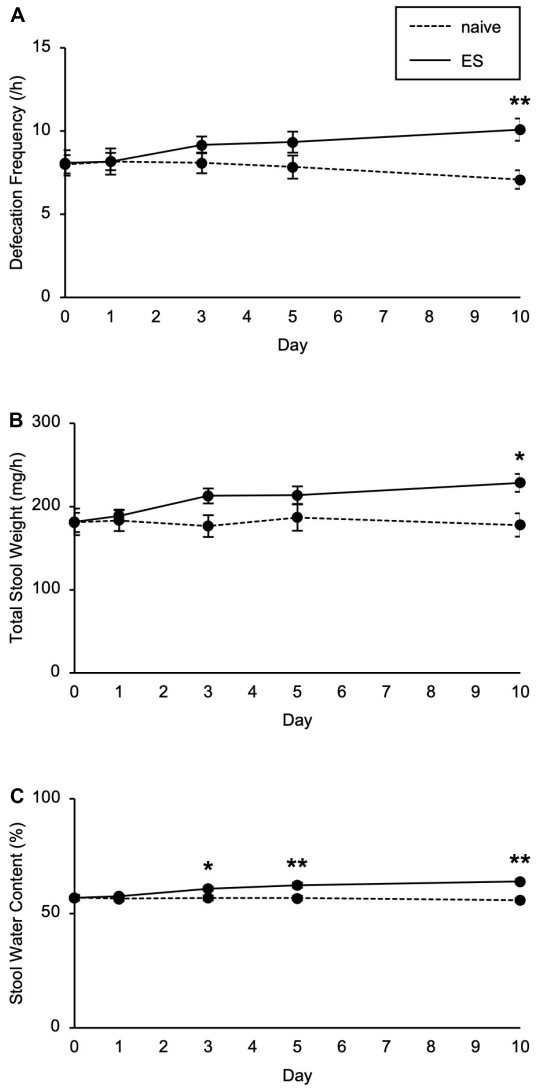

FIGURE 2
Chronic vicarious social defeat stress increased defecation frequency and stool water content. **(A–C)** Defecation frequency **(A)**, total stool weight **(B)**, and stool water content **(C)** for 1 h on different days during the stress session. Data are presented as means ± s.e.m. Data were analyzed using two-way repeated measures ANOVA, followed by Bonferroni's *post hoc* test. $^{*}p < 0.05$, $^{**}p < 0.01$. $n = 12$ for each group.

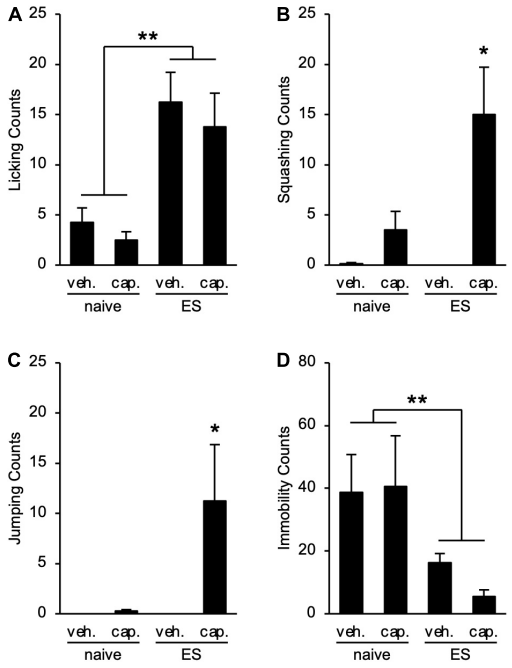

FIGURE 3
Chronic vicarious social defeat stress induces abdominal hyperalgesia. **(A–D)** Visceral pain-related behavior counts in the capsaicin-induced hyperalgesia test. **(A)** Licking; **(B)** Squashing; **(C)** Jumping; **(D)** Immobility. veh.: vehicle; cap.: capsaicin. Data are presented as means ± s.e.m., and analyzed using two-way factorial ANOVA, followed by Bonferroni's *post hoc* test. $^{*}p < 0.05$, $^{**}p < 0.01$. $n = 8$ for each group.

effect of drug: $F_{(1,\ 28)} = 0.7875$, non-significant; interaction effects: $F_{(1,\ 28)} = 0.02452$, non-significant; Figure 3A), and capsaicin administration increased squashing and jumping counts in ES mice (two-way ANOVA; main effect of stress: $F_{(1,\ 28)} = 5.036$, $p = 0.0329$, $F_{(1,\ 28)} = 3.848$, non-significant, respectively; main effect of drug: $F_{(1,\ 28)} = 13.14$, $p < 0.01$, $F_{(1,\ 28)} = 4.206$, $p = 0.0498$, respectively; interaction effects: $F_{(1,\ 28)} = 5.260$, $p = 0.0295$, $F_{(1,\ 28)} = 3.848$, non-significant, respectively; Figures 3B,C), suggesting that cVSDS induces abdominal hyperalgesia. On the other hand, we noted a decrease in immobility counts in ES mice regardless of administration of capsaicin (two-way ANOVA; main effect of stress: $F_{(1,\ 28)} = 11.88$, $p < 0.01$; main effect of drug: $F_{(1,\ 28)} = 0.0003423$, non-significant; interaction effects: $F_{(1,\ 28)} = 0.02772$, non-significant; Figure 3D).

Chronic vicarious social defeat stress did not change intestinal pathological conditions

To clarify the histological status in ES mice, we performed hematoxylin–eosin staining of the small and large intestines. Scores of the epithelial surface damage, crypt damage, the number of inflammatory cells, and the presence of ulceration did not differ between naive and ES mice (Figures 4A,B; Supplementary Table 1), indicating that cVSDS did not alter pathological states. Moreover, the plasma concentration of FITC-dextran, which was administrated orally, was same in ES mice and naive mice (Student's *t*-test: non-significant; Figure 4C), suggesting that cVSDS did not influence intestinal permeability in mice.

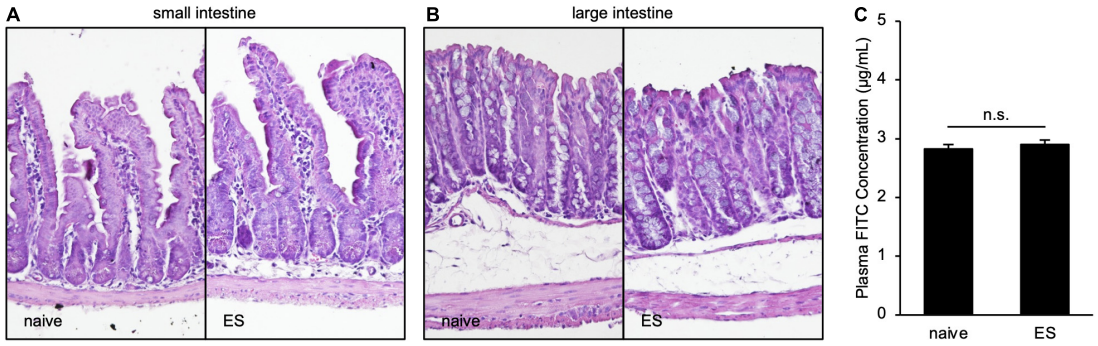

FIGURE 4
Chronic vicarious social defeat stress does not affect pathological states. **(A,B)** Representative images of hematoxylin–eosin staining of small intestine **(A)** and large intestine **(B)**. Histological and inflammatory statuses are evaluated by epithelial surface damage, crypt damage, the number of inflammatory cells, and presence of ulceration. **(C)** Plasm FITC concentration 1 h after the administration of FITC-dextran (MW 4000) on Day 11. Data are presented as means ± s.e.m., and analyzed using Student's *t*-test. $n = 12$ for each group.

Long-term effects of chronic vicarious social defeat stress on intestinal hypermotility and abdominal analgesia

We also tested long-term effects of cVSDS on intestinal conditions (**Figure 5A**). The increased transit ratio in the CMT persisted (Student's *t*-test: $p = 0.0145$; **Figure 5B**), and squashing and jumping behaviors in the CHT were still observed (Student's *t*-test: $p < 0.01$, $p = 0.0258$, respectively; **Figures 5C,D**) 30 days after the stress loading in ES mice. These results suggest that ES mice present chronic abdominal abnormalities.

Keishikashakuyakuto normalized the chronic vicarious social defeat stress-induced intestinal hypermotility

Finally, we determined the effect of keishikashakuyakuto, which is used clinically to treat IBS, on the intestinal motility changes in ES mice. Two days after cVSDS, keishikashakuyakuto decreased the charcoal transit ratio in ES mice in the CMT, but did not affect that of naive mice (two-way ANOVA; main effect of stress: $F_{(1,\ 28)} = 2.797$, non-significant; main effect of drug: $F_{(1,\ 28)} = 5.702$, $p = 0.0239$; interaction effects: $F_{(1,\ 28)} = 4.508$, $p = 0.0427$; **Figure 6**). These results suggest that keishikashakuyakuto modulates intestinal motility.

Discussion

In the current research, we investigated the intestinal conditions of mice exposed to repeated ESs in the cVSDS paradigm, which has played a crucial role in recent preclinical studies as an animal model of MDD and PTSD because of its wide validity in three modes: constructive, face, and predictive (Sial et al., 2016; Yoshioka et al., 2022). We first confirmed that cSDS and/or cVSDS affect physiological and behavioral parameters—such as body weight gain, social behaviors, and plasma corticosterone concentration. Our findings were consistent with previous reports (Warren et al., 2013; Yoshioka et al., 2022). We also found that cVSDS rather than cSDS increased the intestinal transit ratio in the CMT, an effect that persisted 1 month after stress loading, defecation frequency, and stool water content. ES mice also showed visceral pain-related behaviors in the CHT both immediately and one month after exposure to stress. On the other hand, the pathological status and intestinal permeability of the intestine of naive and ES mice did not differ. These results suggest that cVSDS in mice provokes IBS-D-like symptoms such as chronic intestinal peristaltic exacerbations and abdominal hyperalgesia without intestinal lesions. Furthermore, treatment with an IBS-therapeutic, keishikashakuyakuto, induced recovery of the observed intestinal transport abnormality. We therefore propose the cVSDS paradigm as a new animal model of IBS with wide validity.

Conventional animal models of IBS are limited by their requirement for preparation with an acute PS, such as restraint stress, or drug-induced intestinal inflammation (Williams et al., 1988; Qin et al., 2011; Larauche et al., 2012). Besides, other animal models, such as neonatal maternal separation and chronic water avoidance stress paradigms, present intestinal pathological changes (Söderholm et al., 2002; Bradesi et al., 2005; Vannucchi and Evangelista, 2018). Here, we revealed that repeated psychological stress-induced IBS-D-like symptoms without morphological changes and inflammations of the intestine, conferring on this cVSDS paradigm higher constructive and face validities. From the aspect of the gut–brain axis, we consider the hypothesis that the insular cortex plays an important role in determining the phenotype of ES mice as

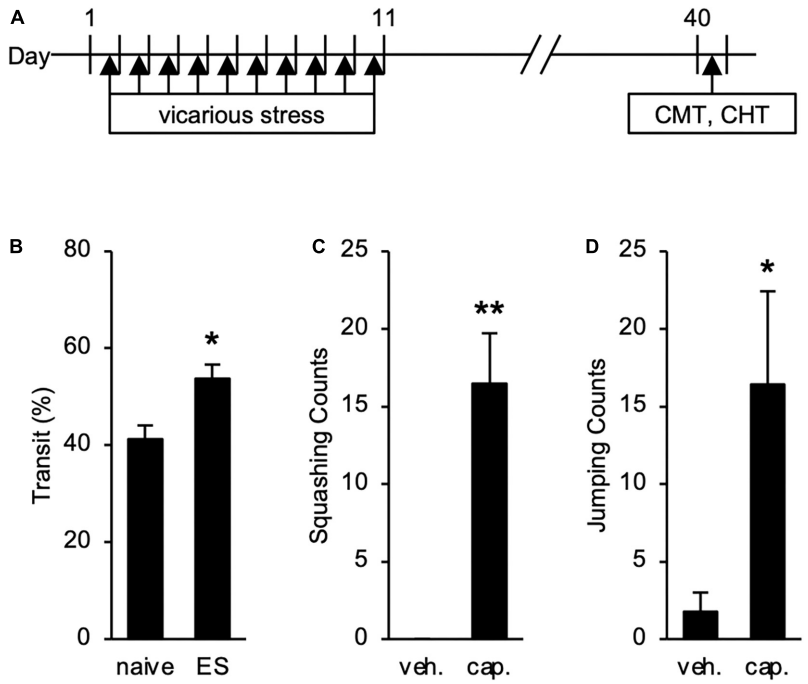

FIGURE 5
Long-term Effects of chronic vicarious social defeat stress (cVSDS) on intestinal peristalsis and abdominal hyperalgesia. **(A)** Experimental design to evaluate long-term effects of cVSDS. CMT: charcoal meal test; CHT: capsaicin-induced hyperalgesia test. **(B)** Intestinal transit ratio in the charcoal meal test. Data are presented as means ± s.e.m., and analyzed using Student's *t*-test. $*p < 0.05$. naive, $n = 6$; ES, $n = 5$. **(C,D)** Visceral pain-related behavior counts in the capsaicin-induced hyperalgesia test. **(C)** Squashing; **(D)** Jumping. veh.: vehicle; cap.: capsaicin. Data are presented as means ± s.e.m., and analyzed using two-way factorial ANOVA, followed by Bonferroni's *post hoc* test. $*p < 0.05$, $**p < 0.01$. naive, $n = 12$; ES, $n = 12$.

the insular cortex is a part of the upper central nervous system controlling digestive functions and is involved in the process of coping with psychological stress. Indeed, it was indicated in some rodent studies that psychological stress activates the insular cortex (Nakatake et al., 2020; Zhang et al., 2022). Therefore, elucidating the functional mechanism underlying IBS-like symptoms in ES mice would substantially lead to understanding the "gut–brain axis." Moreover, how different kinds of stress and individual differences affect intestinal functions is not well known both preclinically and clinically; therefore, creating an IBS-C animal model is keenly anticipated.

We previously reported that cSDS in juvenile mice causes IBS-like symptoms in their adulthood, an animal model of IBS now regarded as both novel and highly validated (Matsumoto et al., 2021). We consider both the cSDS and the cVSDS paradigms to be very useful animal models of IBS in the elucidation of the pathophysiological conditions and the design of therapeutic drugs. Remarkably, early childhood cSDS evokes symptoms at a later stage, while cVSDS does so at either the initial or the later stage; further studies are required to clarify the deferment of onset time. Interestingly, our present result indicates that cSDS did not significantly affect intestinal peristalsis immediately after the stress loading, and a single VSDS contrarily suppressed the motility. This may be due to the

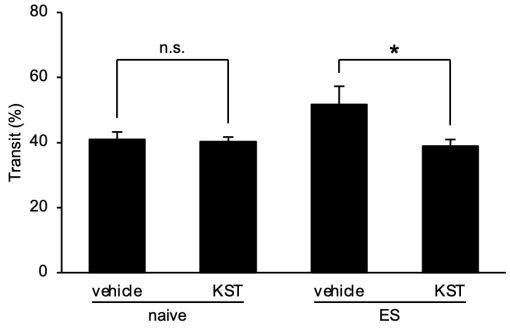

FIGURE 6
Keishikashakuyakuto normalizes chronic vicarious social defeat stress-induced intestinal peristaltic change. Keishikashakuyakuto (KST; 1 g/kg, p.o.) attenuated the intestinal transit ratio in ES mice, but not in naive mice, in the charcoal meal test on day 12. Data are presented as means ± s.e.m., and analyzed using two-way factorial ANOVA, followed by Bonferroni's *post hoc* test. $*p < 0.05$. naive, $n = 10$; ES, $n = 6$.

dominance of the sympathetic nervous system in certain kinds of stress. In the cSDS paradigm, for instance, PS mice showed higher daily consumption of water compared to naive mice (data not shown), suggesting the possibility that cSDS evoked dipsia by activating the sympathetic nervous system. In other words,

the possible dominance of the sympathetic nervous system in PS mice may have suppressed the increase in intestinal transit rate. Further studies are needed to determine the influences of cSDS and cVSDS on the autonomic nervous system.

As aforementioned, IBS patients show recurrent abdominal pain. Here, besides licking of the lower abdomen behaviors induced by cVSDS, ES mice presented squashing and jumping movements in the CHT both immediately and one month after cVSDS, suggesting repeated psychological stress-induced chronic abdominal hyperalgesia. Although previous reports have regarded immobility in the CHT as a visceral pain-related behavior (Eijkelkamp et al., 2007), in ES mice it was significantly low despite administration of capsaicin, because ES mice showed hyperactivity (Yoshioka et al., 2022). We thus propose that ES mice exhibited IBS-D-like symptoms with persistent abdominal pain.

In Oriental medicine, keishikashakuyakuto is an effective treatment of functional gastrointestinal disorders, commonly used for all subtypes of IBS (Saitoh et al., 1999; Oka et al., 2014; Higurashi et al., 2018; Kimura, 2019). According to our results, keishikashakuyakuto controlled the increased intestinal peristalsis in ES mice but did not affect naive mice, suggesting that keishikashakuyakuto not only suppressed intestinal motility but also improved stress-induced diarrhea-like symptom. Hence, we confirmed the predictive validity of the cVSDS paradigm as an animal model of IBS. Additionally, although keishikashakuyakuto is prescribed to relieve abdominal pain (Oka et al., 2014), visceral pain-related behaviors in ES mice tested using the CHT deteriorated with the administration of keishikashakuyakuto (data not shown). This result suggests the possibility that keishikashakuyakuto increases 1) retentivity and/or 2) reactivity of capsaicin in the colon, because keishikashakuyakuto has smooth muscle relaxant actions and raises the extracellular concentration of calcium ions, a key mediator of the capsaicin receptor, transient receptor potential vanilloid 1 (Takayama et al., 2015; Lee et al., 2020). Thus, designing another test system would be required to evaluate the effects of keishikashakuyakuto on abdominalgia.

To date, many IBS animal models have induced organic inflammation in the intestine or have been accompanied by physical stress (Williams et al., 1988; Söderholm et al., 2002; Bradesi et al., 2005; Qin et al., 2011; Larauche et al., 2012; Vannucchi and Evangelista, 2018). Patients with IBS symptoms—for which psychological stress is considered to be a major cause—are often refractory to treatment, amplifying the need to elucidate its pathophysiology. We propose that the present model—induced only by psychological stress—will be an unprecedented and useful animal model.

In conclusion, we demonstrate here for the first time that cVSDS-induced psychological stress alone causes IBS-D-like symptoms in mice. Therefore, we propose the potential of the cVSDS paradigm as a novel unique animal model of IBS with constructive, face, and predictive validities.

Data availability statement

The original contributions presented in this study are included in the article/**Supplementary material**, further inquiries can be directed to the corresponding author/s.

Ethics statement

The animal study was reviewed and approved by the animal welfare committees at the Tokyo University of Science.

Author contributions

TY and MO performed most of the work. KM, TO, TH, MY, SKi, KO, and RK performed the experiments. KM, DY, NH, and SKa provided technical and intellectual advice. AS supervised the project. All authors contributed to the article, agreed to be accountable for all aspects of the work, and approved the submitted version.

Funding

Funding received from the Cyclic Innovation for Clinical Empowerment as part of the Japan Agency for Medical Research and Development (AMED) under Grant Number 17pc0101018h0001.

Conflict of interest

The authors declare that the research was conducted in the absence of any commercial or financial relationships that could be construed as a potential conflict of interest.

Publisher's note

Supplementary material

The Supplementary Material for this article can be found online at: https://www.frontiersin.org/articles/10.3389/fnins.2022.993132/full#supplementary-material

References

Adriani, A., Ribaldone, D. G., Astegiano, M., Durazzo, M., Saracco, G. M., and Pellicano, R. (2018). Irritable bowel syndrome: The clinical approach. *Panminerva Med.* 60, 213–222.

Bai, T., Xia, J., Jiang, Y., Cao, H., Zhao, Y., Zhang, L., et al. (2017). Comparison of the Rome IV and Rome III criteria for IBS diagnosis: A cross-sectional survey. *J. Gastroenterol. Hepatol.* 32, 1018–1025. doi: 10.1111/jgh.13642

Ballou, S., Katon, J., Singh, P., Rangan, V., Lee, H. N., McMahon, C., et al. (2019). Chronic diarrhea and constipation are more common in depressed individuals. *Clin. Gastroenterol. Hepatol.* 17, 2696–2703.

Bradesi, S., Schwetz, I., Ennes, H. S., Lamy, C. M., Ohning, G., Fanselow, M., et al. (2005). Repeated exposure to water avoidance stress in rats: A new model for sustained visceral hyperalgesia. *Am. J. Physiol. Gastrointest. Liver Physiol.* 289, G42–G53. doi: 10.1152/ajpgi.00500.2004

Cryan, J. F., and Dinan, T. G. (2012). Mind-altering microorganisms: The impact of the gut microbiota on brain and behaviour. *Nat. Rev. Neurosci.* 13, 701–712. doi: 10.1038/nrn3346

Du, Y., Gao, X. R., Peng, L., and Ge, J. F. (2020). Crosstalk between the microbiota-gut-brain axis and depression. *Heliyon* 6:e04097.

Eijkelkamp, N., Kavelaars, A., Elsenbruch, S., Schedlowski, M., Holtmann, G., and Heijnen, C. J. (2007). Increased visceral sensitivity to capsaicin after DSS-induced colitis in mice: Spinal cord c-Fos expression and behavior. *Am. J. Physiol. Gastrointest. Liver Physiol.* 293, G749–G757. doi: 10.1152/ajpgi.00114.2007

Golden, S. A., Covington, H. E. III, Berton, O., and Russo, S. J. (2011). A standardized protocol for repeated social defeat stress in mice. *Nat. Protoc.* 6, 1183–1191.

Higurashi, T., Fuyuki, A., Ohkubo, H., Iida, H., Inamori, M., Taguri, M., et al. (2018). The efficacy of the Kampo formula Keishikashakuyakuto for irritable bowel syndrome: A phase 3, multicenter, double-blind, placebo-controlled, randomized controlled trial. *J. Clin. Trials* 8:1000345.

Iñiguez, S. D., Flores-Ramirez, F. J., Riggs, L. M., Alipio, J. B., Garcia-Carachure, I., Hernandez, M. A., et al. (2019). Vicarious social defeat stress induces depression-related outcomes in female mice. *Biol. Psychiatry* 83, 9–17.

Kimura, Y. (2019). Effects of kampo medicine keishikashakuyakuto on large intestine disease in mice. *Tradit. Kampo Med.* 6, 165–172.

Kudryavtseva, N. N., Bakshtanovskaya, I. V., and Koryakina, L. A. (1991). Social model of depression in mice of C57BL/6J strain. *Pharmacol. Biochem. Behav.* 38, 315–320.

Lacy, B. E., Mearin, F., Chang, L., Chey, W. D., Lembo, A. J., Simren, M., et al. (2016). Bowel disorders. *Gastroenterology* 150, 1393–1407.

Larauche, M., Mulak, A., and Taché, Y. (2012). Stress and visceral pain: From animal models to clinical therapies. *Exp. Neurol.* 233, 49–67.

Lee, H. S., Lee, I. H., Kang, K., Park, S. I., Kwon, T. W., and Lee, D. Y. (2020). An investigation of the molecular mechanisms underlying the analgesic effect of Jakyak-Gamcho decoction: A network pharmacology study. *Evid. Based Complement. Alternat. Med.* 2020:6628641. doi: 10.1155/2020/6628641

Li, Z. S., Schmauss, C., Cuenca, A., Ratcliffe, E., and Gershon, M. D. (2006). Physiological modulation of intestinal motility by enteric dopaminergic neurons and the D2 receptor: Analysis of dopamine receptor expression, location, development, and function in wild-type and knock-out mice. *J. Neurosci.* 26, 2798–2807. doi: 10.1523/JNEUROSCI.4720-05.2006

Liang, S., Wu, X., Hu, X., Wang, T., and Jin, F. (2018). Recognizing depression from the microbiota-gut-brain axis. *Int. J. Mol. Sci.* 19:1592.

Matsumoto, K., Takata, K., Yamada, D., Usuda, H., Wada, K., Tada, M., et al. (2021). Juvenile social defeat stress exposure favors in later onset of irritable bowel syndrome-like symptoms in male mice. *Sci. Rep.* 11:16276. doi: 10.1038/s41598-021-95916-5

Matsumoto, K., Yamaba, R., Inoue, K., Utsumi, D., Tsukahara, T., Amagase, K., et al. (2018). Transient receptor potential vanilloid 4 channel regulates vascular endothelial permeability during colonic inflammation in dextran sulphate sodium-induced murine colitis. *Br. J. Pharmacol.* 175, 84–99.

Mayer, E. A. (2011). Gut feelings: The emerging biology of gut-brain communication. *Nat. Rev. Neurosci.* 12, 453–466.

Nakatake, Y., Furuie, H., Ukezono, M., Yamada, M., Yoshizawa, K., and Yamada, M. (2020). Indirect exposure to socially defeated conspecifics using recorded video activates the HPA axis and reduces reward sensitivity in mice. *Sci. Rep.* 10:16881. doi: 10.1038/s41598-020-73988-z

Ng, Q. X., Soh, A. Y. S., Loke, W., Venkatanarayanan, N., Lim, D. Y., and Yeo, W. S. (2019). Systematic review with meta-analysis: The association between post-traumatic stress disorder and irritable bowel syndrome. *J. Gastroenterol. Hepatol.* 34, 68–73.

Oka, T., Okumi, H., Nishida, S., Ito, T., Morikiyo, S., Kimura, Y., et al. (2014). JOPM-EBM Working Team. Effects of Kampo on functional gastrointestinal disorders. *Biopsychosoc. Med.* 8:5. doi: 10.1186/1751-0759-8-5

Palsson, O. S., and Drossman, D. A. (2005). Psychiatric and psychological dysfunction in irritable bowel syndrome and the role of psychological treatments. *Gastroenterol. Clin. North Am.* 34, 281–303.

Qin, H. Y., Wu, J. C., Tong, X. D., Sung, J. J., Xu, H. X., and Bian, Z. X. (2011). Systematic review of animal models of post-infectious/post-inflammatory irritable bowel syndrome. *J. Gastroenterol.* 46, 164–174. doi: 10.1007/s00535-010-0321-6

Rhee, S. H., Pothoulakis, C., and Mayer, E. A. (2009). Principles and clinical implications of the brain-gut-enteric microbiota axis. *Nat. Rev. Gastroenterol. Hepatol.* 6, 306–314. doi: 10.1038/nrgastro.2009.35

Rygula, R., Abumaria, N., Flügge, G., Fuchs, E., Rüther, E., and Havemann-Reinecke, U. (2005). Anhedonia and motivational deficits in rats: Impact of chronic social stress. *Behav. Brain Res.* 162, 127–134. doi: 10.1016/j.bbr.2005.03.009

Rygula, R., Abumaria, N., Flügge, G., Hiemke, C., Fuchs, E., Rüther, E., et al. (2006). Citalopram counteracts depressive-like symptoms evoked by chronic social stress in rats. *Behav. Pharmacol.* 17, 19–29. doi: 10.1097/01.fbp.0000186631.53851.71

Saitoh, K., Kase, Y., Ishige, A., Komatsu, Y., Sasaki, H., and Shibahara, N. (1999). Effects of Keishi-ka-shakuyaku-to (Gui-Zhi-Jia-Shao-Yao-Tang) on diarrhea and small intestinal movement. *Biol. Pharm. Bull.* 22, 87–89. doi: 10.1248/bpb.22.87

Sial, O. K., Warren, B. L., Alcantara, L. F., Parise, E. M., and Bolaños-Guzmán, C. A. (2016). Vicarious social defeat stress: Bridging the gap between physical and emotional stress. *J. Neurosci. Methods* 258, 94–103. doi: 10.1016/j.jneumeth.2015.10.012

Söderholm, J. D., Yates, D. A., Gareau, M. G., Yang, P. C., MacQueen, G., and Perdue, M. H. (2002). Neonatal maternal separation predisposes adult rats to colonic barrier dysfunction in response to mild stress. *Am. J. Physiol. Gastrointest. Liver Physiol.* 283, G1257–G1263. doi: 10.1152/ajpgi.00314.2002

Takayama, Y., Uta, D., Furue, H., and Tominaga, M. (2015). Pain-enhancing mechanism through interaction between TRPV1 and anoctamin 1 in sensory neurons. *Proc. Natl. Acad. Sci. U.S.A.* 112, 5213–5218.

Theiss, A. L., Vijay-Kumar, M., Obertone, T. S., Jones, D. P., Hansen, J. M., Gewirtz, A. T., et al. (2009). Prohibitin is a novel regulator of antioxidant response that attenuates colonic inflammation in mice. *Gastroenterology* 137, 199–208. doi: 10.1053/j.gastro.2009.03.033

Vannucchi, M. G., and Evangelista, S. (2018). Experimental models of irritable bowel syndrome and the role of the enteric neurotransmission. *J. Clin. Med.* 7:4.

Warren, B. L., Vialou, V. F., Iñiguez, S. D., Alcantara, L. F., Wright, K. N., Feng, J., et al. (2013). Neurobiological sequelae of witnessing stressful events in adult mice. *Biol. Psychiatry* 73, 7–14. doi: 10.1016/j.biopsych.2012.06.006

Williams, C. L., Villar, R. G., Peterson, J. M., and Burks, T. F. (1988). Stress-induced changes in intestinal transit in the rat: A model for irritable bowel syndrome. *Gastroenterology* 94, 611–621. doi: 10.1016/0016-5085(88)90231-4

Yoshioka, T., Yamada, D., Kobayashi, R., Segi-Nishida, E., and Saitoh, A. (2022). Chronic vicarious social defeat stress attenuates new-born neuronal cell survival in mouse hippocampus. *Behav. Brain Res.* 416:113536. doi: 10.1016/j.bbr.2021.113536

Zhang, M. M., Geng, A. Q., Chen, K., Wang, J., Wang, P., Qiu, X. T., et al. (2022). Glutamatergic synapses from the insular cortex to the basolateral amygdala encode observational pain. *Neuron* 110, 1993–2008. doi: 10.1016/j.neuron.2022.03.030

frontiers | Frontiers in Neuroscience

TYPE Original Research
PUBLISHED 13 October 2022
DOI 10.3389/fnins.2022.1001544

OPEN ACCESS

EDITED BY
Xiaoming Jin,
Indiana University–Purdue University Indianapolis, United States

REVIEWED BY
Gerard M. Moloney,
University College Cork, Ireland
Jian-jun Chen,
Chongqing Medical University, China

*CORRESPONDENCE
Siddappa N. Byrareddy
sid.byrareddy@unmc.edu

†These authors have contributed equally to this work

SPECIALTY SECTION
This article was submitted to Gut-Brain Axis, a section of the journal Frontiers in Neuroscience

RECEIVED 23 July 2022
ACCEPTED 09 September 2022
PUBLISHED 13 October 2022

CITATION
Olwenyi OA, Johnson SD, Bidokhti M, Thakur V, Pandey K, Thurman M, Acharya A, Uppada S, Callen S, Giavedoni L, Ranga U, Buch SJ and Byrareddy SN (2022) Systems biology analyses reveal enhanced chronic morphine distortion of gut-brain interrelationships in simian human immunodeficiency virus infected rhesus macaques.
Front. Neurosci. 16:1001544.
doi: 10.3389/fnins.2022.1001544

Systems biology analyses reveal enhanced chronic morphine distortion of gut-brain interrelationships in simian human immunodeficiency virus infected rhesus macaques

Omalla A. Olwenyi[1,2†], Samuel D. Johnson[1,2†], Mehdi Bidokhti[1†], Vandana Thakur[1], Kabita Pandey[1,2], Michellie Thurman[1], Arpan Acharya[1], Srijayaprakash Uppada[1], Shannon Callen[1], Luis Giavedoni[3], Udaykumar Ranga[4], Shilpa J. Buch[1] and Siddappa N. Byrareddy[1,5,6*]

[1]Department of Pharmacology and Experimental Neuroscience, University of Nebraska Medical Center, Omaha, NE, United States, [2]Department of Pathology and Microbiology, University of Nebraska Medical Center, Omaha, NE, United States, [3]Department of Biology, Trinity University, San Antonio, TX, United States, [4]Molecular Biology and Genetics Unit, Jawaharlal Nehru Centre for Advanced Scientific Research, Bangalore, India, [5]Department of Genetics, Cell Biology and Anatomy, University of Nebraska Medical Center, Omaha, NE, United States, [6]Department of Biochemistry and Molecular Biology, University of Nebraska Medical Center, Omaha, NE, United States

Background: Commonly used opioids, such as morphine have been implicated in augmented SIV/HIV persistence within the central nervous system (CNS). However, the extent of myeloid cell polarization and viral persistence in different brain regions remains unclear. Additionally, the additive effects of morphine on SIV/HIV dysregulation of gut-brain crosstalk remain underexplored. Therefore, studies focused on understanding how drugs of abuse such as morphine affect immune dynamics, viral persistence and gut-brain interrelationships are warranted.

Materials and methods: For a total of 9 weeks, rhesus macaques were ramped-up, and twice daily injections of either morphine (n = 4) or saline (n = 4) administered. This was later followed with infection with SHIVAD8EO variants. At necropsy, mononuclear cells were isolated from diverse brain [frontal lobe, cerebellum, medulla, putamen, hippocampus (HIP) and subventricular zone (SVZ)] and gut [lamina propria (LP) and muscularis (MUSC) of ascending colon, duodenum, and ileum] regions. Multiparametric flow cytometry was used to were profile for myeloid cell polarity/activation and results corroborated with indirect immunofluorescence assays. Simian human immunodeficiency virus (SHIV) DNA levels were measured with aid of the digital droplet polymerase chain reaction (PCR) assay. Luminex assays were then used to evaluate soluble plasma/CSF biomarker levels. Finally,

changes in the fecal microbiome were evaluated using 16S rRNA on the Illumina NovaSeq platform.

Results: Flow Cytometry-based semi-supervised analysis revealed that morphine exposure led to exacerbated M1 (CD14/CD16)/M2 (CD163/CD206) polarization in activated microglia that spanned across diverse brain regions. This was accompanied by elevated SHIV DNA within the sites of neurogenesis–HIP and SVZ. HIP/SVZ CD16+ activated microglia positively correlated with SHIV DNA levels in the brain (r = 0.548, p = 0.042). Simultaneously, morphine dependence depleted butyrate-producing bacteria, including *Ruminococcus* (p = 0.05), *Lachnospira* (p = 0.068) genera and *Roseburia_sp_831b* (p = 0.068). Finally, morphine also altered the regulation of CNS inflammation by reducing the levels of IL1 Receptor antagonist (IL1Ra).

Conclusion: These findings are suggestive that morphine promotes CNS inflammation by altering receptor modulation, increasing myeloid brain activation, distorting gut-brain crosstalk, and causing selective enhancement of SHIV persistence in sites of neurogenesis.

KEYWORDS

morphine, gut-brain axis, microbiome, microglia, SHIV, neurogenesis, CNS, viral reservoirs

Introduction

Within the United States, the opioid epidemic results in over 125 daily deaths and approximately 70 billion dollars annually diverted toward criminal justice and healthcare systems (Florence et al., 2016; CDC/NCHS, 2018). Currently, the opioid crisis is embodied by recreational and overwhelming addiction to several drugs of abuse. Commonly used drugs of abuse range from prescription painkillers and naturally derived opioids such as morphine, codeine and opium (Rummans et al., 2018; Solimini et al., 2018). In addition, prescription synthetic opioids such as fentanyl, tramadol and carfentanil are also vastly misused (Pérez-Mañá et al., 2018). Interestingly, a significant proportion of opioid consumers are also infected with HIV-1. Morphine synergistically enhances viral loads and worsens HIV/SIV pathogenesis (Nath et al., 2000; Nath, 2002; Zou et al., 2011). In addition, morphine abuse results in remarkable neuropathogenesis characterized by neuronal dysfunction/degeneration that accelerates the occurrence of neuro-AIDS (Nath et al., 2000; Nath, 2002; Zou et al., 2011). Further, morphine administration also exacerbates alterations in gut homeostasis depicted by the disruption of the gastrointestinal epithelial barrier. Subsequently, this leads to elevated microbial translocation, microbial dysbiosis, and systemic immune activation (Meng et al., 2015a,b).

Morphine-mediated multiple organ dysregulation is fostered through several mechanisms, including the skewing of cytokines and chemokines. As a result, this facilitates increased expression of viral entry co-receptors, such as CCR5 and CXCR4 on target cells [CD4+ T cells, myeloid cells (monocytes, macrophages, and microglia)] (Guo et al., 2002; Steele et al., 2003; Kim et al., 2018). During inflammation, peripheral monocytes differentiate, acquiring proinflammatory phenotypes as they traffic and egress into tissues where they differentiate into macrophages (Shi and Pamer, 2011; Teh et al., 2019).

To gain access into the central nervous system (CNS), HIV-1 preferentially infects peripheral pro-inflammatory CD16+ monocyte subsets that subsequently breach the blood-brain barrier (Schechter et al., 2017). By compromising the blood-brain barrier, morphine increases the accessibility of virus-infected cells from the periphery into the CNS (Mahajan et al., 2008; Leibrand et al., 2019). Furthermore, SIV-infected rhesus macaques exposed to morphine exhibit exacerbated monocyte/macrophage influx into the CNS resulting in enhanced neuro-viremia (Bokhari et al., 2011). The compartmentalization of the CNS from the periphery limits the penetration of potent antiretroviral drugs. Consequentially, this offers a sanctuary for ongoing HIV/SIV replication, seeding of the viral reservoir, and persistent inflammation

(Ellero et al., 2017). These events lead to a wide spectrum of cognitive impairments collectively termed as HIV-associated neurocognitive disorders (HAND) (Heaton et al., 2011; Farhadian et al., 2017).

Within the brain, HIV-1 principally infects the microglia (Rock et al., 2004) maintaining a steady state of quiescence and transcriptionally silent latency (Alvarez-Carbonell et al., 2019). However, HIV envelope gp120 and transactivator (Tat) proteins present in the CNS continue to promote neuronal damage despite ongoing viral latency (Tenneti and Lipton, 2000; Kaul and Lipton, 2005). Damaged neurons together with infiltrating proinflammatory macrophages release several proinflammatory cytokines, including interleukin (IL)-1β, IL-6, interferon-gamma (IFN-γ), and tumor necrosis factor-alpha (TNF-α) (Mizuno et al., 1994a,b, 2003). Resultantly, increased neurodegeneration, and augmented IL-1β- and TNF-α-dependent HIV reactivation within microglia occurs (Streit, 2006; Alvarez-Carbonell et al., 2017; Garcia-Mesa et al., 2017). Our laboratory has recently shown that following cART-mediated viral suppression, morphine-dependent SIV-infected rhesus macaques harbored elevated replication-competent reservoirs in the brain myeloid cells (Acharya et al., 2020).

The relative proportions of neuronal and myeloid cell lineages, varies within different brain regions (Ishino et al., 2017; Friedman et al., 2018; Tan et al., 2020). Given such variations, the effect of morphine on myeloid phenotypes and accompanying SIV reservoirs within diverse niches of the brain remains unknown. It is well recognized that the vagus nerve provides a conduit for bi-directional communication between the brain and the gut, highlighted by interjoining the enteric and CNSs (Breit et al., 2018). The production of neuro-immune mediators enables the brain to modulate intestinal functions (Carabotti et al., 2015; Breit et al., 2018). Reciprocally, the gut microbiota secretes metabolites such as short-chain fatty acids that foster optimal brain function (Bonini et al., 1997; Kimura et al., 2011; Dalile et al., 2019; Ma et al., 2019). Additionally, the specific composition of the microbiome can modulate crucial processes, such as neurogenesis in key brain compartments including the hippocampus (HIP) (Dinan and Cryan, 2017; Kelly et al., 2017). In fact, the disruption of the gut microbiome has been linked to several neurodegenerative disorders (Chen et al., 2021), such as Alzheimer's disease (AD) (Kumar et al., 2016; Vogt et al., 2017), Parkinson's disease (Laurent et al., 2013; Paiva et al., 2017), and multiple sclerosis (Jangi et al., 2016). Furthermore, morphine-mediated perturbation of the gut microbiome and simultaneous neuroinflammation have also been associated with dependence and tolerance (Lee et al., 2018). The complex interaction between the gut microbiome, inflammation, and brain-gut immune axis, however, remains poorly understood during HIV/SIV infection.

To address these knowledge gaps, we utilized a systems immunology approach using non-human primates (NHPs) as models for HIV infection. Compared to consenting human study participants, NHPs offer greater flexibility of interrogating changes in diverse tissue compartments (Winkler et al., 2012). HIV has a limited range of host infectivity and does not infect rhesus macaques (Iwanami et al., 2017). To bridge this limitation, we used an engineered chimeric simian human immunodeficiency virus (SHIV) AD8EO clone whose NF-κB binding sites within the long-term repeat (LTR) region were modified to enhance replication fitness (Dave et al., 2020). Following SHIV infection, we conducted comprehensive immune typing to understand phenotypic changes in myeloid cells found in various tissues. Simultaneously, we estimated viral DNA levels within diverse gut and brain regions and evaluated alterations in fecal microbiomes. In addition, changes in soluble factors in the cerebrospinal fluid (CSF) and plasma samples of SHIV-infected rhesus macaques were quantified.

Our findings suggested that morphine administration led to elevated myeloid cell activation across diverse brain regions and disrupted IL-1 regulation in the CNS by lowering the expression of CSF IL-1 receptor antagonist (IL-1ra). Further morphine increased viral persistence, particularly in sites of neurogenesis, while simultaneously disrupting the fecal microbiome. These observations have strong implications on future studies that will aim to dissect mechanisms by which morphine modulates the gut-brain axis.

Materials and methods

Rhesus macaques used and ethical approval for this study

Eight adult male (5–8 years of age) rhesus macaques accommodated within the Department of Comparative Medicine at the University of Nebraska Medical Center (UNMC) core animal facility were utilized for this study (**Supplementary Table 1**). Animals were pair-housed in steel cages within a temperature controlled (∼72° F) and light controlled (12-h light/dark cycle) room. Animals were routinely monitored by experienced staff twice a day. In addition to standard monkey chow (Purina, Gray Summit, MO, USA), their diet was supplemented with fresh fruits and vegetables. Environmental enrichment was also afforded by providing toys, foraging devices, and delicacies such as peanuts and cereals. At the terminal stage of this study, all animals were humanely euthanized by an overdose of a ketamine/xylazine mixture followed by transcardial perfusion with ice-cold PBS. All study procedures were approved by the Institutional Animal Care and Use Committee at UNMC. All study procedures were reviewed and approved by the UNMC IACUC protocol "15-113-01-FC." This protocol was titled "The combinatorial effects of Opiates and promoter-variant strains of HIV-1 subtype C on neuropathogenesis and latency."

Morphine administration and subsequent simian human immunodeficiency virus infection

The overall study design is depicted in **Supplementary Figure 1**. This study included 8 rhesus macaques, four (n = 4) of which were intramuscularly injected with morphine (6 mg/kg/injection) twice a day on weekdays and one time on weekends (12 injections/week). Another four (n = 4) macaques received saline in parallel at same time points (12 injections/week) for 8 weeks. After 8 weeks, all rhesus macaques were intravenously inoculated with 200 $TCID_{50}$ of SHIV AD8EO and its variants with varying 1–3 site of NF-KB sites in the promoter region (Dave et al., 2020). Thereafter, daily morphine or saline exposure was maintained until the end of the study (∼6–8 months). At necropsy, fecal samples, femoral blood, gut, liver, and whole brain tissue samples were collected.

Preparation of peripheral blood mononuclear cells

Femoral blood was collected in K2-EDTA vacutainer tubes (BD, 367841). Within 4 h of collection, blood was centrifuged at 1,200 rpm for 20 min to separate the plasma. The remaining blood cells were layered over a Lymphoprep Density Gradient Medium from STEMCELL Technologies, Germany. Then, peripheral blood mononuclear cells (PBMCs) were isolated by density gradient centrifugal separation (Woollard et al., 2018).

Preparation of liver mononuclear cells

Liver tissue was placed in RPMI immediately upon collection and finely chopped into 1 mm^2 fine pieces using disposable scalpel blades. Following, the finely ground liver tissue (close to 10 g) was placed in digest media (20,000 U collagenase IV, 50 U DNase I, and 20 ml of DPBS) and incubated at 37°C for 30 min with occasional mixing in the Personal HybTm (Stratagene). The digested liver tissue was then filtered using 100 and 40 μm sterile cell strainers (Fisher Scientific, Pittsburgh, PA, USA).

Preparation of gut mononuclear cells

For gut cell isolation, the digestion medium (10,000 U collagenase IV, 25 U DNAse I, and 10 ml DPBS) was prepared in advance for each tissue being processed. Tissue from the duodenum, ileum, and ascending colon were collected at necropsy. Approximately 10 g of lamina propria (LP) and muscularis (MUSC) mucosa sections were surgically excised for each gut section. Washes were then performed using DPBS in a petri dish, and tissues were carefully minced into 1 mm^3 sections. Following this, 10 ml of digestion medium was added, and enzymatic digestion was performed for close to 1.5 h with frequent vortexing at 37°C. Then, 2 ml of FBS was added to each conical tube, and tissues triturated by gently pipetting up and down for additional homogenization. The digested gut tissue sections were then filtered using the 100 and 40 μm sterile cell strainers (Fisher Scientific, Pittsburgh, PA, USA). The filtrate was centrifuged at 1,200 rpm for 6 min and the resultant pellet resuspended in 5 ml of RPMI containing 20% FBS. The resuspended cells were then overlaid on a 60 and 30% Percoll gradient and centrifuged at 2,000 rpm for 30 min without braking. This was followed by targeting the cell layer found between the 30 and 60% interface comprising of lymphocytes and myeloid immune cells. The separated cells were washed with DPBS at 1200 rpm for 6 min and used for further analysis.

Preparation of brain mononuclear cells

Following necropsy, portions of the whole brain tissue were dissected from the frontal lobe, cerebellum, medulla, putamen, HIP, and subventricular zone (SVZ). The examined tissue sections were washed with DPBS to remove any debris and minced into 1 mm^3 pieces using scalpel blades and forceps. Then, 1–2 g of minced brain tissue was added to 50 mL conical tubes containing 10 mL of digestion medium (0.25% trypsin-EDTA + 25 U/mL DNase I in DPBS) and incubated for 1 h at 37°C with occasional mixing. After digestion, 2 mL of FBS was added to inhibit the digestive enzymes. The digestive tissue was triturated using a 25 mL pipette to enhance homogenization. Filtration was then performed using 100 and 40 μm sterile cell strainers (Fisher Scientific, Pittsburgh, PA, USA). The resultant filtrate was centrifuged at 1,600 rpm for 10 min at room temperature and the pellet was resuspended in DPBS. The resuspended cells were overlaid on a 60 and 30% Percoll gradient and centrifuged at 2,000 rpm for 30 min without braking. This was followed by targeting the cell layer found between the 30 and 60% interface comprising of lymphocytes and myeloid cells. The separated cells were washed with DPBS at 1,200 rpm for 6 min and were resuspended in Dulbecco's Modified Eagle's Medium (DMEM) media until further analysis.

Flow cytometry of diverse tissue samples

Myeloid cell phenotyping in mononuclear cells obtained from diverse tissues

Tissue (blood, gut, liver, and gut) mononuclear cells were washed with DPBS and stained with zombie aqua live-dead stain

to exclude dead cells. Then, FC receptor binding antibodies were added to minimize non-specific binding. After subsequent washes, a cocktail of surface receptor binding antibodies (listed in **Supplementary Table 2A**) suspended in BV buffer was added to the cells. Corresponding fluorescent minus one (FMO) tubes alongside compensation controls were also prepared simultaneously. Stained cells were fixed with 1% paraformaldehyde (PFA), and events were acquired using a Fortessa X450 instrument.

Automated and manual analyses of flow cytometry data

Compensated FCS3.0 files were exported from BD Facs Diva onto Flowjo Version 10. Manual gating was then performed using the gating strategies described in **Supplementary Figures 2, 3**. Automated analyses were performed using Flowjo Plugin Downsample version 3.0 to obtain similar events across several samples. After this, concatenations were carried out to obtain a single file. Later, the Flowjo Plugin Fast Fourier Transform-accelerated Interpolation-based t-SNE (FIt-SNE) was then executed on the resultant single concatenated FSC file at the following settings (t-SNE dimensions = 2, Nearest neighbors = Approximate, Perplexity = 20.0, and Maximum iterations = 3000) (Linderman et al., 2017).

Quantification of cell-associated simian human immunodeficiency virus DNA in various tissues

Digital droplet polymerase chain reaction (dd-PCR) was utilized to estimate the amount of SHIV DNA within the tissues. Genomic DNA was extracted using the AllPrep DNA/RNA Mini kit from Qiagen (Cat No./ID: 80204). The levels of genomic DNA were next evaluated using a GE SimpliNano drop spectrophotometer. Then, the Bio-Rad QX200 AutoDG digital droplet PCR system was used to carry out dd-PCR reactions. First, a reaction mixture comprising of: dd-PCR Supermix for probes (no dUTP), 10 μM forward primer, 10 μM reverse primer, 10 μM probe, DNA template, and RNase/DNase free water) was prepared. Then, 22 μl of the reaction mixture was added to each well of a 96-well plate and loaded onto a QX200 Droplet Generator for the generation of liquid droplets followed by heat sealing with a foil (Bio-Rad; Bio-Rad; Cat#181–4040). Amplification was carried out in a C1000 Touch thermal cycler (Bio-Rad, Hercules, CA, USA) under the conditions described in **Supplementary Table 3**. After this, the dd-PCR plates were placed in a QX200 droplet reader (Bio-Rad, Hercules, CA, USA) for droplet count and fluorescence measurements. With the aid of QuantaSoft software, the absolute quantity of DNA per sample (copies/μl) was determined after applying a fluorescence amplitude threshold to exclude negative droplets from the positive droplets containing the amplified products. The normalization for the conserved RPP30 gene was done to yield equivalent copies of SIV gag per million cells. Also, viral RNA levels were estimated using quantitative PCR (qPCR) assays as previously described (Acharya et al., 2020).

Indirect-immunofluorescence assay

Formalin fixed paraffin-embedded brain (HIP) tissues collected from six (11N074, 11N097, 12N060, 12N044, 12N015, and 13L126) different animals were grouped as SHIV+ saline (control $n = 3$) and SHIV+ morphine (infected $n = 3$). The selected tissues were then cut into 5 μm sections, deparaffinized in xylene and re-hydrated in descending grades of ethanol and deionized water. This was later followed by antigen retrieval in tris EDTA buffer (pH, 9.0), and blocking performed with ttPBS (1× PBS with 0.3% Tween 20 and 2 mM sodium azide) containing normal goat serum (S-1000, Vector laboratories, Burlingame, CA, USA). Next, the sections were incubated with unconjugated primary antibodies that comprised of: mouse anti-p27 SIV gag (clone 55-2F12, AIDS research and reference reagent program, Germantown, MD, USA), mouse anti-CD16 clone 2H7 (Novocastra, Newcastle, UK), rabbit CD163 Antibody (EDHu-1) (Novus biological, Centennial, CO, USA) and goat anti-Iba1 (ab5076) Abcam, Cambridge, Ma, USA at 4C overnight. Afterward, the tissues were washed and later stained with conjugated secondary antibodies such as: alexa488 goat anti-rabbit/goat anti-mouse, alexa546 goat anti-mouse and Dylight405 donkey anti-goat (1:200) for 1 h. The tissues were washed thrice with ttPBS, counter stained by DAPI 0.5 ug/ml for 10 min at room temperature, rinsed and mounted in prolong gold antifade reagent (Thermo Fisher, Waltham, MA, USA) (Dave et al., 2018). Images were acquired and quantified by using a Nuance fluorescence microscope equipped with Nuance software v 3.0.2 (Perking-Elmer Winter St Waltham, MA, USA). Quantification of positive cells was performed manually by counting positive staining per field in 10 random selected fields (Micci et al., 2014).

16S rRNA evaluation of the fecal microbiome

Genomic DNA extraction and 16S rRNA gene sequencing

Following the manufacturer's instructions, DNA was extracted from thawed frozen (−80°C) fecal samples collected during necropsy using the Norgen Biotek Corp Stool DNA isolation kit (Catalog number: 27600). Using 341F/805R primers, a 465 bp amplicon was generated by targeting the V3 and V4 regions of the 16S rRNA gene. Then, sequencing was performed on the Illumina MiSeq platform (according to the manufacturer's specifications) at LC Sciences to yield 250 bp paired-end reads in either direction (Johnson et al., 2021).

Microbiome data analysis

The obtained raw data files were demultiplexed, filtered, and processed to merge paired-end reads into a single continuous sequence tag. In contrast to exploiting sequence similarity within the Quantitative Insights Into Microbial Ecology (QIIME) platform, OTU Clustering was performed using the Divisive Amplicon Denoising Algorithm (DADA2). DADA2 reduces background noise and corrects sequencing errors by filtering, dereplication, chimeric filtering, and other methods. This improves data accuracy, species resolution, and reliability of results (Callahan et al., 2016). Taxonomy annotation was performed using the ribosomal database project (RDP) classifier tool for alignment with the corresponding OTU tags (Wang et al., 2007; Cole et al., 2014). Alpha diversity was then determined based on the number of OTUs/species (Chao-1 index) and uniformity (Shannon index). With the aid of both the R vegan package (Oksanen et al., 2016) and GraphPad Prism 9 software, principal component analysis (PCA) based on the weighted UniFrac distance matrix was used to evaluate Beta diversity (test for phylogenetic relatedness) (Motulsky, 2020). Bacterial taxa data were reformatted to serve as an input on the online Galaxy/Hutlab web platform for linear discriminant analysis effect size (LEfSe) analysis for taxa discrimination found in the two studied groups. For this analysis, the cut-offs used were linear discrimination analysis (LDA) $\geq$ 2 and p-values for Kruskal–Wallis and Pairwise Wilcoxon tests set to $\leq$0.05 (Hutlab; Segata et al., 2011).

Luminex high performance for multiple measures of soluble markers in plasma and cerebrospinal fluid

Plasma and CSF were collected at necropsy, frozen and shipped on dry ice for Luminex assays. Monoclonal antibodies were covalently bound to carboxylated Luminex beads following the carbodiimide procedure according to the manufacturer's suggestion and washed and resuspended in PBS-0.5% Tween 20. Efficacy of coupling was confirmed with 1 μg/mL R-phycoerythrin goat anti-mouse IgG (H + L) antibody (Molecular Probes, Inc., Eugene, OR, USA). Commercial kits were run in individual plates with buffers and standards according to manufacturer's directions. Following standardization, frozen samples were thawed quickly and 50 μL aliquots combined with coated beads. The acquisition gate was set between 8,000 and 13,500, and 100 events/region later acquired. Data were analyzed with the MasterPlex QT quantification software (MiraiBio Inc., Alameda, CA, USA). The following analytes were chosen for our analysis: macrophage inflammatory protein 1-alpha (MIP-1α), MIP-1β, Interleukin-6 (IL-6), interferon-γ-inducible protein 10 (IP-10), Interleukin-8 (IL-8), interferon-alpha (IFN-α), IFN-γ, Eotaxin, Interleukin-12p40 (IL-12p40), Interleukin-18 (IL-18), Interferon–inducible T-cell alpha chemoattractant (I-TAC), TNF-α, soluble CD40L (sCD40L), monokine induced by interferon-gamma (MIG), macrophage migration inhibitory factor (MIF), Interleukin-1 receptor a (IL-1Ra), Lymphatic Vessel Endothelial Receptor 1 (LYVE-1), Monocyte Chemoattractant Protein-1 (MCP-1), Regulated upon activation, normal T-cell expressed and presumably secreted (RANTES), Myeloperoxidase (MPO), Indoleamine 2, 3-dioxygenase (IDO), C-reactive protein (CRP) and perforin (**Supplementary Table 2B**). Measures for the levels of each analyte were interpolated from best fitting curves that were generated using commercial standards as previously described (Giavedoni, 2005).

Statistical analysis

Prism V9.0 (GraphPad Software) and R version 3.4.3 were utilized for statistical analysis. Within-group comparisons (saline vs. morphine) were performed using the non-parametric Mann–Whitney U-test. Paired non-parametric tests were also performed using the Wilcoxon test. Also, grouped non-parametric tests were conducted using the Friedman test. For multiple comparisons, one-way analysis of variance (ANOVA) with Holm-Sidak *post hoc* testing was used. For multiple correlations, the cor function was used in R to generate a correlation matrix. p-values obtained within the correlation matrix were corrected for type 1 error using Holm's correction. Following this, the R corrplot function was utilized to generate heatmaps. Also, the frequencies of flow cytometric measures from different brain regions were then plotted using the cerebroViz package (Bahl et al., 2017). Since the SVZ is not defined in cerebroViz, the best anatomical approximation, the caudate nucleus, was used to visualize this region.

Results

The dynamics of viral loads in the plasma and cerebrospinal fluid compartments of morphine-dependent vs. saline-exposed rhesus macaques

During infection, the median peaks of plasma viral load in the morphine- and saline-treated groups were 1,338,500 and 6,430,000 copies per ml, respectively, (p = 0.220) (**Figure 1A**). Similarly, the median peaks of CSF viral load in the morphine and saline groups were 1,008 and 4,224 copies per ml, respectively, (p = 0.88) (**Figure 1B**). The longitudinal geometrical means of plasma and CSF viral loads of morphine and saline-exposed rhesus macaques are presented in **Figures 1C,D** with no

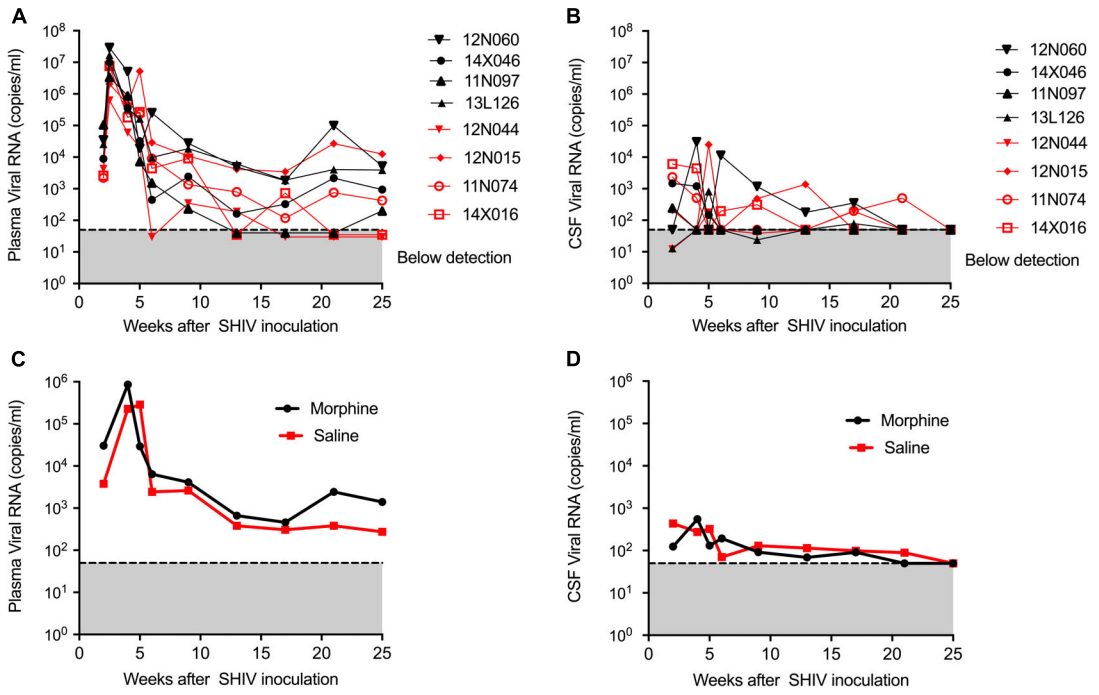

FIGURE 1
Kinetics of Plasma and CSF viral loads of morphine administered SHIVADE08 infected rhesus macaques. Plasma and CSF viral loads were quantified using a quantitative PCR (qPCR) assay. Longitudinal viral load measures in **(A)** plasma and **(B)** CSF of individual animals exposed to either morphine (red tagged) or saline (blue tagged). Geometric means of **(C)** plasma viral loads and **(D)** CSF viral loads were shown. The gray shaded zone displays the limit of detection of the assay (50 copies/ml). No statistical differences were observed between morphine vs. saline exposed SHIV infected rhesus macaques based on Mann–Whitney *U*-test comparisons at 0, 4, 8, 12, 16, 20, and 24-week timepoints.

statistical significance observed. Furthermore, we did not find significant differences in viral DNA and RNA levels in peripheral blood or several tissues examined ($p > 0.05$) (**Supplementary Figure 2**).

Surface marker profile of the brain myeloid lineage in simian human immunodeficiency virus-infected saline or morphine-exposed rhesus macaques

The phenotype of brain myeloid cells is multi-dimensionally altered during different diseases, trauma, and neurodegeneration states (Herz et al., 2017). To gain insights into the global immune landscape of the predominant brain myeloid phenotypes, we profiled pooled cells isolated from different brain regions and evaluated their overall activation status, activation, frequency, and polarity. Thus an 18-parameter flow cytometry panel comprising size and complexity discrimination (FSC vs. SSC), dead cell exclusion (Zombie Aqua), dump lineage exclusion ($CD3^+$, $CD8^+$ NK^+ and $CD20^+$ cells), myeloid lineage markers (CD45 and CD11b), activation state (HLA-DR) and phenotypic markers (CD14, CD64, CD32, DC Sign, CX3CR1, CD206, CD163, and CD16) was utilized. Following event acquisition, manual gating was performed to obtain total brain myeloid cells after excluding dead cells and cells positive for the dump lineage markers (**Supplementary Figure 3**). Next, we used machine learning approaches to identify predominant myeloid cell phenotypes within brain cells. Based on the similitude of individual cell expression profiles, FitSNE projections of total brain myeloid cells segregated into distinct unbiased clusters of resting microglia, activated microglia, and macrophages based on CD45 and CD11b lineage discrimination (**Figure 2A**). As such, resting microglia (CD11b lo CD45 lo), activated microglia (CD11b int CD45 int), and macrophage (CD11b hi CD45 hi) subsets were noted. Our findings revealed that the resting microglia were the most predominant myeloid population in comparison to activated microglia and macrophages ($p < 0.0001$) (**Figure 2B**). Activated microglia expressed higher levels of HLA-DR than the resting microglia (**Figure 2C**). The resting microglia, as expected, demonstrated the lowest levels of all the phenotypic markers. Of note, the activated microglia of the morphine-exposed group expressed higher levels of CD14, CD16, CD163, and CD206 ($p < 0.01$ to $p < 0.0001$) compared to the saline-received group (**Figure 2D**). Similarly, macrophages of the morphine group expressed significantly higher levels

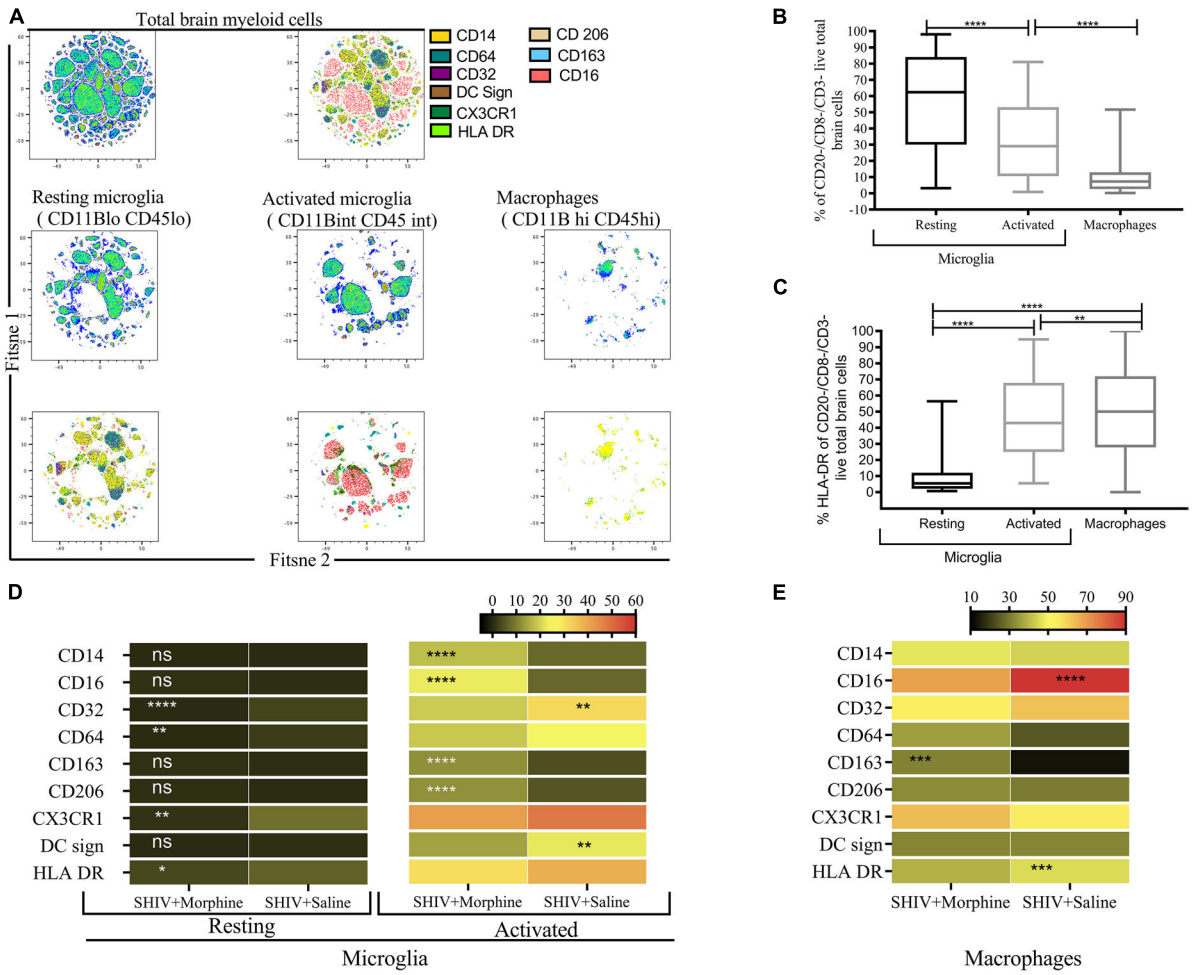

FIGURE 2
Flow Cytometric surface marker analysis reveals divergent brain myeloid phenotypes in SIV infected macaques exposed to either morphine or saline. **(A)** FitSNE projection of different macrophage/microglia phenotype markers expressed on total brain myeloid cells pooled from different brain regions in simian human immunodeficiency virus (SHIV) infected macaques (n = 8) exposed to either morphine or saline. **(B)** Percent frequencies of resting microglia, activated microglia and macrophages within total myeloid cells pooled from different brain regions as denoted by CD45 and CD11B discrimination. Data represent median ± range. **(C)** Evaluation of the extent of HLA-DR expression within resting microglia, activated microglia and macrophages pooled from diverse brain regions. Representative data denote median ± range. **(D)** Comparisons of % frequencies of CD14, CD16, CD32, CD64, CD163, CD206, CX3CR1, DC Sign, and HLA-DR in resting/activated microglia **(E)** macrophages in SHIV infected macaques treated with either morphine or saline. [*$p < 0.05$, **$p < 0.01$, ***$p < 0.001$, ****$p < 0.0001$ using the Wilcoxon test for paired non-parametric differences within groups **(B,C)**]. Mann–Whitney U-tests used for panels **(D,E)**.

of CD163 ($p < 0.001$). Unexpectedly, elevated levels of CD16 and HLA-DR were seen in the saline controls ($p < 0.0001$ and $p < 0.001$) (Figure 2E).

Trends of elevated M1/M2 activated microglia span different brain regions of morphine-exposed rhesus macaques

Recent advances in cell sequencing, mass cytometry, and high parameter flow cytometry have furthered the understanding of the phenotypical heterogeneity of brain myeloid cells within the diverse regions of the brain (Mrdjen et al., 2018; Tan et al., 2020). To gain insights into the landscape of the differences in activated microglial cell activation across the different brain regions, we focused on profiling the expression of CD14, CD163, CD16, and CD206 markers. We observed a significant upregulation of CD14 on the surface of activated microglia, pooled from different brain regions of animals exposed to morphine ($p < 0.0001$) (Figure 2D). During evaluation of regional distribution, we noticed a trend of elevated surface CD14 expression on activated microglia was noticed within all studied regions (frontal lobe, cerebellum, medulla oblongata, SVZ, HIP and putamen) (Figure 3A). Similarly, these niches also contained increased

levels of CD16 activated microglia and CD206 activated microglia in the morphine vs. saline exposed SHIV-infected rhesus macaques (Figures 3B,C) respectively. Remarkably, CD163 activated microglia levels were only visibly elevated in the cerebellum of morphine vs. saline exposed rhesus macaques (Figure 3D).

Frequencies of CD16+ activated microglia correlate with gut/brain simian human immunodeficiency virus DNA levels

Within the diverse regions of brain examined, SHIV DNA levels were highly variable across different sites evaluated. However, in some regions no viral DNA was detected (Figure 4A). Upon normalizing and adjusting for sites where no DNA was detected, morphine exposure was associated with increased levels of SHIV DNA (Figure 4B). A region-based perspective of the modulation of SHIV DNA by morphine revealed no changes in the levels of viral DNA within the brain stem (medulla). Importantly, the bulk of morphine-induced enhancement in the levels of viral DNA appeared in sites of neurogenesis (HIP and the SVZ), (p = 0.0043) (Figure 4C). Myeloid cells have been reported to be the principal HIV/SIV DNA reservoirs in the brain (Wallet et al., 2019). Therefore, we next compared the profiles of activated microglia and macrophages at the sites where the SHIV DNA was detected vs. undetected. The levels of CD32 on activated microglia were elevated in the brain regions where SHIV DNA was detected (Figure 4D). No differences in HLA-DR expression were noted (Figure 4E). Similarly, the levels of

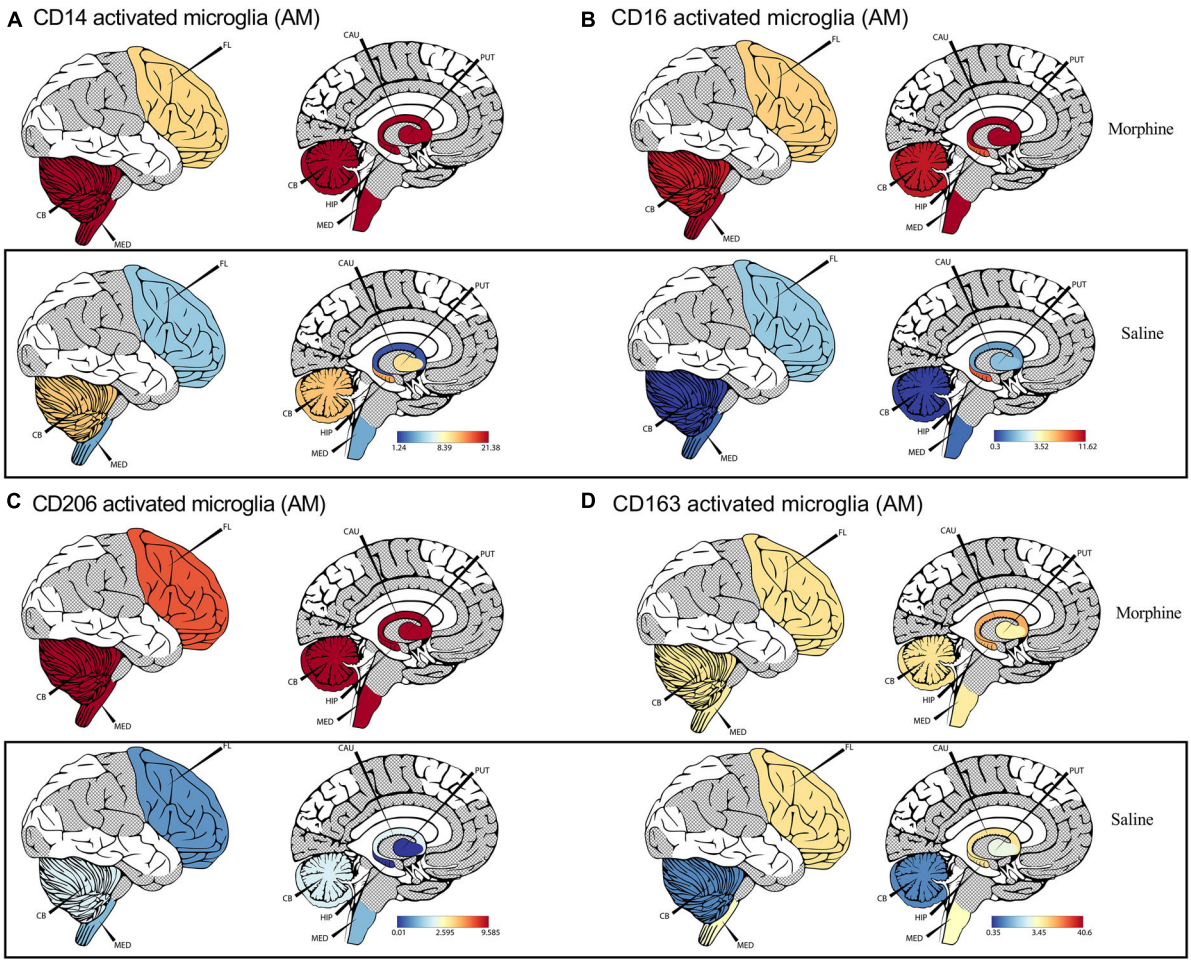

FIGURE 3
Morphine induces differential CD14, and CD163 profiles within diverse brain regions in simian human immunodeficiency virus (SHIV) infected rhesus macaques exposed to saline (n = 4) or morphine (n = 4). **(A)** CerebroViz visualization highlighting the anatomic distribution of **(A)** surface CD14, **(B)** surface CD16, **(C)** surface CD206, **(D)** surface CD163 on activated microglia contained within the frontal lobe (FL), cerebellum (CB), medulla (MED), Putamen (Put), Hippocampus (Hip), Caudate nucleus (CAU) in replacement of the subventricular zone (SVZ) activated microglia for visualization purposes.

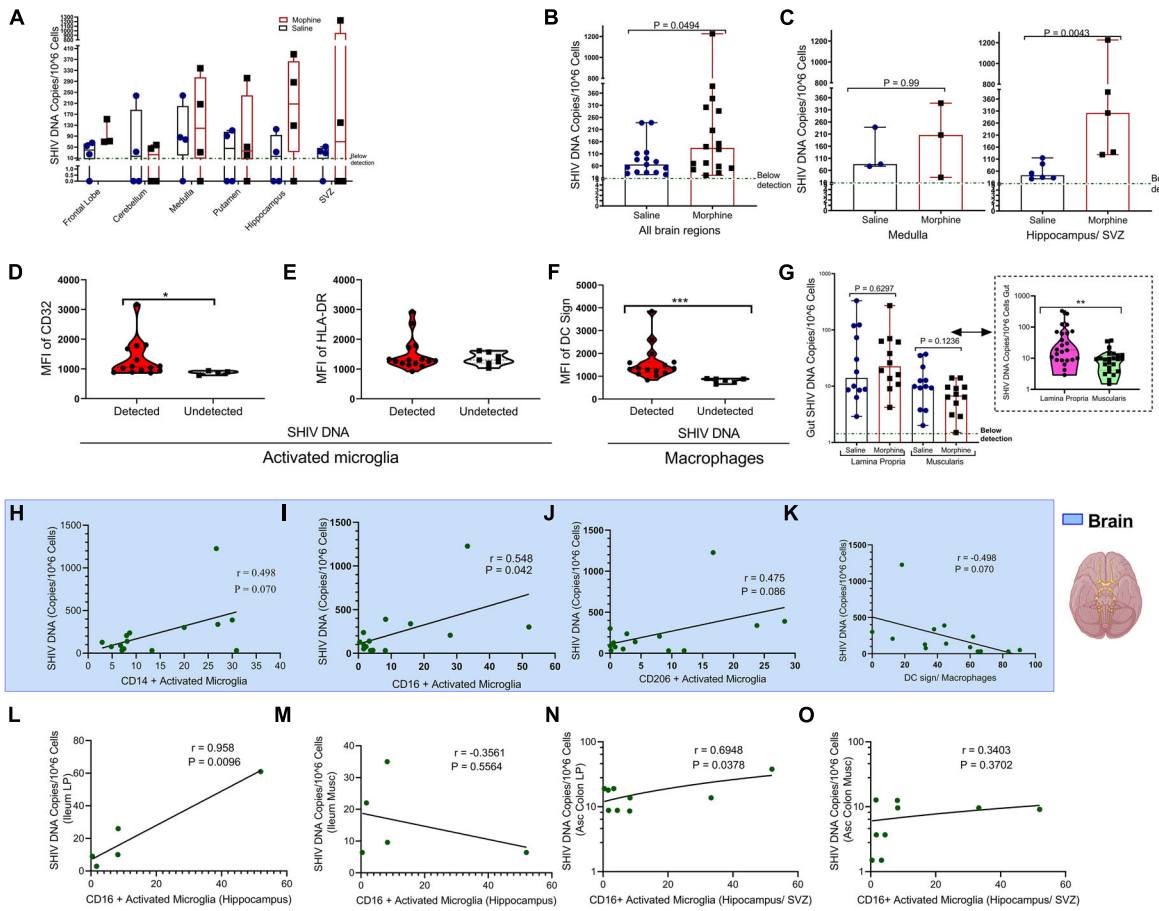

FIGURE 4

Relationship between CD16+ Activated Microglia and either gut or brain simian human immunodeficiency virus (SHIV) DNA. **(A)** Levels of SHIV DNA within the frontal lobe, cerebellum, medulla, putamen, hippocampus, and subventricular zone (SVZ) in morphine vs. saline exposed rhesus macaques. **(B)** Comparison of levels of SHIV DNA pooled within all the brain regions after adjusting for regions in which the virus was not detected. **(C)** Levels of SHIV DNA within the brain stem (medulla) and sites of neurogenesis (hippocampus/SVZ) in morphine vs. saline-treated rhesus macaques. **(D)** Mean Fluorescence Intensity (MFI) of CD32 **(E)** HLA-DR in activated microglia and **(F)** DC Sign in macrophages found within niches of detected and undetected SHIV DNA across the total brain. **(G)** Levels of SHIV DNA within the lamina propria and muscularis mucosa with further stratification of saline and morphine groups. All data represent median ± range in Panels **(A–G)**. **(H)** Association of brain SHIV DNA with CD14+ activated microglia **(I)** CD16+ activated microglia **(J)** CD206 activated microglia, and **(K)** DC Sign macrophages pooled form all brain regions in which SHIV DNA was detected. **(L)** Association between hippocampus CD16+ activated microglia and either SHIV DNA in ileum lamina propria (LP) or **(M)** ileum muscularis (Musc). **(N)** Relationship between CD16+ activated microglia found in neurogenic sites (hippocampus/SVZ) in ascending colon (Asc Colon) LP and **(O)** Asc Colon Musc. (*$p < 0.05$, **$p < 0.01$, ***$p < 0.001$). Mann–Whitney *U*-tests were used for significance in panels **(B–F)**. For panel **(G)**, multiple comparisons were evaluated using one-way ANOVA with Holm-Sidak *post hoc* testing.

DC sign on macrophages were also enhanced in SHIV DNA positive vs. negative brain regions (Figure 4F). In the gut, higher levels of the SHIV DNA were found in the LP vs. the muscularis ($p = 0.01$) (Figure 4G). Remarkably, in the brain, multiple markers of microglial polarity were associated with SHIV DNA. Spearman rank correlation analysis showed that increases in CD16+ activated microglia were accompanied by a significant elevation of brain SHIV DNA ($r = 0.548$, $p = 0.042$) (Figure 4I). Other markers of myeloid polarity expressed on activated microglia, such as CD14 ($r = 0.498$, $p = 0.070$), CD206 ($r = 0.475$, $p = 0.080$), and DC Sign+ brain macrophages ($r = 0.498$, $p = 0.070$) had borderline associations with the brain SHIV DNA (Figures 4H,J,K). Lastly, the viral DNA levels within the ileum LP ($r = 0.958$, $p = 0.0096$) (Figure 4L), not ileum muscularis ($r = -0.3561$, $p = 0.5564$), (Figure 4M) were positively correlated with the CD16+ activated microglia present in the HIP ($r = 0.958$, $p = 0.0096$), (Figure 4L) as opposed to ileum muscularis SHIV DNA ($r = -0.3561$, $p = 0.5564$), (Figure 4M). Finally, % CD16 activated microglia found in the neurogenic niches (HIP and SVZ), were associated with increasing SHIV DNA within the LP ($r = 0.6948$, $p = 0.0378$), (Figure 4N) unlike in

the muscularis (r = 0.3403, p = 0.3702), (Figure 4O) of the ascending colon.

Immunofluorescence corroborates findings indicating that morphine exposure leads to elevated expression of diverse myeloid markers that co-stain with SIV p27

To corroborate our earlier findings using another method (immunofluorescence) to complement our flow cytometry findings, we observed that within the HIP tissue, morphine exposure led to increased expression of CD163 (p = 0.039). In addition, the augmented expression of CD163 was also associated with elevated co-staining with SIVp27 (Supplementary Figures 4A,E). Similarly, morphine exposure also led to increased expression of CD206 (p = 0.0015) (Supplementary Figures 4B,E). Rhesus macaques exposed to morphine also had a marginally statistically significant increased expression of the myeloid activation marker Iba-1 (p = 0.066) that was also shown to increasingly colocalize with SIVp27 (Supplementary Figures 4C,E). Lastly, the expression of CD16 was not statistically different in morphine vs. saline exposed SHIV infected rhesus macaques despite the intensified staining observed in morphine treated animals (Supplementary Figure 4D).

Exposure to morphine was associated with community level depletions of the microbiome in simian human immunodeficiency virus infected rhesus macaques

Key genera of the gut microbiome, collectively termed as the psychobiome (Bates, 2021), are postulated to produce secondary metabolites that foster optimal brain activity and modulate intestinal myeloid lineage activation (Carabotti et al., 2015; Ji et al., 2016). Upon analyzing for average species diversity within the gut habitat (alpha diversity), we found that there were no differences in the number of OTUs/species (Chao-1 index), (p = 0.88) (Figure 5A) and uniformity of species (Shannon index), (p = 0.1143) within morphine-exposed and saline-received rhesus macaques (Figure 5B). Upon evaluating for changes within microbial populations, beta diversity using the principle component analysis of unweighted UniFrac distance matrix revealed that the OTUs of morphine exposed rhesus macaques clustered distinctly from the saline recipient animals (p = 0.0002 based on multiple linear regression) (Figure 5C). Using LEfSE, we observed a unidirectional change that saline exposed animals contained elevated OTUs of families *Brachyspiraceae* and *Desulfovibrionaceae*, genera *Ruminococcus torques* group, *Ruminococcaceae* UCG_008, *Anaerovibrio* and *Lachnospira* [LDA score (log 10) > 2] in comparison to morphine exposed rhesus macaques (Figure 5D).

Morphine selectively depletes key genera and species of the fecal microbiome

Morphine did not induce changes in key HIV-associated genera, such as *Prevotella-9*, (p = 0.200) (Figure 6A), most homologous to *Prevotella copri*, the pathobiont in human microbiomes associated with inflammatory diseases, and *Lactobacillus* (p = 0.114) (Figure 6B), majorly considered anti-inflammatory (Dillon et al., 2016). Further, morphine administration resulted in a reduction of *Brachyspira* (Figure 6C) and *Lachnospira* (Figure 6D), although these differences were not significant (both p = 0.0666). The relative abundance of *Anaerovibrio* (p = 0.028) (Figure 6E) and *Ruminococcaceae* UCG_008 (p = 0.05) (Figure 6F) were significantly lower in the morphine-treated vs. saline recipients. Furthermore, *Rhodospirillales* unclassified species were also significantly reduced in the morphine-treated vs. saline administered rhesus macaques (p = 0.028) (Figure 6G). Lastly *Anaerovibrio* unclassified species (p = 0.028) (Figure 6H) and *Roseburia* species (p = 0.008) (Figure 6I) were significantly depleted. There were no significant depletions in *Faecalibacterium* species (Figure 6J) and *Streptococcus equinus* species (Figure 6K) in the morphine-exposed vs. the saline group (both p = 0.068).

Morphine disrupts the levels of key cytokines and chemokine receptor levels in the cerebrospinal fluid and plasma of rhesus macaques

We additionally tested how exposure to morphine affected soluble factors associated with chemotaxis and inflammation underlying SHIV infection (Figure 7A). No significant differences were observed with several proinflammatory cytokines, such as CRP, TNF-α, IL-6, IL12 p-40, IFN-α, and IFN-γ. Remarkedly, the levels of MIP-1β (p = 0.0469) and IL-1Ra (p = 0.0014) in the CSF were elevated in saline- vs. morphine-treated rhesus macaques. Conversely, the MIG levels were elevated in the CSF of SHIV-infected rhesus macaques that received morphine. In the plasma of SHIV-infected rhesus macaques, the Eotaxin (p = 0.0387) levels were similarly elevated in the morphine- vs. saline-treated animals (Figure 7B). Having observed a reduction in the levels of

MIP-1β and IL-1Ra in morphine-exposed animals, we asked if an association existed between these analytes and found a strong positive correlation (r = 0.8571 and p = 0.0238). We extended the analysis of associations between key cell types localized within brain regions where high levels of SHIV persistence were observed. CD16+ activated microglia (SVZ/HIP) were strongly associated with IL-Ra in the CSF (r = −0.9286 and p = 0.0067) (Figure 7C) and Eotaxin in the plasma (r = 0.8571 and p = 0.0238) (Figure 7D). CD14+ macrophages (SVZ/HIP) were strongly associated also with MIP-1β (r = 0.8214 and p = 0.0341) (Figure 7E), and IL-1Ra (r = 0.7143 and p = 0.0881) in the CSF (Figure 7F). *Prevotella* relative abundance in the fecal microbiome was also positively correlated with MIP-1β (r = 0.8571 and p = 0.0238) (Figure 7G). Evaluation of associations between the key genera of the fecal microbiome and the CD14+ macrophages (SVZ/HIP) highlighted the presence of strong correlations between this cell subset and *Lactobacillus* relative abundance (r = −0.9286 and p = 0.0067) (Figure 7H), *Prevotella* relative abundance (r = 0.9286 and p = 0.0067) (Figure 7I), and *Anaerovibrio* (r = 0.8929 and p = 0.0123) (Figure 7J), respectively.

Discussion

Our results present novel findings on how morphine affects brain myeloid lineage polarization and SHIV persistence in different brain regions. First, we reveal that morphine increases microglia activation traversing M1/M2 polarity within diverse brain regions, while enhancing SHIV persistence particularly in

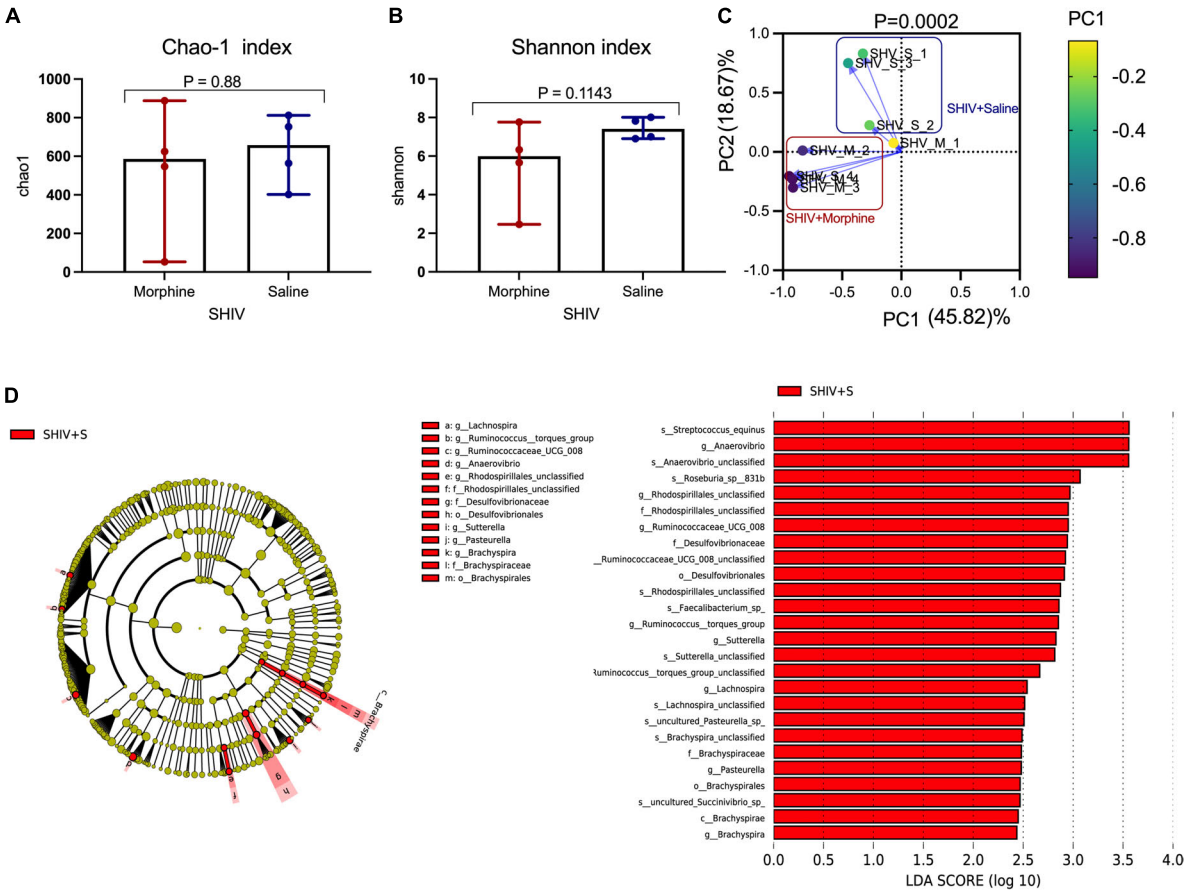

FIGURE 5
Exposure to morphine disorientates gut microbiome homeostasis in simian human immunodeficiency virus (SHIV) infected rhesus macaques. Differences in **(A)** Chao-1 index **(B)** Shannon index as measures pf Alpha diversity in rhesus macaques exposed to either morphine or saline. Mann–Whitney *U*-tests were used to evaluate differences within the two groups in panels **(A,B)**. Data represent median ± range in panels **(A,B)**. **(C)** Weighted UniFrac Principal component analysis showing distinct clustering of SHIV + morphine animals vs. SHIV + saline animals. Variance was reported following the use of PCA in panel **(C)**. **(D)** Cladogram indicating significantly different taxa calculated using linear discriminant analysis effect size (LEfSe) analysis for microbiome discrimination at the community level (class, family, genus, and species) of SHIV + saline (red) vs. SHIV + morphine (blue) rhesus macaques. Side by side, corresponding tabulated linear discriminant analysis (LDA) are also presented with the logarithmic threshold score being set at 2.0. Using the Kruskal–Wallis and pairwise Wilcoxon tests, $p < 0.05$ set as cut-off for differences within the studied groups.

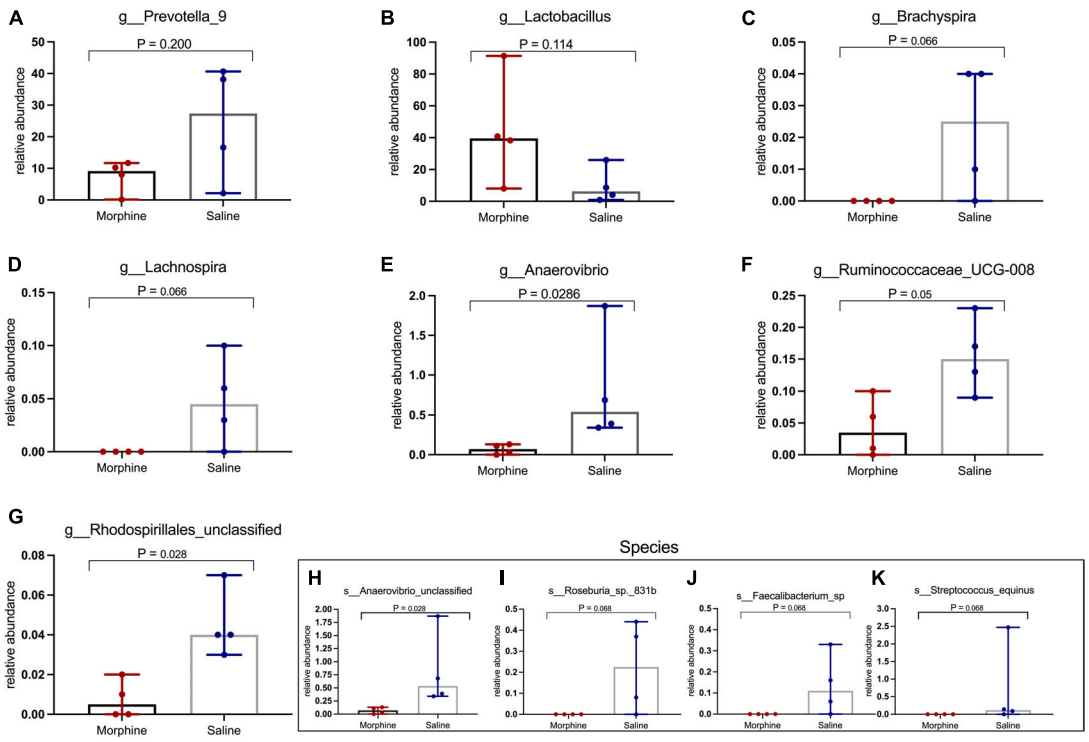

FIGURE 6
In simian human immunodeficiency virus (SHIV) infected rhesus macaques, exposure to morphine leads to reduced distinct genera and species of the fecal microbiota. Genus and Species differences within the fecal microbiomes as detailed by **(A)** *Prevotella-9* genus, **(B)** *Lactobacillus* genus, **(C)** *Brachyspira* genus, **(D)** *Lachnospira* genus, **(E)** *Anaerovibrio* genus, **(F)** *Ruminococcaceae* UCG-008, **(G)** *Rhodospirillales* unclassified, **(H)** *Anaerovibrio* species, **(I)** *Roseburia_sp_831b*, **(J)** *Faecalibacterium* species, **(K)** *Streptococcus equinus* species of SHIV + morphine animals vs. SHIV + saline rhesus macaques. [$p < 0.05$ deemed significant while borderline significance ($p = 0.05$ to $p = 0.07$), all obtained using the Mann–Whitney *U*-test for non-parametric differences within the two classified groups].

sites of neurogenesis. In tandem, morphine also depletes crucial genera of the gut microbiome, which could affect optimal brain function. Finally, we provide extra cues as to how morphine further disorganizes gut-brain crosstalk during SHIV infection.

Similar to several previous reports, we found that resting microglia were the predominant myeloid phenotype in the brain and exhibited a quiescent state. This was characterized by the low expression of cell surface markers, including the lineage markers CD45, CD11B, and the myeloid pan activation marker HLA-DR. Notably, activated microglia/macrophages exhibited elevated levels of these surface molecules (Nimmerjahn et al., 2005; Conrad and Dittel, 2011; Ponomarev et al., 2011; Jurga et al., 2020). Worse still, the increased surface expression of mu-opioid receptors on activated microglia makes this cell type more susceptible to alterations following morphine exposure (Maduna et al., 2019). Hence, we noticed increased plasticity of activated microglia, as shown by elevated surface pro-inflammatory M1 markers (CD14, CD16) and anti-inflammatory M2 markers (CD163 and CD206) in SHIV infected rhesus macaques exposed to morphine. Similarly, morphine was shown to increase myeloid cell activation traversing M1/M2 phenotypes in tissues of cancer patients (Tu et al., 2020).

Interestingly, CD14+ expression on microglia exacerbates the brain's inflammatory milieu, as demonstrated by increased plaques in AD (Liu et al., 2005; Jurga et al., 2020). As predicted, the elevation of CD16 (FcγRIIIA) that promotes pro-inflammatory signaling was accompanied by a concomitant reduction of CD32 (FcγRII) that facilitates anti-inflammatory signaling.

Accumulation of CD163 and CD206 alternative microglia could serve as a means to resolve the burgeoning morphine-mediated inflammatory damage involving phagocytosis of debris, and clearance of haptoglobin complexes (Biswas and Mantovani, 2010; Etzerodt and Moestrup, 2013; Park et al., 2016; Ohgidani et al., 2017). Within dissected brain regions, the observed heterogeneity of morphine-mediated myeloid activation mirrors previous publications that report regional differences in myeloid cell morphology and spatial diversity (Bachiller et al., 2018; Tan et al., 2020). Increased CD14+ and CD163+ expression within the frontal lobe and the cerebellum of morphine-dependent animals could hint at more intense inflammation-induced atrophy within these regions (Hoyer et al., 2017; Israel et al., 2019). Collectively, this further underscore morphine's myeloid skewing toward increased neuro-inflammation as further confirmed by our

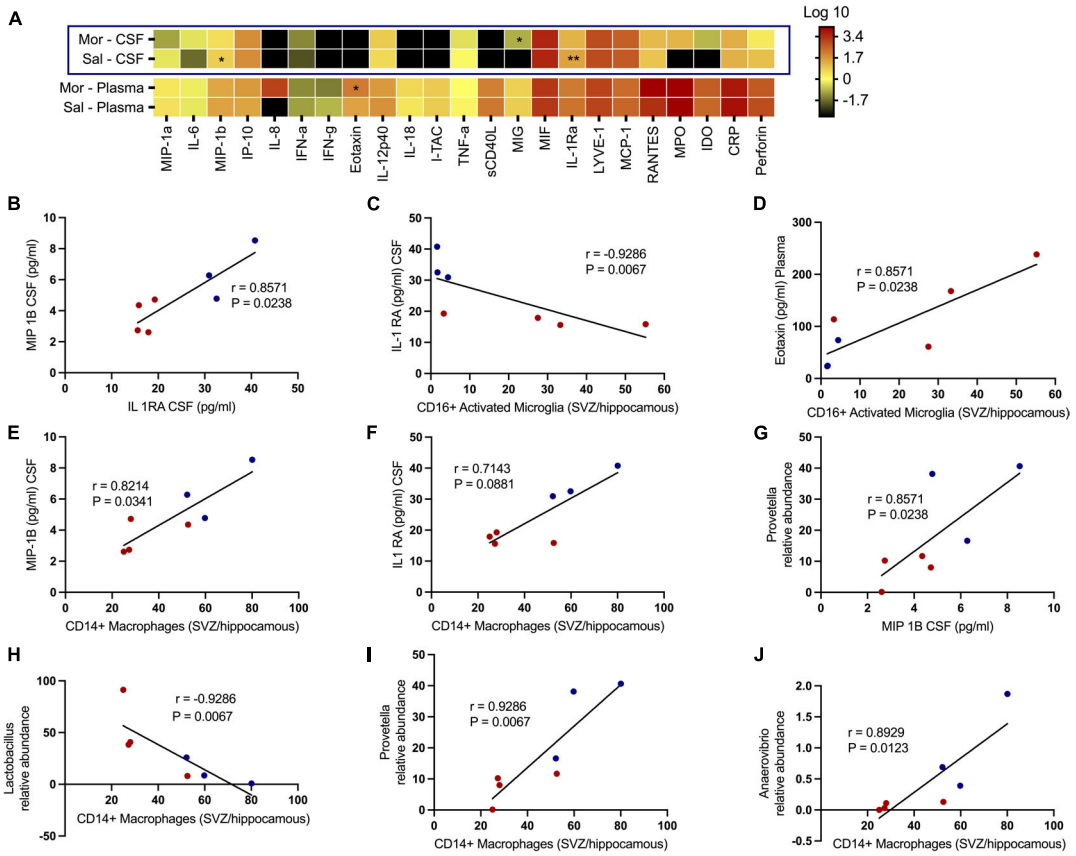

FIGURE 7
Morphine dysregulates chemokine and inflammatory cytokine receptors in plasma/the CNS that intercorrelate with CD16+ activated microglia/CD14+ macrophages in sites of neurogenesis and specific genera of the fecal microbiome further offering credence to morphine's possible effects on interactions of the gut-brain axis. **(A)** Changes within the CSF and plasma soluble factor profiles of simian human immunodeficiency virus (SHIV) infected rhesus macaques exposed to either morphine or saline. Multiple correlations between diverse parameters of the fecal microbiome, brain immune cells and CSF/plasma soluble factor indices as shown by relationships between **(B)** MIP-1B CSF (pg/ml) and IL-1 RA CSF (pg/ml). **(C)** IL-1 RA CSF (pg/ml) and CD16+ activated microglia [subventricular zone (SVZ)/hippocampus]. **(D)** Eotaxin plasma (pg/ml) and CD16+ activated microglia [(SVZ)/hippocampus]. **(E)** MIP-1B CSF (pg/ml) and CD14+ macrophages [(SVZ)/hippocampus]. **(F)** IL-1 RA CSF (pg/ml) and CD14+ macrophages [(SVZ)/hippocampus]. **(G)** *Prevotella* relative abundance and MIP-1B CSF (pg/ml). **(H)** *Lactobacillus* relative abundance and CD14+ macrophages [(SVZ)/hippocampus]. **(I)** *Prevotella* relative abundance and CD14+ macrophages [(SVZ)/hippocampus]. **(J)** *Anaerovibrio* relative abundance and CD14+ macrophages [(SVZ)/hippocampus]. $p < 0.05$ is considered statistically significant. (Red dot points signify morphine treated SIV infected rhesus macaques whilst blue dot points are saline treated SIV infected rhesus macaques). (*$p < 0.05$, **$p < 0.01$, using the Spearman's rank correlation test).

imaging studies that showed elevated myeloid activation based on Iba-1and distorted M1/M2 phenotypes based on CD16, CD163, and CD206 (Sudduth et al., 2013; Hovens et al., 2014; Walker and Lue, 2015).

The decreased levels of the chemokine MIP-1β observed within the CSF of morphine-dependent rhesus macaques is consistent with previous findings (Mahajan et al., 2002). These studies reported that morphine lowers expression of MIP-1β while chemokine receptor CCR5 expression in microglia, hence facilitating viral entry (Mahajan et al., 2002). Likewise, lower levels of CSF IL-1Ra could have implications of less readily available receptor levels, which in turn, could block the binding of the highly inflammatory cytokine IL-1. Subsequently, this may result in the facilitation of morphine-mediated neuroinflammation, further fueling the establishment of neuro-SHIV propagation and persistence (Murray et al., 2015).

The finding that morphine exposure enhances the levels of SHIV DNA at the sites of neurogenesis (HIP and SVZ) and the brain stem (medulla) alludes to the seeding of the viral reservoir in selective brain regions. Along these lines, Perez et al. (2018) and Putatunda et al. (2019) found that viral DNA primarily localizes to similar brain regions (Perez et al., 2018; Putatunda et al., 2019). Myeloid cells have been proposed as the principal viral reservoirs in tissues (Rodrigues et al., 2017; Ko et al., 2019). Remarkably, in sites where we detected viral DNA, increased expression of DC sign+ on brain macrophages could hint at increased viral permissivity (Lee et al., 2001). The significant association between CD16+

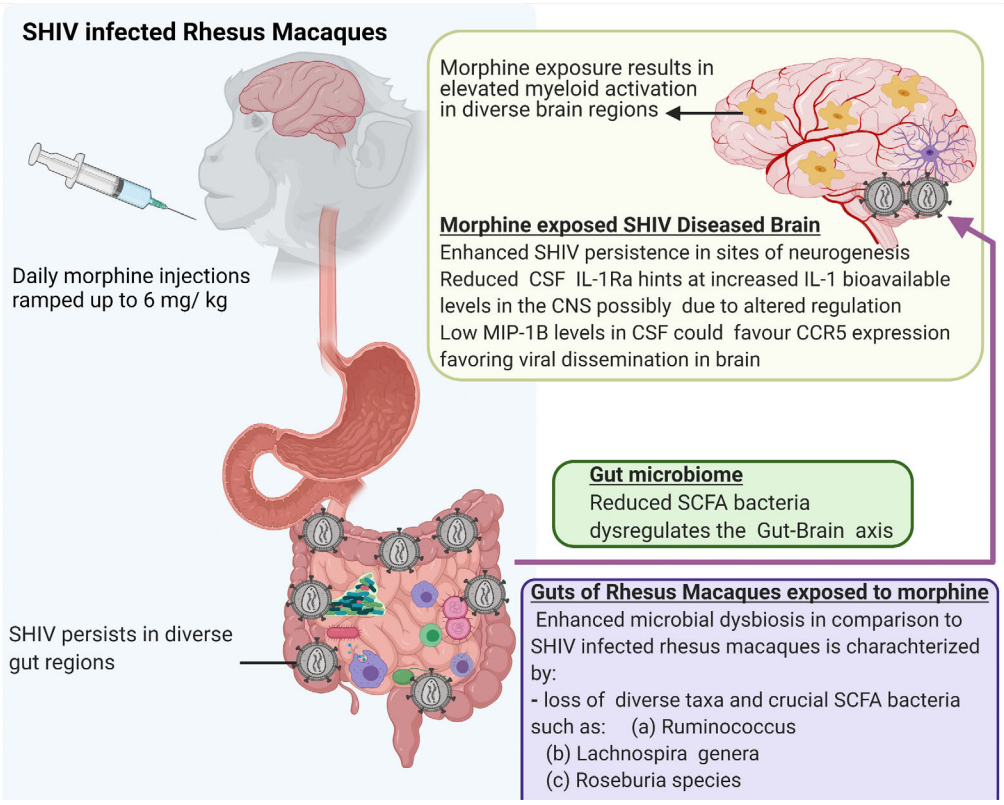

FIGURE 8
Summary of multiple effects of morphine on the gut-brain axis of simian human immunodeficiency virus (SHIV) infected rhesus macaques.

activated microglia and brain SHIV DNA further highlights an association between immune activation and viral persistence in the brain. Our imaging findings are also consistent with the previous reports which showed that CD163, CD206 and CD16 microglia/macrophages harbored HIV DNA (Fischer-Smith et al., 2008; Nowlin et al., 2015; Ko et al., 2019). As such, this further builds on evidence that brain myeloid cells serve as viral reservoirs (Abreu et al., 2019; Mitchell et al., 2019).

The observation that morphine increases viral persistence in sites of neurogenesis points to healthy neurons being crucial for maintaining latency in microglia. Recent reports suggest that optimal communication between healthy neurons and microglia through the mediation of receptors such as CD200 and CX3CL1 are required to maintain pro-viral DNA transcriptionally silent (Alvarez-Carbonell et al., 2020). Further, morphine also alters the homeostasis of the CNS through elevated inflammation and chronic myeloid activation. In combination, this could enhance the generation of damaged neurons which could concomitantly lead to increased amounts quantities of SHIV DNA in sites of neurogenesis.

The observation that increased levels of CD16+ activated microglia at the neurogenic niches were associated with the presence of viral DNA in the ileum LP and the ascending colon LP hints at possible gut-brain crosstalk. Based on the existence of a gut-brain axis, metabolites such as SCFAs secreted by the gut microbiome may influence CNS inflammation and shape microglial maturation (Erny et al., 2015; Meneses et al., 2016; Mertsalmi et al., 2017; Abdel-Haq et al., 2019). It is possible that SIV-associated gut dysbiosis compounded by the effects of morphine could crucially contribute toward CNS dysregulation, particularly at the sites of neurogenesis. The influence of the fecal microbiome on brain functions, such as neurogenesis, was ascertained after fecal transplants obtained from old mice promoted hippocampal neurogenesis in germ-free mice (Kundu et al., 2019). Our findings morphine perturbs the diversity of the gut microbiota at the community level agrees with previous reports that show that morphine distorts the gut bacterial microbiome (Zhang et al., 2019; Johnson et al., 2021). Further, our findings agree with the previous reports that show that morphine exposure causes the depletion of SCFA-producing bacteria (Sindberg et al., 2019; Gicquelais et al., 2020; Johnson et al., 2021).

We noted that specific butyrate secreting bacterial species, such as *Roseburia_sp_831b* species together with *Ruminococcus* and *Lachnospira* majorly represented the depleted SCFA producing bacteria. The secreted metabolites

released by these genera are crucial for the reduction of the gut inflammation (Parada Venegas et al., 2019), production of antimicrobial peptides (AMPs) (Hillman et al., 2020), and the maintenance of the gut barrier function (Peng et al., 2009; Kelly et al., 2015). Unlike our previous study, where we observed that *Prevotella-9* replaced the butyrate-producing bacteria in morphine-exposed, ART-treated, and SIV infected rhesus macaques, we did not notice any fluctuations in *Prevotellaceae* and an associated α-diversity (Johnson et al., 2021). In this study we observed a strong positive association between pro-inflammatory *Prevotella-9* and the CSF MIP-1β/CD14+ macrophages (SVZ/HIP) as opposed to a strong negative correlation between anti-inflammatory *Lactobacillus* and CD14+ macrophages (SVZ/HIP), alluding to elevated gut inflammation and dysbiosis affecting CNS inflammation. These findings similarly highlight processes involved in the loss of gut barrier function, leading to concomitant microbial translocation and the systemic immune activation/inflammation previously reported during morphine enhanced HIV pathogenesis (Meng et al., 2013; Banerjee et al., 2016). Strong associations between proinflammatory gut microbiota and CD14+ macrophages in the SVZ suggests that the expansion of this population is reliant on a highly proinflammatory gut milieu. Collectively, these interrelationships offer additional credence to morphine's ability to perturb the previously reported multiple systems cross-talk that occurs between the gut microbiota, enteric-nervous and brain systems (Lee et al., 2018; Cryan et al., 2019; Zhang et al., 2019).

In summary, we posit that morphine-associated CNS dysregulation is sustained by the loss of the feedback control of pro-inflammatory cytokines such as IL-1, the depletion of the psychobiome and the dysregulation of the gut-brain axis crosstalk that exacerbates the reactivation of the proviral reservoir. Consequentially, this results in a vicious cycle where the recently released viruses infect new and susceptible microglial cells, causing fluctuations in the size of the viral reservoir. Future studies on limiting neuro persistence in morphine abusers should aim at limiting morphine-enhanced defective neuron-microglia crosstalk by targeting receptors such as the CD200 receptor and CX3CL1. In addition, metabolomic screens should be carried out to understand how morphine affects key metabolites involved in optimal crosstalk between the gut microbiome and HIP (Liu et al., 2021). Lastly studies that look at the contribution of other sections of the microbiome such as the virome and fungi toward gut-brain axis crosstalk should also be considered (Townsend et al., 2021; Du Toit, 2022; Leonardi et al., 2022).

Lastly, we acknowledge that a small number of animals were utilized in the present study. In addition, our ability to evaluate the viral reservoirs, especially in the gut compartment is limited by the fact that the study animals were not exposed to cART. Despite these limitations, our study offers new leads suggesting that morphine increases the seeding of the neuro-SHIV reservoirs primarily at the sites of neurogenesis. This is simultaneously accompanied by the elevated brain myeloid cell activation with the M1/M2 polarization spanning across diverse brain regions and a skewed regulation of neuroinflammation. Furthermore, our findings provide novel insights into how morphine affects the gut-brain axis and offer a blueprint that could guide future mechanistic studies focused on dissecting key processes by which HIV affects multiple organ cross-talk during substance abuse (**Figure 8**).

Data availability statement

Microbiome data presented in this study are deposited in the NCBI BioProject database, accession number PRJNA870584. Source code for generating **Figure 3** can be found on: https://github.com/aomalla123/Cerbroviz-code/blob/main/README.md.

Ethics statement

The animal study was reviewed and approved by Institutional Animal Care and Use Committee University of Nebraska Medical Center.

Author contributions

OO, SJ, MB, and SNB designed the study. OO, MB, and SNB designed the flow cytometry panel. OO, SJ, and MB carried out sample acquisition and performed analysis of related data. KP, MT, SJ, and AA carried out estimation of the SIV viral reservoir within diverse gut and brain regions. OO, SJ, and SU were involved in tissue processing. VT performed the immunofluorescence analysis. SJ performed the DNA extraction from fecal material. SJ and OO were involved in microbiome data analysis. LG, MB, and SJ were involved in Luminex evaluations. SC performed macaque studies and morphine administration. UR, SJB, and SNB designed the parent study and solicited funds to support this work. All authors are read, edited, and approved the manuscript.

Funding

This study was supported by the NIH grant R01DA041751 awarded to UR, SNB, and SJB. Further SNB also supported partially by R21MH113455. The funders had no role in designing the study or in the interpretation of the results.

Acknowledgments

We thank the support of the staff and veterinarians of the University of Nebraska Medical Center (UNMC) Department of Comparative Medicine for housing and animal procedures. Lindsey Knight for initial help in animal experiments. We also thank Dave for initial help in virus preparation. We appreciate the efforts of the flow core at UNMC for helping several flow cytometry based experiments. SHIV AD8EO was kind gift from Malcolm A. Martin, NIH.

Conflict of interest

The authors declare that the research was conducted in the absence of any commercial or financial relationships that could be construed as a potential conflict of interest.

Publisher's note

All claims expressed in this article are solely those of the authors and do not necessarily represent those of their affiliated organizations, or those of the publisher, the editors and the reviewers. Any product that may be evaluated in this article, or claim that may be made by its manufacturer, is not guaranteed or endorsed by the publisher.

Supplementary material

The Supplementary Material for this article can be found online at: https://www.frontiersin.org/articles/10.3389/fnins.2022.1001544/full#supplementary-material

SUPPLEMENTARY FIGURE 1
Study design involving treatment of rhesus macaques and intricate detailing of experiments utilized for this study. During the entire course of the study, eight rhesus macaques were given either morphine (n = 4) at 6 mg/kg and saline (n = 4) twice daily and once on weekends. After 8 weeks, rhesus macaques were infected with SHIVADE08. Using fecal samples, the 16s rDNA fecal microbiome was studied using the illumine sequencing platform. Similarly, flow cytometry was utilized to interrogate changes in myeloid modifications found in the brain, gut, and liver. Levels of SHIV DNA were estimated using the digital droplet polymerase chain reaction (dd-PCR) assay across different regions of gut and brain tissues.

SUPPLEMENTARY FIGURE 2
Viral dynamics in peripheral blood and diverse tissues. Differences in Gag DNA levels found in **(A)** PBMC CD4+ T-cells **(B)** Lungs **(C)** Spleen in eight SHIV infected rhesus macaques exposed to either morphine or saline. Differences in Gag RNA levels found in **(E)** PBMC CD4+ T-cells **(F)** Lungs **(G)** Spleen in eight SHIV infected rhesus macaques exposed to either morphine or saline.

SUPPLEMENTARY FIGURE 3
Brain gating strategy used to interrogate brain myeloid (microglia and macrophages) found in diverse brain regions. Various brain regions were dissected and tissue digestion carried out using DNAse and Trypsin and obtained single-cell suspensions analyzed using the BD Fortesssax450. Detailed gating strategy involving an FSCA vs. Time to check the stability of the flow and obtain events only when an expected stream flows were obtained. Using Pulse Geometry scales comprised of FSC-H vs. FSC-A and SSC-H vs. SSC-A dot plots, we excluded doublets. Next, dump gates were used to eliminate unwanted populations. CD8α+ cells and Live Dead exclusion plus CD3+ T-cell removal guided the exclusion of CD3+ T-cells, NK cells, and dead cells. Next, the CD20 dot plots guided the removal of B-cells. Collectively, this ensured that the major populations studied in Brain cells were majorly myeloid cells. CD45 vs. CD11B plots were utilized to guide segregation of resting/activated microglia in addition to macrophages. Fluorescence minus one (FMO) controls were used to guide the proper placement of gates of diverse myeloid cell markers within the resting microglia, activated microglia and macrophages.

SUPPLEMENTARY FIGURE 4
Surface expression of diverse myeloid markers in the hippocampus of SHIV-infected saline or morphine-exposed rhesus macaques. Immunofluorescence images of the hippocampus was stained with different macrophage markers: **(A)** CD163 and **(B)** CD206 (green) together with SIV-p27 (red) and DAPI for nucleus was visualized by fluorescence microscope. **(C)** Single and combined staining for Iba 1 (blue), SIV-p27 (red) and merged co-expression of Iba 1and SIV-p27. **(D)** Single stained CD16, SIV p27 and CD16 (green) co-expressed with p27 in the brain of one representative rhesus macaque. The upper panel indicates SHIV + saline while panel **(E)** represents SHIV + morphine respectively. Quantitative analyses were done by two groups each n = 3 showing the number of cells per mm^2 of tissue that stained positively for the markers of interest ($p < 0.05$ signifies statistical significance as carried out using unpaired T-tests).

References

Abdel-Haq, R., Schlachetzki, J. C. M., Glass, C. K., and Mazmanian, S. K. (2019). Microbiome-microglia connections via the gut-brain axis. *J. Exp. Med.* 216, 41–59. doi: 10.1084/jem.20180794

Abreu, C. M., Veenhuis, R. T., Avalos, C. R., Graham, S., Parrilla, D. R., Ferreira, E. A., et al. (2019). Myeloid and CD4 T Cells Comprise the Latent Reservoir in Antiretroviral Therapy-Suppressed SIVmac251-Infected Macaques. *mBio* 10:e1659–e1619. doi: 10.1128/mBio.01659-19

Acharya, A., Olwenyi, O. A., Thurman, M., Pandey, K., Morsey, B. M., Lamberty, B., et al. (2020). Chronic morphine administration differentially modulates viral reservoirs in SIVmac251 infected rhesus macaque model. *J. Virol.* 95:e1657–e1620. doi: 10.1101/2020.09.09.290700

Alvarez-Carbonell, D., Garcia-Mesa, Y., Milne, S., Das, B., Dobrowolski, C., Rojas, R., et al. (2017). Toll-like receptor 3 activation selectively reverses HIV latency in microglial cells. *Retrovirology* 14:9. doi: 10.1186/s12977-017-0335-8

Alvarez-Carbonell, D., Ye, F., Ramanath, N., Dobrowolski, C., and Karn, J. (2019). The Glucocorticoid Receptor Is a Critical Regulator of HIV Latency in Human Microglial Cells. *J. Neuroimmune Pharmacol.* 14, 94–109. doi: 10.1007/s11481-018-9798-1

Alvarez-Carbonell, D., Ye, F., Ramanath, N., Garcia-Mesa, Y., Knapp, P. E., Hauser, K. F., et al. (2020). Cross-talk between microglia and neurons regulates HIV latency. *PLoS Pathogens* 15:e1008249. doi: 10.1371/journal.ppat.1008249

Bachiller, S., Jiménez-Ferrer, I., Paulus, A., Yang, Y., Swanberg, M., Deierborg, T., et al. (2018). Microglia in Neurological Diseases: A Road Map to Brain-Disease Dependent-Inflammatory Response. *Front. Cell. Neurosci.* 12:488. doi: 10.3389/fncel.2018.00488

Bahl, E., Koomar, T., and Michaelson, J. J. (2017). cerebroViz: an R package for anatomical visualization of spatiotemporal brain data. *Bioinformatics* 33, 762–763. doi: 10.1016/j.euroneuro.2016.09.392

Banerjee, S., Sindberg, G., Wang, F., Meng, J., Sharma, U., Zhang, L., et al. (2016). Opioid-induced gut microbial disruption and bile dysregulation leads to gut barrier compromise and sustained systemic inflammation. *Mucosal Immunol.* 9, 1418–1428. doi: 10.1038/mi.2016.9

Bates, M. (2021). Targeting the Gut to Treat the Brain. *IEEE Pulse* 12, 2–5. doi: 10.1109/MPULS.2021.3094250

Biswas, S. K., and Mantovani, A. (2010). Macrophage plasticity and interaction with lymphocyte subsets: cancer as a paradigm. *Nat. Immunol.* 11, 889–896. doi: 10.1038/ni.1937

Bokhari, S. M., Hegde, R., Callen, S., Yao, H., Adany, I., Li, Q., et al. (2011). Morphine potentiates neuropathogenesis of SIV infection in rhesus macaques. *J. Neuroimmune Pharmacol.* 6, 626–639. doi: 10.1007/s11481-011-9272-9

Bonini, J. A., Anderson, S. M., and Steiner, D. F. (1997). Molecular cloning and tissue expression of a novel orphan G protein-coupled receptor from rat lung. *Biochem. Biophys. Res. Commun.* 234, 190–193. doi: 10.1006/bbrc.1997.6591

Breit, S., Kupferberg, A., Rogler, G., and Hasler, G. (2018). Vagus Nerve as Modulator of the Brain–Gut Axis in Psychiatric and Inflammatory Disorders. *Front. Psychiatry* 9:44. doi: 10.3389/fpsyt.2018.00044

Callahan, B. J., McMurdie, P. J., Rosen, M. J., Han, A. W., Johnson, A. J., and Holmes, S. P. (2016). DADA2: High-resolution sample inference from Illumina amplicon data. *Nat. Methods* 13, 581–583. doi: 10.1038/nmeth.3869

Carabotti, M., Scirocco, A., Maselli, M. A., and Severi, C. (2015). The gut-brain axis: interactions between enteric microbiota, central and enteric nervous systems. *Ann. Gastroenterol.* 28, 203–209.

CDC/NCHS, (2018). *National Vital Statistics System, Mortality*. Atlanta, GA: US Department of Health and Human Services, CDC WONDER, CDC. Available online at: https://wonder.cdc.gov. (accessed September 19, 2022).

Chen, Y., Zhou, J., and Wang, L. (2021). Role and Mechanism of Gut Microbiota in Human Disease. *Front. Cell Infect. Microbiol.* 11:625913. doi: 10.3389/fcimb.2021.625913

Cole, J. R., Wang, Q., Fish, J. A., Chai, B., McGarrell, D. M., Sun, Y., et al. (2014). Ribosomal Database Project: data and tools for high throughput rRNA analysis. *Nucleic Acids Res.* 42:D633–D642. doi: 10.1093/nar/gkt1244

Conrad, A. T., and Dittel, B. N. (2011). Taming of macrophage and microglial cell activation by microRNA-124. *Cell Res.* 21, 213–216. doi: 10.1038/cr.2011.9

Cryan, J. F., O'Riordan, K. J., Cowan, C. S. M., Sandhu, K. V., Bastiaanssen, T. F. S., Boehme, M., et al. (2019). The Microbiota-Gut-Brain Axis. *Physiol. Rev.* 99, 1877–2013. doi: 10.1152/physrev.00018.2018

Dalile, B., Van Oudenhove, L., Vervliet, B., and Verbeke, K. (2019). The role of short-chain fatty acids in microbiota–gut–brain communication. *Nat. Rev. Gastroenterol. Hepatol.* 16, 461–478. doi: 10.1038/s41575-019-0157-3

Dave, R. S., Ali, H., Sil, S., Knight, L. A., Pandey, K., Madduri, L. S. V., et al. (2020). NF-κB Duplications in the Promoter-Variant HIV-1C LTR Impact Inflammation Without Altering Viral Replication in the Context of Simian Human Immunodeficiency Viruses and Opioid-Exposure. *Front. Immunol.* 11:95. doi: 10.3389/fimmu.2020.00095

Dave, R. S., Sharma, R. K., Muir, R. R., Haddad, E., Gumber, S., Villinger, F., et al. (2018). FDC:TFH Interactions within Cervical Lymph Nodes of SIV-Infected Rhesus Macaques. *J. Neuroimmune Pharmacol* 13, 204–218. doi: 10.1007/s11481-017-9775-0

Dillon, S. M., Frank, D. N., and Wilson, C. C. (2016). The gut microbiome and HIV-1 pathogenesis: a two-way street. *AIDS* 30, 2737–2751. doi: 10.1097/QAD.0000000000001289

Dinan, T. G., and Cryan, J. F. (2017). Gut instincts: microbiota as a key regulator of brain development, ageing and neurodegeneration. *J. Physiol.* 595, 489–503. doi: 10.1113/JP273106

Du Toit, A. (2022). Remember the phages. *Nat. Rev. Microbiol.* 20:254. doi: 10.1038/s41579-022-00718-9

Ellero, J., Lubomski, M., and Brew, B. (2017). Interventions for Neurocognitive Dysfunction. *Curr. HIV/AIDS Rep.* 14, 8–16. doi: 10.1007/s11904-017-0346-z

Erny, D., de Angelis, A. L. H., Jaitin, D., Wieghofer, P., Staszewski, O., David, E., et al. (2015). Host microbiota constantly control maturation and function of microglia in the CNS. *Nat. Neurosci.* 18, 965–977. doi: 10.1038/nn.4030

Etzerodt, A., and Moestrup, S. K. (2013). CD163 and inflammation: biological, diagnostic, and therapeutic aspects. *Antioxidants Redox Signal.* 18, 2352–2363. doi: 10.1089/ars.2012.4834

Farhadian, S., Patel, P., and Spudich, S. (2017). Neurological Complications of HIV Infection. *Curr. Infect. Dis. Rep.* 19:50. doi: 10.1007/s11908-017-0606-5

Fischer-Smith, T., Bell, C., Croul, S., Lewis, M., and Rappaport, J. (2008). Monocyte/macrophage trafficking in acquired immunodeficiency syndrome encephalitis: Lessons from human and nonhuman primate studies. *J. Neurovirol.* 14, 318–326. doi: 10.1080/13550280802132857

Florence, C., Luo, F., Xu, L., and Zhou, C. (2016). The economic burden of prescription opioid overdose, abuse and dependence in the United States, 2013. *Medical Care* 54:901. doi: 10.1097/MLR.0000000000000625

Friedman, B. A., Srinivasan, K., Ayalon, G., Meilandt, W. J., Lin, H., Huntley, M. A., et al. (2018). Diverse Brain Myeloid Expression Profiles Reveal Distinct Microglial Activation States and Aspects of Alzheimer's Disease Not Evident in Mouse Models. *Cell Rep.* 22, 832–847. doi: 10.1016/j.celrep.2017.12.066

Garcia-Mesa, Y., Jay, T. R., Checkley, M. A., Luttge, B., Dobrowolski, C., Valadkhan, S., et al. (2017). Immortalization of primary microglia: a new platform to study HIV regulation in the central nervous system. *J. Neurovirol.* 23, 47–66. doi: 10.1007/s13365-016-0499-3

Giavedoni, L. D. (2005). Simultaneous detection of multiple cytokines and chemokines from nonhuman primates using luminex technology. *J. Immunol. Methods* 301, 89–101. doi: 10.1016/j.jim.2005.03.015

Gicquelais, R. E., Bohnert, A. S. B., Thomas, L., and Foxman, B. (2020). Opioid agonist and antagonist use and the gut microbiota: associations among people in addiction treatment. *Sci. Rep.* 10:19471. doi: 10.1038/s41598-020-76570-9

Guo, C.-J., Li, Y., Tian, S., Wang, X., Douglas, S. D., and Ho, W.-Z. (2002). Morphine enhances HIV infection of human blood mononuclear phagocytes through modulation of beta-chemokines and CCR5 receptor. *J. Investig. Med.* 50, 435–442. doi: 10.1136/jim-50-06-03

Heaton, R. K., Franklin, D. R., Ellis, R. J., McCutchan, J. A., Letendre, S. L., Leblanc, S., et al. (2011). HIV-associated neurocognitive disorders before and during the era of combination antiretroviral therapy: differences in rates, nature, and predictors. *J. Neurovirol.* 17, 3–16. doi: 10.1007/s13365-010-0006-1

Herz, J., Filiano, A. J., Smith, A., Yogev, N., and Kipnis, J. (2017). Myeloid Cells in the Central Nervous System. *Immunity* 46, 943–956. doi: 10.1016/j.immuni.2017.06.007

Hillman, E. T., Kozik, A. J., Hooker, C. A., Burnett, J. L., Heo, Y., Kiesel, V. A., et al. (2020). Comparative genomics of the genus Roseburia reveals divergent biosynthetic pathways that may influence colonic competition among species. *Microbial. Genomics* 6:mgen000399. doi: 10.1099/mgen.0.000399

Hovens, I. B., Nyakas, C., and Schoemaker, R. G. (2014). A novel method for evaluating microglial activation using ionized calcium-binding adaptor protein-1 staining: cell body to cell size ratio. *Neuroimmunol. Neuroinflamm.* 1, 82–88. doi: 10.4103/2347-8659.139719

Hoyer, C., Alonso, A., Schlotter-Weigel, B., Platten, M., and Fatar, M. H. I. V. -(2017). Associated Cerebellar Dysfunction and Improvement with Aminopyridine Therapy: A Case Report. *Case Rep. Neurol.* 9, 121–126. doi: 10.1159/000475544

Hutlab, G. (). *LDA Effect Size (LEfSe)*. [Available from: http://huttenhower.sph.harvard.edu/galaxy/ (accessed September 19, 2022).

Ishino, Y., Yetman, M. J., Sossi, S. M., Steinecke, A., Hayano, Y., and Taniguchi, H. (2017). Regional Cellular Environment Shapes Phenotypic Variations of Hippocampal and Neocortical Chandelier Cells. *J. Neurosci.* 37, 9901–9916. doi: 10.1523/JNEUROSCI.0047-17.2017

Israel, S. M., Hassanzadeh-Behbahani, S., Turkeltaub, P. E., Moore, D. J., Ellis, R. J., and Jiang, X. (2019). Different roles of frontal versus striatal atrophy in HIV-associated neurocognitive disorders. *Hum. Brain Mapp.* 40, 3010–3026. doi: 10.1002/hbm.24577

Iwanami, S., Kakizoe, Y., Morita, S., Miura, T., Nakaoka, S., and Iwami, S. (2017). A highly pathogenic simian/human immunodeficiency virus effectively produces infectious virions compared with a less pathogenic virus in cell culture. *Theoretical. Biol. Medical Model.* 14:9. doi: 10.1186/s12976-017-0055-8

Jangi, S., Gandhi, R., Cox, L. M., Li, N., von Glehn, F., Yan, R., et al. (2016). Alterations of the human gut microbiome in multiple sclerosis. *Nat. Commun.* 7:12015. doi: 10.1038/ncomms12015

Ji, J., Shu, D., Zheng, M., Wang, J., Luo, C., Wang, Y., et al. (2016). Microbial metabolite butyrate facilitates M2 macrophage polarization and function. *Sci. Rep.* 6:24838. doi: 10.1038/srep24838

Johnson, S. D., Fox, H. S., Buch, S., and Byrareddy, S. N. (2021). Chronic Opioid Administration is Associated with Prevotella-dominated Dysbiosis in SIVmac251 Infected, cART-treated Macaques. *J. Neuroimmune Pharmacol.* [Eub ahead of print]. doi: 10.1007/s11481-021-09993-4

Jurga, A. M., Paleczna, M., and Kuter, K. Z. (2020). Overview of General and Discriminating Markers of Differential Microglia Phenotypes. *Front. Cell. Neurosci.* 14:198. doi: 10.3389/fncel.2020.00198

Kaul, M., and Lipton, S. A. (2005). Experimental and potential future therapeutic approaches for HIV-1 associated dementia targeting receptors for chemokines, glutamate and erythropoietin. *Neurotoxicity Res.* 8, 167–186. doi: 10.1007/BF03033828

Kelly, C. J., Zheng, L., Campbell, E. L., Saeedi, B., Scholz, C. C., Bayless, A. J., et al. (2015). Crosstalk between microbiota-derived short-chain fatty acids and intestinal epithelial HIF augments tissue barrier function. *Cell Host Microbe* 17, 662–671. doi: 10.1016/j.chom.2015.03.005

Kelly, J. R., Minuto, C., Cryan, J. F., Clarke, G., and Dinan, T. G. (2017). Cross talk: the microbiota and neurodevelopmental disorders. *Front. Neurosci.* 11:490. doi: 10.3389/fnins.2017.00490

Kim, S., Hahn, Y. K., Podhaizer, E. M., McLane, V. D., Zou, S., Hauser, K. F., et al. (2018). A central role for glial CCR5 in directing the neuropathological interactions of HIV-1 Tat and opiates. *J. Neuroinflamm.* 15:285. doi: 10.1186/s12974-018-1320-4

Kimura, I., Inoue, D., Maeda, T., Hara, T., Ichimura, A., Miyauchi, S., et al. (2011). Short-chain fatty acids and ketones directly regulate sympathetic nervous system via G protein-coupled receptor 41 (GPR41). *Proc. Natl. Acad. Sci.U.S.A.* 108, 8030–8035. doi: 10.1073/pnas.1016088108

Ko, A., Kang, G., Hattler, J. B., Galadima, H. I., Zhang, J., Li, Q., et al. (2019). Macrophages but not Astrocytes Harbor HIV DNA in the Brains of HIV-1-Infected Aviremic Individuals on Suppressive Antiretroviral Therapy. *J. Neuroimmune Pharmacol* 14, 110–119. doi: 10.1007/s11481-018-9809-2

Kumar, D. K. V., Choi, S. H., Washicosky, K. J., Eimer, W. A., Tucker, S., Ghofrani, J., et al. (2016). Amyloid-β peptide protects against microbial infection in mouse and worm models of Alzheimer's disease. *Sci. Trans. Med.* 8:340ra72. doi: 10.1126/scitranslmed.aaf1059

Kundu, P., Lee, H. U., Garcia-Perez, I., Tay, E. X. Y., Kim, H., Faylon, L. E., et al. (2019). Neurogenesis and prolongevity signaling in young germ-free mice transplanted with the gut microbiota of old mice. *Sci. Trans. Med.* 11:eaau4760. doi: 10.1126/scitranslmed.aau4760

Laurent, R. S., O'Brien, L. M., and Ahmad, S. T. (2013). Sodium butyrate improves locomotor impairment and early mortality in a rotenone-induced Drosophila model of Parkinson's disease. *Neuroscience* 246, 382–390. doi: 10.1016/j.neuroscience.2013.04.037

Lee, B., Leslie, G., Soilleux, E., O'Doherty, U., Baik, S., Levroney, E., et al. (2001). cis Expression of DC-SIGN allows for more efficient entry of human and simian immunodeficiency viruses via CD4 and a coreceptor. *J. Virol.* 75, 12028–12038. doi: 10.1128/JVI.75.24.12028-12038.2001

Lee, K., Vuong, H. E., Nusbaum, D. J., Hsiao, E. Y., Evans, C. J., and Taylor, A. M. W. (2018). The gut microbiota mediates reward and sensory responses associated with regimen-selective morphine dependence. *Neuropsychopharmacology* 43, 2606–2614. doi: 10.1038/s41386-018-0211-9

Leibrand, C. R., Paris, J. J., Jones, A. M., Masuda, Q. N., Halquist, M. S., Kim, W. K., et al. (2019). HIV-1 Tat and opioids act independently to limit antiretroviral brain concentrations and reduce blood-brain barrier integrity. *J. Neurovirol.* 25, 560–577. doi: 10.1007/s13365-019-00757-8

Leonardi, I., Gao, I. H., Lin, W.-Y., Allen, M., Li, X. V., Fiers, W. D., et al. (2022). Mucosal fungi promote gut barrier function and social behavior via Type 17 immunity. *Cell* 185, 831–46.e14. doi: 10.1016/j.cell.2022.01.017

Linderman, G. C., Rachh, M., Hoskins, J. G., Steinerberger, S., and Kluger, Y. (2017). Efficient algorithms for t-distributed stochastic neighborhood embedding. *arXiv* [Preprint].

Liu, L., Wang, H., Rao, X., Yu, Y., Li, W., Zheng, P., et al. (2021). Comprehensive analysis of the lysine acetylome and succinylome in the hippocampus of gut microbiota-dysbiosis mice. *J. Adv. Res.* 30, 27–38. doi: 10.1016/j.jare.2020.12.002

Liu, Y., Walter, S., Stagi, M., Cherny, D., Letiembre, M., Schulz-Schaeffer, W., et al. (2005). LPS receptor (CD14): a receptor for phagocytosis of Alzheimer's amyloid peptide. *Brain* 128, 1778–1789. doi: 10.1093/brain/awh531

Ma, Q., Xing, C., Long, W., Wang, H. Y., Liu, Q., and Wang, R.-F. (2019). Impact of microbiota on central nervous system and neurological diseases: the gut-brain axis. *J. Neuroinflamm.* 16:53. doi: 10.1186/s12974-019-1434-3

Maduna, T., Audouard, E., Dembélé, D., Mouzaoui, N., Reiss, D., Massotte, D., et al. (2019). Microglia Express Mu Opioid Receptor: Insights From Transcriptomics and Fluorescent Reporter Mice. *Front. Psychiatry* 9:726. doi: 10.3389/fpsyt.2018.00726

Mahajan, S. D., Aalinkeel, R., Sykes, D. E., Reynolds, J. L., Bindukumar, B., Fernandez, S. F., et al. (2008). Tight junction regulation by morphine and HIV-1 tat modulates blood-brain barrier permeability. *J. Clin. Immunol.* 28, 528–541. doi: 10.1007/s10875-008-9208-1

Mahajan, S. D., Schwartz, S. A., Shanahan, T. C., Chawda, R. P., and Nair, M. P. N. (2002). Morphine Regulates Gene Expression of α- and β-Chemokines and Their Receptors on Astroglial Cells Via the Opioid μ Receptor. *J. Immunol.* 169, 3589–3599. doi: 10.4049/jimmunol.169.7.3589

Meneses, G., Bautista, M., Florentino, A., Díaz, G., Acero, G., Besedovsky, H., et al. (2016). Electric stimulation of the vagus nerve reduced mouse neuroinflammation induced by lipopolysaccharide. *J. Inflamm.* 13:33. doi: 10.1186/s12950-016-0140-5

Meng, J., Banerjee, S., Li, D., Sindberg, G. M., Wang, F., Ma, J., et al. (2015a). Opioid Exacerbation of Gram-positive sepsis, induced by Gut Microbial Modulation, is Rescued by IL-17A Neutralization. *Sci. Rep.* 5:10918. doi: 10.1038/srep10918

Meng, J., Sindberg, G. M., and Roy, S. (2015b). Disruption of gut homeostasis by opioids accelerates HIV disease progression. *Front. Microbiol.* 6:643. doi: 10.3389/fmicb.2015.00643

Meng, J., Yu, H., Ma, J., Wang, J., Banerjee, S., Charboneau, R., et al. (2013). Morphine induces bacterial translocation in mice by compromising intestinal barrier function in a TLR-dependent manner. *PloS One* 8:e54040. doi: 10.1371/journal.pone.0054040

Mertsalmi, T., Aho, V., Pereira, P., Paulin, L., Pekkonen, E., Auvinen, P., et al. (2017). More than constipation–bowel symptoms in Parkinson's disease and their connection to gut microbiota. *Eur. J. Neurol.* 24, 1375–1383. doi: 10.1111/ene.13398

Micci, L., Alvarez, X., Iriele, R. I., Ortiz, A. M., Ryan, E. S., McGary, C. S., et al. (2014). CD4 Depletion in SIV-Infected Macaques Results in Macrophage and Microglia Infection with Rapid Turnover of Infected Cells. *PLoS Pathogens* 10:e1004467. doi: 10.1371/journal.ppat.1004467

Mitchell, B. I., Laws, E. I., and Ndhlovu, L. C. (2019). Impact of Myeloid Reservoirs in HIV Cure Trials. *Curr. HIV/AIDS Rep.* 16, 129–140. doi: 10.1007/s11904-019-00438-5

Mizuno, T., Kawanokuchi, J., Numata, K., and Suzumura, A. (2003). Production and neuroprotective functions of fractalkine in the central nervous system. *Brain Res.* 979, 65–70. doi: 10.1016/S0006-8993(03)02867-1

Mizuno, T., Sawada, M., Marunouchi, T., and Suzumura, A. (1994a). Production of interleukin-10 by mouse glial cells in culture. *Biochem. Biophys. Res. Commun.* 205, 1907–1915. doi: 10.1006/bbrc.1994.2893

Mizuno, T., Sawada, M., Suzumura, A., and Marunouchi, T. (1994b). Expression of cytokines during glial differentiation. *Brain Res.* 656, 141–146. doi: 10.1016/0006-8993(94)91375-7

Motulsky, H. (2020). *PRISM 9: Taking your Analyses and Graphs to Higher Dimensions*. Available online at: https://www.graphpad.com/support/faq/prism-900-release-notes/

Mrdjen, D., Pavlovic, A., Hartmann, F. J., Schreiner, B., Utz, S. G., Leung, B. P., et al. (2018). High-dimensional single-cell mapping of central nervous system immune cells reveals distinct myeloid subsets in health, aging, and disease. *Immunity* 48, 380.–395. doi: 10.1016/j.immuni.2018.01.011

Murray, K. N., Parry-Jones, A. R., and Allan, S. M. (2015). Interleukin-1 and acute brain injury. *Front. Cell. Neurosci.* 9:18. doi: 10.3389/fncel.2015.00018

Nath, A. (2002). Human immunodeficiency virus (HIV) proteins in neuropathogenesis of HIV dementia. *J. Infect. Dis.* 186:S193–S198. doi: 10.1086/344528

Nath, A., Anderson, C., Jones, M., Maragos, W., Booze, R., Mactutus, C., et al. (2000). Neurotoxicity and dysfunction of dopaminergic systems associated with AIDS dementia. *J. Psychopharmacol.* 14, 222–227. doi: 10.1177/026988110001400305

Nimmerjahn, A., Kirchhoff, F., and Helmchen, F. (2005). Resting microglial cells are highly dynamic surveillants of brain parenchyma in vivo. *Science* 308, 1314–1318. doi: 10.1126/science.1110647

Nowlin, B. T., Burdo, T. H., Midkiff, C. C., Salemi, M., Alvarez, X., and Williams, K. C. (2015). SIV encephalitis lesions are composed of CD163(+) macrophages present in the central nervous system during early SIV infection and SIV-positive macrophages recruited terminally with AIDS. *Am. J. Pathol.* 185, 1649–1665. doi: 10.1016/j.ajpath.2015.01.033

Ohgidani, M., Kato, T. A., Haraguchi, Y., Matsushima, T., Mizoguchi, Y., Murakawa-Hirachi, T., et al. (2017). Microglial CD206 gene has potential as a state marker of bipolar disorder. *Front. Immunol.* 7:676. doi: 10.3389/fimmu.2016.00676

Oksanen, J., Blanchet, F. G., Friendly, M., Kindt, R., Legendre, P., McGlinn, D., et al. (2016). *Vegan: Community Ecology Package. R package version 2.4-3*. Vienna: R Foundation for Statistical Computing.

Paiva, I., Pinho, R., Pavlou, M. A., Hennion, M., Wales, P., Schütz, A.-L., et al. (2017). Sodium butyrate rescues dopaminergic cells from alpha-synuclein-induced transcriptional deregulation and DNA damage. *Hum. Mol. Genet.* 26, 2231–2246. doi: 10.1093/hmg/ddx114

Parada Venegas, D., De la Fuente, M. K., Landskron, G., González, M. J., Quera, R., Dijkstra, G., et al. (2019). Short Chain Fatty Acids (SCFAs)-Mediated Gut Epithelial and Immune Regulation and Its Relevance for Inflammatory Bowel Diseases. *Front. Immunol.* 10:277. doi: 10.3389/fimmu.2019.00277

Park, H. J., Oh, S. H., Kim, H. N., Jung, Y. J., and Lee, P. H. (2016). Mesenchymal stem cells enhance α-synuclein clearance via M2 microglia polarization in experimental and human parkinsonian disorder. *Acta Neuropathol.* 132, 685–701. doi: 10.1007/s00401-016-1605-6

Peng, L., Li, Z.-R., Green, R. S., Holzman, I. R., and Lin, J. (2009). Butyrate enhances the intestinal barrier by facilitating tight junction assembly via activation of AMP-activated protein kinase in Caco-2 cell monolayers. *J. Nutri.* 139, 1619–1625. doi: 10.3945/jn.109.104638

Perez, S., Johnson, A. M., Xiang, S. H., Li, J., Foley, B. T., Doyle-Meyers, L., et al. (2018). Persistence of SIV in the brain of SIV-infected Chinese rhesus macaques with or without antiretroviral therapy. *J. Neurovirol.* 24, 62–74. doi: 10.1007/s13365-017-0594-0

Pérez-Mañá, C., Papaseit, E., Fonseca, F., Farré, A., Torrens, M., and Farré, M. (2018). Drug Interactions With New Synthetic Opioids. *Front. Pharmacol.* 9:1145. doi: 10.3389/fphar.2018.01145

Ponomarev, E. D., Veremeyko, T., Barteneva, N., Krichevsky, A. M., and Weiner, H. L. (2011). MicroRNA-124 promotes microglia quiescence and suppresses EAE by deactivating macrophages via the C/EBP-α-PU.1 pathway. *Nat. Med.* 17, 64–70. doi: 10.1038/nm.2266

Putatunda, R., Ho, W.-Z., and Hu, W. (2019). HIV-1 and Compromised Adult Neurogenesis: Emerging Evidence for a New Paradigm of HAND Persistence. *AIDS Rev.* 21, 11–22. doi: 10.24875/AIDSRev.19000003

Rock, R. B., Gekker, G., Hu, S., Sheng, W. S., Cheeran, M., Lokensgard, J. R., et al. (2004). Role of microglia in central nervous system infections. *Clin. Microbiol. Rev.* 17, 942–964. doi: 10.1128/CMR.17.4.942-964.2004

Rodrigues, V., Ruffin, N., San-Roman, M., and Benaroch, P. (2017). Myeloid Cell Interaction with HIV: A Complex Relationship. *Front. Immunol.* 8:1698. doi: 10.3389/fimmu.2017.01698

Rummans, T. A., Burton, M. C., and Dawson, N. L. (eds) (2018). *How Good Intentions Contributed to Bad Outcomes: The Opioid Crisis. Mayo Clinic Proceedings.* Amsterdam, NL: Elsevier. doi: 10.1016/j.mayocp.2017.12.020

Schechter, M. E., Andrade, B. B., He, T., Richter, G. H., Tosh, K. W., Policicchio, B. B., et al. (2017). Inflammatory monocytes expressing tissue factor drive SIV and HIV coagulopathy. *Sci. Trans. Med.* 9:eaam5441. doi: 10.1126/scitranslmed.aam5441

Segata, N., Izard, J., Waldron, L., Gevers, D., Miropolsky, L., Garrett, W. S., et al. (2011). Metagenomic biomarker discovery and explanation. *Genome Biol.* 12:R60. doi: 10.1186/gb-2011-12-6-r60

Shi, C., and Pamer, E. G. (2011). Monocyte recruitment during infection and inflammation. *Nat. Rev. Immunol.* 11, 762–774. doi: 10.1038/nri3070

Sindberg, G. M., Callen, S. E., Banerjee, S., Meng, J., Hale, V. L., Hegde, R., et al. (2019). Morphine Potentiates Dysbiotic Microbial and Metabolic Shifts in Acute SIV Infection. *J. Neuroimmune Pharmacol* 14, 200–214. doi: 10.1007/s11481-018-9805-6

Solimini, R., Pichini, S., Pacifici, R., Busardò, F. P., and Giorgetti, R. (2018). Pharmacotoxicology of Non-fentanyl Derived New Synthetic Opioids. *Front. Pharmacol.* 9:654. doi: 10.3389/fphar.2018.00654

Steele, A. D., Henderson, E. E., and Rogers, T. J. (2003). Mu-opioid modulation of HIV-1 coreceptor expression and HIV-1 replication. *Virology* 309, 99–107.

Streit, W. J. (2006). Microglial senescence: does the brain's immune system have an expiration date? *Trends Neurosci.* 29, 506–510. doi: 10.1016/j.tins.2006.07.001

Sudduth, T. L., Schmitt, F. A., Nelson, P. T., and Wilcock, D. M. (2013). Neuroinflammatory phenotype in early Alzheimer's disease. *Neurobiol. Aging* 34, 1051–1059. doi: 10.1016/j.neurobiolaging.2012.09.012

Tan, Y.-L., Yuan, Y., and Tian, L. (2020). Microglial regional heterogeneity and its role in the brain. *Mol. Psychiatry* 25, 351–367. doi: 10.1038/s41380-019-0609-8

Teh, Y. C., Ding, J. L., Ng, L. G., and Chong, S. Z. (2019). Capturing the Fantastic Voyage of Monocytes Through Time and Space. *Front. Immunol.* 10:834. doi: 10.3389/fimmu.2019.00834

Tenneti, L., and Lipton, S. A. (2000). Involvement of activated caspase-3-like proteases in N-methyl-D-aspartate-induced apoptosis in cerebrocortical neurons. *J. Neurochem.* 74, 134–142. doi: 10.1046/j.1471-4159.2000.0740134.x

Townsend, E. M., Kelly, L., Muscatt, G., Box, J. D., Hargraves, N., Lilley, D., et al. (2021). The Human Gut Phageome: Origins and Roles in the Human Gut Microbiome. *Front. Cell Infect. Microbiol.* 11:643214.

Tu, H., Chu, H., Guan, S., Hao, F., Xu, N., Zhao, Z., et al. (2020). The role of the M1/M2 microglia in the process from cancer pain to morphine tolerance. *Tissue Cell* 68:101438. doi: 10.1016/j.tice.2020.101438

Vogt, N. M., Kerby, R. L., Dill-McFarland, K. A., Harding, S. J., Merluzzi, A. P., Johnson, S. C., et al. (2017). Gut microbiome alterations in Alzheimer's disease. *Sci. Rep.* 7:13537. doi: 10.1038/s41598-017-13601-y

Walker, D. G., and Lue, L.-F. (2015). Immune phenotypes of microglia in human neurodegenerative disease: challenges to detecting microglial polarization in human brains. *Alzheimers Res. Therapy* 7:56. doi: 10.1186/s13195-015-0139-9

Wallet, C., De Rovere, M., Van Assche, J., Daouad, F., De Wit, S., Gautier, V., et al. (2019). Microglial Cells: The Main HIV-1 Reservoir in the Brain. *Front. Cell Infect. Microbiol.* 9:362. doi: 10.3389/fcimb.2019.00362

Wang, Q., Garrity, G. M., Tiedje, J. M., and Cole, J. R. (2007). Naive Bayesian classifier for rapid assignment of rRNA sequences into the new bacterial taxonomy. *Appl. Environ. Microbiol.* 73, 5261–5267. doi: 10.1128/AEM.00062-07

Winkler, J. M., Chaudhuri, A. D., and Fox, H. S. (2012). Translating the brain transcriptome in neuroAIDS: from non-human primates to humans. *J. Neuroimmune Pharmacol* 7, 372–379. doi: 10.1007/s11481-012-9344-5

Woollard, S. M., Olwenyi, O. A., Dutta, D., Dave, R. S., Mathews, S., Gorantla, S., et al. (2018). Preliminary Studies on Immune Response and Viral Pathogenesis of Zika Virus in Rhesus Macaques. *Pathogens* 7:70. doi: 10.3390/pathogens7030070

Zhang, L., Meng, J., Ban, Y., Jalodia, R., Chupikova, I., Fernandez, I., et al. (2019). Morphine tolerance is attenuated in germfree mice and reversed by probiotics, implicating the role of gut microbiome. *Proc. Natl. Acad. Sci.* 116, 13523–13532. doi: 10.1073/pnas.1901182116

Zou, S., Fitting, S., Hahn, Y.-K., Welch, S. P., El-Hage, N., Hauser, K. F., et al. (2011). Morphine potentiates neurodegenerative effects of HIV-1 Tat through actions at μ-opioid receptor-expressing glia. *Brain* 134, 3616–3631. doi: 10.1093/brain/awr281

frontiers | Frontiers in Neuroscience

TYPE Original Research
PUBLISHED 04 November 2022
DOI 10.3389/fnins.2022.1034547

OPEN ACCESS

EDITED BY
Chunhui Bao,
Shanghai University of Traditional Chinese Medicine, China

REVIEWED BY
Jan D. Huizinga,
McMaster University, Canada
Ji-Hong Chen,
McMaster University, Canada

*CORRESPONDENCE
Yue Yu
yuyuemd@ustc.edu.cn

SPECIALTY SECTION
This article was submitted to Gut-Brain Axis, a section of the journal Frontiers in Neuroscience

RECEIVED 01 September 2022
ACCEPTED 24 October 2022
PUBLISHED 04 November 2022

CITATION
Liu J, Lv C, Wang W, Huang Y, Wang B, Tian J, Sun C and Yu Y (2022) Slow, deep breathing intervention improved symptoms and altered rectal sensitivity in patients with constipation-predominant irritable bowel syndrome. *Front. Neurosci.* 16:1034547. doi: 10.3389/fnins.2022.1034547

Slow, deep breathing intervention improved symptoms and altered rectal sensitivity in patients with constipation-predominant irritable bowel syndrome

Jie Liu[1], Chaolan Lv[1], Wei Wang[2], Yizhou Huang[3], Bo Wang[3], Jiashuang Tian[2], Chenyu Sun[4] and Yue Yu[1]*

[1]Department of Gastroenterology, The First Affiliated Hospital of USTC, Division of Life Sciences and Medicine, University of Science and Technology of China, Hefei, China, [2]Department of Gastroenterology, Affiliated Anhui Provincial Hospital, Anhui Medical University, Hefei, China, [3]Graduate School of Bengbu Medical College, Bengbu, China, [4]AMITA Health Saint Joseph Hospital Chicago, Chicago, IL, United States

Background and aim: Limited treatment options have been shown to alter the natural course of irritable bowel syndrome (IBS). Slow, deep breathing (SDB) is a common pain self-management intervention. This pilot study aimed to explore the impact of SDB on measures of autonomic and anorectal functions as well as patient-reported symptoms in constipation-predominant IBS (IBS-C).

Methods: Eighty-five IBS-C patients were enrolled in this study and randomly assigned to the experimental group (Group A, n = 42) and the control group (Group B, n = 43). SDB was conducted at six breathing cycles per minute with an inhalation for 4 s and exhalation for 6 s at a ratio of 2:3 and repeated for 30 min during the intervention. All subjects underwent high-resolution anorectal manometry (HRAM) and completed the standardized IBS symptom severity system (IBS-SSS) questionnaire. Meanwhile, changes in stool consistency, weekly frequency of complete spontaneous bowel movements (CSBMs), and weekly frequency of spontaneous bowel movements (SBMs) were recorded. All IBS-C patients received electrocardiogram (ECG) recordings for heart rate variability (HRV) analysis at baseline, weeks 3, 6.

Results: At baseline, no differences were found between Groups A and B. The IBS-SSS score and its five sub-scores of Group B patients were significantly higher at week 6 than those of Group A patients (all $p < 0.001$). Furthermore, compared with Group B patients, Group A patients had a significantly higher threshold volume for the first sensation ($p < 0.001$), desire to defecate ($p = 0.017$), and maximum tolerable volume ($p = 0.018$) at week 6 of the SDB treatment. We also noted significant improvements in stool consistency ($p = 0.002$), weekly SBM frequencies ($p < 0.001$), and weekly

CSBM frequencies (p = 0.018) of Group A patients at week 6 when compared with Group B patients. Finally, the corrected high frequency (HF) of Group A patients was significantly higher than the HF of Group B patients at week 3 ($p < 0.001$) and at week 6 ($p < 0.001$). Likewise, patients in Group A had a significantly higher root mean square of the successive differences (RMSSD) than that of patients in Group B at week 3 ($p < 0.001$) and at week 6 ($p < 0.001$).

Conclusion: We found that a 6-week SDB intervention improved symptoms and altered rectal sensation in IBS-C patients. Moreover, SDB enhanced vagal activity. These findings suggest that the effect of SDB on IBS-C may be due to mechanisms involving autonomic responses.

KEYWORDS

irritable bowel syndrome, constipation, anorectal function, slow deep breathing, autonomic dysfunction

Introduction

Constipation-predominant irritable bowel syndrome (IBS-C), as one of the most common disorders of gut-brain interaction (DGBI), is defined under the Rome IV Diagnostic Criteria as recurrent abdominal pain/discomfort accompanied by changes in defecation habits and/or stool frequency or form (Ford et al., 2017). Globally, it is estimated that more than 11.2% of the population has irritable bowel syndrome (IBS) symptoms, of which IBS-C accounts for nearly a third of all IBS cases (Lacy et al., 2015; Ford et al., 2020). A previous study reported that patients' quality of life could be significantly decreased by IBS-C (Ballou et al., 2019). IBS-C is well known to be linked to dysfunction of autonomic nervous system, visceral hypersensitivity, intestinal bacterial overgrowth, and gut inflammation, etc. (Holtmann et al., 2016). To date, of the approved IBS treatments, few have been confirmed to be effective in improving IBS-C symptoms. Dietary and behavioral interventions, prebiotic and probiotic supplements, spasmolytic agents, osmotic and/or stimulant laxatives, fiber products, and neuromodulators are recognized as common empirically supported therapies for IBS-C (Camilleri, 2021). Some novel drugs, including linaclotide, have been examined in randomized placebo-controlled trials and verified in IBS-C patients, but no pharmacological agent has been shown to alter the natural course of IBS (Black et al., 2020). In addition, there is no consensus on the gold standard treatment for IBS-C. Moreover, a recent meta-analysis revealed that diarrhea or headache was significantly more common in the licensed drugs treatment group than in the placebo group in IBS-C trials (Barberio et al., 2021). Therefore, it is important that, as an emerging area of interest, complementary and alternative medicine (CAM) are adequately investigated to determine its efficacy as a treatment for IBS.

Notably, previous evidences based on the American College of Gastroenterology Task Force demonstrated that IBS symptoms can be alleviated with dynamic psychotherapy, hypnotherapy, and cognitive therapy (American College of Gastroenterology Task Force on Irritable Bowel Syndrome et al., 2009). Slow, deep breathing (SDB) is a self-management intervention that ranks as the second most practiced complementary and alternative health approach according to National Health Interview Survey data (Clarke et al., 2015). SDB is a common component of several non-pharmacological techniques such as relaxation, meditation, hypnotherapy and yoga, which have been applied as a CAM in treating chronic pain syndromes (Nahin et al., 2015). A systematic review of several experimental studies employing somatic pain models and clinical studies of the effects of SDB on chronic pain management established the hypoalgesic effects of SDB on relieving pain symptoms (Jafari et al., 2017). They proposed cognitive, emotional, and autonomic (e.g., increased vagal nerve activity) modulations as potential mechanisms of SDB-mediated pain relief (Jafari et al., 2017).

Vagal afferent signaling can be increased using different levels of SDB (Jafari et al., 2017). The stimulation of pulmonary stretch receptors by deep breathing result in afferent signaling through the vagus nerve, which enhances afferent inputs to the nucleus of the solitary tract in the brain stem. These receptors also synapse with ascending circuits terminating at subcortical and cortical levels (e.g., insular cortex and amygdala) and participate in sensory, emotional, and cognitive processing of signals (Mazzone and Undem, 2016). Meanwhile, this nucleus of the solitary tract project directly and/or indirectly into several brain areas, which play a key role in pain regulation (e.g., periaqueductal gray and locus coeruleus) (Bruehl and Chung, 2004). Thus, on this theoretical basis, several studies have found hypoalgesic and antinociceptive effects of baroreceptor and

vagus nerve stimulation (Busch et al., 2013; Reyes del Paso et al., 2014).

As high sympathetic tone and impaired vagal pathway are implicated in the pathophysiology of IBS and constipation (Tanaka et al., 2008; Liu et al., 2022), it is reasonable to hypothesize that SDB is a potentially effective, complementary lifestyle management in patients with IBS. A previous study found that microvascular endothelial function of IBS patients improved following the SDB intervention (Katherine Jurek et al., 2022). Although these observed improvements were encouraging, up to now, no study has assessed the effectiveness of SDB on anorectal physiological tests for IBS-C patients. The purpose of this pilot study was to explore the impact of SDB on measures of autonomic and rectal sensation as well as patient-reported IBS-C symptoms.

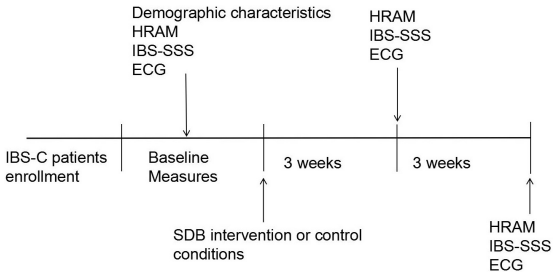

FIGURE 1
The study procedure. IBS-C, irritable bowel syndrome with constipation; HRAM, high-resolution anorectal manometry; ECG, electrocardiography; IBS-SSS, irritable bowel syndrome symptom severity system; SDB, slow, deep breathing.

Materials and methods

Patients

Outpatients (ages 18–65) who met the Rome IV diagnostic criteria (Drossman, 2016) for IBS-C were diagnosed by a gastroenterologist (Y Y) experienced in the diagnosis of DGBI. Subjects were recruited into the study at the Department of Gastroenterology, the First Affiliated Hospital of University of Science and Technology of China (USTC) between July 2019 and January 2022. The exclusion criteria were: (i) patients who practice SDB on a regular basis; (ii) patients with chronic obstructive pulmonary diseases; (iii) patients with a history of any cardiovascular disease, including a heart attack, stroke, myocardial infarction, coronary artery disease, angina, arrhythmias; (iv) patients with a body mass index (BMI) of < 18.5 or > 30 kg/m^2; and (iv) patients who were taking drugs that could affect IBS-C symptoms, such as prebiotic and probiotic supplements, spasmolytic agents, laxatives, and neuromodulators. Subjects were required to refrain from strenuous exercise, avoid caffeine and alcohol for at least 12 h, and fast (for solid food) for 4 h before testing.

This study protocol was approved by the Ethics Committee of the First Affiliated Hospital of USTC (Registration No: 2022-RE-142) and registered in the Chinese Clinical Trial Registry (No. ChiCTR-2200060462). All participants signed a written informed consent before their inclusion into the research.

Experimental protocol

This was a within-subjects experimental study. A total of 90 patients with IBS-C were randomly divided into two groups: Group A and Group B. However, five participants were lost to follow-up due to time difficulties, representing a dropout rate of 6.67% for group A and 4.44% for group B. Finally, 85 IBS-C patients completed this study, including 42 IBS-C patients in the SDB intervention (Group A) and 43 IBS-C patients in the control group (Group B).

All participants completed the standardized irritable bowel syndrome symptom severity system (IBS-SSS) questionnaire and pre- and post-SDB at weeks 3 and 6. Meanwhile, the stool consistency, weekly frequency of complete spontaneous bowel movements (CSBMs), and weekly frequency of spontaneous bowel movements (SBMs) of each patient were recorded. High-resolution anorectal manometry (HRAM) was performed for enrolled constipation-predominant IBS (IBS-C) patients, and all subjects received electrocardiogram (ECG) recording for time-domain heart rate variability (HRV) analysis at baseline, weeks 3, 6. The procedure of this study is depicted in **Figure 1**.

Measurements

Slow, deep breathing intervention

This prospective study was a randomized control trial where subjects were not blinded to the study. Enrolled patients were randomly divided into Group A with a 6-week SDB intervention or Group B with control conditions. Randomization was performed using Randomizer.org while implementing a 1:1 allocation ratio. Patients in Group A were instructed to perform a 30-min SDB at least 5 days per week whereas the control group maintained their regular breathing. In detail, SDB was conducted at six breathing cycles per minute with an inhalation for 4 s and exhalation for 6 s at a ratio of 2:3 and repeated for 30 min during the intervention. Once baseline testing was completed, participants assigned to the SDB group performed all breathing sessions in the gastrointestinal motility room under the supervision of our research team. Practice logs were recorded to ensure that the experimental group met the practice requirements. Participants in both groups were instructed to maintain

their regular diet and exercise regimens (Lee et al., 2021; Gholamrezaei et al., 2022).

High-resolution anorectal manometry

HRAM (MedKinetic, Ningbo, China) was performed for all IBS-C patients as described in our previous study (Liu et al., 2021), Briefly, 1–2 doses of glycerin enema was used to empty the rectum for bowel preparation 30–60 min before the HRAM examination. An eight-channel water-perfused anorectal manometric catheter (GAP-08A; Ningbo Maida Medical Device, Ningbo, China) was employed to measure the anal sphincter pressure and rectal sensation at a 1-cm interval. The device employs the technology of proprietary pressure transduction, which allows every pressure-sensor element to sense pressure over a 2.5-mm length in each of the 12 dispersed radially sectors. Patients were placed in the left lateral position and a catheter was inserted into the rectum after lubrication. The rectoanal inhibitory reflexes (RAIR) was then evaluated by inflating the balloon attached to the tip of the catheter with a hand-held syringe to a volume from 0 to 50 ml. The sensation test was assessed using a rectal balloon distended at a 5 ml interval until the subjects indicated the first sensation. Subsequently, we increased the volume of the balloon in progressive 5-ml increments until the subjects felt a sensation of the desire to defecate and the maximum tolerance. The outcomes for inducing these sensations depended on subject self-reports and the threshold volumes for these sensations were recorded (Lee and Bharucha, 2016).

Questionnaires

IBS-SSS is an internationally validated questionnaire for assessing overall IBS-like symptoms (Francis et al., 1997). The IBS-SSS score is a five subscore visual analog scales (VAS) instrument developed for measuring the intensity of IBS-like symptoms during the preceding 10 days. IBS-SSS consists of five subscores, including abdominal pain intensity and duration, stool frequency and consistency, abdominal distension, and interference with life in general. Each of the five subscores is rated on a 100-point Likert response scale, ranging from 0 (no symptom) to 100 (extremely severe symptoms). Thus, the highest possible total IBS-SSS score is 500 points. The higher the total score, the more severe the patient's IBS-C symptoms. Meanwhile, the stool consistency [evaluated using the Bristol Stool Form Scale (BSFS)], weekly frequency of CSBMs, and weekly frequency of SBMs of each patient were also recorded during this study. The BSFS is a validated 7-point assessment that ranges from 1 [indicating separate, hard lumps, like nuts (hard to pass)] to 7 [indicating watery, no solid pieces (entirely liquid)] (Lewis and Heaton, 1997).

Assessment of autonomic functions

Autonomic functions were evaluated with spectral analysis of HRV time-domain as well as frequency-domain parameters. HRV signals were obtained using an ECG recording (ct-082, Hangzhou Baihui Electrocardiograms, China), whereas each subject's HRV data was analyzed by monitoring R-R intervals with the HRV analysis software V.1.2.0.0 (Cardiotrak Holter system; Hangzhou Baihui Electrocardiograms, China). At baseline and control conditions, high-frequency (HF) power was used to reflect parasympathetic activity. Given the influence of SDB on the respiratory peak, we used the central frequency of respiration peak (CFRP) to correct HF band and eliminate the effect of SDB on respiratory peak shift, which in turn influenced our spectral analysis. The corrected HF area was chosen from CFRP*0.65 to 0.40 Hz (Chang et al., 2013; Li et al., 2018).

The Baevsky Index or Sympathetic Index (SI) was calculated to reflect sympathetic tone using the formula (Ali et al., 2021). The most frequent R-R interval was transformed into mode (Mo), expressed in seconds. A 50 ms bin width was used to calculate the amplitude of mode (AMo), expressed as a percentage of the total number of intervals measured. Variability was represented by MxDMn as the difference between longest (Mx) and shortest (Mn) R-R interval values, expressed in seconds. The SI was expressed as s^{-2}.

Meanwhile, the following time domain HRV parameters were extracted based on the time between the individual R-peaks [the interval between R-peaks is defined as the normal to normal (NN) interval]: (1) standard deviation of NN-intervals (SDNN); (2) root mean square of the successive RR interval differences (RMSSD). In addition, previous study indicated that respiration had a limited impact on RMSSD, which could be used to reflect parasympathetic activity (Hill and Siebenbrock, 2009).

Statistical analysis

All the statistical analyses were performed on SPSS V.19.0 software (IBM Corp, Armonk, NY). Continuous variables are given as mean ± standard deviation. Differences between the two groups were compared using a paired *t*-test for continuous variables and Chi-square test for discontinuous parameters. $P < 0.05$ signified statistical significance.

Results

Participants

A total of 90 IBS-C patients were enrolled in this study and randomly assigned into two groups: the experimental group (Group A) and the control group (Group B). However, five participants (three from group A and two from group B) were lost to follow-up. Of the 85 participants who completed the study, 59 were female and 26 were male, with a mean age of 46.79 ± 12.55 years. No statistical differences in age, gender,

TABLE 1 Demographic characteristics for the two study groups.

	Overall ($N = 85$)	Group A ($n = 42$)	Group B ($n = 43$)	t/χ^2	P
Gender					
Male (n)	26	9	17	3.281	0.070
Female (n)	59	33	26		
Age (years)	46.79 ± 12.55	46.45 ± 11.70	47.12 ± 13.47	0.24	0.809
BMI (kg/m^2)	23.34 ± 3.83	23.86 ± 3.98	22.83 ± 3.65	1.240	0.218
Duration of constipation(months)	34.81 ± 19.63	34.21 ± 10.30	35.40 ± 9.17	0.276	0.783

BMI, body mass index. Participants in group A were treated with slow, deep breathing and participants in group B were controls. No statistically significant difference was noted in age, gender, BMI, and the duration of constipation.

BMI, and the duration of IBS-C were observed among the three groups. These results are shown in Table 1.

Baseline data

Regarding rectal sensitivity, we found no significant differences between RAIR, first sensation, desire to defecate, and maximum tolerable volume of patients in Groups A and B ($p = 0.176$, $p = 0.391$, $p = 0.133$, and $p = 0.073$, respectively). Regarding IBS-C symptoms, we noted no difference in IBS-SSS between patients in Group A and B ($p = 0.568$). Regarding autonomic functions, we found no significant difference between patients in Groups A and B in HF ($p = 0.667$), SI ($p = 0.121$), SDNN ($p = 0.852$), and RMSSD ($p = 0.435$). Meanwhile, BSFS scores ($p = 0.138$), weekly CSBM frequencies ($p = 0.669$), and weekly SBM frequencies ($p = 0.801$) were comparable between the patients in the two groups. These results are summarized in Table 2. In addition, we considered the ranges mentioned in the study by Sun et al. (2014) as the reference. The volumes for the first sensation of 15 patients were below the normal range (20∼90 ml), and five patients were above the normal range. The volumes for the desire to defecate in 12 patients were below the normal range (50∼170 ml), and six patients were beyond the normal range. The volumes for the urge to defecate in eight patients were below the normal range (80∼220 ml), and four patients were beyond the normal range. The maximum tolerable volumes of 14 patients were below the normal range (120∼280 ml), and seven were above the normal range.

Effects of slow, deep breathing on irritable bowel syndrome symptom severity system

As depicted in Figure 2, we observed no significant difference in IBS-SSS total score and five subscale scores at the baseline between Groups A and B (all $p > 0.050$). Meanwhile, we found no significant difference in IBS-SSS total score at week 3 between the two groups (288.57 ± 40.46 vs. 300.00 ± 71.58, $p = 0.369$), whereas the abdominal pain intensity score in Group B was significantly higher than that in Group A at week 3 (43.33 ± 14.59 vs. 56.28 ± 23.20, $p = 0.003$). Notably, patients in Group A had a significantly lower IBS-SSS total score and its five subscores compared to those in Group B after 6 weeks (all $p < 0.001$). These outcomes are shown in Table 3.

Effects of slow, deep breathing on constipation symptoms

We observed no significant differences in the BSFS scores (2.05 ± 0.66 vs. 1.79 ± 0.60, $p = 0.064$), weekly SBM frequencies (1.45 ± 0.55 times vs. 1.56 ± 0.59 times, $p = 0.395$), and weekly CSBM frequencies (1.17 ± 0.38 times vs. 1.23 ± 0.43 times, $p = 0.454$) at week 3 between Groups A and B. However, we found significant improvements in BSFS scores (2.12 ± 0.71 vs. 1.60 ± 0.76, $p = 0.002$), weekly SBM frequencies (2.14 ± 0.84 times vs. 1.47 ± 0.50 times, $p < 0.001$), and weekly CSBM frequencies (1.40 ± 0.54 times vs. 1.14 ± 0.47 times, $p = 0.018$) of Group A patients compared with those of Group B patients at week 6 (Figure 2).

Effects of slow, deep breathing on rectal sensitivity

Maximum tolerable volume was significantly higher in Group A than in Group B at week 3 (244.52 ± 35.90 ml vs. 228.37 ± 35.59 ml, $p = 0.040$). Compared with IBS-C patients in Group B, Group A patients had a significantly higher threshold volume for the first sensation at week 6 of SDB treatments (33.81 ± 8.96 ml vs. 26.16 ± 6.62 ml, $p < 0.001$), desire of defecation (56.79 ± 7.87 ml vs. 52.67 ± 7.66 ml, $p = 0.017$), and maximum tolerable volume (248.33 ± 34.07 ml vs. 229.77 ± 36.68 ml, $p = 0.018$). However, there was no difference in threshold volume for urge to defecate between Group A and Group B at week 3 (108.69 ± 10.42 ml vs. 104.07 ± 12.26 ml, $p = 0.065$) and at week 6 (104.76 ± 9.50 ml vs. 106.63 ± 9.80 ml, $p = 0.375$). Meanwhile, no difference was observed in threshold volume for the first sensation

TABLE 2 Baseline characteristics for the two study groups.

	Overall (N = 85)	Group A (n = 42)	Group B (n = 43)	T	P
Rectal sensitivity					
RAIR (ml)	23.47 ± 5.23	23.92 ± 5.24	22.44 ± 4.80	1.364	0.176
First sensation (ml)	24.47 ± 5.72	23.93 ± 6.00	25.00 ± 5.46	0.862	0.391
Desire of defecation (ml)	51.18 ± 9.99	49.52 ± 9.03	52.79 ± 10.71	1.519	0.133
Urge to defecate (ml)	104.24 ± 10.51	103.45 ± 11.07	105.00 ± 10.00	0.677	0.500
Maximum tolerable volume (ml)	227.76 ± 45.50	218.81 ± 42.27	236.51 ± 47.30	1.818	0.073
Heart rate variability (HRV)					
HF (ms^2)	135.01 ± 38.74	134.60 ± 37.58	135.42 ± 39.81	0.432	0.667
SI (s^{-2})	38.89 ± 7.18	40.12 ± 8.50	37.70 ± 5.44	1.567	0.121
SDNN (ms)	106.99 ± 18.64	106.81 ± 18.53	107.16 ± 18.83	0.187	0.852
RMSSD (ms)	26.45 ± 7.12	25.83 ± 6.24	27.05 ± 7.91	0.784	0.435
IBS-C symptoms					
IBS-SSS	284.00 ± 63.27	280.00 ± 47.52	287.91 ± 75.96	0.574	0.568
BSFS scores	1.64 ± 0.48	1.71 ± 0.46	1.56 ± 0.50	1.497	0.138
SBM frequencies (per week)	1.33 ± 0.59	1.36 ± 0.58	1.30 ± 0.60	0.430	0.669
CSBM frequencies (per week)	1.01 ± 0.42	1.00 ± 0.44	1.02 ± 0.41	0.252	0.801

RAIR, rectoanal inhibitory reflexes; HF, high frequency; SI, Baevsky Index or Sympathetic Index; SDNN, standard deviation of normal to normal intervals; RMSSD, root mean square of the successive differences; BSFS, Bristol Stool Form Scale; CSBM, complete spontaneous bowel movements; SBM, spontaneous bowel movements.

(25.60 ± 5.97 ml vs. 26.05 ± 6.22 ml, p = 0.734), desire of defecation (50.48 ± 6.70 ml vs. 53.02 ± 9.52 ml, p = 0.158) at week 3 between the two groups. In addition, there was no difference in RAIR between Group A and Group B after 3 weeks (22.38 ± 4.84 ml vs. 23.02 ± 5.02 ml, p = 0.550) and 6 weeks (22.50 ± 5.21 ml vs. 22.91 ± 5.03 ml, p = 0.715). These results are shown in **Figure 3**.

Effects of slow, deep breathing on autonomic functions

As summarized in **Table 2**, we found no differences in the HF (p = 0.667), SI (p = 0.121), SDNN (p = 0.852), and RMSSD (p = 0.435) between Group A and Group B at the baseline. Notably, the corrected HF in Group A was significantly higher than the HF in Group B at week 3 (897.19 ± 60.02 ms^2 vs. 126.72 ± 16.62 ms^2, $p < 0.001$) and at week 6 (1270.31 ± 155.61 ms^2 vs. 157.26 ± 14.35 ms^2, $p < 0.001$). However, there was no difference in SI between Group A and Group B at week 3 (38.76 ± 5.88 s^{-2} vs. 36.84 ± 5.32 s^{-2}, p = 0.117) and at week 6 (38.59 ± 6.66 s^{-2} vs. 36.77 ± 4.68 s^{-2}, p = 0.146). Meanwhile, the SDNN in Group A was significantly higher than that in Group B at week 3 (123.07 ± 22.03 ms vs. 104.23 ± 18.90 ms, $p < 0.001$) and at week 6 (136.83 ± 21.24 ms vs. 105.33 ± 17.70 ms, $p < 0.001$). Likewise, patients in Group A had a significantly higher RMSSD than that of patients in Group B at week 3 (33.55 ± 6.39 ms vs. 26.81 ± 5.40 ms, $p < 0.001$) and at week 6 (36.67 ± 5.94 ms vs. 25.40 ± 6.01 ms, $p < 0.001$). These results are shown in **Figure 4**.

Discussion

The results of the current study demonstrated that a 6-week SDB intervention improved symptoms and altered rectal sensation in IBS-C patients. Meanwhile, patients receiving SDB intervention reported a significant improvement in stool consistency and the frequency of bowel movements. Moreover, according to the time-domain and frequency-domain analysis of HRV, SDB enhanced vagal activity in IBS-C. These findings suggest that SDB improved IBS-C symptoms, which may be mediated via enhancement of vagal activity. Notably, the relationship between SDB and its impact on rectal sensation remains largely unknown and scarcely studied in IBS-C patients. Results from this current study support the improved symptoms of a 6-week SDB intervention in IBS-C patients and suggest an increased threshold volume for the first sensation, desire of defecation, and maximum tolerable volume after 6 weeks of SDB intervention compared with control condition. To our knowledge, this is the first clinical trial study to demonstrate the impact of a SDB intervention on rectal sensitivity in patients with IBS-C.

In recent years, as pharmacological agents proven to be effective for the treatment of IBS-C are limited and have potential adverse effects, there has been considerable attention on lifestyle modifications and non-pharmacological interventions for IBS. As a result, complementary measures are frequently recommended but evidence for their effectiveness and adverse effects is scarce (American College of Gastroenterology Task Force on Irritable Bowel Syndrome et al., 2009; Black et al., 2020). This preliminary study shows that

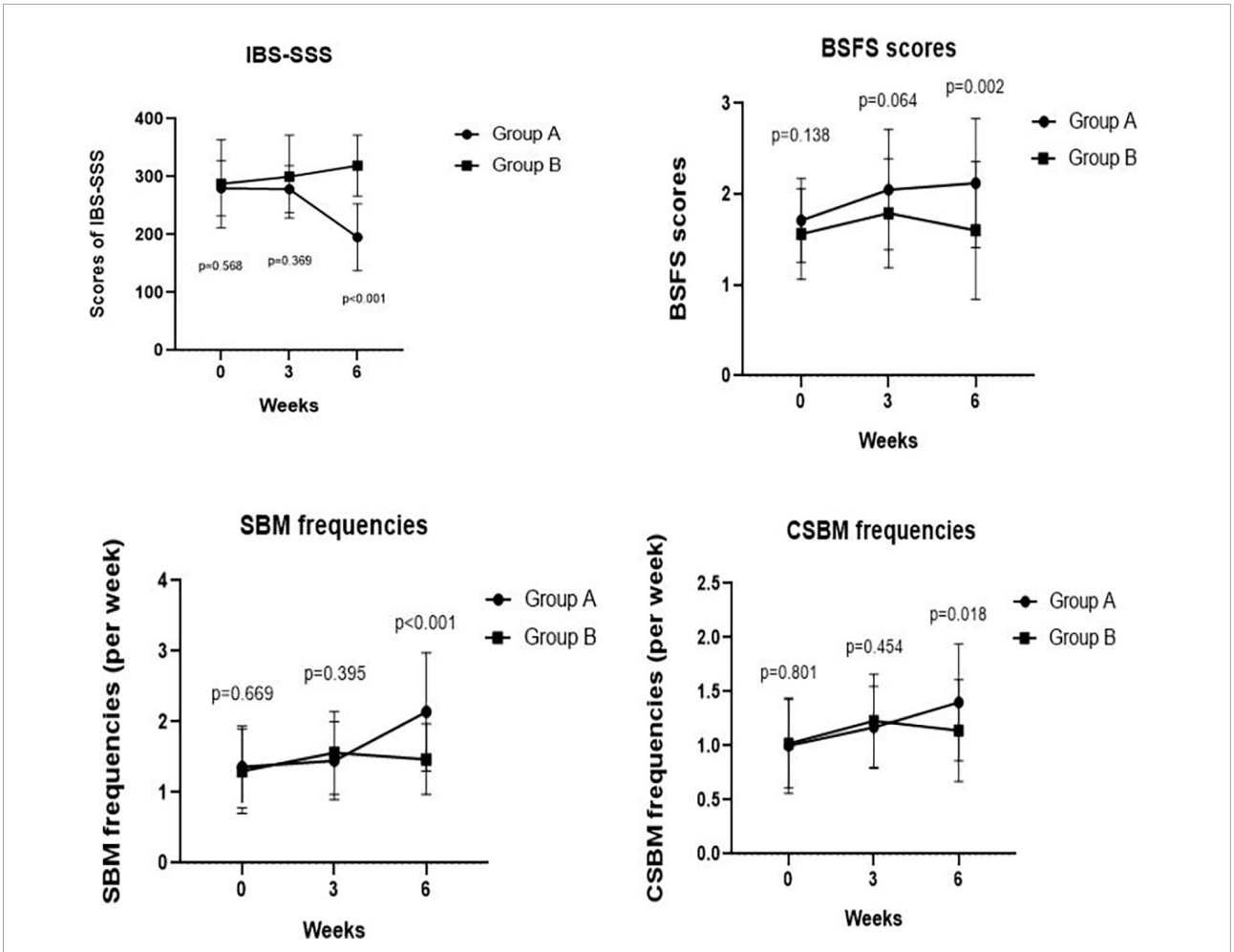

FIGURE 2
Comparing IBS-SSS score, BSFS score, weekly frequency of CSBMs, and weekly frequency of SBMs pre- and post-treatment at weeks 3, 6 between Groups A and B. We found a significant difference in IBS-SSS, BSFS score, weekly frequency of SBMs, weekly frequency of CSBMs post-treatment between Groups A and B at week 6 ($p < 0.001$, $p = 0.002$, $p < 0.001$, and $p = 0.018$, respectively).

TABLE 3 Comparison of IBS symptom between the two study groups.

	3 weeks			6 weeks		
	Group A	**Group B**	***P***	**Group A**	**Group B**	***P***
Abdominal pain intensity	43.33 ± 14.59	56.28 ± 23.20	0.003	40.95 ± 12.46	64.19 ± 14.18	<0.001
Abdominal pain frequency	58.10 ± 11.53	59.07 ± 17.43	0.762	39.52 ± 15.61	64.65 ± 12.97	<0.001
Abdominal distension	60.00 ± 12.49	61.86 ± 17.36	0.573	35.71 ± 14.34	64.65 ± 15.02	<0.001
Dissatisfaction of bowel habit	60.48 ± 14.31	55.81 ± 16.07	0.056	40.00 ± 17.11	61.40 ± 17.67	<0.001
Interference on life in general	67.38 ± 23.48	70.00 ± 37.61	0.702	39.29 ± 19.68	64.19 ± 17.76	<0.001
IBS-SSS total score	288.57 ± 40.46	300.00 ± 71.58	0.369	195.48 ± 57.73	319.07 ± 52.45	<0.001

IBS, irritable bowel syndrome.

SDB is effective for self-management of IBS-C. In our study, of patients receiving SDB intervention exhibited significantly improved IBS-C symptoms after 6 weeks compared with control condition. It could be that SDB is more feasible than other lifestyle managements like yoga, meditation or traditional exercise. For example, SDB can be practiced from various locations with less time commitment and minimal physical effort. Notably, the relationship between SDB and improved IBS symptoms in IBS-C patients may be multi-factorial, and the underlying mechanisms need further investigation.

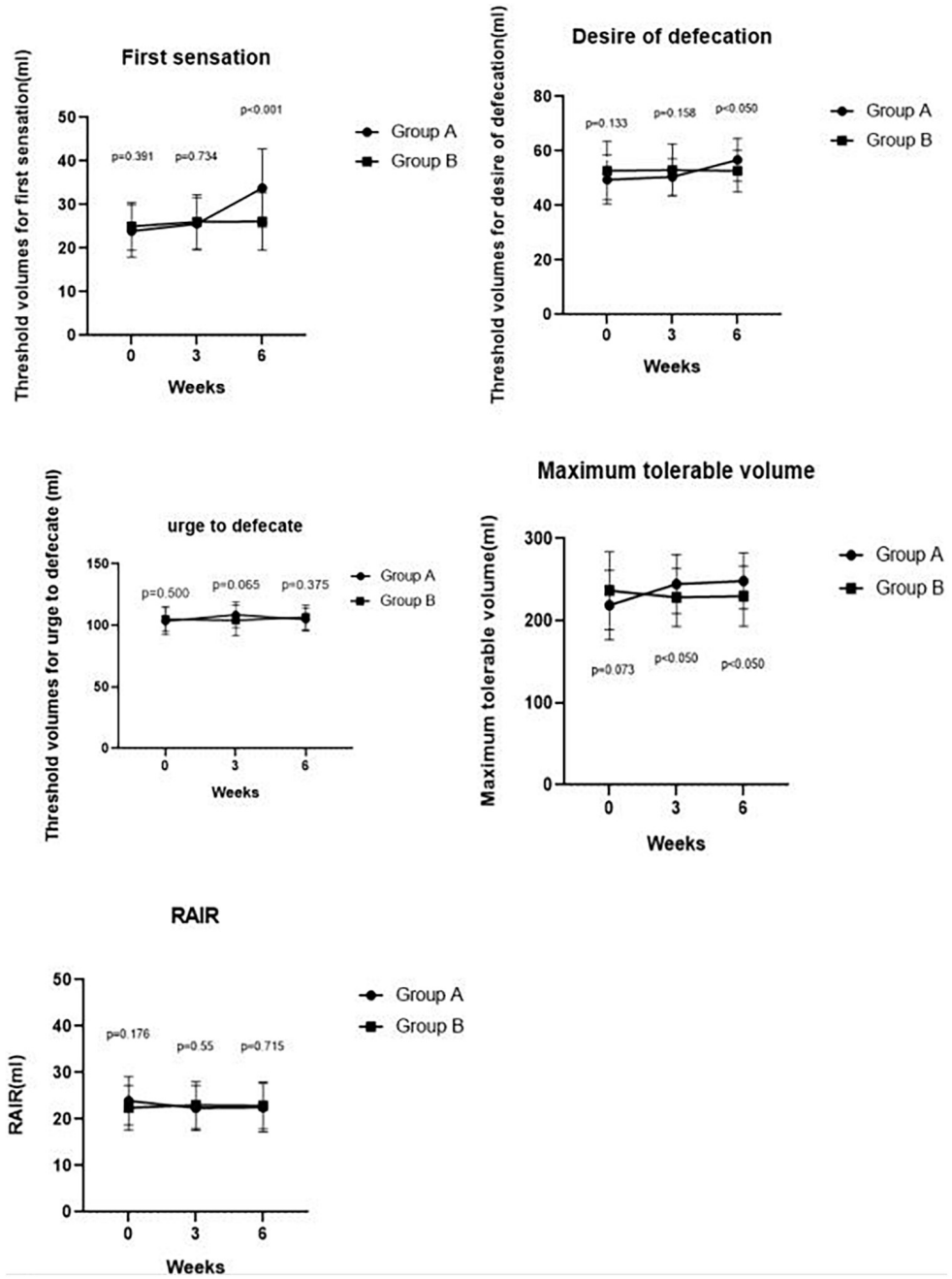

FIGURE 3
Comparing RAIR, threshold volumes for the first sensation, the desire to defecate, urge to defecate and maximum tolerable volume pre-treatment and post-treatment at weeks 3, 6 between Groups A and B. We found a significant difference in the maximum tolerable volume between Groups A and B at week 3 ($p < 0.050$). We also found significant differences in the first sensation, desire to defecate, and maximum tolerable volume between Groups A and Group B at week 6 ($p < 0.001$, $p < 0.050$, and $p < 0.050$, respectively).

Katherine Jurek et al. (2022) found that IBS symptom severity was unaltered after 4 weeks of SDB intervention. However, our study found that IBS-SSS was ameliorated significantly after 6 weeks of SDB treatment. This difference could be attributed to different durations of treatment used in the two studies. However, our outcome of improved IBS symptoms is similar to studies by Silva and Motta (2013) and Zivkovic et al. (2017). Specifically, Silva and Motta (2013) found that the use of breathing exercises increased defecation frequency after 6 weeks for constipation patients but fecal incontinence remained unchanged, concluding that SDB may be a useful treatment for constipation. Similarly, Zivkovic et al. (2017)

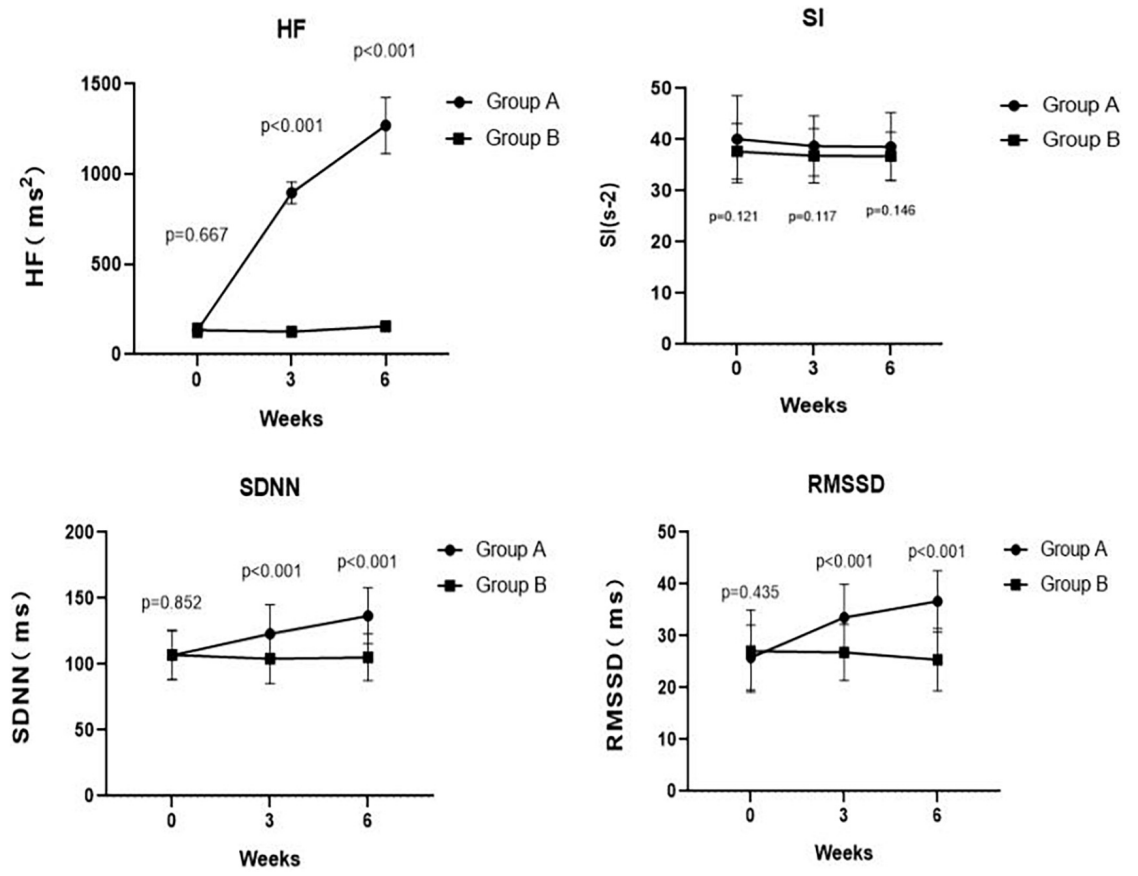

FIGURE 4
Comparing traditional or corrected HF, SI, SDNN, and RMSSD pre- and post-treatment at weeks 3, 6 between Groups A and B. The corrected HF in Group A was significantly higher than the HF in Group B at week 3 ($p < 0.001$) and at week 6 ($p < 0.001$). There was no significant difference in SI between Group A and Group B at week 3 ($p = 0.117$) and at week 6 ($p = 0.146$). At weeks 3, 6, the SDNN in Group A was significantly higher than that in Group B ($p < 0.001$ and $p < 0.001$, respectively). Meanwhile, at weeks 3, 6, the RMSSD in Group A was significantly higher than that in Group B ($p < 0.001$ and $p < 0.001$, respectively).

demonstrated that significant improvement in defecation frequency was experienced after diaphragmatic breathing exercises treatment in children with chronic constipation and fecal incontinence. The authors concluded that breathing exercises could be considered effective complementary therapy for bowel dysfunction. Meanwhile, emerging evidence suggest a positive effect of breath training on gastroesophageal reflux disease (GERD) symptoms, indicating that inspiratory muscle training could train crural fibers, positively influencing the antireflux barrier (Casale et al., 2016). However, it is worth mentioning that the outcome of our present study regarding IBS symptoms was represented only by changes in subjective data. Therefore, the possible mechanism of SDB still needs to be further explored.

Imbalance in autonomic system has been considered a pathophysiological factor for development of IBS. Our previous study (Yu et al., 2019) found that deep breathing training is effective for GERD patients with increasing lower esophageal sphincter pressure and decreasing gastroesophageal acid reflux, which may be mediated by increasing vagal activity. In a randomized controlled trial investigating the effects of SDB on HRV of healthy adults, Lee et al. (2021) found that healthy adults receiving SDB intervention had higher values of alpha to high-beta wave and higher HF value than control group, indicating a significant change in autonomic function between SDB intervention group and control group. However, SDB can induce respiratory peak shifting, and the effect of respiration on HRV is displayed as a respiratory peak, which is located in the HF band. Thus, without the simultaneous analysis of the respiration rate, the changes in HF power should not be regarded as definitive evidence of changes in autonomic balance. To correct the effect of a slow breathing rate on respiratory peak shift, which in turn influences the spectral analysis, we referenced the enhanced method of Li et al. (2018) and used CFRP at 0.65 Hz to correct the conjunction between HF bands of HRV. Our corrected spectral analysis showed that SDB enhanced vagal activity,

which is similar to the results obtained by Chang et al. (2013). Interestingly, no difference was observed in sympathetic activity, which was represented by SI. Meanwhile, to avoid the influence of SDB on HF, the time domain HRV parameters, including SDNN and RMSSD, were extracted based on the time between the individual R-peaks. The outcomes of time-domain analysis in this study shown that SDB increased the RMSSD and indicated that SDB might enhance vagal activity, which is similar to the results obtained by Rovsing et al. (2021).

A recent study by Gholamrezaei et al. (2022) also observed that SDB could decrease visceral pain intensity. Botha et al. (2015) reported that the development of acid-induced esophageal hypersensitivity could be prevented by deep breathing. Visceral hypersensitivity has been confirmed as playing a key role in the pathophysiology of functional gastrointestinal disorders, such as non-cardiac chest pain, heartburn, and IBS (Simrén et al., 2018). Notably, visceral hypersensitivity is regarded as the most important pathophysiological mechanism for the development of IBS. It has been found that IBS patients are more likely to report lower volumes or pressures of first sensation of rectal pain than healthy adults (Whitehead et al., 1990; Bradette et al., 1994). A previous study found no difference in rectal compliance between IBS patients and control subjects and significantly higher sensory threshold of volumes for rectosigmoid discomfort and pain in healthy controls than in IBS patients, indicating the role of visceral hypersensitivity in IBS (Whitehead et al., 1990). Moreover, the phenomenon of hypersensitivity in IBS patients is not only limited to the rectum and colon, but it is also associated with the whole digestive tract, suggesting that alteration of visceral sensation may present as a pan-intestinal phenomenon. Trimble et al. (1995) reported that lower rectal sensory thresholds in IBS patients than in controls and lower sensory threshold volumes for both first sensation and pain evoked by balloon distension of the esophagus. In the current study, we found an increase in maximum tolerable volume to anorectal balloon distension in IBS-C patients after 3 weeks of SDB treatment. Moreover, a higher threshold of volumes for first sensation, desire of defecation, and maximum tolerable volume were observed in IBS-C patients after 6 weeks of SDB treatment compared with the control group. Overall, we detected altered rectal hypersensitivity in constipated IBS patients following SDB, but the effect of SDB on IBS-C warrants further investigation.

Limitations

Some potential shortcomings need to be noted in this study. First, the values of rectal sensory thresholds tested using HRAM were subjectively recorded through patients' self-reports. Therefore, the difference in the sensory threshold may be statistically significant but certainly not clinically significant as we analyzed no subgroup of patients. Second, sensory test in the current study was performed using HRAM with water perfusion, whereas most recent studies were implemented using solid state catheters. Although no differences at rest between the two types of catheters were reported in previous studies, greater sensitivity to rapid pressure changes was observed in solid-state catheters compared with water perfusion, which may lead to different results (Liem et al., 2012; Rasijeff et al., 2017). Finally, the sample size in this study was quite small and therefore large-scale multicenter studies are warranted in the future to explore this relationship. The relationship between SDB and its impact on visceral hypersensitivity in IBS-C also needs further verification.

Conclusion

Overall, we explored the association between SDB and its impact on IBS-C symptoms and rectal sensation in patients with IBS-C. We found improved symptoms and altered rectal sensitivity after a 6-week SDB intervention for patients with IBS-C. Moreover, the effect of SDB on IBS-C symptoms might be mediated by increased vagal modulation.

Data availability statement

The raw data supporting the conclusions of this article will be made available by the authors, without undue reservation.

Ethics statement

The studies involving human participants were reviewed and approved by Ethics Committee of the First Affiliated Hospital of USTC (Registration No: 2022-RE-142). The patients/participants provided their written informed consent to participate in this study.

Author contributions

YY planned the study and revised the manuscript critically. JL, CL, WW, YH, BW, JT, and YY performed the

SDB and HRAM. JL and CL collected and interpreted the data. JL and CS drafted the manuscript. All authors read and approved the final manuscript.

Funding

This study was supported by the External Science and Technology Cooperation Planning Projects of Anhui Province of China (No. 1604b0602021).

Acknowledgments

We appreciate all subjects who participated in this research.

Conflict of interest

The authors declare that the research was conducted in the absence of any commercial or financial relationships that could be construed as a potential conflict of interest.

Publisher's note

References

Ali, M. K., Liu, L., Chen, J. H., and Huizinga, J. D. (2021). Optimizing autonomic function analysis via heart rate variability associated with motor activity of the human colon. *Front. Physiol.* 12:619722. doi: 10.3389/fphys.2021.619722

American College of Gastroenterology Task Force on Irritable Bowel Syndrome, Brandt, L. J., Chey, W. D., Foxx-Orenstein, A. E., Schiller, L. R., Schoenfeld, P. S., et al. (2009). An evidence-based position statement on the management of irritable bowel syndrome. *Am. J. Gastroenterol.* 104(Suppl. 1), S1–S35. doi: 10.1038/ajg.2008.122

Ballou, S., McMahon, C., Lee, H. N., Katon, J., Shin, A., Rangan, V., et al. (2019). Effects of irritable bowel syndrome on daily activities vary among subtypes based on results from the IBS in America survey. *Clin. Gastroenterol. Hepatol.* 17, 2471–2478.e3. doi: 10.1016/j.cgh.2019.08.016

Barberio, B., Savarino, E. V., Black, C. J., and Ford, A. C. (2021). Adverse events in trials of licensed drugs for irritable bowel syndrome with constipation or diarrhea: Systematic review and meta-analysis. *Neurogastroenterol. Motil.* 34:e14279. doi: 10.1111/nmo.14279

Black, C. J., Burr, N. E., and Ford, A. C. (2020). Relative efficacy of tegaserod in a systematic review and network meta-analysis of licensed therapies for irritable bowel syndrome with constipation. *Clin. Gastroenterol. Hepatol.* 18, 1238–1239.e1. doi: 10.1016/j.cgh.2019.07.007

Botha, C., Farmer, A. D., Nilsson, M., Brock, C., Gavrila, A. D., Drewes, A. M., et al. (2015). Preliminary report: Modulation of parasympathetic nervous system tone influences oesophageal pain hypersensitivity. *Gut* 64, 611–617. doi: 10.1136/gutjnl-2013-306698

Bradette, M., Delvaux, M., Staumont, G., Fioramonti, J., Bueno, L., and Frexinos, J. (1994). Evaluation of colonic sensory thresholds in IBS patients using a barostat. Definition of optimal conditions and comparison with healthy subjects. *Dig. Dis. Sci.* 39, 449–457. doi: 10.1007/BF02088327

Bruehl, S., and Chung, O. Y. (2004). Interactions between the cardiovascular and pain regulatory systems: An updated review of mechanisms and possible alterations in chronic pain. *Neurosci. Biobehav. Rev.* 28, 395–414. doi: 10.1016/j.neubiorev.2004.06.004

Busch, V., Zeman, F., Heckel, A., Menne, F., Ellrich, J., and Eichhammer, P. (2013). The effect of transcutaneous vagus nerve stimulation on pain perception–an experimental study. *Brain Stimul.* 6, 202–209. doi: 10.1016/j.brs.2012.04.006

Camilleri, M. (2021). Diagnosis and treatment of irritable bowel syndrome: A review. *JAMA* 325, 865–877. doi: 10.1001/jama.2020.22532

Casale, M., Sabatino, L., Moffa, A., Capuano, F., Luccarelli, V., Vitali, M., et al. (2016). Breathing training on lower esophageal sphincter as a complementary treatment of gastroesophageal reflux disease (GERD): A systematic review. *Eur. Rev. Med. Pharmacol. Sci.* 20, 4547–4552.

Chang, Q., Liu, R., and Shen, Z. (2013). Effects of slow breathing rate on blood pressure and heart rate variabilities. *Int. J. Cardiol.* 169, e6–e8. doi: 10.1016/j.ijcard.2013.08.121

Clarke, T. C., Black, L. I., Stussman, B. J., Barnes, P. M., and Nahin, R. L. (2015). Trends in the use of complementary health approaches among adults: United States, 2002-2012. *Natl. Health Stat. Rep.* 79, 1–16.

Drossman, D. A. (2016). Functional gastrointestinal disorders: History, pathophysiology, clinical features and Rome IV. *Gastroenterology* 150, 1262–1279.e2. doi: 10.1053/j.gastro.2016.02.032

Ford, A. C., Lacy, B. E., and Talley, N. J. (2017). Irritable bowel syndrome. *N. Engl. J. Med.* 376, 2566–2578. doi: 10.1056/NEJMra1607547

Ford, A. C., Sperber, A. D., Corsetti, M., and Camilleri, M. (2020). Irritable bowel syndrome. *Lancet* 396, 1675–1688. doi: 10.1016/S0140-6736(20)31548-8

Francis, C. Y., Morris, J., and Whorwell, P. J. (1997). The irritable bowel severity scoring system: A simple method of monitoring irritable bowel syndrome and its progress. *Aliment. Pharmacol. Ther.* 11, 395–402. doi: 10.1046/j.1365-2036.1997.142318000.x

Gholamrezaei, A., Van Diest, I., Aziz, Q., Pauwels, A., Tack, J., Vlaeyen, J. W. S., et al. (2022). Effect of slow, deep breathing on visceral pain perception and its underlying psychophysiological mechanisms. *Neurogastroenterol. Motil.* 34:e14242. doi: 10.1111/nmo.14242

Hill, L. K., and Siebenbrock, A. (2009). Are all measures created equal? Heart rate variability and respiration – biomed 2009. *Biomed. Sci. Instrum.* 45, 71–76.

Holtmann, G. J., Ford, A. C., and Talley, N. J. (2016). Pathophysiology of irritable bowel syndrome. *Lancet Gastroenterol. Hepatol.* 1, 133–146. doi: 10.1016/S2468-1253(16)30023-1

Jafari, H., Courtois, I., Van den Bergh, O., Vlaeyen, J. W. S., and Van Diest, I. (2017). Pain and respiration: A systematic review. *Pain* 158, 995–1006. doi: 10.1097/j.pain.0000000000000865

Katherine Jurek, M., Seavey, H., Guidry, M., Slomka, E., and Hunter, S. D. (2022). The effects of slow deep breathing on microvascular and autonomic function and symptoms in adults with irritable bowel syndrome: A pilot study. *Neurogastroenterol. Motil.* 34:e14275. doi: 10.1111/nmo.14275

Lacy, B. E., Chey, W. D., and Lembo, A. J. (2015). New and emerging treatment options for irritable bowel syndrome. *Gastroenterol. Hepatol. (N Y)* 11(4 Suppl. 2), 1–19.

Lee, S. H., Lee, H. J., and Park, D. S. (2021). Effects of deep and slow breathing on stress stimulation caused by high-intensity exercise in healthy adults. *Psychol. Health Med.* 26, 1079–1090. doi: 10.1080/13548506.2020.1786138

Lee, T. H., and Bharucha, A. E. (2016). How to perform and interpret a high-resolution anorectal manometry test. *J. Neurogastroenterol. Motil.* 22, 46–59. doi: 10.5056/jnm15168

Lewis, S. J., and Heaton, K. W. (1997). Stool form scale as a useful guide to intestinal transit time. *Scand. J. Gastroenterol.* 32, 920–924. doi: 10.3109/00365529709011203

Li, C., Chang, Q., Zhang, J., and Chai, W. (2018). Effects of slow breathing rate on heart rate variability and arterial baroreflex sensitivity in essential hypertension. *Medicine (Baltimore)* 97:e0639. doi: 10.1097/MD.0000000000010639

Liem, O., Burgers, R. E., Connor, F. L., Benninga, M. A., Reddy, S. N., Mousa, H. M., et al. (2012). Solid-state vs water-perfused catheters to measure colonic high-amplitude propagating contractions. *Neurogastroenterol. Motil.* 24, 345–e167. doi: 10.1111/j.1365-2982.2011.01870.x

Liu, J., Lv, C., Huang, Y., Wang, Y., Wu, D., Zhang, C., et al. (2021). Digital rectal examination is a valuable bedside tool for detecting dyssynergic defecation: A diagnostic study and a meta-analysis. *Can. J. Gastroenterol. Hepatol.* 2021:5685610. doi: 10.1155/2021/5685610

Liu, L., Milkova, N., Nirmalathasan, S., Ali, M. K., Sharma, K., Huizinga, J. D., et al. (2022). Diagnosis of colonic dysmotility associated with autonomic dysfunction in patients with chronic refractory constipation. *Sci. Rep.* 12:12051. doi: 10.1038/s41598-022-15945-6

Mazzone, S. B., and Undem, B. J. (2016). Vagal afferent innervation of the airways in health and disease. *Physiol. Rev.* 96, 975–1024. doi: 10.1152/physrev.00039.2015

Nahin, R. L., Stussman, B. J., and Herman, P. M. (2015). Out-of-pocket expenditures on complementary health approaches associated with painful health conditions in a nationally representative adult sample. *J. Pain* 16, 1147–1162. doi: 10.1016/j.jpain.2015.07.013

Rasijeff, A. M. P., Withers, M., Burke, J. M., Jackson, W., and Scott, S. M. (2017). High-resolution anorectal manometry: A comparison of solid-state and water-perfused catheters. *Neurogastroenterol. Motil.* 29:e13124. doi: 10.1111/nmo.13124

Reyes del Paso, G. A., Montoro, C., Muñóz Ladrón de Guevara, C., Duschek, S., and Jennings, J. R. (2014). The effect of baroreceptor stimulation on pain perception depends on the elicitation of the reflex cardiovascular response: Evidence of the interplay between the two branches of the baroreceptor system. *Biol. Psychol.* 101, 82–90. doi: 10.1016/j.biopsycho.2014.07.004

Rovsing, C., Rovsing, H., Liboriussen, C. H., Jensen, M. K., Andersen, S. S., Andersen, S. S., et al. (2021). Deep breathing increases heart rate variability in patients with rheumatoid arthritis and systemic lupus erythematosus. *J. Clin. Rheumatol.* 27, 261–266. doi: 10.1097/RHU.0000000000001300

Silva, C. A., and Motta, M. E. (2013). The use of abdominal muscle training, breathing exercises and abdominal massage to treat paediatric chronic functional constipation. *Colorectal Dis.* 15, e250–e255. doi: 10.1111/codi.12160

Simrén, M., Törnblom, H., Palsson, O. S., van Tilburg, M. A. L., Van Oudenhove, L., Tack, J., et al. (2018). Visceral hypersensitivity is associated with GI symptom severity in functional GI disorders: Consistent findings from five different patient cohorts. *Gut* 67, 255–262. doi: 10.1136/gutjnl-2016-312361

Sun, X. H., Wang, Z. F., Xin, H. W., Zhu, Y., Wang, X., Luo, J., et al. (2014). Normative values and its clinical significance of the anorectal manometry in Chinese from multi-center study. *Chin. J. Dig.* 34, 597–602.

Tanaka, T., Manabe, N., Hata, J., Kusunoki, H., Ishii, M., Sato, M., et al. (2008). Characterization of autonomic dysfunction in patients with irritable bowel syndrome using fingertip blood flow. *Neurogastroenterol. Motil.* 20, 498–504. doi: 10.1111/j.1365-2982.2007.01039.x

Trimble, K. C., Farouk, R., Pryde, A., Douglas, S., and Heading, R. C. (1995). Heightened visceral sensation in functional gastrointestinal disease is not site-specific. Evidence for a generalized disorder of gut sensitivity. *Dig. Dis. Sci.* 40, 1607–1613. doi: 10.1007/BF02212678

Whitehead, W. E., Holtkotter, B., Enck, P., Hoelzl, R., Holmes, K. D., Anthony, J., et al. (1990). Tolerance for rectosigmoid distention in irritable bowel syndrome. *Gastroenterology* 98(5 Pt 1), 1187–1192. doi: 10.1016/0016-5085(90)90332-U

Yu, Y., Wei, R., Liu, Z., Xu, J., Xu, C., and Chen, J. D. Z. (2019). Ameliorating effects of transcutaneous electrical acustimulation combined with deep breathing training on refractory gastroesophageal reflux disease mediated via the autonomic pathway. *Neuromodulation* 22, 751–757. doi: 10.1111/ner.13021

Zivkovic, V. D., Stankovic, I., Dimitrijevic, L., Kocic, M., Colovic, H., Vlajkovic, M., et al. (2017). Are interferential electrical stimulation and diaphragmatic breathing exercises beneficial in children with bladder and bowel dysfunction? *Urology* 102, 207–212. doi: 10.1016/j.urology.2016.12.038

frontiers | Frontiers in Neuroscience

TYPE Review
PUBLISHED 09 November 2022
DOI 10.3389/fnins.2022.981772

OPEN ACCESS

EDITED BY
Xiaoming Jin,
Indiana University–Purdue University Indianapolis, United States

REVIEWED BY
Yue-Li Sun,
Shanghai University of Traditional Chinese Medicine, China
Chen Chen,
Frontage Laboratories, Inc., United States

*CORRESPONDENCE
Wei Dong
dongwei@swmu.edu.cn
Changshun Bao
bcs756@126.com
Yang Yu
yuyang80@swmu.edu.cn

†These authors have contributed equally to this work and share first authorship

SPECIALTY SECTION
This article was submitted to Gut-Brain Axis, a section of the journal Frontiers in Neuroscience

RECEIVED 29 June 2022
ACCEPTED 24 October 2022
PUBLISHED 09 November 2022

CITATION
Zhang Y, Lang R, Guo S, Luo X, Li H, Liu C, Dong W, Bao C and Yu Y (2022) Intestinal microbiota and melatonin in the treatment of secondary injury and complications after spinal cord injury.
Front. Neurosci. 16:981772.
doi: 10.3389/fnins.2022.981772

Intestinal microbiota and melatonin in the treatment of secondary injury and complications after spinal cord injury

Yiwen Zhang[1,2], Rui Lang[2†], Shunyu Guo[2†], Xiaoqin Luo[1], Huiting Li[3], Cencen Liu[4], Wei Dong[3*], Changshun Bao[2,5,6,7*] and Yang Yu[1,3*]

[1]Department of Human Anatomy and Histoembryology, School of Basic Medical Sciences, Southwest Medical University, Luzhou, China, [2]Department of Neurosurgery, The Affiliated Hospital of Southwest Medical University, Luzhou, China, [3]Key Laboratory of Medical Electrophysiology, Ministry of Education and Medical Electrophysiological Key Laboratory of Sichuan Province, Collaborative Innovation Center for Prevention of Cardiovascular Diseases, Institute of Cardiovascular Research, Southwest Medical University, Luzhou, China, [4]Department of Pathology, People's Hospital of Zhongjiang County, Deyang, China, [5]Sichuan Clinical Research Center for Neurosurgery, The Affiliated Hospital of Southwest Medical University, Luzhou, China, [6]Academician (Expert) Workstation of Sichuan Province, The Affiliated Hospital of Southwest Medical University, Luzhou, China, [7]Neurological Diseases and Brain Function Laboratory, The Affiliated Hospital of Southwest Medical University, Luzhou, China

Spinal cord injury (SCI) is a central nervous system (CNS) disease that can cause sensory and motor impairment below the level of injury. Currently, the treatment scheme for SCI mainly focuses on secondary injury and complications. Recent studies have shown that SCI leads to an imbalance of intestinal microbiota and the imbalance is also associated with complications after SCI, possibly through the microbial-brain-gut axis. Melatonin is secreted in many parts of the body including pineal gland and gut, effectively protecting the spinal cord from secondary damage. The secretion of melatonin is affected by circadian rhythms, known as the dark light cycle, and SCI would also cause dysregulation of melatonin secretion. In addition, melatonin is closely related to the intestinal microbiota, which protects the barrier function of the gut through its antioxidant and anti-inflammatory effects, and increases the abundance of intestinal microbiota by influencing the metabolism of the intestinal microbiota. Furthermore, the intestinal microbiota can influence melatonin formation by regulating tryptophan and serotonin metabolism. This paper summarizes and reviews the knowledge on the relationship among intestinal microbiota, melatonin, and SCI in recent years, to provide new theories and ideas for clinical research related to SCI treatment.

KEYWORDS

spinal cord injury, melatonin, intestinal microbiota, secondary injury, complications, treatment spinal cord injury, treatment

Introduction

SCI is a highly disabling disease caused by various events, including traffic accidents, fall injuries, sports injuries, and tumors triggering spinal cord compression, traction, and contusion (Zhang et al., 2017). Besides the primary injury, the subsequent secondary injury caused by inflammation, edema, free radical peroxidation, local circulatory disorder, abnormal energy metabolism, electrolyte disorder, programmed apoptosis, nitric oxide and endogenous opioid peptides, and accumulation of excitatory neurotransmitters further exacerbate the damage to the spinal cord tissue (Anjum et al., 2020). Furthermore, multiple complications after SCI including respiratory and urinary tract infections, pressure ulcer, deep vein thrombosis and pulmonary embolism, neurogenic bladder, gastrointestinal dysfunction, sexual dysfunction and so on, have become significant causes of death and low quality of life in the recovery period (Rogers and Todd, 2016). The prognosis of SCI is usually related to the degree of primary injury and the treatment of segments, injury time, secondary injury and complications. Surgery to relieve compression after injury (within 24–36 h) is considered an effective and critically effective treatment to improve the prognosis of SCI (Badhiwala et al., 2021). In addition, hyperbaric oxygen, pulse electrical stimulation, mild hypothermia therapy, acupuncture, laser puncture, rehabilitation training, and other therapies could be used to assist in the recovery of function (Huang et al., 2020). Pharmacological treatment, neurotrophic factor therapy, cell transplantation therapy, gene therapy, and intervention in signaling pathways are thought to be potentially efficient in improving the prognosis of SCI, but more clinical trials are still needed to prove their effectiveness (Badhiwala et al., 2021). SCI has different pathological changes in various periods. Acute (= 2–48 h), and sub-acute (=14 days) after SCI, pathological changes such as vascular injury, ionic imbalance, free radical production, lipid peroxidation, accumulation of excitatory neurotransmitters, edema, necrosis and apoptosis occur at this stage (Faden et al., 1989; Oyinbo, 2011; Borgens and Liu-Snyder, 2012; Anjum et al., 2020). In the chronic SCI stage (> 1 month post-injury), characterized by chronic inflammation, axonal loss and maturation of glial scarring (Tran et al., 2018; Quadri et al., 2020). In addition, there are differences between acute and chronic inflammation. Following the primary injury, microglia at the injury site release proinflammatory and chemotactic factors, as well as recruit central granulocytes to mediate acute inflammation. At this time, M1 and M2 macrophages coexist (Zhou et al., 2014; Gensel and Zhang, 2015; Hellenbrand et al., 2021). In the chronic stage, M1 macrophages exist for a long time and mediate chronic inflammation with mature lymphocytes (Bastien and Lacroix, 2014; Schwab et al., 2014). Melatonin (N-acetyl-5-methoxy tryptamine) is an indole hormone secreted by the pineal gland. The pineal gland takes tryptophan in the blood as raw material and synthesizes 5-methoxy-n-acetamide through various enzymatic reactions (Vasey et al., 2021; **Figure 1**). Its secretion is regulated by circadian rhythm, inhibited during the day and active at night. In addition to the pineal gland, melatonin can also come from the intestines, skin, retina, bone marrow, platelets and other structures. However, it acts primarily locally and rarely throughout the whole body *via* blood circulation (Huether, 1993; Bubenik, 2002; Ren et al., 2017).

In terms of dosage, there is little difference between the physiological and pharmacological effects of melatonin, physiological dose provides plasma melatonin levels of the same order of magnitude as a nocturnal peak (less or around 100 pg/ml or 400 pM). Oral administration of 0.3 mg can reach the endogenous level at night (Dubocovich et al., 2010; Claustrat and Leston, 2015). In addition, continuous desensitization of receptors caused by excessive use of melatonin may affect sleep and circadian rhythm (Gerdin et al., 2004; Wurtman, 2006).

Melatonin which the CNS synthesizes has good blood-brain barrier permeability. It determines that melatonin can ensure sufficient concentration when interacting with other CNS parts through blood circulation. Melatonin is known to have a variety of biological functions, including circadian rhythm regulation, anti-inflammatory, free radical scavenging, edema reduction, suppression of the hypothalamic-pituitary endocrine axis, suppression of cancer, stimulation of mitochondrial biogenesis, immunomodulation, blood pressure regulation and the epigenetic regulation, and has therapeutic effects on a variety of secondary injuries after SCI (Giannoulia-Karantana et al., 2006; de Faria Poloni et al., 2011; Mazzoccoli et al., 2011; Xu L.X. et al., 2017; Chang et al., 2018; Onaolapo et al., 2020; Cho et al., 2021; Vasey et al., 2021). Melatonin can also regulate the intestinal biological clock and the types of intestinal microbiota, improve the metabolic disorder caused by intestinal microbiota imbalance after SCI, and indirectly play a role in the recovery of function and the treatment of complications (Paulose et al., 2016). The route of administration and detection method are simple and convenient, which are conducive to investigation and evaluation. The exogenous melatonin can be administered orally or intravenously and its concentration can be assessed by blood, saliva and so on. It is considered a more convenient and accessible approach to provide greater comfort to patients and improve their quality of life (Dermanowski et al., 2022).

The intestinal microbiota can act on the CNS through the microbial gut-brain axis. The normal microbial ecology of the intestinal tract helps the human body generate a range of vitamins, engage in carbohydrate, protein, and lipid metabolism, promote trace element absorption, proper intestinal peristalsis, feces excretion, and prevent the growth of dangerous bacteria (Blaut, 2013). The brain-gut axis seems to provide new discoveries in some CNS diseases. The brain can transmit information from top to bottom *via* the autonomic nervous system, the gut nervous system, the hypothalamus pituitary adrenal axis (HPA), and the meningeal lymphatic

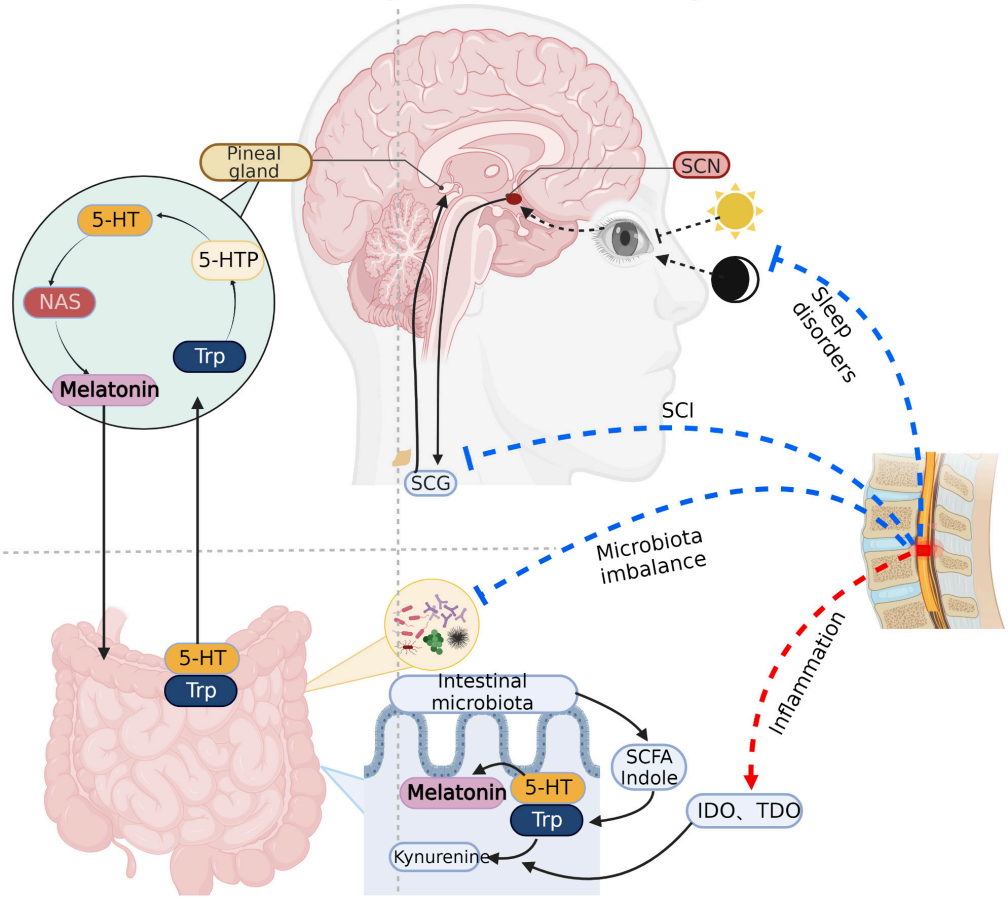

FIGURE 1
Melatonin synthesis: Pineal cells absorb tryptophan (Trp) and produce melatonin through intermediates such as 5-hydroxytryptophan (5-HTP), serotonin and N-acetyl-5-hydroxytryptamine (NAS). Substances such as indole and short chain fatty acids produced by gut microbiota also promote the synthesis of gut-derived melatonin. Light signal regulation of melatonin: Light signal received by the optic apparatus transmits to the supraoptic nucleus (SCN) of the hypothalamus, then it continues to transmit to the sympathetic cervical ganglion (SCG) through the brainstem and spinal cord, and finally arrived at the pineal gland to regulate the secretion of melatonin. Spinal cord direct damage, sleep disorders, microbiota imbalance and inflammatory will inhibit the synthesis and secretion of melatonin after SCI. IDO, Indoleamine 2, 3-dioxygenase; TDO, Tryptophan dioxygenase. Created with BioRender.com.

vessels (Yuan et al., 2021). many neurological diseases, such as depression, multiple sclerosis (MS), Alzheimer's disease (AD), Parkinson's disease, and others, can cause changes in the structure of the intestinal microbiota (Joscelyn and Kasper, 2014; Williams and Murray, 2015; Sun et al., 2018; Anderson et al., 2019). In addition, the intestine can also transmit signals from bottom to top through the vagus and immune pathways (Yuan et al., 2021). Patients with Parkinson's disease have higher levels of lipopolysaccharide (LPS) and lower levels of short-chain fatty acid (SCFA) in the intestine, leading to chronic inflammation in the CNS and promoting disease progression (Keshavarzian et al., 2015; Perez-Pardo et al., 2019). Increasing the percentage of intestinal regulatory T (Treg) cells but decreasing interleukin-17-gamma-delta T cells can alleviate nerve defects and anti-inflammation after stroke (Lee et al., 2020). Intestinal microbiota promotes the occurrence of the intracranial aneurysm by regulating plasma taurine and fatty acid levels (Li et al., 2020). It also improves neuronal degeneration, brain edema and blood-brain-barrier damage by increasing the level of glucagon-like peptide 1 (Li et al., 2018), and improves spatial learning through SCFA after traumatic brain injury (Opeyemi et al., 2021). In addition, the secretion of intestinal bacterial amyloid protein and lipopolysaccharide (LPS) promotes neuroinflammation and causes neuronal death in AD (Pistollato et al., 2016; Kesika et al., 2021). Some studies suggest that regulating stress state and HPA through fecal bacteria transplantation may be significant in treating depression (Liang et al., 2018).

SCI is usually accompanied by the destruction of intestinal ecology through mechanisms associated with disruption

of signals from higher control center, autonomic nerve dysfunction, intestinal barrier permeability change, mesenteric lymph node immune regulation, and long-term use of antibiotics (Cervi et al., 2014; Kigerl et al., 2016; Tate et al., 2016; Jing et al., 2019). Studies have shown that intestinal microbiota modulates the functional recovery after SCI through SCFA and the immune system (Jing et al., 2021b; Rodenhouse et al., 2022). Alternatively, there is evidence that fecal flora transplantation (FMT) may be effective in improving complications such as gastrointestinal dysfunction, bloating and constipation after SCI (Jing et al., 2021a). Furthermore, intestinal microbiota could directly or indirectly participate in the synthesis of melatonin. Melatonin is derived from serotonin (5-hydroxytryptamine, 5-HT). Intestinal bacteria may directly produce SCFAs, which stimulate the production of 5-HT. Then, the 5-HT is successively converted into N-acetyl-5-hydroxytryptamine (NAS) and melatonin by arylalkylamine N-acetyltransferase (AANAT, EC: 2.3.1.87) and acetylserotonin O-methyltransferase (ASMT, EC: 2.1.1.4) (Benabou et al., 2017; **Figure 1**).

As a result, a bidirectional link is observed, in which changes in intestinal microbiota influence the regulation of the melatonergic system, and treatment of melatonin cause changes in microbiota, with both factors contributing to the pathobiology and treatment of SCI. This review aims to describe the potential links among gut microbiota, melatonin, and SCI and to explore the synergistic effects of melatonin and the regulation of gut microbiota in improving the prognosis of SCI.

The relationship between melatonin and intestinal microbiota

Melatonin regulates the recovery of intestinal microbiota disorders

Melatonin affects the composition of intestinal microbiota

Melatonin regulate the intestinal microbiota, which improve the reduction of intestinal operational taxonomic unit (OTU), increase ACE index and Shannon index, decrease Simpson index, increase the diversity and abundance of intestinal microbiota, increase the abundance of firmicum and decrease the abundance of Bacteroides (Ren et al., 2018; Gao T. et al., 2020; Kim et al., 2020). Melatonin also increases Akkermansia flora's abundance (Hagi and Belzer, 2021). In the SCI mouse model, melatonin reduce the abundance of Clostridium and increase the abundance of Lactobacillus (Jing et al., 2019). Also, melatonin could increase the abundance of Myxobacteria and Streptococcus mucophaphagus (Park et al., 2020), protect intestinal barrier and reduce intestinal inflammation. In addition, melatonin enhances the abundance of bacteria and decrease the ratio of firmicum to Bacteroides in a high-fat diet-induced obesity mouse model (Xu P. et al., 2017; Yin et al., 2018). In the ochratoxina induced liver injury model, melatonin increase the abundance of Bacteroides, verrucous microorganisms and actinomycetes, while decrease the abundance of firmicum and Lactobacillus (Zhang H. et al., 2021; Zhao et al., 2021). In terms of microbial metabolism, melatonin significantly reduces the relative abundance of the microbiome in the cysteine and methionine metabolism and peptidoglycan biosynthesis pathway in the restraint stress mouse model, while increasing the relative abundance of the microbiome in the tryptophan metabolism, aminobenzoic acid degradation, renin angiotensin system, γ-aminobutyric acid ergic synapses and type II diabetes pathway (Lin et al., 2021).

Protective effect of melatonin on intestinal barrier

There are three interconnected barriers in the intestine, a biological barrier made up of the intestinal microbiota; an intestinal immune barrier made up of the intestinal lymphatic system; and a physical barrier comprising the voluntary movement of the intestine and the mucosal epithelial system (Gao et al., 2019). The fluorescein isothiocyanate labeled dextran experiment proved that the intestinal permeability in stress state would increase (Jing et al., 2019). Under stress, the number of intestinal goblet cells and intestinal gland proliferating cell nuclear antigen positive cells decreased, which affect mucus secreted and intestinal cells proliferated, and then the repair effect of intestine barrier was damaged. Meanwhile, the activation of nuclear factor-kappaB (NF-κB) pathway induced autophagy and eventually damages the intestinal mechanical barrier (Gao et al., 2019).

The expression of tight junction-related proteins claudin-1, occludin and zonula occludens-1 (ZO-1) decreased in stress models such as SCI and sleep deprivation, and melatonin is effective in improving the reduction of occludin and ZO-1 (Gao et al., 2019; Jing et al., 2019). It suggested that melatonin may strengthen the tight connection between cells, regulate intestinal permeability, repair and maintain the stability of intestinal mechanical barrier, which effectively prevent toxins and other bacterial metabolites in the intestine from entering the blood and cause cascading chain inflammatory reaction. A similar effect was also observed in the oxazolone induced colitis model (Zhao et al., 2021), indicating that melatonin's preservation of the intestinal barrier was not confined to stress damage and that its barrier protective role had a broader application. In addition, melatonin accelerates the emptying effect of the gastrointestinal tract in mice after SCI (Jing et al., 2019), demonstrating that melatonin enhances gastrointestinal function, promotes peristalsis and strengthens the mechanical barrier.

Melatonin regulates intestinal immune function and down-regulates inflammatory response

In prolonged paradoxical sleep deprivation mouse model, with the activation of the HPA, a large amount of cortisol were released into the systemic circulation, which would mediate the disturbance of intestinal microbiota (Galvão Mde et al., 2009), stimulate a cascade of transcription factors and associated signaling pathways. Cortisol activated the protein expression of the signal transducer and activator of transcription 3 (STAT-3)/activator protein 1 (AP-1)/NF-κB pathway, such as phosphorylated-signal transducer and activator of transcription-3 (p-STAT3), AP-1, p-P65 and phosphorylated-inhibitor of nuclear factor-kappaB (p-IκB), while melatonin decreased the expression of the above proteins, suggesting that melatonin suppressed inflammation and autophagy by inhibiting NF-κB pathway (Gao et al., 2021). Research has shown that the stress induces changes in intestinal permeability leading to the secretion of LPS by the intestinal microbiota which in turn activates the TLR4 inflammatory signaling pathway to release of several proinflammatory cytokine such as interleukin-1β (IL-1β), IL-6 and tumor necrosis factor-α (TNF-α) (Ghareghani et al., 2018). In a mouse model of colitis, melatonin inhibited the increase of IL-1β, IL-17 and TNF-α, whereas in TLR4 knockout mice melatonin has been found to fail to inhibit effectively the increased levels of IL-1β, IL-17, and TNF-α (Kim et al., 2020), suggesting that melatonin may suppress the LPS/TLR4 signaling pathway by inhibiting expression of pro-inflammation cytokines. In addition, the expression of anti-inflammatory factors (IL-5, IL-10, IL-22) was regulated by administration of melatonin on in a stress model (Gao et al., 2019, Gao K. et al., 2020; Lin et al., 2021), and further inhibit intestinal inflammation. It was demonstrated that in a mouse model of SCI, melatonin displayed anti-inflammatory effects by reducing the upregulation of IL-17, interferon-gamma (IFN- γ) and monocyte chemoattractant protein-1 (MCP1) (Jing et al., 2019). In the oxazolone induced colitis model, melatonin could inhibit the production of IL-5, IL-13 and their mRNA in type 2 innate lymphocytes (ILC2s) and affect the type 2 immune response (Zhao et al., 2021). Ghareghani et al. (2018) and Xiong et al. (2022) demonstrated that melatonin modulates intestinal immune function through the expression of nod-like receptor-related genes and TLRs. By differential expression gene (DEG) and gene ontology (GO) analysis, *Tlr1*, *Tlr2*, *Tlr7*, *Cd14*, *Naip*, *Cxcl8* and *Nlrp1*, *Nlrp3* gene expression levels were found to be significantly increased in ASMT (a key enzyme in the acetyl serine synthesis melatonin pathway) overexpressing transgenic sheep (Li et al., 2021). It is suggested that melanin plays an important role by regulating anti-inflammatory related factors and signaling pathways. In general, melatonin can regulate the immune response by regulating intestinal TLRs and nod like receptors, and affect the type 2 immune response by inhibiting ILC2s. It also inhibits the STAT-3/AP-1/NF-κB pathway, down-regulating the release of inflammatory factors and up-regulating anti-inflammatory factors, suppressing the intestinal inflammatory response and setting the stage for ecological recovery of the microbiota.

Intestinal microbiota affects melatonin secretion

Melatonin is abundant in the gastrointestinal tract, with approximately 10–100 times more melatonin in the gastrointestinal tissues than in the blood and 400 times more in the gut than in the pineal gland (Huether, 1993; Bubenik, 2002). Intestinal microbiota can affect melatonin secretion through a variety of mechanisms. High dietary fiber diet promoted the increase of intestinal short chain fatty acid concentration and 5-HT concentration in serum and intestinal mucosa, and promoted the up-regulation of tryptophan hydroxylase (TPH1) mRNA level (Zhuo et al., 2021). Besides, intestinal microbial metabolites, short chain fatty acids such as propionic acid and butyric acid, and tryptophan metabolite indoles can promote the production of 5-HT, which in turn further affects melatonin secretion *via* AANAT and ASMT (Gao et al., 2018; **Figure 1**).

Intestinal microbial sulfatase can promote melatonin secretion (Ervin et al., 2020). The experiments in zebrafish have proved that probiotics and dark conditions can increase the mRNA expression of melatonin receptor genes, mainly melatonin-1 related receptor genes (*Mtnr1ba* and *Mtnr1bb*) (Lutfi et al., 2021). The disturbance of intestinal microbiota affect the absorption of vitamins, which cause deficiencies in enzyme cofactors. In addition, the disruption of intestinal microbiota induces intestinal inflammatory reaction. Inflammatory and deficiencies of enzymatic cofactors would trigger the kynurenine metabolic pathway, promoting the synthesis of tryptophan into kynurenine and inhibiting the synthesis of tryptophan into 5-hydroxytryptamine and melatonin (Rudzki et al., 2021).

Spinal cord injury and intestinal microbiota

The imbalance of intestinal microbiota has been proved to be related to various CNS diseases. Firmicutes and Bacteroides are two phylum of intestinal microbiota, both of them contain probiotics and opportunistic pathogens, which have dual effects on human body (Wexler and Goodman, 2017; Heintz-Buschart and Wilmes, 2018). Intestinal microbiota can produce short-chain fatty acids by metabolizing dietary fiber (Markowiak-Kopeć and liżewska, 2020). Previous studies found that obese people have higher level of Firmicutes and lower level of Bacteroides (Ley et al., 2005, 2006). In addition, another study found that obese people have higher levels of SCFA

(Schwiertz et al., 2010), proving that the level of SCFA is directly proportional to Firmicutes.

Studies have confirmed that intestinal microbiota is disordered after SCI, which is manifested by the decrease of the abundance of Firmicutes, with or without the increase of bacteroides, resulting in the change of the ratio of Firmicutes to Bacteroides, this change in microbiota structure affects the production of short-chain fatty acids (Gungor et al., 2016; Zhang et al., 2018; Jing et al., 2019; Bazzocchi et al., 2021; Rodenhouse et al., 2022), this appears to be associated with severe inflammation and complex infection after SCI. There are significant differences in intestinal microbiota composition in patients after SCI in the acute and chronic stages. There is greater abundance of genus Sutterella in the acute stage, it may be related to more severe inflammation (Santoru et al., 2017). In the chronic stage, it had lower abundances of the Burkholderiaceae family. But with the increase of exercise, the abundance of Burkholderiaceae increases. It suggests that long-term inactivity after SCI may lead to this difference (Li et al., 2022). The changes in intestinal microbiota after SCI are related to the degree of injury. In American Spinal Injury Association Impairment Scale (AIS) A or B patients, the abundance of lactobacillus is higher, and in AIS C or D patients, Bacteroides, Faecalibacterium, Lachnospiraceae are more abundant (Bazzocchi et al., 2021). A study of patients with complete spinal cord injury (CTSCI) and incomplete spinal cord injury (ITSCI) has found that the abundance of Synergistetes is significantly different between CTSCI and ITSCI. Coriobacteriae, Eubacterium, and Cloacibacillus is more abundant in CTSCI, Lactobacillaceae, Lachnospiraceae, Eubacteria, Clostridium, and Sutterella is more abundant in ITSCI (Yu et al., 2021). Different levels of SCI will also lead to the different intestinal microbiota. Zhang et al. (2018) found that the abundance of Bacteroides is higher in quadriplegia patient, while Acidaminococcaceae, Blautia, Porphyromonadaceae, and Lachnoclostridium is higher in paraplegia patient. Another study pointed out that the Firmicutes in T10 is low, while actinomycetes in T4 and T10 are increased (Du et al., 2021).

The causes of intestinal microbiota imbalance after spinal cord injury

Control interruption of advanced center, autonomic nerve function, and intestinal nerve function disorder

The regulation of intestinal function is actually co-regulated by sympathetic, parasympathetic and enteric nervous system (ENS) (Furness et al., 2014). After SCI, the injured ascending and descending neurons cannot dominate the lower neurons below the injured segment, nor can they transmit the information of lower neurons to the brain. The interruption of the control of the advanced center leads to the loss of gastrointestinal and bladder sympathetic control, smooth muscle dysfunction, impaired intestinal movement, fecal retention or incontinence (Holmes et al., 2020), and these variables are maintained throughout the acute to chronic phase of SCI. It has been studied to exclude the influence of sympathetic and parasympathetic on intestinal tract by injuring the high level thoracic spinal cord, in the mice with T8 SCI, it found that the number of nitroergic nerve cells decreased, and the number of acetylcholine decreased although the proportion of acetylcholinergic nerve did not change significantly (Lefèvre et al., 2020). Another study found that nitroergic and cholinergic neurons decreased in the mice with T3 SCI (White et al., 2020). These results suggest that the ENS is damaged after SCI, which lead to the destruction of colonic content secretion, propulsion and local reflex regulation related to colonic segmentation (Furness et al., 2014).

Immune regulation and inflammation of mesenteric lymph node gut-associated lymphoid tissue

Gut-associated lymphoid tissue (GALT) is innervated by the sympathetic nerve of the spinal cord. The loss of control of the sympathetic nerve destroys the immune homeostasis of GALT after SCI (Straub et al., 2006), further affecting the regulation of the intestinal immune system on the intestinal microbiota. Kigerl et al. (2016) found that the expression of TNF, IL-10, IL-1β, and transforming growth factor-β (TGF-β) is increased in mesenteric lymph nodes on the third day after SCI, and Li et al. (2022) found that different flora changes in the feces of patients in the acute stage of SCI compared with those in the chronic stage. In 8-week SCI animals, it has been found that IL-1β is significantly associated with 23 OTUs, and 12 OTUs were found to be significantly correlated to IL-12. Although macrophage inflammatory protein 2 is especially related to the difference in microbial diversity, no significant OTU is detected (O'Connor et al., 2018). It indicates that the occurrence of acute and chronic inflammation after SCI mediates the destruction of intestinal ecology.

Changes in intestinal epithelial barrier dysfunction

Intestinal epithelial barrier dysfunction has proved after SCI (Liu et al., 2020, 2021). The change leads to more opportunities for bacteria and their metabolites to enter the circulation, cause enterogenous infection, and further lead to the disorder of flora. Studies have shown that SCI affects the intestinal epithelial barrier and induces intestinal disturbances, leading to delayed motor recovery in mice (Kigerl et al., 2016).

Long-term use of antibiotics

Numerous studies have reported that many antibiotics exert anti-inflammatory and neuroprotective effects in different central and peripheral nervous system disorders, including SCI.

But long-term use of antibiotics may further aggravate the disturbance of intestinal microbiota after SCI, inducing the increase of firmicum, Proteus and Actinobacillus the decrease of Bacteroides, and affecting the functional recovery after SCI (Jing et al., 2019; Bazzocchi et al., 2021; Rodenhouse et al., 2022). However, as an antibiotic, dimethylaminocycline has largely ignored its negative effects on intestinal microbiota and systemic immune response after SCI, which may be related to its direct anti-inflammatory, anti-oxidation, anti-anxiety, and neuroprotective properties (Schmidt et al., 2021).

Improving the dysfunctional flora structure is beneficial to the functional recovery after spinal cord injury

Short-chain fatty acid regulate the inflammatory process and inhibit the neurotoxicity and secondary injury of microglia

Microglia can rapidly transform into activated macrophages and produce toxic molecules that mediate lipid peroxidation, eventually leading to subsequent tissue damage and axonal contraction after SCI (Busch et al., 2009; Kigerl et al., 2009). Moreover, glial cells increase pain hypersensitivity by releasing various signal molecules, such as proinflammatory cytokines (DeLeo and Yezierski, 2001; Watkins et al., 2001; Hanisch, 2002). Short-chain fatty acids have strong anti-inflammatory effects on macrophages (Park et al., 2005; Chen et al., 2007) and inhibit CNS inflammation through the brain-gut axis. Patients with SCI have significantly lower levels of butyric acid producing bacteria, and the decreased butyric acid levels lead to reduce inhibition of microglia, resulting in microglia-mediated neurotoxicity, which may also be responsible for the persistent triggering of neuropathic pain. Low butyric acid levels may affect long-term functional recovery after SCI (Gungor et al., 2016). Another study demonstrated that probiotic-transplanted mice could reduce inflammatory response by increasing the production of SCFAs, which modulate gut immunological and barrier functions by inhibiting NF-κB signaling (Jing et al., 2021b; **Figure 2**). At the early stage of SCI, the level of Firmicutes decreases and Bacteroides increases, which affect the production of SCFA (Jing et al., 2021a). However, most studies of FMT for SCI have chosen in the chronic phase of SCI. Therefore, the alteration of intestinal flora after the intervention of intestinal flora in the acute phase of SCI need to be studied in depth.

Adjustment of flora structure to improve the function after spinal cord injury

It is suggested that probiotic transplantation to reconstitute the intestinal microbiota is beneficial in promoting functional recovery after SCI. In mice involved in the transplantation of probiotics to reconstitute the gut microbiota after SCI, the action evoked potential (MEP) amplitude was significantly higher in the probiotic-transplanted mice than in the SCI group. In addition, the number of NeuN + cells, NF-200 - positive cells, and the expression of synapsin increased in probiotic-transplanted mice, which suggested that probiotic transplantation may promote the survival of neurons and axonal regeneration after SCI (Jing et al., 2021a; **Figure 2**). On the other hand, transplantation of probiotics before SCI could reduce the loss of function after injury, and can effectively improve the flora structure disorder caused by antibiotics, which is considered to be positive significance for the recovery of neural function after SCI (Rodenhouse et al., 2022).

Intestinal microbiota contributes to the treatment of autonomic nervous function complications

There are many related chronic complications after SCI, such as intestinal dysfunction, bladder dysfunction and sexual dysfunction (**Figure 3**), severely impair the quality of life. Studies have shown that compared with other complications, patients with SCI want to solve the problem of intestinal dysfunction (Glickman and Kamm, 1996; Lynch et al., 2001; Anderson, 2004; Zhang et al., 2018). Neurogenic motor gut dysfunction usually occurs after SCI, and it can be further classified into upper motor meta gut syndrome (UMN) and lower motor gut syndrome (LMN). In the mouse model, the mice that recovered the structure of intestinal microbiota after fecal microbiota transplantation showed faster gastrointestinal transit through barium gavage followed by X-ray imaging (Jing et al., 2021b).

After SCI, neurogenic bladder would also occur, resulting in urinary retention and incontinence, which further cause urinary system infection. It has been reported that the annual urinary tract infection rates of upper motor neuron intestinal syndrome group and lower motor neuron intestinal syndrome group were 3.0 ± 1.8 and 2.6 ± 1.8, respectively (Gungor et al., 2016). It has been proved that the transplantation of intestinal microbiota could improve refractory urinary tract infection (Tariq et al., 2017; Biehl et al., 2018; Magruder et al., 2019, 2020), which may be related to the change of dominant bacteria inhibiting the growth and colonization of pathogenic bacteria, but it still needs more in-depth research and prospective studies to explore the molecular mechanisms and confirm. C. J. Worby summarized that the influence of intestinal microbiota of urinary tract infection may come from three aspects. Firstly, the causative organisms of urinary tract infections come from the gut microbiota. Furthermore, a specific gut microbiota provides a suitable living environment for urinary tract infections. Eventually disturbances in the gut microbiota modulate the immune system (Worby et al., 2022). Therefore, improving the gut microbiota positively affects urinary tract infections.

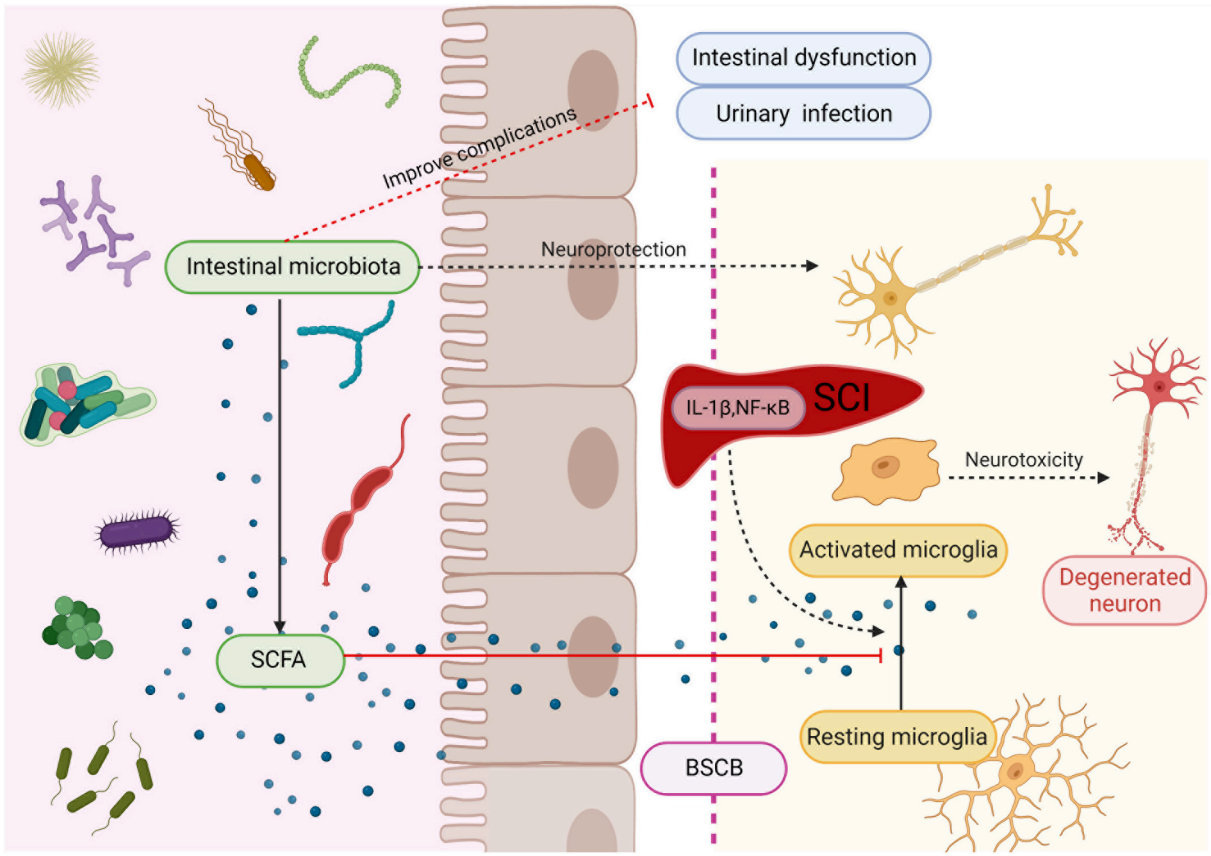

FIGURE 2
Intestinal microbiota protects neuron and improves complications after SCI. Microbiota secretes SCFA to regulate maturation and activation of microglia, thereby suppressing their neurotoxicity. Created with BioRender.com.

The relationship between spinal cord injury and melatonin

Effect of spinal cord injury on melatonin secretion

SCI in different spinal cord segments lead to significantly disparate degrees of melatonin secretion. Studies have shown that the level of cortisol in thoracic SCI was higher, and the level of melatonin in cervical SCI was lower (Thøfner Hultén et al., 2018). It was found that melatonin levels were significantly lower in patients with completed cervical SCI than in the thoracolumbar SCI group and the normal group. Furthermore, melatonin levels appear to differ between patients with complete and incomplete SCI, but *in vivo* and *in vitro* experimental verification is lacking, and this hypothesis requires further experimental validation (Whelan et al., 2020). It has been previously confirmed that the secretion rhythm of melatonin is related to the suprachiasmatic nucleus (SCN) of the hypothalamus (Cardinali and Pévet, 1998). The nerve from SCN to the pineal gland passes through the upper part of the cervical spinal cord and connects with the preganglionic cells of the sympathetic cervical ganglion (SCG) (Møller and Baeres, 2002), which indicates that melatonin secretion is related to cervical spinal cord segments (**Figure 1**).

In addition, the change of melatonin secretion level may be related to sleep disorders after SCI (Hultén et al., 2020). An investigation on sleep disorders in patients with cervical myelopathy reported that spinal cord compression and area reduction were independent risk factors for sleep disorders. Therefore, patients with compression SCI caused by spinal canal stenosis are prone to sleep disorders, and subsequently affect melatonin secretion (Kim et al., 2021).

Melatonin has a beneficial effect on the treatment of spinal cord injury

Melatonin has been proved by many studies to improve motor function recovery after SCI (Shen et al., 2017; Jing et al., 2019; Li et al., 2019; Wang K. et al., 2019; Xu et al., 2019;

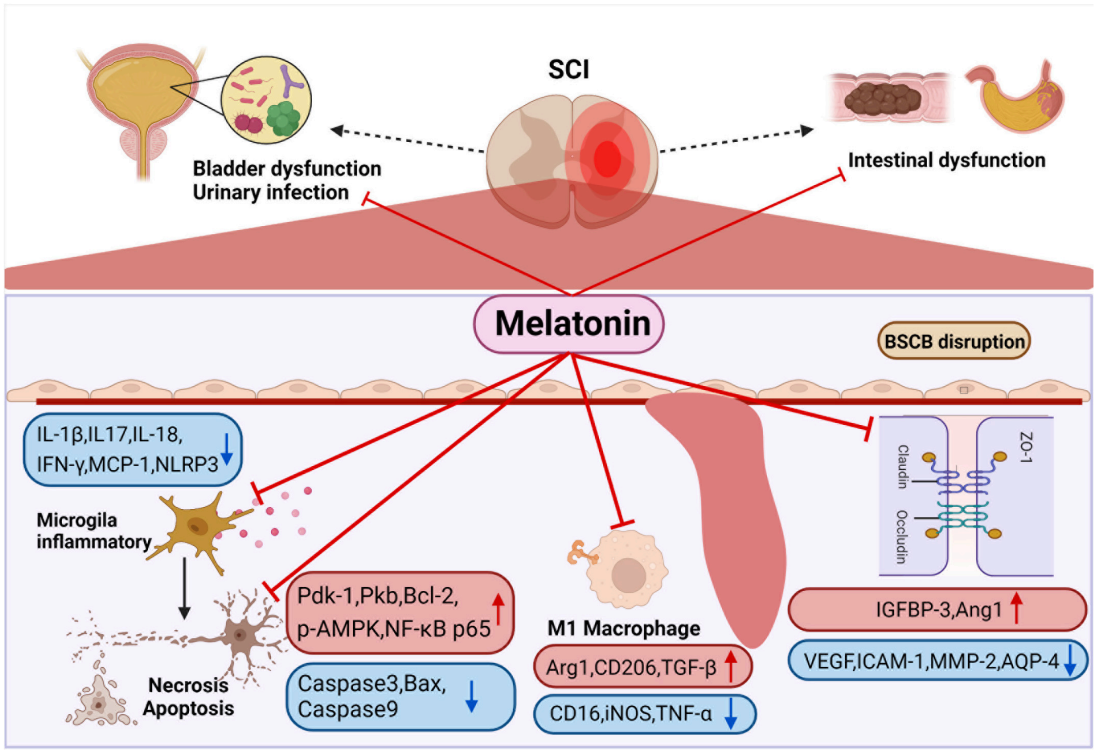

FIGURE 3
Smooth muscle dysfunction leads to constipation and fecal incontinence after SCI. Melatonin can enhance intestinal motility to promote emptying. It can also improve colonizing dominant bacteria abundance to reduce the probability of urinary infection. Melatonin inhibits the activation of M1 macrophage after SCI, the release of a variety of inflammatory factors are suppressed, and at the same time regulates apoptosis-related proteins to inhibit the apoptosis of nerve cells. In addition, melatonin regulates channel-related proteins to maintain the stability of blood-spinal cord barrier and reduce edema. Created with BioRender.com.

Gao K. et al., 2020; Majidpoor et al., 2020; Yang et al., 2020; Bi et al., 2021a), which is closely related to the anti-inflammatory, anti-apoptotic, tissue edema reducing, blood spinal cord barrier (BSCB) protection and nerve remodeling functions of melatonin (**Figure 3**). It was demonstrated that melatonin treatment significantly reduced the relative abundance of Clostridium perfringens, markedly increased the relative abundance of Lactobacillus, and dramatically improved function after SCI (Jing et al., 2019). In addition, melatonin can be used in combination with various treatment methods to treat SCI. For instance, polylactic acid glycolic acid copolymer sustained-release microspheres with melatonin and laponite hydrogel for mixed injection to treat SCI (Zhang M. et al., 2021). The use of melatonin in extracellular vesicles of stem cells reduces the levels of N6 methyladenosine modification (m6A) and methyltransferase 3 (METTL3) in SCI, and enhances the stability of USP29mRNA in MSCs, which also promote stem cell proliferation, differentiation, neurosphere formation and secretion of neurotrophic factors (Li et al., 2017; Zheng et al., 2017). In general, melatonin plays the role of anti-inflammatory, anti-apoptotic, tissue edema reducing, blood polar core barrier protection and nerve remodeling functions in acute and sub-acute stages.

Neuroprotective function of melatonin

Melatonin was effective in ameliorating neuronal apoptosis and consequently protecting neurons after SCI (Jing et al., 2017; Shen et al., 2017; Zheng et al., 2017; Li et al., 2019; Xu et al., 2019; Gao K. et al., 2020; Bi et al., 2021a). It has been found that melatonin treatment significantly increased the expression of apoptosis-related proteins, including phosphatidylinositol 3 kinase (PI3K) p85 and PI3K downstream proteins (phosphoinositide-dependent kinase-1, protein kinase B and NF-κB p65). The up-regulation of PI3K downstream protein was inhibited after using melatonin inhibitor luzindole, which indicates that melatonin inhibits apoptosis after SCI by activating PI3K pathway (Bi et al., 2021a,b). In addition, some studies found that melatonin down regulated the expression of Caspase3 and caspase9 after SCI, and the expression levels of autophagy marker protein (beclin-1), LC-3b and SITR1/AMPK signal pathway related proteins (SIRT1 and p-AMPK) increased significantly. The above effects disappeared after using SIRT1 inhibitor EX527, which indicates that melatonin can regulate

autophagy and apoptosis through SIRT1/AMPK (Gao K. et al., 2020). Li et al. (2019) also demonstrated that melatonin enhances the autophagy of spinal cord neurons through PI3K/AKT/mTOR signaling pathway. Furthermore, melatonin significantly increased p-LRP6, β-catenin and LEF-1, the level of pro-apoptotic protein Bax was down-regulated, and the anti-apoptotic protein Bcl-2 was up-regulated, indicating that melatonin *via* Wnt/β- Catenin signaling pathway to regulate autophagy and apoptosis (Shen et al., 2017; **Figure 3**).

Melatonin down regulates the inflammatory response after spinal cord injury

Melatonin treatment can significantly reverse the expression of inflammatory related factors after SCI, such as IL-17 and IFN-γ, MCP-1 (Jing et al., 2019), NOD-like receptor protein 3 (NLRP3), IL-1 β, and caspase-1 (Xu et al., 2019; Yang et al., 2020). Some studies have pointed out that melatonin can inhibit inflammation after SCI *via* TLR4/NF-κB and NOX2/TXNIP signaling pathways (Paterniti et al., 2017; Majidpoor et al., 2020). Majidpoor et al. (2021) found that melatonin decreased the activities of NLRP3, apoptosis associated spotted protein and caspase-1, down regulated the level of IL-1 β and IL-18. The sensitivity of different segmental injuries to melatonin treatment is different. Among them, T6 is the most sensitive to melatonin treatment, except for T6, melatonin treatment does not affect the level of NLRP3 after SCI. IL-18 does not change only after melatonin treatment for T1 segmental injury (Majidpoor et al., 2021), which is undoubtedly interesting, but the reasons for this deserve further study.

However, few studies are concluding that melatonin has different sensitivity in different segments, which still needs to be further verified by other experiments. Zhang et al. (2019) found that melatonin treatment after SCI reduced M1 microglia markers (CD16, iNOS, TNF-a), but increased the levels of the M2 microglia markers (Arg1, CD206, TGF-β), which proves that melatonin promotes the differentiation of macrophages toward M2 type after SCI. In addition, melatonin inhibits the aggregation of microglia and thus the activation and proliferation of microglia and astrocytes (Paterniti et al., 2017; Yang et al., 2020; **Figure 3**).

Melatonin improves local blood circulation and edema, and maintained the stability of the blood spinal cord barrier

Studies have shown a reduction in the endothelial marker protein CD31 after SCI, suggesting damage to the blood-spinal cord barrier, and administration of melatonin increased the proportion of CD31-labeled vessels, suggesting that melatonin is effective in reducing the permeability of the blood-spinal cord barrier after SCI (Jing et al., 2017). Wang K. et al. (2019) proved that melatonin enhance the level of angiopoietin 1 (Ang1), reduce the expression of vascular endothelial growth factor (VEGF), adhesion factor intercellular adhesion molecule 1 and BSCB related factor matrix metallopeptidase 2 through insulin-like growth factor binding protein-3 (IGFBP-3), indicating that melatonin can maintain the stability of BSCB through interaction with IGFBP3 (**Figure 3**). Besides this, studies in animals have shown that melatonin administration reduces tissue edema after SCI. Xu et al. (2019) demonstrated that the water content of spinal cord tissue decreased significantly after melatonin administration and that melatonin downregulated the expression of the aquaporin aquaporin-4 (Li et al., 2014; Liu et al., 2015).

Melatonin prevents the down-regulation of neuroplasticity after spinal cord injury

Melatonin treatment after SCI significantly increased the mRNA and protein expression levels of growth associated protein-43 (GAP-43), synapsin1, Neurofilament 200 (NF200) and Postsynaptic density protein 95 (PSD-95) (Bi et al., 2021a), which play an important role in the process of neuronal remodeling. Moreover, brain-derived neurotrophic factor (BDNF) is the neuronal plasticity promoter, which affects neuronal remodeling through synapsin1 and GAP-43 protein. After SCI, the expression of BDNF, synapsin1 and GAP-43 in the spinal cord decreases, while melatonin can partially reverse the decrease of them, suggesting that melatonin has a protective effect on neural plasticity after SCI (Jing et al., 2017).

Conclusion

The complications after SCI greatly impact quality of life and life expectancy, especially constipation and fecal incontinence caused by gastrointestinal and bladder dysfunction (Glickman and Kamm, 1996; Lynch et al., 2001; Anderson, 2004; Zhang et al., 2018). The intestinal microbiota is closely related to gastrointestinal dysfunction. After SCI, the loss of advanced central control of the sympathetic nerve, the destruction of intestinal immune homeostasis, the impairment of intestinal barrier function, inflammation and the use of antibiotics will lead to the imbalance of intestinal microbiota and further cause gastrointestinal dysfunction. Regulating the structural disorder of intestinal microbiota can effectively inhibit the secondary injury after SCI, improve function, treat gastrointestinal dysfunction, and have a positive effect on urinary tract infection, which is undoubtedly very important for treating complications and the improvement of patients' quality of life. Melatonin not only effectively blocks the secondary injury process after SCI, but also promotes the recovery of intestinal microbiota structure. It plays a synergistic role in intestinal microbiota to improve the prognosis of SCI.

Melatonin plays an important role in the treatment of acute and subacute SCI, including anti-apoptosis, anti-inflammation, anti-free radical damage, alleviating edema, protecting BSCB, promoting neurons, reducing the accumulation of astrocytes,

and further affecting disease's development in the chronic phase, such as regulating chronic inflammation and reducing scar formation. Intestinal microbiota can promote neuronal survival and axonal regeneration, secrete SCFA to regulate inflammation and immune function, and has positive significance for the treatment of complications after SCI.

There is no direct research proving that melatonin and intestinal microbiota have synergistic effects on the treatment of SCI. However, some studies have proved the synergy between the two from the side. Intestinal microbiota down regulates NF-κB pathway by short-chain fatty acids in SCI. Melatonin is also proved that down-regulate the signal expression of the same pathway. On the other hand, melatonin can modulate the intestinal barrier and motor function to regulate the structure of the intestinal flora. In addition, some studies have confirmed that the positive effect of melatonin on SCI is reduced after the use of antibiotics. It also indirectly shows that the two have a synergistic effect on the recovery of SCI. Therefore, melatonin and gut microbiota may act synergistically in the treatment of SCI and further studies will be needed to confirm their role and underlying mechanisms.

The disorder of intestinal microbiota after SCI occurs in the acute stage. However, in the current study, FMT mostly occurs in the chronic stage after SCI. Therefore, whether early use of FMT and melatonin to regulate the structure of intestinal microbiota and produce significant therapeutic effects on SCI is worthy of further study.

In addition, Majidpoor et al. found that different sensitivity of melatonin treatment in different injured segments (Majidpoor et al., 2021). Few study has reached similar conclusions, so the underlying mechanism deserves further study.

The intestinal tract contains a variety of flora and abundant lymphoid tissue, which has a strong immunomodulatory function. Gut-derived Treg cells have been confirmed to feature in the prognosis of stroke, and studies have confirmed that programmed death protein 1 (PD-1) and CC-chemokine ligand 28 (CCL28) regulate Treg cells (Wang P. et al., 2019; He et al., 2021). In addition, melatonin also has a regulatory effect on Treg cells (Álvarez-Sánchez et al., 2015; Glebezdina et al., 2019). Therefore, the combined effect of melatonin and gut microbiota whether further affect the prognosis of SCI through Treg cells is worthy of in-depth study.

This review discusses the relationship among melatonin, intestinal microbiota and SCI, and summarizes the progress of melatonin and intestinal microbiota in treating SCI. By elucidating the link among melatonin, the brain-gut axis and SCI, new insights and ideas for the treatment of SCI are provided, furthering the development of SCI treatment.

Author contributions

YZ, YY, CB, and WD conceived the perspective of the work. YZ, RL, and SG drafted the manuscript. HL and CL designed the figures. All authors revised and approved the final version of the manuscript.

Funding

This work was supported by the National Natural Science Foundation of China (31871031 and 32170968 to WD), the Fund of Key Laboratory of Medical Electrophysiology in 2021 (KeyME-2021-01 to YY), China Postdoctoral Science Foundation (2021M692700 to YY), and Sichuan Science and Technology Program (22ZDYF3809 to YY and 22ZDYF3783 to WD).

Conflict of interest

The authors declare that the research was conducted in the absence of any commercial or financial relationships that could be construed as a potential conflict of interest.

Publisher's note

References

Álvarez-Sánchez, N., Cruz-Chamorro, I., López-González, A., Utrilla, J. C., Fernández-Santos, J. M., Martínez-López, A., et al. (2015). 'Melatonin controls experimental autoimmune encephalomyelitis by altering the t effector/regulatory balance'. *Brain Behav. Immun.* 50, 101–114. doi: 10.1016/j.bbi.2015.06.021

Anderson, G., Rodriguez, M., and Reiter, R. J. (2019). 'Multiple sclerosis: Melatonin, orexin, and ceramide interact with platelet activation coagulation factors and gut-microbiome-derived butyrate in the circadian dysregulation of mitochondria in glia and immune cells'. *Int. J. Mol. Sci.* 20:5500. doi: 10.3390/ijms20215500

Anderson, K. D. (2004). 'Targeting recovery: Priorities of the spinal cord-injured population'. *J. Neurotrauma* 21, 1371–1383.

Anjum, A., Yazid, M. D., Fauzi Daud, M., Idris, J., Ng, A. M. H., Selvi Naicker, A., et al. (2020). Spinal cord injury: Pathophysiology, multimolecular interactions, and underlying recovery mechanisms'. *Int. J. Mol. Sci.* 21:7533. doi: 10.3390/ijms21207533

Badhiwala, J. H., Wilson, J. R., Witiw, C. D., Harrop, J. S., Vaccaro, A. R., Aarabi, B., et al. (2021). 'The influence of timing of surgical decompression for acute spinal cord injury: A pooled analysis of individual patient data'. *Lancet Neurol.* 20, 117–126.

Bastien, D., and Lacroix, S. (2014). 'Cytokine pathways regulating glial and leukocyte function after spinal cord and peripheral nerve injury'. *Exp. Neurol.* 258, 62–77. doi: 10.1016/j.expneurol.2014.04.006

Bazzocchi, G., Turroni, S., Bulzamini, M. C., D'Amico, F., Bava, A., Castiglioni, M., et al. (2021). 'Changes in gut microbiota in the acute phase after spinal cord injury correlate with severity of the lesion'. *Sci. Rep.* 11:12743. doi: 10.1038/s41598-021-92027-z

Benabou, M., Rolland, T., Leblond, C. S., Millot, G. A., Huguet, G., Delorme, R., et al. (2017). 'Heritability of the melatonin synthesis variability in autism spectrum disorders'. *Sci. Rep.* 7:17746. doi: 10.1038/s41598-017-18016-3

Bi, J., Shen, J., Chen, C., Li, Z., Tan, H., Sun, P., et al. (2021a). 'Role of melatonin in the dynamics of acute spinal cord injury in rats'. *J. Cell. Mol. Med.* 25, 2909–2917. doi: 10.1111/jcmm.16325

Bi, J., Sun, P., Feng, E., Shen, J., Chen, C., Tan, H., et al. (2021b). 'Melatonin synergizes with methylprednisolone to ameliorate acute spinal cord injury'. *Front. Pharmacol.* 12:723913. doi: 10.3389/fphar.2021.723913

Biehl, L. M., Cruz Aguilar, R., Farowski, F., Hahn, W., Nowag, A., and Wisplinghoff, H. (2018). Fecal microbiota transplantation in a kidney transplant recipient with recurrent urinary tract infection. *Infection* 46, 871–874. doi: 10.1007/s15010-018-1190-9

Blaut, M. (2013). 'Ecology and physiology of the intestinal tract'. *Curr. Top. Microbiol. Immunol.* 358, 247–272.

Borgens, R. B., and Liu-Snyder, P. (2012). 'Understanding secondary injury'. *Q. Rev. Biol.* 87, 89–127.

Bubenik, G. A. (2002). 'Gastrointestinal melatonin: Localization, function, and clinical relevance'. *Dig. Dis. Sci.* 47, 2336–2348.

Busch, S. A., Horn, K. P., Silver, D. J., and Silver, J. (2009). 'Overcoming macrophage-mediated axonal dieback following CNS injury'. *J. Neurosci.* 29, 9967–9976. doi: 10.1523/JNEUROSCI.1151-09.2009

Cardinali, D. P., and Pévet, P. (1998). 'Basic aspects of melatonin action'. *Sleep Med. Rev.* 2, 175–190.

Cervi, A. L., Lukewich, M. K., and Lomax, A. E. (2014). 'Neural regulation of gastrointestinal inflammation: Role of the sympathetic nervous system'. *Auton. Neurosci.* 182, 83–88.

Chang, C. C., Huang, T. Y., Chen, H. Y., Huang, T. C., Lin, L. C., Chang, Y. J., et al. (2018). 'Protective effect of melatonin against oxidative stress-induced apoptosis and enhanced autophagy in human retinal pigment epithelium cells'. *Oxid. Med. Cell. Longev.* 2018:9015765. doi: 10.1155/2018/9015765

Chen, P. S., Wang, C. C., Bortner, C. D., Peng, G. S., Wu, X., Pang, H., et al. (2007). 'Valproic acid and other histone deacetylase inhibitors induce microglial apoptosis and attenuate lipopolysaccharide-induced dopaminergic neurotoxicity'. *Neuroscience* 149, 203–212. doi: 10.1016/j.neuroscience.2007.06.053

Cho, J. H., Bhutani, S., Kim, C. H., and Irwin, M. R. (2021). 'Anti-inflammatory effects of melatonin: A systematic review and meta-analysis of clinical trials'. *Brain Behav. Immun.* 93, 245–253.

Claustrat, B., and Leston, J. (2015). 'Melatonin: Physiological effects in humans'. *Neurochirurgie* 61, 77–84.

de Faria Poloni, J., Feltes, B. C., and Bonatto, D. (2011). Melatonin as a central molecule connecting neural development and calcium signaling. *Funct. Integr. Genom.* 11, 383–388. doi: 10.1007/s10142-011-0221-8

DeLeo, J. A., and Yezierski, R. P. (2001). 'The role of neuroinflammation and neuroimmune activation in persistent pain'. *Pain* 90, 1–6.

Dermanowski, M. M., Hejduk, A., Kuczyńska, J., Wichniak, A., Urbańska, A., and Mierzejewski, P. (2022). 'Assessment of dim light melatonin onset based on plasma and saliva samples'. *Chronobiol. Int.* 39, 626–635.

Du, J., Zayed, A. A., Kigerl, K. A., Zane, K., Sullivan, M. B., and Popovich, P. G. (2021). 'Spinal cord injury changes the structure and functional potential of gut bacterial and viral communities'. *mSystems* 6:e01356–20. doi: 10.1128/mSystems.01356-20

Dubocovich, M. L., Delagrange, P., Krause, D. N., Sugden, D., Cardinali, D. P., and Olcese, J. (2010). 'International union of basic and clinical pharmacology. LXXV. nomenclature, classification, and pharmacology of G protein-coupled melatonin receptors'. *Pharmacol. Rev.* 62, 343–380. doi: 10.1124/pr.110.002832

Ervin, S. M., Simpson, J. B., Gibbs, M. E., Creekmore, B. C., Lim, L., Walton, W. G., et al. (2020). 'Structural insights into endobiotic reactivation by human gut microbiome-encoded sulfatases'. *Biochemistry* 59, 3939–3950. doi: 10.1021/acs.biochem.0c00711

Faden, A. I., Demediuk, P., Panter, S. S., and Vink, R. (1989). 'The role of excitatory amino acids and NMDA receptors in traumatic brain injury'. *Science* 244, 798–800.

Furness, J. B., Callaghan, B. P., Rivera, L. R., and Cho, H. J. (2014). 'The enteric nervous system and gastrointestinal innervation: Integrated local and central control'. *Adv. Exp. Med. Biol.* 817, 39–71.

Galvão Mde, O., Sinigaglia-Coimbra, R., Kawakami, S. E., Tufik, S., and Suchecki, D. (2009). Paradoxical sleep deprivation activates hypothalamic nuclei that regulate food intake and stress response. *Psychoneuroendocrinology* 34, 1176–1183. doi: 10.1016/j.psyneuen.2009.03.003

Gao, J., Xu, K., Liu, H., Liu, G., Bai, M., Peng, C., et al. (2018). 'Impact of the gut microbiota on intestinal immunity mediated by tryptophan metabolism'. *Front. Cell. Infect. Microbiol.* 8:13. doi: 10.3389/fcimb.2018.00013

Gao, K., Niu, J., and Dang, X. (2020). 'Neuroprotection of melatonin on spinal cord injury by activating autophagy and inhibiting apoptosis via SIRT1/AMPK signaling pathway'. *Biotechnol. Lett.* 42, 2059–2069.

Gao, T., Wang, Z., Cao, J., Dong, Y., and Chen, Y. (2020). 'Melatonin attenuates microbiota dysbiosis of jejunum in short-term sleep deprived mice'. *J. Microbiol.* 58, 588–597. doi: 10.1007/s12275-020-0094-4

Gao, T., Wang, Z., Cao, J., Dong, Y., and Chen, Y. (2021). Melatonin ameliorates corticosterone-mediated oxidative stress-induced colitis in sleep-deprived mice involving gut microbiota. *Oxid. Med. Cell. Longev.* 2021:9981480. doi: 10.1155/2021/9981480

Gao, T., Wang, Z., Dong, Y., Cao, J., Lin, R., Wang, X., et al. (2019). 'Role of melatonin in sleep deprivation-induced intestinal barrier dysfunction in mice'. *J. Pineal Res.* 67:e12574. doi: 10.1111/jpi.12574

Gensel, J. C., and Zhang, B. (2015). 'Macrophage activation and its role in repair and pathology after spinal cord injury'. *Brain Res.* 1619, 1–11.

Gerdin, M. J., Masana, M. I., and Dubocovich, M. L. (2004). 'Melatonin-mediated regulation of human MT(1) melatonin receptors expressed in mammalian cells'. *Biochem. Pharmacol.* 67, 2023–2030.

Ghareghani, M., Reiter, R. J., Zibara, K., and Farhadi, N. (2018). 'Latitude, vitamin d, melatonin, and gut microbiota act in concert to initiate multiple sclerosis: A new mechanistic pathway'. *Front. Immunol.* 9:2484. doi: 10.3389/fimmu.2018.02484

Giannoulia-Karantana, A., Vlachou, A., Polychronopoulou, S., Papassotiriou, I., and Chrousos, G. P. (2006). 'Melatonin and immunomodulation: Connections and potential clinical applications'. *Neuroimmunomodulation* 13, 133–144. doi: 10.1159/000097258

Glebezdina, N. S., Olina, A. A. I., Nekrasova, V., and Kuklina, E. M. (2019). 'Molecular mechanisms of control of differentiation of regulatory T-lymphocytes by exogenous melatonin'. *Dokl. Biochem. Biophys.* 484, 13–16. doi: 10.1134/S1607672919010058

Glickman, S., and Kamm, M. A. (1996). 'Bowel dysfunction in spinal-cord-injury patients'. *Lancet* 347, 1651–1653.

Gungor, B., Adiguzel, E., Gursel, I., Yilmaz, B., and Gursel, M. (2016). 'Intestinal microbiota in patients with spinal cord injury'. *PLoS One* 11:e0145878. doi: 10.1371/journal.pone.0145878

Hagi, T., and Belzer, C. (2021). 'The interaction of akkermansia muciniphila with host-derived substances, bacteria and diets'. *Appl. Microbiol. Biotechnol.* 105, 4833–4841. doi: 10.1007/s00253-021-11362-3

Hanisch, U. K. (2002). 'Microglia as a source and target of cytokines'. *Glia* 40, 140–155.

He, X., Lin, S., Yang, L., Tan, P., Ma, P., Qiu, P., et al. (2021). 'Programmed death protein 1 is essential for maintaining the anti-inflammatory function of infiltrating regulatory T cells in a murine spinal cord injury model'. *J. Neuroimmunol.* 354:577546. doi: 10.1016/j.jneuroim.2021.577546

Heintz-Buschart, A., and Wilmes, P. (2018). 'Human gut microbiome: Function matters'. *Trends Microbiol.* 26, 563–574.

Hellenbrand, D. J., Quinn, C. M., Piper, Z. J., Morehouse, C. N., Fixel, J. A., and Hanna, A. S. (2021). 'Inflammation after spinal cord injury: A review of the critical timeline of signaling cues and cellular infiltration'. *J. Neuroinflamm.* 18:284. doi: 10.1186/s12974-021-02337-2

Holmes, G. M., Hubscher, C. H., Krassioukov, A., Jakeman, L. B., and Kleitman, N. (2020). 'Recommendations for evaluation of bladder and bowel function in

pre-clinical spinal cord injury research'. *J. Spinal Cord Med.* 43, 165–176. doi: 10.1080/10790268.2019.1661697

Huang, H., Young, W., Skaper, S., Chen, L., Moviglia, G., Saberi, H., et al. (2020). 'Clinical neurorestorative therapeutic guidelines for spinal cord injury (IANR/CANR version 2019)'. *J. Orthop. Translat.* 20, 14–24. doi: 10.1016/j.jot.2019.10.006

Huether, G. (1993). 'The contribution of extrapineal sites of melatonin synthesis to circulating melatonin levels in higher vertebrates'. *Experientia* 49, 665–670. doi: 10.1007/BF01923948

Hultén, V. D. T., Biering-Sørensen, F., Jørgensen, N. R., and Jennum, P. J. (2020). 'A review of sleep research in patients with spinal cord injury'. *J. Spinal Cord Med.* 43, 775–796.

Jing, Y., Yu, Y., Bai, F., Wang, L., Yang, D., Zhang, C., et al. (2021b). 'Effect of fecal microbiota transplantation on neurological restoration in a spinal cord injury mouse model: Involvement of brain-gut axis'. *Microbiome* 9:59. doi: 10.1186/s40168-021-01007-y

Jing, Y., Bai, F., and Yu, Y. (2021a). 'Spinal cord injury and gut microbiota: A review'. *Life Sci.* 266:118865.

Jing, Y., Bai, F., Chen, H., and Dong, H. (2017). 'Melatonin prevents blood vessel loss and neurological impairment induced by spinal cord injury in rats'. *J. Spinal Cord Med.* 40, 222–229. doi: 10.1080/10790268.2016.1227912

Jing, Y., Yang, D., Bai, F., Zhang, C., Qin, C., Li, D., et al. (2019). 'Melatonin treatment alleviates spinal cord injury-induced gut dysbiosis in mice'. *J. Neurotrauma* 36, 2646–2664. doi: 10.1089/neu.2018.6012

Joscelyn, J., and Kasper, L. H. (2014). 'Digesting the emerging role for the gut microbiome in central nervous system demyelination'. *Mult. Scler.* 20, 1553–1559.

Keshavarzian, A., Green, S. J., Engen, P. A., Voigt, R. M., Naqib, A., Forsyth, C. B., et al. (2015). 'Colonic bacterial composition in Parkinson's disease'. *Mov. Disord.* 30, 1351–1360.

Kesika, P., Suganthy, N., Sivamaruthi, B. S., and Chaiyasut, C. (2021). 'Role of gut-brain axis, gut microbial composition, and probiotic intervention in Alzheimer's disease'. *Life Sci.* 264:118627.

Kigerl, K. A., Gensel, J. C., Ankeny, D. P., Alexander, J. K., Donnelly, D. J., and Popovich, P. G. (2009). 'Identification of two distinct macrophage subsets with divergent effects causing either neurotoxicity or regeneration in the injured mouse spinal cord'. *J. Neurosci.* 29, 13435–13444.

Kigerl, K. A., Hall, J. C., Wang, L., Mo, X., Yu, Z., and Popovich, P. G. (2016). 'Gut dysbiosis impairs recovery after spinal cord injury'. *J. Exp. Med.* 213, 2603–2620.

Kim, J., Oh, J. K., Kim, S. W., Yee, J. S., and Kim, T. H. (2021). 'Risk factors for sleep disturbance in patients with cervical myelopathy and its clinical significance: A cross-sectional study'. *Spine J.* 21, 96–104. doi: 10.1016/j.spinee.2020.09.002

Kim, S. W., Kim, S., Son, M., Cheon, J. H., and Park, Y. S. (2020). 'Melatonin controls microbiota in colitis by goblet cell differentiation and antimicrobial peptide production through Toll-like receptor 4 signalling'. *Sci. Rep.* 10:2232. doi: 10.1038/s41598-020-59314-7

Lee, J., d'Aigle, J., Atadja, L., Quaicoe, V., Honarpisheh, P., Ganesh, B. P., et al. (2020). 'Gut microbiota-derived short-chain fatty acids promote poststroke recovery in aged mice'. *Circ. Res.* 127, 453–465. doi: 10.1161/CIRCRESAHA.119.316448

Lefèvre, C., Bessard, A., Aubert, P., Joussain, C., Giuliano, F., Behr-Roussel, D., et al. (2020). 'Enteric nervous system remodeling in a rat model of spinal cord injury: A pilot study'. *Neurotrauma Rep.* 1, 125–136. doi: 10.1089/neur.2020.0041

Ley, R. E., Bäckhed, F., Turnbaugh, P., Lozupone, C. A., Knight, R. D., and Gordon, J. I. (2005). 'Obesity alters gut microbial ecology'. *Proc. Natl. Acad. Sci. U.S.A.* 102, 11070–11075.

Ley, R. E., Turnbaugh, P. J., Klein, S., and Gordon, J. I. (2006). 'Microbial ecology: Human gut microbes associated with obesity'. *Nature* 444, 1022–1023.

Li, C., Chen, X., Qiao, S., Liu, X., Liu, C., Zhu, D., et al. (2014). Melatonin lowers edema after spinal cord injury. *Neural Regen. Res.* 9, 2205–2210. doi: 10.4103/1673-5374.147954

Li, G., Lv, D., Yao, Y., Wu, H., Wang, J., Deng, S., et al. (2021). 'Overexpression of ASMT likely enhances the resistance of transgenic sheep to brucellosis by influencing immune-related signaling pathways and gut microbiota'. *FASEB J.* 35:e21783. doi: 10.1096/fj.202100651R

Li, H., Sun, J., Du, J., Wang, F., Fang, R., Yu, C., et al. (2018). 'Clostridium butyricum exerts a neuroprotective effect in a mouse model of traumatic brain injury via the gut-brain axis'. *Neurogastroenterol. Motil.* 30:e13260. doi: 10.1111/nmo.13260

Li, H., Xu, H., Li, Y., Jiang, Y., Hu, Y., Liu, T., et al. (2020). 'Alterations of gut microbiota contribute to the progression of unruptured intracranial aneurysms'. *Nat. Commun.* 11:3218. doi: 10.1038/s41467-020-16990-3

Li, J., Van Der Pol, W., Eraslan, M., McLain, A., Cetin, H., Cetin, B., et al. (2022). 'Comparison of the gut microbiome composition among individuals with acute or long-standing spinal cord injury vs. able-bodied controls'. *J. Spinal Cord Med.* 45, 91–99.

Li, Y., Guo, Y., Fan, Y., Tian, H., Li, K., and Mei, X. (2019). 'Melatonin enhances autophagy and reduces apoptosis to promote locomotor recovery in spinal cord injury via the PI3K/AKT/mTOR signaling pathway'. *Neurochem. Res.* 44, 2007–2019. doi: 10.1007/s11064-019-02838-w

Li, Z., Li, X., Chan, M. T. V., Wu, W. K. K., Tan, D., and Shen, J. (2017). 'Melatonin antagonizes interleukin-18-mediated inhibition on neural stem cell proliferation and differentiation'. *J. Cell. Mol. Med.* 21, 2163–2171. doi: 10.1111/jcmm.13140

Liang, S., Wu, X., Hu, X., Wang, T., and Jin, F. (2018). 'Recognizing depression from the microbiota-gut-brain axis'. *Int. J. Mol. Sci.* 19:1592.

Lin, R., Wang, Z., Cao, J., Gao, T., Dong, Y., and Chen, Y. (2021). 'Role of melatonin in murine "restraint stress"-induced dysfunction of colonic microbiota'. *J. Microbiol.* 59, 500–512. doi: 10.1007/s12275-021-0305-7

Liu, X., Liang, F., Song, W., Diao, X., Zhu, W., and Yang, J. (2021). 'Effect of Nrf2 signaling pathway on the improvement of intestinal epithelial barrier dysfunction by hyperbaric oxygen treatment after spinal cord injury'. *Cell Stress Chaperones* 26, 433–441. doi: 10.1007/s12192-020-01190-1

Liu, X., Liang, F., Zhang, J., Li, Z., Yang, J., and Kang, N. (2020). 'Hyperbaric oxygen treatment improves intestinal barrier function after spinal cord injury in rats'. *Front. Neurol.* 11:563281. doi: 10.3389/fneur.2020.563281

Liu, X., Wang, Y., Yang, J., Liu, Y., Zhou, D., Hou, M., et al. (2015). Anti-edema effect of melatonin on spinal cord injury in rats. *Biomed. Pap. Med. Fac. Univ. Palacky Olomouc Czech. Repub.* 159, 220–226. doi: 10.5507/bp.2015.012

Lutfi, E., Basili, D., Falcinelli, S., Morillas, L., Carnevali, O., Capilla, E., et al. (2021). 'The probiotic lactobacillus rhamnosus mimics the dark-driven regulation of appetite markers and melatonin receptors' expression in zebrafish (*Danio rerio*) larvae: Understanding the role of the gut microbiome'. *Comp. Biochem. Physiol. B Biochem. Mol. Biol.* 256:110634. doi: 10.1016/j.cbpb.2021.110634

Lynch, A. C., Antony, A., Dobbs, B. R., and Frizelle, F. A. (2001). 'Bowel dysfunction following spinal cord injury'. *Spinal Cord* 39, 193–203.

Magruder, M., Edusei, E., Zhang, L., Albakry, S., Satlin, M. J., Westblade, L. F., et al. (2020). 'Gut commensal microbiota and decreased risk for *Enterobacteriaceae* bacteriuria and urinary tract infection'. *Gut Microbes* 12:1805281. doi: 10.1080/19490976.2020.1805281

Magruder, M., Sholi, A. N., Gong, C., Zhang, L., Edusei, E., Huang, J., et al. (2019). 'Gut uropathogen abundance is a risk factor for development of bacteriuria and urinary tract infection'. *Nat. Commun.* 10:5521. doi: 10.1038/s41467-019-13467-w

Majidpoor, J., Khezri, Z., Rostamzadeh, P., Mortezaee, K., Rezaie, M. J., Fathi, F., et al. (2020). 'The expressions of NLRP1, NLRP3, and AIM2 inflammasome complexes in the contusive spinal cord injury rat model and their responses to hormonal therapy'. *Cell Tissue Res.* 381, 397–410. doi: 10.1007/s00441-020-03250-5

Majidpoor, J., Mortezaee, K., Khezri, Z., Fathi, F., Zali, A., Derakhshan, H. B., et al. (2021). 'The effect of the "segment" of spinal cord injury on the activity of the nucleotide-binding domain-like receptor protein 3 inflammasome and response to hormonal therapy'. *Cell Biochem. Funct.* 39, 267–276. doi: 10.1002/cbf.3574

Markowiak-Kopeć, P., and liżewska, K. (2020). 'The effect of probiotics on the production of short-chain fatty acids by human intestinal microbiome'. *Nutrients* 12:1107.

Mazzoccoli, G., Carughi, S., Sperandeo, M., Pazienza, V., Giuliani, F., and Tarquini, R. (2011). 'Neuro-endocrine correlations of hypothalamic-pituitary-thyroid axis in healthy humans'. *J. Biol. Regul. Homeost. Agents* 25, 249–257.

Møller, M., and Baeres, F. M. (2002). 'The anatomy and innervation of the mammalian pineal gland'. *Cell Tissue Res.* 309, 139–150.

O'Connor, G., Jeffrey, E., Madorma, D., Marcillo, A., Abreu, M. T., Deo, S. K., et al. (2018). 'Investigation of microbiota alterations and intestinal inflammation post-spinal cord injury in rat model'. *J. Neurotrauma* 35, 2159–2166. doi: 10.1089/neu.2017.5349

Onaolapo, O. J., Onaolapo, A. Y., Olowe, O. A., Udoh, M. O., Udoh, D. O., and Nathaniel, T. I. (2020). 'Melatonin and melatonergic influence on neuronal transcription factors: Implications for the development of novel therapies for

neurodegenerative disorders'. *Curr. Neuropharmacol.* 18, 563–577. doi: 10.2174/1570159X18666191230114339

Opeyemi, O. M., Rogers, M. B., Firek, B. A., Janesko-Feldman, K., Vagni, V., Mullett, S. J., et al. (2021). 'Sustained dysbiosis and decreased fecal short-chain fatty acids after traumatic brain injury and impact on neurologic outcome'. *J. Neurotrauma* 38, 2610–2621. doi: 10.1089/neu.2020.7506

Oyinbo, C. A. (2011). 'Secondary injury mechanisms in traumatic spinal cord injury: A nugget of this multiply cascade'. *Acta Neurobiol. Exp.* 71, 281–299.

Park, J. S., Woo, M. S., Kim, S. Y., Kim, W. K., and Kim, H. S. (2005). 'Repression of interferon-gamma-induced inducible nitric oxide synthase (iNOS) gene expression in microglia by sodium butyrate is mediated through specific inhibition of ERK signaling pathways'. *J. Neuroimmunol.* 168, 56–64. doi: 10.1016/j.jneuroim.2005.07.003

Park, Y. S., Kim, S. H., Park, J. W., Kho, Y., Seok, P. R., Shin, J. H., et al. (2020). 'Melatonin in the colon modulates intestinal microbiota in response to stress and sleep deprivation'. *Intest. Res.* 18, 325–336. doi: 10.5217/ir.2019.00093

Paterniti, I., Campolo, M., Cordaro, M., Impellizzeri, D., Siracusa, R., Crupi, R., et al. (2017). 'PPAR-α modulates the anti-inflammatory effect of melatonin in the secondary events of spinal cord injury'. *Mol. Neurobiol.* 54, 5973–5987. doi: 10.1007/s12035-016-0131-9

Paulose, J. K., Wright, J. M., Patel, A. G., and Cassone, V. M. (2016). 'Human gut bacteria are sensitive to melatonin and express endogenous circadian rhythmicity'. *PLoS One* 11:e0146643. doi: 10.1371/journal.pone.0146643

Perez-Pardo, P., Dodiya, H. B., Engen, P. A., Forsyth, C. B., Huschens, A. M., Shaikh, M., et al. (2019). 'Role of TLR4 in the gut-brain axis in Parkinson's disease: A translational study from men to mice'. *Gut* 68, 829–843. doi: 10.1136/gutjnl-2018-316844

Pistollato, F., Sumalla Cano, S., Elio, I., Masias Vergara, M., Giampieri, F., and Battino, M. (2016). 'Role of gut microbiota and nutrients in amyloid formation and pathogenesis of Alzheimer disease'. *Nutr. Rev.* 74, 624–634.

Quadri, S. A., Farooqui, M., Ikram, A., Zafar, A., Khan, M. A., Suriya, S. S., et al. (2020). 'Recent update on basic mechanisms of spinal cord injury'. *Neurosurg. Rev.* 43, 425–441.

Ren, W., Liu, G., Chen, S., Yin, J., Wang, J., Tan, B., et al. (2017). 'Melatonin signaling in T cells: Functions and applications'. *J. Pineal Res.* 62:12394. doi: 10.1111/jpi.12394.

Ren, W., Wang, P., Yan, J., Liu, G., Zeng, B., Hussain, T., et al. (2018). 'Melatonin alleviates weanling stress in mice: Involvement of intestinal microbiota'. *J. Pineal Res.* 64:12448. doi: 10.1111/jpi.12448

Rodenhouse, A., Talukder, M. A. H., Lee, J. I., Govindappa, P. K., O'Brien, M., Manto, K. M., et al. (2022). 'Altered gut microbiota composition with antibiotic treatment impairs functional recovery after traumatic peripheral nerve crush injury in mice: Effects of probiotics with butyrate producing bacteria'. *BMC Res. Notes* 15:80. doi: 10.1186/s13104-022-05967-8

Rogers, W. K., and Todd, M. (2016). 'Acute spinal cord injury'. *Best Pract. Res. Clin. Anaesthesiol.* 30, 27–39.

Rudzki, L., Stone, T. W., Maes, M., Misiak, B., Samochowiec, J., and Szulc, A. (2021). 'Gut microbiota-derived vitamins - underrated powers of a multipotent ally in psychiatric health and disease'. *Prog. Neuropsychopharmacol. Biol. Psychiatry* 107:110240. doi: 10.1016/j.pnpbp.2020.110240

Santoru, M. L., Piras, C., Murgia, A., Palmas, V., Camboni, T., and Liggi, S. (2017). 'Cross sectional evaluation of the gut-microbiome metabolome axis in an Italian cohort of IBD patients'. *Sci. Rep.* 7:9523.

Schmidt, E. K. A., Raposo, P. J. F., Torres-Espin, A., Fenrich, K. K., and Fouad, K. (2021). 'Beyond the lesion site: Minocycline augments inflammation and anxiety-like behavior following SCI in rats through action on the gut microbiota'. *J. Neuroinflamm.* 18:144. doi: 10.1186/s12974-021-02123-0

Schwab, J. M., Zhang, Y., Kopp, M. A., Brommer, B., and Popovich, P. G. (2014). 'The paradox of chronic neuroinflammation, systemic immune suppression, autoimmunity after traumatic chronic spinal cord injury'. *Exp. Neurol.* 258, 121–129. doi: 10.1016/j.expneurol.2014.04.023

Schwiertz, A., Taras, D., Schäfer, K., Beijer, S., Bos, N. A., Donus, C., et al. (2010). 'Microbiota and SCFA in lean and overweight healthy subjects'. *Obesity* 18, 190–195.

Shen, Z., Zhou, Z., Gao, S., Guo, Y., Gao, K., Wang, H., et al. (2017). 'Melatonin inhibits neural cell apoptosis and promotes locomotor recovery via activation of the Wnt/β-catenin signaling pathway after spinal cord injury'. *Neurochem. Res.* 42, 2336–2343.

Straub, R. H., Wiest, R., Strauch, U. G., Härle, P., and Schölmerich, J. (2006). 'The role of the sympathetic nervous system in intestinal inflammation'. *Gut* 55, 1640–1649.

Sun, M. F., Zhu, Y. L., Zhou, Z. L., Jia, X. B., Xu, Y. D., Yang, Q., et al. (2018). 'Neuroprotective effects of fecal microbiota transplantation on MPTP-induced Parkinson's disease mice: Gut microbiota, glial reaction and TLR4/TNF-α signaling pathway'. *Brain Behav. Immun.* 70, 48–60. doi: 10.1016/j.bbi.2018.02.005

Tariq, R., Pardi, D. S., Tosh, P. K., Walker, R. C., Razonable, R. R., and Khanna, S. (2017). 'Fecal microbiota transplantation for recurrent clostridium difficile infection reduces recurrent urinary tract infection frequency'. *Clin. Infect. Dis.* 65, 1745–1747. doi: 10.1093/cid/cix618

Tate, D. G., Forchheimer, M., Rodriguez, G., Chiodo, A., Cameron, A. P., Meade, M., et al. (2016). 'Risk factors associated with neurogenic bowel complications and dysfunction in spinal cord injury'. *Arch. Phys. Med. Rehabil.* 97, 1679–1686.

Thøfner Hultén, V. D., Biering-Sørensen, F., Jørgensen, N. R., and Jennum, P. J. (2018). 'Melatonin and cortisol in individuals with spinal cord injury'. *Sleep Med.* 51, 92–98.

Tran, A. P., Warren, P. M., and Silver, J. (2018). 'The biology of regeneration failure and success after spinal cord injury'. *Physiol. Rev.* 98, 881–917.

Vasey, C., McBride, J., and Penta, K. (2021). 'Circadian rhythm dysregulation and restoration: The role of melatonin'. *Nutrients* 13:3480. doi: 10.3390/nu13103480

Wang, K., Li, M., Jin, L., Deng, C., Chen, Z., Chen, H., et al. (2019). 'Retracted article: Melatonin protects spinal cord injury by up-regulating IGFBP3 through the improvement of microcirculation in a rat model'. *RSC Adv.* 9, 32072–32080. doi: 10.1039/c9ra04591k

Wang, P., Qi, X., Xu, G., Liu, J., Guo, J., Li, X., et al. (2019). 'CCL28 promotes locomotor recovery after spinal cord injury via recruiting regulatory T cells'. *Aging* 11, 7402–7415.

Watkins, L. R., Milligan, E. D., and Maier, S. F. (2001). 'Spinal cord glia: New players in pain'. *Pain* 93, 201–205.

Wexler, A. G., and Goodman, A. L. (2017). 'An insider's perspective: *Bacteroides* as a window into the microbiome'. *Nat. Microbiol.* 2:17026.

Whelan, A., Halpine, M., Christie, S. D., and McVeigh, S. A. (2020). 'Systematic review of melatonin levels in individuals with complete cervical spinal cord injury'. *J. Spinal Cord Med.* 43, 565–578. doi: 10.1080/10790268.2018.1505312

White, A. R., Werner, C. M., and Holmes, G. M. (2020). 'Diminished enteric neuromuscular transmission in the distal colon following experimental spinal cord injury'. *Exp. Neurol.* 331:113377. doi: 10.1016/j.expneurol.2020.113377

Williams, R., and Murray, A. (2015). 'Prevalence of depression after spinal cord injury: A meta-analysis'. *Arch. Phys. Med. Rehabil.* 96, 133–140.

Worby, C. J., Olson, B. S., Dodson, K. W., Earl, A. M., and Hultgren, S. J. (2022). Establishing the role of the gut microbiota in susceptibility to recurrent urinary tract infections. *J. Clin. Invest.* 132:158497. doi: 10.1172/jci158497

Wurtman, R. (2006). 'Ramelteon: A novel treatment for the treatment of insomnia'. *Expert Rev. Neurother.* 6, 957–964.

Xiong, X., Bao, Z., Mi, Y., Wang, X., and Zhu, J. (2022). 'Melatonin alleviates neonatal necrotizing enterocolitis by repressing the activation of the NLRP3 inflammasome'. *Gastroenterol. Res. Pract.* 2022:6920577. doi: 10.1155/2022/6920577

Xu, G., Shi, D., Zhi, Z., Ao, R., and Yu, B. (2019). 'Melatonin ameliorates spinal cord injury by suppressing the activation of inflammasomes in rats'. *J. Cell. Biochem.* 120, 5183–5192.

Xu, L. X., Lv, Y., Li, Y. H., Ding, X., Wang, Y., Han, X., et al. (2017). 'Melatonin alleviates brain and peripheral tissue edema in a neonatal rat model of hypoxic-ischemic brain damage: The involvement of edema related proteins'. *BMC Pediatr.* 17:90. doi: 10.1186/s12887-017-0824-x

Xu, P., Wang, J., Hong, F., Wang, S., Jin, X., Xue, T., et al. (2017). 'Melatonin prevents obesity through modulation of gut microbiota in mice'. *J. Pineal Res.* 62:12399. doi: 10.1111/jpi.12399

Yang, Z., Bao, Y., Chen, W., and He, Y. (2020). 'Melatonin exerts neuroprotective effects by attenuating astro- and microgliosis and suppressing inflammatory response following spinal cord injury'. *Neuropeptides* 79:102002. doi: 10.1016/j.npep.2019.102002

Yin, J., Li, Y., Han, H., Chen, S., Gao, J., Liu, G., et al. (2018). 'Melatonin reprogramming of gut microbiota improves lipid dysmetabolism in high-fat diet-fed mice'. *J. Pineal Res.* 65:e12524. doi: 10.1111/jpi.12524

Yu, B., Qiu, H., Cheng, S., Ye, F., Li, J., Chen, S., et al. (2021). 'Profile of gut microbiota in patients with traumatic thoracic spinal cord injury and its clinical implications: A case-control study in a rehabilitation setting'. *Bioengineered* 12, 4489–4499. doi: 10.1080/21655979.2021.1955543

Yuan, B., Lu, X. J., and Wu, Q. (2021). 'Gut microbiota and acute central nervous system injury: A new target for therapeutic intervention'. *Front. Immunol.* 12:800796. doi: 10.3389/fimmu.2021.800796

Zhang, C., Zhang, W., Zhang, J., Jing, Y., Yang, M., Du, L., et al. (2018). 'Gut microbiota dysbiosis in male patients with chronic traumatic complete spinal cord injury'. *J. Transl. Med.* 16:353. doi: 10.1186/s12967-018-1735-9

Zhang, H., Yan, A., Liu, X., Ma, Y., Zhao, F., Wang, M., et al. (2021). 'Melatonin ameliorates ochratoxin A induced liver inflammation, oxidative stress and mitophagy in mice involving in intestinal microbiota and restoring the intestinal barrier function'. *J. Hazard. Mater.* 407:124489. doi: 10.1016/j.jhazmat.2020.124489

Zhang, J., Li, S., and Wu, Y. (2017). 'Recovery of spinal cord injury following electroacupuncture in rats through enhancement of Wnt/β-catenin signaling'. *Mol. Med. Rep.* 16, 2185–2190. doi: 10.3892/mmr.2017.6801

Zhang, M., Bai, Y., Xu, C., Lin, J., Jin, J., Xu, A., et al. (2021). 'Novel optimized drug delivery systems for enhancing spinal cord injury repair in rats'. *Drug Deliv.* 28, 2548–2561. doi: 10.1080/10717544.2021.2009937

Zhang, Y., Liu, Z., Zhang, W., Wu, Q., Zhang, Y., Liu, Y., et al. (2019). 'Melatonin improves functional recovery in female rats after acute spinal cord injury by modulating polarization of spinal microglial/macrophages'. *J. Neurosci. Res.* 97, 733–743. doi: 10.1002/jnr.24409

Zhao, Z. X., Yuan, X., Cui, Y. Y., Liu, J., Shen, J., Jin, B. Y., et al. (2021). 'Melatonin mitigates oxazolone-induced colitis in microbiota-dependent manner'. *Front. Immunol.* 12:783806. doi: 10.3389/fimmu.2021.783806

Zheng, B., Hao, D., Guo, H., and He, B. (2017). 'Melatonin alleviates acute spinal cord injury in rats through promoting on progenitor cells proliferation'. *Saudi Pharm. J.* 25, 570–574.

Zhou, X., He, X., and Ren, Y. (2014). 'Function of microglia and macrophages in secondary damage after spinal cord injury'. *Neural Regen. Res.* 9, 1787–1795.

Zhuo, Y., Cao, M., Gong, Y., Tang, L., Jiang, X., Li, Y., et al. (2021). 'Gut microbial metabolism of dietary fibre protects against high energy feeding induced ovarian follicular atresia in a pig model'. *Br. J. Nutr.* 125, 38–49. doi: 10.1017/S0007114520002378

frontiers | Frontiers in Neuroscience

TYPE Original Research
PUBLISHED 07 December 2022
DOI 10.3389/fnins.2022.1019590

OPEN ACCESS

EDITED BY
Yi-Hung Chen,
China Medical University, Taiwan

REVIEWED BY
Ronglin Cai,
Anhui University of Chinese Medicine, China
Paloma Birmann,
Federal University of Pelotas, Brazil
Zhenzhen Xue,
China Academy of Chinese Medical Sciences, China

*CORRESPONDENCE
Yin Shi
flysy0636@163.com
Yuan Lu
luyuan_sh@163.com

SPECIALTY SECTION
This article was submitted to Gut-Brain Axis, a section of the journal Frontiers in Neuroscience

RECEIVED 15 August 2022
ACCEPTED 15 November 2022
PUBLISHED 07 December 2022

CITATION
Bao C, Huang J, Wu H, Ma Y, Zhou H, Chen L, Yang D, Liu H, Shi Y and Lu Y (2022) Moxibustion alleviates depression-like behavior in rats with Crohn's disease by inhibiting the kynurenine pathway metabolism in the gut-brain axis.
Front. Neurosci. 16:1019590.
doi: 10.3389/fnins.2022.1019590

Moxibustion alleviates depression-like behavior in rats with Crohn's disease by inhibiting the kynurenine pathway metabolism in the gut-brain axis

Chunhui Bao[1,2], Jin Huang[3], Huangan Wu[1,2], Yueying Ma[3], Hongyu Zhou[3], Liming Chen[1], Dandan Yang[4], Huirong Liu[1,2], Yin Shi[1,2]* and Yuan Lu[1,2]*

[1]Yueyang Hospital of Integrated Traditional Chinese and Western Medicine, Shanghai University of Traditional Chinese Medicine, Shanghai, China, [2]Key Laboratory of Acupuncture and Immunological Effects, Shanghai University of Traditional Chinese Medicine, Shanghai, China, [3]Shanghai University of Traditional Chinese Medicine, Shanghai, China, [4]Hong Kong Baptist University, Hong Kong, Hong Kong SAR, China

Background: Moxibustion is a potential therapy for inflammatory bowel disease-related depression, but its specific mechanism of action is unclear. This study aimed to investigate the molecular mechanism by which moxibustion alleviates depressive behavior in rats with Crohn's disease (CD).

Methods: The CD rat model was established with 2,4,6-trinitrobenzenesulfonic acid. Treatment with moxibustion was applied to Tianshu (ST25, bilateral), Qihai (CV6), and Baihui (GV20) acupoints, and the effect of moxibustion was compared with that of the combination of moxibustion plus indoleamine-2,3-dioxygenase 1 (IDO1) inhibitor, 1-methyltryptophan (1-MT). The effects of moxibustion and moxibustion plus 1-MT combination on colonic inflammation and depressive behavior (assessed by forced swimming test, sucrose preference test, and open field test) were investigated. The changes in IDO1, TNF-α, and IL-1β in rat colon and hippocampus were assessed by Western blot (WB). Gas chromatography-mass spectrometry, immunofluorescence staining, and WB were applied to detect kynurenine pathway (KP) metabolites, hippocampal neuronal activity, and microglia activation, respectively.

Results: Both moxibustion and moxibustion plus 1-MT combination significantly alleviated intestinal inflammation and depressive behavior, downregulated the levels of IDO1 in the colon and hippocampus, and inhibited inflammation-inducing factors IL-1β and TNF-α, as well as the kynurenine/tryptophan (KYN/TRP) ratio of KP metabolites, and upregulated the kynurenic acid (KYNA)/KYN ratio and the KYNA/quinolinic acid (QUIN) ratio in the hippocampus in rats with CD; Hippocampal ionized calcium-binding adaptor molecule-1 (Iba-1), c-fos protein expression, activated microglia,

and neuronal activation was also significantly reduced by moxibustion and moxibustion plus 1-MT. The addition of 1-MT did not significantly increase the therapeutic effect of moxibustion.

Conclusion: Moxibustion can improve depressive behavior in rats with CD, which may be related to its regulation of KP metabolism in the gut-brain axis and inhibition of hippocampal microglia activation and neuronal activation.

KEYWORDS

moxibustion, Crohn's disease, depression, gut-brain axis, tryptophan-kynurenine metabolism

Introduction

Crohn's disease (CD), a type of inflammatory bowel disease (IBD), is a chronic inflammatory disease of the gastrointestinal tract characterized by abdominal pain, diarrhea, and weight loss. In recent decades, the prevalence of CD in China has shown an increasing trend (Zhao et al., 2013; Ng et al., 2016). This may be related to several factors including genetic, environmental, dietary, and infection-related factors (Ananthakrishnan, 2015). There is currently no definitive cure for CD (Kaplan, 2015). The disease course is marked by frequent relapses, which greatly affects the life and work of patients. Emotional and psychological factors are known to play an important role in inducing the recurrence of CD (van der Have et al., 2014).

According to two systematic reviews (Mikocka-Walus et al., 2016; Neuendorf et al., 2016), the rate of depression in patients with IBD (21.2%) is almost twofold higher than that in the general population, and the rate of depression in patients with CD may be as high as 24.4%. The prevalence of depression in patients with active CD may even exceed 40%. Many researchers have explained the mechanism of the interaction between IBD and depression through a bidirectional gut-brain interaction (Gracie et al., 2018, 2019). Brain-gut interaction refers to the linkage between the emotional and cognitive centers of the brain with the peripheral control and function of the gastrointestinal tract; it is a bi-directional crosstalk between the central nervous system and the gastrointestinal tract (Wang and Wang, 2016). Tryptophan (TRP) metabolism plays an important role in the gut-brain axis mechanism (O'Mahony et al., 2015). At least 90% of the tryptophan intake in the body is converted to kynurenine for the next step of metabolism, known as the kynurenine pathway (KP) (Badawy, 2017). Clinical studies have shown an association between TRP metabolism and IBD severity (Nikolaus et al., 2017). Dysfunction of key enzymes in the KP was also shown to be associated with IBD and depressive behavior in animal models as well as humans; for example, indoleamine-2,3-dioxygenase 1 (IDO1), a key rate-limiting enzyme in KP metabolism (O'Mahony et al., 2015). Two important metabolites of KP, i.e., kynurenic acid (KYNA) and quinolinic acid (QUIN), have opposite effects on CNS neuronal activity (neurotoxic and neuroprotective properties, respectively) (Chen and Guillemin, 2009). These metabolites can cross the blood-brain barrier to reach the central nervous system; imbalance in the level between KYNA and QUIN has received the most attention in patients with brain dysfunction such as depression (Savitz et al., 2015b; Liu et al., 2018). Specifically, QUIN is mainly metabolized in microglia and has a strong neurotoxic effect on the hippocampus (Lugo-Huitron et al., 2013). Hippocampus is a major component of the brain's limbic system and is strongly linked to depression (Sheline et al., 2019). Our group demonstrated a close association of increased gray matter volume in the hippocampus and other emotion-related brain areas with depression and anxiety in CD patients (Bao et al., 2015). These findings suggest that the effect of activation of KP on hippocampal function may be one of the key mechanisms of depression in CD.

Treatment of CD with acupuncture and moxibustion has been a popular research area in recent years. Previous work by our team has shown that moxibustion or moxibustion combination with acupuncture can alleviate disease activity (Bao et al., 2014, 2022), and improve serological markers of inflammation (Bao et al., 2014, 2022), immunity (Zhao et al., 2015), and tight junction protein expression in the intestinal wall (Bao et al., 2011; Shang et al., 2015) in CD. In addition, we have also demonstrated that acupuncture can improve depression (Bao et al., 2021) and peripheral KP metabolism (Bao et al., 2016, 2021) in CD, and that the effects of electroacupuncture and moxibustion on brain function in CD patients are related to the brain steady-state afferent processing network and the default mode network, respectively (Bao et al., 2017). Therefore, we speculate that moxibustion may be one of the promising therapies for IBD-related depression; however, the mechanism by which it alleviates depression in CD is still unclear.

This study aimed to investigate the mechanism by which moxibustion alleviates depression in rats with CD. 2,4,6-trinitrobenzenesulfonic acid (TNBS)-induced CD model rats were treated with moxibustion at the Tianshu (ST25, bilateral), Qihai (CV6), and Baihui (GV20) acupoints to investigate

whether moxibustion can reduce the depressive behavior by affecting KP metabolism in the gut-brain axis. First, depressive behavioral tests, intestinal inflammation, and IDO1 levels were measured and the correlation between depressive behavior and intestinal inflammation levels was assessed; then, hippocampal KP metabolism inflammation-inducing factor levels, key rate-limiting enzyme IDO1 content, and KP metabolites, hippocampal neuronal activity, and microglia activation were investigated.

Materials and methods

Laboratory animals

Clean grade male SD rats, weighing 150 ± 20 g, were obtained from the Animal Experiment Center of Shanghai University of Traditional Chinese Medicine. All rats were raised in SPF-grade feeding rooms in a controlled environment (temperature: 20–25°C, humidity: 40–70%, 12 h light/12 h dark cycle), and acclimatized for 1 week. Animals with normal diet and behavior and without adverse effects were included in the experiment [Experimental Animal Use License: SCXK (Shanghai) 2017-0005]. The experimental protocol complied with the national standard of the People's Republic of China for ethical review of experimental animal welfare GB/T 358922018 and was approved by the Animal Experimentation Ethics Committee of the Shanghai University of Traditional Chinese Medicine (No. PZSHUTCM200918016).

Model and methods of interventions

Preparation of model

The CD rat models were established according to the academically accepted protocol described by Morris et al. (1989), using 2,4,6-trinitrobenzene sulfonic acid (TNBS, No. P2297, Sigma, USA

Sigma, Novus Biologicals, Invitrogen, Abcam.). Rats were anesthetized by intraperitoneal injection of 2% sodium pentobarbital solution at 0.25 ml/100 g on days 1, 8, 15, and 22, respectively, after 24 h of fasting. Afterward, a mixture of 5% TNBS and 50% ethanol (2:1 ratio) was administered as an enema at a dose of 0.3 ml/100g. After the enema, the rats were held upside-down suspended by lower limbs for 3 min under anesthesia. Rats in the control group were anesthetized by the same method and administered an equal amount of saline by enema.

After the completion of modeling, three rats in the modeling and control groups were randomly selected and tested for depression-related behavior. Rats were sacrificed by neck dislocation under anesthesia, and the colon was harvested for hematoxylin-eosin (HE) staining and histopathologic scoring to evaluate whether the model establishment was successful. A schematic illustration of the experimental procedure is presented in **Figure 1**.

Grouping and intervention

Experiment I

Rats were randomly divided into 4 groups (n = 8/group) after 7 days of acclimatization, and therapeutic interventions were performed after modeling. Rats in the moxibustion group were treated with moxibustion at ST25, CV6, and GV20. These acupoints were selected with reference to previous studies (Bao et al., 2011; Zhao et al., 2019). The moxa strips were made of refined moxa velvet with a diameter of 0.5 cm (Hanyi, Henan Nanyang Han Medicine Moxa Co. Ltd.), ignited, and then applied at 2–3 cm vertically above the acupoints of the rats. The order of moxibustion was ST25 and CV6 first, followed by GV20. The treatment frequency was once every 10 min, once a day, for a total of 7 times (Bao et al., 2019). In the sham group, the moxa strips were not lit and the rest of the operation was the same as in the moxibustion group. Rats in the control group and the model group received no treatment and were only fastened in the same way as rats in the moxibustion group.

Experiment II

Rats were randomly divided into 5 groups (n = 8/group) after 7 days of acclimatization to the environment. The treatment intervention was performed for 7 days at the end of modeling, once a day, and the modalities of moxibustion were the same as in Experiment 1. In the 1-MT + moxibustion group, the IDO1 inhibitor 1-MT (No. 860646, Sigma, USA) was prepared as 10% 1-MT solution and 1 ml of the solution was injected intraperitoneally into rats with CD half an hour before each moxibustion, and 1 ml of 0.9% saline was injected intraperitoneally into the moxibustion group every day before moxibustion as the control. Rats in the 1-MT group were administered intraperitoneal injection of 1 ml per day, and rats in the control and model groups were administered intraperitoneal injection of 1 ml of 0.9% saline per day.

Specimen collection and processing

At the end of the intervention, rats in each group were weighed and then fasted for 24 h (with free access to water). Sample collection was performed on the following day. Rats were anesthetized with 2% sodium pentobarbital solution (0.25 ml/100 g intraperitoneally) according to their body mass. Three rats in each group were randomly selected for brain perfusion; hippocampal tissues were collected and soaked in 4% paraformaldehyde and fixed in a refrigerator at 4°C for 24 h for immunofluorescence staining and Western blot assay. After the remaining rats were anesthetized, a 2-cm section of the colon was laid flat on filter paper, and fixed by 4% paraformaldehyde immersion for colon bulk scoring, HE staining, and Western blot assay.

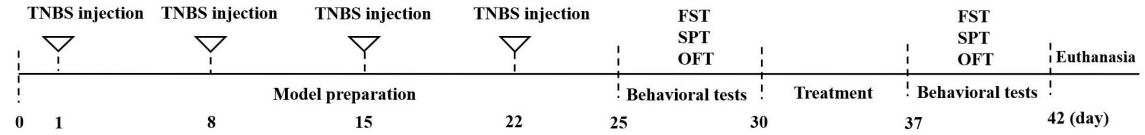

FIGURE 1
Experimental procedure.

Assessment of body weight and intestinal inflammation

Body weight

The increase in body weight at the end of the intervention in each group was compared with that at baseline.

Disease activity index

Rats were evaluated in terms of percentage loss of body mass, fecal traits, and blood in stool, referring to the method of calculating disease activity described by Murthy et al. (1993).

Macroscopic damage scoring of tissues

The morphology of colon was examined in each group, and then dissected along the longitudinal axis of the mesentery and washed with PBS solution to examine the gross morphology of the colonic mucosa. The Colonic Mucosal Damage Index (CMDI) was observed visually by referring to Paiotti et al. (2012), including vascular congestion and edema on the surface of the intestinal wall, ulceration, thickness of the intestinal wall, and adhesions.

Colonic histopathologic score

Colonic tissues from each group were subjected to HE staining and histopathological changes such as colonic mucosal epithelium, intestinal glands, inflammatory cell infiltration, and granulation tissue proliferation were observed under light microscopy. The grading was performed according to the method developed by Appleyard and Wallace (1995).

Depressive behavior tests

Forced swimming test

The forced swimming experiment was adapted from Petit-Demouliere et al. (2005). Rats were placed in transparent cylindrical (50 cm high, 30 cm diameter) buckets filled with water at a temperature of (23 ± 1)°C and a depth of 30–33 cm, with one rat in each bucket. Rats in the water were neither able to touch the bottom with the hind paws to support the body nor able to climb the barrel wall with the front paws. The cumulative resting time of the rats in the water was recorded, which was the time when the rats floated motionless on the water surface or kept their heads out of the water with only slight movement of the limbs to maintain the body balance. The behavioral performance of the rats was recorded for 6 min and the cumulative immobility time of the rats at the water surface during the last 5 min was analyzed. Each rat was tested individually.

Sucrose preference test

The sucrose preference test was adapted from Ko et al. (2020). All animals were trained to adapt and learn to drink sugar water for 48 h before the start of the test. One bottle of 1% sucrose water and one bottle of pure water for experimental animals were placed in each cage for the first 24 h, and the positions of the two bottles were exchanged around the second 24 h. At the end of adaptation period, all rats were taken off water for 4 h and then the sucrose preference test was performed. All rats were kept in a single cage during the experiment and provided two pre-weighed bottles of water, one bottle of 1% sucrose water and another bottle of pure water for experimental animals. The position of the two bottles was changed after 1 h; after 2 h, the two bottles were taken away and weighed. Sucrose preference ratio = total sucrose consumption/[total pure water consumption (g) + total sucrose consumption (g)] × 100%.

Open field test

The total path of the open field test was calculated as described by Walsh and Cummins (1976). Three days before the start of the experiment, the rats were stroked in the experimental environment for 5 min every day. During the test, each rat was placed at the center of a 100 × 100 × 50 cm open field box, and the movements of the rats were tracked using the Digbeth animal behavior video tracking analysis system for 5 min. Then the rats were removed, the bottom of the box and the four walls were cleaned, and the residual odor of the experiment was removed with 35% ethanol. A quiet environment was maintained during the test, and the rats in each group were tested alternately. After the completion of the test, the total path traveled for each rat's activity was analyzed.

Hematoxylin-eosin staining

Colonic specimens from rats were fixed in 10% formalin for 48 h and dehydrated by passage through a graded ethanol

series. The specimens were paraffin-embedded, sectioned, and dewaxed by immersion in xylene. The dewaxed slices were dehydrated by passage through different concentrations of ethanol. The slices were placed in an aqueous hematoxylin solution and eosin staining solution. The slides were placed in xylene for 3 min × 2 times transparent, sealed with neutral gum, then placed in an oven at 65°C for 15 min. Photographs were obtained through a microscope (NIKON Corporation, ECLIPSE Ci) and histopathologic scoring was performed.

Western blot

Cell lysates were separated by 10% sodium dodecyl sulfate-polyacrylamide gel electrophoresis, transferred to nitrocellulose membranes, and incubated with primary anti-Iba1 antibody (#17198, CST), c-fos antibody (NBP2-50037, Novus Biologicals), IDO1 antibody (PA5-107329, Invitrogen), GAPDH antibody (#5174, CST) for 2 h, followed by incubation with secondary anti-Goat anti-mouse IgG (1:1000, A0216, Beyotime) and Goat anti-rabbit IgG (1:1000, A0208, Beyotime) for 1 h at 37°C. The ECL luminescent solution was added to the front of the membrane for 5 min in the darkroom to visualize the protein, which was placed in an imaging system (Tanon, Tanon-5200) for scanning to detect the reaction bands.

Immunofluorescent staining

Hippocampus specimens from rats were rinsed with saline at 4°C, fixed in 10% formalin for 24 h, paraffin embedded, and sliced. The slices were dewaxed in xylene, soaked in graded alcohol series for 5 min, and rinsed in tap water for 10 min, respectively. 0.01 M sodium citrate buffer solution was used for high-pressure repair for 15 min, and drops of primary anti-Iba-1 antibody (1:100, ab283319, Abcam), c-fos antibody (1:100, ab214672, Abcam) were added to the wet box and incubated overnight at 4°C. The slices were rinsed thrice with PBS for 3 min each and incubated with the corresponding secondary antibodies donkey anti-mouse IgG (1:500, A0460, Biyuntian) and goat anti-rabbit IgG (1:500, A0423, Biyuntian). DAPI (1:5000 dilution) was added to the anti-quench sealer, sealed, stored in the refrigerator at −20°C, and photographed by fluorescence microscopy (NIKON, ECLIPSE Ni).

Statistical analysis

Continuous variables exhibiting homogenous variance and normal distribution were presented as mean ± standard deviation and between-group differences were assessed using one-way ANOVA, with *post-hoc* LSD test used for multiple comparisons; paired test was used for within-group comparisons. Continuous variables with non-normal distribution or inhomogenous variance were presented as median (interquartile range), and between-group differences were assessed using the Kruskal–Wallis *H* test; the Nemenyi test was used for multiple comparisons, while the Wilcoxon rank sum test was used for within-group comparisons. The correlation between intestinal inflammation and depressive behavior in each group was analyzed using a typical correlation. Experimental images were analyzed using ImageJ (NIH, USA) as well as Analyze Skeleton (2D/3D) and FracLac plug-in packages. Statistical analyses were performed using SPSS 24.0 (IBM, USA). *P*-values < 0.05 were considered indicative of statistical significance.

Results

Experiment I

Assessment of body weight and intestinal inflammation

The increase in body weight of rats in the model group was significantly lower than that in the control group ($P < 0.01$). A significant increase in weight gain was observed after moxibustion treatment ($P < 0.05$) (**Figure 2A**). The disease activity index (DAI) score, CMDI score, and colonic histopathologic score in the model group were significantly higher than those in the control group ($P < 0.01$ for all), but all were reversed after moxibustion treatment ($P < 0.01$ for all), and significantly superior to those in the sham group ($P < 0.01$, $P < 0.05$, $P < 0.01$, respectively) (**Figures 2B–E**). This suggests that moxibustion significantly reduced abnormally high DAI score, CMDI score, and colonic histopathologic score, as well as accelerated weight gain in depressed rats with CD.

Behavioral evaluation of depression in rats

To evaluate whether the modeling was successful and to assess the therapeutic effect of moxibustion, we performed behavioral tests on rats. In the sucrose preference test (SPT), rats in the model group had a significantly lower sucrose preference ratio compared with the control group ($P < 0.05$), and rats in the moxibustion group had a significantly higher sucrose preference ratio after treatment ($P < 0.01$), which was significantly better than that in the sham group ($P < 0.05$) (**Figure 3A**). Moxibustion significantly reduced the floating time of rats ($P < 0.05$) which was significantly better than that in the sham group ($P < 0.05$) (**Figure 3B**). In terms of open field test (OFT), the total path in the model group was significantly reduced compared with the control group ($P < 0.01$), and the total path was significantly increased after applying moxibustion ($P < 0.01$) and significantly better than that in the sham group ($P < 0.05$) (**Figures 3C, D**). The results suggest that moxibustion can effectively alleviate the depressive state of rats with CD.

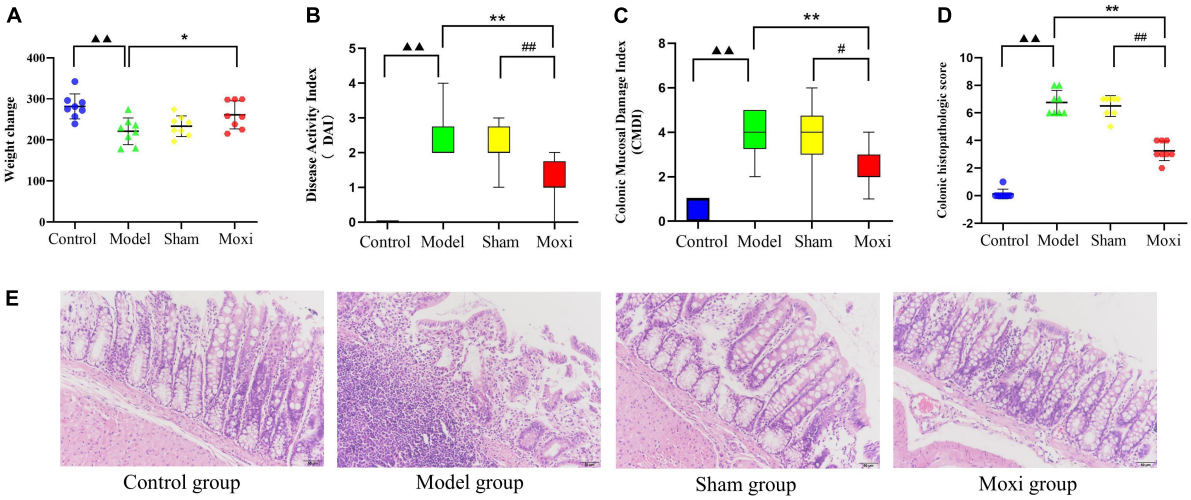

FIGURE 2
Effect of moxibustion on weight gain and improvement of intestinal inflammation levels. **(A)** Change in body weight, **(B)** Disease activity index (DAI) score, **(C)** Colonic Mucosal Damage Index (CMDI) score, and **(D)** Colonic histopathologic score. **(E)** Hematoxylin-eosin (HE)-stained sections of colon tissue of rats in each group. $n = 8$ per group. $^{▲▲}P < 0.01$ vs. control group; $^{*}P < 0.05$, $^{**}P < 0.01$ vs. model group; $^{\#}P < 0.05$, $^{\#\#}P < 0.01$ vs. sham group.

Correlation analysis of intestinal inflammation and depressive behavior in each group

The sucrose preference ratio of rats also showed a significant positive correlation with body weight gain ($r = 0.514$, $P < 0.01$). The sucrose preference ratio and total path showed a significant negative correlation with DAI score, CMDI score, and histopathologic score. The floating time of rats showed a significant positive correlation with DAI score ($r = 0.583$, $P < 0.001$) and histopathologic score ($r = 0.42$, $P < 0.05$).

Protein expression levels of IDO1, IL-1β, and TNF-α in the colon

Colon IDO1 protein expression in the model group was significantly greater than that in the control group ($P < 0.01$), suggesting high expression of IDO1, a key rate-limiting enzyme for KP metabolism, and accelerated KP metabolism. Compared with the model group, the expression of IDO1 protein was significantly decreased in the moxibustion group ($P < 0.01$), and the expression was lower than that in the sham group ($P < 0.01$) (**Figures 4A, B**). The expression of colonic IL-1β protein and TNF-α protein was significantly higher in the model group compared to the control group ($P < 0.01$ for both), suggesting that the increased expression level of IDO1-inducing factor (IDO1 is a rate-limiting enzyme of intestinal KP metabolism) is a potential cause of IDO1 activation. Compared with the model group, the expression of both proteins was significantly reduced after moxibustion treatment ($P < 0.01$ for both), and the expression was lower compared to that in the sham group ($P < 0.01$, both) (**Figures 4A, C, D**). These findings suggested that moxibustion significantly inhibited intestinal inflammation in depressed rats with CD, reduced the high expressions of IDO1-inducing factors IL-1β protein and TNF-α protein, and inhibited the activation of IDO1 protein, which may slow down the metabolism of KP.

Experiment I

Assessment of body weight and intestinal inflammation

The body weight of rats in the model group was significantly lower than that in the control group ($P < 0.01$), while the DAI score, CMDI score, and colonic histopathologic score were significantly higher than those in the control group ($P < 0.01$ for *all*). After the intervention, DAI score (**Figure 5B**), CMDI score (**Figure 5C**), and colonic histopathologic score in the moxibustion group, 1-MT group, and 1-MT + moxibustion group were significantly lower than those in the model group (**Figures 5D, E**) ($P < 0.01$ for all except DAI score in the 1-MT group, $P < 0.05$); the body weight of rats in the moxibustion group and 1-MT + moxibustion group showed a significant increase ($P < 0.01$) (**Figure 5A**). The differences between the three groups were not significant. These findings suggested that moxibustion, 1-MT, or the combination of both significantly reduced the abnormally high DAI score, CMDI score, and colonic histopathologic score in depressed rats with CD. Moxibustion and moxibustion combined with 1-MT also contributed to the increase in body mass, but the addition of 1-MT to moxibustion did not significantly increase the effect.

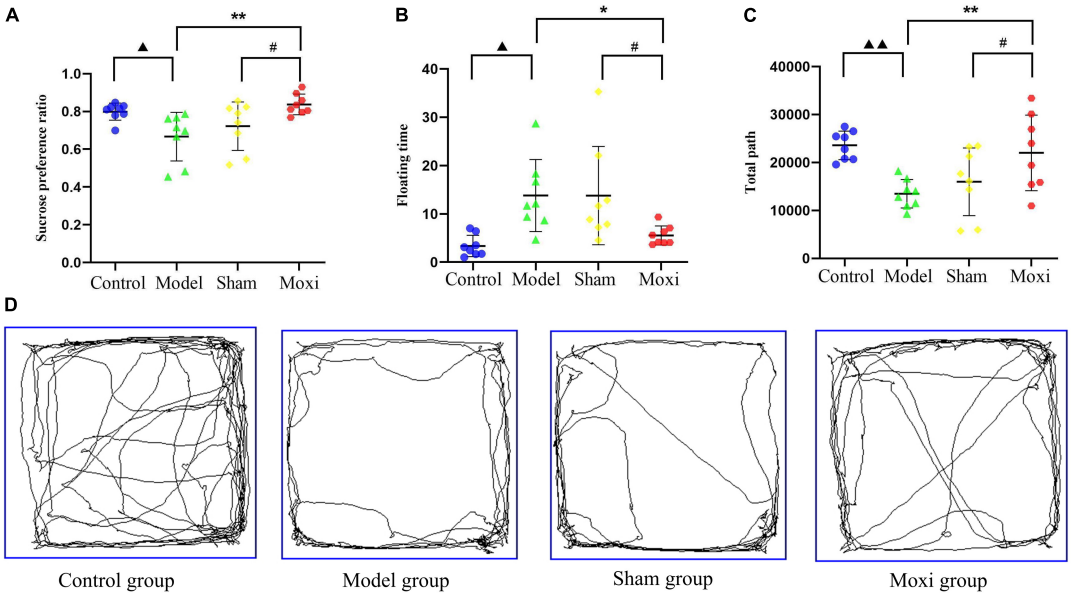

FIGURE 3
Effect of moxibustion on alleviating depression-like behavior. **(A)** Sucrose preference ratio, **(B)** Floating time, **(C)** Total path, and **(D)** Activity trajectory in the open field experiment of rats in each group. $n = 8$ per group. $^{▲}P < 0.05$ vs. control group, $^{▲▲}P < 0.01$ vs. control group; $^{*}P < 0.05$, $^{**}P < 0.01$ vs. model group; $^{\#}P < 0.05$ vs. sham group.

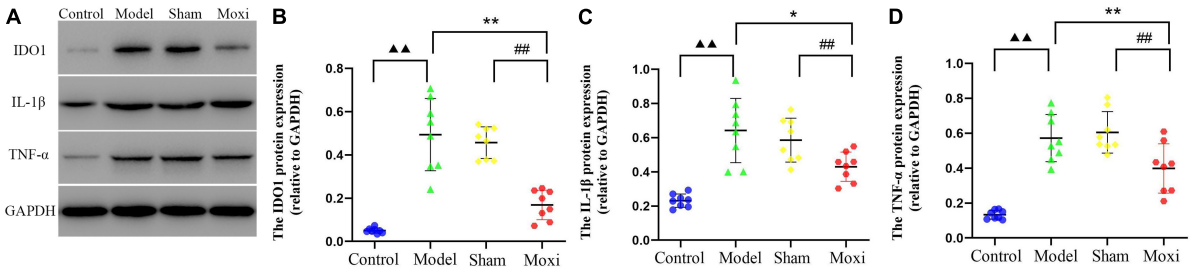

FIGURE 4
Effect of moxibustion on protein expressions of IDO1, IL-1β, and TNF-α in the colon. **(A)** Western blot bands of IDO1, IL-1β, and TNF-α protein expression, **(B)** IDO1 protein, **(C)** IL-1β protein, and **(D)** TNF-α protein expression in the colon of rats in each group. $n = 8$ per group. $^{▲▲}P < 0.01$ vs. control group; $^{*}P < 0.05$, $^{**}P < 0.01$ vs. model group; $^{\#\#}P < 0.01$ vs. moxibustion group.

Behavioral evaluation of depression in rats

The sucrose preference index and the total path of the open field test in the model group were significantly lower than those in the control group ($P < 0.01$ for both), while the floating time was significantly higher ($P < 0.01$), suggesting a depressive state in the rat model of CD. After the intervention, the sucrose preference index in the moxibustion group and the 1-MT group was significantly higher than that in the model group ($P < 0.05$ for both) (Figure 6A); the floating time was significantly decreased in the moxibustion group, the 1-MT group, and the 1-MT + moxibustion group ($P < 0.05$, $P < 0.05$, $P < 0.01$, respectively) (Figure 6B), and the total path of the open-field test was significantly increased ($P < 0.01$, $P < 0.05$, $P < 0.01$, respectively) (Figures 6C, D). However, there was no significant difference between moxibustion group, 1-MT group, and 1-MT + moxibustion group in this respect. These findings suggested that moxibustion, 1-MT, and 1-MT + moxibustion all significantly alleviated depressive behavior in rats with CD, and that the addition of 1-MT to moxibustion did not significantly increase the effect.

Morphology of hippocampal neuronal cell activity and microglia

The Iba1 microglia in the resting state was branched, with yellow or brownish-yellow cells, mainly distributed in the cytoplasm and intercellular stroma. Compared with the control group, Iba1 expression was increased in the cerebral cortex of the model group rats, and the cell protrusions were retracted

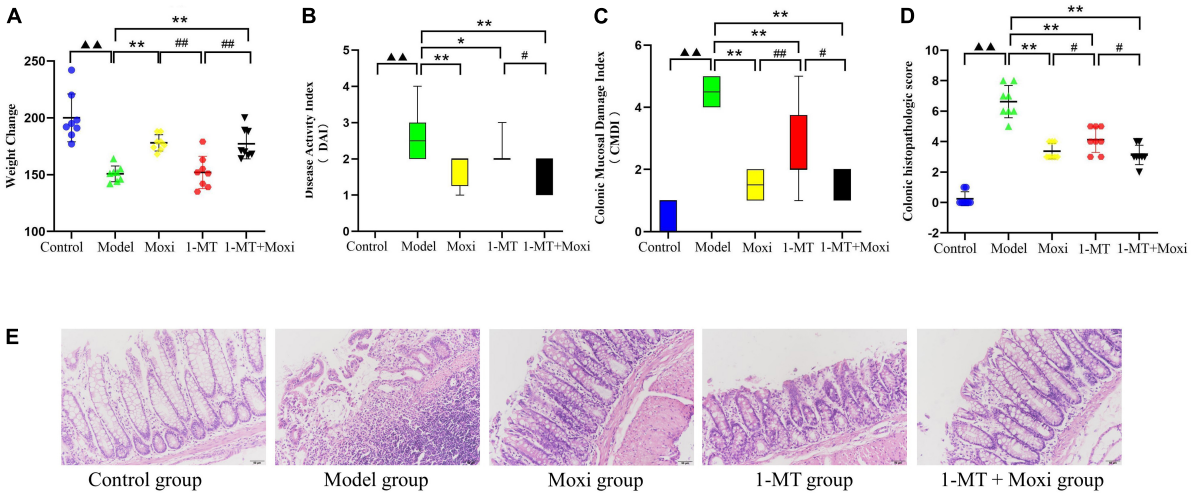

FIGURE 5
Effects of moxibustion, 1-MT, or a combination of both on weight gain and improvement of intestinal inflammation levels. **(A)** Change in body weight, **(B)** Disease activity index (DAI) score, **(C)** Colonic Mucosal Damage Index (CMDI) score, and **(D)** Colonic histopathologic score. **(E)** Hematoxylin-eosin (HE)-stained sections of colon tissue of rats in each group. $n = 8$ per group. $^{▲▲}P < 0.01$ vs. control group; $^{*}P < 0.05$, $^{**}P < 0.01$ vs. model group; $^{\#}P < 0.05$, $^{\#\#}P < 0.01$ vs. 1-MT group.

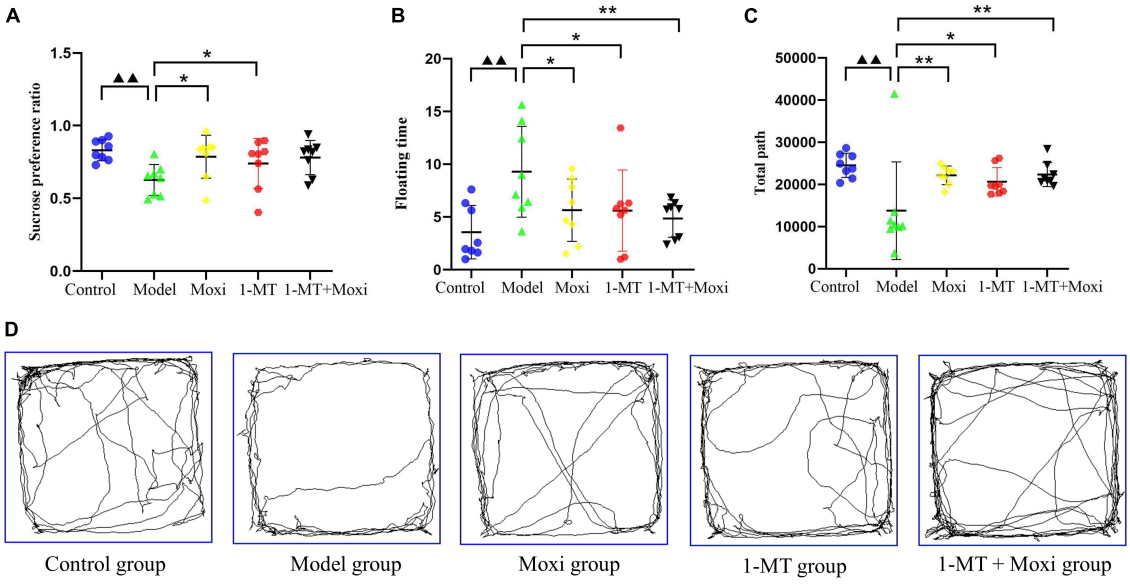

FIGURE 6
Effects of moxibustion, 1-MT, or a combination of both on alleviating depression-like behavior. **(A)** Sucrose preference ratio, **(B)** Floating time of rats in each group; **(C)** Total path, and **(D)** Activity trajectory of rats in the open field experiment of rats in each group. $n = 8$ per group. $^{▲▲}P < 0.01$ vs. control group; $^{*}P < 0.05$, $^{**}P < 0.01$ vs. model group.

with an amoeboid appearance, indicating successful induction of microglia activation; a large number of c-fos neurons were also seen expressed as oval and round brown neurons. After 1-MT, moxibustion, and 1-MT + moxibustion interventions, microglia activation in the hippocampus was reduced in the three groups, and neuronal activation was also reduced, which was improved compared with the model group (Figure 7).

Detection of biomarkers in hippocampal neuronal cell and microglia

Hippocampal c-fos protein and Iba-1 protein expressions in the model group were significantly higher than those in the control group ($P < 0.01$ for both), suggesting abnormal increase in neuronal activity and microglia activation in the hippocampus of depressed rats with CD. After the intervention,

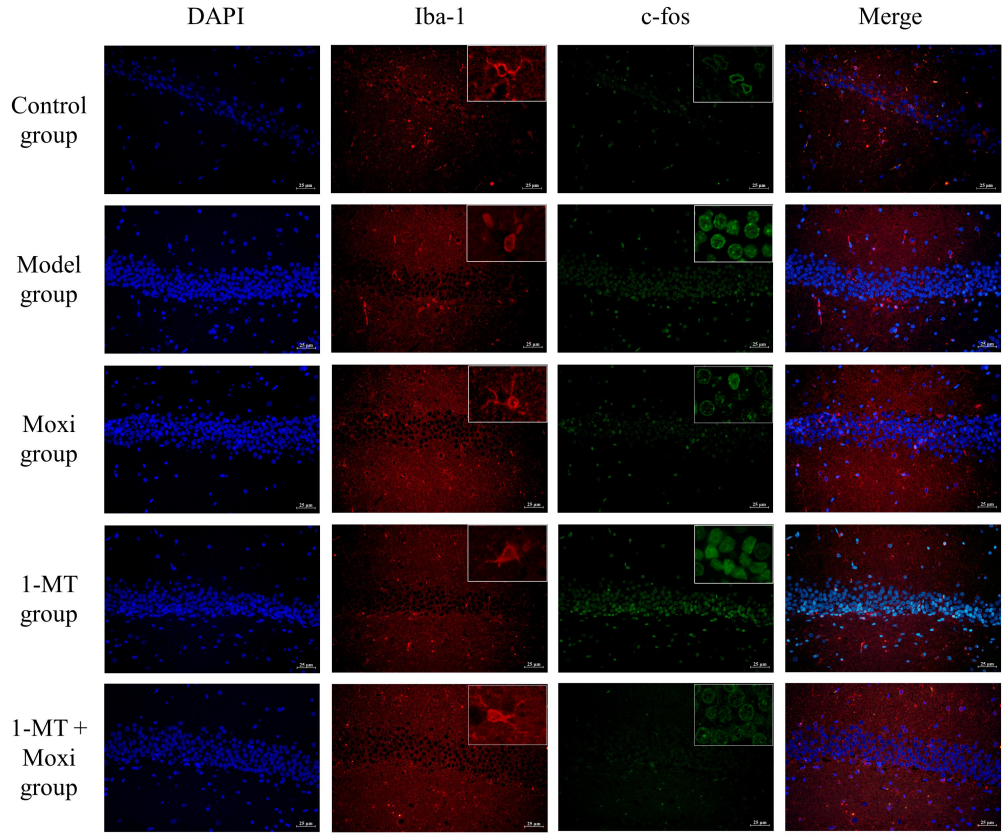

FIGURE 7
Effects of moxibustion, 1-MT, or a combination of both on improving hippocampal neuronal activity and microglia activation morphology in each group of rats. Representative images of immunofluorescence staining of hippocampal slices for DAPI (blue, nuclei indicator), Iba-1 (red), TLR4 (green), Iba-1 (red) + TLR4 (green). $n = 3$ per group.

hippocampal Iba-1 protein expression ($P < 0.01$ for both) and c-fos protein ($P < 0.01$ for both) were significantly decreased in the moxibustion group and the 1-MT + moxibustion group compared with the model group, while there was no significant change in the Iba-1 protein expression. There was no significant difference between the moxibustion group and the 1-MT + moxibustion group with respect to hippocampal c-fos protein or Iba-1 protein expression (**Figures 8A–C**). These findings suggested that moxibustion, 1-MT, and 1-MT + moxibustion all significantly reduced the abnormally high expression of hippocampal c-fos and Iba-1 protein in the depressed rats with CD and inhibited the abnormal activation of neurons and microglia, while the combination of moxibustion and 1-MT did not significantly enhance the effect.

Detection of hippocampal kynurenine pathway

The hippocampal KYN/TRP ratio in the model group was significantly higher than that in the control group ($P < 0.01$), and the KYNA/KYN ratio and KYNA/QUIN ratio were significantly lower than that in the control group ($P < 0.01$, both), suggesting that the balance between KYNA and QUIN was disrupted by increased hippocampal KP metabolism in depressed rats with CD. After the intervention, compared with the model group, the expression of hippocampal KYN/TRP ratio was significantly decreased ($P < 0.01$ for *all*), and the KYNA/KYN ratio was significantly increased ($P < 0.05$ for *all*) in the moxibustion group, 1-MT group, and 1-MT + moxibustion group. In addition, the KYNA/QUIN ratio was also significantly increased ($P < 0.05$, both) in the moxibustion group and 1-MT + moxibustion group; however, the differences between these two groups were not statistically significant. There was no significant difference between the model group and the control group, or between the hippocampal QUIN/KYN ratios after the intervention (**Figures 8D–G**). The results indicated that there was increased hippocampal KP metabolism, an imbalance between KYNA and QUIN metabolism, and an increased KYNA/QUIN ratio in the depressed rats with CD compared to the control group. Both moxibustion and 1-MT + moxibustion significantly decreased the hippocampal KYN/TRP ratio and increased KYNA/KYN and KYNA/QUIN ratios in CD depressed rats, suggesting a slowing down of that KP metabolism after the intervention; in

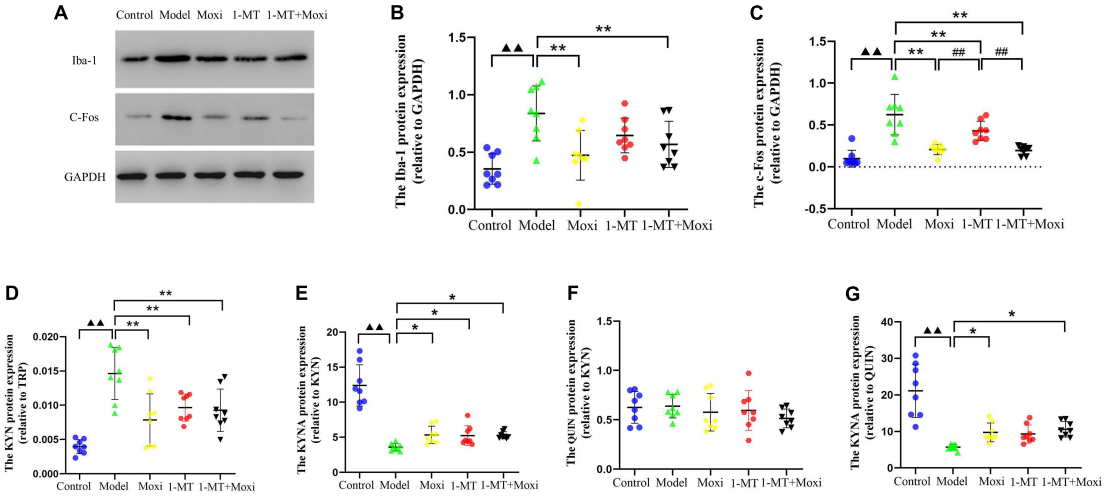

FIGURE 8
Effects of moxibustion, 1-MT, or a combination of both on improving hippocampal neuronal activity and microglia activation markers in each group of rats. **(A)** Western blot bands of Iba-1 and c-fos protein expression, **(B)** Iba-1 protein expression, **(C)** c-fos protein expression, **(D)** KYN/TRP ratio, **(E)** KYNA/KYN ratio, **(F)** QUIN/KYN ratio, and **(G)** KYNA/QUIN ratio in the hippocampus of rats in each group. $n = 8$ per group. ▲▲$P < 0.01$ vs. control group; *$P < 0.05$, **$P < 0.01$ vs. model group; ##$P < 0.01$ vs. 1-MT group.

addition, the combination of moxibustion and 1-MT did not increase the effect.

Protein expression of IDO1—The key rate-limiting enzyme of kynurenine pathway metabolism

Hippocampal IDO1 protein expression in the model group was significantly higher than that in the control group ($P < 0.01$). After the intervention, hippocampal IDO1 protein expression in the 1-MT group, moxibustion group, and 1-MT + moxibustion group were significantly decreased compared with the model group ($P < 0.01$ for all). Hippocampal IDO1 protein expression in the moxibustion group and 1-MT + moxibustion group was lower than that in the 1-MT group ($P < 0.05$, $P < 0.01$, respectively). However, there was no significant difference between the 1-MT + moxibustion and moxibustion groups in this respect (Figure 9). This suggested that moxibustion, 1-MT, and 1-MT + moxibustion all significantly reduced the abnormally high expression of IDO1 protein in the hippocampus of the depressed rats with CD. Moxibustion and 1-MT + moxibustion were more effective than 1-MT, but the combination of moxibustion and 1-MT did not significantly increase the effect of moxibustion.

Content of kynurenine pathway's key rate-limiting enzyme IDO1 regulatory factor—TNF-α and IL-1β

The protein expression of TNF-α and IL-1β in the hippocampus of rats in the model group was significantly higher than that in the control group ($P < 0.01$, both). After the intervention, the hippocampal TNF-α protein expression significantly decreased in the moxibustion group and the 1-MT + moxibustion group compared with the model group ($P < 0.01$, both), and IL-1β protein also significantly decreased, as well as IL-1β protein significantly decreased in the 1-MT group. Compared with the 1-MT group, the hippocampal TNF-α protein expression was lower in the moxibustion and moxibustion + 1-MT groups ($P < 0.05$ for both), while there was no significant difference between the three groups. This suggested that moxibustion and 1-MT + moxibustion significantly reduced hippocampal TNF-α protein in depressed rats with CD, and the effect of the combination was better than that of 1-MT alone. Moxibustion, 1-MT, and 1-MT + moxibustion all significantly reduced the abnormally high expression of IL-1β protein in the hippocampus of depressed rats with CD. The use of 1-MT did not significantly increase the inhibitory effect of moxibustion on TNF-α protein and IL-1β protein.

Discussion

In this study, rats with CD exhibited some behavioral changes akin to those observed in depression. The potential mechanism may involve the gut-brain axis in hippocampal KP metabolism accompanied by hippocampal neuronal activation and increased microglia activity. In contrast, the excessive metabolism of tryptophan by the KP pathway caused by activation of intestinal IDO1 may be one of the important factors contributing to the increase in hippocampal KP metabolites. Our findings suggest that the potential mechanism of action of moxibustion and the combination of moxibustion

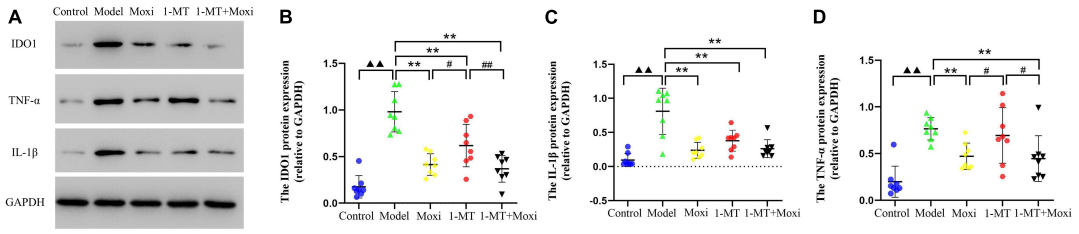

FIGURE 9
Effects of moxibustion, 1-MT, or a combination of both on protein expression of IDO1, IL-1β, and TNF-α in the hippocampus. **(A)** Western blot bands of IDO1, IL-1β, and TNF-α protein expression, **(B)** IDO1 protein expression, **(C)** TNF-α protein expression, and **(D)** IL-1β protein expression in the hippocampus of rats in each group. $n = 8$ per group. $^{▲▲}P < 0.01$ vs. control group; $^{**}P < 0.01$ vs. model group; $^{\#}P < 0.05$, $^{\#\#}P < 0.01$ vs. 1-MT group.

with 1-MT is through inhibition of the IDO1 and the KP metabolic pathway that mediates the "crosstalk" between the gut and the brain. The depressive behaviors of the restrained rat were greatly reversed by moxibustion or moxibustion + 1-MT. Moreover, the combination of moxibustion and 1-MT was found to be less effective than moxibustion alone. A schematic illustration of the mechanism by which moxibustion alleviates TNBS-induced depressive behavior in rats with CD is shown in **Figure 10**.

Compared with the control group, the body weight, sucrose preference index, and total path of the open field test were significantly reduced in the model group, but significantly increased after moxibustion treatment; while the DAI score, CMDI score, colonic histopathologic score, and floating time were significantly increased in the model group rats, and significantly reduced after moxibustion treatment. As in rather, TNBS used in the modeling process can cause serious damage to intestinal function affecting both digestion and absorption, and induce depressive manifestations. Intestinal inflammation showed a significant correlation with depression, suggesting that the two develop in parallel. The more severe the intestinal inflammation, the more pronounced was the depression-like behavior. This supports further research into the potential mechanisms between intestinal inflammation and depressive behaviors. On the other hand, IDO1 protein, a key rate-limiting enzyme of KP, has been extensively studied in the control of mood and behavior as well as psychopathogenesis. IDO1 has been shown to be activated by inflammatory cytokines such as IFN-γ, TNF-α, and IL-1β. Studies have found reduced circulating levels of TRP in cancer patients treated with IL-2 or IFN-α (Capuron et al., 2002). Some studies have also found elevated inflammatory cytokines in some depressed patients (Maes, 1995). In the study by Kim et al. (2012) and Lawson et al. (2013), IDO1 pharmacological inhibition or knockdown was found to alleviate depressive behavior in rats. Interestingly, in this study, the expressions of IDO1, IL-1β, and TNF-α proteins of the model group were significantly higher than that of the control, but they became significantly lower after moxibustion or moxibustion + 1-MT, although the addition of 1-MT did not result in a significant enhancement of the effect of moxibustion. This suggested that the therapeutic effect of moxibustion may be mediated *via* decrease in IDO1 protein and its inducing factors IL-1β protein and TNF-α protein, thus reducing intestinal inflammation and depressive behavior by inhibiting KP. Both moxibustion and 1-MT may have a similar mechanism of action; therefore, the addition of 1-MT to moxibustion failed to increase the effect. TRP is one of the eight essential amino acids in the human body. TRP content in the diet is degraded through three main pathways after entering the human body, with the vast majority of TRP ingested into the human body being converted through the IDO1-mediated KP pathway (Agus et al., 2018). IDO1 plays an essential role in KP. Therefore, we hypothesized that the anti-depression effects of moxibustion are mainly mediated through KP and have synergistic effects of multiple metabolites.

After TRP is absorbed through the intestine, part of it is metabolized into subsequent products in the intestine, liver, and other organs, and part of it directly enters the blood circulation (Gracie et al., 2019). TRP, KYN, and some of the products can penetrate the blood-brain barrier (Cervenka et al., 2017). In the intracerebral environment, IDO1 is expressed mainly on microglia and astrocytes. Approximately 40% of the KYN content in the brain is synthesized in the brain and the rest is derived from plasma (Gal and Sherman, 1980). As expected, hippocampal neuronal activity, microglia activation, c-fos protein, Iba-1 protein, and IDO1 protein were significantly reduced by moxibustion or moxibustion combined with 1-MT treatment, which suggests that moxibustion may improve depressive behavior by inhibiting IDO1 protein production, mediating KP, and by modulating neuronal activation and microglia activation. Owing to the similar mechanisms of action of moxibustion and 1-MT, the combination of the two failed to increase the effect.

Previous studies (Ogyu et al., 2018) have revealed KP disorders in depressed patients with reduced levels of KYNA and KYN and elevated levels of QUIN in patients who were not taking antidepressants. These findings suggested the involvement of the KP pathway in the development of

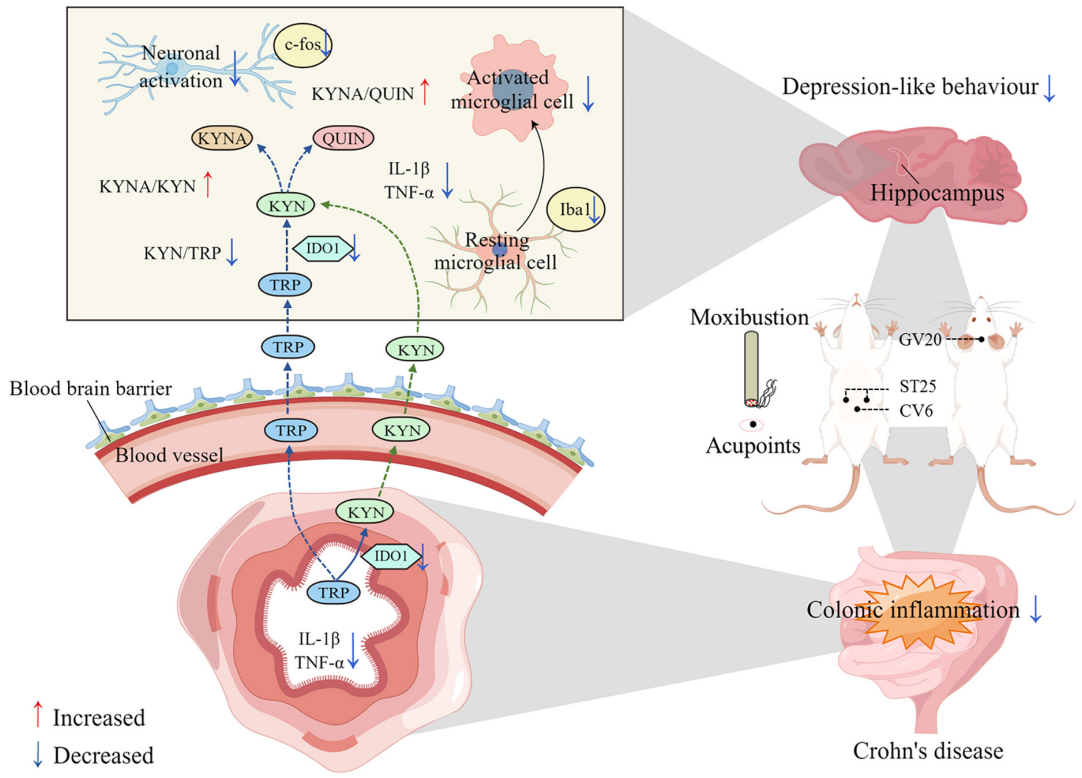

FIGURE 10
Schematic illustration of this research: the potential mechanism by which moxibustion inhibits gut-brain axis kynurenine pathway (KP) metabolism in the treatment of 2,4,6-trinitrobenzenesulfonic acid (TNBS)-induced depressive behavior in rats with Crohn's disease (CD). The mechanism of action of moxibustion at ST25, CV6, and GV20 to improve depression-like behavior and intestinal inflammation in rats with CD may be due to the reduction of intestinal inflammatory cytokines, such as IL-1β and TNF-α, after moxibustion treatment. These inflammatory factors further reduced the activation of intestinal IDO1 and inhibited the excessive degradation of TRP to KYN in the intestine. KYN crosses the blood-brain barrier through the gut-brain axis and enters the brain, where it is further metabolized to KYNA and QUIN. In contrast, the increased ratio of KYNA/KYN and KYNA/QUIN, reduced microglia activation and neuronal activity in hippocampus after moxibustion intervention may be one of the mechanisms by which moxibustion alleviates depression-like behavior in rats with CD.

depression. The principal metabolite of KP, QUIN, is mainly produced in microglia (Guillemin et al., 2005), and is an agonist of *N*-methyl-D-aspartate (NMDA) receptors and a neuroexcitatory toxin found mainly in the forebrain (Schwarcz et al., 2012). Available evidence suggests that a series of neurotoxic effects caused by excessive activation of NMDA receptors in glutamate receptors is one of the important mechanisms of depression (Murrough et al., 2017). Among the NMDA receptor subtypes, the subtypes 2A and 2B show the highest affinity for QUIN and are widely distributed in the hippocampus. Moreover, quinolinate phosphoribosyl transferase (QPRT) activity is low in the hippocampus, and QUIN is difficult to metabolize in the hippocampus; therefore, the neurotoxicity of QUIN is most likely to affect the hippocampus (Lugo-Huitron et al., 2013). As a result, we speculate that the depressive behavior in CD model rats may be stimulated by dyshomeostasis of KP in hippocampal regions.

Studies have shown that the effect of acupuncture on depressive behaviors may be related to the regulation of the KP pathway. Kwon et al. (2012) induced an inflammatory depression model in mice with BCG vaccine and acupunctured the Sanyinjiao (SP6) and Shenmen (HT7) acupoints in mice. They found that acupuncture reduced depressive behaviors in the model mice and affected both serum KP and hippocampal dopamine. Li et al. (2019) found a reduction of depressive behavior in moxibustion rats in a similar model, and observed a strong correlation between hippocampal Kyn/Trp ratio and behavioral scores. Consistent with the above, the model group in our study showed a significantly increased KYN/TRP ratio and significantly decreased KYNA/KYN and KYNA/QUIN ratios compared to the control group; however, all of these metabolite ratios were reversed by moxibustion or co-treatment with 1-MT. Several studies have supported the association of KYN/TRP with CD disease activity, C-reactive protein, hematocrit (Gupta et al., 2012), and other important indices. Several studies have used KYNA/QUIN as a putative neuroprotective factor. Serum KYNA/QUIN was lower in depressed patients and showed a negative correlation with low pleasure, while a

positive correlation was observed with hippocampal and amygdala volume in depressed patients (Savitz et al., 2015a,b). Therefore, our findings demonstrated that moxibustion may alleviate depressive behaviors in rats by modulating KP in the hippocampus. The mechanisms of action of moxibustion and 1-MT may be similar, so the combination of the two failed to increase the effect.

In summary, our findings suggested that moxibustion may be beneficial in improving inflammation and metabolic disorders in the hippocampal region by reducing excessive activation of hippocampal neurons and microglia, thereby inhibiting KP. The current study established a TNBS-induced model of CD and showed that depression in CD may be associated with neurotransmitter disturbances along the gut-brain axis. KP products can be modulated by moxibustion, suggesting that metabolic changes and behavior in the central nervous system may be influenced by moxibustion through KP along the gut-brain axis, which may result in improvement in depressive behavior. Our study provides a theoretical basis for early intervention for depressive behaviors, and contributes to the understanding of the mechanisms of depression and even other neuropsychiatric disorders.

However, some limitations of our study should be acknowledged. First, the pain induced by insertion of the needle for administration of each dose is liable to induce stress (Jin et al., 2019). Secondly, the immunofluorescence and Western blot assay used in the study were restricted to the analysis of protein expression, and RT-PCR was not applied to detect the corresponding gene expression levels. In addition, the effects of moxibustion intervention on NMDA receptors in microglia and neurotransmitter metabolism need to be further studied. Third, no IDO1 activator was applied in this study to further validate the effect of moxibustion. Fourth, gut microbes are also involved in one of the pathways of tryptophan metabolism (Agus et al., 2018), and future studies should investigate whether moxibustion affects IBD depression through additional pathways.

Conclusion

In the present study, moxibustion at ST25, CV6, and GV20 acupoints alleviated CD depression-like behavior, which may be related to the inhibition of intestinal pro-inflammatory factors as well as IDO1 expression, which in turn inhibited excessive KP metabolism of tryptophan, thereby attenuating the effect of KP metabolites in the gut-brain axis and inhibiting hippocampal neuronal activation and microglia activation. The mechanism by which moxibustion alleviates depressive behavior in rats with TNBS-induced colitis may involve the bidirectional regulatory mechanism between the brain and the gut. Although moxibustion is not considered as a routine antidepressant therapy, our study provides evidence for the clinical application of moxibustion as an adjunctive treatment for CD-related depression.

Data availability statement

All datasets generated for this study are included in the article/supplementary material.

Ethics statement

This animal study was reviewed and approved by the Experimental Animal Ethics Committee of the Shanghai University of Traditional Chinese Medicine (No. PZSHUTCM200918016).

Author contributions

CB conceptualized the study and designed the experiments. LC, DY, JH, and YM performed the experiments. HZ performed the data analysis. CB and JH drafted this manuscript. HW, HL, YS, and YL supervised the study and gave critical revision of the manuscript. All authors approved the final version of the manuscript.

Funding

This work was supported by the Shanghai Rising-Star Program (19QA1408100), the National Key Basic Research Program of China (2015CB554500), and National Natural Science Foundation of China (81904303).

Acknowledgments

We thank Yunjia Gu, Mengfan Cui, Kunli Liu, and Xiyin Zhang for their help in the preparation of the animal models and sample collection. We also thank Figdraw for providing the drawing tool.

Conflict of interest

The authors declare that the research was conducted in the absence of any commercial or financial relationships that could be construed as a potential conflict of interest.

Publisher's note

References

Agus, A., Planchais, J., and Sokol, H. (2018). Gut microbiota regulation of tryptophan metabolism in health and disease. *Cell Host Microbe* 23, 716–724. doi: 10.1016/j.chom.2018.05.003

Ananthakrishnan, A. N. (2015). Epidemiology and risk factors for IBD. *Nat. Rev. Gastroenterol. Hepatol.* 12, 205–217. doi: 10.1038/nrgastro.2015.34

Appleyard, C. B., and Wallace, J. L. (1995). Reactivation of hapten-induced colitis and its prevention by anti-inflammatory drugs. *Am. J. Physiol.* 269(1 Pt 1), G119–G125. doi: 10.1152/ajpgi.1995.269.1.G119

Badawy, A. A. (2017). Kynurenine pathway of tryptophan metabolism: Regulatory and functional aspects. *Int. J. Tryptophan Res.* 10:1178646917691938. doi: 10.1177/1178646917691938

Bao, C. H., Liu, P., Liu, H. R., Wu, L. Y., Shi, Y., Chen, W. F., et al. (2015). Alterations in brain grey matter structures in patients with Crohn's disease and their correlation with psychological distress. *J. Crohns Colitis* 9, 532–540. doi: 10.1093/ecco-jcc/jjv057

Bao, C. H., Wang, C. Y., Li, G. N., Yan, Y. L., Wang, D., Jin, X. M., et al. (2019). Effect of mild moxibustion on intestinal microbiota and NLRP6 inflammasome signaling in rats with post-inflammatory irritable bowel syndrome. *World J Gastroenterol.* 25, 4696–4714. doi: 10.3748/wjg.v25.i32.4696

Bao, C. H., Wu, L. Y., Shi, Y., Wu, H. G., Liu, H. R., Zhang, R., et al. (2011). Moxibustion down-regulates colonic epithelial cell apoptosis and repairs tight junctions in rats with Crohn's disease. *World J. Gastroenterol.* 17, 4960–4970. doi: 10.3748/wjg.v25.i32.4696

Bao, C. H., Zhao, J. M., Liu, H. R., Lu, Y., Zhu, Y. F., Shi, Y., et al. (2014). Randomized controlled trial: Moxibustion and acupuncture for the treatment of Crohn's disease. *World J. Gastroenterol.* 20, 11000–11011. doi: 10.3748/wjg.v20.i31.11000

Bao, C. H., Zhong, J., Liu, H. R., Gu, Y. P., Wu, P., Gu, K., et al. (2021). [Effect of acupuncture-moxibustion on negative emotions and plasma tryptophan metabolism in patients with Crohn's disease at active stage]. *Zhongguo Zhen Jiu* 41, 17–22. doi: 10.13703/j.0255-2930.20200814-k0003

Bao, C., Liu, P., Liu, H., Jin, X., Calhoun, V. D., Wu, L., et al. (2016). Different brain responses to electro-acupuncture and moxibustion treatment in patients with Crohn's disease. *Sci. Rep.* 6:36636. doi: 10.1038/srep36636

Bao, C., Wang, D., Liu, P., Shi, Y., Jin, X., Wu, L., et al. (2017). Effect of electro-acupuncture and moxibustion on brain connectivity in patients with Crohn's disease: A resting-state fMRI study. *Front. Hum. Neurosci.* 11:559. doi: 10.3389/fnhum.2017

Bao, C., Wu, L., Wang, D., Chen, L., Jin, X., Shi, Y., et al. (2022). Acupuncture improves the symptoms, intestinal microbiota, and inflammation of patients with mild to moderate Crohn's disease: A randomized controlled trial. *EClinicalMedicine* 45:101300. doi: 10.1016/j.eclinm.2022.101300

Capuron, L., Ravaud, A., Neveu, P. J., Miller, A. H., Maes, M., and Dantzer, R. (2002). Association between decreased serum tryptophan concentrations and depressive symptoms in cancer patients undergoing cytokine therapy. *Mol. Psychiatry* 7, 468–473. doi: 10.1038/sj.mp.4000995

Cervenka, I., Agudelo, L. Z., and Ruas, J. L. (2017). Kynurenines: Tryptophan's metabolites in exercise, inflammation, and mental health. *Science* 357:eaaf9794.

Chen, Y., and Guillemin, G. J. (2009). Kynurenine pathway metabolites in humans: disease and healthy States. *Int. J. Tryptophan Res.* 2, 1–19. doi: 10.1126/science.aaf9794

Gal, E. M., and Sherman, A. D. (1980). L-kynurenine: Its synthesis and possible regulatory function in brain. *Neurochem. Res.* 5, 223–239. doi: 10.1007/BF00964611

Gracie, D. J., Guthrie, E. A., Hamlin, P. J., and Ford, A. C. (2018). Bi-directionality of brain-gut interactions in patients with inflammatory bowel disease. *Gastroenterology* 154, 1635.e–1646.e. doi: 10.1053/j.gastro.2018.01.027

Gracie, D. J., Hamlin, P. J., and Ford, A. C. (2019). The influence of the brain-gut axis in inflammatory bowel disease and possible implications for treatment. *Lancet Gastroenterol. Hepatol.* 4, 632–642. doi: 10.1016/S2468-1253(19)30089-5

Guillemin, G. J., Smythe, G., Takikawa, O., and Brew, B. J. (2005). Expression of indoleamine 2,3-dioxygenase and production of quinolinic acid by human microglia, astrocytes, and neurons. *Glia* 49, 15–23. doi: 10.1002/glia.20090

Gupta, N. K., Thaker, A. I., Kanuri, N., Riehl, T. E., Rowley, C. W., Stenson, W. F., et al. (2012). Serum analysis of tryptophan catabolism pathway: Correlation with Crohn's disease activity. *Inflamm. Bowel Dis.* 18, 1214–1220. doi: 10.1002/ibd.21849

Jin, H., Guo, J., Liu, J., Lyu, B., Foreman, R. D., Shi, Z., et al. (2019). Autonomically mediated anti-inflammatory effects of electrical stimulation at acupoints in a rodent model of colonic inflammation. *Neurogastroenterol. Motil.* 31:e13615. doi: 10.1111/nmo.13615

Kaplan, G. G. (2015). The global burden of IBD: From 2015 to 2025. *Nat. Rev. Gastroenterol. Hepatol.* 12, 720–727. doi: 10.1038/nrgastro.2015.150

Kim, H., Chen, L., Lim, G., Sung, B., Wang, S., McCabe, M. F., et al. (2012). Brain indoleamine 2,3-dioxygenase contributes to the comorbidity of pain and depression. *J. Clin. Invest.* 122, 2940–2954. doi: 10.1172/JCI61884

Ko, C. Y., Yang, Y. B., Chou, D., and Xu, J. H. (2020). The ventrolateral periaqueductal gray contributes to depressive-like behaviors in recovery of inflammatory bowel disease rat model. *Front. Neurosci.* 14:254. doi: 10.3389/fnins.2020.00254

Kwon, S., Lee, B., Yeom, M., Sur, B. J., Kim, M., Kim, S. T., et al. (2012). Modulatory effects of acupuncture on murine depression-like behavior following chronic systemic inflammation. *Brain Res.* 1472, 149–160. doi: 10.1016/j.brainres.2012.07.009

Lawson, M. A., Parrott, J. M., McCusker, R. H., Dantzer, R., Kelley, K. W., and O'Connor, J. C. (2013). Intracerebroventricular administration of lipopolysaccharide induces indoleamine-2,3-dioxygenase-dependent depression-like behaviors. *J. Neuroinflammation* 10:87. doi: 10.1186/1742-2094-10-87

Li, H., Sang, L., Xia, X., Zhao, R., Wang, M., Hou, X., et al. (2019). Therapeutic duration and extent affect the effect of moxibustion on depression-like behaviour in rats via regulating the brain tryptophan transport and metabolism. *Evid. Based Complement. Alternat. Med.* 2019:7592124. doi: 10.1155/2019/7592124

Liu, H., Ding, L., Zhang, H., Mellor, D., Wu, H., Zhao, D., et al. (2018). The metabolic factor kynurenic acid of kynurenine pathway predicts major depressive disorder. *Front. Psychiatry* 9:552. doi: 10.3389/fpsyt.2018.00552

Lugo-Huitron, R., Ugalde, M. P., Pineda, B., Pedraza-Chaverri, J., Rios, C., and Perez-de, L. C. V. (2013). Quinolinic acid: An endogenous neurotoxin with multiple targets. *Oxid. Med. Cell. Longev.* 2013:104024. doi: 10.1155/2013/104024

Maes, M. (1995). Evidence for an immune response in major depression: A review and hypothesis. *Prog. Neuropsychopharmacol. Biol. Psychiatry* 19, 11–38. doi: 10.1016/0278-5846(94)00101-m

Mikocka-Walus, A., Knowles, S. R., Keefer, L., and Graff, L. (2016). Controversies revisited: A systematic review of the comorbidity of depression and anxiety with inflammatory bowel diseases. *Inflamm. Bowel Dis.* 22, 752–762. doi: 10.1097/MIB.0000000000000620

Morris, G. P., Beck, P. L., Herridge, M. S., Depew, W. T., Szewczuk, M. R., and Wallace, J. L. (1989). Hapten-induced model of chronic inflammation and ulceration in the rat colon. *Gastroenterology* 96, 795–803.

Murrough, J. W., Abdallah, C. G., and Mathew, S. J. (2017). Targeting glutamate signalling in depression: Progress and prospects. *Nat. Rev. Drug Discov.* 16, 472–486. doi: 10.1038/nrd.2017.16

Murthy, S. N., Cooper, H. S., Shim, H., Shah, R. S., Ibrahim, S. A., and Sedergran, D. J. (1993). Treatment of dextran sulfate sodium-induced murine colitis by intracolonic cyclosporin. *Dig. Dis. Sci.* 38, 1722–1734. doi: 10.1007/BF01303184

Neuendorf, R., Harding, A., Stello, N., Hanes, D., and Wahbeh, H. (2016). Depression and anxiety in patients with inflammatory bowel disease: A systematic review. *J. Psychosom. Res.* 87, 70–80. doi: 10.1016/j.jpsychores.2016.06.001

Ng, S. C., Leung, W. K., Shi, H. Y., Li, M. K., Leung, C. M., Ng, C. K., et al. (2016). Epidemiology of inflammatory bowel disease from 1981 to 2014: Results from a territory-wide population-based registry in Hong Kong. *Inflamm. Bowel Dis.* 22, 1954–1960. doi: 10.1097/MIB.0000000000000846

Nikolaus, S., Schulte, B., Al-Massad, N., Thieme, F., Schulte, D. M., Bethge, J., et al. (2017). Increased tryptophan metabolism is associated with activity of inflammatory bowel diseases. *Gastroenterology* 153, 1504.e–1516.e. doi: 10.1053/j.gastro.2017.08.028

Ogyu, K., Kubo, K., Noda, Y., Iwata, Y., Tsugawa, S., Omura, Y., et al. (2018). Kynurenine pathway in depression: A systematic review and meta-analysis. *Neurosci. Biobehav. Rev.* 90, 16–25. doi: 10.1016/j.neubiorev.2018.03.023

O'Mahony, S. M., Clarke, G., Borre, Y. E., Dinan, T. G., and Cryan, J. F. (2015). Serotonin, tryptophan metabolism and the brain-gut-microbiome axis. *Behav. Brain Res.* 277, 32–48. doi: 10.1016/j.bbr.2014.07.027

Paiotti, A. P., Ribeiro, D. A., Silva, R. M., Marchi, P., Oshima, C. T., Neto, R. A., et al. (2012). Effect of COX-2 inhibitor lumiracoxib and the TNF-alpha antagonist etanercept on TNBS-induced colitis in Wistar rats. *J. Mol. Histol.* 43, 307–317. doi: 10.1007/s10735-012-9400-8

Petit-Demouliere, B., Chenu, F., and Bourin, M. (2005). Forced swimming test in mice: a review of antidepressant activity. *Psychopharmacology (Berl)* 177, 245–255. doi: 10.1007/s00213-004-2048-7

Savitz, J., Drevets, W. C., Smith, C. M., Victor, T. A., Wurfel, B. E., Bellgowan, P. S., et al. (2015a). Putative neuroprotective and neurotoxic kynurenine pathway metabolites are associated with hippocampal and amygdalar volumes in subjects with major depressive disorder. *Neuropsychopharmacology* 40, 463–471. doi: 10.1038/npp.2014.194

Savitz, J., Drevets, W. C., Wurfel, B. E., Ford, B. N., Bellgowan, P. S., Victor, T. A., et al. (2015b). Reduction of kynurenic acid to quinolinic acid ratio in both the depressed and remitted phases of major depressive disorder. *Brain Behav. Immun.* 46, 55–59. doi: 10.1016/j.bbi.2015.02.007

Schwarcz, R., Bruno, J. P., Muchowski, P. J., and Wu, H. Q. (2012). Kynurenines in the mammalian brain: When physiology meets pathology. *Nat. Rev. Neurosci.* 13, 465–477. doi: 10.1038/nrn3257

Shang, H. X., Wang, A. Q., Bao, C. H., Wu, H. G., Chen, W. F., Wu, L. Y., et al. (2015). Moxibustion combined with acupuncture increases tight junction protein expression in Crohn's disease patients. *World J. Gastroenterol.* 21, 4986–4996. doi: 10.3748/wjg.v21.i16.4986

Sheline, Y. I., Liston, C., and McEwen, B. S. (2019). Parsing the hippocampus in depression: Chronic stress, hippocampal volume, and major depressive disorder. *Biol. Psychiatry* 85, 436–438. doi: 10.1016/j.biopsych.2019.01.011

van der Have, M., van der Aalst, K. S., Kaptein, A. A., Leenders, M., Siersema, P. D., Oldenburg, B., et al. (2014). Determinants of health-related quality of life in Crohn's disease: A systematic review and meta-analysis. *J. Crohns Colitis* 8, 93–106. doi: 10.1016/j.crohns.2013.04.007

Walsh, R. N., and Cummins, R. A. (1976). The open-field test: A critical review. *Psychol. Bull.* 83, 482–504.

Wang, H. X., and Wang, Y. P. (2016). Gut microbiota-brain axis. *Chin. Med. J. (Engl)* 129, 2373–2380. doi: 10.4103/0366-6999.190667

Zhao, C., Bao, C., Li, J., Zhu, Y., Wang, S., Yang, L., et al. (2015). Moxibustion and acupuncture ameliorate crohn's disease by regulating the balance between Th17 and treg cells in the intestinal mucosa. *Evid. Based Complement. Alternat. Med.* 2015:938054. doi: 10.1155/2015/938054

Zhao, J., Ng, S. C., Lei, Y., Yi, F., Li, J., Yu, L., et al. (2013). First prospective, population-based inflammatory bowel disease incidence study in mainland of China: The emergence of "western" disease. *Inflamm. Bowel Dis.* 19, 1839–1845. doi: 10.1097/MIB.0b013e31828a6551

Zhao, J., Tian, H., Song, H., Wang, X., Luo, T., Ai, L., et al. (2019). Effect of electroacupuncture on reuptake of serotonin via miRNA-16 Expression in a rat model of depression. *Evid. Based Complement. Alternat. Med.* 2019:7124318. doi: 10.1155/2019/7124318

frontiers | Frontiers in Neuroscience

TYPE Review
PUBLISHED 09 March 2023
DOI 10.3389/fnins.2023.934341

OPEN ACCESS

EDITED BY
Chunhui Bao,
Shanghai University of Traditional Chinese Medicine, China

REVIEWED BY
Na Liu,
The Second Affiliated Hospital of Xi'an Jiaotong University, China
Jirada Sringean,
Chulalongkorn Centre of Excellence for Parkinson's Disease and Related Disorders, Thailand

*CORRESPONDENCE
Jingyu Zhao
✉ jingyuzhao2010@163.com
Changchun Ji
✉ jichangchun1984@163.com

†These authors have contributed equally to this work

SPECIALTY SECTION
This article was submitted to Gut-Brain Axis, a section of the journal Frontiers in Neuroscience

RECEIVED 02 May 2022
ACCEPTED 07 February 2023
PUBLISHED 09 March 2023

CITATION
Sun Z, Wang X, Feng S, Xie C, Xing Y, Guo L, Zhao J and Ji C (2023) A review of neuroendocrine immune system abnormalities in IBS based on the brain–gut axis and research progress of acupuncture intervention. *Front. Neurosci.* 17:934341. doi: 10.3389/fnins.2023.934341

A review of neuroendocrine immune system abnormalities in IBS based on the brain–gut axis and research progress of acupuncture intervention

Zhangyin Sun[1,2†], Xuejiao Wang[1,2†], Shangsheng Feng[3], Chaoju Xie[1,2], Yu Xing[1,2], Liang Guo[1,2], Jingyu Zhao[4*] and Changchun Ji[2,5*]

[1]College of Acupuncture and Moxibustion, Shaanxi University of Traditional Chinese Medicine, Xianyang, China, [2]Department of Acupuncture and Moxibustion, Shaanxi Hospital of Traditional Chinese Medicine, Xi'an, China, [3]MOE Key Laboratory of Biomedical Information Engineering, Xi'an Jiaotong University, Xi'an, China, [4]Department of Acupuncture and Moxibustion, Xi'an Hospital of Traditional Chinese Medicine, Xi'an, China, [5]Department of Acupuncture and Moxibustion, Shaanxi Provincial Institute of Traditional Chinese Medicine, Xi'an, China

Irritable bowel syndrome (IBS) is a common digestive disorder observed in clinics. Current studies suggest that the pathogenesis of the disease is closely related to abnormal brain–gut interactions, hypokinesia, visceral sensory hypersensitivity in the gastrointestinal tract, and alterations in the intestinal microenvironment. However, it is difficult for a single factor to explain the heterogeneity of symptoms. The Rome IV criteria emphasized the holistic biologic-psycho-social model of IBS, suggesting that symptoms of the disease are closely related to neurogastroenterology and various abnormalities in brain–gut interaction. This study comprehensively reviewed the relationship between the brain–gut axis and IBS, the structure of the brain–gut axis, and the relationship between the brain–gut axis and intestinal microenvironment, and discussed the relationship between the abnormal regulation of the nervous system, endocrine system, and immune system and the incidence of IBS on the basis of brain–gut axis. In terms of treatment, acupuncture therapy can regulate the neuroendocrine-immune system of the body and improve the intestinal microenvironment, and it has the advantages of safety, economy, and effectiveness. We study the pathogenesis of IBS from local to global and micro to macro, and review the use of acupuncture to treat the disease as a whole so as to provide new ideas for the treatment of the disease.

KEYWORDS

irritable bowel syndrome, brain-gut axis, neural signal regulation, endocrine system, immune system, acupuncture

1. Introduction

Irritable bowel syndrome (IBS) is a complex functional gastrointestinal disorder characterized by abdominal pain, abdominal distension, and intestinal disorders that do not involve structural and biochemical abnormalities of the gastrointestinal tract (Ford et al., 2020). The Rome IV criteria classify patients with IBS into four subtypes based on their abnormal bowel movement traits: diarrheal IBS (IBS with diarrhea, IBS-D), constipated IBS

(IBS with constipation, IBS-C), mixed IBS (IBS-M), and unclassified IBS (IBS-U) (Drossman, 2016). The global prevalence of IBS is approximately 11.2 % (Lovell and Ford, 2012). IBM seriously affects the quality of life of patients due to its high prevalence, recurrent symptoms, and susceptibility to complications, such as peptic ulcers, chronic liver disease, depression, and anxiety (Lai et al., 2021). In addition, it has led to a significant increase in the global healthcare burden (Black and Ford, 2020; Sperber et al., 2021).

The pathogenesis of IBS is multifactorial, which also has an important role in gene regulation, but the specific pathogenesis has not been fully elucidated. The disease is thought to be closely associated with abnormal brain–gut interactions, gastrointestinal hypokinesis, visceral sensory hypersensitivity, and intestinal microenvironmental disorders, indicating that a single factor cannot adequately explain the complexity of IBS symptoms. Therefore, treatment is mostly focused on improving gastrointestinal symptoms for different subtypes of IBS, currently involving analgesics, prokinetics, antidiarrheal agents, and psychotherapy (Ford et al., 2018; Arokiadoss and Weber, 2021). This can temporarily alleviate symptoms, but recurrence and varying degrees of side effects can occur (Aziz and Simrén, 2021), which are of great concern for clinical practitioners. Therefore, a fuller understanding of the pathogenesis of IBS is necessary to seek targeted therapies.

As IBS research progressed, it was defined by Rome IV as a disorder of gut–brain interactions (Schmulson and Drossman, 2017). For the understanding of the etiology and clinical features of IBS, Rome IV emphasizes a holistic biopsychosocial model, suggesting that the development of IBS symptoms is closely related to neurogastroenterology and multifaceted abnormalities in brain–gut interaction (Drossman and Hasler, 2016). The brain–gut axis maintains central and local homeostasis in the gut by integrating the neural, endocrine, and immune systems to form a bidirectional regulatory pathway and by connecting closely with the gut microbiota. Abnormalities in any of the brain–gut pathways may lead to the disruption of homeostatic balance and eventually induce IBS (Person and Keefer, 2021), in which neurological, endocrinological, and immunological factors intersect to produce symptoms that are the characteristic manifestation of the disease (Buckley et al., 2016). Therefore, understanding IBS from the perspective of abnormal regulation of the neuroendocrine-immune system in the brain–gut axis can facilitate the understanding of its pathogenesis.

2. Brain–gut axis

The brain–gut axis is a bidirectional information exchange system that integrates brain and intestinal functions, thereby effectively maintaining homeostasis in these organs (Carabotti et al., 2015). Different studies have confirmed that abnormal brain–gut interactions are closely related to IBS. Therefore, a deep understanding of the brain–gut axis would facilitate the elucidation of the pathogenesis of IBS. In the following sections, we highlight the basic architecture of the brain–gut axis and subsequently explore the relationship between the brain–gut axis and the intestinal microenvironment.

2.1. Basic architecture of the brain–intestine axis

Brain–gut interactions occur not only directly through neural pathways but also indirectly through humoral pathways (Bercik et al., 2012). First, the neural pathway of brain–gut interaction is a bidirectional interaction pathway linking the central nervous system (CNS) and the enteric nervous system (ENS). It is generally accepted that the regulation of gastrointestinal motility by the nervous system is achieved through three-level coordinated actions. Level 1 is the local regulation of the ENS, which consists of two plexuses: the interosseous plexus, which innervates the motility of the intestinal smooth muscle, and the submucosal plexus, which regulates intestinal mucosal sensation, secretion, and absorption. The sensory neurons, interneurons, and motor neurons of the ENS are interconnected to form separate, independent functions that integrate and process information similar to those of the brain and the spinal cord. Level 2 occurs in the anterior vertebral ganglion, which receives and regulates information from both the ENS and the CNS. Level 3 occurs in the CNS, which is composed of various centers at all levels of the brain and the spinal cord. They receive various incoming information during changes in the internal and external environment, integrate, and then transmit the regulatory information from the vegetative nervous and the neuroendocrine systems to the ENS, and act directly on gastrointestinal effector cells to regulate smooth muscle, glands, and blood vessels. This neuro-endocrine network linking the gastrointestinal tract to the CNS at different levels is the structural basis for the realization of brain–gut axis function (Bonaz and Bernstein, 2013).

Second, the humoral pathway mainly involves two bidirectional regulatory pathways and brain–gut peptides. Among them, the bidirectional regulatory pathways, namely, the hypothalamic-pituitary-adrenal axis (HPA) and the hypothalamic-autonomic nervous system axis (HANS), are the main pathways involved in physiological and psychological stress responses (Stasi et al., 2012).

In addition, brain and intestinal peptides are hormones that regulate the movement of the gallbladder and bile ducts, such as gastrokinetic hormone, cholecystokinin, and glucagon. These peptides are highly distributed in the gastrointestinal and nervous systems, and hence, they are called brain and intestinal peptides. Brain and intestinal peptides of the gastrointestinal and nervous systems regulate the complex functions of the gastrointestinal tract, such as movement, sensation, secretion, and absorption through endocrine, neurosecretory, and paracrine secretory peptides (Wu I. X. Y. et al., 2019). Different types of intestinal peptides, such as 5-hydroxytryptamine (5-HT), substance P (SP), calcitonin gene-related peptide, vasoactive intestinal peptide, somatostatin, neuropeptide Y, and cholecystokinin, can act on the central nervous and the enteric nervous systems, such that both systems can jointly regulate the functions of the gastrointestinal tract. In addition, different brain and intestinal peptides have different mechanisms of action, and most brain and intestinal peptides do not act on IBS in isolation. There are complex interconnections between various brain and intestinal peptides, which are jointly involved in the regulation of the physiological activities of the gastrointestinal tract.

2.2. Relationship between the brain–gut axis and the intestinal microenvironment

In the brain–gut interaction, neurological dysfunction can lead to alterations in the intestinal microenvironment (Li et al., 2020). This is composed of the microbiota, local immune system, and epithelium of the single-cell layer, which can effectively regulate homeostasis in the body and consequently maintain normal physiological functions of the gastrointestinal tract (Fay et al., 2017). Therefore, the relationship between the brain–gut axis and the intestinal microenvironment was explored from three perspectives: the intestinal microbiota, intestinal immune system, and intestinal mucosal permeability (the relationship between the brain–gut axis and the intestinal flora is shown in Figure 1).

In recent years, studies on the pathogenesis of IBS have focused on the brain–gut axis, intestinal microecological relationships (Hillestad et al., 2022), and intestinal microbiota disorders (Aziz et al., 2017). The brain–gut axis integrates the neural, endocrine, and immune systems, forming a bidirectional regulatory pathway that maintains the homeostasis of brain and gut functions. The gut microbiota is an important player in the brain–gut bidirectional information exchange system. On the one hand, its interaction with the ENS and neurological and endocrine signaling pathways profoundly affects the brain–gut communication function (Martin et al., 2018); and on the other hand, it can influence the brain–gut axis function through direct and body circulation pathways. This indicates that the gut microbiota and the brain–gut axis are closely linked and interact with each other, thereby forming a complex brain–gut microbiota network to maintain normal gut function.

The brain–gut axis can influence the host gut flora, and similarly, the gut microbiota can effectively regulate some of the functions of the brain–gut axis (Khlevner et al., 2018). First, the brain–gut axis can influence the intestinal microbiota. On the one hand, the response signals from the CNS are transmitted to the smooth muscle layer of the intestine through the relevant fibers, thereby influencing gastrointestinal motility and secretion and regulating the intestinal flora environment (Mayer et al., 2014). On the other hand, stress and emergency stimulation of the host CNS will have an impact on the intestinal flora. It has been reported that neuroinflammation induced by traumatic brain injury through the brain–gut pathway results in impaired intestinal motility and increased intestinal mucosal permeability (Hanscom et al., 2021). Second, the intestinal microbiota can maintain the functional homeostasis of the host gut and participate in the regulation of neurological development as well as mood, appetite, cognition, and behavior in the host (Mu et al., 2016). The decrease in the number and diversity of gut flora is closely associated with neurological dysfunctions in the host, such as abnormalities in mood and behavior. Through the blood circulatory pathway, gut microbiota and its metabolites, such as short-chain fatty acids, neurotransmitters, and their precursors can influence the expression levels of neurotransmitters, precursors, and their receptors in the CNS, thus regulating brain function, cognition, and behavior (Cryan et al., 2020). Moreover, improving the disturbance of the intestinal microbiota and reconfiguring intestinal homeostasis may facilitate the recovery of the neurological function of an organism (O'Hagan et al., 2017). Bidirectional communication takes place between the brain and the gut, and the involvement of the gut microbiota has recently been discovered. An abundance of symbiotic microorganisms inhabit the lumen of the gastrointestinal tract and signal the immune and endocrine systems of the host through the secretion of metabolites such as short-chain fatty acids (SCFAs), amino acids, and polyamines. The aim of our study was to investigate specific types of microbiota-derived metabolites, specifically bile acids, short-chain fatty acids, vitamins, amino acids, serotonin, and hypoxanthines, which are all implicated in the pathogenesis of IBS.

Dysregulation of the microbial-gut-brain axis can exacerbate various CNS disorders through the expression of abnormal metabolites, such as SCFAs. Microbiota-derived metabolites play a central role in the communication between microbes and their hosts, with SCFAs probably being the most studied.

Short-chain fatty acids (SCFAs), mainly derived from the fermentation of dietary fiber, play a key role in host gut metabolism and immune function. Stress increases fecal acetate and total SCFA levels as well as colonic *FFAR2* and *FFAR3* expressions. Moreover, SCFA supplementation ameliorated acute stress-induced elevated body temperature and corticosterone levels in chronically stressed mice. Similar changes were found in colonic MR gene expression, although stress-induced increases in hippocampal MR gene expression were not affected. In addition, no differences in GR gene expression were found in any of the tissues investigated, and these differences may have disappeared over time. Sustained decreases in *CRFR1*, *CRFR2*, and *MR* expressions were observed in the group that received SCFA injections alone, and SCFA also had antidepressant and anxiolytic effects (Van De Wouw et al., 2018). Overall, these results suggest that SCFAs can down-regulate stress signaling and HPA axis responses, a critical pathway for microbe-gut-brain axis communication (Wiley et al., 2016). Studies using germ-free (GF) mice lacking all microbes provide compelling and consistent evidence that the microbiota is essential for brain development. GF mice exhibit altered expression of neurotransmitters and their receptors and neurotrophic factors in the brain, exhibit region-specific gene expression, and have an impaired blood–brain barrier. Even hippocampal neurogenesis and neuroplasticity in mice were affected by the absence of the gut microbiota. The maturation of oligodendrocytes is inhibited by specific gut microbial metabolites that alter myelin formation patterns in the limbic system. Therefore, a healthy, stable, and diverse intestinal microbiota is essential for normal brain–gut interactive communication.

In addition, the CNS directly affects the intestinal microbiota through stress-mediated virulence gene expression and indirectly through ANS-mediated intestinal motility, intestinal immune regulation, and secretion (Osadchiy et al., 2019). The top-down effect of the brain on the gut microbiota was also confirmed in a recent clinical randomized controlled trial (Jacobs et al., 2021).

The CNS damage increases intestinal mucosal permeability. For example, a large release of norepinephrine from cecum sympathetic nerves, altered cecal mucin production, and cupped cell numbers were observed in rats with brain injury, and this affected the intestinal microbiota and permeability (Houlden et al., 2016). We reviewed the literature and found that ANS dysfunction is seen after brain injury, and this exaggerates sympathetic

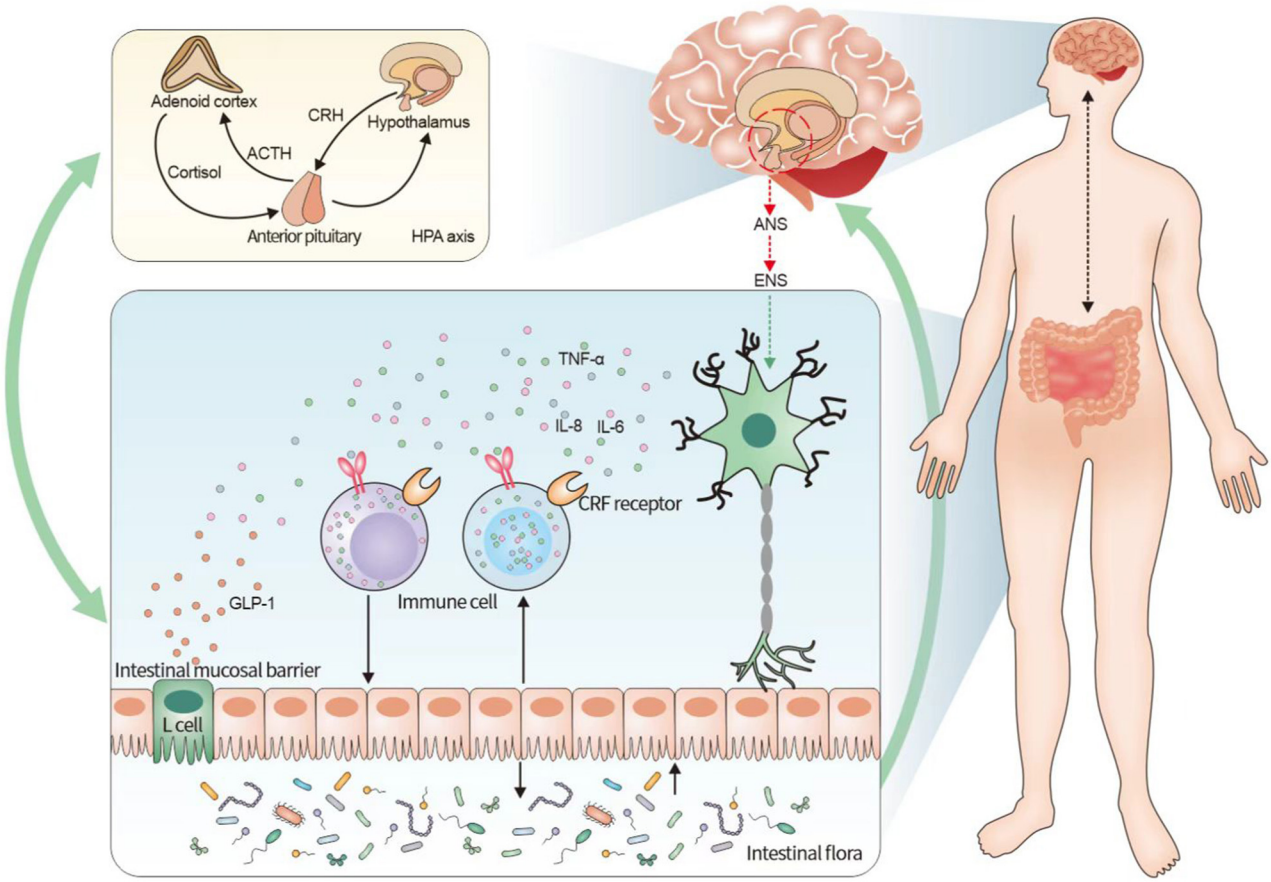

FIGURE 1
Relationship between irritable bowel syndrome and the neuroendocrine-immune system based on the brain–gut axis. The figure illustrates that the pathogenesis of irritable bowel syndrome can be understood in terms of the neuroendocrine-immune network system of the brain–gut axis. The brain–gut axis connects the ENS and the CNS and activates the endocrine system mainly by initiating the HPA axis in the CNS, while the endocrine system has a bidirectional regulation with the intestinal immune system, and the intestinal mucosal barrier, immune cells, and intestinal flora are involved in the intestinal immune system, among which the intestinal flora forms another bidirectional regulation with the brain–gut axis. It indicates that the neuroendocrine-immune system of the brain–gut axis influences the pathogenesis of IBS, and the three systems form a multidimensional and bidirectional regulation among themselves. CRF, adrenocorticotropin-releasing factor; HPA, hypothalamus-pituitary-adrenal; IBS, irritable bowel syndrome.

activation (Purkayastha et al., 2019). In addition, under stressful stimuli, large amounts of neurotransmitters and receptors, such as norepinephrine and catecholamines, are released in the peripheral circulation (Zhang et al., 2020), and these regulate intestinal mucosal permeability.

Furthermore, the close relationship between HPA axis activation, a key humoral pathway in the brain–gut axis, and intestinal permeability has been demonstrated in clinical trials (Arciniega-maptinez et al., 2022). First, adrenocorticotropin-releasing factor (CRF) released by the HPA axis can increase intestinal permeability (Lyte et al., 2011). Second, the gut microbiome involves the blood–brain barrier (BBB) in its interactions with the peripheral and neuroimmune systems, and on the BBB, the gut microbiome can interact with the CNS and regulate body function. Bacteria can release the microbiome and its factors directly into the body's circulation and bloodstream. Once in the blood, the microbiome and its factors can alter peripheral immune cells to facilitate interaction with the BBB and eventually with other elements of the neurovascular unit. Bacteria and their factors or cytokines and other immunologically active substances released from peripheral sites under the influence of the microbiome can cross the BBB, alter the integrity of the BBB, change the rate of BBB transport, or induce the release of neuroimmune substances from barrier cells (Logsdon et al., 2018). In addition, metabolites produced by the microbiome, such as short-chain fatty acids, can cross the BBB to affect brain function. Through these and other mechanisms, microbiome–BBB interactions can influence the disease process, as reported for multiple sclerosis (Dopkins et al., 2018). Preclinical studies provide evidence that the BBB is altered when animals are subjected to experimental intestinal infections or when animals lack a normal gut microbiome.

In addition, the ENS has an important role in gastrointestinal peristalsis, digestion, secretion, and regulation of intestinal mucosal

permeability (Furness, 2012). The ENS plays a key role in regulating pH in the gastrointestinal lumen and consequently intestinal inflammation, which is strongly associated with increased mucosal permeability (Tanaka et al., 2016).

With the exploration of the gut–brain axis, it was found that alpha synucleinopathy can be transmitted in both directions in the brain and the intestine. The pathology of PD [Parkinson's disease (PD)] is characterized by alpha synucleinopathy, which proves that the brain–gut axis also plays an important role in the pathogenesis of PD. In addition, the presence of a large microbiota in the gut, which is involved in the formation and transmission of alpha synucleinopathy, suggests that dysbiosis of the gut microbiota is closely related to the progression of PD.

3. Abnormal neural signal regulation

The cerebro-intestinal axis is a neuroendocrine network that connects the gastrointestinal system with the CNS, and it involves three main nervous systems: the CNS, ANS, and ENS. The gastrointestinal tract is the only organ in the body that is innervated by the CNS, ANS, and ENS, and its functional activities are neurologically regulated by these three systems. The impaired functions of any of the systems can cause gastrointestinal tract dysfunction and mediate the development of IBS.

3.1. ANS dysfunction

The ANS is part of the peripheral efferent nervous system that regulates the activity of the visceral and vascular smooth muscle, the cardiac muscle, and the glands. The sympathetic and parasympathetic nervous systems, under the control of the cerebral cortex and the hypothalamus, both antagonize and coordinate the physiological activities of the organs. The structure of the autonomic nervous system (ANS) can be divided into central and peripheral parts. The ANS is mainly distributed in the visceral, cardiovascular, and glandular bodies, whose central part is also located in the brain and the spinal cord. The peripheral part includes visceral motor (efferent) and visceral sensory (afferent) fibers, which constitute the visceral motor and visceral sensory nerves, respectively.

The ANS plays an important role in the brain–gut axis as a bridge between the central and the enteric nervous systems; hence, it is able to regulate the movement and sensation of the intestine. There are changes in autonomic function in patients with IBS that may be associated with autonomic dysfunction (Salvioli et al., 2015). The ANS comprises two nervous systems, sympathetic and parasympathetic, whose structures and functions are integrated into the brain–gut axis and work together to maintain functional homeostasis in the intestine. On the one hand, the sympathetic nervous system inhibits gastrointestinal motility and secretion, while the parasympathetic nervous system plays a stimulatory and pro-secretory role in smooth muscle. Sympathetic–parasympathetic imbalance causes altered bowel habits in patients with IBS. On the other hand, the modulation of visceral sensitivity by both is closely related to abdominal pain in IBS (De Winter et al., 2016). The parasympathetic afferent pathway begins in the vagus nerve and ends in the nucleus tractus solitarius, which transmits pain signals to the corticolimbic layer. The sympathetic afferent pathway mediates pain signals primarily through the spinal cord, first to the thalamus and then to the sensory cortex and pain stroma. The signal also travels to specific areas of the brain, such as the hippocampus, the amygdala, the prefrontal cortex, and finally to the hypothalamus (Fukudo, 2013). In addition, important tissues and organs in the CNS can interact with the HPA axis and the ANS. These central regions, which regulate intestinal function, are involved in both emotions (e.g., mood, anxiety, and pain) and cognitive behaviors (e.g., memory and decision-making), such that the dysfunction of the ANS directly or indirectly controls the development and progression of IBS disease.

3.2. CNS dysfunction

The CNS is composed of the brain and the spinal cord (the brain and the spinal cord are the central parts of various reflex arcs) and is the most dominant part of the human nervous system. It receives afferent information from all parts of the body, which is integrated and processed into coordinated motor efferents or stored in the CNS to become the neural basis for learning and memory.

Brain dysfunction has an important relationship with the development of IBS. Some key sites in the CNS associated with emotion-pain regulation are structurally altered in patients with IBS (Aziz and Simrén, 2021). For example, Sheehan et al. (2011) found a correlation between the activity of the cingulate gyrus and the pain-related cerebral cortex in patients with IBS and the clinical symptoms of IBS. Increased neuronal activity has been reported in the medial prefrontal cortex, the insula, and the anterior cingulate gyrus, which are brain regions associated with visceral pain in patients with IBS (Grinsvall et al., 2021), and a larger area of excitation was observed in brain regions associated with nociceptive processing (e.g., the prefrontal cortex, the anterior cingulate gyrus, the thalamus, etc.,) (Seminowicz et al., 2010). Similarly, in a cohort study, the IBS group exhibited extensive structural changes in the brain compared with that in the controls, and these changes in the brain included a reduction or increase in gray matter volume in multiple regions of the sensorimotor, central executive, and default mode networks, and these changes were strongly associated with chronic visceral pain (Öhlmann et al., 2021). Another study found that spontaneous activity in the amygdala and the anterior insula was significantly increased in patients with IBS, while spontaneous activity in sensorimotor areas tended to reduce (Hong et al., 2013). Moreover, cognitive-behavioral treatment reduced activity in the anterior cingulate gyrus, the amygdala, and the hypothalamus, suggesting that spontaneous activity of the brain may be associated with some symptoms of IBS. In addition, patients with IBS have smaller volumes in the bilateral superior frontal gyrus, the bilateral insular gyrus, the bilateral amygdala, the left cingulate gyrus, the left rectus gyrus, the left shell nucleus, and the brainstem, and larger volumes in the left postcentral gyrus (Labus et al., 2014), which are mostly part of the limbic system and are crucial for the body to perceive visceral injurious stimuli, pain production, emotional processing,

and emotion regulation. Thus, CNS abnormalities can lead to visceral pain and emotional abnormalities in patients with IBS.

3.3. ENS dysfunction

The ENS consists of the ganglia contained in the gastrointestinal tract, the biliopancreatic system, and the network between them, which can connect the gastrointestinal tract with the CNS and ANS. On the one hand, it transmits sensory information to the brain through neurons, nerve fibers, and neurotransmitters connected to the central nerve, such that the activities of the intestine are regulated by the center. On the other hand, it has considerable autonomic functions to locally regulate the motility, secretion, and blood flow, as well as water and electrolyte transport of the intestine. The ENS consists of the ganglia and the biliopancreatic system contained in the gastrointestinal tract as well as the network between the ganglia and biliopancreatic system that connects the gastrointestinal tract to the CNS and ANS.

On the one hand, it transmits sensory information to the brain through neurons, nerve fibers, and neurotransmitters connected to the central nerve, such that the activities of the intestine are regulated by the center. On the other hand, it has considerable autonomic functions to locally regulate the motility, secretion, blood flow, as well as water and electrolyte transport of the intestine.

When the intestine is stimulated by mechanical dilatation, stress, inflammation, and allergens, chromophores release 5-HT as a paracrine signal acting on intestinal mast cells, spinal afferent cells, and neurons in the ENS. Intestinal mast cells release multiple mediators of paracrine signaling, including histamine and serine proteases, chymotrypsin and trypsin, and serotonin. Some of these mediators diffuse to receptors at the afferent injury-sensitive and mechanosensitive end of the spectrum and are known to cause abdominal pain and distention that may lead to IBS (Wood, 2020). In addition, 5-HT acts on spinal afferent neurons to mediate central responses to intestinal stimuli, as well as on 5-HT receptors on enteric neurons to influence intestinal sensory and motor functions. In IBS-D model rats, the total number of the ganglia and neurons in the submucosal plexus of the small intestine increased, the proportion of excitatory neurons (cholinergic neurons and vasoactive intestinal peptide neurons) increased, and the proportion of inhibitory neurons (nitrogenergic neurons) in the intermuscular plexus decreased (Li et al., 2016). Such morphological changes in the ENS are consistent with accelerated intestinal transmission and increased secretion in IBS-D.

The enteric nervous system (ENS) contains many neurotransmitters or brain intestinal peptides and can regulate intestinal function through a variety of neurotransmitters. When the internal environment of the gastrointestinal tract is altered, the intrinsic primary sensory neurons can be modified to produce strong sensory signals and transmitted upward to cause discomfort in the body. Therefore, the activation of primary neurons in the enteric plexus is one of the mechanisms associated with visceral hypersensitivity in IBS. Studies on enteric neurotransmitters and their complex signaling pathways as well as the interaction between enteric neurons and peripheral glial cells and Cajal mesenchymal cells have led to a better understanding of the functional regulation of the ENS in the pathogenesis of IBS (Zhang et al., 2019; Matheis et al., 2020). Therefore, ENS abnormalities are associated with the development of IBS.

4. Endocrine system abnormalities

The brain–gut axis has an important role in the development of IBS, and patients with IBS have hyperfunction of the HPA axis and impaired function of the endocrine system, which leads to abnormalities in an organism. Although there are many factors that affect the endocrine system, those with important roles include adrenocorticotropin-releasing factor (CRF), corticosteroids, and glucagon-like peptide 1 (GLP-1).

4.1. CRF

Adrenocorticotropin-releasing factor (CRF) is an important hormone associated with the body's response to stress. It is a major mediator of stress responses in the brain–gut axis, while the HPA axis is key to maintaining homeostasis and is responsible for various responses in the endocrine system. CRF plays a key role in the activation of the HPA axis under basal and stressful conditions (Chen et al., 2012). It may also explain the higher levels of adrenocorticotropic hormone and cortisol in patients with IBS, compared with that in healthy subjects (Distrutti et al., 2016). CRF exerts its biological effects by activating CRF1 and CRF2 receptors (CRFR1 and CRFR2), stimulating colonic motility, and inducing visceral hypersensitivity responses (Nozu and Okumura, 2015). CRFR1 is commonly found in the regions of the brain associated with pressure and nociceptive circuits, including the paraventricular nucleus, the ventricles, and the amygdala (Reyes et al., 2008). Toll-like receptor 4 (TLR4) or IL-1 receptor antagonists block abnormal visceral pain and increase intestinal permeability caused by CRF (Nozu et al., 2018). CRF receptor (CRF-R) signaling has critical roles in stress-related alterations in gastrointestinal function, stimulation of the colonic enteric nervous system, secretory motor function, intestinal permeability, and visceral hypersensitivity (Tache et al., 2018). In addition, Labus et al. found that peripheral administration of CRF1 receptor antagonists in patients with IBS reduced abdominal pain and anxiety (Labus et al., 2014). In addition, CRF receptors were found in interosseous nerves, sensory nerves, sympathetic nerves, intestinal chromophores, and immune cells in the guts of animals and humans. This suggests that the central and peripheral CRF system regulates the body's response to stress and modulates the syndromes that occur in IBS (Chen et al., 2012; Nozu and Okumura, 2015). In the immune context, CRF and CRF receptors are present in immune cells in the intestine. Stress, through the local CRF system, activates intestinal immune cells, leading to intestinal pro-inflammatory cytokine release, increased permeability, mucin secretion, and visceral allergy (Chatoo et al., 2018).

4.2. Corticosteroids

Corticosteroids are steroids produced by the adrenal cortex, and they mostly include hormones, such as glucocorticoids, mineralocorticoids, and sex hormones. They are readily absorbed by the gastrointestinal tract and are highly bound to proteins and play an important role in the treatment of intestinal disorders (Kapugi and Cunningham, 2019). Salt corticosteroids (MR) and glucocorticoids (GR) are steroid hormones that act in the stress system model through salt corticosteroid and glucocorticoid receptors (MRs and GRs, respectively), mediating the roles of adrenal hormones, such as cortisol, in the initiation and termination of the stress response, respectively. Corticosterone, which is the stress hormone in the amygdala, induces visceral hypersensitivity through the actions of GR and MR (Myers and Greenwood-Van Meerveld, 2012). It has been demonstrated that higher cortisol levels in patients with IBS positively correlated with psychological stress levels (Videlock et al., 2016). In addition, glucocorticoids, including endogenous cortisol, inhibit the production and activity of many inflammatory cells, as well as redistribute them to other parts of the body, resulting in fewer circulating immune cells (Ericson-Neilsen and Kaye, 2014). Chronic stress induces alterations in the expression of GR and CRH, leading to increased visceral pain and colonic permeability, while exposure to environmental enrichment suppresses stress-induced changes within the brain–gut axis to prevent visceral and somatic hypersensitivity and colonic hyperpermeability (Orock et al., 2021). All these indicate that the central signaling of corticosteroids is a potential target for the treatment of intestinal dysfunction in IBS.

4.3. GLP-1

Ingestion of certain foods is a predisposing factor for certain IBS symptoms (Simren et al., 2001). It has been shown that reducing the consumption of fermentable oligosaccharides, disaccharides, monosaccharides, and polyols (FODMAPs) may alleviate the symptoms of bloating, abdominal pain, and osmotic diarrhea in IBS (Barrett et al., 2010; Zahedi et al., 2018). Intestinal secretion of glucagon is an important physiological response that occurs in the intestine after eating. The secretion of glucagon-like peptide 1 (GLP-1) by L cells, expression of the surface receptor TGR5 by intestinal L cells, and induction of GLP-1 release from enteroendocrine cells by the TGR5 agonist 6α-ethyl-23(S)-methylcholic acid (EMCA, INT-777) inhibits glucagon secretion and gastric emptying and suppresses food uptake (Thomas et al., 2009). One study demonstrated that the glucagon-like peptide-1 receptor agonist ROSE-010 reduced pain during IBS episodes (Touny et al., 2022). However, GLP-1 acts on the enteric nervous system by reducing excitatory cholinergic neurotransmitters and regulating nitric oxide release through presynaptic GLP-1Rs (Amato et al., 2010). In addition, GLP-1 can initiate colonic enteric neurons and the vagus nerve (Amato et al., 2010); the vagus nerve is involved in the pathophysiological processes of IBS; hence, GLP-1 may influence the central regulation of visceral pain sensitivity. Interestingly, GLP-1 also modulates cytokines secreted by the GI tract and alters the central CRF pathway that regulates stress-induced alterations in colonic transit (Nakade et al., 2007).

5. Abnormal immune system

Current studies have confirmed the existence of an immune-activated state and the involvement of brain–gut interaction in the development of IBS. The immune system is an essential link in the neuroendocrine-immune network system, and IBS acts through immune cells, immune factors, and intestinal mucosal immune aspects and thus affects the whole system.

5.1. Immunocytes

Mast cells (MC), an intrinsic component of the neuroimmune axis, are present at elevated levels in IBS mucosal samples (Buhner and Schemann, 2012; Lee and Lee, 2016; Krammer et al., 2019). Although other immune cells may be involved in the pathophysiological process of IBS (Uranga et al., 2020), mast cells are important cellular mediators of local nerve fiber sensitization (Casado-Bedmar and Keita, 2020). The chronic inflammation of the intestinal mucosa in patients with IBS increases intestinal epithelial permeability. This leads to increased exposure of intestinal mucosa to intestinal contents, causes mast cell activation and degranulation to release large amounts of inflammatory mediators (Nogueira et al., 2017), stimulates visceral sensory neurons, causes the release of neuropeptides, and participates in pathophysiological processes, such as pain perception and cognition, through HANS upregulation mode (Skaper et al., 2014; Mackey et al., 2016). Similarly, mast cells can be activated by neuropeptides, such as SP, leading to the release of protein hydrolases, as a stress response to pain. Therefore, IBS is considered a brain–gut axis disease (Casado-Bedmar and Keita, 2020; Labanski et al., 2020). IBS biopsies showed an increased number of mast cells in the lamina propria, compared with that observed in the healthy controls (Krammer et al., 2019), and increased concentrations of products secreted by mast cells, such as histamine, proteases, cytokines, and prostaglandins, in patients with IBS activate intestinal neurons (Balestra et al., 2012). In addition, MC activation is associated with CRF, and it leads to increased visceral hypersensitivity and intestinal permeability by acting on mast cells and causing degranulation and release of trypsin-like enzymes, tumor necrosis factor-α, and histamine (Zhang et al., 2016; Tache et al., 2018). This effect may be due to the involvement of neuroendocrine-immune interaction mechanisms in the pathogenesis of IBS (Jarret et al., 2020).

In addition, the feedback response of the immune system induced by the HPA downregulation pattern can cause low-grade inflammation after which the colon is more susceptible to the effects of stress on intestinal nerve function (Wouters et al., 2016). The activated immune system in patients with IBS, as evidenced by increased expression of colonic mucosal cytokines and increased release of pro-inflammatory cytokines from monocytes isolated from peripheral blood, especially in patients with IBS-D, is specific to the gastrointestinal tract (Vicario et al., 2015; Van De Wouw et al., 2018). Increased humoral immunoreactivity in the jejunal

mucosa of patients with IBS-D was identified by microarray analysis, which correlated with the activation of B lymphocytes and the production of immunoglobulins.

5.2. Immune factors

Evidence of immune activation in IBS includes elevated levels of pro-inflammatory cytokines, such as interleukin-6 (IL-6), IL-8, and tumor necrosis factor-α (Brzozowski et al., 2016; Seyedmirzaee et al., 2016; Ivashkin et al., 2021). On the one hand, the cytokines have neuromodulatory effects and can stimulate the excitation of intestinal mucosal pro-secretory neurons, which can also lead to changes in intestinal functions (e.g., contraction, absorption, and secretion). In addition, IL-6 releases the sympathetic brake by suppressing the presynaptic inhibition of norepinephrine release. On the other hand, visceral pain can be evoked after cytokine excitation of enteric neurons (Buckley et al., 2016), making cytokines an important cause of visceral pain-mediated IBS (Atmaramani et al., 2020).

It has been reported that the levels of anti-inflammatory cytokines (e.g., IL-10 and transforming growth factor beta) decreased in IBS colon and rectal biopsies (Coëffier et al., 2010; Ivashkin et al., 2021). Probiotics, as living microorganisms, can modulate the immune system, leading to the upregulation of anti-inflammatory cytokines and growth factors, and can interact with the brain–gut axis by regulating endocrine and neurological functions (Atmaramani et al., 2020). Thus, immune factors play an important role in the pathogenesis of IBS as intermediate transmitters or different "links" in the regulation of the neuroendocrine-immune network.

5.3. Intestinal mucosal immunity

The intestinal mucosal immune system is composed of intestinal epithelial cells, intestinal interepithelial lymphocytes, lymphocytes of the lamina propria, intestinal submucosal-collecting lymph nodes, and various monocytes, which directly participate in intestinal immune regulation. Some studies have confirmed the presence of abnormal mucosal immunity in patients with IBS (Aerssens et al., 2008), and stress factors are thought to be strongly associated with the development of IBS (Elsenbruch and Enck, 2016). Stress regulates the intestinal immune system by triggering the brain–gut axis to produce neurotransmitters and hormones. Secretory immunoglobulin A (SIgA) is the most important immunoglobulin on the mucosal surface of the intestine, and stress can cause the upregulation or downregulation of SIgA levels, thus affecting intestinal immunity (Campos-Rodríguez et al., 2013). SIgA production is regulated by stress (Brawner et al., 2020) and pIgR expression (Jarillo-Luna et al., 2015), and the immunoglobulin-pIgR complex (Diga-pIgR and PIGA-pIgR) is transported cellularly through the intestinal epithelium. Upon reaching the tip of these cells, pIgR is cleaved, releasing sIgA, and a pIgR-derived polypeptide into the intestinal lumen (Brandtzaeg, 2013). Therefore, SIgA and pIgR protect the intestinal epithelium from pathogens and regulate the intestinal inflammatory response to maintain homeostasis *in vivo*. In addition, visceral nerve fibers are distributed in the submucosa (Meissner's plexus) and mucosal plexus, which contain nerve endings that can contact antigen-presenting cells to control intestinal immune responses (De Jonge, 2013; Jacobson et al., 2021). These indicate that the IBS mucosal immune system also plays a significant role in the CNS.

6. Discussion

Irritable bowel syndrome (IBS) is a common functional gastrointestinal disorder that has a significant impact on the quality of life of patients due to its high prevalence, severity, and recurrence; hence, effective interventions are urgently needed. The efficacy of current interventions does not meet the clinical requirements of patients because the pathophysiology of the disease is not fully understood in terms of etiology and heterogeneity of symptoms. Therefore, it is necessary to have a comprehensive understanding of the disease toward the development of targeted interventions for improved clinical treatment.

Under the social–psychological–biological model advocated by Rome IV, this study highlights the pathogenesis of IBS from the perspective of abnormal regulation of the neuroendocrine-immune system of the brain–gut axis. In addition, it finds that a complex system consisting of several systems, such as the nervous, immune, and endocrine systems, participates in the regulation of the brain–gut axis. IBS may occur if there is a problem in a certain link, which may also trigger the dysfunction of other systems, resulting in the diversity and severity of IBS symptoms.

Traditional Chinese medicine is a medical theory system gradually formed and developed in long-term medical practice. In the long-term clinical use of TCM against digestive system diseases, we have discovered a close relationship between the brain and the intestine. Interestingly, this relationship is validated by the brain–gut axis theory from current microscopic studies, which suggest that there is a theoretical basis for the efficacy of TCM acupuncture therapy against IBS. Modern studies have shown that TCM acupuncture therapy can effectively regulate the functional levels of the brain–gut axis in rats with IBS (Sun et al., 2015), suggesting that TCM acupuncture therapy is a potential complementary alternative therapy for IBS.

In recent years, acupuncture therapy has attracted the attention of medical researchers in China and abroad because of its safety, efficiency, and green features. In particular, its efficacy in regulating gastrointestinal dysfunction and extraintestinal conditions has been favored by clinical medical practitioners worldwide. A large number of clinical studies have confirmed that acupuncture therapy contributes to the management of IBS, such as systematic evaluation studies demonstrating the effectiveness of acupuncture therapy (Wu Y. et al., 2019) and randomized controlled clinical trials investigating its feasibility and efficacy (Pei et al., 2020; Qi et al., 2021; Shen et al., 2022).

In addition, different studies have confirmed that acupuncture can modulate IBS from the intestinal and dorsal root ganglion perspectives (Jin et al., 2021), brain functional interconnections and effects (Ma et al., 2020), and at the level of the brain–gut axis (Zhu et al., 2017), and expert treatment consensus opinions have been formed (Zhu et al., 2017). In conclusion, acupuncture therapy can effectively treat IBS and modulate gastrointestinal symptoms and concomitant mood disorders in patients.

Irritable bowel syndrome (IBS) is a complex functional gastrointestinal disease, and it is difficult to dissect the complexity of the disease from the perspectives of abnormal brain–gut interactions, hypokinetic and visceral sensory hypersensitivity, and altered intestinal microenvironment alone. Rather, clinical workers can understand IBS from a holistic bio-psycho-social model, which has the following five guiding implications for patients and researchers: (1) the combination of anti-anxiety and depression drugs can be used to treat irritable bowel syndrome in clinical work, providing a new way of thinking for the clinical treatment of the disease; (2) the treatment can be done from the perspective of treating the bowel from the brain; (3) acupuncture can be used to treat irritable bowel syndrome from the aspect of anxiety and depression; (4) keeping patients away from stressors to avoid long-term stimulation can be a treatment method; and (5) patients can be provided with stress training, psychological training, and positive meditation to prevent later relapse or frequent relapse.

Author contributions

CJ and JZ: study concept and design. ZS, XW, and CJ: search for information. ZS and XW: draft of the manuscript. All authors contributed to the article and approved the submitted version.

Funding

This study was supported by grants from the National Natural Science Foundation of China (82074560), the Shaanxi Province Natural Science Basic Research Program Project (2020JM-697), the Shaanxi Province Innovation Capacity Support Program (2020KJXX-075), and the Shaanxi Provincial Traditional Chinese Medicine Administration Scientific Research Project (JCMS064).

Acknowledgments

The authors would like to thank Shanbo Ma, Kun Zhang, and Xiaocun Yang for their help during the discussion and revision.

Conflict of interest

The authors declare that the research was conducted in the absence of any commercial or financial relationships that could be construed as a potential conflict of interest.

Publisher's note

All claims expressed in this article are solely those of the authors and do not necessarily represent those of their affiliated organizations, or those of the publisher, the editors and the reviewers. Any product that may be evaluated in this article, or claim that may be made by its manufacturer, is not guaranteed or endorsed by the publisher.

References

Aerssens, J., Camilleri, M., Talloen, W., Thielemans, L., Göhlmann, H. W., Van Den Wyngaert, I. et al. (2008). Alterations in mucosal immunity identified in the colon of patients with irritable bowel syndrome. *Clin. Gastroenterol. Hepatol.* 6, 194–205. doi: 10.1016/j.cgh.2007.11.012

Amato, A., Cinci, L., Rotondo, A., and Serio, R. Faussone-aussone-pellegrini, M. S., Vannucchi, M. G., and Mulè, F. (2010). Peripheral motor action of glucagon-like peptide-1 through enteric neuronal receptors. *Neurogastroenterol. Motil.* 22, 664–e203. doi: 10.1111/j.1365-2982.2010.01476.x

Arciniega-maptinez, I. M., Resendiz albor, A. A., Cárdenas jaramillo, L. M., Gutlerrez-meza, J. M., Falfan-valencia, R., Arroyo, B. M. et al. (2022). CD4.(+)/IL-4(+) lymphocytes of the lamina propria and substance P promote colonic protection during acute stress. *Mol. Med. Rep.* 25, 1–10. doi: 10.3892/mmr.2021.12579

Arokiadoss, A., and Weber, H. C. (2021). Targeted pharmacotherapy of irritable bowel syndrome. *Curr. Opin. Endocrinol. Diabetes Obes.* 28, 214–221. doi: 10.1097/MED.0000000000000618

Atmaramani, R. R., Black, B. J. de la Peña, J. B., Campbell, Z. T., Pancrazio, J. J., and B. J. (2020) Conserved expression of Nav1, 7. and Nav1.8 contribute to the spontaneous and thermally evoked excitability in IL-6 and NGF-sensitized adult dorsal root ganglion neurons *in vitro*. *Bioengineering.* 7, 44. doi: 10.3390/bioengineering7020044

Aziz, I., and Simrén, M. (2021). The overlap between irritable bowel syndrome and organic gastrointestinal diseases. *Lancet Gastroenterol. Hepatol.* 6, 139–148. doi: 10.1016/S2468-1253(20)30212-0

Aziz, I., Törnblom, H., and Simrén, M. (2017). Small intestinal bacterial overgrowth as a cause for irritable bowel syndrome: guilty or not guilty? *Curr. Opin. Gastroenterol.* 33, 196–202. doi: 10.1097/MOG.0000000000000348

Balestra, B., Vicini, R., Cremon, C., Zecchi, L., Dothel, G., Vasina, V., et al. (2012). Colonic mucosal mediators from patients with irritable bowel syndrome excite enteric cholinergic motor neurons. *Neurogastroenterol. Motil* 24, 1118–e570. doi: 10.1111/nmo.12000

Barrett, J. S., Gearry, R. B., Muir, J. G., Irving, P. M., Rose, R., Rosella, O., et al. (2010). Dietary poorly absorbed, short-chain carbohydrates increase delivery of water and fermentable substrates to the proximal colon. *Aliment. Pharmacol. Ther.* 31, 874–882. doi: 10.1111/j.1365-2036.2010.04237.x

Bercik, P., Collins, S. M., and Verdu, E. F. (2012). Microbes and the gut-brain axis. *Neurogastroenterol. Motil.* 24, 405–413. doi: 10.1111/j.1365-2982.2012.01906.x

Black, C. J., and Ford, A. C. (2020). Global burden of irritable bowel syndrome: trends, predictions and risk factors. *Nat. Rev. Gastroenterol. Hepatol.* 17, 473–486. doi: 10.1038/s41575-020-0286-8

Bonaz, B. L., and Bernstein, C. N. (2013). Brain-gut interactions in inflammatory bowel disease. *Gastroenterology.* 144, 36–49. doi: 10.1053/j.gastro.2012.10.003

Brandtzaeg, P. (2013). Secretory IgA: designed for anti-microbial defense. Front. *Immunol.* 4, 222. doi: 10.3389/fimmu.2013.00222

Brawner, K. M., Yeramilli, V. A., Kennedy, B. A., Patel, R. K., and Martin, C. A. (2020). Prenatal stress increases IgA coating of offspring microbiota and exacerbates necrotizing enterocolitis-like injury in a sex-dependent manner. *Brain Behav. Immun.* 89, 291–299. doi: 10.1016/j.bbi.2020.07.008

Brzozowski, B., Mazur-Bialy, A., Pajdo, R., Kwiecien, S., Bilski, J., Zwolinska-Wcislo, M., et al. (2016). Mechanisms by which stress affects the experimental and clinical inflammatory bowel disease (IBD): role of brain-gut axis. *Curr. Neuropharmacol.* 14, 892–900. doi: 10.2174/1570159X14666160404124127

Buckley, M. M., O'Brien, R., Devlin, M., Creed, A. A., Rae, M. G., Hyland, N. P., et al. (2016). Leptin modifies the prosecretory and prokinetic effects of the inflammatory cytokine interleukin-6 on colonic function in Sprague-Dawley rats. *Exp. Physiol.* 101, 1477–1491. doi: 10.1113/EP085917

Buhner, S., and Schemann, M. (2012). Mast cell-nerve axis with a focus on the human gut. *Biochim. Biophys. Acta.* 1822, 85–92. doi: 10.1016/j.bbadis.2011.06.004

Campos-Rodríguez, R. Godinez-victoria, M., Abarca-rojano, E., Pacheco-yépez, J., Reyna-garfias, H., Barbosa-cabrera, R. E., and Drago-serrano, M. E. (2013). Stress modulates intestinal secretory immunoglobulin A. *Front. Integr. Neurosci.* 7, 86. doi: 10.3389/fnint.2013.00086

Carabotti, M., Scirocco, A., Maselli, M. A., and Severi, C. (2015). The gut-brain axis: Interactions between enteric microbiota, central and enteric nervous systems. *Ann. Gastroenterol.* 28, 203–209.

Casado-Bedmar, M., and Keita, Å. V. (2020). Potential neuro-immune therapeutic targets in irritable bowel syndrome. *Therap. Adv. Gastroenterol.* 13, 1756284820910630. doi: 10.1177/1756284820910630

Chatoo, M., Li, Y., Ma, M. A., Coote, Z., and Du, J. J., and Chen, X. (2018). Involvement of corticotropin-releasing factor and receptors in immune cells in irritable bowel syndrome. *Front. Endocrinol.* 9, 21. doi: 10.3389/fendo.2018.00021

Chen, X. Q., Kong, F. P., Zhao, Y., and Du, J. Z. (2012). High-altitude hypoxia induces disorders of the brain-endocrine-immune network through activation of corticotropin-releasing factor and its type-1 receptors. *Zhongguo Ying Yong Sheng Li Xue Za Zhi*. 28, 481–487.

Coëffier, M., Gloro, R., Boukhettala, N., Aziz, M., Lecleire, S., Vandaele, N., et al. (2010). Increased proteasome-mediated degradation of occludin in irritable bowel syndrome. *Am. J. Gastroenterol.* 105, 1181–8. doi: 10.1038/ajg.2009.700

Cryan, J. F., O'Riordan, K. J., Sandhu, K., Peterson, V., and Dinan, T. G. (2020). The gut microbiome in neurological disorders. *Lancet Neurol.* 19, 179–194. doi: 10.1016/S1474-4422(19)30356-4

De Jonge, W. J. (2013). The Gut's little brain in control of intestinal immunity. *Gastroenterol.* 2013, 630159. doi: 10.1155/2013/630159

De Winter, B. Y., Deiteren, A., and De Man, J. G. (2016). Novel nervous system mechanisms in visceral pain. *Neurogastroenterol. Motil.* 28, 309–315. doi: 10.1111/nmo.12785

Distrutti, E., Monaldi, L., Ricci, P., and Fiorucci, S. (2016). Gut microbiota role in irritable bowel syndrome: new therapeutic strategies. World J. *Gastroenterol.* 22, 2219–2241. doi: 10.3748/wjg.v22.i7.2219

Dopkins, N., Nagarkatti, P. S., and Nagarkatti, M. (2018). The role of gut microbiome and associated metabolome in the regulation of neuroinflammation in multiple sclerosis and its implications in attenuating chronic inflammation in other inflammatory and autoimmune disorders. *Immunology*. 154, 178–185. doi: 10.1111/imm.12903

Drossman, D. A. (2016). Functional gastrointestinal disorders: history, pathophysiology, clinical features and Rome IV. *Gastroenterology* 150:1262–79. doi: 10.24890/pc

Drossman, D. A., and Hasler, W. L. (2016). Rome IV-functional GI disorders: disorders of gut-brain interaction. *Gastroenterology* 150, 1257–1261. doi: 10.1053/j.gastro.2016.03.035

Elsenbruch, S., and Enck, P. (2016). Psychobiological mechanisms in the pathophysiology of chronicvisceral pain. *Schmerz*. 30, 407–411. doi: 10.1007/s00482-016-0130-9

Ericson-Neilsen, W., and Kaye, A. D. (2014). Steroids: pharmacology, complications, and practice delivery issues. *Ochsner J.* 14, 203–207. doi: 10.1142/9781848168305_0013

Fay, K. T., Ford, M. L., and Coopersmith, C. M. (2017). The intestinal microenvironment in sepsis. *Biochim. Biophys. Acta Mol. Basis Dis.* 1863, 2574–2583. doi: 10.1016/j.bbadis.2017.03.005

Ford, A. C., Moayyedi, P., Chey, W. D., Harris, L. A., Lacy, B. E., Saito, Y. A., et al. (2018). American college of gastroenterology monograph on management of irritable bowel syndrome. *Am. J. Gastroenterol.* 113, 1–18. doi: 10.1038/s41395-018-0084-x

Ford, A. C., Sperber, A. D., Corsetti, M., and Camilleri, M. (2020). Irritable bowel syndrome. *Lancet*. 396, 1675–1688. doi: 10.1016/S0140-6736(20)31548-8

Fukudo, S. (2013). Stress and visceral pain: focusing on irritable bowel syndrome. *Pain*. 154, S63–S70. doi: 10.1016/j.pain.2013.09.008

Furness, J. B. (2012). The enteric nervous system and neurogastroenterology. *Nat. Rev. Gastroenterol. Hepatol.* 9, 286–294. doi: 10.1038/nrgastro.2012.32

Grinsvall, C., Van Oudenhove, L., Dupont, P., Ryu, H. J., Ljungberg, M., Labus, J. S., et al. (2021). Altered structural covariance of insula, cerebellum and prefrontal cortex is associated with somatic symptom levels in irritable bowel syndrome (IBS). *Brain Sci.* 11, 1580. doi: 10.3390/brainsci11121580

Hanscom, M., Loane, D. J., and Shea-Donohue, T. (2021). Brain-gut axis dysfunction in the pathogenesis of traumatic brain injury. *J. Clin. Invest.* 131, 12. doi: 10.1172/JCI143777

Hillestad, E. M. R., Van Der Meeren, A., Nagaraja, B. H., Bjørsvik, B. R., Haleem, N., Benitez-Paez, A., et al. (2022). Gut bless you: the microbiota-gut-brain axis in irritable bowel syndrome. *World J. Gastroenterol.* 28, 412–431. doi: 10.3748/wjg.v28.i4.412

Hong, J. Y., Kilpatrick, L. A., Labus, J., Gupta, A., Jiang, Z., Ashe-Mcnalley, C., et al. (2013). Patients with chronic visceral pain show sex-related alterations in intrinsic oscillations of the resting brain. J. *Neurosci.* 33, 11994–12002. doi: 10.1523/JNEUROSCI.5733-12.2013

Houlden, A., Goldrick, M., Brough, D., and Vizi, E. S. LéNáRT, N., Martinecz, B. et al. (2016). Brain injury induces specific changes in the caecal microbiota of mice *via* altered autonomic activity and mucoprotein production. *Brain Behav. Immun.* 57, 10–20. doi: 10.1016/j.bbi.2016.04.003

Ivashkin, V., Poluektov, Y., Kogan, E., Shifrin, O., Sheptulin, A., Kovaleva, A., et al. (2021). Disruption of the pro-inflammatory, anti-inflammatory cytokines and tight junction proteins expression, associated with changes of the composition of the gut microbiota in patients with irritable bowel syndrome. *PLOS ONE*. 16, e0252930. doi: 10.1371/journal.pone.0252930

Jacobs, J. P., Gupta, A., Bhatt, R. R., Brawer, J., Gao, K., Tillisch, K., et al. (2021). Cognitive behavioral therapy for irritable bowel syndrome induces bidirectional alterations in the brain-gut-microbiome axis associated with gastrointestinal symptom improvement. *Microbiome*. 9, 236. doi: 10.1186/s40168-021-01188-6

Jacobson, A., Yang, D., Vella, M., and Chiu, I. M. (2021). The intestinal neuro-immune axis: crosstalk between neurons, immune cells, and microbes. *Mucosal Immunol.* 14, 555–565. doi: 10.1038/s41385-020-00368-1

Jarillo-Luna, R. A., Rivera-Aguilar, V., and Pacheco-Yépez, J. Godínez-victoria, M., Oros- pantoja, R., Miliar-garcía, A., and Campos-rodríguez, R. (2015). Nasal IgA secretion in a murine model of acute stress. The possible role of catecholamines. *J. Neuroimmunol.* 278, 223–31. doi: 10.1016/j.jneuroim.2014.11.009

Jarret, A., Jackson, R., Duizer, C., Healy, M. E., Zhao, J., Rone, J. M., et al. (2020). Enteric nervous system-derived IL-18 orchestrates mucosal barrier immunity. *Cell* 180, 50–63.e12. doi: 10.1016/j.cell.2019.12.016

Jin, D., Liu, Y., Lv, S., Qi, Q., Li, M., Wang, Y., et al. (2021). Electroacupuncture and moxibustion modulate the BDNF and TrkB expression in the colon and dorsal root ganglia of IBS rats with visceral hypersensitivity. *Evid. Based Complement Alternat Med.* 2021, 8137244. doi: 10.1155/2021/8137244

Kapugi, M., and Cunningham, K. (2019). Corticosteroids. *Orthop. Nurs.* 38, 336–339. doi: 10.1097/NOR.0000000000000595

Khlevner, J., Park, Y., and Margolis, K. G. (2018). Brain-gut axis: clinical implications. *Gastroenterol. Clin. North Am.* 47, 727–739. doi: 10.1016/j.gtc.2018.07.002

Krammer, L., Sowa, A. S., and Lorentz, A. (2019). Mast cells in irritable bowel syndrome: a systematic review. *J. Gastrointestin. Liver Dis.* 28, 463–472. doi: 10.15403/jgld-229

Labanski, A., Langhorst, J., Engler, H., and Elsenbruch, S. (2020). Stress and the brain-gut axis in functional and chronic-inflammatory gastrointestinal diseases: a transdisciplinary challenge. *Psychoneuroendocrinology*. 111, 104501. doi: 10.1016/j.psyneuen.2019.104501

Labus, J. S., Dinov, I. D., Jiang, Z., Ashe-Mcnalley, C., Zamanyan, A., Shi, Y., et al. (2014). Irritable bowel syndrome in female patients is associated with alterations in structural brain networks. *Pain*. 155, 137–149. doi: 10.1016/j.pain.2013.09.020

Lai, Y. T., Chen, C. Y., and Bair, M. J. (2021). Epidemiology, clinical features, and prescribing patterns of irritable bowel syndrome in Taiwan. *Front. Pharmacol.* 12, 788795. doi: 10.3389/fphar.2021.788795

Lee, K. N., and Lee, O. Y. (2016). The role of mast cells in irritable bowel syndrome. *Gastroenterol. Res. Pract*. 2016, 2031480. doi: 10.1155/2016/2031480

Li, S., Fei, G., Fang, X., Yang, X., Sun, X., Qian, J., et al. (2016). Changes in enteric neurons of small intestine in a rat model of irritable bowel syndrome with diarrhea. *J. Neurogastroenterol. Motil.* 22, 310–320. doi: 10.5056/jnm15082

Li, X. J., You, X. Y., Wang, C. Y., Li, X. L., Sheng, Y. Y., Zhuang, P. W., et al. (2020). Bidirectional Brain-gut-microbiota Axis in increased intestinal permeability induced by central nervous system injury. *CNS Neurosci. Ther.* 26, 783–790. doi: 10.1111/cns.13401

Logsdon, A. F., Erickson, M. A., Rhea, E. M., Salameh, T. S., and Banks, W. A. (2018). Gut reactions: how the blood-brain barrier connects the microbiome and the brain. *Exp. Biol. Med.* 243, 159–165. doi: 10.1177/1535370217743766

Lovell, R. M., and Ford, A. C. (2012). Global prevalence of and risk factors for irritable bowel syndrome: a meta-analysis. *Clin. Gastroenterol. Hepatol.* 10, 712–721.e4. doi: 10.1016/j.cgh.2012.02.029

Lyte, M., Vulchanova, L., and Brown, D. R. (2011). Stress at the intestinal surface: catecholamines and mucosa-bacteria interactions. *Cell Tissue Res.* 343, 23–32. doi: 10.1007/s00441-010-1050-0

Ma, K., Liu, Y., Shao, W., Sun, J., Li, J., Fang, X., et al. (2020). Brain functional interaction of acupuncture effects in diarrhea-dominant irritable bowel syndrome. *Front. Neurosci.* 14, 608688. doi: 10.3389/fnins.2020.608688

Mackey, E., Ayyadurai, S., and Pohl, C. S. D' Costa, S., Li, Y., and Moeser, A. J. (2016). Sexual dimorphism in the mast cell transcriptome and the pathophysiological responses to immunological and psychological stress. *Biol. Sex Differ.* 7, 60. doi: 10.1186/s13293-016-0113-7

Martin, C. R., Osadchiy, V., Kalani, A., and Mayer, E. A. (2018). The brain-gut-microbiome axis. *Cell. Mol. Gastroenterol. Hepatol.* 6, 133–148. doi: 10.1016/j.jcmgh.2018.04.003

Matheis, F., Muller, P. A., Graves, C. L., Gabanyi, I., Kerner, Z. J., Costa-Borges, D., et al. (2020). Adrenergic signaling in muscularis macrophages limits infection-induced neuronal loss. *Cell*. 180, 64–78.e16. doi: 10.1016/j.cell.2019.12.002

Mayer, E. A., Knight, R., Mazmanian, S. K., Cryan, J. F., and Tillisch, K. (2014). Gut microbes and the brain: Paradigm shift in neuroscience. *J. Neurosci*. 34, 15490–15496. doi: 10.1523/JNEUROSCI.3299-14.2014

Mu, C., Yang, Y., and Zhu, W. (2016). Gut microbiota: the brain peacekeeper. *Front. Microbiol*. 7, 345. doi: 10.3389/fmicb.2016.00345

Myers, B., and Greenwood-Van Meerveld, B. (2012). Differential involvement of amygdala corticosteroid receptors in visceral hyperalgesia following acute or repeated stress. *Am. J. Physiol. Gastrointest. Liver Physiol*. 302, G260–G266. doi: 10.1152/ajpgi.00353.2011

Nakade, Y., Tsukamoto, K., Iwa, M., Pappas, T. N., and Takahashi, T. (2007). Glucagon like peptide-1 accelerates colonic transit via central CRF and peripheral vagal pathways in conscious rats. *Auton. Neurosci.* 131, 50–56. doi: 10.1016/j.autneu.2006.06.007

Nogueira, L. T., Costa, D. V., Gomes, A. S., Martins, C. S., Silva, A. M., Coelho-Aguiar, J. M., et al. (2017). The involvement of mast cells in the irinotecan-induced enteric neurons loss and reactive gliosis. *J. Neuroinflammation*. 14, 79. doi: 10.1186/s12974-017-0854-1

Nozu, T., Miyagishi, S., Nozu, R., Takakusaki, K., and Okumura, T. (2018). Altered colonic sensory and barrier functions by CRF: roles of TLR4 and IL-1. *J. Endocrinol*. 239, 241–252. doi: 10.1530/JOE-18-0441

Nozu, T., and Okumura, T. (2015). Corticotropin-releasing factor receptor type 1 and type 2 interaction in irritable bowel syndrome. *J. Gastroenterol*. 50, 819–830. doi: 10.1007/s00535-015-1086-8

O'Hagan, C., Li, J. V., Marchesi, J. R., Plummer, S., Garaiova, I., Good, M. A., et al. (2017). Long-term multi-species *Lactobacillus* and *Bifidobacterium* dietary supplement enhances memory and changes regional brain metabolites in middle-aged rats. *Neurobiol. Learn. Mem*. 144, 36–47. doi: 10.1016/j.nlm.2017.05.015

Öhlmann, H., Koenen, L. R., Labrenz, F., Engler, H., Theysohn, N., Langhorst, J., et al. (2021). Altered brain structure in chronic visceral pain: specific differences in gray matter volume and associations with visceral symptoms and chronic stress. *Front. Neurol*. 12, 733035. doi: 10.3389/fneur.2021.733035

Orock, A., Louwies, T., Ligon, C. O., Mohammadi, E., and Greenwood-Van Meerveld, B. (2021). Environmental enrichment prevents stress-induced epigenetic changes in the expression of glucocorticoid receptor and corticotrophin releasing hormone in the central nucleus of the amygdala to inhibit visceral hypersensitivity. *Exp. Neurol*. 345, 113841. doi: 10.1016/j.expneurol.2021.113841

Osadchiy, V., Martin, C. R., and Mayer, E. A. (2019). Gut microbiome and modulation of CNS function. *Compr. Physiol*. 10, 57–72. doi: 10.1002/cphy.c180031

Pei, L., Geng, H., Guo, J., Yang, G., Wang, L., Shen, R., et al. (2020). Effect of acupuncture in patients with irritable bowel syndrome: a randomized controlled trial. *Mayo Clin. Proc*. 95, 1671–1683. doi: 10.1016/j.mayocp.2020.01.042

Person, H., and Keefer, L. (2021). Psychological comorbidity in gastrointestinal diseases: update on the brain-gut-microbiome axis. *Prog. Neuropsychopharmacol. Biol. Psychiatry*. 107, 110209. doi: 10.1016/j.pnpbp.2020.110209

Purkayastha, S., Stokes, M., and Bell, K. R. (2019). Autonomic nervous system dysfunction in mild traumatic brain injury: a review of related pathophysiology and symptoms. *Brain Inj*. 33, 1129–1136. doi: 10.1080/02699052.2019.1631488

Qi, L. Y., Wang, Y., Wang, L. Q., She, Y. F., Shi, G. X., Li, Y., et al. (2021). Acupuncture for the treatment of diarrheal-predominant irritable bowel syndrome: study protocol for a pilot randomized controlled trial. *Trials*. 22, 253. doi: 10.1186/s13063-021-05211-x

Reyes, B. A., Valentino, R. J., and Van Bockstaele, E. J. (2008). Stress-induced intracellular trafficking of corticotropin-releasing factor receptors in rat locus coeruleus neurons. *Endocrinology* 149, 122–130. doi: 10.1210/en.2007-0705

Salvioli, B., Pellegatta, G., Malacarne, M., Pace, F., Malesci, A., Pagani, M., et al. (2015). Autonomic nervous system dysregulation in irritable bowel syndrome. *Neurogastroenterol. Motil*. 27, 423–430. doi: 10.1111/nmo.12512

Schmulson, M. J., and Drossman, D. A. (2017). What is new in Rome IV. *J. Neurogastroenterol. Motil*. 23, 151–163. doi: 10.5056/jnm16214

Seminowicz, D. A., Labus, J. S., Bueller, J. A., Tillisch, K., Naliboff, B. D., Bushnell, M. C., et al. (2010). Regional gray matter density changes in brains of patients with irritable bowel syndrome. *Gastroenterology*. 139, 48–57.e2. doi: 10.1053/j.gastro.2010.03.049

Seyedmirzaee, S., Hayatbakhsh, M. M., Ahmadi, B., Baniasadi, N., Bagheri Rafsanjani, A. M., Nikpoor, A. R., et al. (2016). Serum immune biomarkers in irritable bowel syndrome. *Clin. Res. Hepatol. Gastroenterol*. 40, 631–637. doi: 10.1016/j.clinre.2015.12.013

Sheehan, J., Gaman, A., Vangel, M., and Kuo, B. (2011). Pooled analysis of brain activity in irritable bowel syndrome and controls during rectal balloon distension. *Neurogastroenterol. Motil.* 23, 336–346. doi: 10.1111/j.1365-2982.2010.01635.x

Shen, J. H., Ye, Y. M., and Li, S. S. (2022). Acupuncture for diarrhea-predominant irritable bowel syndrome: a randomized control study. *World J. Acupuncture-Moxibustion* 32, 123–130. doi: 10.1016/j.wjam.2022.02.003

Simren, M., Mansson, A., Langkilde, A. M., Svedlund, J., Abrahamsson, H., Bengtsson,U., et al. (2001). Food-related gastrointestinal symptoms in the irritable bowel syndrome. *Digestion*. 63, 108–115. doi: 10.1159/000051878

Skaper, S. D., Facci, L., and Giusti, P. (2014). Mast cells, glia and neuroinflammation: partners in crime? *Immunology*. 141, 314–327. doi: 10.1111/imm.12170

Sperber, A. D., Bangdiwala, S. I., Drossman, D. A., Ghoshal, U. C., Simren, M., Tack, J., et al. (2021). Worldwide prevalence and burden of functional gastrointestinal disorders, results of Rome foundation global study. *Gastroenterology*. 160, 99–114.e3. doi: 10.1053/j.gastro.2020.04.014

Stasi, C., Rosselli, M., Bellini, M., Laffi, G., and Milani, S. (2012). Altered neuro-endocrine-immune pathways in the irritable bowel syndrome: the top-down and the bottom-up model. *J. Gastroenterol*. 47, 1177–1185. doi: 10.1007/s00535-012-0627-7

Sun, J., Wu, X., Meng, Y., Cheng, J., Ning, H., Peng, Y., et al. (2015). Electro-acupuncture decreases 5-HT, CGRP and increases NPY in the brain-gut axis in two rat models of diarrhea-predominant irritable bowel syndrome (D-IBS). *BMC Complement. Altern. Med*. 15, 340. doi: 10.1186/s12906-015-0863-5

Tache, Y., Larauche, M., Yuan, P. Q., and Million, M. (2018). Brain and gut CRF signaling: Biological actions and role in the gastrointestinal tract. *Curr. Mol. Pharmacol*. 11, 51–71. doi: 10.2174/1874467210666170224095741

Tanaka, F., Tominaga, K., Fujikawa, Y., Nagami, Y., Kamata, N., Yamagami, H., et al. (2016). Concentration of glial cell line-derived neurotrophic factor positively correlates with symptoms in functional dyspepsia. *Dig. Dis. Sci*. 61, 3478–3485. doi: 10.1007/s10620-016-4329-5

Thomas, C., Gioiello, A., Noriega, L., Strehle, A., Oury, J., Rizzo, G., et al. (2009). TGR5-mediated bile acid sensing controls glucose homeostasis. *Cell Metab*. 10, 167–177. doi: 10.1016/j.cmet.2009.08.001

Touny, A. A., Kenny, E., Månsson, M., Webb, D. L., and Hellström, P. M. (2022). Pain relief and pain intensity response to GLP-1 receptor agonist ROSE-010 in irritable bowel syndrome; clinical study cross-analysis with respect to patient characteristics. *Scand. J. Gastroenterol*. 57, 783–791. doi: 10.1080/00365521.2022.2041084

Uranga, J. A., Martínez, V., and Abalo, R. (2020). Mast cell regulation and irritable bowel syndrome: effects of food components with potential nutraceutical use. *Molecules*. 25, 4314. doi: 10.3390/molecules25184314

Van De Wouw, M., Boehme, M., Lyte, J. M., Wiley, N., and Strain, C. O'sullivan, O. et al. (2018). Short-chain fatty acids: microbial metabolites that alleviate stress-induced brain-gut axis alterations. *J. Physiol.* 596, 4923–4944. doi: 10.1113/JP276431

Vicario, M., González-Castro, A. M., Martínez, C., Lobo, B., Pigrau, M., Guilarte, M., et al. (2015). Increased humoral immunity in the jejunum of diarrhoea-predominant irritable bowel syndrome associated with clinical manifestations. *Gut*. 64, 1379–1388. doi: 10.1136/gutjnl-2013-306236

Videlock, E. J., Shih, W., Adeyemo, M., Mahurkar-Joshi, S., Presson, A. P., Polytarchou, C., et al. (2016). The effect of sex and irritable bowel syndrome on HPA axis response and peripheral glucocorticoid receptor expression. *Psychoneuroendocrinology* 69, 67–76. doi: 10.1016/j.psyneuen.2016.03.016

Wiley, J. W., Higgins, G. A., and Athey, B. D. (2016). Stress and glucocorticoid receptor transcriptional programming in time and space: Implications for the brain-gut axis. *Neurogastroenterol. Motil.* 28, 12–25. doi: 10.1111/nmo.12706

Wood, J. D. (2020). Serotonergic integration in the intestinal mucosa. *Curr. Pharm. Des*. 26, 3010–3014. doi: 10.2174/1381612826666200612161542

Wouters, M. M., Vicario, M., and Santos, J. (2016). The role of mast cells in functional GI disorders. *Gut*. 65, 155–168. doi: 10.1136/gutjnl-2015-309151

Wu, I. X. Y., Wong, C. H. L., Ho, R. S. T., Cheung, W. K. W., Ford, A. C., Wu, J. C. Y., et al. (2019). Acupuncture and related therapies for treating irritable bowel syndrome: overview of systematic reviews and network meta-analysis. *Therap. Adv. Gastroenterol.* 12, 1756284818820438. doi: 10.1177/1756284818820438

Wu, Y., He, H., Cheng, Z., Bai, Y., and Ma, X. (2019). The role of neuropeptide Y and peptide YY in the development of obesity *via* gut-brain axis. *Curr. Protein Pept. Sci*. 20, 750–758. doi: 10.2174/1389203720666190125105401

Zahedi, M. J., Behrouz, V., and Azimi, M. (2018). Low fermentable oligo-di-mono-saccharides and polyols diet vs. general dietary advice in patients with diarrhea-predominant irritable bowel syndrome: a randomized controlled trial. *J. Gastroenterol. Hepatol*. 33, 1192–1199. doi: 10.1111/jgh.14051

Zhang, B., Ma, M. A., Rachmin, S., He, I., Baral, M., Choi, P., et al. S. et al. (2020). Hyperactivation of sympathetic nerves drives depletion of melanocyte stem cells. *Nature*. 577, 676–681. doi: 10.1038/s41586-020-1935-3

Zhang, L., Song, J., and Hou, X. (2016). Mast cells and irritable bowel syndrome: from the bench to the bedside. *J. Neurogastroenterol. Motil.* 22, 181–192. doi: 10.5056/jnm15137

Zhang, L., Wang, R., Bai, T., Xiang, X., Qian, W., Song, J., et al. (2019). EphrinB2/ephB2-mediated myenteric synaptic plasticity: mechanisms underlying the persistent muscle hypercontractility and pain in post-infectious IBS. *FASEB J*. 33, 13644–13659. doi: 10.1096/fj.201901192R

Zhu, X., Liu, Z., Niu, W., Wang, Y., Zhang, A., Qu, H., et al. (2017). Effects of electroacupuncture at ST25 and BL25 in a Sennae-induced rat model of diarrhoea-predominant irritable bowel syndrome. *Acupunct. Med*. 35, 216–223. doi: 10.1136/acupmed-2016-011180

Frontiers in Neuroscience

Provides a holistic understanding of brain function from genes to behavior

Part of the most cited neuroscience journal series which explores the brain - from the new eras of causation and anatomical neurosciences to neuroeconomics and neuroenergetics.

Discover the latest Research Topics

See more →

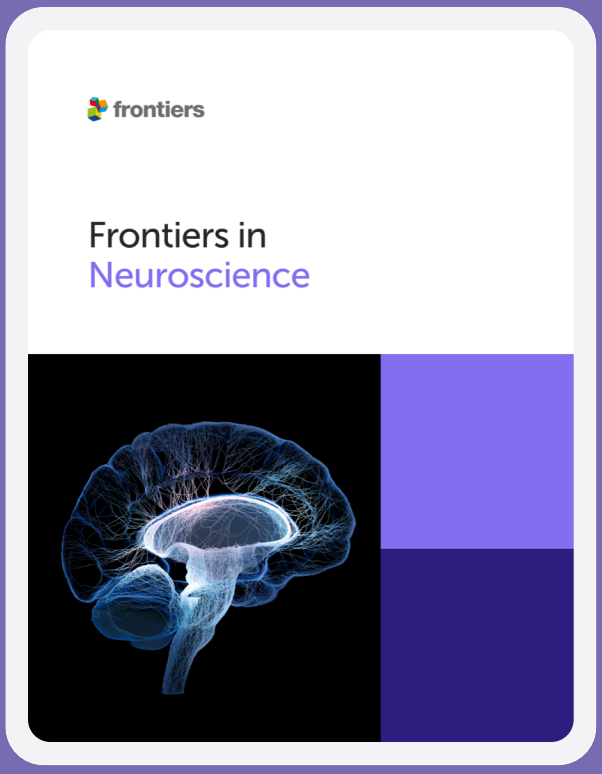

Frontiers

Avenue du Tribunal-Fédéral 34
1005 Lausanne, Switzerland
frontiersin.org

Contact us

+41 (0)21 510 17 00
frontiersin.org/about/contact